COMPUTATIONAL CIVIL ENGINEERING 2006

F. Paulet-Crainiceanu, C. Ionescu, H. Barbat

editors

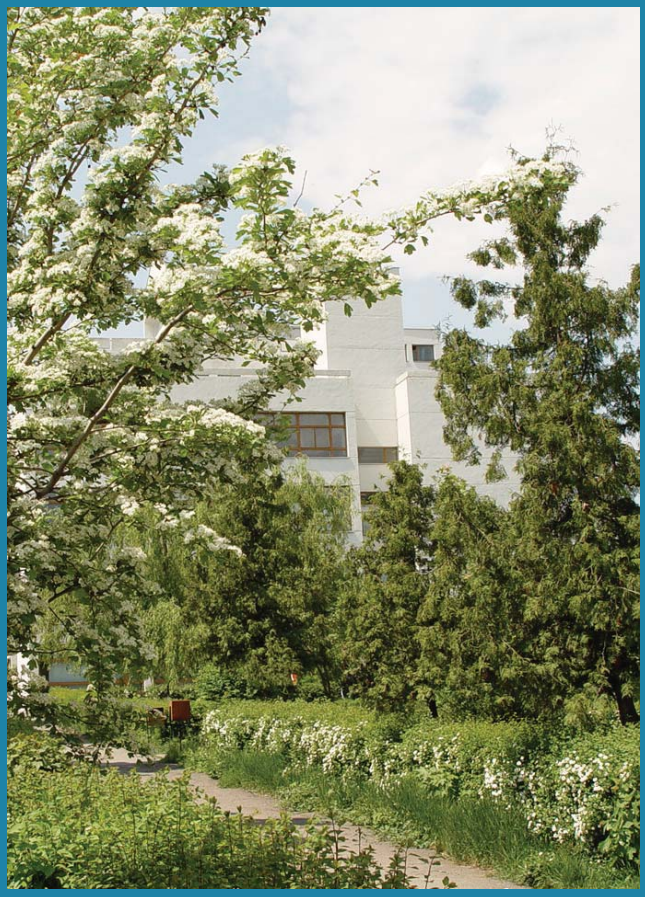

EDITURA SOCIETATII ACADEMICE "MATEI - TEIU BOTEZ"

Iasi, 2006

International Symposium

“Computational Civil Engineering 2006”

Iaşi, România, May 26, 2006

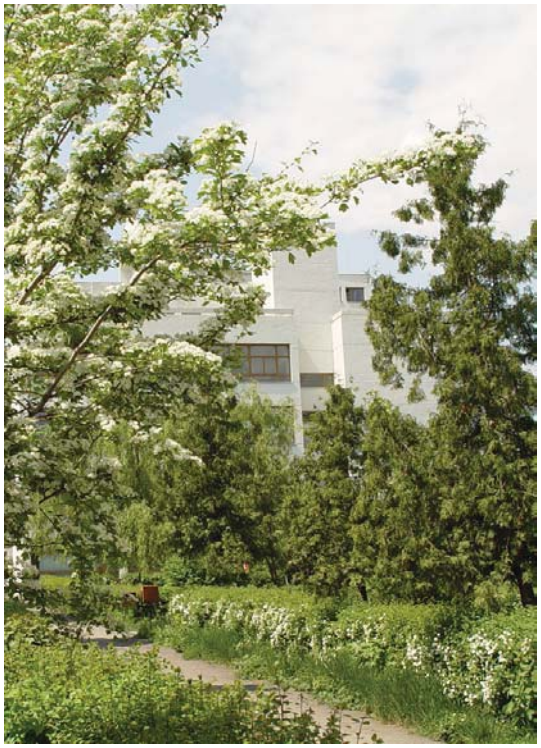

F. Paulet-Crainiceanu, C. Ionescu, H. Barbat
Editors

EDITURA SOCIETĂŢII ACADEMICE "MATEI-TEIU BOTEZ"
Iaşi, 2006

"Computational Civil Engineering. 2006", International Symposium
Iaşi, România, May 26, 2005
F. Paulet-Crainiceanu, C. Ionescu, H. Barbat
Editors

Descrierea CIP a Bibliotecii Naționale a României

COMPUTATIONAL CIVIL ENGINEERING. INTERNATIONAL SYMPOSIUM (2006 ; Iaşi)

Computational civil engineering - 2006 : 26 mai, Iaşi / editors: Fideliu Păuleț-Crăiniceanu, Constantin Ionescu, Horia Barbat. - Iaşi : Editura Societății Academice "Matei - Teiu Botez", 2006

Bibliogr.

ISBN (10) 973-7962-89-3 ; ISBN (13) 978-973-7962-89-8

I. Păuleț-Crăiniceanu, Fideliu (ed.)
II. Ionescu, Constantin (ed.)
III. Barbat, Horia (ed.)

004:624(063)

Computerized processing: F. Păuleț-Crăiniceanu

Historical moments from Civil Engineering technical education in Moldova

- **Midle Age and the beginning of Modern Age**

- "Schola latină" (Latin School) from Cotnari (1562-1563) (during the ruling of the voivode Eraclide "the Despot").
- Superior College (also named "Vasilian Collage" or "Vasilian Academy" after the voivode Vasile Lupu) from the Trei Ierarhi Monastery in Iaşi (1634-1653).
- "Şcoala Domnească" (Royal or Voivodal School) from Iaşi (1714).

- **XIXth Century**

- "Şcoala de ingineri hotarnici" (School of Land Surveyors) in Romanian language from Iaşi (1813-1820) created by Gheorghe Asachi. This is the first testimony of engineering technical education in Romanian language in Iaşi.
- "Academia Mihăileană" ("Mihailean Academy", after the voivode Mihail Sturdza) from Iaşi (1834-1848). Through the Mihailean Academy, durable foundations for Romanian Higher education were laid.
- Mihail Kogălniceanu (politician, historian, writer and journalist) makes the project for organizing in Iaşi an "Applicative School for Roads, Bridges and Buildings" („Şcoala de aplicație pentru drumuri, poduri şi zidiri"). This is the first project of a polytechnic school in Romania (1850).

- **XXth Century**

- Inside the University of Iaşi, the next Applied Sciences sections are created: Electrotechnic, Industrial Chemistry, and Agricultural Chemestry (1912).
- The „Gheorghe Asachi" Polytechnical School from Iaşi (1937) containing the next Faculties: Electrotechnic, Industrial Chemistry, and Agriculture is formed.
- The Faculty of Civil Engineering is established (1941).
- The Polytechnical School from Iaşi is divided in 1948 into:
  - „Ion Ionescu de la Brad" Agronomical Institute from Iaşi;
  - „Gheorghe Asachi" Polytechnical Institute of Iaşi, with the Faculties: Industrial Chemistry, Civil Engineering, Electromechanics and Mechanics.

Establishment of the Faculty of Civil Engineering of Iaşi

***Based on the Decree-Law no. 989 from November 13, 1941, published in „The Official Monitor" no. 270, at the „Gh. Asachi" Polytechnical School from Iaşi the Faculty of Civil Engineering is established*.**

In „The Official Monitor", part I, no. 118 from May 23, 1942, the Faculty of Civil Engineering of Iaşi's structural organization is published. The general specialization is that of Civil Engineer and the Faculty had the next positions: six Professors and six Associate Professors for general subjects, four Professors for specialty subjects (Bridges I – wood and masonry, Bridges II – metallic constructions, Railways, Roads) and five Associate Professors for specialty subjects (Drawing for Civil Engineering; Topography, Geodesy and Land Survey; Construction Materials' Technology; Architecture; Navigations and Land Reclamation). During the next years, other subjects have been added: Civil Engineering Constructions, Geotechnics, Reinforced Concrete, Foundations, and Urbanism. Under this organizational structure, the Faculty acted until the education reform in 1948.

Professor **Anton Şesan** (1916-1969)

ANTON ŞESAN
1916 - 1969

Professor Anton Şesan was born on December 26, 1916, in Carapciu – Storojineț, a village in Hotin County (now in Republic of Moldova), from a family of intellectuals. He followed the high school in Rădăuți and then the Polytechnic School from Bucharest.

In 1940 he obtains the Civil Engineer diploma and, in a short time, he became the manager of a construction company. In 1943 he takes the Assistant Professor position in Strength of Materials at the "Gh. Asachi" Polytechnic Institute of Iaşi. In 1945 he becomes Associate Professor in Civil Engineering and, in 1948, Deputy Professor in Structural Statics. In 1951 he is promoted to full Professor in Structural Statics. In his activity he also taught Structural Dynamics and Structural Design in Plastic Domain.

He was the head of the Structural Statics and Strength of Materials Department, Vice-Dean, Vice-Rector and Ph.D. adviser. Also, he has been the manager of the Constructions Researches Institute (INCERC) Iaşi Branch from 1957 (when this branch have been established) until the end of his life.

Anton Şesan was a great Professor, a real promoter of science and researches, a developer of new fields and techniques in Civil Engineering. He created strong bases for the future of the Faculty of Civil Engineering of Iaşi, and many generations of students, researchers and faculties were powerfully influenced by him.

He introduces the new, at that time, notion of *factorial moments* and a version of Displacement Method, the *Active Moments Method*. He generalizes the Moments Distribution Method in the plastic domain and was a pioneer in mathematical modeling and in computerized structural design. Professor Şesan was a forerunner in the use of probabilistic approach for building safety.

The most important realizations of Professor Anton Şesan are linked with antiseismic protection of Civil Engineering structures. He proposed *Earthquake Engineering* as a topic for students. The theoretical studies he conducted were doubled by experimental researches. Together with a team of faculties and researchers from INCERC he realized three shaking tables (600 KN, 150 KN and 5 KN) that made Iaşi the most important research center in Romania and one of the most important in Eastern Europe.

Professor Anton Şesan published more than 140 scientific papers.

Department of Structural Mechanics,

Faculty of Civil Engineering of Iaşi

Professor **Alexandru Negoiță** (1916-1998)

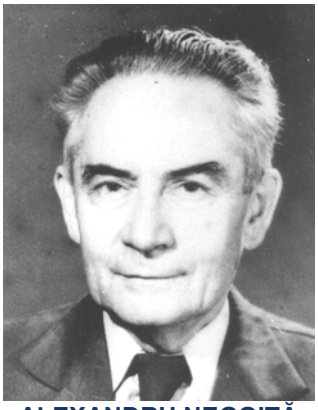

ALEXANDRU NEGOIȚĂ
1916 - 1998

Part of the elite of Romanian technical higher education, Professor Alexandru Negoiță was a model for many generations of students. He initiated many fundamental and applied sciences research directions.

He was born in Ciurea, a village in Iaşi County on June 19, 1916. In 1934 he graduates the National High School from Iaşi and in 1940 he graduates the Faculty of Civil Engineering from the Polytechnic University of Bucharest.

For 12 years he worked for very important building and design companies. Then, for 26 years, he worked in research field, being at one moment the general manager of the Civil Engineering Research Institute.

From 1952, Alexandru Negoiță becomes Associate Professor and from 1961 Professor in the staff of the Faculty of Civil Engineering from Cluj-Napoca. For a period of time he had been the Dean of that Faculty. From 1971 he moves to Iaşi, as a Professor at the Faculty of Civil Engineering Iaşi. A member of the Structural Mechanics Department, Professor Negoiță was elected, between 1971 and 1982, the head of department.

Professor Alexandru Negoiță taught subjects as: Civil and Industrial Buildings; Strength of Materials; Earthquake Engineering, History of Techniques in Constructions; Theory of Structures. After the 1977 earthquake he convinced the authorities to allow the initiation of Earthquake Engineering as a topic for students in Civil Engineering. He also taught Earthquake Engineering for two years at the Faculty of Civil Engineering from Oran in Algeria.

He published more than 300 scientific papers and participated to more than 200 research projects in Romania and outside. One of his books, "Applications of Earthquake Engineering" was awarded the "Anghel Saligny" prize from the Romanian Academy.

He organized and participated to many scientific meetings were he received high appreciations. Alexandru Negoiță was a member of many national and international professional associations. He was the Ph.D. adviser for more than 65 graduate students and was a member of the Romanian Ministry of Education commission for titles and diplomas awards.

In 1997, Professor Alexandru Negoiță receives the title of *Doctor Honoris Causa* from the Technical University of Cluj-Napoca.

Professor **Lucian Strat**

"Computational Civil Engineering 2006", International Symposium
Iaşi, România, May 26, 2006

Some aspects of the contribution of Professor Anton Sesan to Romanian construction school

Florin Macavei

Department of Structural Mechanics, Technical University of Civil Engineering of Bucharest, Romania

Summary

Some aspects of the Professor Anton Sesan's contribution to Romanian construction school are presented.

After a short description of the factorial moments operators, the factorial determinants are presented as operators for solving the plane and space framed contours as well as the plane and space framed structures. The connection with frontal method for finite element analysis is pointed out.

Some aspects concerning the seismic station are presented.

KEYWORDS: factorial moments, factorial determinants operators, frontal method.

1. INTRODUCTION

Professor Anton Sesan was a great personality. He created a valuable school of Statics of Structures, Strength of Materials, Dynamics of Structures and Earthquake Engineering.

Professor Anton Sesan pointed out the importance of the theoretical research in connection with the experimental investigations.

2. THE STRUCTURE AS A WHOLE

As a member of the Statics and Strength of Materials Department whose head was Professor Anton Sesan, I learned that any structure must be considered as a whole. The extraction of a joint (Figure 1) in order to be investigated experimentally in detail is incorrect. The behavior of the extracted joint is different from the behavior of the same joint of the structure. The results are falsified.

The same rule he applied to people. Anybody has to be considered as a whole. It is wrong to consider only one or some aspects.

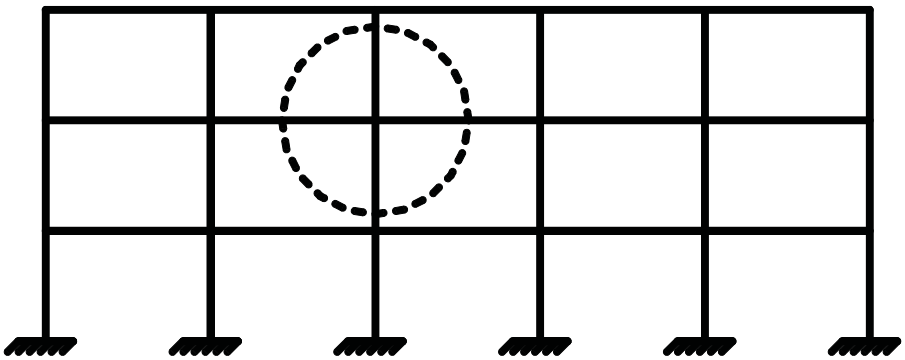

Figure 1. Extraction of a joint

3. FACTORIAL MOMENTS OPERATORS

Professor Anton Sesan introduced the factorial moments operators. He expressed the differential relations among the flexural functions in a generalized form (discontinuities, any loads, variable inertia moment etc). Expressing the external actions as factorial moments of suitable order it can be written the expression of any flexural function as a sum of factorial moments of the corresponding order.

Sesan A. and Ciongradi I. [3] generalized the factorial moments for Dynamics of beams with distributed mass.

4. FACTORIAL DETERMINANTS

The factorial determinant operator was conceived in 1967. It was presented in 1967 and 1968 at Scientific Seminary of Statics and Strength of Materials Department.

It was published by Anton Sesan, Adrian Vulpe and Florin Macavei in 1969, [4] and 1971 [5].

This type of determinant applies to rectangular matrices. Examples :

- a row determinant is equal to the sum of the elements
- a column determinant is equal to the product of the elements divided by the factorial of the number of elements
- a determinant with two columns and "n" identical rows is equal to Newton's binomial divided by n! (Figure 2,a)

For a space contour, the elements of the factorial determinant are (3×3) submatrices.

$$\begin{vmatrix} a & b \\ a & b \\ a & b \\ a & b \\ a & b \end{vmatrix} = \frac{a^5}{5!} + \frac{a^4 b}{4!1!} + \frac{a^3 b^2}{3!2!} + \frac{a^2 b^3}{2!3!} + \frac{a b^4}{1!4!} + \frac{b^5}{5!}$$

a) The connection with binomial formula

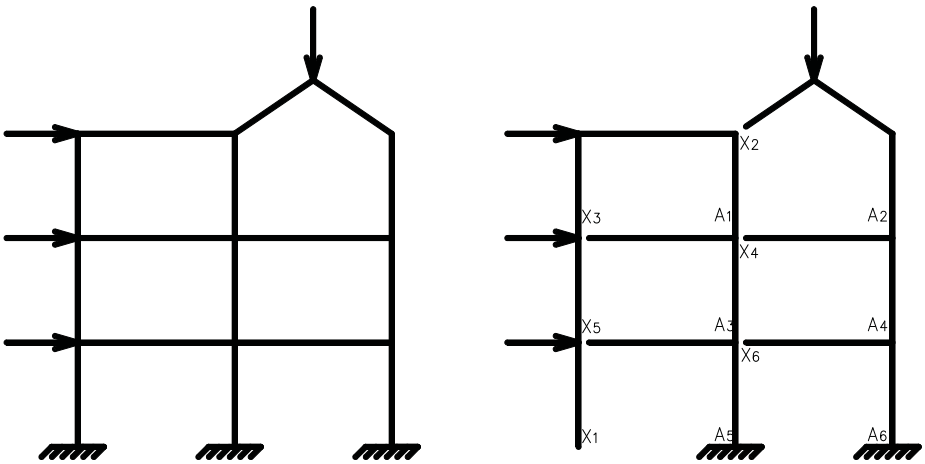

b) The successive elimination of the structure portions

Figure 2. Factorial determinants

A plane or a space structure is solved by successive elimination of the structure portions. These portions are contours (Figure 2,b).

The writing and the solving of the system of equations is made interwined. The unknows are eliminated successively, each X_i being expressed in terms of unknowns X_j ($j > i$), by putting conditions of continuity at A_i .

Actually, the force method is used.

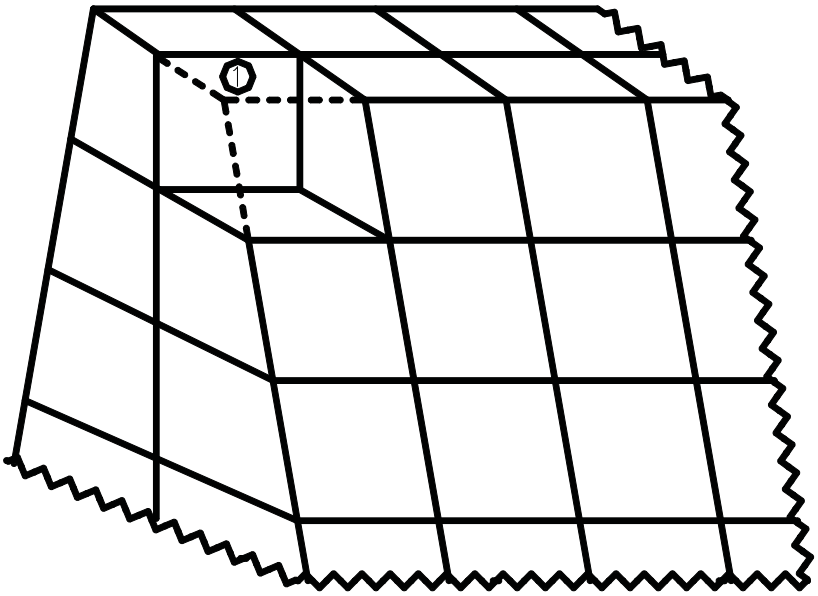

a) The elimination of the first element

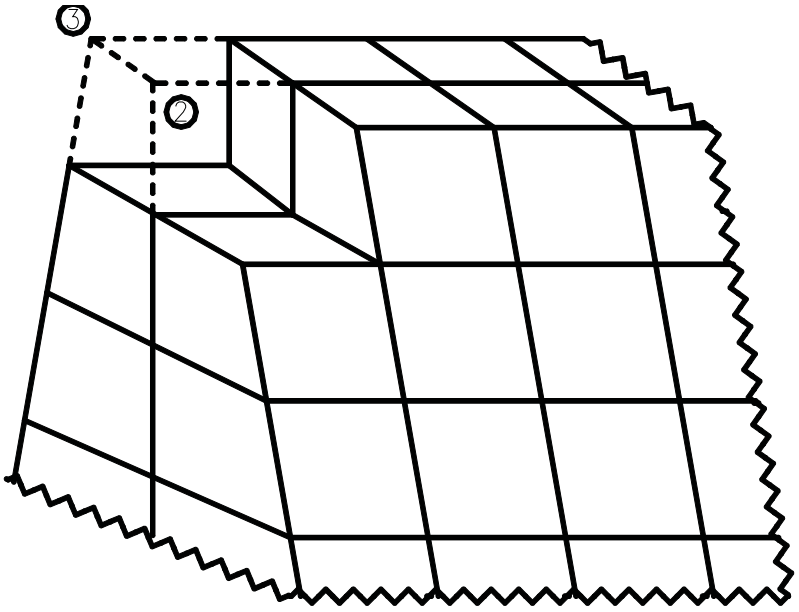

b) The elimination of the second element

Figure 3. The frontal method

5. THE FRONTAL METHOD

In frontal method [1], the displacement method is used, namely the finite element analysis. The writing and the solving of the system of equations is made intertwined. In each step are generated only the equations necessary in that step (Figure 3).

For a certain numbering of the elements, the first substructure contains only the first element, the second substructure contains the first two elements, but with internal joints incident only to the second element, [2], and so on.

The numbering of the elements is important.

6. THE SEISMIC STATION

Since 1966 I lived in the house of Gheorghe Asachi Street, at number 7. From the window of my room I could see the Seismic Station. It was a great opportunity.

This seismic station is the first in Romania and in this part of Europe.

References

1. Irons, B. M. A frontal solution program for finite element analysis, *Int. J. Num. Meth. Eng*., Vol. 2, 1970.
2. Macavei, F. *Contributii la determinarea raspunsului dinamic al structurilor spatiale*. Teza de doctorat, ICB, Bucuresti, 1983.(in Romanian)
3. Sesan, A.,Ciongradi, I. Momente exponentiale pentrui determinarea functiilor incovoierii a barelor cu masa distribuita, *Buletinul IPI*, Tomul XI (XV), Fasc. 1-2, 1965.(in Romanian)
4. Sesan, A., Vulpe, A., Macavei F. Use of the “factorial moments” operators in the solving of space contours, *Buletinul IPI*, Tomul XV (XIX), Fasc. 3-4, 1969.
5. Sesan, A., Vulpe, A., Macavei F. Factorial determinants in solving the space contours, *Instituto Lombardo – Accademia di Scienze e Lettere, Rendiconti*, Vol. 105, Milano, 1971.

Table of Contents

***
Historical moments from Civil Engineering technical education in Moldova i

***
Establishment of the Faculty of Civil Engineering of Iaşi i

Department of Structural Mechanics, Faculty of Civil Engineering of Iaşi
Professor Anton Şesan (1916-1969) ii

Lucian Strat
Professor Alexandru Negoiță (1916-1998) iii

Florin Macavei
Some aspects of the contribution of Professor Anton Sesan to Romanian construction school iv

Table of Contents 3

1. Păuleț-Crăiniceanu, F., Ionescu, C., Barbat, H.
Achievements and performances in Computational Civil Engineering 7

2. Mata, P.A., Barbat, A.H., Oller, S.M.
Seismic analysis of structures incorporating energy dissipating devices by means of numerical methods 25

3. Mata, P.A., Barbat, A.H., Oller, S.M.
Numerical simulation of the seismic behavior of passively controlled precast concrete buildings 38

4. Carreño, M.L., Cardona, O.D., Barbat, A.H.
Holistic evaluation of the seismic risk in urban centers 51

5. Faleiro, J., Barbat, A., Oller, S.
Nonlinear Analysis of Reinforced Concrete Frames 69

6. Brozovsky, J., Fojtik, T., Martinec, P.
Impact of fine aggregates replacement by fluidized fly ash to resistance of concretes to aggressive media 100

7. Brozovsky, J., Martinec, P., Brozovsky, jr., J.
Time flow of gypsumfree cements strength development 107

8. Kratochvil, A., Brozovsky, J.
The optimization of properties of self-compacting concrete by the combination of fine filler 113

9. Minch, M., Trochanowski, A.
Boundary element method numerical modeling of RC plane stress cracked plate 123

10. Minch, M., Trochanowski, A.
The numerical model for reinforced concrete structures and analysis using finite elements method 136

11. Szołomicki, J.
Numerical modelling for homogenization of masonry structures 147

12. Boroń, J.
About some important changes in applied structural optimization 156

13. Proca, G.E.
A database for elements' and structures' computation 166

14. Rotberg, R.
Thermal composites design 171

15. Amariei, C., Filip, V.
A generalization of the moments distribution method for the structure computation in the postelastic field 181

16. Campian, C., Pernes, P.
Finite element model for composite steel-concrete column 189

17. Zach, J., Kminova, H., Horky, O.
Determination of temperature course in concrete during hydration 198

18. Dósa, A., Popa, L.
High order beam elements for the stability and non-linear analysis of frame structures 204

19. Popa, L.
The analysis of frame structures with non-prismatic beams 212

20. Kozlovská, M., Kozák P.
Computer aided tool for personal protection equipment generation 216

21. Bašková, R.
Computational modeling of building process time behaviour 225

22. Struková, Z.
Electronic portal for occupational health and safety management on building site 238

23. Brozovsky jr., J., Kolos, I., Materna, A.
Non-linear constitutive model for mortar 245

24. Radinschi, I., Ciobanu, B.
Implementation of computational methods in Physics learning 251

25. Másilková, L.
Indoor climate in contemporary buildings 257

26. Iancovici, M.
Correlations of earthquake ground motion and energy distributions in one-story irregular building structures 265

27. Musil, R.
Building system loads and its climatic data 277

28. Sokolar, R.
Utilization of the Statistical Method of Planned Experiment (PLANEX) for research of building materials properties 286

29. Lungu, I., Boţi, N.
Soil improvement in the design of the foundation rehabilitation 292

30. Boţi, N., Lungu, I., Boţi, I.
Evaluation of the geotechnical risk in the hilly zones within the city of Iaşi 299

31. Brandejsová, H., Novotný, M.
Present trends and potentialities in designing of log-houses external walls 307

32. Fojtík, T., Vymazal, T., Žižková, N., Petránek, V.
Technical, environmental and security criteria of new building materials parameters evaluation 313

33. Brosteanu, M., Brosteanu, T.
Selection of theoretical method for lateral load analysis of brick shear walls structures 321

34. Nevrivova, L.,
Using computer technology for laboratory results (data) evaluation 328

35. Chiorean, C.G.
A computer program for advanced analysis of semi-rigid steel space frames 336

36. Chiorean, C.G.
A computer program for M-N-Φ and N-M-M analysis of reinforced concrete sections 345

37. Šikula, O.
CFD simulation of indoor climate 360

38. Vasilescu, A.
Remarks on the Geometrical Non-Linear Analysis of Cyclic Symmetrical Structures 369

39. Doležílková, H.
Computer modelling and simulation of carbon dioxide indoor concentration 375

40. Berkowski, P.
Some examples of structural optimization problems modelling 383

41. Barbuta, M., Petru, M., Nour, D.S.
Computer simulation on reinforced concrete beams subjected to flexure 393

42. Ungureanu, N., Vrabie, M., Moga, A., Ungureanu, C.
Some aspects regarding the design and building of the retaining walls systems made of precast concrete blocks 401

43. Vulpe, A., Carausu, A.
Modeling and evaluation of seismically induced damages by functional and stochastic models 412

44. Coveianu, M., Bîtcă, D.
Design of compressed elements simulated with elements of initial deflection equivalent to buckling curves A,B,C 427

45. Prodescu, A., Bîtcă, D.
Studies regarding the computation of vibrating frequencies for steel taintor (radial) gates 435

46. Vlad, I.A.
Teaching and learning Applied Mechanics by aid of computers 443

47. Žižková, N.
New screed materials for external thermal insulation composite systems 449

48. Petránek, V.
Coating of concrete structures exposed to corrosive media 456

49. Diaconu, D., Vasilescu, D., Palamaru, G., Mihai, C., Diaconu, A.C., Popa, T.
Iassy contributions to the development of Earthquake Engineering 464

50. Comisu, C.C.
Real-time damage monitoring system by modal testing of highway bridges 490

51. Voiculescu, D.
Useful calculation of buckling length for steel columns 500

52. Voiculescu, D., Preda, D.
“HE” column sizing under complex actions 505

53. Teleman, E.C., Axinte, E., Silion, R.
Trends of actual computer assistance for laboratory studies in boundary layer wind tunnel 509

54. Ionescu, C., Popa, R.
The importance of databases for the efficient exploitation of bridges within an administrative unit 519

55. Ionescu, C., Nicuță, A.
Information and dissemination in Bridge Engineering 525

56. Păuleț-Crăiniceanu, F.
Steps in Structural Robotics implementation 531

"Computational Civil Engineering 2006", International Symposium
Iaşi, România, May 26, 2006

Achievements and performance in Computational Civil Engineering

Fideliu Păuleț-Crăiniceanu[1], Constantin Ionescu[1], Horia Barbat[2]

[1]"Gh. Asachi" Technical University of Iaşi, România
[2]Universitat Politècnica de Catalunya, Barcelona, Spain

Summary

In Civil Engineering, computers are becoming from major tools to vital tools. The international symposium "Computational Civil Engineering" held every year in Iaşi, Romania is proving the above statement. The multitude and diversity of themes, methodologies and applications show that this symposium is a result of a necessity and of a practical approach in Civil Engineering.

Through the gathering of researchers' achievements and points of view, Computational Civil Engineering symposium is a real platform for scientific expression and it is helping people involved in Civil Engineering field in obtaining news and knowledge.

At the same time the organizers of Computational Civil Engineering 2006 are very proud of the large participation number and also of the high quality of science and technology reflected in the papers of proceedings.

Computational Civil Engineering 2006 was also an opportunity for remembering some great Professors from the Faculty of Civil Engineering of Iaşi and also to celebrate the 65th anniversary from the establishment of higher education in construction field in Moldova.

KEYWORDS: civil engineering, computer aided design, computer aided engineering, computer programming, computer-based education, computational methods, databases, computer aided management.

1. INTRODUCTION

The use of computer in Civil Engineering is becoming more and more a vital fact. It is almost unconceivable to obtain efficiency and fast results in research, design, realization and maintenance in Civil Engineering domain without the use of computers and computer applications (software).

In turn, the increasing dependency on computers is generating concerns about the reliability of all involved factors (power supply, computer security,

communications means, software accuracy, training and responsibility of users etc.).

The above two statements together with similar approaches from other engineering domains have generated the need of a new terminology that took form as *Computational Civil Engineering* [1], shortened as *CCE*. Historians of Civil Engineering might get countless proves of early forerunner in this field and they will be of a real help in showing interesting, exotic, unknown, etc. professional facts and people that put the basics of the named field.

Therefore, a group of three enthusiasts from Romania and Spain decided to organize a small symposium [1] that latter repeated [2-4] and may become a tradition that is a platform for impressive researches and a chance for researchers to integrate more in the scientific Civil Engineering community. Books and CDs with the proceedings have been issued, see Figure 1.

Figure 1. Proceedings of Computational Civil Engineering International Symposiums (covers of books and CDs)

A synthetic statistics of the participations to the Computational Civil Engineering symposium is shown in Table 1.

From the gained experience, the organizers of Computational Civil Engineering international symposiums have detected some general important themes of the

field: Computer Aided Design and Engineering, Computer Programming for Civil Engineering, Computer-Based Education, Computational Methods in Civil Engineering, Databases in Civil Engineering, and Computer Aided Management in Civil Engineering. Other directions could be identified, too. For the moment the papers were not classified conforming to the themes, but it might be useful in the future.

Table 1. Evolution of participation at CCE Symposiums

	No of authors	No of countries	No of papers	No of pages
CCE 2003	38	3	28	239
CCE 2004	42	5	28	266
CCE 2005	40	2	29	297
CCE 2006	84	5	57	539

Computational Civil Engineering 2006 was also an opportunity for remembering some great Professors from Faculty of Civil Engineering of Iaşi, Figure 2, and also to celebrate the 65th anniversary from the establishment of higher education in construction field in Moldova [5-9].

Figure 2. CCE2006. The two remembered Professors

At the same time it should be fair to stress the importance and support given by the Faculty of Civil Engineering from the "Gh. Asachi" Technical University of Iaşi, Romania [10], by the "Matei-Teiu Botez" Academic Society from Iaşi, Romania and its publishing house [11] to the Computational Civil Engineering

symposiums. Also, it might be of interest to show that many papers published under CCE's care are also published in the international, internet based, scientific journal "Intersecții/Intersections" [12].

2. ACHIEVEMENTS AND PERFORMANCE IN COMPUTATIONAL CIVIL ENGINEERING

In what follows, this paper tries to identify the achievements and performances brought by the participants to the Computational Civil Engineering 2006 [1] and to see also some perspective reflected in the published papers.

Mata, Barbat, and Oller [13] study the nonlinear dynamic response of civil structures with energy dissipating devices. They employ the Simo-Vu Quoc formulation for beams and rods capable of undergoing large strains and displacements. The cross section of the beam is divided into an orthogonal non–homogeneous grid of cells, the sectional forces are decomposed fiber by fiber and the corrected sectional forces and moments are then obtained by integration over the section area. Concrete's behavior is simulated employing a damage model based on the Kachanov theory for degrading materials, while the energy dissipating devices are simulated using a rod element with only one Gauss integration point. This model shows ability to predict the response of the elastic rod even for large displacements and rotations. Nonlinear seismic response of a planar frame was investigated and the effectiveness of the models and devices is underlined.

The same authors are enlarging their above analysis and applications [14]. Disadvantages associated with the traditional precast concrete structures (as low global structural damping coefficient, important P-Δ effects and non-ductile connecting joints) are at the base of the study. Using the theory developed in [13], a software tool has been created. The non-linear seismic response of a 2D and of a 3D typical precast buildings with damping devices is performed. Trials are leading to improved response and the corresponding characteristics of passive devices.

Urban seismic risk evaluation is proposed from a holistic point of view by Carreño, Cardona and Barbat [15]. The proposed risk evaluation is performed using a set of input descriptors (divided into social fragility descriptors and lack of resilience descriptors). Total risk depends on the physical risk and impact risk. Compared to previous works, the new model provides a more solid theoretical and analytical support, preserves the use of indicators and fuzzy sets or membership functions in a different way and facilitates the comparison of

risk among cities. Seismic hazard and the physical exposure have been included into the physical risk variables. Calculation of total risk was performed for Bogota and Barcelona.

A very extensive study [16] is referring to modeling the damage response of multi-storey reinforced concrete frames. The authors, Faleiro, Barbat and Oller, start from the model of elastic beam-column with inelastic hinges at the ends. Degradation of concrete is estimated through Continuum Damage Mechanics and a proposed global damage index. Theoretical basics are explained at large. Numerical implementation of the method is exposed. Examples of numerical applications are also shown and very good precision of the model is confirmed. Therefore the proposed method is an excellent tool for the seismic damage evaluation, reliability, and safety assessment of exiting structures.

Brozovsky, Fojtik and Martinec [17] are studying the use of fluid combustion ashes as additives and replacement of fine grained aggregate in concrete resistant to aggressive media, chlorides and sulphates in particular. A 24 months period of monitoring of concrete samples under aggressive media has been performed. Analysis of the composition and recipes with ashes weighting 0-50% as replacement of natural aggregates were investigated. It was found that 50% solution was suitable for resistance to aggressive media.

In [18], Brozovsky, Martinec and Brozovsky jr. are focused on long term behavior of gypsumfree cements, a problem shown to be less systematically investigated until this study. The investigations have been done on two types of cements and monitoring the tensile bending strength, compression strength, and the propagation rate of ultrasonic pulses at ages of 1, 2, 3, 7, 28 days and 1, 2, 3, years. Conclusions show clear behavior of the monitored parameters.

Optimization of self-compacting concrete is studied by Kratochvil and Brozovsky in [19]. Experiments were carried out for verification of the possibility of affecting the concrete mixture properties combination of different types of fillers (ground granulated furnace slag, fly ash, ground limestone and silica fume, stone powder). Best compounds are underlined for studied cases while other tests are in the views of authors.

Minch and Trochanowski [20] present a Boundary Element Method model of reinforced concrete plane stress plate formulated in terms of general functions, expending a previous model referring to beams. After hypotheses, differential equations for displacements, differential equations of visco-elastic plates, and boundary elements method's basics, the incremental approach is shown. A general flowchart, the corresponding computer program and a numerical example are also added, showing very good accuracy of the proposed method.

The same team as before [21] analyzes cracked reinforced concrete structures by using Finite Element Method. Non-linear behavior of concrete and steel is reviewed. The proposed non-linear method is detailed. An analysis of a RC panel element is performed and comparisons of different solutions are underlined.

The very difficult problem of numerically modeling of masonry structures is deal by Szołomicki in [22]. The study is unifying the equivalent elastic properties, strength envelope and different failure patterns of masonry material. A formulation of volume element is stated and the model for damage of joints and bricks is presented. The finite element is implemented and a numerical application is performed.

In [23], Boroń is dealing with structural optimization as one of the main topics for research in Civil Engineering. In the first part, as a show for the technologies from 80's, an example of scalar optimization for a water tank is presented. Then, the paper is focusing on application of genetic algorithms (micro-GA) on multi-criterion optimization techniques. A flowchart and an application to a four bar plane truss are also shown. In conclusions the author is stressing the challenging matter of optimization in the globalization era.

Proca [24] is presenting an initiative for creating a database for structural design based on norms, codes and regulations in Romania. A first part shows the logical chain of phases in structural design. Then, for a chosen standard, a database for better application is implemented. Similar approach is intended for other standards.

In [25], Rotberg is dealing with thermal design of composite multilayered materials, particularly of the composite plates. Theoretical aspects about thermal stresses are shown. Details on numerical calculations and results for a laminate plate are revealed. A computer program was elaborated and used for the performed analysis.

For post-elastic domain of structural computation, a generalization of moment distribution method is proposed by Amariei and Filip [26]. Based on a previous study started by regretted Prof. Sesan the generalization is performed. The detailed developed algorithm and flowchart are presented. Computer program calculations are suggested for future progress.

Campian and Pernes, [27], describe models using finite element method for composite steel-concrete columns. Firstly, based on standardized procedures, an experimental work was performed on 12 columns. Numerical models were applied using DRAIN-2DX computer program. Very good agreements (less

then 5%) between the two analyses were observed, commented and graphically presented.

Because of the strong implications on mechanical properties and durability of concrete, determination of temperatures in concrete during hydration is studied by Zach, Kminova and Horky, [28]. Firstly, the time-history process of hydration heat release is presented for an experimental case. Then the heat transfer coefficient determination is theoretically demonstrated. Calculation of temperature course in concrete structure during hydration for a model of tunnel lining with wall thickness of 0.5 m is presented. The paper reveals that it is possible to predict the temperature course in massive concrete during hydration.

In [29], Dósa and Popa deal with high order Euler-Bernuolli beam elements (p-version of Finite Element Method) for the stability and non-linear analysis of frame structures. Formulation and equations used in beam elements together with the tangent stiffness matrix are presented. Numerical analyses referring to buckling, and to post-critical behavior of the Roorda L-frame are performed. Conclusions stress that the numerical analyses on elements with polynomial degree six eliminates the necessity of dividing the beams and lead to precision of results.

Popa [30] is focusing on frame structures with non-prismatic beams. Particularly, the flexibility coefficients calculation is on the views. The equivalent beam notion is introduced and theoretical calculations are performed. A numerical example with an "H" cross-section beam with a linear longitudinal variation illustrates the procedure, shown to be simple and easy to apply.

In [31], Kozlovská and Kozák deal with personal protection equipment problem in construction industry. After a general view, the analysis is focused on the large number of inputs (regulations; personal protection equipment; hazards; operations; selection criteria) and on requirements or outputs (hazard analysis; personal protection equipment character, type, application condition and list; information on possible dangers, hazard re-evaluation). An algorithm and a flowchart solving the requirements are shown. A time-saving software tool was elaborated and an example of use is presented.

Computational model of time behavior for building processes is studied by Bašková, [32]. A special attention is given to internal time structure of building processes, usually ignored by classical network analysis from the management system. Detailed computational models are presented and improvements compared to classical applications are revealed.

Struková, [33], presents an internet based portal for health and safety management on building site. The portal is designed to be a communication channel, a working tool for managers and also a feedback for health and safety at construction site. The structure of the portal contains sections on trainings, safety coordination, personal protection work resources, accidents, machines and equipments, noise, and hazardous substances. Each section contains rubrics on terms, legislation, main activities, documents and agenda. The portal is interactive and can be accessed and serviced by internet. Images from the portal are shown. Conclusions underline the importance of the developed tool regarding the contribution to health and safety.

In [34], Brozovsky jr., Kolos, and Materna are proposing a non-linear constitutive model for mortar. The model is based on the one-dimensional equivalent stress-strain relationship and assumes different behavior in tension and in compression. A numerical analysis is also presented. For better validation of the model, future analyses and comparisons with experimental results are in the views of authors.

For improvement of Physics' learning in higher education, Radinschi and Ciobanu [35] propose implementation of some computer based methods. Firstly, the strong relation between Mathematics and Physics is presented, together with relatively poor math skills that students show. "Teaching-while quizzing" tests are presented as a solution for better learning. Questions, exercises, demonstrations and tools have been developed to stress the visualization of Physics concepts. Computer based tests are now used and results show students' superior performances.

Másilková [36] is analyzing the indoor climate in contemporary buildings, especially the humidity problems arising. In the first part, the authors is studying the ventilation problems in modern buildings. Examples of computation on natural ventilation (infiltration/exfiltration) and mechanical ventilation into apartment flats are presented. Supplementary heat consumption needed for ventilation is evaluated for different situations.

Correlations of earthquake ground motion and energy distributions in one-story irregular building structures are the themes in [37] investigated by Iancovici. The problem of non-symmetrical, irregular, with non-coincident centers of mass and stiffness building is thoroughly analyzed. Energy based concept for earthquake action is adopted and bi-directional ground motion is taken into account.

Musil, [38] is treating the building system loads and its climatic data as a stochastic system, to which the input data is very important. The author analyzes the building system as a part of the environment. Consumption of

water, waste water production, production of solid waste, and electricity consumption are identified as inputs for the system. Then the activities inside of building and their time development are analyzed. Climatic data and meteorological annual changes are studied and modeled for use in computer programs.

Sokolar, [39], is using the Statistical Method of Planned Experiment (PLANEX) for research of building materials properties. The method is helping in showing the influence of parameters involved in the experiment on the properties of the analyzed products. Application is made on the experiments for fine fly ash from black coal used as a basic raw material for ceramic tiles. In this case the parameters and properties refer to pressing pressure, firing shrinkage, water absorption, bending strength and bulk density. A system of polynomial equation is connecting the variables in the process. Graphical results are among the output data of the computer program.

The design of the foundation rehabilitation is studied by Lungu and Boți, [40]. Attention is given on soil improvement. For old buildings, typical foundations' degradations are identified: erosion of the stone foundation; partial crumbling of brickworks foundations; rot of wood foundations; moisture damage on stone and brick infrastructures; fissures, cracks, fractures into the foundation elements due to uneven settlements. The plastic pressure as a reference pressure in the deformation at the limit state is analyzed and its application to foundation rehabilitation process is shown. For soils with reduced cohesion, and soils with high permeability, jet grouting is determined to be a good solution.

In [41], N. Boți, Lungu and I. Boți, are performing an evaluation of the geotechnical risk for a building planned in one of the hilly zones within the City of Iaşi, Romania. A geotechnical survey, the building's characteristics are shown. General geotechnical and hydrological conditions of the site are presented. Also, previous and actual geotechnical conditions are exposed. Then, geotechnical tests and a thorough slope stability analysis are performed. Land slides were predicted and, therefore, foundation of the future building should be a difficult task.

Designing of log-houses external walls is in the views of Brandejsová and Novotný, [42]. They show that wood houses are most complaining to Life Cycle Assessment standard requirements. Environmental as comfort aspects are presented. However, important observations regarding the quality of building this king of houses are issued. Incorrect details of wood work are shown. Thermo vision analyses of wood walls are performed and proposed for further researches.

Fojtík, Vymazal, Žižková and Petránek, [43], are proposing technical, environmental and security criteria for new building materials parameters evaluation. The Failure Mode and Effects Analysis Method is at the base of the presented analysis. The method is effective in quality management. The main steps of the method are shown and evaluation of risk factors is exposed. Application of the method to design and development of concrete is performed.

In [44], M. Brosteanu, and T. Brosteanu are referring to selection of theoretical method for lateral load analysis of brick shear walls structures. In introduction, the European and Romanian rules and standards on masonry buildings are reviewed. The main categories of walls layout are presented. Five methods of static analysis are revealed and comparisons between them and the experimental data are performed. Based on comparisons and on the scope of analysis, recommendations for choosing a method are issued.

Processing the large amount of data resulted after laboratory tests is the topic treated by Nevrivova in [45]. The author was dealing with this kind of problem when trying to obtain new possibilities to produce lightweight heat insulating fire brick material on basis of waste products. The experimental procedure is detailed, stressing on the variety of parameters. Necessity of computerized data processing is shown. The algorithm and the Visual Basic program for Excel together with some graphical and numerical results are presented.

Chiorean, [46], presents a computer program for advanced analysis of semi-rigid steel space frames. This program is taking into account material and geometrical nonlinearities in a new and efficient manner. Rigid floor diaphragm, large displacements and semi-rigid joints are also considered. Formulation of plasticity in the cross-section is expressed gradually, by smooth force-strain curves numerically calibrated. Theoretical considerations, the algorithm and the computer program are presented. An application on a steel framed structure used in literature is proving the quality of the work.

The same author, [47], has also elaborated a computer program for M-N-Φ and N-M-M analysis of reinforced concrete sections. The program is suitable for complex cross-sections of arbitrary shape and curved edges, with or without openings. The paper proposes to use an iterative procedure based on arc-length constraint equations to determine the biaxial strength of an arbitrary composite steel-concrete cross-section. Mathematical formulation and solution of the problem are shown. Numerical examples reveal the large possibilities and the accuarcy of the method and of the computer program.

Computational Fluid Dynamics is used by Šikula, [48], for simulation of indoor climate. The necessity of creating and controlling the climate in the buildings is underlined. Details of theoretical and experimental assessment of vertical

temperature distribution in a room are presented. Vertical distribution of temperature curves go together with explanations. The experimental data, for a heated room, are compared with numerical results from a computer program.

Vasilescu, in [49], is dealing with geometrical non-linear analysis of cyclic symmetrical structures. This type of structures is relatively often met and their particularities could be used in analysis. A modified Newton-Raphson procedure and the corresponding algorithm are presented. It is stated that the procedure is well suited for cyclic symmetrical structures with mild geometrical non-linearities. Strong non-linear cyclic symmetrical structures are in the views for further studies.

In [50], Doležílková is treating the problem of modelling and simulation of carbon dioxide indoor concentration. The importance of buildings' inside climate is stressed. The analysis is focused on indoor air quality, pollutants and mainly on carbon dioxide. Five different computer programs are compared in terms of characteristics, inputs and outputs. One of the software is chosen and presented in depth. Applications for determining the carbon dioxide concentration in the rooms of a flat for three input situations using the software are developed. Consequently, ventilation procedures could be applied.

Structural optimization modeling is the topic for Berkowski, [51]. Mathematical formulation and the programming techniques of the optimization problems are presented. Discrete synthesis of steel frame is implemented in a computer program for second-order analysis (P-delta effect) and an example for a two bay frame structure is shown. Then shape optimization of sections under Saint-Venant torsion and a corresponding graphical computer program are described. After that, another method, evolutionary structural optimization, and examples are introduced.

Barbuta, Petru, and Nour perform a computer simulation on reinforced concrete beams subjected to flexure, [52]. In parallel with experimental work, Finite Element analyzes are shown. The subject of study is a 1500 mm long simple supported beam with a 90x120 mm section symmetrically loaded with two forces. The algorithm and a computer program were done for generating input data of commercial FEM software. Comparisons between experiments and FEM analysis show good agreements.

The design and building of the retaining walls systems made of precast concrete blocks is the object of the paper [53]. The authors, N. Ungureanu, Vrabie, Moga, and A. Ungureanu, show the value and complexity of retaining walls in Civil Engineering. A solution for erecting such walls is the use precast units. A simple to apply design procedure, based on only one parameter, is exposed. Vault-shape structures made from precast blocks are analyzed. Details of

design computations and limit stress considerations are issued. Advantages of the method are revealed.

Evaluation of seismically induced damages and their modeling by functional and stochastic models are treated by Vulpe and Carausu, [54]. Seismic damage indexes and damage functionals, based on fragility and vulnerability concepts, are described. Then, probabilistic assessment of seismic damage in hysteretic structures is analyzed. Fragility and vulnerability models for seismic damage assessment are studied. The same is performed for stochastic models for seismic damages of structures.

Coveianu and Bîtcă, in [55], present a proposal of design for compressed elements based on simulations with elements of initial deflection equivalent to buckling curves A,B,C. The estimation of the equivalent deflection and also the calculation of initial deflection for compressed elements with a square pipe steel section are shown. Conclusions reveal that the proposed method could very well describe the non-linear phenomena taking place in compressed elements.

Computation of vibrating frequencies for steel taintor (radial) gates is studied by Prodescu and Bîtcă, [56]. The importance of the study to the safety of hydraulic systems is shown. A real case about a deep radial gate is described and analyzed. A FEM model is developed. First 24 periods and frequencies of vibrations for three different hypotheses are revealed. Also, the first three modes of vibrations are illustrated. Conclusions show the influence of bearing conditions to the modes of vibrations.

Use of computers in teaching and learning Applied Mechanics is treated by Vlad, [57]. The study is generated by the need for improved teaching and by the "mathematically un-adapted" students that are a growing problem in Academic field. New and simple computational tools are regarded as a mean for solving the needs. The dialogue between students and instructors can also be improved through computer applications, some of them residing on Internet. The role of the mathematical programming environments in teaching and learning is underlined. Example of the use of such mathematical tool is referring to the stress tensor component functions in a prismatic dam acted by the hydrostatic pressure and body (gravitational) forces.

New screed materials, using waste materials, for external thermal insulation composite systems are proposed by Žižková, [58]. Insulation composite systems used for thermal insulations are presented, the main objective being the observation of fixing materials. The materials used in the study are shown. Processability, adhesiveness, strengths, frost resistance coefficient and thermal conductivity coefficient were monitored. Parametric test taking into account the

composition of waste materials (e.g. fly-ash, crushed limestone washing) are detailed and results are graphically expressed. Conclusions show that, when the substitution of original material by waste material is appropriate, the new material is having the same or even better properties than reference materials.

In a paper titled "Coating of concrete structures exposed to corrosive media", [59], Petránek is performing researches link to resins used for protecting structural elements. Causes of corrosion and strategies of protection for reinforced concrete are reviewed. Instead of usual fillers, waste materials were used in coating tests: fly ash, slag, and wastes from the washing of crushed aggregates. As binders, vinyl-ester, polyester and polyurethane have been used. All test result values exceeded the values required for coating, the limit for filling being the workability of the fresh coating. The best compositions were selected.

D. Diaconu, Vasilescu, Palamaru, Mihai, A.C. Diaconu, and Popa, perform a vast review of the City of Iassy's contributions to the development of Earthquake Engineering in Romania. The paper, [60], is a remembering of the forerunners and of their works in the field of the Civil Engineering in general, and in the field of Earthquake Engineering in particular. The referred researches have been carried out in Iasi both within the Branch of National Institute for Research and Development in Civil Engineering (INCERC) and the Faculty of Civil Engineering. Revealed contributions covered: determination of dynamic characteristics of structures; Civil Engineering structures (large panel structures; masonry structures; structures made of three-dimensional precast elements; monolithic or partially prefabricated framed structures; lamellar framed structures; structures with monolithic vertical diaphragms and precast flat slabs; structures with frames and thinned structural walls and structures with central or multiple cores; rural buildings made up of local materials); structures for industry (single-story and multi-story industrial buildings; special constructions); unique constructions of national importance; seismic isolation and equipment-structure interaction; rehabilitation of the existing buildings; improvement of the dynamic-seismic interaction among different building materials and members; seismic qualification of technological equipment and facilities; cooperation. A large number of photos accompany the comments.

In [61] Comisu is proposing a real-time damage monitoring system of highway bridges based on modal testing. A proposed composition for a mobile test laboratory is also shown in contrast to the actual state of subjective observations that lead to the identification of a bridge state. Benefits, objectives, deliverables and expected scientific impact of the proposals are analyzed. The scientific program and introduced innovation are revealed.

Voiculescu, [62], is dealing with calculation of buckling length for steel columns. A computer program based on a data sheet processor is presented. The input data is shown to be easy and graphical part very useful. Theoretical considerations are detailed. Instances from the use of the computer GUI and results are shown. The program can be also very useful in pre-design stage for structures.

Dimensioning "HE" type steel columns under complex actions is the subject treated by Voiculescu and Preda in [63]. The calculation are done by the help of a program written for a data sheet processor. The data is input using a database of section types and other helping windows. Graphical parts are also easing the user work. The program can verify the strength and the general stability. Further developments are in views of authors.

Teleman, Axinte and Silion are presenting some trends of actual computer assistance for laboratory studies in boundary layer wind tunnel, [64]. Climatic changes and developments in the theory of Wind Engineering are at the base of the study. New, modern approaches for assessment of wind actions are extensively revealed. The paper show that modeling the wind flow is a complex task containing, among others, the structure of the wind flow, the wind turbulence, the time scales and the integral length scales. Then, problems linked to the measurements that must be performed in the boundary layer wind tunnel are described: acquisition techniques; power spectral densities analysis; turbulence intensity analysis; cross correlation of the longitudinal and transversal turbulence.

In [65], Ionescu and Popa are dealing with the efficiency that database could provide for bridges management. The importance of bridges in a country infrastructure is shown. Computerization of activities for the administrative infrastructure network is underlined. For a chosen administrative unit, the amount of data and tasks are detailed. Comment and statistics about the roads and bridges network are issued. Conclusions outline that databases and actual data are at the base of improved administration of the brides and roads network.

Ionescu and Nicuță are treating the problem of information and dissemination in Bridge Engineering, [66]. For general scientific creation feedback system, there are mainly three identified (sub)systems: the information system, the creation system and the dissemination system. Resources, people and activities involved in the information system and their connections are presented in a diagram and then commented. A similar approach is performed for the dissemination system. Analysis of the publication types is carried out. A special attention is given to the scientific journals.

The general goal of the author of [67] is to show that a new concept, Structural Robotics, can be implemented in Civil Engineering. Components of this new concept are studied as separated and necessary steps. Some progresses done when Structural Active Control has been intensively and extensively studied are presented. The newly introduced Structural Active Hinges are detailed and shown to be practically realizable. Analytical models and numerical applications to simple structures are presented and good results are obtained. Future directions are also seen.

3. CONCLUSIONS

During the last four years Computational Civil Engineering has emerged as a new and strong aspect of the Civil Engineering domain. This is proved by the four symposiums organized in Iasi, Romania [1-4] and also by the quality, quantity and diversity of papers published with those occasions.

Meeting as *Computational Civil Engineering 2006* are chances to offer opportunities for remembering forerunners and their great works [5-9].

Though the meaning of Computational Civil Engineering is somehow fuzzy, it is generally accepted that computers and their use play a major role in Civil Engineering as for the rest of society. From the gained experience, some general important themes as: Computer Aided Design and Engineering, Computer Programming for Civil Engineering, Computer-Based Education, Computational Methods in Civil Engineering, Databases in Civil Engineering, and Computer Aided Management in Civil Engineering have been detected to be parts of the domain.

The large number of contributed papers to sustain the Computational Civil Engineering [11-67] shows that this infrastructure-like sub-domain is an important factor for Civil Engineers, a platform for meeting, exchanging opinions and experience, a good opportunity to make the Civil Engineering community more adaptive and competitive.

References

1. Ionescu, C., Păuleț-Crăiniceanu, F., Barbat, H. (editors), *Computational Civil Engineering*, Editura Societății Academice "Matei-Teiu Botez", Iaşi, 2003, ISBN 973-7962-27-3
2. Păuleț-Crăiniceanu, F., Ionescu, C., Barbat, H. (editors), *Computational Civil Engineering 2004*, Editura Societății Academice "Matei-Teiu Botez", Iaşi, 2005, ISBN 973-7962-50-8
3. Păuleț-Crăiniceanu, F., Ionescu, C., Barbat, H. (editors), *Computational Civil Engineering 2005*, Editura Societății Academice "Matei-Teiu Botez", Iaşi, 2005, ISBN 973-7962-65-5

4. Păuleț-Crăiniceanu, F., Ionescu, C., Barbat, H. (editors), *Computational Civil Engineering 2006*, Editura Societății Academice "Matei-Teiu Botez", Iaşi, 2006, ISBN (10) 973-7962-89-3; ISBN (13) 978-973-7962-89-8.
5. ***, Historical moments from Civil Engineering technical education in Moldova, *Computational Civil Engineering 2006,* Editura Societății Academice "Matei-Teiu Botez", Iaşi, 2006, ISBN (10) 973-7962-89-3 ; ISBN (13) 978-973-7962-89-8, pg. i
6. ***, Establishment of the Faculty of Civil Engineering of Iaşi, *idem,* pg. i
7. (Department of Structural Mechanics, Faculty of Civil Engineering of Iaşi), Professor Anton Şesan (1916-1969), *idem,* pp. ii-iii
8. Strat, L., Professor Alexandru Negoiță (1916-1998), *idem,* pp. iii-iv
9. Macavei, F., Some aspects of the contribution of Professor Anton Sesan to Romanian construction school, *idem,* pp. iv-viii
10. Faculty of Civil Engineering of Iaşi, http://www.ce.tuiasi.ro/
11. Editura Societății Academice „Matei-Teiu Botez", ("Matei-Teiu Botez" Publishing House) http://www.ce.tuiasi.ro/edituraSAMTB/
12. *Intersecții/Intersections*, International Journal, http://www.ce.tuiasi.ro/intersections/
13. Mata, P.A., Barbat, A.H., Oller, S.M., Seismic analysis of structures incorporating energy dissipating devices by means of numerical methods, *idem,* pp.25-37
14. Mata, P.A., Barbat, A.H., Oller, S.M., Numerical Simulation of the Seismic behavior of passively controlled precast concrete buildings, *idem,* pp. 38-50
15. Carreño, M.L., Cardona, O.D., Barbat, A.H., Holistic evaluation of the seismic risk in urban centers, *idem,* pp.51-68
16. Faleiro, J., Barbat, A., Oller, S., Nonlinear Analysis of Reinforced Concrete Frames, *idem,* pp.69-99
17. Brozovsky, J., Fojtik, T., Martinec, P., Impact of fine aggregates replacement by fluidized fly ash to resistance of concretes to aggressive media, *idem,* pp.100-106
18. Brozovsky, J., Martinec, P., Brozovsky, jr., J., Time flow of gypsumfree cements strength development, *idem,* pp.107-112
19. Kratochvil, A., Brozovsky, J., The optimization of properties of self-compacting concrete by the combination of fine filler, *idem,* pp.113-122
20. Minch, M., Trochanowski, A., Boundary element method numerical modeling of RC plane stress cracked plate, *idem,* pp.123-135
21. Minch, M., Trochanowski, A., The numerical model for reinforced concrete structures and analysis using finite elements method, *idem,* pp.136-146
22. Szołomicki, J., Numerical modelling for homogenization of masonry structures, *idem,* pp.147-155
23. Boroń, J., About some important changes in applied structural optimization, *idem,* pp.156-165
24. Proca, G.E., A database for elements' and structures' computation, *idem,* pp.166-170
25. Rotberg, R., Thermal composites design, *idem,* pp.171-180
26. Amariei, C., Filip, V., A generalization of the moments distribution method for the structure computation in the postelastic field, *idem,* pp.181-188
27. Campian, C., Pernes, P., Finite element model for composite steel-concrete column, *idem,* pp.189-197
28. Zach, J., Kminova, H., Horky, O., Determination of temperature course in concrete during hydration, *idem,* pp.198-203

29. Dósa, A., Popa, L., High order beam elements for the stability and non-linear analysis of frame structures, *idem,* pp.204-211
30. Popa, L., The analysis of frame structures with non-prismatic beams, *idem,* pp.212-215
31. Kozlovská, M., Kozák P., Computer aided tool for personal protection equipment generation, *idem,* pp.216-225
32. Bašková, R., Computational modeling of building process time behaviour, *idem,* pp.226-237
33. Struková, Z., Electronic portal for occupational health and safety management on building site, *idem,* pp.238-244
34. Brozovsky jr., J., Kolos, I., Materna, A., Non-linear constitutive model for mortar, *idem,* pp.245-250
35. Radinschi, I., Ciobanu, B., Implementation of computational methods in Physics learning, *idem,* pp.251-256
36. Másilková, L., Indoor climate in contemporary buildings, *idem,* pp.257-264
37. Iancovici, M., Correlations of earthquake ground motion and energy distributions in one-story irregular building structures, *idem,* pp.265-276
38. Musil, R., Building system loads and its climatic data, *idem,* pp.277-285
39. Sokolar, R., Utilization of the Statistical Method of Planned Experiment (PLANEX) for research of building materials properties, *idem,* pp.286-291
40. Lungu, I., Boți, N., Soil improvement in the design of the foundation rehabilitation, *idem,* pp.292-298
41. Boți, N., Lungu, I., Boți, I., Evaluation of the geotechnical risk in the hilly zones within the city of Iași, *idem,* pp.299-306
42. Brandejsová, H., Novotný, M., Present trends and potentialities in designing of log-houses external walls, *idem,* pp.307-312
43. Fojtík, T., Vymazal, T., Žižková, N., Petránek, V., Technical, environmental and security criteria of new building materials parameters evaluation, *idem,* pp.313-320
44. Brosteanu, M., Brosteanu, T., Selection of theoretical method for lateral load analysis of brick shear walls structures, *idem,* pp.321-327
45. Nevrivova, L., Using computer technology for laboratory results (data) evaluation, *idem,* pp.328-335
46. Chiorean, C.G., A computer program for advanced analysis of semi-rigid steel space frames, *idem,* pp.336-345
47. Chiorean, C.G., A computer program for M-N-Φ and N-M-M analysis of reinforced concrete sections, *idem,* pp.346-359
48. Šikula, O., CFD simulation of indoor climate, *idem,* pp.360-368
49. Vasilescu, A., Remarks on the Geometrical Non-Linear Analysis of Cyclic Symmetrical Structures, *idem,* pp.369-374
50. Doležílková, H., Computer modelling and simulation of carbon dioxide indoor concentration, *idem,* pp.375-382
51. Berkowski, P., Some examples of structural optimization problems modelling, *idem,* pp.383-392
52. Barbuta, M., Petru, M., Nour, D.S., Computer simulation on reinforced concrete beams subjected to flexure, *idem,* pp.393-400

53. Ungureanu, N., Vrabie, M., Moga, A., Ungureanu, C., Some aspects regarding the design and building of the retaining walls systems made of precast concrete blocks, *idem,* pp.401-411
54. Vulpe, A., Carausu, A., Modeling and evaluation of seismically induced damages by functional and stochastic models, *idem,* pp.412-426
55. Coveianu, M., Bîtcă, D., Design of compressed elements simulated with elements of initial deflection equivalent to buckling curves A,B,C, *idem,* pp.427-434
56. Prodescu, A., Bîtcă, D., Studies regarding the computation of vibrating frequencies for steel taintor (radial) gates, *idem,* pp.435-442
57. Vlad, I.A., Teaching and learning Applied Mechanics by aid of computers, *idem,* pp.443-448
58. Žižková, N., New screed materials for external thermal insulation composite systems, *idem,* pp.449-456
59. Petránek, V., Coating of concrete structures exposed to corrosive media, *idem,* pp.457-463
60. Diaconu, D., Vasilescu, D., Palamaru, G., Mihai, C., Diaconu, A.C., Popa, T., Iassy contributions to the development of Earthquake Engineering, *idem,* pp.464-489
61. Comisu, C.C., Real-time damage monitoring system by modal testing of highway bridges, *idem,* pp.490-499
62. Voiculescu, D., Useful calculation of buckling length for steel columns, *idem,* pp.500-504
63. Voiculescu, D., Preda, D., "HE" column sizing under complex actions, *idem,* pp.505-509
64. Teleman, E.C., Axinte, E., Silion, R., Trends of actual computer assistance for laboratory studies in boundary layer wind tunnel, *idem,* pp.509-518
65. Ionescu, C., Popa, R., The importance of databases for the efficient exploitation of bridges within an administrative unit, *idem,* pp.519-524
66. Ionescu, C., Nicuță, A., Information and dissemination in Bridge Engineering, *idem,* pp.525-530
67. Păuleț-Crăiniceanu, F., Steps in Structural Robotics implementation *idem,* pp.531-539

"Computational Civil Engineering 2006", International Symposium
Iaşi, România, May 26, 2006

Seismic analysis of structures incorporating energy dissipating devices by means of numerical methods

Pablo Mata A[1], Alex H. Barbat[2] and Sergio Oller M[3]

[1]*TechnicalUniversity of Catalonia.Edificio C1, Campus Norte UPC. Gran Capitán s/n. Barcelona 08034, Spain . Email: pmata@cimne.upc.edu*
[2] *Technical University of Catalonia, Spain.. Email: alex.barbat@upc.edu*
[3] *Technical University of Catalonia, Spain.. Email: sergio.oller@upc.edu*

Summary

The nonlinear dynamic response of civil structures with energy dissipating devices is studied. The structure is modeled using the Vu Quoc–Simo formulation for beams in finite deformation. The effects of shear stresses are considered, allowing rotating the local system of each beam independently of the position of the beam axis. The material nolinearity is treated at material point level with an appropriated constitutive law for concrete and fiber behavior for steel reinforcements and stirrups. The simple mixing theory is used to treat the resulting composite. The equation of motion of the system as well as the conservation laws are expressed in terms of sectional forces and generalized strains and the dynamic problem is solved in the finite element framework. A specific kind of finite element is proposed for modeling the energy dissipating devices. Several tests were conducted to validate the ability of the model to reproduce the nonlinear response of concrete structures subjected to earthquake loading.

KEYWORDS: seismic analysis, beam model, numerical methods.

1. INTRODUCTION

In the traditional approach to earthquake engineering design, the computations are carried out on the basis of linear elastic static analysis. The nonlinear behavior and energy dissipation can be accounted for in a trivial manner by a force-based approach, analyzing the elastic response spectra of a single degree of freedom system, *SDF*, and the so called reduction factor method for introducing the material ductility. A more rational concept, the displacement based approach, turns toward the design based on the critical limit states of the elements [Davenne et.al. 2003]. Both design procedures are based on the study of a *SDF* system or simplified substitute structures, which are not capable to account for the load redistribution inside the structures due to local non-linearity. This is one of the major drawbacks preventing a realistic description of the global and local behavior of the structure up to the failure [Davenne et.al. 2003]. By other hand, additional improvements

can be done if energetic concepts are taken into account. The passive control of structures takes advantages of the possibility of dissipate energy in specific devices alleviating the stresses in the main structural elements and controlling the lateral displacements of the whole structure.

One choice to perform realistic analysis of structures equipped with energy dissipating devices for seismic loading is employing nonlinear time history analysis assuming physical descriptions for the materials and applying transient loadings on the structure in terms of natural or simulated ground motions. The model employed for the structure should be able to simulate the changes of configuration of the structure during the dynamic action, especially for the case of flexible structural behavior. Additionally, appropriated constitutive laws have to be provided for the materials of the elements and for dissipating devices.

In this work the latter is achieved modeling the structure by mean of employing the Simo-Vu Quoc formulation for beams and rods capable of undergoing large strains and displacements [Simo et.al. 1985]. Each beam section is meshed into a grid of cells, each of them corresponding to a fiber directed along the beam axis. The material associated with a fiber can be composed by several components, employing the simple mixing theory for the treatment of the resulting composite [Oller, et.al. 1997]. The incorporation of energy dissipating devices is obtained developing a special rod element with only one integration point. Appropriated one-dimensional constitutive laws or strain–stress relationships are provided for the element. Numerical examples are studied to validate the ability of the model for simulating the dynamic response of structures subjected to seismic loading.

2. KINEMATIC OF BEAMS IN FINITE STRAIN

Nonlinear analysis of three-dimensional beam–like structural systems subjected to very large displacements is a problem frequently encountered in earthquake engineering. The 3D beam formulation employed here makes use of the equilibrium equations in terms of stress resultants in order to deduce on the energy conjugate strain measure through application of the virtual work principle. The Newmark method is employed for integrating the equations of motion in the dynamic linearized version [Simo et.al. 1985, 1986; Ibrahimbegovic, 1995].

2.1 Kinematics' Description

A typical cross section of the beam will be associated with a orthonormal basis vector, $\{t_i(S,t)\}_{i=1,2,3}$ of a moving frame attached to its centroid, where $S \in [0, L] \subset R$ denotes the curvilinear coordinate along the line of centroids of the undeformed beam, $t \in R$ is a time parameter. The $t_3(S)$ component remains

normal to the section all time. The fixed (so called material description) reference axis of the same section is denoted by $\{E_i(S,0)\}_{i=1,2,3}$ so that $\{t_i(S,0)\}_{i=1,2,3} \equiv \{E_I(S)\}_{I=1,3}\ \forall S \in [0,L]$. The fixed spatial basis is denoted by $\{e_i(S,0)\}_{i=1,2,3}$. See figure 1. The orientation of the moving frame $\{t_i(S,t)\}_{i=1,2,3}$ along $S \in [0,L]$, and through time $t \in R$ is specified by an orthogonal transformation $\Lambda(S,t) = \Lambda_{iJ}(S,t) e_i \otimes E_J$ such that $t_I(S,t) = \Lambda(S,t) E_I = \Lambda_{iJ}(S,t) e_i$. The position $x_0 \in R^3$ of the centroid of the cross section is defined by the map: $x_0 = \phi_0 = \phi_{0i}(S,t) e_i$. Here $\Lambda(S,t) \in SO(3)$ the special orthogonal (Lie) group having the following property: $\Lambda\Lambda^t = 1$. The derivatives of the orthogonal transformation are summarized in the following formulas [Simo et.al. 1985, 1986]:

Derivatives of the moving frame

Spatial	Material	
$\frac{\partial \Lambda(S,t)}{\partial S} = \Omega(S,t)\Lambda(S,t)$	$\frac{\partial \Lambda(S,t)}{\partial S} = \Lambda(S,t)K(S,t)$	(1)
$\frac{\partial \Lambda(S,t)}{\partial t} = W(S,t)\Lambda(S,t)$	$\frac{\partial \Lambda(S,t)}{\partial t} = \Lambda(S,t)\bar{W}(S,t)$	
$\Omega = \begin{bmatrix} 0 & -\omega_3 & \omega_2 \\ \omega_3 & 0 & -\omega_1 \\ -\omega_2 & \omega_1 & 0 \end{bmatrix}$	$K = \begin{bmatrix} 0 & -k_3 & k_2 \\ k_3 & 0 & -k_1 \\ -k_2 & k_1 & 0 \end{bmatrix}$	(2)
$\omega = \omega_1 e_1 + \omega_2 e_2 + \omega_3 e_3 = k_1 t_1 + k_2 t_2 + k_3 t_3$	$k = k_1 E_1 + k_2 E_2 + k_3 E_3$	(3)
$w = w_1 e_1 + w_2 e_2 + w_3 e_3 = \bar{w}_1 t_1 + \bar{w}_2 t_2 + \bar{w}_3 t_3$	$w = \bar{w}_1 E_1 + \bar{w}_2 E_2 + \bar{w}_3 E_3$	(4)

where $\Omega(S,t), W(S,t), K(S,t), \bar{W}(S,t)$ are the spatial and material representation of the curvature tensors and spins of the cross section respectively. Note that $K + K^t = 0$, $\Omega + \Omega^t = 0$.

2.2 Stress Resultant and Couples

Denoting by $P = T_I \otimes E_I$ the non symmetric first Piola–Kirchhoff stress tensor, the stress resultant *n* and the spatial stress couple *m* over a cross section $\Gamma \subset R^2$ in the current configuration, are defined according with the equation (5) as:

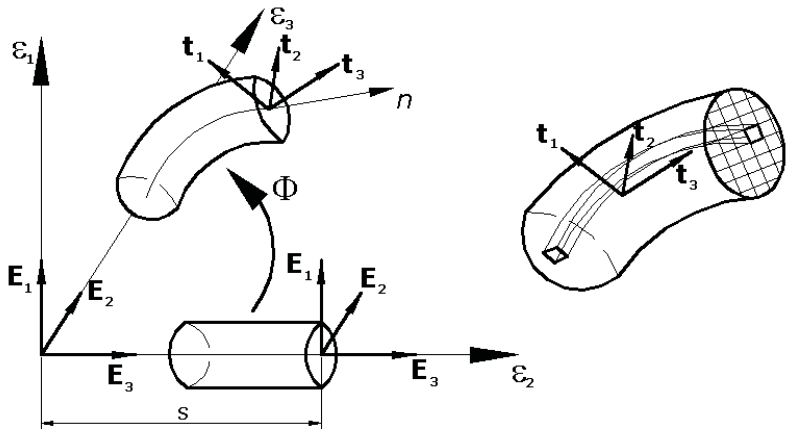

Figure 1: Kinematics of beams in finite strain for fiber sections.

$$n = \int_{\Gamma} T_3 d\Gamma, \qquad m = \int_{\Gamma} (x - \phi_0(S,t)) \times T_3 d\Gamma \tag{5}$$

The material version of the stress resultants and couples are obtained pulling back *n, m* to the reference configuration by mean of Λ [Simo et.al. 1985]. Appropriated strain measurements conjugated to the corresponding stress resultant and couples are obtained trough the *stress power equivalence* [Simo et.al. 1986], equation (6).

$$\int_{\Gamma \times [0,L]} P : \dot{F} d\Gamma dS = \int_{[0,L]} [n \cdot \overset{\nabla}{\gamma} + m \cdot \overset{\nabla}{\omega}] dS = \int_{[0,L]} [N \cdot \dot{\Gamma} + M \cdot \dot{\kappa}] dS \tag{6}$$

where $\dot{F}$ is the time derivative of the deformation gradient and a superimposed dot denotes time differentiation. Here, $\overset{\nabla}{(\bullet)} = (\partial/\partial t)(\bullet) - w \times (\bullet)$ denotes the *co-rotated rate,* that is, the rate measured by an observer attached to the moving frame. The corresponding strain measurements are given by the equation (7).

$$\gamma = \partial \phi_0(S,t) / \partial t - t_3; \quad \Gamma = \Lambda^t \, \partial \phi_0(S,t) / \partial t - E_3; \quad \text{k} = \Lambda^t \omega \tag{7}$$

2.3 Weak Form: Inertia Operator

The system of partial differential equations to be solved consists of the balance laws and constitutive equations expressed in local form. Considering any arbitrary admissible variation $\eta(S) = (\eta_0(S), \vartheta(S))$ of the spatial configuration of the rod (φ, Λ), and multiplying them by the local form of the balance laws, after several mathematical procedures, it is possible to obtain the weak form of the equilibrium equations (for a detailed description consult Simo et.al. 1986, 1988):

$$G_{dyn}(\vartheta,\eta) := \int_{[0,L]} \left\{ A_\rho \ddot{\varphi}_0 \cdot \eta_0 + [I_\rho \dot{w} + w \times (I_\rho w)] \cdot \vartheta \right\} dS + G(\vartheta,\eta) \equiv 0 \quad (8)$$

where

$$G(\vartheta,\eta) := \int_{[0,L]} \left\{ N \cdot \Lambda^t [\frac{\partial \eta_0}{\partial S} - \vartheta \times \frac{\partial \phi_0}{\partial S}] + M \cdot \Lambda^t \frac{\partial \vartheta}{\partial S} \right\} dS - \int_{[0,L]} (\tilde{n} \cdot \eta + \tilde{m} \cdot \vartheta) dS \equiv 0 \quad (9)$$

and A_ρ and I_ρ are the sectional density of area and Inertia dyadic, respectively.

2.4 Time Integration

The Newmark's method is employed to integrate the linearized system obtained from the weak form. The novelty of the proposed approach lies in the treatment of the rotational part which relies crucially on the use of the discrete counterpart of the *exponential map* in the special group *SO(3)*. The basic problem concerning the discrete time stepping update is that given a configuration of displacements and rotation tensor $\varphi_n := (d_n, \Lambda_n)$, linear and angular velocities and accelerations, (v_n, w_n), (a_n, α_n) in the time step *n* obtain the updated configuration in the time step *n+1*. The algorithm employed is summarized in the equations (10), (11) and (12) for the material description of the dynamic variables, Δt is the length of the time step. It is interesting to note that the updating procedure for the rotational part of the dynamic variables have to be carried out in the material description due to the fact that this configuration is time independent and the base point on the rotational manifold stays fixed [Makinen, 2001].

Implicit time stepping algorithm, (material description)

Translation	Rotation	
$d_{n+1} = d_n + u_n$	$\Lambda_{n+1} = \Lambda_n \exp[\Theta_n] \equiv \exp[\theta_n]\Lambda_n$	(10)
$u_n = (\Delta t) v_n + (\Delta t)^2 [(0.5-\beta) a_n + \beta a_{n+1}]$	$\Theta_n = (\Delta t) W_n + (\Delta t)^2 [(0.5-\beta) A_n + \beta A_{n+1}]$	(11)
$v_{n+1} = v_n + \Delta t [(1-\gamma) a_n + \gamma a_{n+1}]$	$W_{n+1} = W_n + \Delta t [(1-\gamma) A_n + \gamma A_{n+1}]$	(12)

Working on the linearized form of the equation (9) and employing standard techniques of the finite element method, is possible to obtain the discrete version of the system of equation [Simo et al, 1988]:

$$LG^i_{dyn\ n+1} = \sum_{I,J=1}^{N} \eta_I \cdot [P_I(\varphi^{(i)}_{n+1}) + K_{IJ}(\Lambda_n, \varphi^{(i)}_{n+1}) \Delta \varphi^{(i)}_{J,n+1}] = 0 \quad (13)$$

$$K_{IJ}(\Lambda_n, \varphi_{n+1}^{(i)}) := M_{IJ}(\Lambda_n, \Lambda_{n+1}^{(i)}) + S_{IJ}(\varphi_{n+1}^{(i)}) + G_{IJ}(\Lambda_{n+1}^{(i)}) + L_{IJ}(\Lambda_{n+1}^{(i)}) \qquad (14)$$

where P_I and K_{IJ} are the vector of residual forces and the stiffness matrix respectively. The matrix K_{IJ} have contributions from the inertia, material and geometric terms M_{IJ}, S_{IJ} and (G_{IJ}, L_{IJ}) respectively. A step-by-step iterative Newton-Rapson scheme with a predictor–corrector method is employed to obtain the dynamic response of the system.

3. MULTIFIBERS BEAM ELEMENTS

The cross section of the beam is divided into an orthogonal non–homogeneous grid of cells as it is shown in Figure 2. This avoid the formulation of constitutive laws using sectional forces and displacements or moments and curvatures, which is the traditional way to solve the problem but valid only in certain particular cases [Oller and Barbat, 2006]. The sectional forces are decomposed fiber by fiber, in stress tensor which are corrected according with the constitutive laws given for the materials of the fiber and using the simple mixing theory to treat the resulting composite [Car, Oller et.al. 2000]. The corrected sectional forces and moments are then obtained by integration over the section area. The obtained sectional forces and moments are then used to compute the residual forces, in order to iterate for equilibrium if necessary (see Figure 2).

3.1 Constitutive Laws

In this work the concrete behavior is simulated employing a damage model based on the Kachanov theory for degrading materials. The model can take into account different properties for tension or compression. The steel reinforcements and stirrups are modeled employing elastic–plastic fiber behavior. Both models are thermodynamically sustainable avoiding the representation of the behavior of the materials in an approximated form based mainly on experimental studies. Strain localization is expected to occur in some members and therefore, a regularization of the dissipated energy is carried out at constitutive level to obtain objectivity in the response of the whole structure [Hanganu et.al. 2002].

3.1.1 Damage constitutive model for concrete

The damage model has a rigorous but relatively simple formulation strictly based on thermodynamics [Simo and Ju, 1987]. The model is formulated in the material configuration with no temperature time variations. The free energy presents the following form:

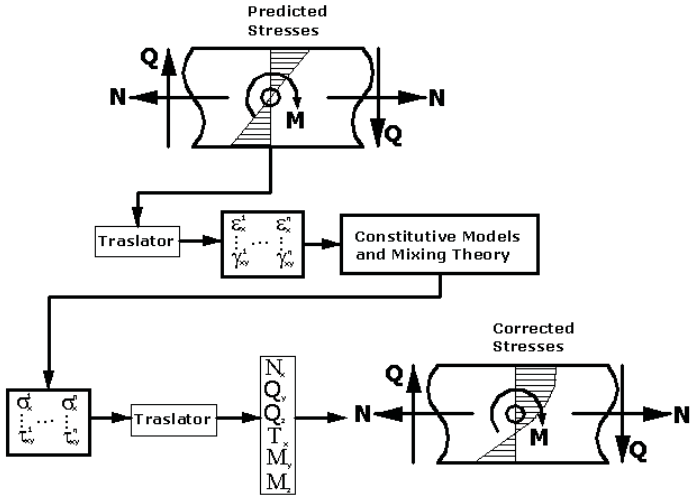

Figure 2: Iterative process at Integration point level in each section.

$$\psi(\varepsilon,d)=(1-d)\psi_0(\varepsilon)=(1-d)(\frac{1}{2\rho_0}\varepsilon^T\sigma_0)=(1-d)(\frac{1}{2\rho_0}\varepsilon^T C_0\varepsilon) \tag{15}$$

where ε is the strain tensor, $d\ (0\le d\le 1)$ is the internal damage variable, ρ_0 is the density in the material configuration, C_0 is the elastic constitutive tensor in the initial undamaged state. The fulfillment of the Clasius Planck inequality provide the constitutive law and dissipation, $\dot{\Xi}_m$, according to equation (16).

$$\sigma=(1-d)C_0\varepsilon; \qquad \dot{\Xi}_m=-\frac{\partial\Psi}{\partial d}\dot{d}\ge 0 \tag{16}$$

The damage yield criterion is defined in function of the free energy of the undamaged material as: $F=K(\sigma_0)\sqrt{2\rho_0\Psi_0}-1$, where $K(\sigma_0)$ is a function of the principal stresses and takes into account the ability of the model to consider different traction and compression properties [Barbat, et.al. 1997]. See Figure 3. Finally, the tangent constitutive tensor is given [Oller et.al. 1997] by

$$\delta\sigma=C^D\delta\varepsilon=[(1-d)\underset{=}{I}-\frac{dG(\bar{\sigma})}{d\bar{\sigma}}\sigma^0\otimes\frac{\partial\bar{\sigma}}{\partial\sigma^0}]C^0\delta\varepsilon=(I-D)C^0\delta\varepsilon \tag{17}$$

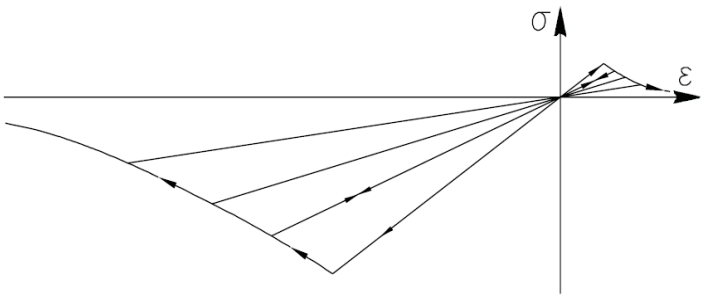

Figure 3: Local damage model with different tension–compression properties.

3.1.2 Constitutive model for steel reinforcements and stirrups

The steel of the bar reinforcements and stirrups is simulated by mean of employing a constitutive law for fibers. The fibers are treated as an orthotropic material with the steel's elastic modulus in the direction of the reinforcement and the concrete's elastic modulus in the other two directions. The Poisson coefficient is taken equal to zero to avoid introducing lateral interaction between concrete and steel reinforcements. After the yield criterion has been reached the plastic flux is oriented in the direction of the fiber [Car et.al. 2000].

3.1.3 Simple mixing theory for materials

The behavior of the composite is defined according to the fractional part of the total volume of the compounding substances (see Figure 4). It also assumes that in each material point all the components contribute with their own constitutive law in the assigned volume proportion. This allows combining materials with different constitutive behavior. In this work it is assumed that all phases in the mixture have the same strain field. The stress state of the composite is obtained starting from a hyper elastic model satisfying the dissipation condition of the second principle of thermodynamics, for n materials components, each of them with a volume proportion k_c, mass density m_c and free energy ψ_c, the stress is given by the equation (18) [Car et.al. 2000].

$$\sigma = \sum_{c=1}^{n} k_c m_c \frac{\partial \psi_c}{\partial \varepsilon} = \sum_{c=1}^{n} k_c m_c (\sigma)_c \tag{18}$$

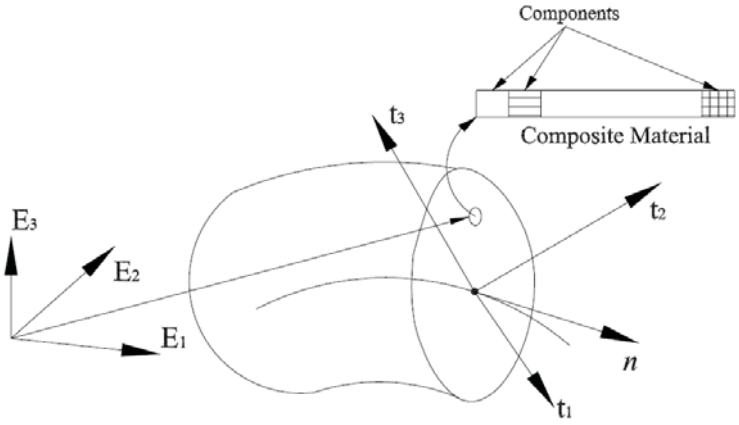

Figure 4: Each fiber of the section has assigned a composite material.

3.2 Energy Dissipating Devices

The energy dissipating devices are simulated using a rod element with only one Gauss integration point. The rotational degrees of freedom are released in both ends of the beam to obtain only relative displacements in the device. The constitutive law employed for dissipating devices corresponds to a bilinear plasticity, but any other one dimensional description can be employed, for example in Mata et.al. (2006), a constitutive description for elastomers to be employed in energy dissipating devices is given.

4. NUMERICAL EXAMPLES

In this section three numerical examples validating the proposed formulation for rods in the geometric and material nonlinear range are presented and explained. The first two examples correspond to the nonlinear elastic response of a rod in static and dynamic range. The third one corresponds to the study of a typical flexible and low damped concrete building, which is equipped with energy dissipating devices.

4.1 Elastic Large Bending of a Rod

This example presents the geometrically nonlinear analysis of a rectilinear cantilever beam with a bending moment, M, applied at the free end (Figure 5). See Ibrahimbegovic (1995) for more details. For the chosen data the values of the free end bending moments that turns the reference rectilinear line into the corresponding circle is 20π, if the applied moment is increased again the another smaller circle is formed at $M = 40\pi$. The beam is modeled employing 40 quadratic

finite elements with two Gauss integration point to avoid shear locking in the response. It is possible to observe the ability of the model to predict the response of the elastic rod even for large displacements and rotations.

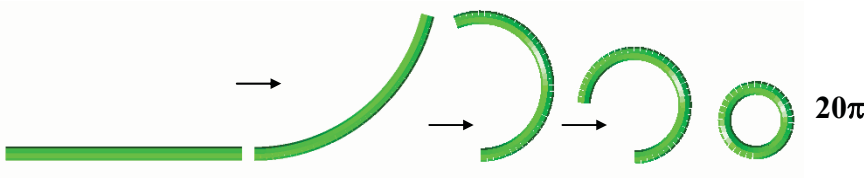

Figure 5: Nonlinear elastic bending of rod.

4.2 Dynamic Analysis of Beam: Large Rotations

The same beam of the previous example has been subjected to an imposed rotation of π at the clamped end. The dynamic response is obtained for a density mass of 3.0×10^{-5} Kg/cm^3, the result of the simulation allows to see the versatility of the formulation for predicting the complex configurations of the system during the motion. The rotational inertia terms are considered in the formulation allowing enhancing the prediction of the dynamic response for the case of large rotations, as it can be seen in Figure 6.

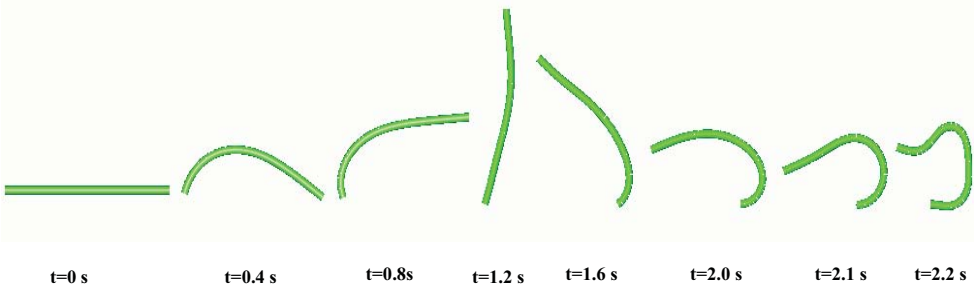

Figure 6: Nonlinear dynamic response of rod subjected to an applied rotation.

4.3 Nonlinear Seismic Response of Planar Frame

In this work the seismic nonlinear response of a typical concrete industrial building is studied. The building has a bay width of 20 m and 24 m of inter–axes length. The story high is 10 m. The concrete of the beam is H–50, (50 Mpa, ultimate compression), with an elastic modulus of 35.000 Mpa for the beam and H–30 for the concrete of the columns. It has been assumed a Poison coefficient of 0.2 for both concretes. The steel bar reinforcements considered in the study and the fiber discretization of the sections are those shown in Figure 7. The ultimate tensile

stress for the steel is 510 Mpa. The dimensions of the columns are 60x60 cm^2. The beam has a variable section with an initial high of 80 cm on the supports and 120 cm in the middle of the span.

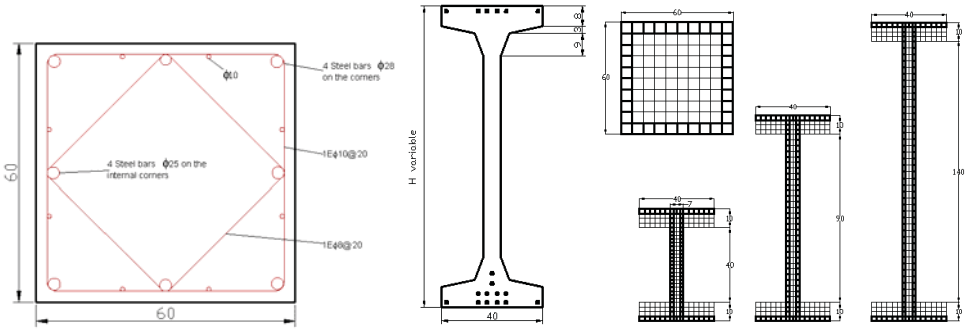

Figure 7: Columns and beam reinforcements and fiber model of the sections.

The permanent loads considered are 2000 N/m^2 and the weight of upper half of the closing walls, that is, 270,000 N. The employed acceleration record is the N–S component of the *El Centro* earthquake, 1940. The section of the energy dissipating devices was designed for yielding with an axial force of 300.000 N and for a relative displacement between the two ending nodes of 1.0 mm. The length of the dissipating devices is of 2.5 m (see Figure 8).

In Figure 9 it is possible to see the contribution of the dampers to reduce the displacements response. The obtained reduction is the order of 51% minimizing the P–Δ effects. The maximum acceleration shows a reduction of the order of 30% compared with the case where no devices are incorporated.

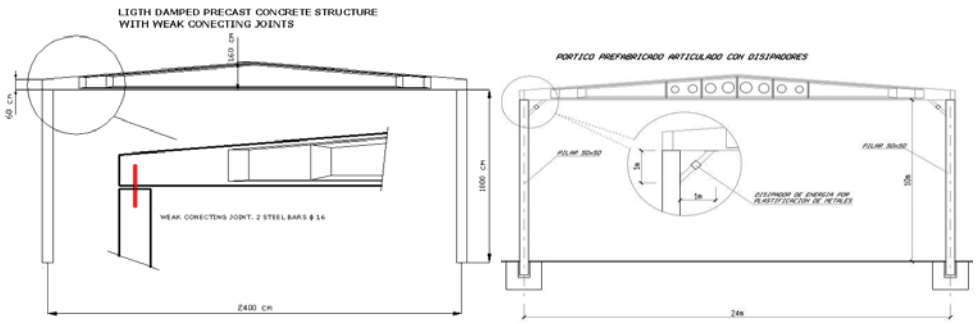

Figure 8: Precast industrial building without and with dissipators.

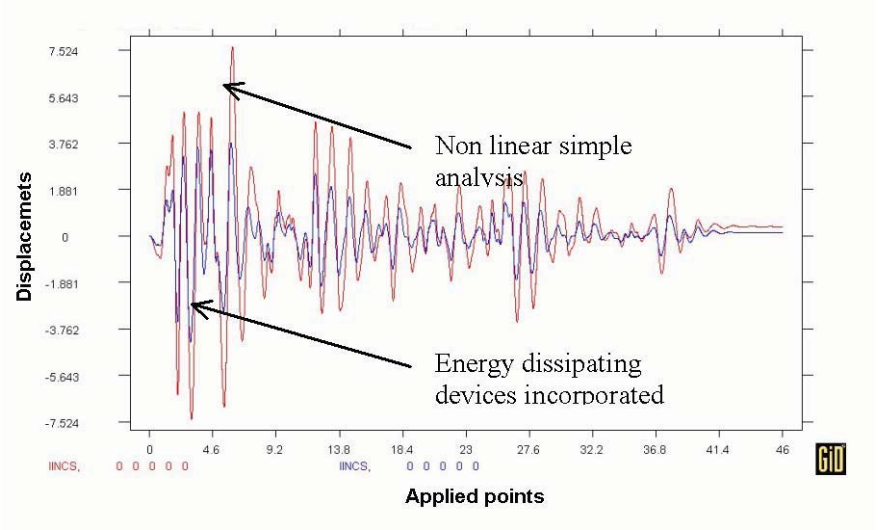

Figure 9: Displacements time history.

5. CONCLUSIONS

The geometrically exact formulation due to Vu–Quoc and Simo for beams and the use of appropriated constitutive laws for materials provides a useful tool to simulate the earthquake effects on concrete structures. A detailed study of the seismic response of structures requires taking into account the geometric and material nonlinear behavior of the structure for including the ductility demand on structural members, softening behavior, energy dissipation and the P-Δ effect. The plastic energy dissipating devices allows the improvement of the seismic behavior of flexible and low damped concrete structure studied in this work. From the presented studies it is possible to see that the use of plastic energy dissipating devices reduces the displacement response about 50% and the acceleration response 30% for the N–S component of the *El Centro* 1940 earthquake record.

6. ACKNOWLEDGMENTS

This work has been partially supported by: The University of Chile, Project FONDECYT nº 1970732; Ministerio de Ciencia y Tecnología, Spain, Project: "Numerical simulation of the seismic behavior of structures with energy dissipation systems", Contract nº: BIA2003 - 08700 - C03 – 02; and Integrated R&D Project of the EC "LessLoss–Risk Mitigation for Earthquakes and Landslides" funded by

the European Commission, Directorate General of Research under the Contract nº GOCE-CT-2003-505448.

7. REFERENCES

Barbat A. H, Oller S, Oñate E and Hanganu A. (1997). Viscous damage model for Timoshenko beam structures. *International Journal of Solids and Structures.* Vol. 34. Nº 30. pp. 3953—3976.

Car J, Oller. S and Oñate E. (2000). Modelo constitutivo continuo para el estudio del comportamiento mecánico de los materiales compuestos. *International Center for Numerical Methods in Engineering, CIMNE, Barcelona, Spain. PhD Thesis.* (In Spanish).

Davenne L, Ragueneau F, Mazars J and Ibrahimbegovic. A. (2003). Efficient approaches to finite element analysis in earthquake engineering. *Computers & Structures* 81, 1223—1239.

Hanganu Alex D., Oñate E. and Barbat A.H. (2002). A finite element methodology for local/global damage evaluation in civil engineering structures. *Computers & Structures* 80, 1667—1687.

Ibrahimbegovic A. (1995). On the finite element implementation of geometrically nonlinear Reissner's beam theory: three-dimensional curved beam elements. *Computer Methods in Applied Mechanic and Engineering.* 122, 11—26.

Makinen J. (2001). Critical Study of Newmark scheme on manifold of finite rotations. *Computer Methods in Applied Mechanic Engineering.*191, 817—828.

Mata P., Boroschek R., Barbat A.H. and Oller S. (2006). High damping rubber model for energy dissipating devices. *Journal of Earthquake Engineering*, JEE, (accepted for publication).

Oller S. and Barbat A.H. (2006). Moment-curvature damage model for bridges subjected to seismic loads. *Computer Methods in Applied Mechanic Engineering.* (In Press).

Simo J.C, and Vu–Quoc L. (1985). A finite strain beam formulation, Part I. *Computer Methods in Applied Mechanic Engineering.* 49, 55–70

Simo J.C, and Vu–Quoc L. (1986). A three dimensional finite strain rod model, Part II: Computational aspects. *Computational Methods in Applied Engineering.* 58, 79—116.

Simo J.C, and Vu–Quoc L. (1988). On the dynamic in space of rods undergoing large motions–A geometrically exact approach. *Computer Methods in Applied Mechanic Engineering.* 66, 125—161.

"Computational Civil Engineering 2006", International Symposium
Iaşi, România, May 26, 2006

Numerical simulation of the seismic behavior of passively controlled precast concrete buildings

Pablo Mata A[1], Alex H. Barbat[2] and Sergio Oller M[3]

[1]*Technical University of Catalonia.Edificio C1, Campus Norte UPC. Gran Capitán s/n. Barcelona 08034, Spain . Email: pmata@cimne.upc.edu*
[2] *Technical University of Catalonia, Spain.. Email: alex.barbat@upc.edu*
[3] *Technical University of Catalonia, Spain.. Email: sergio.oller@upc.edu*

Summary

The poor performance of some precast structures have limited their use in seismic zones due to their low level of structural damping, P-Δ effects and low ductility of de structural joints. These characteristics allow proposing the use of passive dissipating devices for improving their behavior. The seismic response of two precast buildings is studied in this work. The response of the structures equipped with energy dissipators is compared with the non-controlled case. The first structure is a low damped industrial precast concrete building with low ductility connecting joints. The second one is a 3D frame typically built in urban areas. The structures are simulated using the Simo's formulation for beams. Each beam section is meshed in a secondary grid of fibers along the beam axis. The materials of each fiber can be composed of several components having appropriated constitutive laws. The simple mixing theory is used to treat the resulting composite. A special kind of element is developed for modeling the dissipating devices. The results obtained in this work allow validating the use of passive control for improving the seismic performance of precast structures.

KEYWORDS: seismic analysis, beam model, numerical methods.

1. INTRODUCTION

The use of precast concrete structures in seismic areas have been frequently limited, by the lack of confidence about their performance in seismic regions as well as by the absence of seismic design provisions or specific codes for analysis and design of critical zones in the structure, i.e. the connecting joints. Due to these reasons, the recognized advantages of precast concrete construction over cast-in-place methods, which commonly are mainly referred only to construction aspects (quality control, velocity of erection), have captured the most of the attention by the researchers, while its structural efficiency is overlooked. The poor performance of several precast parking structures in the 1994 Northridge Earthquake due to incorrect design detailing has probably increased the lack of confidence on such

structural systems, contributing to further restrictions on precast usage in seismic zones. In the last years some alternative concepts for the analysis and design of precast concrete structures in seismic zones have been investigated as opposed to the frequently accepted criteria of "emulation of cast-in-place concrete" [Pampanin, 2003].

Among the most frequently noted disadvantages associated with the traditional precast concrete structures [Mata, Barbat et.al. 2004] are:

- Low *global structural damping coefficient*. On the one hand, the 5% of the global structural damping frequently associated to conventional cast in place concrete structures is not necessarily the most appropriated value for precast ones, which could have considerably smaller values, of the order of 2%, with the consequent amplifications in the dynamic response.
- Important *PΔ effects* for the case of some flexible structures. The precast industry tends to generate more flexible elements mainly designed for permanent death load and, therefore, PΔ effects could be increased for lateral loading paths.
- *Non ductile connecting joints*. The conventional seismic design is not directly applicable to the case of precast concrete structures, because the connecting joints are not monolithic. Furthermore, the joints are points where the ductility demand is important and, therefore, they are critical points of the structure where it is expected that damage concentrate. Additionally, a zone where damage is concentrated presents softens mechanical behavior and it can be identified with a plastic hinge in the structure. As it is well known, only a limited number of plastic hinges can be developed in the structure before a structural behavior corresponding to a mechanism is obtained.

By other hand, the effectiveness of passive control techniques is well recognized for reducing the dynamic response of structures subjected to seismic actions. It is possible to improve the seismic behavior of precast concrete structures by using energy dissipation devices to absorb a part of the energy induced by earthquakes and to concentrate the damage in specific zones.

One choice to perform realistic analysis of structures equipped with energy dissipating devices for seismic loading is by means of employing material and geometrical nonlinear time history analysis assuming appropriated constitutive descriptions for the materials and applying acceleration records to the base of the structure. The numerical model should be able to simulate the changes of configuration of the structure during the earthquake, especially for the case of flexible structures.

In this work the latter is achieved by mean of employing the Simo-Vu Quoc formulation for beams, which is capable of undergoing large strains and displacements [Simo et.al. 1985]. Each beam section is meshed into a grid of fibers

directed along the beam axis. Two kinds of materials are employed: concrete and steel. For describing the mechanical behavior of concrete, a local damage constitutive model based on Kachanov´s theory is used. Reinforcing steel bars are treated using a fiber plastic model. The material associated with a fiber is treated by means the simple mixing theory [Oller et.al. 1997]. The incorporation of energy dissipating devices is obtained developing a special rod element.

In this paper the numerical simulation of the dynamic response of two typical precast concrete building subjected to earthquake loads, using passive energy dissipating devices is carried out. Both structures present the deficiencies previously described. The first one corresponds to a plane frame employed to build industrial buildings. The second one is a three-dimensional concrete frame corresponding a building constructed in urban areas. Nonlinear behavior for both frame structures and energy dissipating devices are considered in the computational simulations.

2. NUMERICAL TOOL

A specific software package, *PLCDYN Plastic Concrete Dynamic*, has been developed to simulate the nonlinear behavior of civil engineering structures including those based on beam elements. The developed code allows solving problems in many different areas of the mechanic of solids: static, dynamic, with material and geometric non-linearity, thermally coupled problems and composite based structures [Car et.al. 2000].

For the case of beam like structures the geometrically exact formulation due to Simo–Vu Quoc is implemented. The kinematical assumptions of the model allow simulating finite strains and large displacements and rotations during the dynamic action [Ibrahimbegovic, 1995; Simo et.al. 1985, 1986, 1988; Mata et.al. 2005]. For dynamic analysis a Newmark scheme, which update consistently all the dynamic variables associated with finite rotations, has been implemented [Simo et.al. 1989].

Each beam section of the elements is meshed into a secondary grid of quadrilaterals for including a non-homogeneous distribution of materials. Each quadrilateral corresponds to a fiber oriented along the centroid axis of the beam. See Figure 1. The material of each fiber is composed by several components, having each of them its own constitutive law. By this way, it is possible to consider the steel reinforcement as one of the components of the composite located in the quadrilaterals on the boundary of the section. The resulting composite is treated according to the *simple mixing theory* [Car et.al. 2000], which impose the same strain field for all components in a material point. The stress field is recovered for each component according to its constitutive law, the total stress is determined

supposing that each component contributes to the total stress according to its volumetric participation in the mixture.

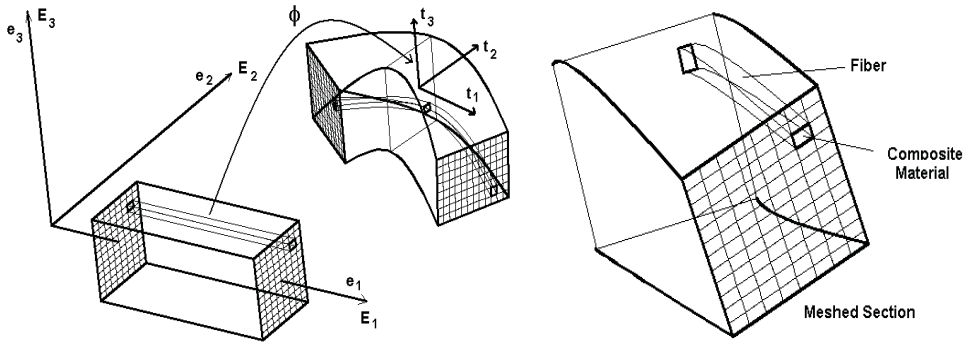

Figure 1: Kinematics of beams and grid of quadrilaterals in each section.

The sectional forces and moments are obtained integrating the stresses over the whole section in each integration point. This kind of approximation avoids the development or employment of constitutive laws based on force–displacement for the element, which is the most common way to model the nonlinear beam behavior, but this kind of laws are valid only for a certain geometry of sections or mechanical behaviors of the beams [Barbat et.al. 1997]. Sectional forces and moments are then used to check global equilibrium of the dynamical system. The iterative process is repeated until convergence is obtained.

2.1 Constitutive laws for materials

The failure of concrete for different strain or stress conditions is simulated employing an *isotropic damage model* based on fundamental thermo dynamical principles [Barbat et.al. 1997]. This model is able to simulate in a simple and efficient fashion one of the basic features of the concrete behavior: *degradation*, strain softening under tension–compression stress states. Figure 2 shows the shape of the damage criterion in the principal stress space employed for the concrete. In this figure it is possible to see that the model takes into account different properties for tension or compression states. The resulting integration algorithm for this model is simple and suitable for large-scale computations. In this category, nonlinear behavior is monitored through a single internal scalar variable, called *damage* or *degradation* [Hanganu et.al. 2002].

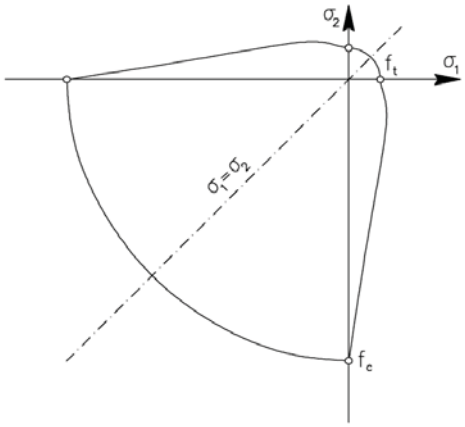

Figure 2: Kinematics of beams and grid of quadrilaterals in each section.

Steel bar reinforcements and stirrups are modeled by mean of the *plastic fiber behavior* model. The model consists in an orthotropic material with a steel elastic modulus in the direction of the reinforcement and concrete properties in the other two directions. Plastic flow is oriented along the fiber once the yielding criterion is reached [Car et.al. 2000].

2.2 Strain localization

Strain localization is expected to occur when large incursion in the nonlinear range are attained by the structure [Hanganu et.al. 2002]. The objectivity of the response is obtained by means of carrying out a regularization the dissipated energy in each integration point considering the characteristic length of the finite element where the is strain localization have place. In this way the maximum dissipated energy by a material is limited by its fracture energy. This corrective procedure became the global structural response objective but the length of the zone where strains are localized is still mesh dependent.

2.3 Dissipating device element

The energy dissipating devices are modeled by mean of a bi–pinned rod element with only one integration point in the middle of the rod span. The bi–pinned condition of the ending nodes allows obtaining displacements in the direction of the axes element and, therefore, only axial strains have place. Specific one-dimensional constitutive laws have to be provided for the element. In this work, only devices with plasticity as constitutive law will be employed but the developed element can be employed with any other kind of constitutive relation, e.g. [Mata et.al. 2006].

3. NUMERICAL SIMULATIONS

3.1 Precast concrete industrial frame

The nonlinear seismic response of a typical plane precast industrial building, Figure 3, is studied. The building has a bay width of 24 m and 12 m of inter–axes length. The story high is 12 m. The concrete of the structure is H–35, (35 Mpa, ultimate compression), with an elastic modulus of 290.000 Mpa. It has been assumed a Poison coefficient of 0.2. The steel reinforcement of the sections considered in the study corresponds to the 10% of the sectional area and the quadrilateral discretization of the sections is presented in the same figure for each element. The ultimate tensile stress for the steel is 510 Mpa. The dimensions of the columns are 60x60 cm^2. The beam has a variable section with an initial high of 60 cm on the supports and 160 cm in the middle of the span.

The permanent loads considered are 1050 N/m^2 and the weight of upper half of the closing walls (432,000 N). The employed acceleration record is the N–S component of the El Centro earthquake, 1940.

The energy dissipating devices were simulated by means of employing the previously described model to obtain only axial force in each element. The properties of the dissipating devices were designed for yielding with an axial force of 150.000 N and for a relative displacement between the two ending nodes of 1.5 mm. The length of the devices was of 2,00 m.

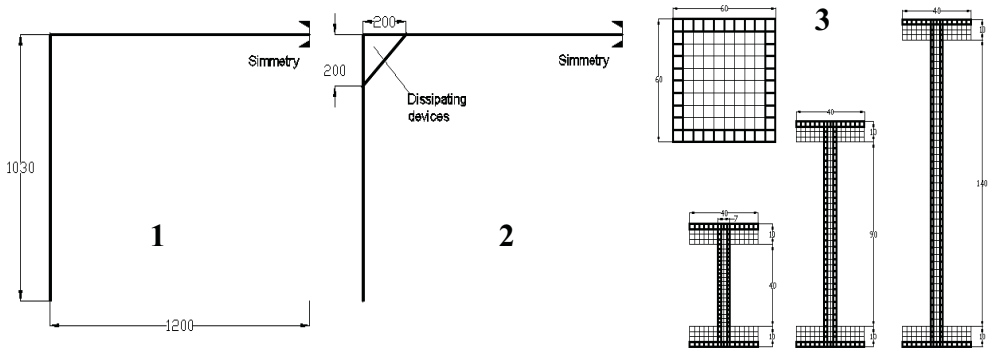

Figure 3: Half part of 2D precast industrial frame. 1: Normal frame 2: Energy dissipating devices incorporated (diagonal elements). 3: Numerical model of Column and beam sections.

A nonlinear static analysis has been performed on the structure with and with out energy dissipating devices. A sequence of imposed displacements with sinusoidal

form is applied on the upper corner of the structure. The results are summarized in figure 4 where base shear is draw as function of the top displacement. In this figure it is possible to see that the controlled structure increments its stiffness and resistance when compared with the non-controlled case. Additionally, more energy dissipating capacity is obtained for the controlled structure as it can be evidenced from the greater hysteretic cycles obtained.

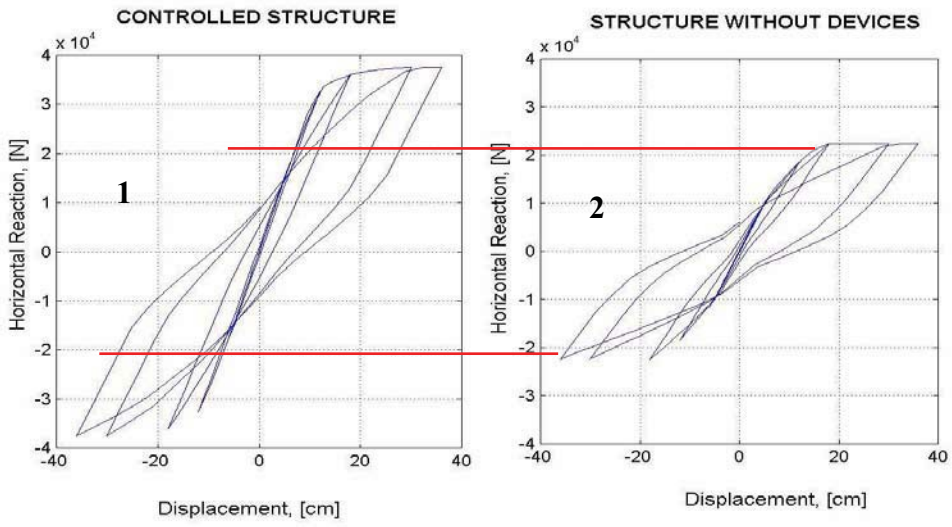

Figure 4: Hysteretic cycles. 1: Structure. 2: Energy dissipating devices.

By other hand, ductility of the structure is increased when control devices are employed as it can be seen in Figure 5.

The results of the numerical simulations allow seeing that the employment of plastic dissipating devices contributes to improve the seismic behavior of the structure for the case of the employed seismic record. Figure 6 shows the hysteretic cycles obtained for the structure with and with out devices. For the case of the whole structure the cycles are obtained from the lateral displacement of the upper beam–column joint and the horizontal reaction (base shear) in the columns. It is possible to appreciate that the non-controlled structure (bare frame) presents greater lateral displacements and a more structural damage is observed, (greater hysteretic area than for the controlled case). In the case of the structure equipped with dissipator a stiffer response is obtained and a part of the dissipated energy is concentrated in the controlling devices as expected.

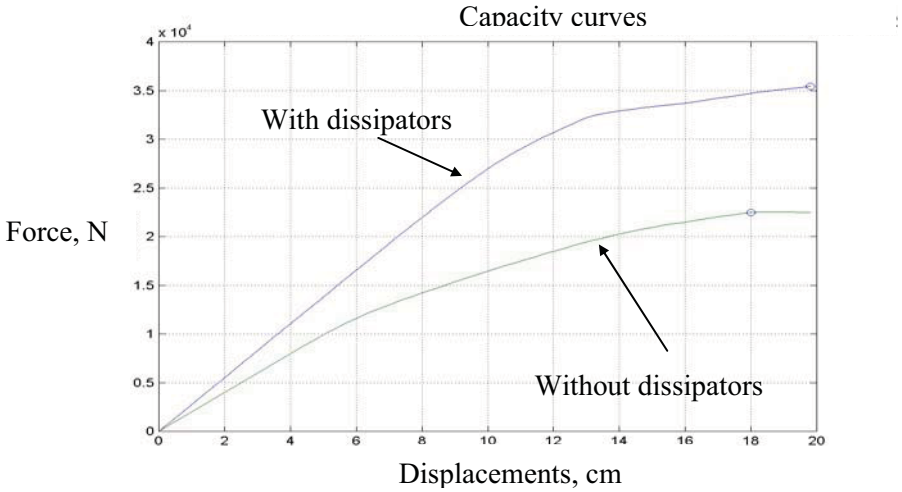

Figure 5: Capacity curves.

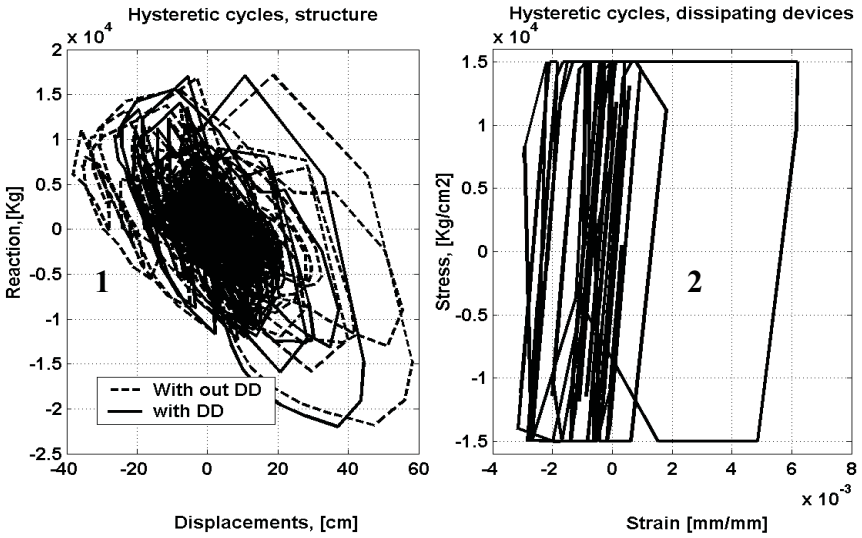

Figure 6: Hysteretic cycles. 1: Structure. 2: Energy dissipating devices.

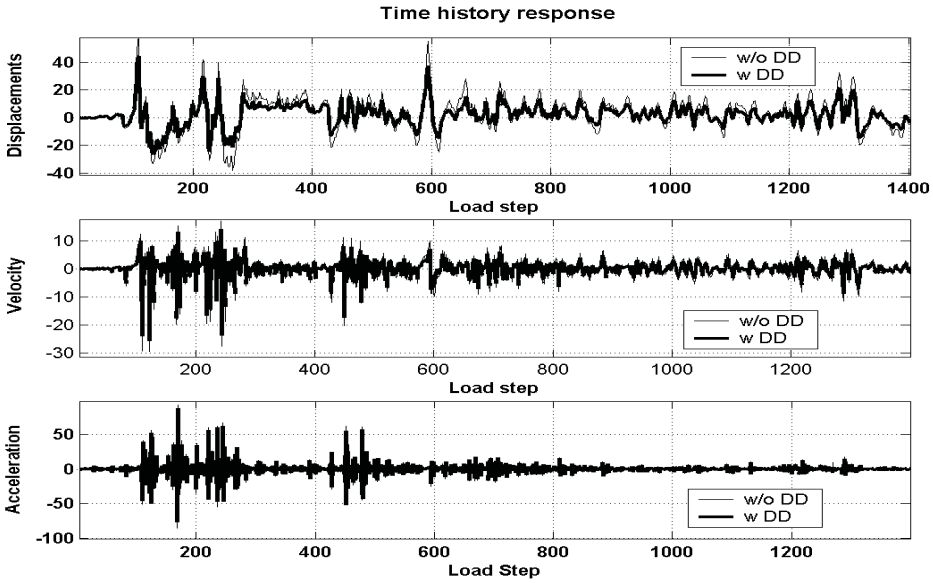

Figure 7: Time history response of the structure with and with out dissipating devices.

Figure 7 shows the time history responses of the upper beam–column joint. A reduction of 12 % is obtained for the maximum lateral displacement compared with the bare frame. Acceleration and velocity are controlled in the same way, but only 4 and 5 % percent of reduction is obtained. A possible explanation for the low effectiveness of the dissipators is that the devices only contribute to increase the ductility of the beam – column joint with out alleviating the base shear demand on the columns due to their dimensions and location in the structure. By other hand, joints are critical points in precast structures and therefore, the employment of dissipators combined with a careful design of the columns can help to improve the seismic their behavior.

3.2 Precast concrete building

The nonlinear seismic response of a precast building constructed in urban areas is studied. See Figure 8. The building has one bay and two stories of 6 and 3 m width, respectively. The concrete of the structure is H–25, (25 Mpa, ultimate compression), with an elastic modulus of 25.000 Pa. It has been assumed a Poison coefficient of 0.2. The steel bar reinforcements considered in the study are those corresponding to the 8% of the sectional area for elements near to the joint (25 % of the column or beam length), and 4% for elements in the middle part of the span. The ultimate tensile stress for the steel is 510 Mpa. The dimensions of the columns are 30x30 cm^2. The beams have a section of 15x30 cm^2.

The permanent loads considered are the weight of the concrete floors, a live load of 2500 N/m^2 and the weight of the closing walls, (432,000 N). The employed acceleration record is the same as before in the direction X and the same record scaled by 0.3 in the orthogonal direction.

No accidental or structural eccentricities were considered in this work, but it is possible to do it modifying the mass density of the beams or adding another structural element in the same of the planar frames.

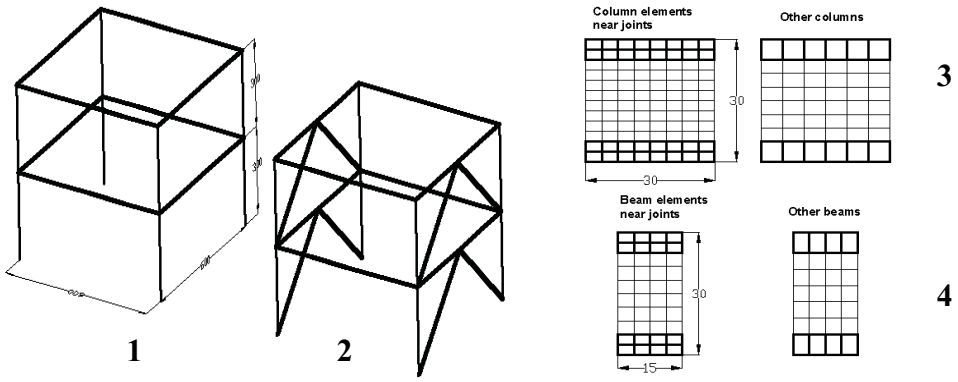

Figure 8 : 1 : 3D Frame. 2: Dissipating devices incorporated. 3, 4: Column and beams sections.

Several numerical simulations were carried out to obtain an optimized combination of the characteristic of the energy dissipation devices for knowing what is the yielding level, F_y, stiffness, K, and yielding displacement, D_y, which give a biggest protection level to the structure. The properties of the employed energy dissipating devices are summarized in Table 1.

Table 1: Parameters of the energy dissipation devices

Device Characteristics		Device Characteristics		Device Characteristics		Device Characteristics		Device Characteristics	
F_y, (N)	1000	F_y, (N)	2000	F_y, (N)	3000	F_y, (N)	4000	F_y, (N)	5000
D_y, (mm)	1.250	D_y, (mm)	1.250	D_y, (mm)	1.250	D_y, (mm)	1.250	D_y, (mm)	1.250
F_y, (N)	1000	F_y, (N)	2000	F_y, (N)	3000	F_y, (N)	4000	Fy, (N)	5000
D_y, (mm)	2.500	D_y, (mm)	2.500	D_y, (mm)	2.500	D_y, (mm)	2.500	Dy, (mm)	2.500
F_y, (N)	1000	F_y, (N)	2000	F_y, (N)	3000	F_y, (N)	4000	F_y, (N)	5000
D_y, (mm)	5.000	D_y, (mm)	5.000	D_y, (mm)	5.000	D_y, (mm)	5.000	D_y, (mm)	5.000

The results of the simulation are expressed in terms of maximum top and middle floor displacements; base shear and over-tuning moment are presented simultaneously as function of the type of employed device in figure 9. From this figure it is possible to see that even when the biggest benefits in terms of the selected global variables are attained for different device characteristics, the more advantageous characteristics are related with flexible devices (K=8000 N/mm) with a medium yielding displacement (approx. 2.5 mm) and yielding force around the 4000 N.

Therefore, the selected properties of the dissipators were: Plastic yielding for a axial force of 4000 N, relative yielding displacement between the two ending nodes of 2.50 mm. The length of the dissipating devices is of 6.7 m. The dissipating devices only were incorporated in the direction where the strongest ground acceleration record is applied.

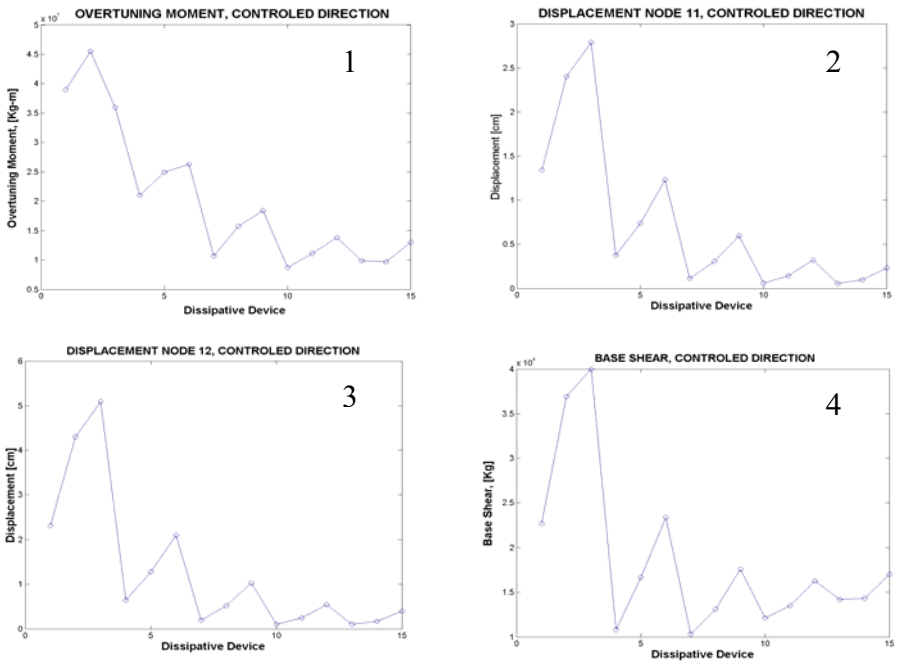

Figure 9: Maximum response for each energy dissipating device. 1: Over–tuning Moment. 2: Top floor displacement. 3: Middle floor displacement. 4: Base shear.

4. CONCLUSIONS

The seismic behavior of two typical precast concrete structures is studied employing a numerical code, which incorporate a geometrically exact finite strain formulation for rods using appropriated constitutive laws for materials. The simple mixing rule is employed to treat the resulting composites. The fiber beam model presented in this work provides a useful tool to simulate the earthquake effects on structures. A specific plastic energy dissipating device element is employed in the simulations. The advantages of employing dissipating devices to protect and improve the seismic behavior of flexible and low damped precast structures with non ductile connecting joints is studied for the 2D and 3D cases presented here. From the results it is possible to see that several numerical simulation are required to validate the best choice for selecting the mechanical characteristics of the control devices to ensure the biggest improvements in the seismic response of the controlled structure.

5. ACKNOWLEDGMENTS

This work has been partially supported by: The University of Chile, Project FONDECYT nº 1970732; Ministerio de Ciencia y Tecnología, Spain, Project: "Numerical simulation of the seismic behavior of structures with energy dissipation systems", Contract nº: BIA2003 - 08700 - C03 – 02; and the Integrated R&D Project of the EC "LessLoss–Risk Mitigation for Earthquakes and Landslides" funded by the European Commission, Directorate General of Research under the Contract nº GOCE-CT-2003-505448.

6. REFERENCES

Barbat. A. H, Oller. S, Oñate. E and Hanganu. A. (1997). Viscous damage model for Timoshenko beam structures. *International Journal of Solids and Structures*. Vol. 34. Nº 30. pp. 3953–3976.

Car. J, Oller. S and Oñate E. (2000). Modelo constitutivo continuo para el estudio del comportamiento mecánico de los materiales compuestos. *International Center for Numerical Methods in Engineering, CIMNE, Barcelona, Spain. PhD Thesis.* (In Spanish).

Davenne. L, Ragueneau. F, Mazars. J and Ibrahimbegovic. A. (2003). Efficient approaches to finite element analysis in earthquake engineering. *Computers and Structures* 81. 1223-1239.

Hanganu Alex D., Oñate E. and Barbat A.H. (2002). A finite element methodology for local/global damage evaluation in civil engineering structures. *Computers & Structures* 80, 1667—1687.

Ibrahimbegovic. A. (1995). On the finite element implementation of geometrically nonlinear Reissner's beam theory: three-dimensional curved beam elements. *Computer Methods in Applied Mechanic and Engineering*. 122, 11-26.

Mata A. P, Barbat A and Oller S. (2004). Improvement of the seismic behavior of precast concrete structures by means of energy dissipating devices. *Third European Conference on Structural Control, 3ECSC. 12-15 July, Vienna University of Technology,* Vienna, Austria.

Mata A. P, Oller. S and Barbat A. (2005). Numerical tool for nonlinear seismic analysis of buildings with energy dissipating systems. *9th World Seminar on Seismic Isolation, Energy Dissipation and Active Vibration Control of Structures,* Kobe, Japan, June 13-16.

Mata P., Boroschek R., Barbat A.H. and Oller S. (2006). High damping rubber model for energy dissipating devices. *Journal of Earthquake Engineering, JEE*, (accepted for publication).

Pampanin S. (2003). Alternative design philosophies and seismic response of precast concrete buildings. *Fib. News. Structural Concrete*, 4, Nº 4.

Simo. J.C, and Vu–Quoc L. (1985). A finite strain beam formulation, Part I. *Computer Methods in Applied Mechanic Engineering.* 49, 55–70

Simo. J.C, and Vu–Quoc L. (1986). A three dimensional finite strain rod model, Part II: Computational aspects. *Computational Methods in Applied Engineering*. 58, 79–116.

Simo. J.C, and Vu–Quoc L. (1988). On the dynamic in space of rods undergoing large motions–A geometrically exact approach*. Computer Methods in Applied Mechanic Engineering.* 66, 125–161.

"Computational Civil Engineering 2006", International Symposium
Iaşi, România, May 26, 2006

Holistic evaluation of the seismic risk in urban centers

Martha L. Carreño[1], Omar D. Cardona[2] and Alex H. Barbat[3]

[1] *Technical University of Catalonia, C/ Gran Capitán SN, Módulo C 1, 08904 Barcelona, Spain*
[2] *Universidad Nacional de Colombia, Carrera 27 64-60, Manizales, Colombia*
[3] *Technical University of Catalonia, C/ Gran Capitán SN, Módulo C 1, 08904 Barcelona, Spain*

Summary

In the past, the concept of risk has been defined in a fragmentary way in many cases, according to each scientific discipline involved in its appraisal. At nowadays, the risk is defined, for management purposes, as the potential economic, social and environmental consequences of hazardous events that may occur in a specified period of time. From the perspective of this article, risk requires a multidisciplinary evaluation that takes into account not only the expected physical damage, the number and type of casualties or economic losses, but also the conditions related to social fragility and lack of resilience conditions, which favors the second order effects when a hazard event strike a urban centre. The urban seismic risk evaluation is proposed from a holistic point of view; that is an integrated and comprehensive approach to guide decision-making. Evaluation of the potential physical damage is the first step of this method. Subsequently, a set of social context conditions that aggravate the physical effects are also considered. In the method here proposed, the holistic risk evaluation is based on urban risk indicators. According to this procedure, a physical risk index is obtained, for each unit of analysis, from existing loss scenarios, whereas the total risk index is obtained by factoring the former index by an impact factor, based on variables associated with the socio-economic conditions of each unit of analysis. Finally, examples of the model application are given for two urban centers: Bogotá and Barcelona

KEYWORDS: risk evaluation, seismic risk, urban centers.

1. METHODOLOGY OF EVALUATION

The report Natural Disasters and Vulnerability Analysis [UNDRO, 1980] proposed the unification of disaster related definitions as hazard (H), vulnerability (V), exposed elements (E) and risk (R) and suggested one expression to associating them, that is considered a standard at present

$$R = E \cdot H \cdot V \tag{1}$$

Based on this formulation several methodologies for risk assessment have been developed from different perspectives in the last decades, and recently a holistic approach for the case of urban centers [Cardona and Hurtado 2000; Masure, 2003].

Cardona (2001) developed a conceptual framework and a model for seismic risk analysis of a city from a holistic perspective. It considers both "hard" and "soft" risk variables of the urban centre, taking into account exposure, socio-economic characteristics of the different districts of the city and their disaster coping capacity or degree of resilience. The model was made to guide the decision-making in risk management, helping to identify the critical zones of the city and their vulnerability from different professional disciplines.

This article presents an alternative method for urban risk evaluation based on Cardona's model [Cardona, 2001; Barbat and Cardona, 2003], using a holistic approach and describing seismic risk by means of indices. Expected building damage and losses in the infrastructure, obtained from future loss scenarios are basic information for the evaluation of physical risk in each unit of analysis. Starting from these data, a physical damage index is obtained. The holistic evaluation of risk by means of indices is achieved affecting the physical risk with an impact factor or aggravating coefficient, obtained from contextual conditions, such as the socio-economic fragility and the lack of resilience, that aggravate initial physical loss scenario. Available data about these conditions at urban level are necessary to apply the method. An explanation of the model is made ahead and also some examples of application for the cities of Bogotá, Colombia, and Barcelona, Spain, are described to illustrate the benefits of this approach that contributes to the effectiveness of risk management, inviting to the action identifying the hard and soft weaknesses of the urban centre. Figure 1 shows the theoretical framework for the alternative model.

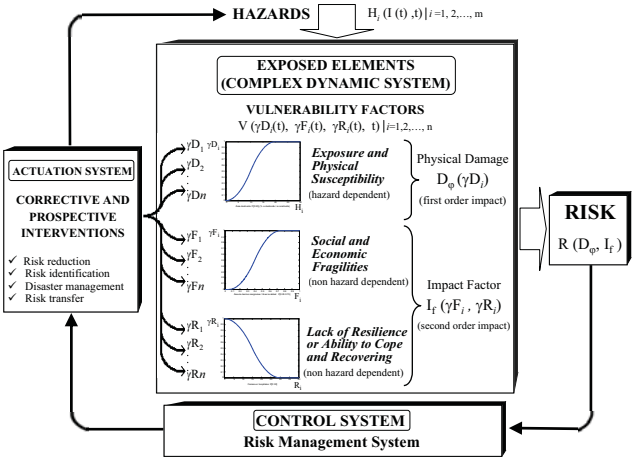

Figure 1: Model for holistic approach of disaster risk (adapted from Cardona and Barbat, 2000)

From a holistic perspective risk, R, is a function of the potential physical damage, D_j, and an impact factor, I_f. The former is obtained from the susceptibility of the exposed elements, γ_{Di}, to hazards, H_i, regarding their potential intensities, I, of events in a period of time t, and the latter depends on the social fragilities, γ_{Fi}, and the issues related to lack of resilience, γ_{Ri}, of the disaster prone socio-technical system or context. Using the meta-concepts of the theory of control and complex system dynamics, to reduce risk it is necessary to intervene in corrective and prospective way the vulnerability factors and, when it is possible, the hazards directly. Then risk management requires a system of control (institutional structure) and an actuation system (public policies and actions) to implement the changes needed on the exposed elements or complex system where the risk is a social process.

In this paper the proposed holistic evaluation of risk is performed using a set of input variables, herein denominated descriptors. They reflect the physical risk and the aggravating conditions that contribute to the potential impact. Those descriptors, listed forward, are obtained from the loss scenarios effects and from socio-economic and coping capacity information of the exposed context [Barbat and Cardona, 2003; Carreño et al., 2005]. The obtainment or calculation of these descriptors is not the objective of this paper. More information on this subject can be found in Carreño et al. (2005). They are only input information data. The socio-economic fragility and the lack of resilience are a set of factors (related to indirect or intangible effects) that aggravate the physical risk (potential direct effects). Thus, the total risk depends on the physical risk, and the indirect effects expressed as a factor

$$R_T = R_F\left(1+F\right) \tag{2}$$

In this equation, known as Moncho's equation, R_T is the total risk index, R_F is the physical risk index and F is the impact factor. This coefficient, F, depends on the weighted sum of a set of aggravating factors related to the socio-economic fragility, F_{FSi}, and the lack of resilience of the exposed context, F_{FRj}

$$F = \sum_{i=1}^{m} w_{FSi} \times F_{FSi} + \sum_{j=1}^{m} w_{FRj} \times F_{FRj} \tag{3}$$

where w_{FSi} and w_{FRj} are the weights or influences of each i and j factors and m and n are the total number of descriptors for social fragility and lack of resilience respectively.

The aggravating factors F_{FSi} and F_{FRj} are calculated using transformation functions shown in the figures 2 and 3. These functions standardize the gross values of the descriptors transforming them in commensurable factors. The weights w_{FSi} and w_{FRj}

represent the relative importance of each factor and are calculated by means of the Analytic Hierarchy Process (AHP). It is used to derive ratio scales from both discrete and continuous paired comparisons [Saaty, 1980, 2001].

The physical risk, R_F, is evaluated in the same way, using the transformation functions showed in the Figure 3

$$R_F = \sum_{i=1}^{p} w_{RFi} \times F_{RFi} \tag{4}$$

where p is the total number of descriptors of physical risk index, F_{RFi} are the component factors and w_{RFi} are their weights respectively. The factors of physical risk, F_{RFi}, are calculated using the gross values of physical risk descriptors such as the number of deaths, injured or the destroyed area, and so on. The transformation functions take values between 0 and 1 (see figures 2, 3 and 4).

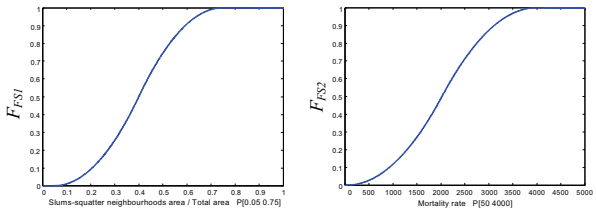

Figure 2: Examples of transformation functions used for the social fragility factors

It is estimated that the indirect effects of hazard events, sized by the factor F in equation 2, can be the same order of the direct effects. According to the Economic Commission for Latin America and the Caribbean (ECLAC), it is estimated that the indirect economic effects of a natural disaster depend on the type of phenomenon. The order of magnitude of the indirect economic effects for a "wet" disaster (as one caused by a flood) could be of 0.50 to 0.75 of the direct effects. In the case of a "dry" disaster (caused by an earthquake, for example), the indirect effects could be about the 0.75 to 1.00 of the direct effects, due to the kind of damage (destruction of livelihoods, infrastructure, housing, etc.). This means that the total impact, R_T, could be between 1.5 and 2 times R_F. In this method, the maximum value selected was the latter. For this reason, the impact factor, F, takes values between 0 and 1 in equation 2, in this case.

In order to develop the transformation functions sigmoid functions were used (see figures 2 to 4). The maximum and minimum values (for the values 1 or 0 of each factor) were fixed using existing information about disasters as well as experts opinions. For the lack of resilience descriptors, related to the level of development of the community and the emergency planning or preparedness, a linear relation

was assumed. Table 1 presents the variables used to reflecting the social fragility and the lack of resilience in the estimation of *F*.

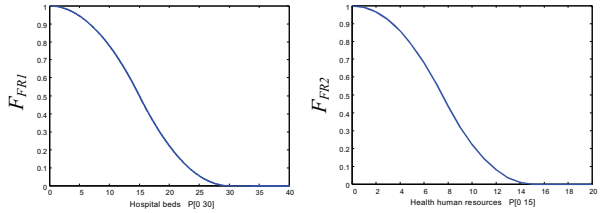

Figure 3: Examples of transformation functions used for the lack of resilience factors

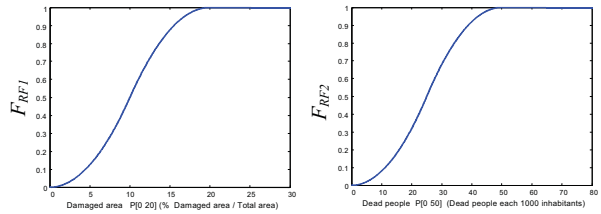

Figure 4: Examples of transformation functions used for the physical risk factors

Figures 2 to 4 show the values of the descriptors in the x-axis of the transformation functions. The corresponding factors, or scaled values, are given in the y-axis. Table 2 presents the initial measurement units of each descriptor of social fragility and resilience. Table 3 shows the descriptors of the physical risk. The factors for a city are obtained in each case using the transformation functions of the aforesaid figures and the variables with the units of tables above-mentioned.

Table 1: Descriptors used to evaluate the impact factor F

Aspect	Descriptor
Social fragility	Slums-squatter neighbourhoods
	Mortality rate
	Delinquency rate
	Social disparity index
	Population density
Lack of resilience	Hospital beds
	Health human resources
	Public space
	Rescue and firemen manpower
	Development level
	Preparedness emergency planning

Table 2: Aggravating descriptors, their units and identifiers

Descriptor		Units
X_{FS1}	Slums-squatter neighbourhoods	Slum-squatter neighbourhoods area / Total area
X_{FS2}	Mortality rate	Number of deaths each 10000 inhabitants
X_{FS3}	Delinquency rate	Number of crimes each 100000 inhabitants
X_{FS4}	Social disparity index	Index between 0 y 1
X_{FS5}	Population density	Inhabitants / Km^2 of build area
X_{FR1}	Hospital beds	Number of hospital beds each 1000 inhabitants
X_{FR2}	Health human resources	Health human resources each 1000 inhabitants
X_{FR3}	Public space	Public space area/ Total area
X_{FR4}	Rescue and firemen manpower	Rescue and firemen manpower each 10000 inhabitants
X_{FR5}	Development level	Qualification between 1 and 4
X_{FR6}	Emergency planning	Qualification between 0 and 2

Figure 5 shows the process of calculation of the total risk index for the units of analysis, R_T, starting from the factors of physical risk, F_{RFi}, and of aggravating, F_{FSi} and F_{RFi}, and using the weights w_{RFi}, w_{FSi} and w_{FRi} of each factor. These weights take values according to the expert opinion for each studied city applying the Analytic Hierarchical Process (AHP). Using the factors obtained applying the functions of figures 2 to 4, the physical risk index is calculated by applying equation 4, the impact factor by means of equation 3 and, finally, the total risk is calculated by means of equation 2.

This new model improves conceptual and methodological aspects of the first Cardona's proposal, refining the applied numerical techniques and turning it into a more versatile tool. The conceptual improvements provide a more solid theoretical and analytical support to the new model, eliminating unnecessary and dubious aspects of the previous method, given more transparency and applicability in some cases. The new approach preserves the use of indicators and fuzzy sets or membership functions, proposed originally, but in a different way. It also improves the procedure of normalization and calculates the final indices in an absolute (non relative) manner. This feature facilitates the comparison of risk among cities. Finally, the earlier model takes into account descriptors of physical risk, seismic hazard, physical exposure, socio-economic fragility, and lack of resilience; in the new approach, seismic hazard and the physical exposure have been eliminated because they are redundant due to they have been included into the physical risk variables.

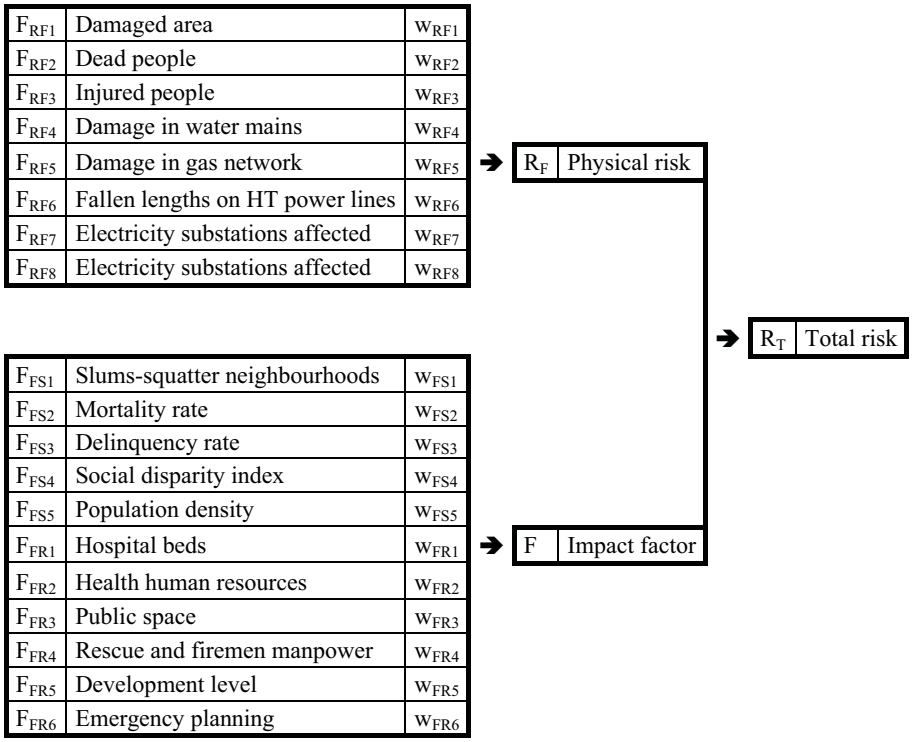

Figure 5: Factors of physical risk, social fragility and lack of resilience and their weights

Table 3: Physical risk descriptors, their units and identifiers

Descriptors		Units
X_{RF1}	Damaged area	Percentage (damaged area / build area)
X_{RF2}	Dead people	Number of dead people each 1000 inhabitants
X_{RF3}	Injured people	Number of injured people each 1000 inhabitants
X_{RF4}	Ruptures in water mains	Number of ruptures / Km^2
X_{RF5}	Rupture in gas network	Number of ruptures / Km^2
X_{RF6}	Fallen lengths on HT power lines	Metres of fallen lengths / Km^2
X_{RF7}	Telephone exchanges affected	Vulnerability index
X_{RF8}	Electricity substations affected	Vulnerability index
X_{RF9}	Damage in the road network.	Damage index

2. EXAMPLE OF APPLICATION: SEISMIC RISK OF BOGOTÁ

In Bogotá, the capital of Colombia, the localities are political-administrative subdivisions of the urban territory, with clear competences in financing and application of resources. They were created with the objective of attending in an effective way the necessities of the population of each territory. Since 1992,

Bogotá has 20 localities which can be seen in Figure 6: Usaquén, Chapinero, Santafé, San Cristóbal, Usme, Tunjuelito, Bosa, Ciudad Kennedy, Fontibón, Engativa, Suba, Barrios Unidos, Teusaquillo, Mártires, Antonio Nariño, Puente Aranda, Candelaria, Rafael Uribe, Ciudad Bolívar y Sumapaz. In this study, only 19 of these localities are considered, because the locality of Sumapaz corresponds to the rural area.

As it is well known, the seismic hazard is the most significant threat for Bogotá. The scenario of seismic physical risk illustrated also in Figure 6 was used as a starting point for the application of the model. It displays the mean damaged area in predefined cells or zones considering a strong near field earthquake with 0.2g acceleration at the bedrock [Universidad de Los Andes, 1996].

Tables 4 and 5 show the weights computed using the AHP, for the components of the physical risk and for the aggravating factors, respectively. The weights are calculated in Carreño et al. (2005). Tables 6 show the values of the descriptors used in this application, which represent the physical risk. Table 7 shows the values of the factors of physical risk obtained by applying the functions of the Figure 4. The aggravating factors due to the social fragility and the lack of resilience are obtained by the applying the functions of figures 2 and 3. Table 8 shows the results for the physical risk, the impact factor and the total risk of each locality and the average values for the city.

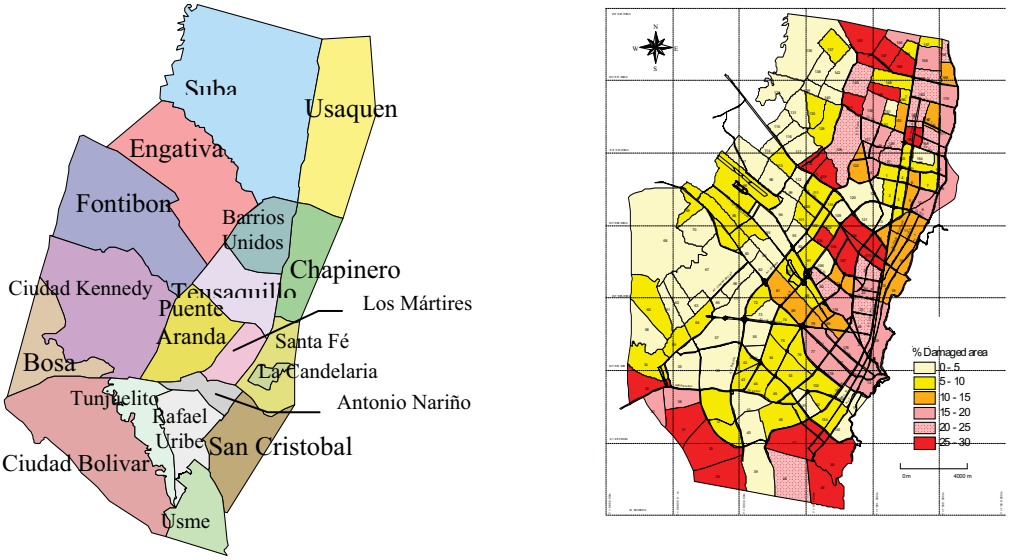

Figure 6: Political-administrative division of Bogotá, and scenario of physical seismic risk, Universidad de Los Andes (1996)

Table 4: Physical risk descriptors, their units and identifiers

Factor	Weight	Weight value
F_{RF1}	w_{RF1}	0.31
F_{RF2}	w_{RF2}	0.10
F_{RF3}	w_{RF3}	0.10
F_{RF4}	w_{RF4}	0.19
F_{RF5}	w_{RF5}	0.11
F_{RF6}	w_{RF6}	0.11
F_{RF7}	w_{RF7}	0.04
F_{RF8}	w_{RF8}	0.04

Table 5: Weights for the factors of the aggravating conditions

Factor	Weight	Weight value
F_{FS1}	w_{FS1}	0.18
F_{FS2}	w_{FS2}	0.04
F_{FS3}	w_{FS3}	0.04
F_{FS4}	w_{FS4}	0.18
F_{FS5}	w_{FS5}	0.18
F_{FR1}	w_{FR1}	0.06
F_{FR2}	w_{FR2}	0.06
F_{FR3}	w_{FR3}	0.04
F_{FR4}	w_{FR4}	0.03
F_{FR5}	w_{FR5}	0.09
F_{FR6}	w_{FR6}	0.09

Table 6: Descriptor values of the physical risk, R_F

Locality	X_{RF1}	X_{RF2}	X_{RF3}	X_{RF4}	X_{RF5}	X_{RF6}	X_{RF7}	X_{RF8}
Usaquen	15.1186	4	27	2	0	24	0.7	0.83
Chapinero	5.0302	5	27	5	0	81	0.77	0.9
Santafé	6.6070	3	16	7	0	63	0.62	0.9
San Cristóbal	4.9278	2	13	4	0	34	0.68	0.9
Usme	10.5870	0	1	1	1	14	0.67	0.9
Tunjuelito	3.5494	0	1	1	0	7	0.58	0.7
Bosa	4.2461	2	12	3	1	42	0.73	0.9
Ciudad Kennedy	4.8198	0	2	1	0	11	0.54	0.7
Fontibón	5.3163	1	7	1	0	5	0.64	0.7
Engativa	6.8777	1	5	1	0	3	0.66	0.8
Suba	13.8449	2	13	1	0	19	0.66	0.77
Barrios Unidos	12.2659	4	27	2	1	45	0.75	0.9
Teusaquillo	10.2985	8	41	4	0	36	0.74	0.9
Mártires	7.0283	6	30	2	0	18	0.66	0.7
Antonio Nariño	4.0287	0	2	2	0	17	0.67	0.8
Puente Aranda	5.7006	1	6	2	0	20	0.69	0.7
Candelaria	8.9515	9	44	6	0	81	0.67	0.9
Rafael Uribe	3.2433	1	11	2	0	29	0.65	0.9
Ciudad Bolívar	8.8908	1	11	1	1	21	0.64	0.9

Table 7: Factors, F_{RF}, and the physical risk index, R_F

Locality	F_{RF1}	F_{RF2}	F_{RF3}	F_{RF4}	F_{RF5}	F_{RF6}	F_{RF7}	F_{RF8}	R_F
Usaquen	0.881	0.0128	0.259	0.08	0	0.0288	0.7	0.83	0.386
Chapinero	0.127	0.02	0.259	0.5	0	0.328	0.77	0.9	0.264
Santafé	0.218	0.0072	0.091	0.82	0	0.198	0.62	0.9	0.314
San Cristobal	0.121	0.0032	0.0601	0.32	0	0.0578	0.68	0.9	0.175
Usme	0.557	0	0.00036	0.02	0.08	0.0098	0.67	0.9	0.253
Tunjuelito	0.063	0	0.00036	0.02	0	0.0025	0.58	0.7	0.076
Bosa	0.090	0.0032	0.0512	0.18	0.08	0.0882	0.73	0.9	0.152
Ciudad Kennedy	0.116	0	0.00142	0.02	0	0.0061	0.54	0.7	0.092
Fontibón	0.141	0.0008	0.0174	0.02	0	0.0012	0.64	0.7	0.105
Engativa	0.237	0.0008	0.00889	0.02	0	0.0004	0.66	0.8	0.139
Suba	0.811	0.0032	0.0601	0.02	0	0.0181	0.66	0.77	0.326
Barrios Unidos	0.701	0.0128	0.259	0.08	0.08	0.101	0.75	0.9	0.350
Teusaquillo	0.529	0.0512	0.589	0.32	0	0.0648	0.74	0.9	0.366
Mártires	0.247	0.0288	0.32	0.08	0	0.0162	0.66	0.7	0.186
Antonio Nariño	0.081	0	0.00142	0.08	0	0.145	0.67	0.8	0.116
Puente Aranda	0.162	0.0008	0.0128	0.08	0	0.02	0.69	0.7	0.126
Candelaria	0.401	0.0648	0.658	0.68	0	0.328	0.67	0.9	0.426
Rafael Uribe	0.0526	0.0008	0.043	0.08	0	0.042	0.65	0.9	0.103
Ciudad Bolívar	0.395	0.0008	0.043	0.02	0.08	0.022	0.64	0.9	0.206
Bogotá	*0.41*	*0.0039*	*0.0536*	*0.092*	*0.04*	*0.0379*	*0.664*	*0.8630*	*0.2246*

Table 8: Total risk of Bogotá

Locality	R_F	F	R_T
Usaquen	0.386	0.309	0.505
Chapinero	0.264	0.245	0.329
Santafé	0.314	0.478	0.464
San Cristóbal	0.175	0.707	0.298
Usme	0.253	0.797	0.454
Tunjuelito	0.076	0.587	0.121
Bosa	0.152	0.701	0.258
Ciudad Kennedy	0.092	0.643	0.150
Fontibón	0.105	0.358	0.142
Engativa	0.139	0.521	0.211
Suba	0.326	0.369	0.446
Barrios Unidos	0.350	0.302	0.456
Teusaquillo	0.366	0.193	0.436
Mártires	0.186	0.325	0.246
Antonio Nariño	0.116	0.407	0.163
Puente Aranda	0.126	0.391	0.175
Candelaria	0.426	0.631	0.694
Rafael Uribe	0.103	0.635	0.169
Ciudad Bolivar	0.206	0.700	0.350
Bogotá	*0.225*	*0.663*	*0.374*

Figures 7 to 11 display graphically the results of the holistic evaluation of the seismic risk of Bogotá using the proposed model. These figures show that the locality of Candelaria has the most critical situation from the point of view of the physical and total seismic risk, because its impact factor is significant, although it is not the highest of the city. The localities with greater impact factor are Usme, San Cristóbal, Bosa and Ciudad Bolivar, whereas the lowest values are those of Barrios Unidos, Chapinero and Teusaquillo. High values of the greater physical risk index, in addition to Candelaria, are the localities of Usaquén, Barrios Unidos and Teusaquillo, whereas the physical risk index is less in Ciudad Kennedy and Tunjuelito. The greater values of total risk index appear in the localities of Candelaria, Usaquen, Santafé and Barrios Unidos, and the smaller values are those of Ciudad Kennedy, Fontibón and Tunjuelito.

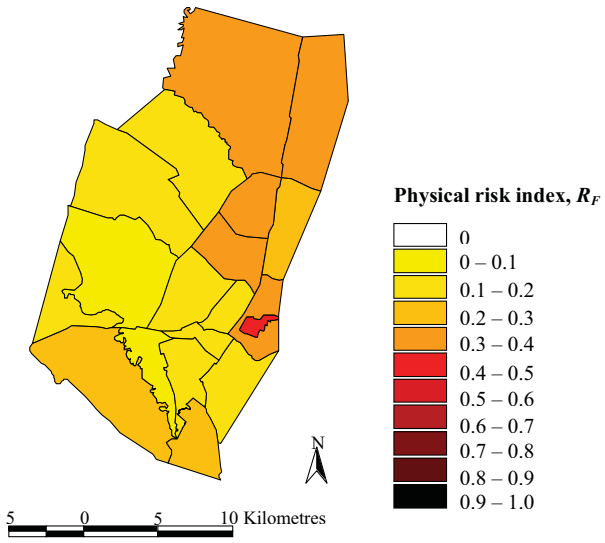

Figure 7: Physical risk index, R_F, for the localities of Bogotá

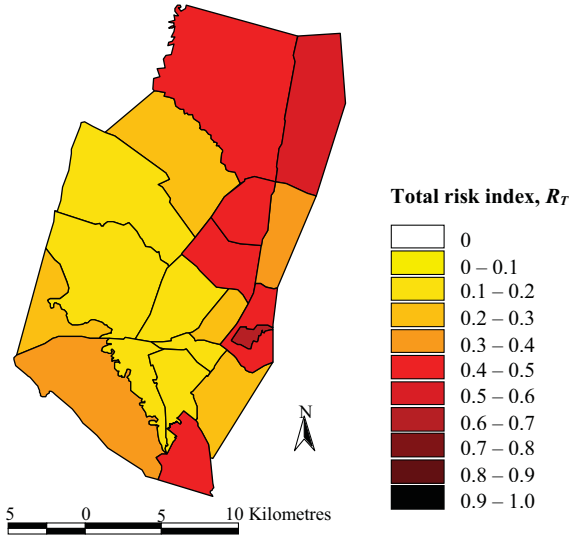

Figure 8: Total risk index, R_T, for the localities of Bogotá

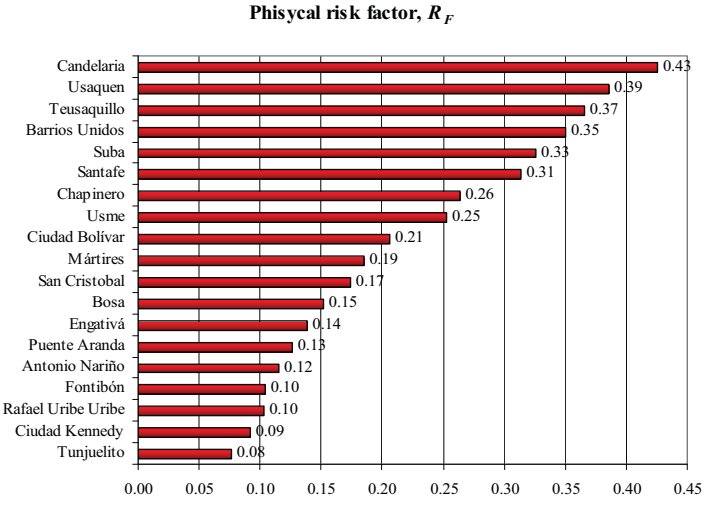

Figure 9: Physical risk index for the localities of Bogotá, in descendent order

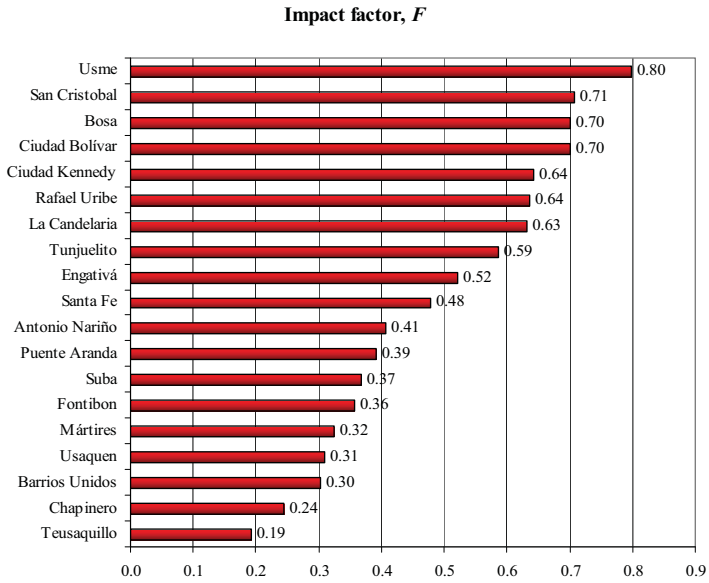

Figure 10: Impact factor for the localities of Bogotá, in descendent order

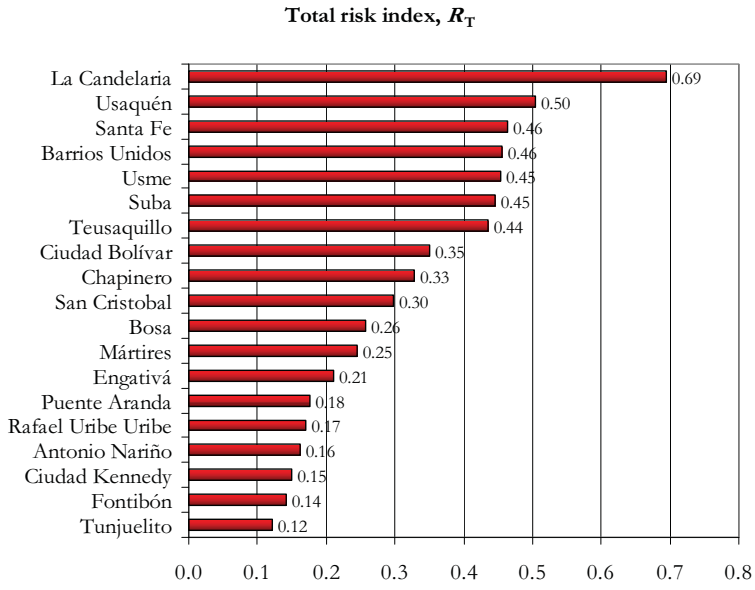

Figure 11: Total risk index for the localities of Bogotá, in descendent order

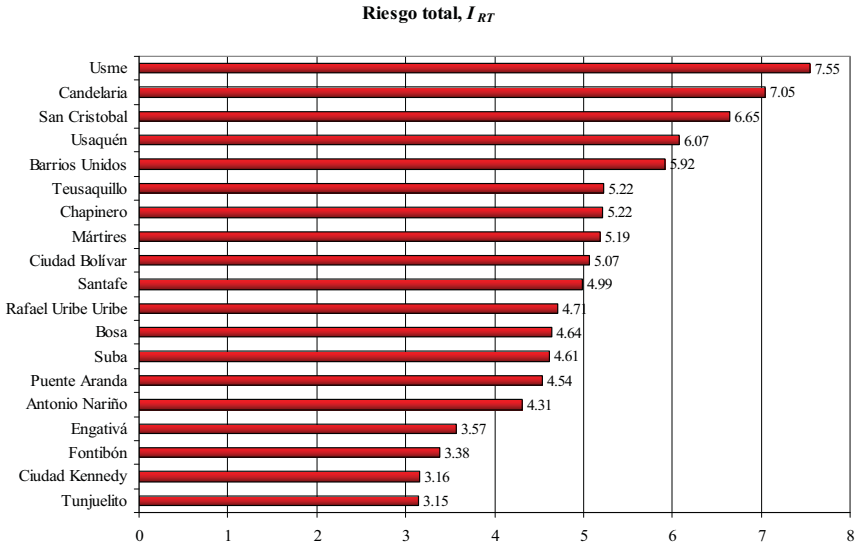

Figure 12: Total risk index for the localities of Bogotá, obtained with the Cardona's model

3. EXAMPLE OF APPLICATION: SEISMIC RISK OF BARCELONA

The city of Barcelona, Spain, is subdivided in ten districts (see Figure 13), which are directed by a Mayor. The districts have management competences in subjects like urbanism, public space, infrastructure maintenance, etc. They are: Ciutat Vella, Eixample, Sants-Montjuïc, Les Corts, Sarrià-Sant Gervasi, Gràcia, Horta-Guinardó, Nou Barris, Sant Andreu and Sant Martí. The districts are subdivided in 38 neighbourhoods or large statistical zones. Barcelona is also subdivided in 248 small statistical zones (ZRP). The physical risk index was calculated from a probabilistic risk scenario developed in the framework of the Risk-UE project [ICC/CIMNE, 2004]. This scenario was calculated considering the 248 small ZRP zones. The impact factor was calculated by district, due to the availability of data at this level only.

Figures 14 to 16 show the results for the physical risk index, the impact factor and the total risk index for Barcelona using the model proposed above. Details about the calculation can be seen in Carreño et al. (2005, 2006).

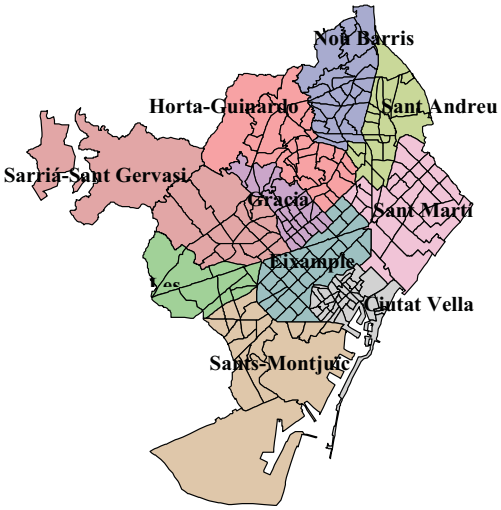

Figure 13: Territorial division of Barcelona

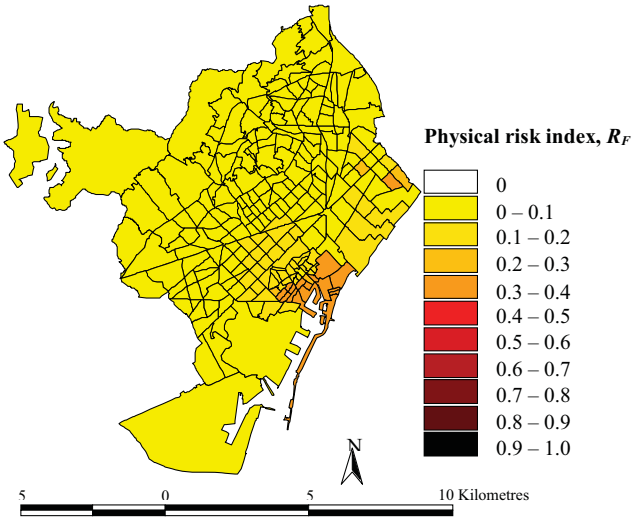

Figure 14: Physical risk index for Barcelona, using the 248 small statistical zones (ZRP)

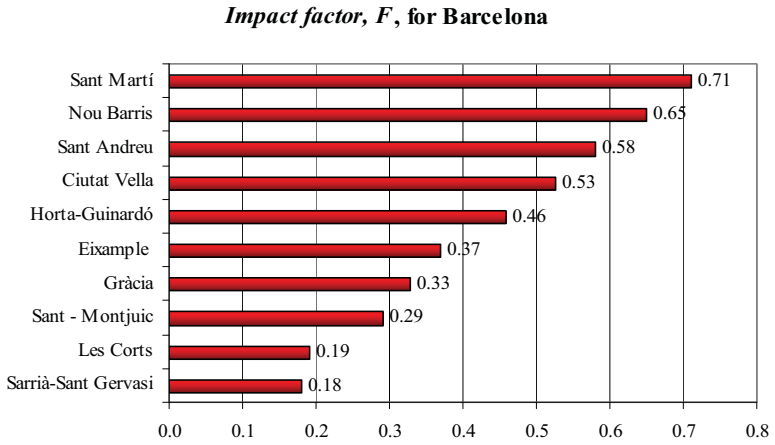

Figure 15: Impact factor for the districts of Barcelona

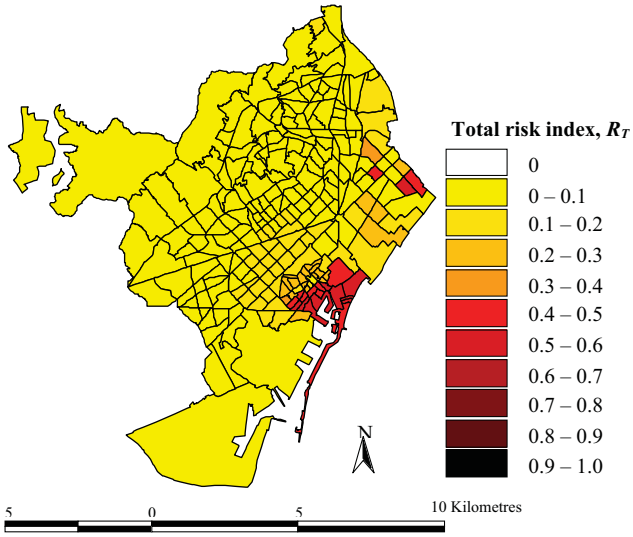

Figure 16: Total risk index for Barcelona, using the 248 small statistical zones (ZRP)

5. CONCLUSIONS

Risk estimation requires a multidisciplinary approach that takes into account not only the expected physical damage, the number and type of casualties or economic losses, but also other social, organizational and institutional factors related to the development of communities that contribute to the creation of risk. At the urban level, for example, vulnerability seen as an internal risk factor should be related not

only to the level of exposure or the physical susceptibility of the buildings and infrastructure material elements potentially affected, but also to the social fragility and the lack of resilience of the exposed community. The absence of institutional and community organization, weak preparedness for emergency response, political instability and the lack of economic health in a geographical area contribute to increased risk increasing. Therefore, the potential negative consequences are not only related to the impact of the hazardous event as such, but also to the capacity to absorb the impact and the control of its implications in a given geographical area.

For the modelling, a simplified but multidisciplinary representation of urban seismic risk has been suggested, based on the parametric use of variables that reflect aspects or factors of such risk. This parametric approach is not more than a model formulated in the most realistic possible form, to which corrections or alternative figures may be continuously introduced. The consideration of physical aspects allowed the construction of a physical risk index. Also, the contextual variables (social, economic, etc.) allowed the construction of an impact factor. The former is built from the information about the seismic scenarios of physical damage (direct effects) and the latter is the result from the estimation of aggravating conditions (indirect effects) based on descriptors and factors related to the social fragility and the lack of resilience of the exposed elements.

This new model for holistic evaluation of risk facilitates the integrated risk management by the different stakeholders involved on risk reduction decision-making. It permits the follow-up of the risk situation and the effectiveness and efficiency of the prevention and mitigation measures can be easily achieved. Results can be verified and the mitigation priorities can be established as regards the prevention and planning actions to modify those conditions having a greater influence on risk in the city. Once the results have been expressed in graphs for each locality or district, it is easy to identify the most relevant aspects of the total risk index, with no need for further analysis and interpretation of results. Finally, this method allows to compare risk among different cities around the world and to perform a multi-hazard risk analysis.

6. ACKNOWLEDGEMENTS

The authors express gratitude to the Inter-American Development Bank (IDB) for the financial support through the Information and Indicators Program for Disaster Risk Management for Latin America and the Caribbean (ATN/JF-7907-RG Operation) and to the Ministry of Education and Science of Spain, project "Desarrollo y aplicación de procedimientos avanzados para la evaluación de la vulnerabilidad y del riesgo sísmico de estructuras" – EVASIS – (REN2002-03365/RIES).

References

Barbat, A. H. and Cardona, O. D., Vulnerability and Disaster Risk Indices from Engineering Perspective and Holistic Approach to Consider Hard and Soft Variables at Urban Level, IDB/IDEA Program on Indicators for Disaster Risk Management, http://idea.unalmzl.edu.co, Universidad Nacional de Colombia, Manizales, 2003.

Cardona, O. D., Estimación Holística del Riesgo Sísmico utilizando Sistemas Dinámicos Complejos. Doctoral Thesis, Universidad Politécnica de Cataluña, Barcelona, Spain, 2001. (in Spanish)

Cardona, O. D. and Barbat, A. H., El Riesgo Sísmico y su Prevención, Calidad Siderúrgica, Madrid, Spain, 2000. (in Spanish)

Cardona, O.D. and Hurtado J.E., "Modelación Numérica para la Estimación Holística del Riesgo Sísmico Urbano, Considerando Variables Técnicas, Sociales y Económicas" 1er Congreso de Métodos Numéricos en Ciencias Sociales, CIMNE-UPC, Noviembre 2000, Barcelona, Spain, 2000. (in Spanish)

Carreño, M. L., Cardona, O. D. and Barbat, A., Sistema de indicadores para la evaluación de riesgos, Monografías de Ingeniería Sísmica, Editor A.H. Barbat, Monografía CIMNE IS-52, 2005. (in Spanish)

Carreño, M.L., Cardona, O.D. and Barbat A.H., Urban seismic risk evaluation: a holistic approach, Natural Hazards (in press), 2006.

Carreño, M.L., Cardona, O.D. and Barbat A.H., Seismic risk evaluation for an urban centre, 250th anniversary of the 1755 Lisbon earthquake, Lisboa, Portugal, 2005.

ICC/CIMNE, An Advanced Approach to Earthquake Risk Scenarios with Applications to Different European Towns, WP08 Application to Barcelona, RISK-UE Project. 2004.

Masure, P., Variables and indicators of vulnerability and disaster risk for land-use and urban or territorial planning, IDB/IDEA Program on Indicators for Disaster Risk Management, http://idea.unalmzl.edu.co Universidad Nacional de Colombia, Manizales, 2003.

Saaty, T. L., The Analytic Hierarchy process, McGraw-Hill Book Co., N.Y., 1980.

Saaty T. L., Decision making for leaders the analytic hierarchy process for decisions in a complex world, Pittsburgh RWS, USA., 2001.

UNDRO (1980), Natural Disasters and Vulnerability Analysis, Report of Experts Group Meeting, Geneva.

Universidad de Los Andes (1996), Microzonificación Sísmica de Santa Fe de Bogotá, Ingeominas, 17 volumenes, Bogotá, Colombia. (in Spanish)

"Computational Civil Engineering 2006", International Symposium
Iaşi, România, May 26, 2006

Nonlinear Analysis of Reinforced Concrete Frames

Jeovan Faleiro[1], Alex Barbat[1] and Sergio Oller[1]

[1] *Escuela Técnica Superior de Ingenieros de Caminos, Canales y Puertos, Techinical University of Catolonia, 08034, Barcelona Spain*

Summary

This paper develops an improved analytical model for predicting the damage response of multi-storey reinforced concrete frames modeled as an elastic beam-column with two inelastic hinges at its ends. The damage is evaluated in the hinges, using the concentrated damage concepts and a new member damage evaluation method for frame members, which leads to a meaningful global damage index of the structure. A numerical procedure for predicting the damage indexes of the structures using matrix structural analysis, plastic theory and continuum damage model is also developed. The method is adequate for the prediction of the failure mechanisms. Numerical examples are finally included

KEYWORDS: Damage estimation; Global damage; Plastic-damage model; Reinforced concrete frames.

1. INTRODUCTION

The constitutive models based on the Continuum Damage Mechanics and the development of the numerical techniques enables to retake existing structural models and improve their capacity of evaluating the global damage state of reinforced concrete building. Plastic theory can be used as mathematical framework to treat permanent strains. However, in particular geomaterials, such as concrete, permanent strains are caused by microcracking, what leads to permanent stiffness degradation. In those cases, the plasticity theory itself is not satisfactory to represent the stiffness degradation, and therefore it is necessary to use another tool, the Continuum Damage Mechanics.

Using the works of Kachanov (1958), Continuum Damage Mechanics became one of the most studied subjects in Solids Mechanics. The main idea is defining a new damage internal variable which describes the evolution of microcracks and microvoids and their influence on the behaviour of the material. This simple and general idea has been used for modelling, until the local fracture, most of the construction materials. Initially introduced for metals, the Continuum Damage Mechanics was later adapted to materials such as concrete (Oller 2001). Currently there are some models in which plasticity and damage are coupled (Simo and Ju

1987; Lucciomi et al. 1996). This approach has the advantage of allowing the development of constitutive independent laws which simulate materials in which the plastic deformation is not significant, as in the case of concrete, ceramic and ceramic composites.

Nowadays, Continuum Mechanics is still not the most suitable analysis framework for certain civil engineering structures, like framed structures which are usually modelled by means of bar elements, while continuum mechanics is used mostly in the case of finite elements models of the structure. Perhaps the main inconvenience in the use of finites elements consists in the fact that the most of the results obtained will be useless or of little practical utility for the structural designer. In this article we use the computational advantages of the matrix formulation for framed building structures, together with the complexity of the plastic-damage constitutive models.

Nonetheless, plasticity theory has been successfully adapted to frame analysis using the concept of lumped plasticity models, in which it is assumed that plastic effects can be concentrated at special locations called plastic hinges. This approach can be justified since in frame analysis the deformation is usually concentrated at or very near the end of the beams, and these are the only results of the frames analysis usually used by the structural designer.

Using the lumped plasticity model, Cipollina et al. (1995) and Flórez-López (1995) adapted the damage models to frame analysis in which the damage is concentrated on plastic hinges, the concentrated damage model. A value of the concentrated damage at the hinge equal to 1 reflects complete loss of strength while a value 0 means no damage. However, this method has the inconvenient that only refers to the damage at the hinge, and do not take into account the effect of cumulative plastic deformations under cyclic loading. Another inconvenient is that, once the concentrated damage index is located at the end of the frame member, is not possible to determine the real damage state of the member.

Based on method proposed by Hanganu et al. (2002), we will present one global damage evaluation method based on continuum mechanics principles in which the label “member damage” will be applied only to damage indices describing the state of frame member while the “global” damage indices will refers to state of whole structure. Both damage indices, member and global, presented herein are independently from the chosen constitutive models for the structural material.

This feature converts the proposed member and global damage indices into a powerful general tool for structural assessment. Moreover, it is applicable directly to both static and dynamic analysis and to estimate the damage produced by seismic actions in reinforced concrete building structures.

This paper will describe the procedure to use plastic-damage models in frame analysis, with application to reinforced concrete structures, in accordance with the

classic theories of Continuum Damage Mechanics and classic theories of plasticity. These theories will give support to the implementation of the member and global damage indices. What distinguishes this work from others is the fact the complete plastic-damage constitutive model, as well as the global damage, is here implemented into a frame analysis algorithm, which is briefly outlined. Finally, we will validate the method trough analysis of framed structures, as a single story bay frame structure, a simply supported reinforced concrete beam, and by a 2 story bay reinforced concrete frame structure.

2. BASIC DEFINITIONS

Let us consider a plane frame with b elements, connected into n nodes. The displacement of the structure is studied during a time interval $[0,T]$. At time $t=0$ the state of the structure is denoted as 'initial or undeformed configuration'. The configuration of the structure will be called 'deformed' for any $t>0$. As a reference, we will consider a couple of orthogonal coordinate axes X and Y to define the position of each node in any configuration. During the deformation of the structure, this coordinate system is assumed to be stationary.

Beams or columns extremities define the frame elements, where joints i and joint j indicate an element. Conventionally, the direction of each element is defined by the $i-j$ nodes. Each joint has three degrees of freedom. For example, the generalized nodal displacement in a node i s can be defined as $\{\mathbf{u}_i\}^T=\{q_1 \quad q_2 \quad q_3\}$, where q_1, q_2 and q_3 indicate the node displacement in the directions X and Y, and the node rotation with respect to the initial configuration, respectively. In this article $\{\bullet\}$ indicates a column matrix and $[\bullet]$ indicates a quadratic matrix.

For each element b, the generalized displacement vector for nodes $i-j$ can be defined as $\{\mathbf{q}_b\}^T=\{\mathbf{u}_i^T \quad \mathbf{u}_j^T\}=\{q_1 \quad q_3 \quad q_2 \quad q_4 \quad q_5 \quad q_6\}$ and the global displacement $\{\mathbf{U}\}$ of the structure is

$$\{\mathbf{U}\}^T=\{\mathbf{u}_1^T \quad \mathbf{u}_2^T \quad .... \quad \mathbf{u}_n^T\} \tag{1}$$

The generalized deformations $\{\mathbf{\Phi}_b\}$ of the beam b can be defined as

$$\{\mathbf{\Phi}_b\}^T=\{\phi_i \quad \phi_j \quad \delta\} \tag{2}$$

where ϕ_i and ϕ_j indicate rotations of the member at the ends i and j respectively and δ is its elongation.

The generalized deformations $\{\mathbf{\Phi}_b\}$ can be expressed in terms of the global displacement $\{\mathbf{U}\}$ by

$$\{\mathbf{\Phi}_b\} = [\mathbf{B}_b]\{\mathbf{U}\} \tag{3}$$

where $[\mathbf{B}_b]$ .is the global displacement transformation matrix.

The generalized "effective" stress vector of the frame element b is defined as

$$\{\mathbf{M}_b\}^{\mathrm{T}} = \{m_i \quad m_j \quad n\} \tag{4}$$

which contains the final forces of the member, where m_i and m_j are the moments at the ends of the member and n indicates the axial force. The internal force is the sum of all generalized effective stress $\{\mathbf{M}_b\}$

$$\{\mathbf{F}_{int}\} = \sum_{b=1}^{3n} [\mathbf{B}_b]^{\mathrm{T}} \{\mathbf{M}_b\} \tag{5}$$

The structure is subject to concentrated forces and moments only on the nodes, grouped into a vector $\{\mathbf{F}_{ext}\}$

$$\{\mathbf{F}_{ext}\}^{\mathrm{T}} = \{ \underbrace{f_1, f_2, f_3}_{\text{forces on node 1}} \quad ..... \quad \underbrace{f_{3n-2}, f_{3n-1}, f_{3n}}_{\text{forces on node } n} \} \tag{6}$$

Using now the expressions of the inertial and internal forces, the equation of quasi-static equilibrium of the nodes is expressed as:

$$\{\mathbf{F}_{ext}\} - \{\mathbf{F}_{int}\} = 0 \tag{7}$$

The relation between generalized stress and the history of deformations can be expressed as follows:

$$\{\mathbf{M}_b\} = [\mathbf{S}_b^e(\mathbf{\Phi}_b)]\{\mathbf{\Phi}_b\} \text{ or } \{\mathbf{\Phi}_b\} = [\mathbf{F}_b^e(\mathbf{M}_b)]\{\mathbf{M}_b\} \tag{8}$$

where $[\mathbf{S}_b^e(\mathbf{\Phi}_b)]$ and $[\mathbf{F}_b^e(\mathbf{M}_b)]$ indicate the local elastic stiffness and flexibility matrices, respectively. They are defined according to the deformed configuration of the member.

In the case of small deformations, the elastic stiffness and flexibility matrices remain constant. In this context, the equation (8) can be rewritten as

$$[\mathbf{M}_b] = [\mathbf{S}_b^e]\{\mathbf{\Phi}_b\} \text{ or } \{\mathbf{\Phi}_b\} = [\mathbf{F}_b^e]\{\mathbf{M}_b\} \tag{9}$$

with $[\mathbf{S}_b^e] = [\mathbf{F}_b^e]^{-1}$ being the stiffness elastic matrix.

Inserting equation (9) into (7) and expanding the expression as a function of displacements:

$$\underbrace{\left(\sum_{b=1}^{nelements} [\mathbf{B}_b]^{\mathrm{T}} : [\mathbf{S}_b] : [\mathbf{B}_b] \right)}_{Internal\ Force} : \{\mathbf{U}\} = \{\mathbf{F}_{ext}\} \tag{10}$$

$\sum [\mathbf{B}_b^{\mathrm{T}}] : [\mathbf{S}_b^e] : [\mathbf{B}_b] = [\mathbf{K}^e]$ is the global stiffness matrix.

3. CONCENTRATED PLASTICITY APPROACH FOR FRAME MEMBERS

For many reinforced concrete cross sectional shapes, the spread of plasticity starting from the ends of the members along the length is not very significant, and the deformation is concentrated at or very near the cross sections of the ends (Deierlein 2001). Therefore, we will assume that all the plasticity is concentrated at the end cross section. We also assume that the plastification of the end cross section is sudden, rather than gradual or fiber-by-fiber, and that the material behaves in a perfectly elastic plastic manner.

3.1 Lumped plasticity model

A constitutive equation can be obtained relating the generalized stress $\{\mathbf{M}_b\}$ with the generalized deformations $\{\mathbf{\Phi}_b\}$ by using the 'lumped dissipation model, considering plasticity, hardening or any other energy dissipation. Energy dissipation is assumed to be concentrated only at the hinges, while beam-column behaviour always remains elastic. With these concepts, we can express the member deformations as:

$$\{\mathbf{\Phi}_b\} = [\mathbf{F}_b^e] : \{\mathbf{M}_b\} + \{\mathbf{\Phi}_b^p\} \tag{11}$$

The term $[\mathbf{F}_b^e] : \{\mathbf{M}_b\} = \{\mathbf{\Phi}^e\}$ corresponds to the beam-column elastic deformations, while $\{\mathbf{\Phi}_b^p\}$ is called 'plastic hinge deformations':

$$\{\mathbf{\Phi}_b^p\}^{\mathrm{T}} = \{\phi_i^p \quad \phi_j^p \quad \delta^p\} \tag{12}$$

where ϕ_i^p and ϕ_j^p represent the plastic rotations of the member at the ends i and j respectively, and δ^p is its plastic elongation.

Using the generalized stress $\{\mathbf{M}_b\}$ from the equation (11), we will obtain:

$$\left\{\mathbf{M}_b\right\} = \left[\mathbf{S}_b^e\right] : \left(\left\{\mathbf{\Phi}_b\right\} - \left\{\mathbf{\Phi}_b^p\right\}\right) \tag{13}$$

Equation (13), assumes that plastic hinges produce when the load on structure increases, until the structure becomes unstable (or a mechanism) due to the development of various plastic hinges. Once a mechanism formed, the structure continues to deform until the final instability is detected by the singularity of the global stiffness matrix.

3.2 Internal variable evolution laws and plastic functions

For the internal variables defined in Equation(12), the plastic deformation evolution laws (Cipollina et al. 1995) is:

$$\begin{aligned} \dot{\phi}_i^p &= \dot{\lambda}_i^p \frac{\partial f_i}{\partial m_i} \quad \dot{\phi}_j^p = \dot{\lambda}_j^p \frac{\partial f_j}{\partial m_j} \\ \dot{\delta}^p &= \dot{\lambda}_i^p \frac{\partial f_i}{\partial n} + \dot{\lambda}_j^p \frac{\partial f_j}{\partial n} \end{aligned} \tag{14}$$

where $f_i \le 0$ and $f_j \le 0$ are the yield functions of hinges i and j, respectively. These functions depend on the generalized stress $\{\mathbf{M}_b\}$ and also depend on the internal variables and plastic multipliers $\dot{\lambda}_i^p$ and $\dot{\lambda}_j^p$. The plastic multipliers according to the Kuhn-Tucker conditions are:

$$\text{No plasticity} \begin{cases} \dot{\lambda}_i^p = 0 \text{ if } f_i < 0 \quad \text{or} \quad \lambda_i^p \dot{f}_i < 0 \\ \dot{\lambda}_j^p = 0 \text{ if } f_j < 0 \quad \text{or} \quad \lambda_j^p \dot{f}_j < 0 \end{cases} \tag{15}$$

$$\text{Plasticity increment} \begin{cases} \dot{\lambda}_i^p \neq 0 \text{ if } f_i = 0 \text{ and } \lambda_i^p \dot{f}_i = 0 \\ \dot{\lambda}_j^p \neq 0 \text{ if } f_j = 0 \text{ and } \lambda_j^p \dot{f}_j = 0 \end{cases} \tag{16}$$

To plastic multiplier strictly positive, we will consider that the plastic deformation is ‘active’; otherwise it will be called ‘passive’.

3.2.1 Plastic functions

The yield criterion or plastic function at any end is usually a function of the bending moment at the end cross section. Simple plastic functions for initial yield may be of the following type:

$$f_{\mathrm{i}}(m_i) = \left|m_i\right| - m_y \le 0 \qquad f_{\mathrm{j}}(m_j) = \left|m_j\right| - m_y \le 0 \tag{17}$$

where m_y is the yield moment or plastic moment..

For those cases where the influence of the force is considered, the yield function proposed by Argyris et al. (1982) is:

$$f_i(m_i) = \frac{|m_i|}{m_y} + \left(\frac{n}{n_y}\right)^2 - \alpha \le 0 \qquad f_j(m_j) = \frac{|m_j|}{m_y} + \left(\frac{n}{n_y}\right)^2 - \alpha \le 0 \qquad (18)$$

where n_y is the yield force limit (see Figure 1).

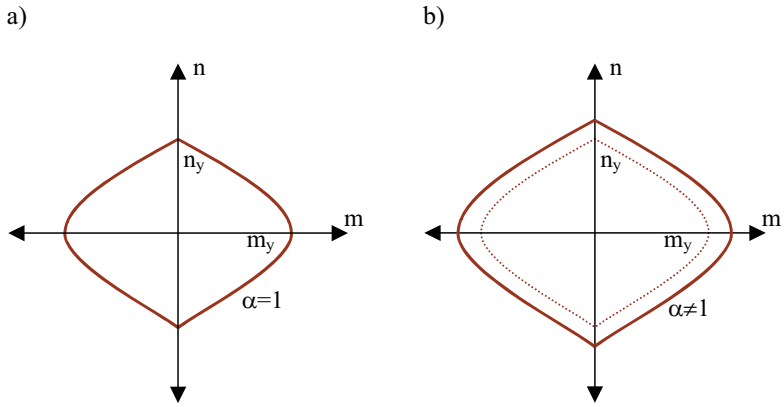

Figure 1 - Yield Surface in m-n space: a) without hardening, b) with hardening.

It is also possible to describe yield functions that take hardening or softening into account. For example, if we consider the hardening as functions of the plastic rotations of the member, Equation (17) can be rewritten as (Flórez-López 1999):

$$f_i(m_i) = \left|m_i - c\phi_i^p\right| - m_y \le 0 \qquad f_j(m_j) = \left|m_j - c\phi_j^p\right| - m_y \le 0 \qquad (19)$$

where c is a constant which indicates a material characteristic.

Despite the fact that the yield surface is the same for the hinges *i* and *j*, the plastic multipliers are independent of each other. This indicates the possibility that for the same element, one of the extremities is being plastified while the other extremity is not. However, the equilibrium at the nodes must be verified by equation (7), which requires the use of some interactive method, such as the Newton-Raphson method, in order to be solved.

4. CONTINUOUS DAMAGE MODEL

We will review some basic concepts of continuum mechanics necessary for the subsequent development of the concentrated damage concepts (Simo and Ju 1987).

Physically, degradation of the material properties is the result of the initiation, growth, and coalescence of microcracks or microvoids. Within the context of continuum mechanics, one may model this process by introducing an internal damage variable that can be a scalar or a tensorial quantity.

Let us consider $\mathbf{C}$, a fourth-order tensor, which characterizes the state of damage and transforms the homogenized tensor $\boldsymbol{\sigma}$ into the effective stress tensor $\overline{\boldsymbol{\sigma}}$ (or vice versa), clearly:

$$\overline{\boldsymbol{\sigma}} = \mathbf{C}^{-1} : \boldsymbol{\sigma} \tag{20}$$

For the isotropic damage case, the mechanical behaviour of microcracks or microvoids is independent of their orientation, and depends only on a scalar variable d. For that reason, $\mathbf{C}$ will simply reduce to $\mathbf{C} = (1-d)\mathbf{I}$, where $\mathbf{I}$ is the rank four-identity tensor, and equation (20) becomes:

$$\overline{\boldsymbol{\sigma}} = \frac{\boldsymbol{\sigma}}{(1-d)} \tag{21}$$

where d is the damage parameter, $\boldsymbol{\sigma}$ the Cauchy stress tensor and $\overline{\boldsymbol{\sigma}}$ is the effective stress tensor, both at time t. Here, $d \in (0,1]$ is a given constant.

The coefficient $1-d$ dividing the stress tensor in equation (21) is a *reduction factor* associated with the amount of damage in the material, initially introduced by Kachanov. The value $d = 0$ corresponds to the undamaged state, whereas a value $d = 1$ corresponds to a *damaged* state. The value $d = 1$ defines complete local rupture. Another possible interpretation is that physically the damage parameter d is the ratio of damage surface area over total (nominal) surface area at a local material point.

4.1 Flexibility matrix of damaged member

Considering the existence of variables, which represent the concentrated damage at the b frame element, which can be defined as (Flórez-López 1993; Faleiro 2004)

$$\{\mathbf{D}\}^T = \{d_i \quad d_j \quad d_a\} \tag{22}$$

where d_i and d_j are a measure of the bending concentrated damage of hinges i and j, respectively, and d_a indicates the measure of axial damage of the member.

These variables can take values between zero, no damage, and one, completely damaged. In the same way as the plasticity, we define that all bending concentrated damage parameters are concentrated at the nodes.

Now, supposing existence of a flexibility matrix of a damaged member $\{\mathbf{F}^d\}$, we have (Faleiro 2005)

$$\underbrace{\{\mathbf{\Phi}_b\} = [\mathbf{F}_b^d]\{\mathbf{M}_b\}}_{\begin{Bmatrix}\phi_i\\ \phi_j\end{Bmatrix}=\begin{bmatrix}f_{11} & f_{12}\\ f_{21} & f_{22}\end{bmatrix}\begin{Bmatrix}m_i\\ m_j\end{Bmatrix}} \tag{23}$$

$$[\mathbf{F}^d] = \frac{L}{6EI}\begin{bmatrix}\dfrac{2}{(1-d_i)} & -1\\ -1 & \dfrac{2}{(1-d_j)}\end{bmatrix} \tag{24}$$

$[\mathbf{F}^d]$ represents the flexibility matrix of a damaged member and its inverse is the stiffness matrix of a damaged member $[\mathbf{S}^d] = [\mathbf{F}^d]^{-1}$. If we also include the axial damage influence and redefine the stiffness matrix as a function of concentrated damage vector $\{\mathbf{D}_b\}$ for a element b, in small displacements, we have (Faleiro 2005)

$$\left[\mathbf{S}_b^d\left(\mathbf{D}_b\right)\right] = \mathrm{k}\begin{bmatrix}12(1-d_i) & 6(1-d_i)(1-d_j) & 0\\ 6(1-d_i)(1-d_j) & 12(1-d_j) & 0\\ 0 & 0 & \dfrac{EA(1-d_i)}{kL}\end{bmatrix} \tag{25}$$

$$k = \frac{1}{4-(1-d_i)(1-d_j)}\frac{EI}{L}$$

It can be observed that in the case where $\{\mathbf{D}_b\}$ is equal to zero, $[\mathbf{S}_b^d]$ reduces to the standard stiffness elastic matrix, $[\mathbf{S}_b^d\left(\mathbf{D}_b = \mathbf{0}\right)] \Rightarrow [\mathbf{S}_b^e]$. If one of the bending concentrated damage variables takes value equal to one, while the other bending concentrated damage and the axial damage are equal to zero, then $[\mathbf{S}_b^d\left(\mathbf{D}_b\right)]$ becomes the stiffness matrix of an elastic member with an internal hinge at the end, on the left or the right.

For the case where both bending concentrated damage variables acquire values equal to one, while the axial damage is equal to zero, we obtain the stiffness matrix of an elastic truss bar where only the axial force remains. Furthermore, the stiffness

matrix of a damaged member $[\mathbf{S}_b^d]$ obtained has the same shape as presented by Flórez-López (1999).

4.2 Damage evolution law

To apply the Continuum Damage Mechanics concepts to the frame analysis, it is necessary to adapt the theory as a function of the deformations at the hinges i and j, as well as the deformation due to the elongation δ. In addition, another necessary condition is that the variable evolutions should be independent of each other.

4.2.1 Free energy potential

Extending the free energy definition $\mathbf{\Psi} = \frac{1}{2}\boldsymbol{\varepsilon} : \mathbf{C} : \boldsymbol{\varepsilon}$ (Malvern, 16), and redefining its as a function of generalized elastic deformations $\{\mathbf{\Phi}_b^e\}$ of one b frame element and of it elastic stiffness matrix $[\mathbf{S}_b^e]$, we obtain the free energy potential as (Faleiro 2004)

$$\mathbf{\Psi}(\mathbf{\Phi}_b^e) = \mathbf{\Psi}_b^0 = \frac{1}{2}\{\mathbf{\Phi}_b^e\} : [\mathbf{S}_b^e] : \{\mathbf{\Phi}_b^e\} \tag{26}$$

By rewriting (26) in terms of the rotations ϕ_i and ϕ_j at the ends of the element, as well as the elongation δ, we obtain

$$\mathbf{\Psi}_b^0 = \frac{1}{2}\left(4\frac{EI}{L}\phi_i + 2\frac{EI}{L}\phi_j\right)\phi_i + \frac{1}{2}\left(4\frac{EI}{L}\phi_j + 2\frac{EI}{L}\phi_i\right)\phi_j + \frac{1}{2}\frac{\mathrm{EA}}{\mathrm{L}}\delta^2 \tag{27}$$

In equation (27) we may observe that the free energy potential is the sum of the energies obtained by the rotations at the i and j nodes plus the elongation δ, in such a way that the free energy potential can be redefined as (Faleiro 2004)

$$\mathbf{\Psi}_b^0 = \mathbf{\Psi}_i^0 + \mathbf{\Psi}_j^0 + \mathbf{\Psi}_\delta^0 \tag{28}$$

Where

$$\mathbf{\Psi}_i^0 = \frac{1}{2}\left(4\frac{EI}{L}\phi_i + 2\frac{EI}{L}\phi_j\right)\phi_i \tag{29}$$

$$\mathbf{\Psi}_j^0 = \frac{1}{2}\left(4\frac{EI}{L}\phi_j + 2\frac{EI}{L}\phi_i\right)\phi_j \tag{30}$$

And

$$\Psi_{\delta}^{0} = \frac{1}{2}\frac{EA}{L}\delta^{2} \ . \tag{31}$$

once, $m_i = 4\frac{EI}{L}\phi_i + 2\frac{EI}{L}\phi_j$, $m_j = 4\frac{EI}{L}\phi_j + 2\frac{EI}{L}\phi_i$, $n = \frac{EA}{L}\delta$, we can express Ψ_i^0, Ψ_j^0, and Ψ_{δ}^{0} in terms of the moments at the ends and m_j, and the axial force n as

$$\Psi_i^0 = \frac{1}{2} m_i \phi_i \tag{32}$$

$$\Psi_j^0 = \frac{1}{2} m_j \phi_j \tag{33}$$

$$\Psi_{\delta}^{0} = \frac{1}{2} n\delta \ . \tag{34}$$

4.2.2 Energy norm for undamaged structure and damage evolution

Now the undamaged energy norm vector τ^b is defined in the same way as the free energy; that is, as a function of the rotations ϕ_i and ϕ_j at the ends of the element and by the elongation δ, following the (Simo 12) similarity formulation (Faleiro 2004)

$$\begin{aligned}
\tau_i^b &= \sqrt{2\Psi_i^0} = \sqrt{\left(4\frac{EI}{L}\phi_i + 2\frac{EI}{L}\phi_j\right)\phi_i} \\
\tau_j^b &= \sqrt{2\Psi_j^0} = \sqrt{\left(4\frac{EI}{L}\phi_j + 2\frac{EI}{L}\phi_i\right)\phi_j} \\
\tau_{\delta}^{b} &= \sqrt{2\Psi_{\delta}^{0}} = \sqrt{\frac{EA}{L}\delta^{2}}
\end{aligned} \tag{35}$$

We then characterize the state of damage in the frame element by the means of a damage criterion, with the following functional form

$$\begin{aligned}
g_i\left(\tau_i^b, r_i^b\right)_t &= \left(\tau_i^b\right)_t - \left(r_i^b\right)_t \le 0 \\
g_j\left(\tau_j^b, r_j^b\right)_t &= \left(\tau_j^b\right)_t - \left(r_j^b\right)_t \le 0 \\
g_{\delta}\left(\tau_{\delta}^{b}, r_{\delta}^{b}\right)_t &= \left(\tau_{\delta}^{b}\right)_t - \left(r_{\delta}^{b}\right)_t \le 0
\end{aligned} \tag{36}$$

Here, the subscript *t* refers to value at current time $t \in \mathbb{R}_+$, r_i^b, r_j^b and r_{δ}^{b} are the damage threshold at current time for the rotations ϕ_i and ϕ_j and the elongation

δ, respectively. We can consider the existence of one vector r_0, for $t=0$, which denotes the initial damage threshold before any loading is applied, defined as

$$\left\{r_0^b\right\}=\sqrt{\left\{\mathbf{M}_y\right\}:\left[\mathbf{S}_b\right]^{-1}:\left\{\mathbf{M}_y\right\}}=\begin{bmatrix}\left(r_i^b\right)_0\\ \left(r_j^b\right)_0\\ \left(r_\delta^b\right)_0\end{bmatrix}\Rightarrow\begin{cases}\left(r_i^b\right)_0=\left(r_j^b\right)_0=\sqrt{\dfrac{L}{3EI}}{m_y}^2\\ \left(r_\delta^b\right)_0=\sqrt{\dfrac{L}{EA}}{n_y}^2\end{cases} \tag{37}$$

where m_y and n_y are the bending moment and axial force limits. The vector r_0 can be considered as a property characteristic of the element, in way that we must have $r_t^b \geq r_0^b$.

Condition (equation (36)) states that damage in the element is initiated when the *energy norm* vector τ^b exceeds the initial damage threshold r_0. For the isotropic case, we define the evolution of the damage variables by

$$\dot{\mathbf{D}}_t^b=\dot{\lambda}^d H(\tau_t^b,\mathbf{D}_t^b)=\begin{cases}\dot{d}_i=\dot{\lambda}_i^d\left(\left(\tau_i^b\right)_t,d_i\right)\\ \dot{d}_j=\dot{\lambda}_j^d\left(\left(\tau_j^b\right)_t,d_j\right)\\ \dot{d}_a=\dot{\lambda}_\delta^d H\left(\left(\tau_\delta^b\right)_t,d_a\right)\end{cases};\ \dot{r}_t^b=\dot{\lambda}^d=\begin{cases}\left(\dot{r}_i^b\right)_t=\dot{\lambda}_i^d\\ \left(\dot{r}_j^b\right)_t=\dot{\lambda}_j^d\\ \left(\dot{r}_\delta^b\right)_t=\dot{\lambda}_\delta^d\end{cases} \tag{38}$$

where $\dot{\lambda}_i^d \geq 0$, $\dot{\lambda}_j^d \geq 0$ and $\dot{\lambda}_\delta^d \geq 0$ are *damage consistency* parameters that define damage loading/unloading conditions according to the Kuhn-Tucker relations

$$\begin{aligned}&\dot{\lambda}_i^d \geq 0;\quad g_i\left(\left(\tau_i^b\right)_t,\left(r_i^b\right)_t\right)\leq 0;\quad \dot{\lambda}_i^d g_i=0\\ &\dot{\lambda}_j^d \geq 0;\quad g_j\left(\left(\tau_j^b\right)_t,\left(r_j^b\right)_t\right)\leq 0;\quad \dot{\lambda}_j^d g_j=0\\ &\dot{\lambda}_\delta^d \geq 0;\quad g_\delta\left(\left(\tau_\delta^b\right)_t,\left(r_\delta^b\right)_t\right)\leq 0;\quad \dot{\lambda}_\delta^d g_\delta=0\end{aligned} \tag{39}$$

Let us now analyze the concentrated damage evolution at hinge i. Conditions (39) are standard for problems involving unilateral constraint. If $g_i<0$, the damage criterion is not satisfied, and by condition $(39)_3$, $\dot{\lambda}_i=0$, hence, the damage rule (38) implies that $\dot{d}_i=0$ and no further damage occurs. If, on the other hand, $\dot{\lambda}_i^d>0$, further damage (loading) is taking place, condition $(39)_3$ now implies that $g_i=0$. In this event the value of $\dot{\lambda}_i$ can be determined by the damage consistency condition, i.e.

$$g_i\left(\left(\tau_i^b\right)_t,\left(r_i^b\right)_t\right)=\dot{g}_i\left(\left(\dot{\tau}_i^b\right)_t,\left(r_i^b\right)_t\right)=0\Rightarrow\dot{\lambda}_i^d=\left(\dot{\tau}_i^b\right)_t \tag{40}$$

Finally, $\left(r_i^b\right)_t$ can be given by the expression

$$\left(r_i^b\right)_t = \max\left\{\left(r_i^b\right)_0, \max_{s\in(0,t)}\left(\tau_i^b\right)_s\right\} \tag{41}$$

By applying to the other parameters, we obtain

$$r_t^b = \max\left\{r_0^b, \max_{s\in(0,t)}\left(\tau_\Phi^b\right)_s\right\} = \begin{cases} \max\left\{\left(r_i^b\right)_0, \max_{s\in(0,t)}\left(\tau_i^b\right)_s\right\} \\ \max\left\{\left(r_j^b\right)_0, \max_{s\in(0,t)}\left(\tau_j^b\right)_s\right\} \\ \max\left\{\left(r_\delta^b\right)_0, \max_{s\in(0,t)}\left(\tau_\delta^b\right)_s\right\} \end{cases} \tag{42}$$

If now we consider that $H(\tau_t^b, \mathbf{D}_t^b)$ in condition (38) is independent of the vector $\{\mathbf{D}_t^b\}$ and assuming that the existence of one function monotonic G, such that $H(\tau_t^b) = \partial G(\tau_t^b)/\partial(\tau_t^b)$, the damage criterion defined in (36) can now be rewritten in relation as a function of G, i.e. at hinge i, by $g_i\left(\tau_i^b, r_i^b\right)_t = G\left(\tau_i^b\right)_t - G\left(r_i^b\right)_t \le 0$. In this way, the flow rule (38) and loading/unloading conditions (39) become

$$\left\{\dot{\mathbf{D}}_t^b\right\} = \dot{\lambda}^d \frac{\partial G(\tau_t^b, r_t^b)}{\partial \tau_t^b} = \begin{cases} \dot{d}_i = \dot{\lambda}_i^d \dfrac{\partial G\left(\left(\tau_i^b\right)_t, \left(r_i^b\right)_t\right)}{\partial\left(\tau_i^b\right)_t} \\ \dot{d}_j = \dot{\lambda}_j^d \dfrac{\partial G\left(\left(\tau_j^b\right)_t, \left(r_j^b\right)_t\right)}{\partial\left(\tau_j^b\right)_t} \\ \dot{d}_a = \dot{\lambda}_\delta^d \dfrac{\partial G\left(\left(\tau_\delta^b\right)_t, \left(r_\delta^b\right)_t\right)}{\partial\left(\tau_\delta^b\right)_t} \end{cases} \quad ; \quad \dot{r}_t^b = \dot{\lambda}^d = \begin{cases} \left(\dot{r}_i^b\right)_t = \dot{\lambda}_i^d \\ \left(\dot{r}_j^b\right)_t = \dot{\lambda}_j^d \\ \left(\dot{r}_\delta^b\right)_t = \dot{\lambda}_\delta^d \end{cases} \tag{43}$$

$$\begin{aligned} &\dot{\lambda}_i^d \ge 0; \quad g_i\left(\left(\tau_i^b\right)_t, \left(r_i^b\right)_t\right) \le 0; \quad \dot{\lambda}_i^d g_i = 0 \\ &\dot{\lambda}_j^d \ge 0; \quad g_j\left(\left(\tau_j^b\right)_t, \left(r_j^b\right)_t\right) \le 0; \quad \dot{\lambda}_j^d g_j = 0 \\ &\dot{\lambda}_\delta^d \ge 0; \quad g_\delta\left(\left(\tau_\delta^b\right)_t, \left(r_\delta^b\right)_t\right) \le 0; \quad \dot{\lambda}_\delta^d g_\delta = 0 \end{aligned} \tag{44}$$

Carrying through the integration in the time of the rate concentrated damage vector, the result is an expression that indicates the evolution of the damage variables as

$$\left\{\mathbf{D}_t^b\right\} = G\left(\tau_t^b\right) = \begin{cases} d_i = G\left(\left(\tau_i^b\right)_t\right) \\ d_j = G\left(\left(\tau_j^b\right)_t\right) \\ d_a = G\left(\left(\tau_\delta^b\right)_t\right) \end{cases} \tag{45}$$

The function G can be defined in relation with of the type of analysis. In our work, one expression used was the exponential softening proposed by Oller (2001)

$$G\left(\left(\tau_k^b\right)_t\right) = 1 - \frac{\left(\tau_k^b\right)_t}{\left(r_k^b\right)_0} e^{A\left(1-\frac{\left(r_k^b\right)_0}{\left(\tau_k^b\right)_t}\right)}; A = \frac{1}{\frac{g_f}{\left(r_k^b\right)_0^2} - \frac{1}{2}}; k \in \left(i, j, \delta\right); \tag{46}$$

where the parameter g_f represents the fracture energy of the material, parameter derived from fracture mechanics as $g_f = G_f / l_c$, where G_f is the fracture energy and l_c can be defined as the characteristic length of the fractured member (Oller 2001) or alternatively as $l_c = \sqrt{A}$ where A is the element section area (Salamy et al. 2005).

5. PLASTIC-DAMAGE MODEL FOR REINFORCED CONCRETE FRAMES

Elastic damage or elastic plastic laws are not sufficient to represent the constitutive behaviour of reinforced concrete. In some damage models, during the loading/unloading process, a zero stress corresponds to a zero strain and the value of the damage is thus overestimated (Figure 2b).

An elastic plastic relation is not valid either, even with softening, (Figure 2a), as the unloading curve follows the elastic slope. A correct plastic-damage model should be capable of representing the softening behaviour; the damage law reproduces the decreasing of the elastic modulus, while the plasticity effect accounts for the irreversible strains (Figure 2c). There are three ways to represent this behaviour (Luccioni 2003):

One of these ways, based on a plastic-damage coupled model, evaluates the damage and the plastic behaviours at the same time. The free energy can be expressed as the sum of elastic energy with the plastic energy, both of them influenced by the damage parameter

$$\mathbf{\Psi} = \mathbf{\Psi}_e(\varepsilon, d) + \mathbf{\Psi}_p(\lambda^p, d) \tag{47}$$

Another option to assume the free energy to be the sum of the elastic energy with the plastic energy and one term dependent of the damage. The result is that the dissipation energy is influenced by the damage parameter as the plasticity parameter

$$\boldsymbol{\Psi} = \boldsymbol{\Psi}_e(\varepsilon, d) + \boldsymbol{\Psi}_p(\lambda^p) + \boldsymbol{\Psi}_d(\lambda^d) \tag{48}$$

$$\boldsymbol{\Xi}_d = \boldsymbol{\Psi}\dot{d} - \lambda^p \lambda^d \tag{49}$$

The last option is to consider that damage and plasticity are uncoupled following their own laws independently; this way can be used when there are permanent deformations.

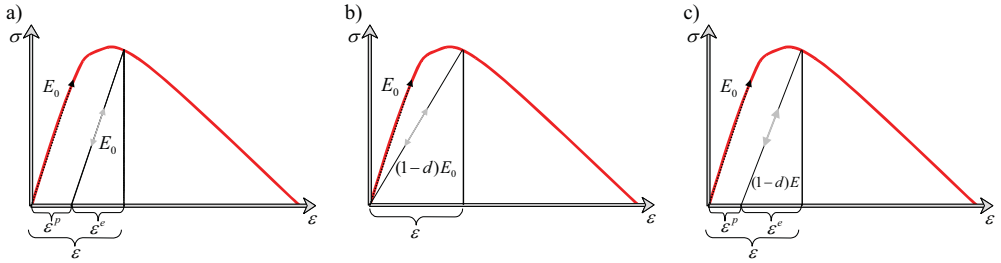

Figure 2 - Loading-unloading behaviour: simulated behaviours and experimental behaviour

5.1 Plastic-damage model

5.1.1 Thermodynamic references

As commented before, in the concrete of reinforced concrete elements, the damage effect modifies the constitutive plastic equation for small deformations by the degradation of the stiffness. New constitutive equation is formulated without time variation of temperature for thermodynamically stable problems, using the following mathematical formulation for the free energy constituted by elastic and plastic terms (Oller 2001, Faleiro et al. 2004)

$$\boldsymbol{\Psi}\left(\boldsymbol{\Phi}^e, \mathbf{D}, q^p, q^d\right) = \boldsymbol{\Psi}^e\left(\boldsymbol{\Phi}^e, \mathbf{D}, q^d\right) + \boldsymbol{\Psi}^p\left(q^p\right) \tag{50}$$

where $\boldsymbol{\Psi}^p$ is a plastic potential function and $\boldsymbol{\Psi}^e\left(\boldsymbol{\Phi}^e, \mathbf{D}, q^d\right)$ is the initial elastic stored energy. Additionally, q^p and q^d indicate the suitable set of internal (plastic and damage, respectively) variables and the elastic deformations $\{\boldsymbol{\Phi}^e\}$ is the free variable in the process.

For stable thermical state problems, the Clausius-Duhem dissipation inequality is valid and takes the form

$$\dot{\Xi} = \{\mathbf{M}\} : \{\dot{\mathbf{\Phi}}^e\} - \dot{\mathbf{\Psi}} \geq 0 \tag{51}$$

This inequality is valid for any loading-unloading stage. Taking the time derivative of equation (50) and substituting into (51) the following equation is obtained for dissipation

$$\dot{\Xi} = \left[\{\mathbf{M}\} - \frac{\partial \mathbf{\Psi}}{\partial \mathbf{\Phi}^e} \right] : \{\dot{\mathbf{\Phi}}\} + \frac{\partial \mathbf{\Psi}}{\partial \mathbf{\Phi}^e} : \{\dot{\mathbf{\Phi}}^p\} - \frac{\partial \mathbf{\Psi}}{\partial q^d} \dot{q}^d - \frac{\partial \mathbf{\Psi}}{\partial q^p} \dot{q}^p \geq 0 \tag{52}$$

In order to guarantee the unconditional fulfilment of the Clausius-Duhem inequality, the multiplier of $\{\dot{\mathbf{\Phi}}\}$ representing an arbitrary temporal variation of the free variable must be null. This condition provides the constitutive law of the damage problem

$$\left[\{\mathbf{M}\} - \frac{\partial \mathbf{\Psi}}{\partial \mathbf{\Phi}^e} \right] \geq 0 \qquad \forall \{\dot{\mathbf{\Phi}}\} \tag{53}$$

from where the final generalized stress of member can be defined as

$$\{\mathbf{M}_b\} = \frac{\partial \mathbf{\Psi}_b}{\partial \mathbf{\Phi}_b^e} \tag{54}$$

Once imposed the condition $\{\mathbf{\Phi}_b^e\} = \{\mathbf{\Phi}_b\} - \{\mathbf{\Phi}_b^p\}$, the free energy for an elastic-plastic frame element with stiffness degradation can be written for small deformations as

$$\mathbf{\Psi}_b \left(\mathbf{\Phi}_b^e, \mathbf{D}_b, q^p, q^d \right) = \frac{1}{2} \left(\{\mathbf{\Phi}_b\} - \{\mathbf{\Phi}_b^p\} \right) : \left[\mathbf{S}_b^d \left(\mathbf{D}_b \right) \right] : \left(\{\mathbf{\Phi}_b\} - \{\mathbf{\Phi}_b^p\} \right) + \mathbf{\Psi}_b^p \left(q^p \right) \tag{55}$$

where the stiffness matrix of the damaged member $\mathbf{S}_b^d \left(\mathbf{D}_b \right)$ is the same matrix defined in (25). By replacing this last equation in (54) one arrives at the expression for plastic-damage analysis (Cipollina et al. 1995, Flórez-López 1995, Faleiro et al. 2004)

$$\{\mathbf{M}_b\} = \left[\mathbf{S}_b^d \left(\mathbf{D}_b \right) \right] : \left(\{\mathbf{\Phi}_b\} - \{\mathbf{\Phi}_b^p\} \right) \tag{56}$$

6. MEMBER AND GLOBAL DAMAGE INDICES

6.1 Member damage index

The idea for the member damage index definition stemmed from a macroscale analogy with the continuous damage model definition. Thus, the starting point for deducing the member damage index is by the assumptions that we can express the free energy $\mathbf{\Psi}_b$ of a member with the non-damaged free energy $\mathbf{\Psi}_b^0$, defined in equation (31), as:

$$\mathbf{\Psi}_b = (1 - D_b^M)\mathbf{\Psi}_b^0 \tag{57}$$

where D_b^M is the member damage index. The free energy $\mathbf{\Psi}_b$ of a member can be defined in terms of the concentrated damage vector $\{\mathbf{D}_b\}$ as

$$\mathbf{\Psi}_b\left(\mathbf{D}_b\right) = \frac{1}{2}\{\mathbf{\Phi}_b\} : \left[\mathbf{S}_b^d\left(\mathbf{D}_b\right)\right] : \{\mathbf{\Phi}_b\} \tag{58}$$

considering

$$\left[\mathbf{S}_b^d\left(\mathbf{D}_b\right)\right] : \{\mathbf{\Phi}_b\} \cong \begin{Bmatrix} (1-d_i)m_i \\ (1-d_i)m_i \\ (1-d_i)m_i \end{Bmatrix} \tag{59}$$

and using (34) and (59), equation (58) can be rewritten as

$$\mathbf{\Psi}_b\left(\mathbf{D}_b\right) = (1-d_i)\mathbf{\Psi}_i^0 + (1-d_j)\mathbf{\Psi}_j^0 + (1-d_a)\mathbf{\Psi}_\delta^0 \tag{60}$$

Solving (57) for D_b^M, we obtain

$$D_b^M = 1 - \frac{\mathbf{\Psi}_b\left(\mathbf{D}_b\right)}{\mathbf{\Psi}_b^0} = 1 - \frac{(1-d_i)\mathbf{\Psi}_i^0 + (1-d_j)\mathbf{\Psi}_j^0 + (1-d_a)\mathbf{\Psi}_\delta^0}{\mathbf{\Psi}_i^0 + \mathbf{\Psi}_j^0 + \mathbf{\Psi}_\delta^0} \tag{61}$$

$$D_b^M = \frac{d_i\mathbf{\Psi}_i^0 + d_j\mathbf{\Psi}_j^0 + d_a\mathbf{\Psi}_\delta^0}{\mathbf{\Psi}_i^0 + \mathbf{\Psi}_j^0 + \mathbf{\Psi}_\delta^0} \tag{62}$$

which is the expression for member damage index for a frame member.

6.2 Global damage index

The global damage index can be defined as the sum of all free energy $\mathbf{\Psi}_b$ of a structure divided by the sum of the non-damaged free energy $\mathbf{\Psi}_b^0$

$$D_G = 1 - \frac{\sum_{b=1}^{3n} \Psi_b(\mathbf{D}_b)}{\sum_{b=1}^{3n} \Psi_b^0} = 1 - \frac{\sum_{b=1}^{3n} \{\Phi_b\} : \left[\mathbf{S}_b^d(\mathbf{D}_b)\right] : \{\Phi_b\}}{\sum_{b=1}^{3n} \{\Phi_b\} : [\mathbf{S}_b^e] : \{\Phi_b\}} \tag{63}$$

where D_G is the global damage index. Replacing $[\mathbf{S}_b^e]\{\Phi_b\} = \{\bar{\mathbf{M}}_b\}$, as well as $[\mathbf{S}_b^d(\mathbf{D}_b)]\{\Phi_b\} = \{\mathbf{M}_b\}$, and assuming that $\{\Phi_b\}^{\mathrm{T}} = \{\mathbf{U}\}^{\mathrm{T}}[\mathbf{B}_b]$, equation (63) becomes

$$D_G = 1 - \frac{\sum_{b=1}^{3n} \{\Phi_b\} : \left[\mathbf{S}_b^d(\mathbf{D}_b)\right] : \{\Phi_b\}}{\sum_{b=1}^{3n} \{\Phi_b\} : [\mathbf{S}_b^e] : \{\Phi_b\}} = 1 - \frac{\{\mathbf{U}\}^{\mathrm{T}} \sum_{b=1}^{3n} [\mathbf{B}_b]^{\mathrm{T}} \{\mathbf{M}_b\}}{\{\mathbf{U}\}^{\mathrm{T}} \sum_{b=1}^{3n} [\mathbf{B}_b]^{\mathrm{T}} \{\bar{\mathbf{M}}_b\}} \tag{64}$$

$$D_G = 1 - \frac{\{\mathbf{U}\}^{\mathrm{T}} \{\mathbf{F}_{int}^D\}}{\{\mathbf{U}\}^{\mathrm{T}} \{\mathbf{F}_{int}\}} \tag{65}$$

where $\{\mathbf{F}_{int}\}$ is the linear internal forces vector should the material preserve its original characteristics and undergo the actual deformation, and $\{\mathbf{F}_{int}^D\}$ is the nonlinear internal forces vector in the actual deformation. This global damage index is similar to that proposed by Hanganu et al. (2002) and Barbat et al. (1998) for finite element analysis.

The global damage index, as well as member damage index, is basically tools for assessing the state of a structure. However, unlike the member damage index, which refers only to the damaged state of a member, the global damage index gives a measure of the structural stiffness loss, since the nonlinear internal forces $\{\mathbf{F}_{int}^D\}$ can be influenced not only by the damage but also by the plasticity.

7. NUMERICAL IMPLEMENTATION OF THE PLASTIC-DAMAGE MODEL

The most important results obtained by using the proposed model are: Deformations $\{\mathbf{\Phi}\}$, stresses $\{\mathbf{M}\}$, internal forces $\{\mathbf{F}_{int}\}$, plastic deformations $\{\mathbf{\Phi}^p\}$ or/and concentrated damage vector $\{\mathbf{D}\}$ the member damage index and global damage index and, if necessary, the remaining internal variables and their associated forces for each member of the structure.

These results are obtained by using the equilibrium equations (7) (quasi-static problems) together with the state law (56) in accordance with the internal variables evolution laws (16), and (44).

Table 1 shows the implicit Newmark time integration scheme used for quasi-static problems.

Table 1 - Nonlinear time integration scheme (Newmark)

A. First iteration (passage from time instant t to time instant $t+1$)
Update relevant matrices in the time t+1

$$\left[\mathbf{K}_t^{(1)}\right] = \sum_{b=1}^{nelements} \left[\mathbf{B}_b^T\right] : \left[\mathbf{S}_b^d\left(\mathbf{D}_b^{t-1}\right)\right] : \left[\mathbf{B}_b\right]$$

Compute:

$$\left\{\hat{\mathbf{F}}_{t+1}^{(1)}\right\} = \left\{\mathbf{F}_{ext}\right\} - \left[\mathbf{K}_t^{(1)}\right]\left\{\mathbf{U}_{t-1}\right\}\ ;\ \left\{\mathbf{D}\right\}_t^{(1)} = \left\{\mathbf{D}\right\}_{t-1} \quad ;\quad \left\{\mathbf{\Phi}^p\right\}_t^{(1)} = \left\{\mathbf{\Phi}^p\right\}_{t-1}$$

B. Loop over global convergence iterations: nth iteration
1.Calculate the first approximations for the iteration n:

$$\left[\mathbf{J}\right] = -\left|\frac{\partial \hat{\mathbf{F}}_t^{(n)}}{\partial \mathbf{U}_t^{(n)}}\right|\ ;\ \left\{\Delta\mathbf{u}_{t+1}^{(n)}\right\} = \left[\mathbf{J}\right]^{-1}\left\{\hat{\mathbf{F}}_t^{(n)}\right\}\ ;\ \left\{\mathbf{U}_t^{(n)}\right\} = \left\{\mathbf{U}_t^{(n-1)}\right\} + \left\{\Delta\mathbf{u}_t^{(n)}\right\}$$

2. Compute the member stresses and internal variables:

$$\left\{\mathbf{\Phi}_b\right\}_t^n = \left[\mathbf{B}_b\right]\left\{\mathbf{U}_t^n\right\}\ ;\ \left\{\mathbf{M}_b\right\}_t^n = \left[\mathbf{S}_b\left(\mathbf{D}_b\right)_t^n\right] : \left(\left\{\mathbf{\Phi}_b\right\}_t^n - \left\{\mathbf{\Phi}_b^p\right\}_t^n\right)$$

3.Updates relevant matrices

$$\left\{\mathbf{F}_{int}^D\right\}_t^{(n)} = \sum_{b=1}^{nelements} \left[\mathbf{B}_b^T\right] : \left\{\mathbf{M}_b\right\}_t^n \quad ;\ \left\{\hat{\mathbf{F}}_t^{(n)}\right\} = \left\{\mathbf{F}_{ext}\right\} - \left\{\mathbf{F}_{int}^D\right\}_t^{(n)}$$

3. If the residual forces norm $\left\|\hat{\mathbf{F}}_t^{(n)}\right\| / \left\|\mathbf{F}_{ext}(t)\right\| \le TOL$, end of iterations and beginning of the computations in the next time step. If not, back to step 1 and proceed calculating.

Let us now focus our attention on the calculation of the member stresses and of the internal variables (Table 1.B.2).

The plastic and damage parameters can be calculated separately, as explained in Section 5. This assumption comes from the observation that damage is linked with the concrete, while plastification is related with the steel.

Therefore, the damage and the plastic evolution can be determined by the equations (35)-(45) for damage and equation (14)- for the plastic behaviour. Table 2 shows the procedure for determining the parameters.

Table 2 - Procedure to the determinations of the damage and plastic parameters.

I. For each b elements at nth iteration:

1. Generalized deformations at the step: $\left\{\boldsymbol{\Phi}_b\right\}_t^{(n)} = \left[\mathbf{B}_b\right] : \left\{\mathbf{U}\right\}_t^{(n)}$

2. Verification of the evolution of the damage:

i. Update of the internal variables: $\left\{\mathbf{D}_b\right\}_t^{(n)} = \left\{\mathbf{D}_b\right\}_t^{(n-1)} \quad ; \quad \left\{\mathbf{r}_b\right\}_t^{(n)} = \left\{\mathbf{r}_b\right\}_t^{(n-1)}$

ii. Determination of the undamaged energy norm vector: $\boldsymbol{\tau}_\Phi^b = \sqrt{\left\{\boldsymbol{\Phi}_b\right\}_t^{(n)} : \mathbf{S}_b : \left\{\boldsymbol{\Phi}_b\right\}_t^{(n)}}$

iii. Verification of the evolution of the damage:

If $g\left(\tau_\Phi^b, \left(\mathbf{r}_b\right)_t^{(n)}\right) \le 0$ No damage evolution →3.

iv. Update of damage variable: $\left\{\mathbf{D}_b\right\}_t^{(n)} = G\left(\tau_\Phi^b\right)$

v. Update of damage threshold: $\left\{\mathbf{r}_b\right\}_t^{(n)} = \left\{\boldsymbol{\tau}_\Phi^b\right\}$

3. Verification of the evolution of the plastic variable:

i. Determination of generalized effective 'trial' stress and update of internal variables:

$\left\{\Delta\boldsymbol{\Phi}_b^p\right\}_0 = \left\{\boldsymbol{\Phi}_b^p\right\}_t^{(n-1)} \quad ; \quad \left\{\Delta q^p\right\}_0 = \left\{q^p\right\}_t^{(n-1)}$

ii. Plastic evolution $k = k+1$:

$\left\{\bar{\mathbf{M}}_b^{trial}\right\}_k = \left[\mathbf{S}_b\right] : \left(\left\{\boldsymbol{\Phi}_b\right\}_t^{(n)} - \left\{\Delta\boldsymbol{\Phi}_b^p\right\}_{k-1}\right)$

iii. Verification of flow conditions and determination of plastic multiplier

$\left(\dot{\lambda}_i^p\right)_k = 0$ if $f\left[\left(\bar{m}_i^{trial}\right)_{k-1} - \left(\Delta q^p\right)_{k-1}\right]_i < 0$ or $\left(\lambda_i^p\right)_k \left[\dot{f}_i\right]_{k-1} < 0$

$\left(\dot{\lambda}_j^p\right)_k = 0$ if $f\left[\left(\bar{m}_j^{trial}\right)_{k-1} - \left(\Delta q^p\right)_k\right]_j < 0$ or $\left(\lambda_j^p\right)_k \left[\dot{f}_j\right]_{k-1} < 0$

No plasticity evolution →4.

$\left(\dot{\lambda}_i^p\right)_k \neq 0$ if $f\left[\left(\bar{m}_i^{trial}\right)_{k-1} - \left(\Delta q^p\right)_{k-1}\right]_i = 0$ or $\left(\lambda_i^p\right)_k \left[\dot{f}_i\right]_{k-1} = 0$

$\left(\dot{\lambda}_j^p\right)_k \neq 0$ if $f\left[\left(\bar{m}_i^{trial}\right)_{k-1} - \left(\Delta q^p\right)_{k-1}\right]_j = 0$ or $\left(\lambda_j^p\right)_k \left[\dot{f}_j\right]_{k-1} = 0$

Plastic evolution→3.iv

iv. Update of plastic variables and of the generalized effective 'trial' stress:

v. Back to 3.ii

4. End of the process of plastic correction

$\left\{\boldsymbol{\Phi}_b^p\right\}_t^{(n)} = \left\{\Delta\boldsymbol{\Phi}_b^p\right\}_k \quad ; \quad \left\{q^p\right\}_t^{(n)} = \left\{\Delta q^p\right\}_k$

5. Achievement of the final generalized stress on the step n:

$\left\{\mathbf{M}_b\right\}_t^{(n)} = \left[\mathbf{S}_b\left(\mathbf{D}_b\right)_t^{(n)}\right] : \left(\left\{\boldsymbol{\Phi}_b\right\}_t^{(n)} - \left\{\boldsymbol{\Phi}_b^p\right\}_t^{(n)}\right)$

6. End of integration process of the constitutive equation.

8. NUMERICAL EXAMPLES

8.1 Example 1: Model validation using a simple framed structure

The objective of this first example is to validate the proposed model and to evaluate the related concentrated damage and the global damage index of a structure. For this reason, we will analyze the results obtained by means of the proposal nonlinear frame analysis method in comparison with results obtained by means of a more refined finite element (FE) model.

The analyzed frame is 4 m high and 4 m wide loaded with two point forces (Figure 3a). The columns have a 8,43 cm x 5,62 cm cross section, the horizontal beam is 5,62 cm thick and 12,65 cm wide.

Two FE models have been considered (Oller et al. 1996), the first one was modeled using the Timoshenko 3-noded beams elements to represent the structure (see Figure 3d) and the second was modeled using 75 2D 8-noded quadrilateral elements (see Figure 3e).

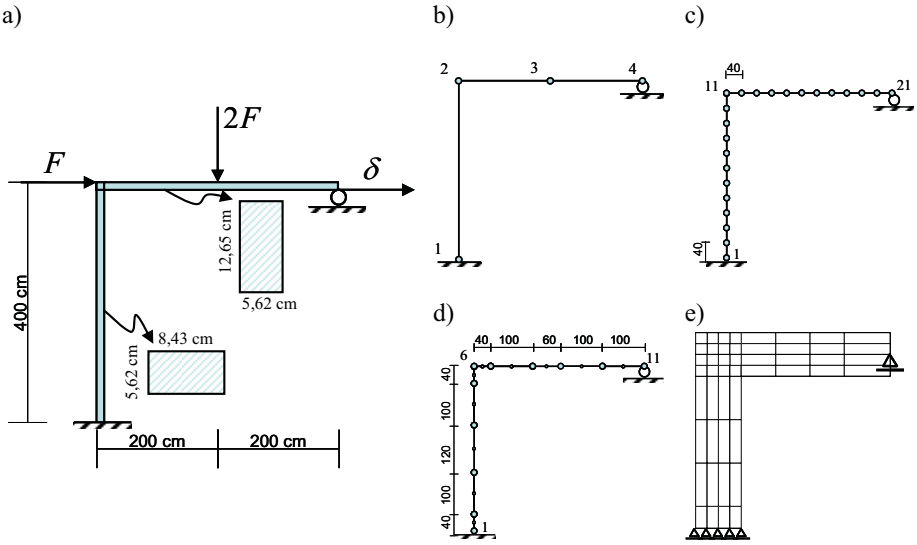

Figure 3 - Geometry of the studied frame. a) Geometry and cross section b) numeration of the nodes of for frame with 3 elements , c) numeration of the nodes of for frame with 20 elements; d) FE mesh using Timoshenko 3-noded beams elements, e) FE mesh using 2D 8-noded quadrilateral elements.

Three frames models have been considered; the first one the frame was discretized by only 3 frame elements, one to defines the column and two to defines the beam (see Figure 3a), the second frame the column and the beam are represented by 10

frame elements (see Figure 3c) and the in last frame, it was adopted the same division of the 3-noded beams elements described in Figure 3d.

In all cases, elastic modulus was $E = 2.110^5\,\text{MPa}$ while for the frame analysis it was assumed that the ultimate moment were $m_u = 45\,\text{kNm}$, for the beam, and $m_u = 20\,\text{kNm}$ for the column. The material was assumed a perfect elastoplastic law, such that, once reaches the elastic limit $\sigma_y = 200\,\text{MPa}$, it yields indefinitely at constant stress.

Figure 4 shows the results of the evolution of the force versus the displacement in the left upper corner of the frame obtained by each model, where we can notice that the results obtained with the proposed frame analysis model are in a good agreement with the results obtained by using the FE model.

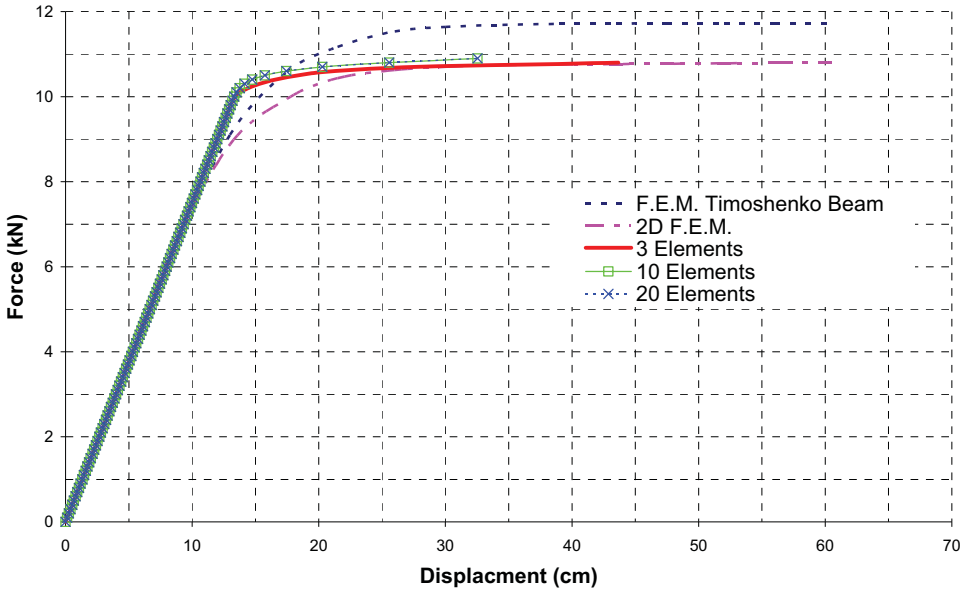

Figure 4 - Comparison of the force-displacement curve for FEM results with results obtained by using the proposed plastic-damage model.

The evolution of the moment at the column base is shown in Figure 5, where a comparison is made among the results obtained with the proposed method for different frame models.

The evolution of global damage index for each frame is shown in Figure 6. We also monitored the concentrated damage at the base and the top of the columns for each frame, once it is clearly expected that the structure will fail due to the weakening of the column. Studying together these three graphs we can analyze the behaviour of each frame.

Observing the results in Figures 8 and 9 we can conclude that, although the concentrated damage effect in the frame analysis influences on the deformation and load capacity, it is the plasticity by means of the plastic hinges, and not the damage, what conditions the numerical stability of the structural analysis.

This behaviour is in agreement with the assumptions that the structure continues to deform until the final instability is detected by the singularity of the global stiffness matrix, caused basically by the increment of the number of the plastic hinges in the frame than by the evolution of the damage.

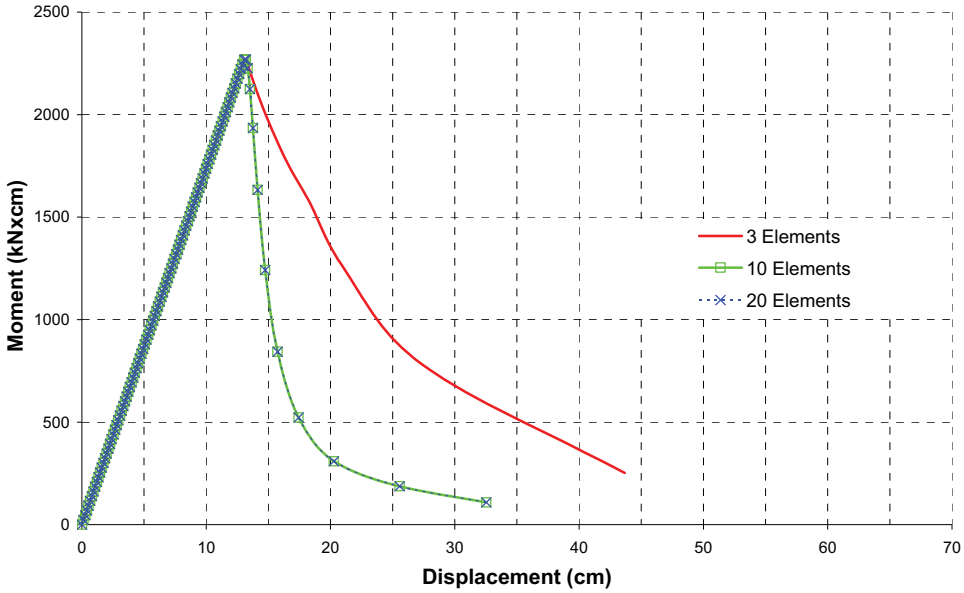

Figure 5 – Moment on the column base versus displacement at the left upper corner.

We can notice that before the concentrated damage beginning, all frames present a perfect plastic behaviour, represented by a straight horizontal line (see Figure 5). When the analysis stops, at $\delta \cong 44$ cm for the 3 elements frame and at $\delta \cong 33$ cm for the others frames, the stiffness matrix becomes singular due to the presence of hinges (i.e, the nodes 3 and 1 in the first frame), and we can no longer perform the structural analysis.

This statement also can be confirmed by the fact that the damage at the column base is less than the global damage index for all cases (see Figure 5). The same curves are obtained for the frames modeled with 10 and 20 elements for both force-displacement relation (Figure 4), moment-displacement relation (Figure 5), global damage index evolutions and evolutions of the damage for the columns (see Figure 6).

Analyzing the damage in the frame modeled with 3 elements, the beginning of the concentrated damage at the top of the column is closer to the beginning of the concentrated damage at its base, and both have almost the same final value. Meanwhile, for the frame with 10 elements and with 20 elements, the damage at the top begins at very high loads while the damage at the base begins almost at the same instant when plasticity begins. In both frames the final value obtained for the concentrated damage at the base is higher than the value obtained at the top of the column.

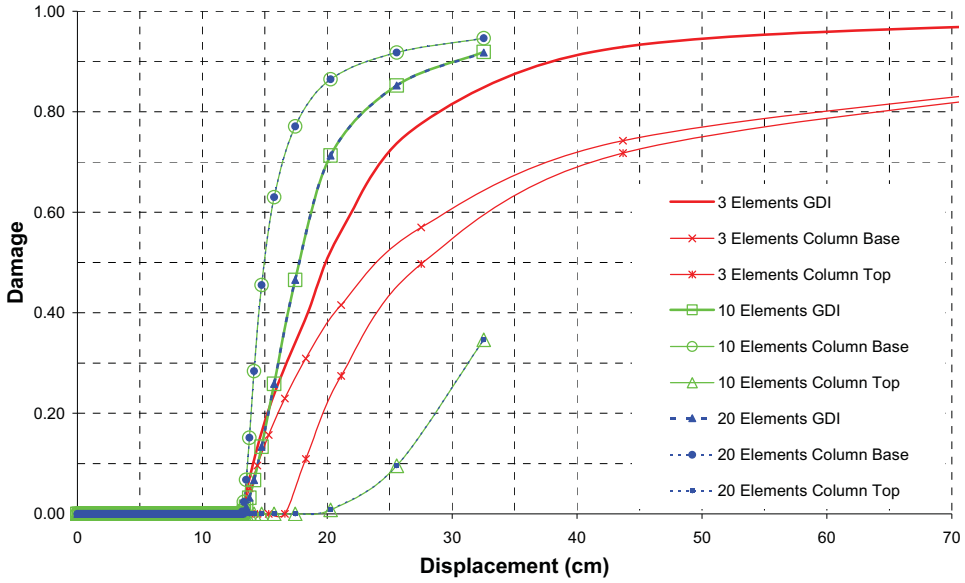

Figure 6 – Evolution of the global damage index (GDI) and the concentrated damage at the base and at the top of the column.

For the frame modeled with three elements, it can be seen clearly that the evolution of the global damage index is not related only due to the concentrated damage evolution but also to the plasticity evolution at the hinges.

We can also notice that for both the frames modeled with 10 elements and with 20 elements, the global damage index rapidly reaches high values for low deformations, what implies that the concentrated damage has more influence on the structural collapse than the plastic hinges, that is, the structure has little tendency to deform.

This can be due to the fact that the column and the beams are composed by several elements, dispersing the effect of the plasticity, while the damage is more concentrated at the base of the column. In conclusion, the behaviour of the

structure can be influenced by the number of elements and, therefore, the results obtained are smaller than it is expected.

8.2 Example 3: Model validation using a reinforced concrete framed structure

The objective of this example is to compare the results obtained by using the plastic-damage model described in this paper with the results of a quasi-static laboratory test performed by Vechio and Emara (1992) on a reinforced concrete frame.

Barbat et al. (1997) have already performed a numerical simulation of the behaviour of the tested frame, but using a viscous damage model, implemented in a finite element program. A complete description of the geometrical and mechanical characteristics of the frame, as well as of the loads, is given in Figure 7.

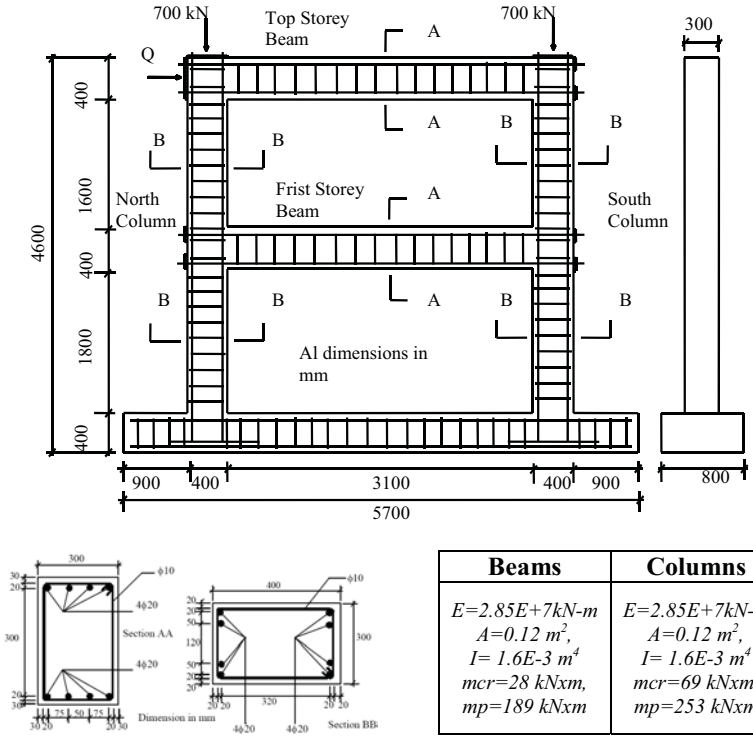

Beams	Columns
E=2.85E+7kN-m *A=0.12 m^2,* *I= 1.6E-3 m^4* *mcr=28 kNxm,* *mp=189 kNxm*	*E=2.85E+7kN-m* *A=0.12 m^2,* *I= 1.6E-3 m^4* *mcr=69 kNxm,* *mp=253 kNxm*

Figure 7 - Description of the geometrical and mechanical characteristics of the frame of Example 3

The laboratory test consisted in applying a total axial load of 700 kN to each column and in maintaining this load in a force controlled mode throughout the test, which thus produced their pre-compression. A horizontal force was afterwards

applied on the beam of the second floor, in a displacement-controlled mode, until the ultimate capacity of the frame was achieved (Vechio and Emara 1992).

In the numerical analysis of the frame the plastic constitutive equation used only takes into account the bending moments (equation (17)), while the lineal damage equation proposed by Oller (2001) has been considered for determining the damage variable evolution, using in this case a fracture energy G_f equal to 250N/m.

The curves in Figure 7 relate the horizontal forces and the displacements of the second floor beam and correspond to the load-unload laboratory test case and to the computer simulation using a viscous damage model (Barbat et al. 1997) and the plastic-damage model proposed in the present paper.

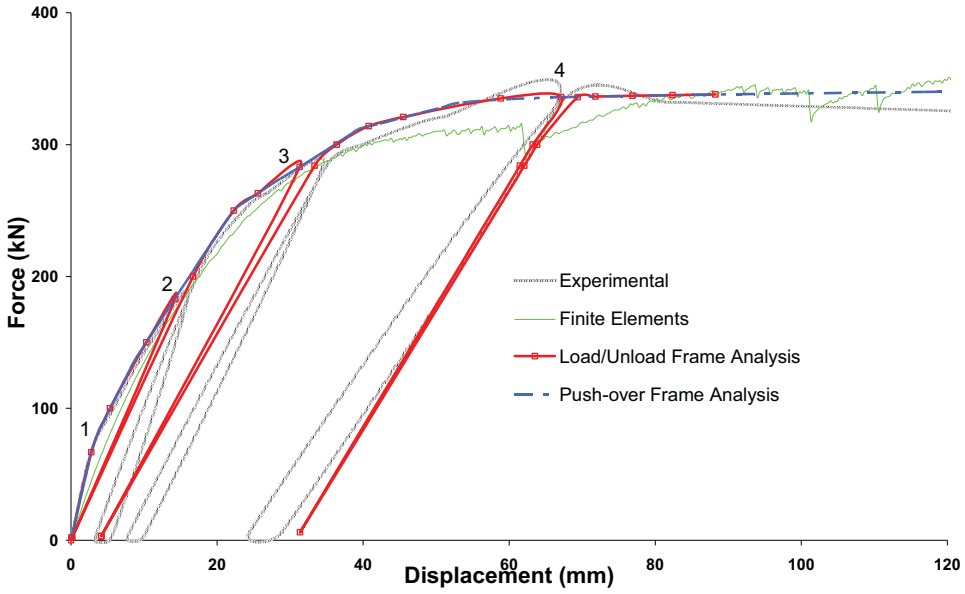

Figure 8 - Comparison of the experimental results with results obtained by using the frame analysis with the proposed platic-damage model, and a finite element model.

The results are reasonably in agreement, taking into account the little computational effort required by the calculation of the model. In the first load-unload cycle, marked by point number two in Figure 8, the presence of residual deformations can be observed in the experimental curve, while in the numerical curve this does not occur. This is because the plastic-damage model still not reach the plastic limit and the plastic deformations are assumed to occur only after the yielding of the reinforcement.

Nevertheless, when one of the elements reaches the plastic limit, it is possible to observe the influence of the plastic hinge on the curve. This situation is noticeable

by the residual deformations represented in the subsequently unload-load cycles, at points three and four in Figure 8. However, in the laboratory test, non-negligible permanent deformations occurred before this, probably because of the inelastic strains and cracking of the concrete. A plastic-damage model taking into account this and other effects (such as confinement of the concrete, shear and dead loads) is under development.

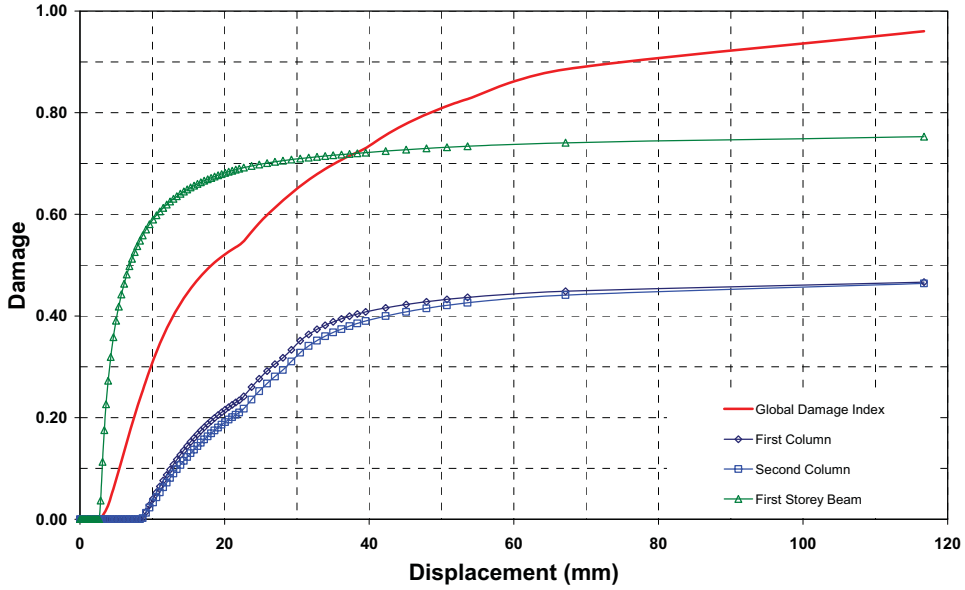

Figure 9 – Evolution of the global damage and the member damage indexes at the first floor.

Analysing the damage evolution at the first floor, shown in Figure 9, and at the second floor, Figure 10, we can notice that the member damage begins in the first storey beam, followed almost simultaneously by damage of the second-story beam, after that, the damage in the first floor columns occurs and, finally, only after a considerable increase of the deformation, the damage begins in the second floor columns. This behaviour is in agreement with the evolution of the damage observed in the laboratory test.

The effect of the damage in the first storey beam can also be detected in the force-displacement curve by the point 1 in Figure 8), which indicates the end of the elastic phase of the structure. However, in the first unload process of the frame, (point 2 in Figure 8) indicates that, at this moment, there is only damage in the frame model, aspect which is confirmed by the fact that the unload line returns to zero. At this point, as it was observed in the laboratory test, the damage occurs only

at the first-story beam, at the second-story beam and at the columns of the first floor.

In the laboratory test, the structure looses stiffness because the propagation of the cracks throughout all the members at the point 2. However, in the frame analysis, the structure looses stiffness only when the plastic effect begins, for loads closer to point 3, when yielding begins in the first floor at the base of both columns.

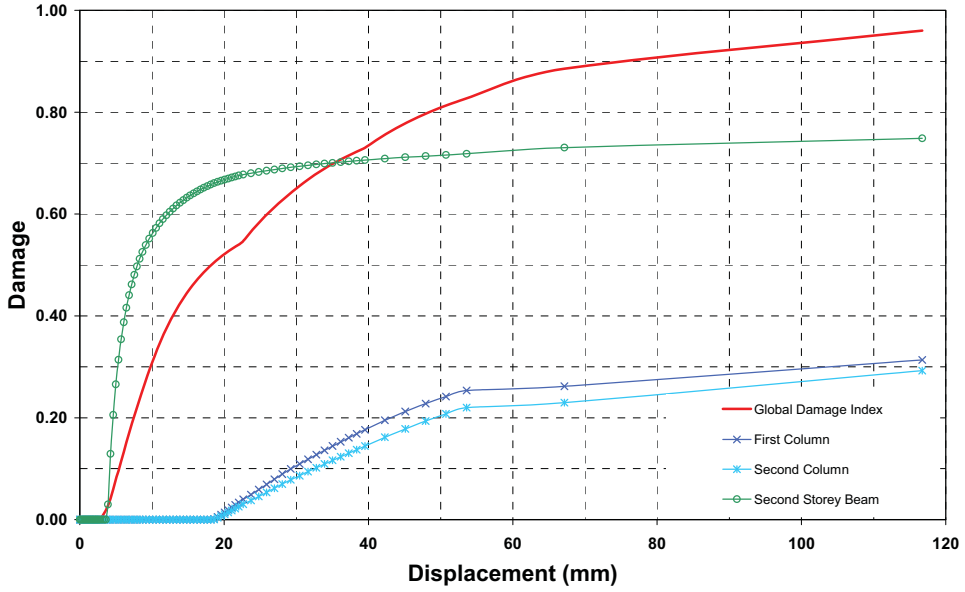

Figure 10 - Evolution of the global damage and the member damage indexes at the second floor

In the laboratory test, the first yielding was detected at the bottom of the longitudinal reinforcement at the end of the first-story beam, followed by the yielding at the base of both columns of the first floor. In contrast, in the frame analysis the first yielding is detected at the base of both columns of the first floor, followed by the yielding of the first-story beam. These differences in the sequence of the yielding can be explained by the fact that in frame analysis the plastification of the end cross section of the members is sudden, and not gradual, or fiber-by-fiber, as observed in the first-story beam in the laboratory test.

The occurrence of the perfect plastic hinge at the first-storey beam and at the base of the first and second columns of the first floor implies a change of the static configuration for the whole structure, resulting in a slight change of the member damage indexes. This behaviour can also be observed by the change in curvature of the global damage index curve. Physically, this can be interpreted as the failure of

the concrete in compression of the first floor columns and of the beams and the ensuing redistribution of the stresses towards the steel.

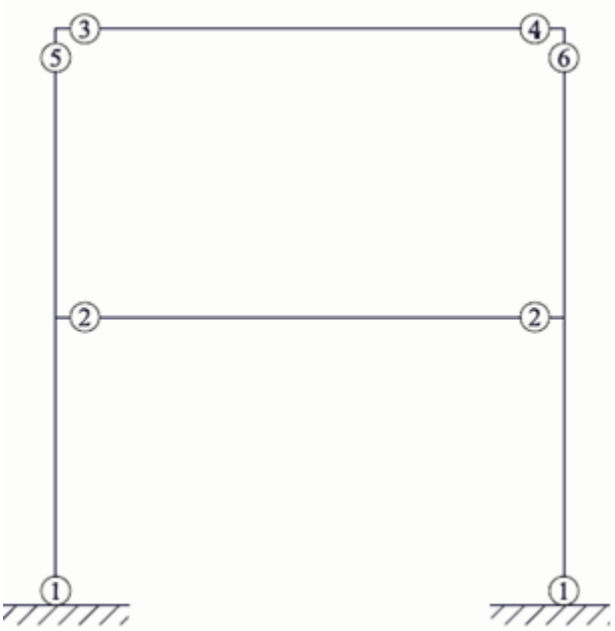

Figure 11 – Sequence of formation of the plastics hinge within the frame.

Figure 11 shows the sequence of formation of the plastic hinges in the frame analysis. Although it is different from the sequence observed in the laboratory test, the final result is the same. Nevertheless, the final deformation obtained in the frame analysis is less than in the laboratory tests because the structural analysis can no longer be perform due the presence of various plastic hinges.

9. CONCLUSIONS

A general framework for the nonlinear analysis of frames based on the Continuum Damage Mechanics and Plasticity Theory has been developed. The plastic-damage model developed in this paper assumes that plasticity and damage are uncoupled, have their own laws and that both are concentrated at ends of the frame members. Within this framework, many kinds of materials and loading conditions have been considered. Even the loading-unloading process has been simulated, and the values obtained provide satisfactory results when compared with laboratory tests, especially for reinforced concrete building.

The proposed model proves to be an effective tool for the numerical simulation of the collapse of frames. It could be a valuable alternative when other types of analyse, such as those based on multi-layer models, appear to be too expensive or impractical due to the size and complexity of the structure. The proposed model for reinforced concrete frames exhibited a very good precision confirmed by the examples included in the paper.

The global damage index has proved to be a powerful and precise tool for identifying the failure load and the structural mechanism leading to failure of reinforced concrete frame structures. This index, together with the member and the concentrated damage indexes, provides accurate quantitative measures for evaluating the state of any component of a damaged structure and of the overall structural behaviour. It is an excellent tool for the seismic damage evaluation, reliability, and safety assessment of exiting structures and which can also be used in the evaluation of the repair or retrofitting strategies.

References

1. A Hanganu, E. Oñate& A. Barbat, A finite element methodology for local/global damage evaluation in civil engineering structures. Computer and Structures, 80 (2002),pp. 1667-1687.
2. B. Luccioni, Apuntes de mecánica de daño continuo. Departamento de Resistencia de los Materiales y Estructuras a la Engeniería, Universidade Politécnica de Catalunya, 2003.
3. B. Luccioni, S. Oller & R. Danesi, Coupled plastic-damage model. Comput. Methods Appl. Mech. Engrg. 129 (1996),pp. 81-89
4. Barbat, M. Cervera, A. Hanaganu, C. Cirauqui, & E. Oñate, Failure pressure evaluation of the containment building of a large dry nuclear power plant. Nuclear Engineering and Design, 180 (1998), pp. 251-270.
5. C. Simo & J. Ju, Stress and strain based continuum damage models. Part I and II. Int. J. Solids Strucutres 23 (1987), pp. 821-869.
6. Cipolina, A. López Inojosa & J. Flórez-López, A simplified damage mechanics approach to nonlinear analysis of frames. Computer & Structures, 54 (1995) (6), pp. 1113-1126.
7. F. J. Vecchio & M. B. Emara, Shear deformations in reinforced concrete frames. ACI Structural Journal, 89, (1992)(1), pp. 45-46.
8. G. G. Deierlein, J. F. Hajjar & , A. Kavinde , Material nonlienar analysis of strucutres: a concentrated plasticity approach. Strucutural Engineering Report No. ST-01-10, Department of Civil Engineering, University of Minesota, 2001.
9. H. Barbat, S. Oller, E. Oñate & A. Hanganu, Viscous damage model for timoshenko beam structures. International Journal of Solids Structures, 34 (1997), (30), pp. 3953-3976.
10. J. C. Simo & T. J. R. Hughes , Computational Inelasticity. New York: Springer Verlag, 1998.
11. J. Faleiro, A. Barbat & S. Oller, (2005). Plastic Damage Model for Nonlinear Reinforced Concrete Frame Analysis. VIII International Conference on Computational Plasticity, COMPLAS VIII, 2 (2005),pp. 906-909.
12. J. Faleiro, A. Barbat & S. Oller, Aplicação de modelos de dano e plasticidade concentrado para o calculo matricial de estruturas de concreto armado. 47º Congresso Brasileiro do Concreto, 1 (2005), pp 201.
13. J. Faleiro, A. Barbat & S. Oller, Plasticidade e dano em pórticos de concreto Armado. 46º Congresso Brasileiro do Concreto, 1 (2004), pp 80-86
14. J. Flórez-López, Plasticidad y fractura en estructuras aporticadas. Monografías CIMNE, Barcelona, 1999.

15. J. Flórez-López, Simplified model of unilateral damage for reinforced concrete frames. Journal of Structural Engineering, ASCE. 121 (1995),p. 12.
16. J. Flórez-López,. Modelos de daño concentrado para la simulación numérica del colapso de pórticos planos. Revista Internacional de Métodos Numéricos para Cálculo y Diseño en Ingeniería, 9 (1993) (2),pp. 123-139.
17. J.H. Argyris, B. Boni & M. Kleiber, Finite element analysis of two and three – dimensional elasto-plastic frames – the natural approach. Computer Methods in Applied Mechanics an Engineering, 35 (1982),pp. 221-248.
18. L. M. Kachanov, On Creep Rupture Time, Div. Eng. Sci., 8 (1958), pp. 26–31.
19. L. Malvern, Introduction to the mechanics of a continuos medium. Prentice Hall, Englewood Cliffs, 1969.
20. M. Jirásek & Z. P. Bazant, Inelastic analysis of structures. New York: John Willey & Sons, 2002
21. M. R. Salamy, H. Kobayashi & S. Unjoh, Experimental and analytical study on RC deep beams. Second International Conference on Concrete & Development, 2005.
22. M. S. Álvares, Aplicação de um modelo de dano localizado a estruturas de barras em concreto armado. Universidade Católica de Goiás <http://www.ucg.br>. Manuel_da_Silva_Álvares.pdf, jully 20, 2004.
23. M. S. Álvares, Estudo de um modelo de dano para o concreto: formulação indentificação paramétrica e aplicação com emprego do método dos elementos finitos. Departamento de Estruturas, Escola de Engenharia de São Carlos – USP, São Carlos, Brazil, 1993.
24. S. Oller, B. Luccioni & A. Barbat, Un Método de Evaluación del Daño Sísmico en Estructuras de Hormigón Armado. Revista Internacional de Métodos Numéricos para Cálculo y Diseño en Ingeniería, 12 (1996) (2),pp. 215-238.
25. S. Oller, Fractura mecánica – un enfoque global. CIMNE: Barcelona, 2001.
26. W. Chen, Plasticity in reinforce concrete. Mac Graw Hill, 1982.

"Computational Civil Engineering 2006", International Symposium
Iaşi, România, May 26, 2006

Impact of fine aggregates replacement by fluidized fly ash to resistance of concretes to aggressive media

Jiri Brozovsky, Tomas Fojtik and Petr Martinec

Institute of Building Materials and Components , Faculty of Civil Engineering, Brno University of Technology, 602 00Brno, Czech Republic

Summary

Fluidized fly ashes constitute a part of industrial waste used in building material production on a small scale up to now. Concrete production is one of fluidized fly ashes application field. This paper presents findings concerning testing of concrete with addition of fluid combustion ashes as to aggressive media resistance - chlorides and sulphates in particular. Fine grained aggregate has been replaced by deposit ash (0 to 50 %). This ash originates from black coal fluid combustion in the TZ Trinec Power Plant. Concrete samples have been exposed for a period of 24 months.

KEYWORDS: fluidized bed ash combustion, concrete resistance, resistance to chlorides, sulphates, raw material.

1. INTRODUCTION

Paper Industrial ashes exploitation for building material production continues permanently in the course of many years. One of wastes exploitable with concrete production is also fluid combustion ash. To use these ash concretes in practice there is necessary to know not only their basic physical–mechanical characteristics but also other properties, among others their resistance to aggressive media. Our research works have been focused on monitoring of concrete chloride/sulphate resistance after addition of deposit fluid combustion ash.

2. FLUIDIZED BED ASH CHARACTERISTICS

Fluid ashes originate in the course of flue gases desulphurization based on direct mixing of fuel with desulphurising reagent (generally lime or dolomite in some cases) before combustion or during it. There are many production processes; most of them are patent covered. Generally all these processes are based on calcination of present desulphurising reagent to CaO and its subsequent reaction with sculpture oxides along with oxidation of sulfur dioxide to sculpture trioxide. This reaction

results in mixture of original fuel ash, unreacted desulphurising reagent (CaO with $CaCO_3$ remains, as the case may be), calcium sulfate, ash matter product reaction with CaO, and unburned fuel. Since fluid combustion temperatures are lower than classic combustion ones, unreacted CaO is present in the form of so called burned lime, therefore reactive lime. Fluid ashes are also typical for their low volume of melt.

As a result of flue gases transport from the furnace space particular fractions of this mixture are separated; fine parts are drifted by flue gases in the form of light ashes, remaining more coarse parts in the furnace space. Solid substances are removed using common technologic procedures (cyclone washers, filters). That is why each fluid combustion unit products in principle fluid ashes of two kinds: furnace space ash (indicated as deposit ash for instance), and light ash (indicated as cyclone ash, filter ash, and so on). Characteristics of both these ashes are different as to physical properties (granulometry, specific surface, density, powder density) as well as chemical and mineralogical composition even if they originate from identical fluid combustion and desulphurization technologic procedure. As well as with classic ash also both kinds of fluid ashes feature disadvantage of unequal properties namely chemical composition, density, and other parameters due to combustion process instability and variability of input component properties (coal and desulphurising reagent).

3. INPUT RAW MATERIAL AND CONCRETE COMPOSITION: BASIC DATA

Material used for concrete production:

Cement : CEM I 42.5 from the Mokra Cement Mill

Aggregates :

- *fine* - mined; Bratčice Gravel Pit; fraction 0 to 4,
- *coarse* - crushed; Olbramovice Gravel Pit, fraction 4 / 8, and 8 / 16.

Ash : deposit fluidized bed ash of black coal fluid combustion from the TZ Trinec Power Plant; see the Table 1 for ash chemical/physical composition.

Mixing Water : in agreement with EN 1008.

Table 1. Trinec ash chemical/ phase composition

A. Chemical composition			
Tested components	Component share [%]	Tested components	Component share [%]
SiO_2	53.5	MnO	0.1
Al_2O_3	21.5	K_2O	2.6
Fe_2O_3	5.8	Na_2O	0.2
TiO_2	0.9	S	2.5
CaO	6.7	C	2.6
MgO	3.2	Annealing loss	0.46
B. Phase composition			
Ash contains considerable volume of β–silica. Only small volume of anhydride has been detected. That is why there is possible to assume low share of partly decomposed potassic feldspar (orthoclase) and lesser share of illite and hematite.			

Testing of concrete with deposit fluid ash as partial replacement of fine aggregates has been carried out using 3 kind of concrete with variable ash content and ashless concrete mixture as reference test sample. See the Table No. 2 for composition of particular concrete mixtures.

Table 2. Concrete mixture composition for experimental works

Concrete mixture composition per $1m^3$ of finished product	B0 Tr	B20 Tr	B30 Tr	B50 Tr
CEM I 42.5 R cement	330	330	330	330
Sand 0 to 4 mm from the Bratčice Gravel Pit	756	605	529	378
Ash from the Chvaletice Power Plant	0	151	227	378
Aggregates 8 to16 mm from the Olbramovice Gravel Pit	1069	1069	1069	1069
Mixing Water	199	199	199	199

4. WORK METHODICS

To investigate concrete resistance to corrosion there were prepared test specimens (blocks 40 × 40 × 160 mm each) conformable to the CSN 73 1340 Standard.

After manufacturing the test specimens have been placed into moist environment for 24 hours followed - after form removal and before exposition to corrosive medium - by placing into water bath at 19 to 21 °C. After 28 hour hardening the specimens have been exposed to corrosive medium action. Selection of parameters under evaluation is based on the CSN 73 1340 Standard.

Tested specimens will be monitored in light of parameters as follows:

- appearance (visually)
- density (EN 12390-7 Standard)
- ultrasonic pulses velocity (EN 12504-4 Standard)

– dynamic modulus of elasticity E_{bu} (CSN 731371 Standard)

– compression strength f_{cc} (EN 196-1 Standard)

– tensile strength under flexure (EN 196-1 Standard)

Specimen strength has been destructive tested before exposition to corrosive medium and after 3, 9, 15, 18, and 24 months of exposition.

Corrosive environment effect during other time periods has been evaluated based on both ultrasonic pulse speed variation and dynamic moduluses of elasticity.

Corrosive media:

– sulphates - sodium sulphate solution (10,000 mg of SO_4^{2-} in 1 litre)

– chlorides - 5 % solution of NaCl

5. FINDINGS OF CONCRETE RESISTANCE MONITORING

See the Figure. 1 to 4 for variation in compression strength, and dynamic moduluses of elasticity depending upon concrete kind, exposition time period, and corrosive medium.

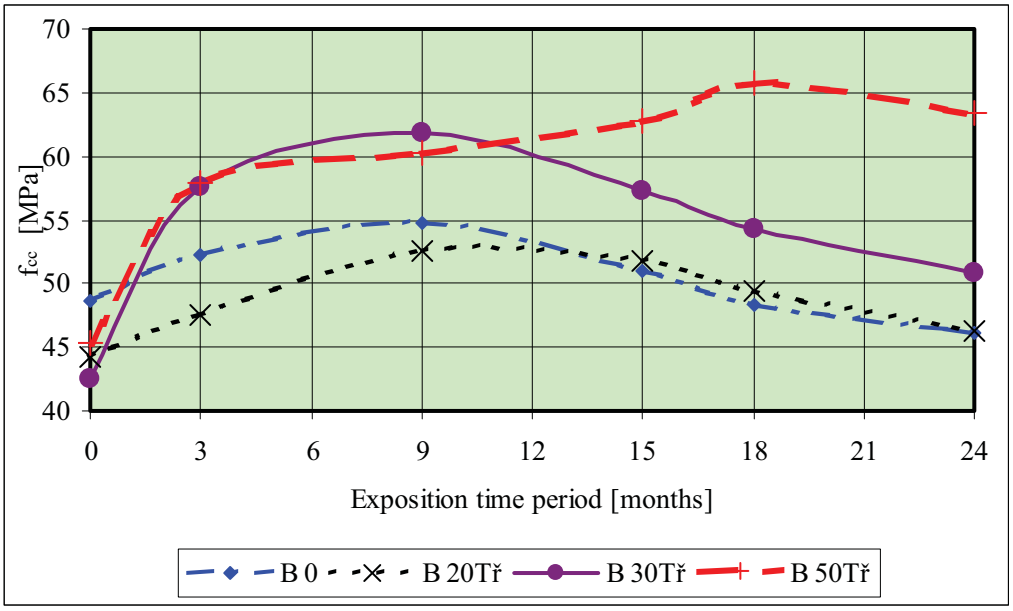

Figure 1. Compression strength curve depending upon exposition time period in aggressive chloride environment

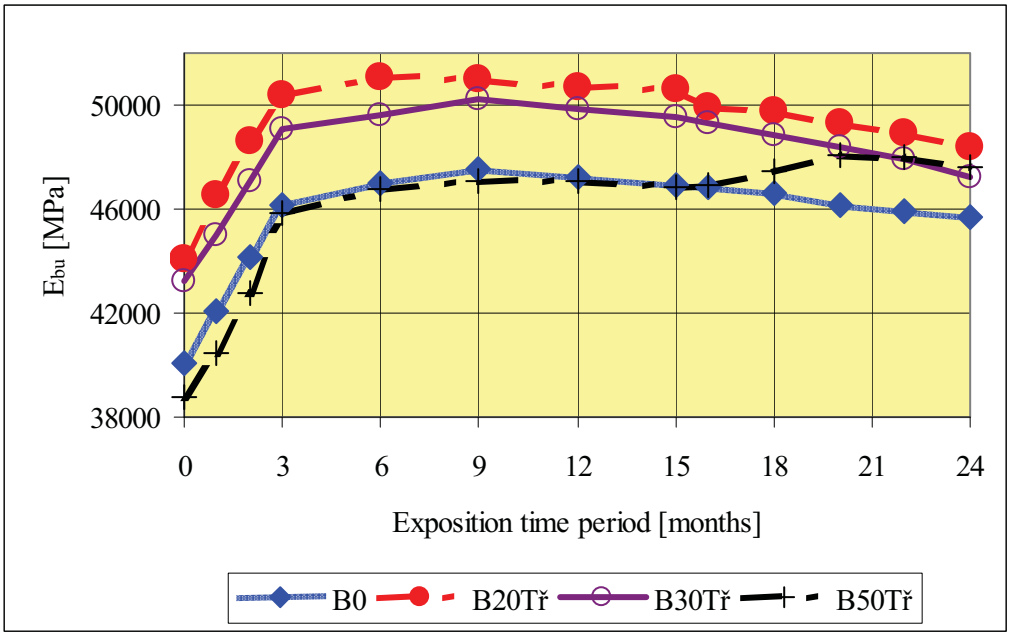

Figure 2. Concrete modulus of elasticity variations depending upon exposition time period in aggressive chloride environment

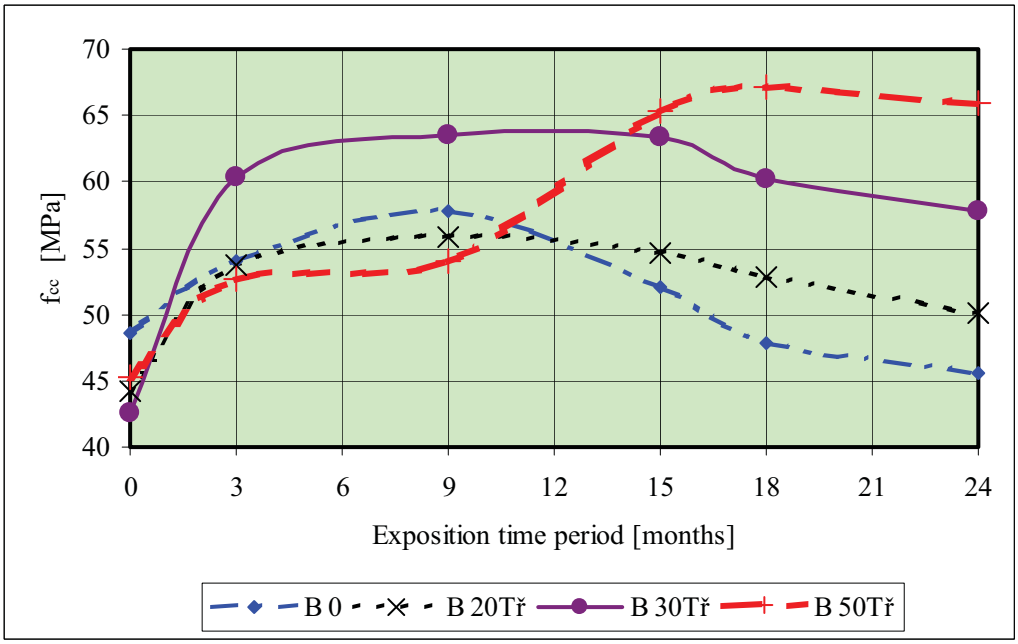

Figure 3. Compression strength curve depending upon exposition time period in aggressive sulphate environment

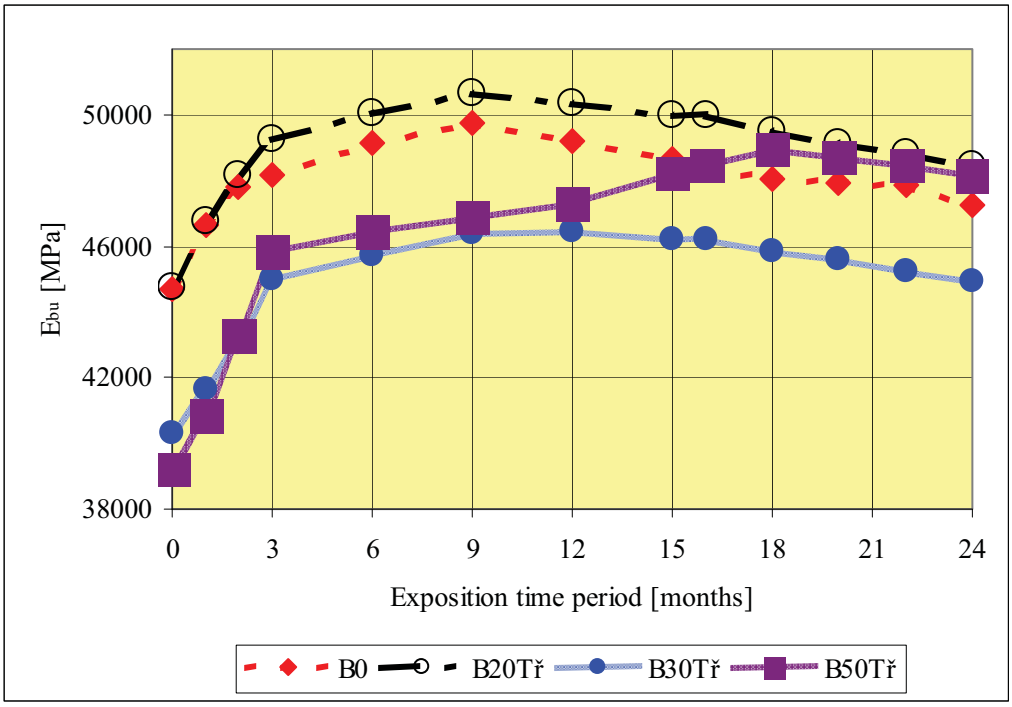

Figure 4. Dynamic modulus of elasticity curve depending upon exposition time period in aggressive sulphate environment

6. CONCLUSIONS

To evaluate concrete resistance to aggressive medium (chlorides in this instance - 12 months evaluation time period according to the CSN 73 1340 Standard) there is necessary to ensure that no one parameter under monitoring shall decrease during this interval.

6.1 Resistance to Chlorides

Based on monitoring results as mentioned above there is possible to state that tested concretes with 50 % of fluid combustion ashes (place of origin: TZ Trinec Co.) as replacement of natural aggregates are resistant to chlorides.

Other tested concretes including reference ashless concrete are unfit to stand up to chlorides by reason of monitored parameter deterioration before expiration of 12 months exposition (6 to 9 months). Concrete with 50 % of deposit fluid ash shown highest resistance; on the other hand concrete where 20 % of fine aggregates have been replaced with fluid combustion ash shown least resistance.

6.2 Resistance to Sulphates

There is possible to treat tested concrete with 50 % of fluid combustion ash (replacement of fine natural aggregates) as resistant to sulphates.

Other tested concretes including reference ashless concrete are unfit to stand up to sulphates by reason of monitored parameter deterioration before expiration of 12 months exposition (6 to 9 months). Concrete with 50 % of deposit fluid ash shown highest resistance; on the other hand concrete where 20 % of fine aggregates have been replaced with fluid combustion ash shown least resistance.

ACKNOWLEDGEMENTS

The work was supported by by the MSM 0021630511 plan: Progressive Building Materials with Utilization of Secondary Raw Materials and their Impact on Structures Durability and the GAČR 103/05/H044project.

References

1. Drochytka R.: et al.: Progressive Building Materials with Utilization of Secondary Raw Materials and their Impact on Structures Durability. Brno University of Technology, Final report of the project VVZ CEZ MSM: 0021630511, Brno 2005. Brozovsky J.: Subtask 3 (in Czech).
2. Adamek,J.- Brozovsky, J. : Influence of fine aggregates partial substitution by fly ash from fluid combustion on concrete durability. *In Proceedings of the 3 rd International Conference : Concrete and Concrete Structures*, University of Žilina,Slovakia 2002
3. Brozovsky, J. and Martinec,P. Durabbility of concrete with fly ash. *In Proceedings of the 2^{d} International Conference on Concrete and Reinforced Concrete: Concrete and reinforced concrete – developement trends*. NIIZHB, Moscow, Russia, Vol. 4, 2005. (in Russian).
4. Brozovsky, J. and Brozovsky, J., jr. Reinforced concrete structure investigation before its repair´. *In Proceedings of the 2^{d} International Conference on Concrete and Reinforced Concrete: Concrete and reinforced concrete – developement trends*. NIIZHB, Moscow, Russia, Vol. 4, 2005 (in Russian).
5. Brozovsky,J., Zach, J., Brozovsky,J., Jr. Durability of concrete made from recycled aggregates *In Proceedings of the International RILEM JCI Seminar Concrete Durability And Service Life Planning: Curing, Crack Control, Performance In Harsh Environments*, Ein-Bokek, Dead Sea, Israel, 2006
6. EN 12504-4 Testing concrete – Part 4: Determination of Ultrasonic Pulse Velocity
7. EN 196-1 Methods of Testing Cement - Part 1: Determination of Strength
8. EN 12390-7 Testing Hardened Concrete – Part 7: Density of Hardened Concrete
9. CSN 73 1340 Concrete Constructions. Tests of Corrosion Resistance of Concrete. General Requirements
10. CSN 73 1371 Method of Ultrasonic Pulse Testing of Concrete
11. EN 1008 Mixing Water for Concrete. Specification for Sampling, Testing and Assessing the Suitability of Water, Including Water Recovered from Processes in the Concrete Industry, as Mixing Water for Concrete

"Computational Civil Engineering 2006", International Symposium
Iaşi, România, May 26, 2006

Time flow of gypsumfree cements strength development

Jiri Brozovsky[1], Petr Martinec[2] and Jiri Brozovsky, jr[3]

[1,2] *Institute of Building Materials and Components , Faculty of Civil Engineering, Brno University of Technology, 602 00Brno, Czech Republic*
[3] *Department of Building Mechanics, Faculty of Civil Engineering, VSB-Technical University of Ostrava, 708 33 Ostrava, Czech Republic*

Summary

In the paper the results of the investigation of the long – term growth of the strength of gypsumfree cements are presented. It was found that the compression strength exhibits a continuously rising tendency, even though the strength increases with time are small. The tensile bending strengths of gypsumfree cements attain their maxima at the age of 3 and 7 days, respectively and then continuously decrease.

KEYWORDS: gypsumfree cement, strength, long – term strengths, tensile bending strength, compressive strength.

1. INTRODUCTION

The solution of this complex of problems is not an end in itself, because the results of tests on gypsumfree cements carried out not only by the author, but also in other organizations e.g. (UD Brno, CVUT Prague, BUT Brno, VUPS Ostrava) have proved that with time there occurs, in certain cases, a decrease of the tensile bending strengths. So far none has been systematically investigating this problem. This is given by the fact that in practical everyday civil engineering compression strength is mostly used as the rating of carriageways.

2. INVESTIGATION OF THE DEVELOPMENT OF GYPSUMFREE CEMENTS STRENGTHS ON PASTES AND STANDARD MORTAR

For the monitoring of long – term strengths of gypsumfree cements have been carried out tests of two gypsumfree cements Prachovice with different admixture contents of the setting regulation system. This was carried out on one hand on test specimens prepared from cement paste, on the other hand on test specimens prepared from standard mortar. In order to eliminate the influence of the specimen

size onto the results of the tests have been uniformly used standard test specimen with dimensions 0,04 x 0,04 x 0,16m.

The results of the tests of strengths and specific weights of the cement paste and standard mortar are presented in Table 1.

Table 1. Results of strength tests on gypsumfree cements for cement paste and standard mortar

KORTAN FN [% weight]		0,5		0,6	
Na_2CO_3 [% weight]		1,8		1,8	
TYPE OF MIX		CEMENT PASTE w = 0,24	STANDARD MORTAR w = 0,33	CEMENT PASTE w = 0,24	STANDARD MORTAR w = 0,33
tensile bending strength σ_{po} [N/mm]	1 day	11,37	5,13	10,85	5,59
	2 days	12,41	8,27	11,31	8,55
	3 days	13,79	9,28	13,26	10,20
	7 days	14,59	10,44	14,13	11,98
	28 days	13,55	10,39	13,13	11,29
comp-ression strength σ_{pd} [N/mm^2]	1 day	55,5	31,0	54,5	32,6
	2 days	58,5	45,6	57,7	42,7
	3 days	60,7	50,2	60,4	46,0
	7 days	69,8	54,0	69,0	56,3
	28 days	76,6	63,0	75,8	65,1
density D [kg/m^3]	1 day	2 245	2 317	2 237	2 317
	2 days	2 250	2 326	2 249	2 332
	3 days	2 261	2 331	2 268	2 332
	7 days	2 263	2 338	2 263	2 334
	28 days	2 268	2 343	2 265	2 335
specific weight ρ [kg/m^3]		2 610	2 640	2 540	2 640
		2 520	2 620	2 570	2 650
		2 510	2 640	2570	2 630
	∅	2 547	2 633	2 560	2 640

3. MONITORING THE LONG – TERM GROWTH OF GYPSUMFREE CEMENTS STRENGTHS

For monitoring the long – term growth of gypsumfree cements strengths have been prepared test specimen from standard mortar in such quantities as to allow to follow the development of strengths during a period of at least 3 years – for every age 9 test specimens were tested.

For the tests was employed gypsumfree cement prepared from MALOMERICE clinker ground to a specific surface 632 m^2kg^{-1} which contained 0,5% Ligrasol and 0,7% referred to the weight of the clinker.

Two types of cement have been tested:

- sample R1 – without supplementary admixtures
- sample R1 – with a supplementary quantity of Na_2CO_3 – 1,2% weight from the clinker weight.

The following parameters have been determined:

- tensile bending strength
- compression strength
- propagation rate of ultrasonic pulses in cements at an age of 1, 2, 3, 7, 28 days and 1, 2, 3, years.

The sample has been stored for entire period in a standard environment, i.e. in the form of water storage. The results of the tests are presented in table 2 and graphically illustrated in figure 1 and 2.

Table 2. Results of strength tests and measurements of ultrasonic pulses propagation rates for various age of gypsumfree cements

Gypsumfree cement clinker Malomerice 632 m^2kg^{-1} 0,5%LIGRASOL + 0,7% Na_2CO_3		without supplementary admixtures	+ 1,2 % Na_2C0_3 referred to clinker weight
tensile bending strength σ_{po} [N/mm^2]	1 day	5,96	8,37
	2 days	10,37	9,46
	3 days	13,39	12,30
	7 days	13,81	12,52
	28 days	12,96	11,75
	1 year	11,57	10,11
	2years	11,02	9,66
	3 years	10,39	8,84
COMPRESSION strength σ_{pd} [N/mm^2]	1 day	38,7	46,3
	2 days	55,2	53,1
	3 days	58,4	55,4
	7 days	63,1	60,4
	28 days	70,9	68,7
	1 year	88,0	85,1
	2years	88,8	87,2
	3 years	90,5	95,1

Gypsumfree cement clinker Malomerice 632 m^2kg^{-1} 0,5%LIGRASOL + 0,7% Na_2CO_3		without supplementary admixtures	+ 1,2 % Na_2C0_3 referred to clinker weight
ultrasonic pulse velocity V[m/s]	1 day	4 414	4 679
	2 days	4 635	------
	3 days	-----	4 767
	7 days	-----	------
	28 days	4903	4 880
	1 year	4 962	4 942
	2years	4 975	4 949
	3 years	4 990	4 967

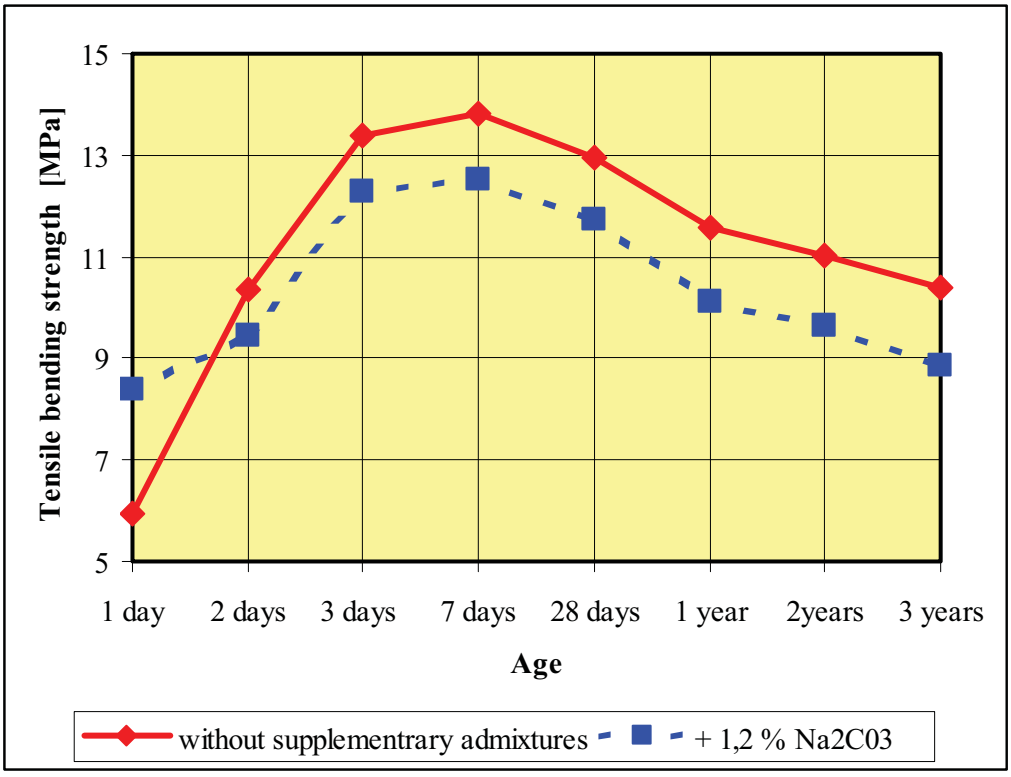

Figure 1. Long-term tensile bending strength of gypsumfree cements in relation to time

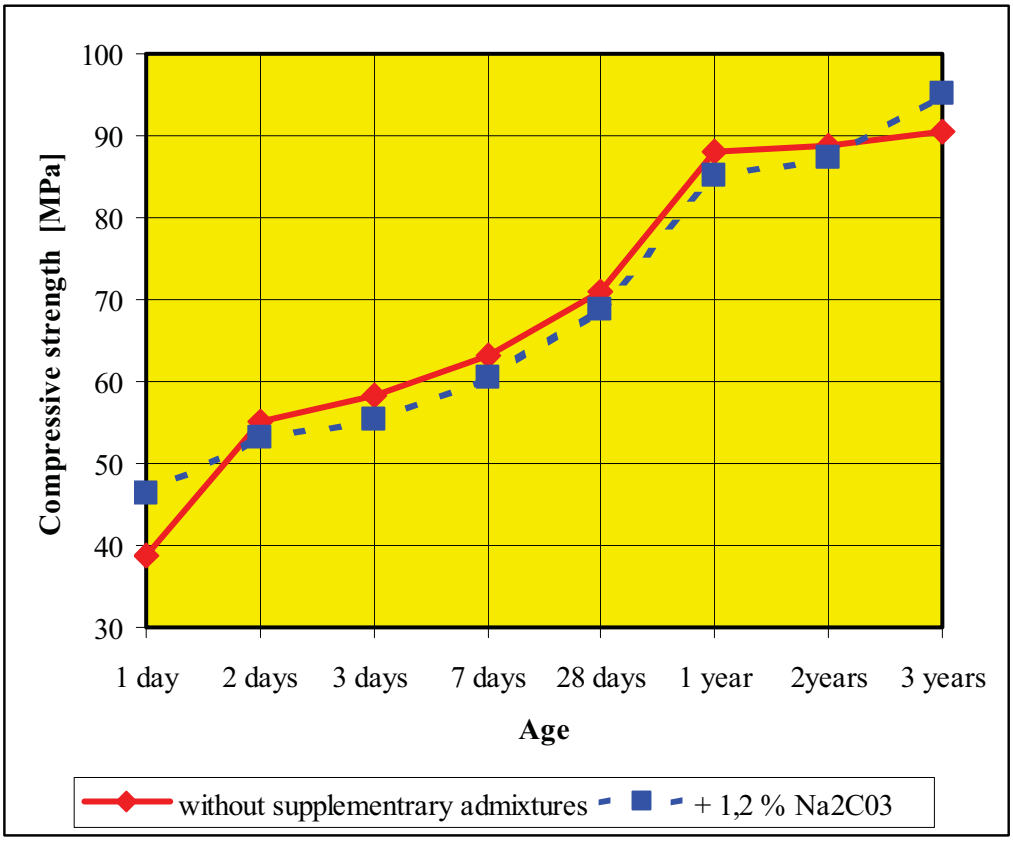

Figure 2. Long-term compressive strength of gypsumfree cements in relation to time

The tensile bending strength of gypsumfree cements attains its maximum at the age 7 days, and then its systematic decrease occurs. For the determination of reasons for this descreares were carried out physical and chemical tests for determining the mineralogical composition of the cements and the microstructure at the age of 3 years. The sample was in fact subjected to X – ray diffraction analysis and the microstructure was photographed on and electron scanning microscope.

The results of the X – ray diffraction analysis are presented in Table 3.

Table 3. Results of the X – ray diffraction analysis of GFC samples

Marking of sample	Identified minerals
R1 - 1	*quartz, calcite, portlandite, β - C_2S, C_3S, C_4AH_{13}*
R1 - 6	*quartz, calcite, portlandite, β - C_2S, C_3S, C_4AH_{13}*
R2 - 1	*quartz, calcite, portlandite, C_4AH_{13}, muscovite*
R2 - 2	*quartz, calcite, portlandite, C_4AH_{13}, CSH II, clay minerals - traces*

4. CONCLUSIONS

Long term tests of GFC have shown that the tensile bending strength after the attainment of their maxima after 7 days continuously decrease during next period and at the age 3 years approach the values that have been obtained at the age of 2 and 1 day, respectively.

After one year the growth of the GFC compressive strength is considerably slowed down, but no tendencies to a decrease of these values have been determined.

The determination of the ultrasonic pulse rates in the tested GFC samples exhibits in relation to time a continuously increasing tendency. From this can be concluded that no deterioration of the microstructure by cracks take place.

Studies of the mineralogical composition and the microstructure have also identified no anomalies that could lead to a decrease of the long-term tensile bending strength values.

ACKNOWLEDGEMENTS

The work was supported by the MSM 0021630511 plan: Progressive Building Materials with Utilization of Secondary Raw Materials and their Impact on Structures Durability and the GAČR 103/04/0169 project.

References

1. Drochytka R.: et al. Progressive Building Materials with Utilization of Secondary Raw Materials and their Impact on Structures Durability. Brno University of Technology, *Final report of the project VVZ CEZ MSM: 0021630511, Brno 2005*. Brozovsky J.: Subtask 3 (in Czech).
2. Brozovsky, J. Investigation of the utilization and preparation of concretes with highly early strength values ,VA Brno, 1994, (in Czech),
3. Brozovsky, J. Concrete with gypsumless cement- research results and experience of utilization in practice. *In : Proceedings of the 1st Conference on Concrete and Reinforced Concrete*, Moscow, Russia, 2001 (in Russian)
4. Brozovsky, J., Brozovsky, J. jr. : Concrete with gypsum free cement – basic characteristics *In : Proceedings of the Intenational Symposium on Non – Traditional Cement & Concrete*, Brno, Czech Republic, 2002
5. Brozovsky, J., Matejka, O. and Martinec, P. Concrete Interlocking Paving Blocks Compression strength Determination U sing Non-Destructive Methods. *In Proceedings of the 8th International Conference of the Slovenian Society for Non-Destructive Testing »Application of Contemporary Non-Destructive Testing in Engineering«,* Portorož, Slovenia*, 2005*
6. EN 12504-4 Testing concrete – Part 4: Determination of Ultrasonic Pulse Velocity
7. EN 196-1 Methods of Testing Cement - Part 1: Determination of Strength
8. EN 12390-7 Testing Hardened Concrete – Part 7: Density of Hardened Concrete
9. CSN 73 1371 Method of Ultrasonic Pulse Testing of Concrete

"Computational Civil Engineering 2006", International Symposium
Iaşi, România, May 26, 2006

The optimization of properties of self-compacting concrete by the combination of fine filler

Ales Kratochvil[1] and Jiri Brozovsky[2]

[1,] *Transport Research Centre, 636 00 Brno, Czech Republic*
[2] *Institute of Building Materials and Components , Faculty of Civil Engineering, Brno University of Technology, 602 00Brno, Czech Republic*

Summary

Our partner Virginia Transport Research Council (VTRC) has provided the Transport Research Centre (CDV) with information about rules applied for technology of self-compacting concrete (SCC) in the USA[1, 2]. According to these sources preferably in the USA ground blast furnace slag and fly ash (only after careful composition test) ,as the filler into concrete mixture for SCC is used. Concrete mixtures containing different types of fillers are frequently used for the production of SCC. The applicable advantage is that the certain kind of filler modifies certain properties of concrete mixture or hardened concrete.

In the Czech Republic, for SCC stoned dust removers (fillers) ground blast furnace slag, fly ash, ground limestone and silica fume are used as concrete mixture fillers. The following experiments were carried out for verification of the possibility of affecting the concrete mixture properties and SCC, by combination of different types of fillers, following tests were carried out.

KEYWORDS: self-compacting concrete, filler, ground blast furnace slag, fly ash, ground limestone, silica fume.

1. TESTS

For verification of rheological properties of experimental concrete mixture, we carried out modified tests by slumping of the cone (Abrams), then by L-box, J-ring and Orimet tests.

1.1 Slump test

When testing, Abrams cone must be placed with the smaller base on the smooth pad 750 x 750 mm and is filled up to the top edge with concrete mixture without compacting. Then by lifting of taper the slumping of concrete mixture on the pad can be carried out. We measure time needed for concrete mixture to be slumped into a cake of diameter 500 mm (T_{50}) and final diameter of the cake (M)

1.2. L – box test

Testing method simulates concrete mixture penetration through reinforcement. For the measurements we used the instrument whose diagram is on fig. 1 .During the test vertical part of the instrument is filled up with concrete mixture and by lifting of sliding gate the mixture can freely leak out over inserted ribbed steel bars (in the present case 3x profile 12 mm with axial distance 50 mm)into horizontal part of 4 L – box. We measure time T_{40} ie. time when the face of concrete mixture in horizontal part of the instrument reaches the distance 400 mm from sliding door and time T_{60} ie. time when the front of concrete mixture reaches the end of L box horizontal part. When the movement ends, we subtract further values H1 (the height of concrete mixture column in 2/3 of horizontal part of the instrument) and H2 (the height of concrete mixture column by the opening of vertical part of instrument).The ratio H1/H2 determines the movement locking of mixture through reinforcement

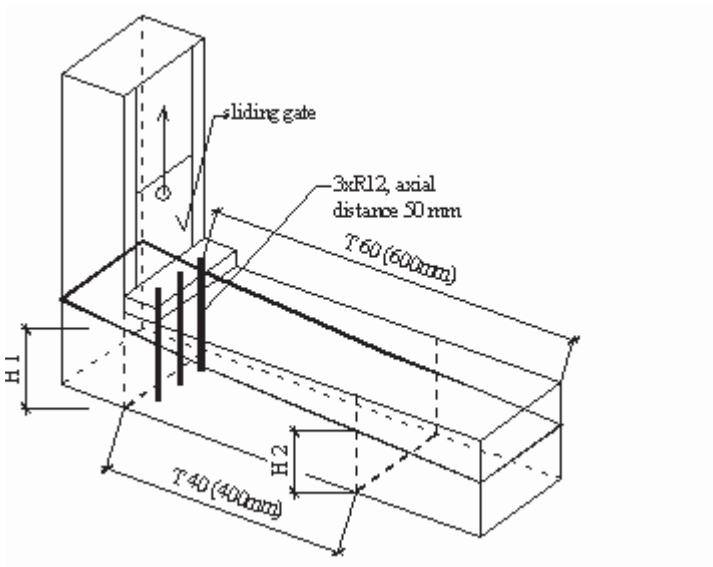

Figure 1. L - box

1.3. Orimet test

We measure the flow through swaged opening of the plant. The test results give us the information, technically accurate enough, about mixture viscosity. (fig.2)

1.4. The combination of Orimet and J – ring tests

Testing procedure described in the preceding paragraph is in this case completed with apparatus that enables to assess locking of mixture through reinforcement – J – ring test (fig.3) Basically it means the annulus inserted in constant distance of spiky steel bars of the same profile. The distance of bars as well as applied annulus profile depending on the max. used aggregate granule differs . J-ring test apparatus is placed centric under the opening of Orimet during the test. We again measure the flow time of concrete mixture throw the opening of Orimet and visually assess the locking of concrete mixture movement through J-ring.

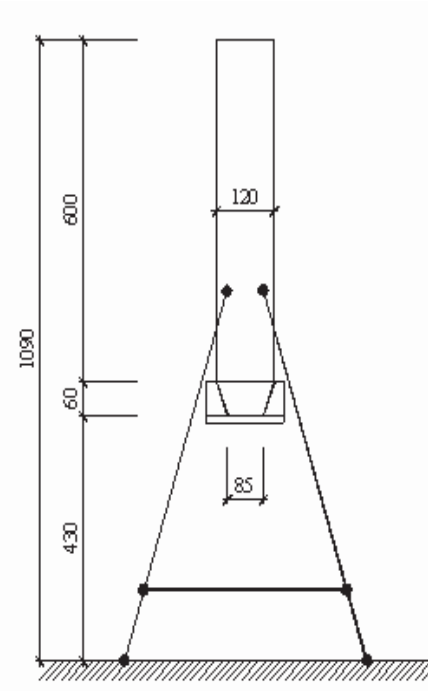

Figure 2. Orimet

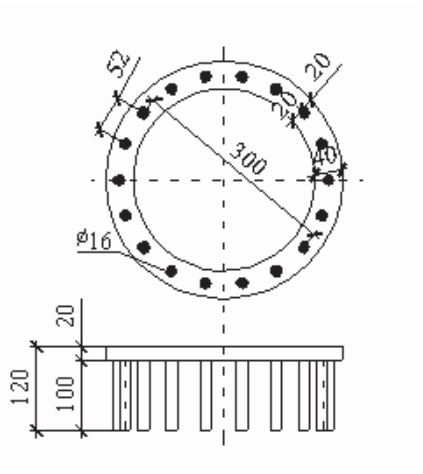

Figure 3. J - ring

Table 1. Experimental concrete mixtures and material properties [kg/m^3]

Mix No.	I	II	III	IV	V	VI	VII	VIII	IX	X
Cement Mokra 42,5 R	404	406	391	399	406	402	402	401	402	396
Sand 0-4, Tovacov	829	710	743	817	710	703	703	762	703	693
Aggregate 4-8, Tovacov	232	233	225	229	233	231	231	230	231	228
Aggregate8-16, Tovacov	556	558	537	548	558	552	552	551	552	544
Stone powder	162	-	-	-	-	100	-	120	100	-
Ground granulated blast furnace slag	-	284	-	-	-	181	-	-	-	139
Fly ash	-	-	215	-	-	-	100	100	-	99
Silica fume	-	-	-	159	-	-	-	-	-	40
Ground limestone fines	-	-	-	-	284	-	181	-	181	-
Admixture (Sika5– 600)	4,0	4,0	3,9	-	4,0	4,0	4,0	4,0	4,0	4,0
Admixture (Sika 3 neu)	-	-	-	12	-	-	-	-	-	-
Mixing water	182	183	210	189	183	191	191	190	191	203
C-W ratio w [v/(c+m)]	0,32	0,27	0,35	0,34	0,27	0,28	0,28	0,31	0,28	0,30
Mix No.	XI	XII	XIII	XIV	XV	XVI	XVII	XVIII	XIX	XX
Cement Mokra 42,5 R	398	406	406	409	406	402	402	396	394	390
Sand 0-4, Tovacov	696	710	710	778	710	703	703	693	690	683
Aggregate 4-8, Tovacov	229	233	233	235	233	231	231	228	227	225
Aggregate8-16,Tovacov	547	558	558	563	558	553	553	544	542	537
Stone powder	-	41	20	-	-	-	-	-	-	-
Ground granulated blast furnace slag	179	243	264	225	274	261	251	238	217	195
Fly ash	99	-	-	-	-	-	-	-	-	-
Silica fume	-	-	-	-	10	20	30	40	59	78
Ground limestone fines	-	-	-	-	-	-	-	-	-	-
Admixtur (Sika5– 600)	4,0	4,0	4,0	4,1	4,1	4,0	4,0	4,0	3,9	3,9
Mixing water	199	183	183	174	183	191	191	203	207	215
C-W ratio w [v/(c+m)]	0,29	0,27	0,27	0,27	0,27	0,28	0,28	0,30	0,31	0,32

These treated compound formulas were applied for sample production to test strength an frost resistance (beam : 100 x 100 x 400mm).For verification of resistance against water and defrost elements (CHRL) , testing cubes with the side of 150 mm were produced. Bending strength and tensile compression fraction tests were gradually carried out on the beam. Frost resistance of hardened concrete was observed by the decrease of sample resistance after 75 and 150 freezing cycles [4], and the measurement of concrete water resistance and CHRL in individual steps after 25 freezing cycles in some cases up to the total 250 cycles were carried out(5).

3. OBSERVED FINE FILLERS

To verify concrete mixture properties modified by various types and combinations following materials were used:

- silica fume (SF), Oravské ferozlitiarenské závody, a.s.,Istebné (Slovakai, specific surface 230 568 $cm^2.g^{-1}$
- ground blast furnace slag (GGBS),Kotouč Štramberk, S= 629 $cm^2.g^{-1}$
- ground limestone (L), specific surface 4 857 $cm^2.g^{-1}$
- fly ash (FA), power plant Chvaletice, specific surface 2 426 $cm^2.g^{-1}$
- stone powder (SP), from quarry Zelešice, specific surface 4 345 $cm^2.g^{-1}$

4. TEST RESULTS

The graphical representation of concrete compression strength test results of basic compound formulas set is shown in fig.4.The strength of dispersion after 28 days of maturing (water placing) was cca 40 % of max. measured value depending on the type of applied fine filler. The highest strength was achieved at samples produced from concrete mixture using silica fume as the fine filler (81 MPa after 90 days).

For tensile strength under bending (Fig.5) the dispersion test results of basic compound formulas after 90 days were similar (cca 35 % of max. measured value) and the highest strength was achieved at samples no.II and VI.(7.82 a 7.15 MPa). In graphs representing the comparison of concrete compound formulas show that entire dose of fine filler necessary for achievement of demanded rheological mixture properties is secured by silica fume.

The measurement results in this case confirm preceding experiences, that so high silica fume doses (159 kg/m^3 of fresh concrete) result in massive decrease of concrete durability (see graphs in fig.6 and 7).On the contrary very favorable results from durability point of view showed samples produced from concrete, that contained combination of stone dust removers and ground blast furnace slag as fine fillers. The concrete produced only with slag admixture showed outstanding chemical resistance (3% NaCl solution), but determination results of its frost resistance at higher number of freezing cycles were distinctively worse. Equal results were obtained from frost and chemical resistance point of view from samples where an admixture ground limestone was used.

Graphs of developments of tensile strength under bending and tensile compression at these formulas are shown in figure 11 and 12. From the course of individual curves, it is evident, that expected increase of strength SCC, depending on increasing silica fume dose, did not become apparent. The reason might be on relatively high volumes of ground blast furnace slag applied in these mixtures for achievement of their rheological properties in fresh state. High doses of slag might at least partially suppress the effect of the strength increase of SCC by silica fume .From the graph in the fig.13 on the contrary it is evident considerable effect of

silica fume dose on SCC chemical resistance. Considerable increase of sample damage with 3%NaCl solution occurred when we had higher number of freezing cycles and doses over 10 % of silica fume in SCC (referring to concrete weight). On the contrary, the dose of silica fume no has effect on frost resistance of SCC (fig.14).

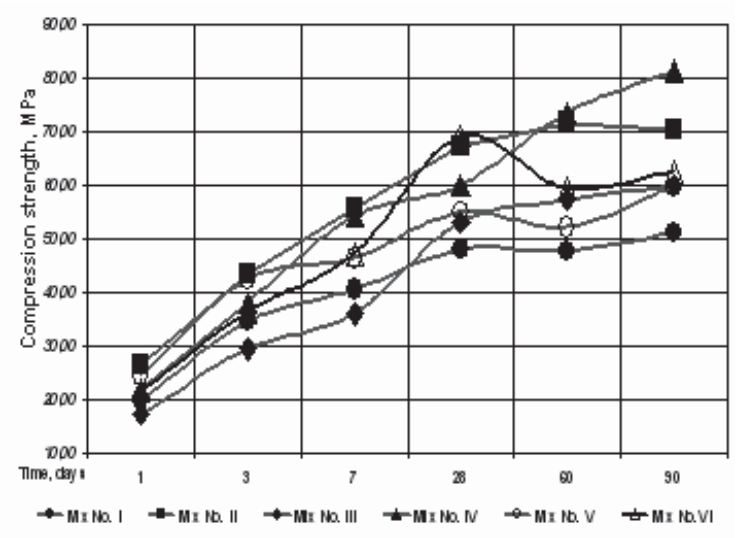

Figure 4. Compressive strength gain with time

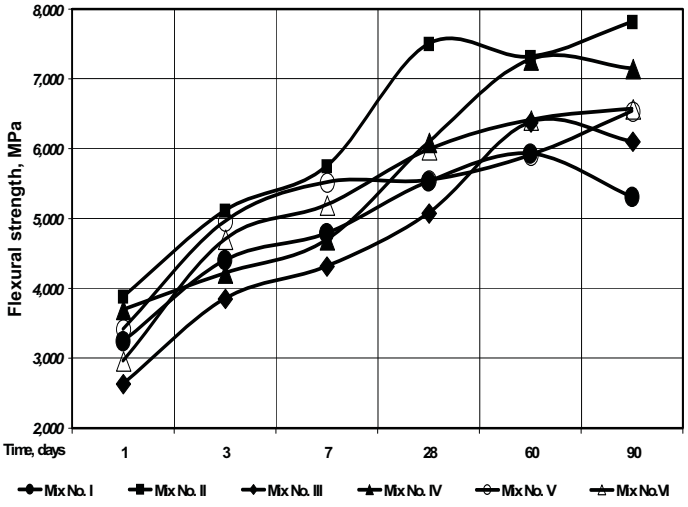

Figure 5. Tensile strength under bending gain with time

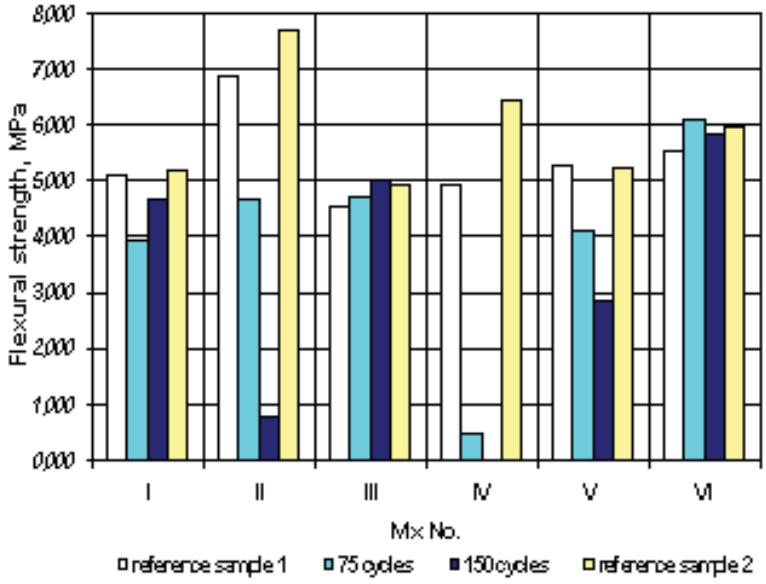

Figure 6. Frost resistance - Tensile strength (8)

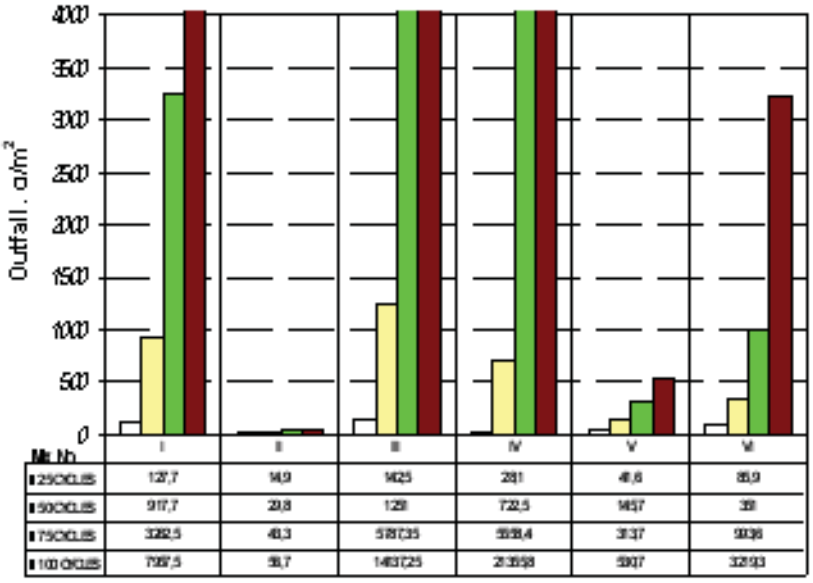

Figure 7. Chemical resistance (3 % NaCl solution) (9)

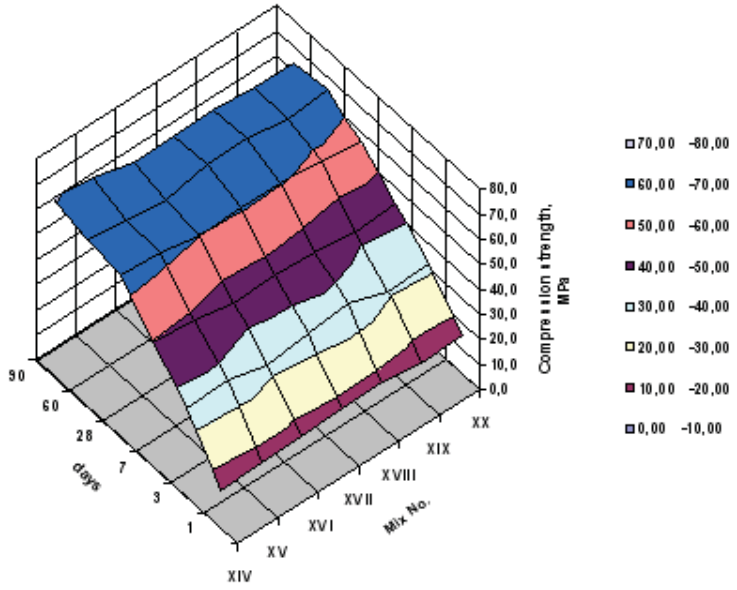

Figure 8. Compressive strength gain with time (11)

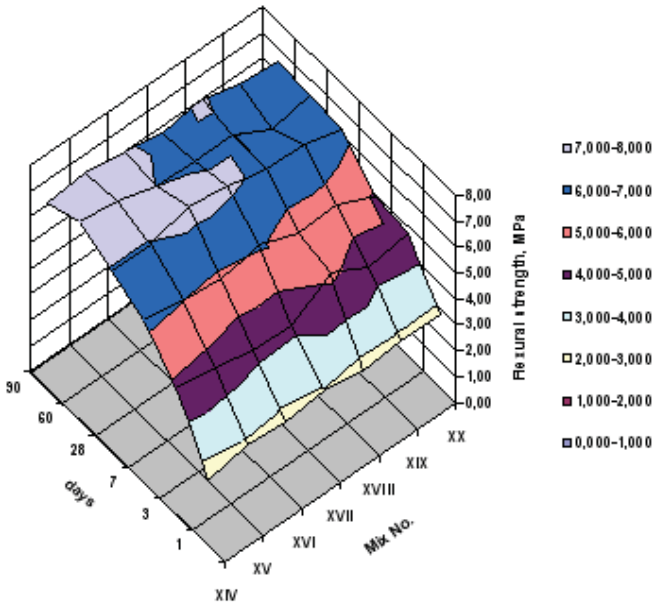

Figure 9. Tensile strength under bending gain with time (12)

5. CONCLUSIONS

The results of the performed tests show that there is a favorable effect of GGBS on strength values SCC as well as on chemical resistance of these concrete. However before concluding on unambiguous positive assessment, in that case it is necessary to wait for final durability (frost) test results.

From frost resistance point of view, the most favorable results of already finished tests, were achieved from compound formulas no.I,III a VI and then all compound formulas observed within assessment of silica fume dose effect on SCC (concrete mixtures no.XIV up to XX).Different frost resistance results at the samples produced from concrete mixtures no.II a XIV (both mixtures contained GGBS as a filler) might be caused by various volumes of blast furnace slag in both compound formulas.

This presumption will have to be verified by other tests. Comparing the compound formulas of concrete mixtures showing the highest frost resistance of produced SCC with the achieved chemical resistance is evident, that the highest durability was achieved at mixtures marked no.V, XIV, XV and XVI. The performed tests results showed that the usage of higher silica fume doses in concrete mixtures is not the best solution from the durability of self compacting point of view.

Foreign experiences and the performed tests results show that optimization of SCC proportion with consideration of demanded properties of fresh concrete mixture and resulting properties of hardened concrete require complete knowledge of individual characteristic of concrete mixture components in the course of all technological cycle of concrete production. E.g according to American experience, durability of SCC using fly ash as filler is possible to be increased by concrete mixture aeration.

In that case it is however necessary to pay high attention to their rheological properties because higher air content influences mobility of mixtures as well as its other properties. As fine filler in the Czech Republic for utilization in SCC seems to be highly perspective combination GGBS with stone powder, respectively with fly ash, when taking into consideration the current prices.

To evaluate concrete resistance to aggressive medium (chlorides in this instance - 12 months evaluation time period according to the CSN 73 1340 Standard) there is necessary to ensure that no one parameter under monitoring shall decrease during this interval.

Acknowledgements

In this article results of a research intention MD ČR 0-44994575 are presented: Sustainable transport - chance for the future and the financial support of the

Ministry of Education, Youth and Sports, project No. 1M680470001, within activities of the CIDEAS research centre.

References

1. Publication NO. FHWA-RD-00-025: Portland-Cement Concrete Rheology and Workability: Final Report, Federal Highway Administration, November 2001
2. Publication NO. 1574: Materials and Construction. Advances in Concrete and Concrete Pavement Construction. Transportation Research Board, National Research Council, Washington D.C., 1997
3. CSN EN 12350-2 Testing fresh concrete – Part 2: Slump test
4. ČSN 73 1322 Determination of frost resistance of concrete
5. ČSN 73 1326 Resistance of cement concrete surface to water and defrosting chemicals

"Computational Civil Engineering 2006", International Symposium
Iaşi, România, May 26, 2006

Boundary element method numerical modeling of RC plane stress cracked plate

M. Minch and A. Trochanowski

Institute of Civil Engineering
Technical University of Wroclaw
pl. Grunwaldzki 11, 50-377 Wrocław, Poland

Summary

In this paper different methods of distribution solution of RC cracked of the plane stress plates are shown. The differential equation of the cracked plates, using the classical variational method of Lagrange is worked out. The displacements equations with the boundary conditions and compatibility conditions in the crack are obtained. The total differential equations in the class of the two-dimensional general vector functions are shown. In this model the effect of discontinuity general deformation vector is taken into account. As the next the viscoelastic plate model has been derived by the variational method of Gurtin in the space of general function. The numerical results of an approximate method of solutions with boundary element method are shown.

1. INTRODUCTION

The RC concrete plates are non-homogeneous. Therefore the response of so heterogeneous structures and additionally defects caused by cracks in concrete to applied actions is generally nonlinear, due to nonlinear constitutive relationships of the materials, known as mechanical nonlinearity and to second order effects of normal forces, known as geometrical nonlinearity. Regard of defects in form of cracks treated as continuous functions, which are usually based on the continuum mechanics approach, gives unsatisfied solution because of summation of assumption errors and solution errors. Therefore the proper mathematical modeling of plate is so important since the final error appears solely in solution phase.

This paper contains a mathematical model of a reinforced concrete plane stress plate formulated in terms of general functions. The physical hypothesis about discontinuous change of displacement vector, caused by cracking of extension zone in the concrete, was taken in the model. Such assumptions and first investigation for distribution model of RC beam with cracks were made by Borcz in 1963 [1]. This paper expands distribution beam Borcz's model for RC cracked plane stress plates.

The assumption of distribution theory of Schwartz [2] affords possibilities for precise mathematical description of discontinuity of the plate. Fundamental for understanding of the next consideration are the general distributions of Dirac's-δ with given density on the curve $\Lambda \in R^2$ and following properties:

$$\langle \mathbf{y}\, \delta_\Lambda, \mathbf{j} \rangle = \int_\Lambda \mathbf{y}(\mathbf{x})\mathbf{j}(\mathbf{x}) d\Lambda \text{ , where } \mathbf{x} = (x_1, x_2) . \tag{1}$$

$$\left\langle D^\alpha(\boldsymbol{\chi}(\mathbf{x})\delta_\Lambda), \boldsymbol{\varphi}(\mathbf{x}) \right\rangle = (-1)^{|\alpha|} \int_\Lambda \boldsymbol{\chi}(\mathbf{x}) D^\alpha \boldsymbol{\varphi}(\mathbf{x}) d\Lambda \text{ , where } \alpha = (\alpha_1 + \alpha_2) \text{ , } |\alpha| = \alpha_1 + \alpha_2 . \tag{2}$$

Here the functions $\boldsymbol{\psi}(\mathbf{x})$, $\boldsymbol{\varphi}(\mathbf{x})$ and $\boldsymbol{\chi}(\mathbf{x})$ are continuous functions on the curve Λ in the space R^2 .

The functionals formulated above for unitary density of function $\boldsymbol{\psi}(\mathbf{x})$ and $\boldsymbol{\chi}(\mathbf{x})$ have the analogue filtering property as for the general distribution of Dirac's-δ. It means that the $\boldsymbol{\psi}(\mathbf{x})$ and $\boldsymbol{\chi}(\mathbf{x})$ have the value of function $\boldsymbol{\varphi}(\mathbf{x})$ or its derivatives respectively for the arguments $\mathbf{x}$ belong to the curve Λ .

The arbitrary plane stress plate is considered. The plate has arbitrary homogeneous boundary conditions and is arbitrary forced, see fig. 1. The region of plate Ω is divided by the curve Λ, means the crack, in two zones Ω_1 and Ω_2 with bound $\partial\Omega_1$ and $\partial\Omega_2$. The curve Λ has two ends Λ_1 and Λ_2. The normal external direction cosines of edge Λ of regions Ω_1 and Ω_2 have different sign. The considered model can be easy generalized to any amount of cracks Λ.

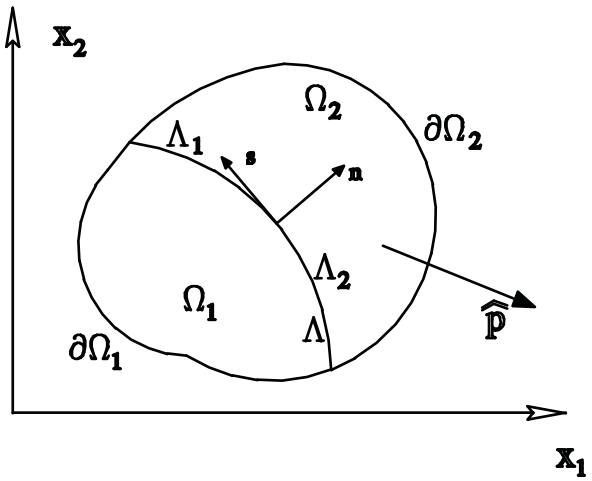

Fig. 1. Scheme of plane stress plate with crack Λ

2. DIFFERENTIAL EQUATION FOR DISPLACEMENT

The discontinuous variational problem of surface integral for displacement was solved. The equilibrium equations, constitutive law and strain equations are assumed to be represented by well-known theory of elasticity relations. We are looking for the extreme of the functional of strain energy U_s with set of permissible displacement value $\mathbf{u}(\mathbf{x})$, where $\mathbf{b}(\mathbf{x})$ means body forces:

$$J[\mathbf{u}(\mathbf{x})] = \int_{\Omega} U_s(\mathbf{u}(\mathbf{x}))d\Omega - \int_{\Omega} \mathbf{b}(\mathbf{x})\mathbf{u}(\mathbf{x})d\Omega - \int_{\partial\Omega} \mathbf{p}(\mathbf{x})\mathbf{u}(\mathbf{x})d\partial\Omega, \tag{3}$$

where $\mathbf{u}(\mathbf{x})$ means displacement vector and $\mathbf{b}(\mathbf{x})$ body forces respectively. The searching function $\mathbf{u}(\mathbf{x})$ is in the class of function $\mathbf{u} \in C^2(\Omega/\Lambda)$ (for $\mathbf{x} \in \Lambda$ function $\mathbf{u}(\mathbf{x})$ has singularity).

Applying Green's transformation with well known relations stress-strain-displacement **S**-**E**-**u** we obtain differential equation of plate in plane stress:

$$\mu(\nabla^2 + \frac{3\lambda + 2\mu}{\lambda + 2\mu}\, grad\, div)\, \mathbf{u}(\mathbf{x}) + \mathbf{b}(\mathbf{x}) = 0\ , \tag{4}$$

associated with combination of elementary boundary conditions:

$$\widetilde{\mathbf{P}}(\mathbf{u}(\mathbf{x})) = \mathbf{p}(\mathbf{x})\ , \qquad \text{for } \mathbf{x} \in \Omega_1 \cup \Omega_2\ , \tag{5}$$

and compatibility condition in the crack:

$$[\widetilde{\mathbf{P}}(\mathbf{u}(\mathbf{x}))]_{\Lambda} = 0\ , \qquad \text{for } \mathbf{x} \in \Lambda_1\Lambda_2\ , \tag{6}$$

where λ and μ are Lame' constants, $\widetilde{\mathbf{P}}$ means operator of surface tension:

$$\widetilde{\mathbf{P}}(.) = \mu(\widetilde{\nabla} + \frac{2\lambda}{\lambda + 2\mu}\, \mathbf{1}\, div)(.)\mathbf{n}\ , \tag{7}$$

where **1** is a unitary tensor, whereas **n** represents normal vector external to the edge $\partial\Omega$.

Here [.]$_\Lambda$ means difference of left and right side limit of expression in square braces on the curve Λ.

Constitutive law of defect is assumed to be represented as follows (see beam analogy of Borcz [1]):

$$[\mathbf{u}(\mathbf{x})]_{\Lambda_1\Lambda_2} = \mathbf{r}(\mathbf{x}) , \text{ with condition } \frac{\partial \mathrm{r}}{\partial \mathrm{s}}(\Lambda_1) = \frac{\partial \mathrm{r}}{\partial \mathrm{s}}(\Lambda_2) = 0 . \tag{8}$$

Here $\mathbf{r}(\mathbf{x})$ means density of defect as a continuous function for $\mathbf{x} \in \Lambda_1\Lambda_2$ and $[\mathbf{u}]_\Lambda = 0$ for $\mathbf{x} \notin \Lambda_1\Lambda_2$. Equation (8) satisfies compatibility condition in the crack, where the displacement vector has a jump on a bound of crack. Here the assumption of internal crack $\Lambda_1\Lambda_2$ was taken. This can be easy proved. Hence on the remaining part of curve Λ the condition $[\mathbf{u}]_\Lambda = 0$ yields, for $\mathbf{x} \notin \Lambda_1\Lambda_2$. Moreover the second condition (8) in the essential way completes the definition of the defect.

It can be easily shown that using Eq. (1)-(2) and Eq. (5)-(8) differential equation (4) has the following form (see [3]).

$$\mu\left\langle (\nabla^2 + \frac{3\lambda + 2\mu}{\lambda + 2\mu}\ grad\ div)\mathbf{u}(\mathbf{x}), \boldsymbol{\varphi} \right\rangle + \left\langle \mathbf{b}(\mathbf{x}), \boldsymbol{\varphi} \right\rangle = \int_{\partial\Omega} [\mathbf{u}(\mathbf{x})\widetilde{\mathbf{P}}(\boldsymbol{\varphi}) + (\mathbf{p}(\mathbf{x}) - \widetilde{\mathbf{P}}(\mathbf{u}(\mathbf{x}))\boldsymbol{\varphi}] d\partial\Omega +$$

$$+ \int_{\Lambda_1\Lambda_2} \mathbf{r}(\mathbf{x})\widetilde{\mathbf{P}}(\boldsymbol{\varphi}) d\Lambda . \tag{9}$$

Using functional way of description with distribution in form of Dirac's-δ we can write final general differential equation of RC cracked plate in plane stress, appropriate boundary and compatibility conditions in the crack respectively:

$$\mu(\nabla^2 + \frac{3\lambda + 2\mu}{\lambda + 2\mu}\ grad\ div)\mathbf{u}(\mathbf{x}) = -\widetilde{\mathbf{P}}(\mathbf{r}(\mathbf{x})\delta_\Lambda) + (\mathbf{p}(\mathbf{x}) - \widetilde{\mathbf{P}}(\mathbf{u}(\mathbf{x}))\delta_{\partial\Omega_1} + \widetilde{\mathbf{P}}[(\widetilde{\mathbf{u}}(\mathbf{x}) - \mathbf{u}(\mathbf{x}))\delta_{\partial\Omega_2}]$$

$$\tag{10}$$

where $\mathbf{b}(\mathbf{x})$ was taken in following form: $\mathbf{b}(\mathbf{x}) = \widetilde{\mathbf{P}}(\widetilde{\mathbf{u}}(\mathbf{x}))\delta_{\partial\Omega_2}$.

The assumption of the jump of displacement vector $\mathbf{u}(\mathbf{x})$ was proved by experimental study [1]. Density of defect also known as constitutive law of crack opening, is the function of tension vector $\mathbf{N}$ acting in the crack:

$$\mathbf{r}(\mathbf{x}) = \mathbf{r}^0(\mathbf{x}) - \mathbf{r}^1(\mathbf{x})\Im(\mathbf{N}(\mathbf{x}))\big|_{\Lambda} \quad , \quad \mathbf{x} \in \Lambda_1\Lambda_2 \quad . \tag{11}$$

Here $\mathbf{r}^0$ describes residual general deformations whereas $\mathbf{r}^1\Im(\mathbf{N})$ elastic general deformations respectively.

The zone of plate Ω_1 is connected with another one Ω_2 by means of reinforcement bars appearing in the cracks. So, the edges of the cracks are not free from tensions at the points of connections.

The components **r** of Eq. (11) are given from RC element tests as well as from general assumption of crack theory and equilibrium conditions in the crack.

Using definition of convolution and Green function satisfying equation $\Delta\Delta\mathbf{G}(\mathbf{x}) = \delta(\mathbf{x})$ the solution of Eq. (10) is described in following form:

$$\mathbf{u}(\mathbf{x}) = \int_{\Lambda_1\Lambda_2} [\mathbf{r}^0(\mathbf{y}) + \mathbf{r}^1(\mathbf{y})\Im(\mathbf{N})]\widetilde{\mathbf{P}}(\mathbf{G}(\mathbf{x},\mathbf{y}))d\Lambda +$$

$$+ \int_{\partial\Omega} \{\widetilde{\mathbf{P}}(\mathbf{G}(\mathbf{x},\mathbf{y}))[\mathbf{u}(\mathbf{y}) - \tilde{\mathbf{u}}(\mathbf{y})] - \mathbf{G}(\mathbf{x},\mathbf{y})[\widetilde{\mathbf{P}}(\mathbf{u}(\mathbf{y})) - \mathbf{p}(\mathbf{y})]\} d\partial\Omega \quad . \tag{12}$$

Here the curvilinear integrals for the edge Λ can be interpreted as a some external force modeling the defect. It can be proved [3] that for plane stress these integrals are the normal and tangential dipole forces cause the jump of displacement vector in the crack. The acting forces are self-balanced and do not cause the increments of external loading of construction.

The final solution of singular integro-differential Eq. (12) describes an accurate mathematical model of cracked RC in plane stress.

The presented solution includes the discontinuity of general deformations in the crack places and simultaneously satisfying continuity of general tension vector on both sides of the defect Λ. Such formulated model of RC cracked plate will be solved with the help of boundary element method (BEM).

3. DIFFERENTIAL EQUATION OF VISCOELASTIC PLATE

The same way as in chapter 2 was applied to describe solution of viscoelastic plane stress plate. The equilibrium equations in form: *div* **S** + **b** = **0**, and geometrical relations in form: $\mathbf{E} = \frac{1}{2}(\nabla\mathbf{u} + \nabla\mathbf{u}^{\mathbf{T}}) = \widetilde{\nabla}\mathbf{u}$.

The set of field equations is fulfilled in the space $\Omega \times [0,\infty)$, where $[0,\infty)$ is time interval. The initial condition of strains' tensor has to be added $\mathbf{E}(\,.\,,0) = \mathbf{E}^0$, for $t = 0$.

The physical law well known as Boltzmann type is taken in following form:

$$\mathbf{1}*\mathbf{S} = \psi_1 * \mathbf{E} + \frac{1}{2}(\psi_2 - \psi_1)*\mathbf{1}\ tr\ \mathbf{E} - \mathbf{F}\ , \quad \text{where:} \tag{13}$$

$$\mathbf{F} = \psi_1 * \mathbf{E}^0 + \frac{1}{2}(\psi_2 - \psi_1)*\mathbf{1}\ tr\ \mathbf{E}^0\ , \tag{14}$$

with convolution rule: $f(t)*g(t) = \int_0^t f(t-\tau)g(\tau)d\tau$. Here the functions ψ_1 and ψ_2 are the functions of relaxation.

The discontinuous viscoelastic variational problem of Gurtin type, in the some way as considered in chapter 2, was solved. The equilibrium equations, Boltzmann constitutive law, strain equations and initial condition are assumed to be represented by well-known theory of elasticity relations.

Analogue to the functional (3) we are looking for the extreme of the functional of strain energy U_v with set of permissible displacement value **u**(**x**):

$$J[\mathbf{u}(\mathbf{x},t)] = \int_\Omega U_v(\mathbf{u}(\mathbf{x},t))d\Omega - \int_\Omega \mathbf{1}*\mathbf{b}(\mathbf{x},t)*\mathbf{u}(\mathbf{x},t)d\Omega - \int_{\partial\Omega} \mathbf{1}*\tilde{\mathbf{p}}(\mathbf{x},t)*\mathbf{u}(\mathbf{x},t)d\partial\Omega\ , \tag{15}$$

Applying Green's transformation with material and field relations we obtain differential equation of plate in plane stress:

$$\mathbf{1}*\mathbf{S} = \psi_1 * \mathbf{E} + \frac{1}{2}(\psi_2 - \psi_2)*\mathbf{1}\ tr\ \mathbf{E} - \mathbf{F}\ , \tag{16}$$

associated with combination of elementary boundary conditions for free and fixed edges respectively:

$$[\widetilde{\mathbf{P}}(\mathbf{u}(\mathbf{x})) - \mathbf{1} * \widetilde{\mathbf{p}}(\mathbf{x})]\Big|_{\partial\Omega_1} = 0 \quad \vee \quad \delta\mathbf{u}(\mathbf{x})\Big|_{\partial\Omega_2} \quad , \tag{17}$$

and compatibility condition in the crack:

$$[\widetilde{\mathbf{N}}(\mathbf{u}(\mathbf{x},t))]_{\Lambda} = 0 \ , \qquad \text{for } \mathbf{x} \in \Lambda_1\Lambda_2 \ , \tag{18}$$

where $\widetilde{\mathbf{N}}$ means viscoelastic operator as the analogy of surface tension from theory of elasticity:

$$\widetilde{\mathbf{P}}(.) = \mu(\widetilde{\nabla} + \frac{2\lambda}{\lambda + 2\mu}\ \mathbf{1}\ div)(.)\mathbf{n} \ , \tag{19}$$

Taking constitutive law of cracks (8) and applying functional way of description with δ of Dirac's type, the final general differential equation of viscoelastic RC cracked plate in plane stress, appropriate boundary, compatibility and initial conditions respectively, can be written as follows:

$$\begin{aligned} &[\psi_1 * \nabla^2 + \frac{1}{2}(\psi_1 + \psi_2) * grad\ div]\mathbf{u}(\mathbf{x},t) + \mathbf{1} * \mathbf{b}(\mathbf{x},t) - div\ \mathbf{F} = \\ &= -\widetilde{\mathbf{N}}(\mathbf{r}(\mathbf{x},t)\delta_{\Lambda}) + [\mathbf{1} * \widetilde{\mathbf{p}}(\mathbf{x},t) - \widetilde{\mathbf{N}}(\mathbf{u}(\mathbf{x},t))]\delta_{\partial\Omega_1} + \widetilde{\mathbf{N}}[(\widetilde{\mathbf{u}}(\mathbf{x},t) - \mathbf{u}(\mathbf{x},t))]\delta_{\partial\Omega_2} \ . \end{aligned} \tag{20}$$

Here the constitutive law of crack opening is expanded as a rule valid additionally in time. Note, that the final solution (20) is similar to elastic solution (10), difference occurs only for relaxation function with λ and μ as a time depended function.

The solution of Eq. (20) is possible with help of elastic solution as a first approximation of viscoelastic solution. It denotes the solution of "associated" elastic problem $\mathbf{u}(\mathbf{x},t)$ from Eq. (12) can be used to convolutions' solution of viscoelastic static problem of RC cracked plain stress as follows:

$$\mathbf{u}(\mathbf{x},t) = \int_0^t \frac{\partial\mathbf{u}(\mathbf{x},\tau)}{\partial\tau}\ \varphi(t-\tau)d\tau \ , \tag{21}$$

where φ is the function with the combination of relaxation and creep functions.

4. MODELING BY BOUNDARY ELEMENT METHOD

Deformation behaviour depends on the history of the loading as well as nonlinearity of material properties. Hence, equations and definitions of the boundary element method in rate form according to the Brebbia [4] formulations were assumed. According to small strains' theory, total strain rate for inelastic problem can be divided into an elastic and inelastic part of total strain rate tensor respectively. Herein, the inelastic strains mean any kinds of strain field that can be considered as initial strains, that is, plastic or viscoplastic strain rate, creep strain rate, thermal strain rate and strain rate due to other causes. So now, we can write (see also [3]) the equations of considered problem with non-linear BEM formulations for fictitious traction vector **p** and body forces **b**, finally leading to initial stresse $\boldsymbol{\sigma}^{\mathrm{p}}$:

$$\mathbf{H}\dot{\mathbf{u}} - \mathbf{A}\dot{\mathbf{p}} = \mathbf{B}\dot{\sigma}^{p} + \mathbf{F}\dot{\mathbf{x}} + \dot{\mathbf{Q}}\ (\dot{\mathbf{x}}) \quad , \tag{22}$$

where: **u** - displacement vector,
X - vector of unknown edge traction,
p - vector of fictitious traction,
$\boldsymbol{\sigma}^{\mathrm{p}}$ - vector of initial stresses,
H, **A** - the same matrices as for elastic analysis,
B - matrix due to the inelastic stress integral,
F - matrix refers to the fundamental function cause by forcing traction with vector **X**, that is, modeling density of crack opening for plane stress ,
Q - matrix of bond, bond-slip relations and other displacements due to aggregate interlock and dowel action of reinforcement in the crack, related to displacement **u**.

5. THE INCREMENTAL COMPUTATIONS

The results' correctness depends on the choice of right type boundary or finite elements respectively and a careful discretization of the structure. The influence of the above on the problem to be studied cannot be neglected. The appropriate simulation of the load-carrying behavior of RC structure is more important then the accuracy of the numerical calculations. The question what kind of numerical methods, boundary or finite elements should be preferably chosen cannot be

answered satisfactorily. Equations (22) must be solved numerically with iterative and incremental techniques. Iteration results due the fact that the right sides of equations depend directly on searching functions. In addition searching functions depend indirectly on physical law. The incremental computation is caused by rate form of Eq. (22). For iteration and incremental computations the modified Newton-Raphson method was applied.

For the computation of plate the behaviour of concrete is taken as well known stress-strain Madrid parabola. The stress-strain relation of steel bars was taken as a well-known elasto-plastic relation from uniaxial tests.

The creep of concrete was taken from the Bažant's [5] rheological model. This model is most suitable for concrete structures because the parameters can be calculated only from the concrete composition (for basic and drying creep as well as shrinkage). The creep function of Bažant is shown below (f_c' means the 28 days compressive strength of concrete):

$$J(t,\tau) = \frac{1}{E_o(f_c')}[1 + \varphi_1(f_c')(\tau^{-m(f_c')} + \alpha)(t-\tau)^{n(f_c')}] \tag{23}$$

After cracking of concrete, the tensile forces in the cracked area are transmitted by bond to the reinforcement consisting of steel bars. Along the segments of broken adhesion the steel bar co-operates with the concrete trough the tangential stresses distributed on the perimeter of the bar. The slip is defined as a relative displacement between reinforcement bars and surrounding concrete. The increment of tensile stresses in the steel bar was approximated by the third-degree curve. Hence, the tangential stresses and bond-slip relationships, as representation of the stiffness of the bond has been found to be in the agreement to tests of Dörr [6], (that is, the second-degree distribution along the segment l_f , where l_f means distance between cracks).

The time-dependence of bond in the loaded state exhibits a similar behavior as concrete in compression (see [7]). The presupposition similar to the linear creep theory of concrete in compression is used for bond creep with bond creep coefficient φ_b. Naturally, in accordance to τ-Δ relationship of Dörr [6], bond creep cannot be described with linear theory. The model of Rotasy [7] was applied to describe the creep of the bond in the cracked concrete.

The development of "rotating cracks" is considered as single cracks treated as the boundary element where the direction of the crack has to be assumed in accordance with the previous step of the main direction of the tensile stresses.

A program for Boundary Element Analysis named PLATE for planar structure was designed. The route through a PLATE analysis includes following procedures is shown below:

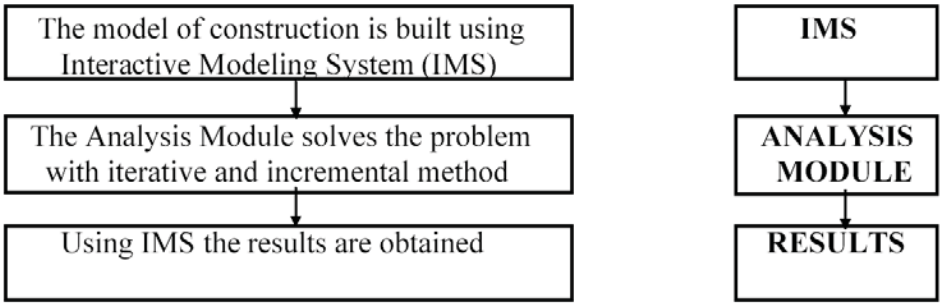

The way of applying iterative and incremental technique in the Analysis Module is shown below in the block diagram:

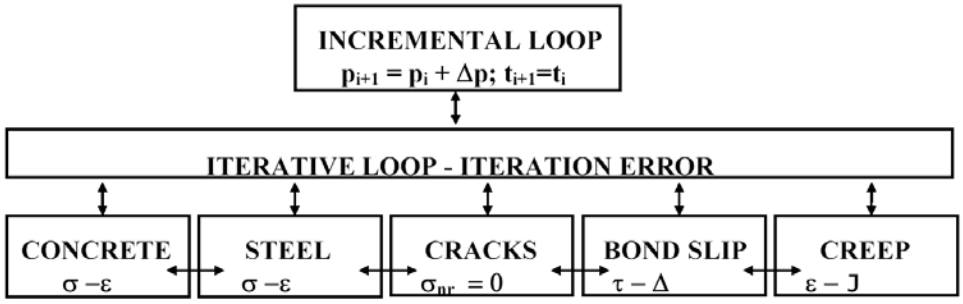

6. NUMERICAL EXAMPLE

The results of simply supported square panel WT3, tested by Leonhardt and Walther [8], were taken to check BEM solution for plain stresses. The panel was reinforced horizontally in different way for bottom and top part. The bottom zone (Ra_1) had 2ϕ8 mm bars each 6 cm fixed in 4 rows, the top zone and vertical bars (Ra_2) were 2ϕ5 mm each 26 cm.

In Fig.2 the experiment received load-midspan deflection relation of the panel as compared to the results of BEM and other authors ([9] and [10]) FEM numerical calculations.

Fig.3 shows the dependence of the time and loading levels on the crack width a_f for panel WT3.

7. CONCLUSIONS

The numerical results obtained for the problems of panels indicated that the presented methods are capable to predict sufficiently and satisfactorily response of reinforced concrete planar structure.

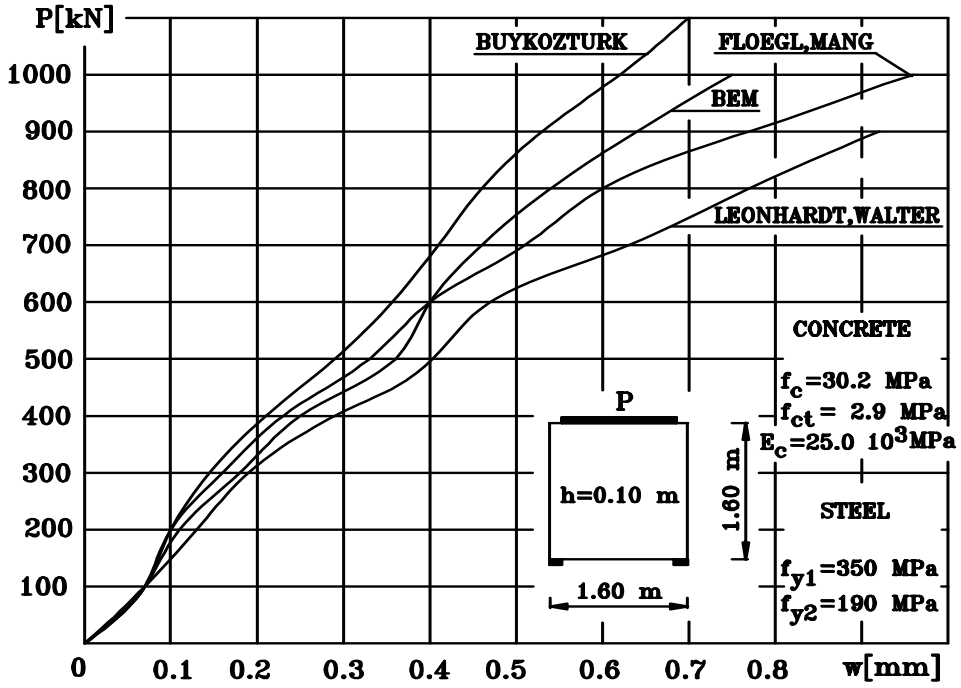

Fig.2. Comparison of calculated load-midspan deflection relations with the test result of panel WT3 [8].

For the computation of planar structure the behavior of concrete should be considered in the biaxial domain. The concrete properties are influenced by many different factors. Therefore the biaxial stress-strain relation and the failure criterion of concrete depend on the results of the tests that are performed to obtain these relations. The biaxial tests of Kupfer [11] for short time loading and proportionally increasing load proved to be the most reliable. Different authors have used these test results to develop analytical formulation of the failure and deformation behavior of the concrete. Link [12] developed an incremental formulation for the tangent stiffness of the concrete on the basis of Kupfer's tests. The stresses are normalized in terms of the uniaxial cylinder strength; therefore the formulation can be used for different grades of concrete. The failure criterion cannot be used as plasticity condition, because it describes a boundary for the maximum stresses and does not allow any statements about the plastic deformations.

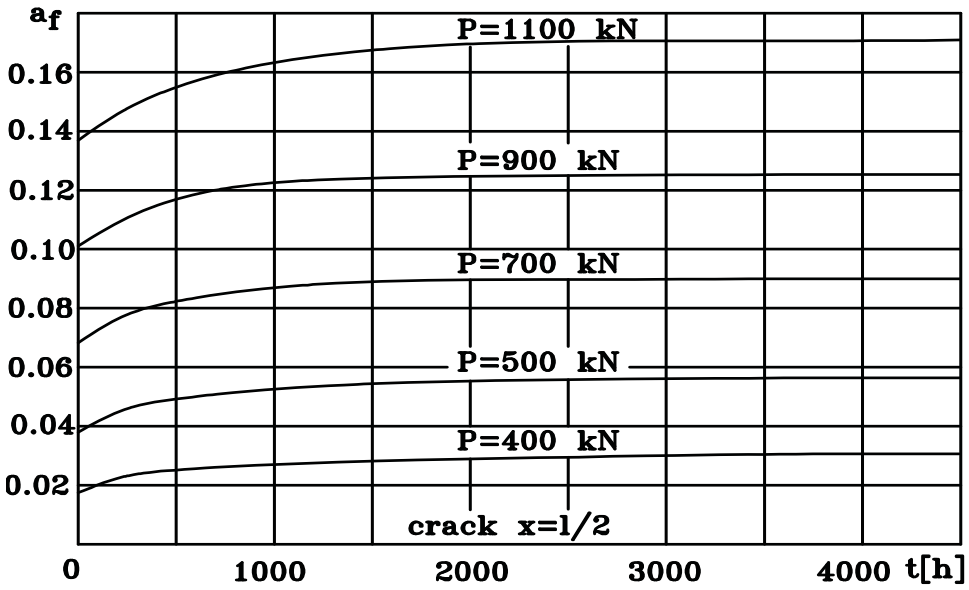

Fig. 3. The dependence of the time and loading levels on the crack width a_f for x=l/2.

The problem of crack propagation can be solved by evaluating Rice's integral along the contour of the crack top zones, where for different specimens the stress intensity factor could be found (see [13]).

Reference

1. BORCZ, A. - *"Podstawy teorii zarysowanych płyt żelbetowych"*. TNEB, Warszawa, 1963.
2. SCHWARTZ, L. - *"Theorie des distributions"*. Paris, 1966.
3. MINCH, M. - Boundary Element Analysis of RC Slabs and Panels. *Proceedings of the Twenty-Fourth Midwestern Mechanics Conference*, Iowa State University, Iowa USA, ISU-ERI-Ames-95002, Developments in Mechanics, **18**. 81-84 (1995).
4. BREBBIA, C. A., TELLES, J. and WRÓBEL, L. - *"Boundary element techniques - theory and applications in engineering."* Springer Verlag, Berlin - New York, 1984.
5. BAŽANT, Z. and PANULA, L. - Practical prediction on time-dependent deformations of concret,. *Mater. and Struct. Res. and Testing*, **11(65)**, 307-329 (1978).
6. DÖRR, K., and MEHLHORN, G. - Berechnung von Stahlbetonscheiben im Zustand II bei Annahme eines wirklichekeitsnahen Werkstoffverhaltens., *Forschungsberichte aus dem Institut für Massivbau der Technischen Hochschule Darmstadt*, H.**39**, (1979).
7. ROTASY, F.S. and KEEP, B. - *"Untersuchung der zeit- und lastabhängigen Schlupfentwicklung von einbetonierten Bewehrungsstählen"*. Institut für Bausoffe, Massivbau und Brandschutz, TU Braunschweig, 1982.
8. LEONHARDT, and F., WALTHER, R. - *"Wandartige träger"*. Deutscher Ausschuss für Stahlbeton, H. **178**, Verlag Wilhelm Ernst & Sohn, Berlin, 1966.

9. BUYKOZTURK, O. - Nonlinear analysis of reinforced concrete structures., *Computers and Structures*, **7**, 149-156 (1977).
10. FLOEGL, H. and MANG, H. A. - On tension stiffening in cracked reinforced concrete slabs and shells considering geometric and physical nonlinearity., *Ing-Arch.,* **51**, 215-242 (1981)
11. KUPFER, H. - Das Verhalten des Betons unter mehrachsiger Kurzzeitbelastung unter besonderer Berücksichtigung der zweiachsigen Beanspruchung, *Deutscher Ausschuss für Stahlbeton,* **229**, 269-274 (1973).
12. LINK, J. - Eine Formulierung des zweiaxialen Verformungs- und Bruchverhaltens von Beton und deren Anwendung auf die wirklichkeitsnahe Berechnung von Stahlbetonplatten., *Deutscher Ausschuss für Stahlbeton*, **270**, (1976).
13. MINCH, M. and TROCHANOWSKI, A. - The numerical model for reinforced concrete structure., *Creep and Coupled Processes*, IVth International Symposium, Bialystok, Poland, 173-178 (1992).

"Computational Civil Engineering 2006", International Symposium
Iaşi, România, May 26, 2006

The numerical model for reinforced concrete structures and analysis using finite elements method

M. Minch and A. Trochanowski

Institute of Civil Engineering
Technical University of Wroclaw
pl. Grunwaldzki 11, 50-377 Wrocław, Poland

Summary

The purpose of this paper is to review model for finite element techniques for non-linear crack analysis of reinforced concrete beams and slabs. The non-linear behavior of concrete and steel were described. Some calculations of "self-stress" for concrete and reinforced concrete beam was made. Current computational aspects are discussed. Several remarks for future studies are also given.

The numerical model of the concrete and reinforced concrete was described. The paper shows the results of calculations on a reinforced concrete plane stress panel with cracks. The non-linear, numerical model of calculations of reinforced concrete was assumed. Using finite elements method some calculations were made. The results of calculations like displacements, stresses and cracking are shown on diagrams. They were compared with experimental results and other finding. Some conclusions about the described model and results of calculation are shown.

1. NON-LINEAR BEHAVIOR OF CONCRETE AND STEEL

Reinforced concrete structures exhibit very complicated behavior different from steel structures. The structural system is composed of different materials, such as cement, steel bars, aggregate etc. Moreover each material shows various physical phenomena.

The non-linear behavior of entire structures can be considered to be accumulated from cracking of concrete, non-linear material properties of concrete under compression, time-dependent deformations due to creep and shrinkage, bond behavior, yielding and strain hardening of steel essentially. Progressive cracking of concrete is surely the most important component of the non-linear response of reinforced concrete structures in normal service state.

The experiments [3,4] show that under cyclic loads concrete and reinforced concrete structures response like linear-elastic materials. The linear-elastic behavior of concrete elements under cyclic loads is the base to assume that total deformations is the sum of elastic, residual, plastic and creep deformations as show on Fig. 1.

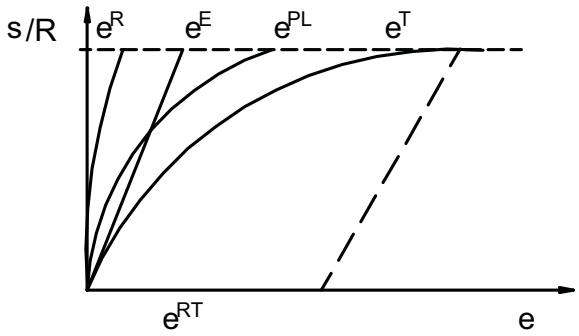

Fig. 1. Stress-strain relationship for concrete.

The total residual ε^{RT} deformation is the sum:

$$\varepsilon^{RT} = \varepsilon^{R} + \varepsilon^{PL} + \varepsilon^{R\varphi} \tag{1}$$

where:

ε^{RT} - residual deformation,
ε^{PL} - plastic deformation,
$\varepsilon^{R\varphi}$ - creep deformation.

The creep deformation described using Rush [2] theory. It was assumed that residual creep deformation is 80% of total. The non-linear residual ε^{R} deformation, because of plane cross section, gives "self-stress" σ^{R} inside the element:

$$\int \sigma^{R}\, dF = 0, \qquad \int \sigma^{R} z\, dF = 0 \quad . \tag{2}$$

Using the equilibrium of forces and moments in the cross section (Eq. 2), the constants A, B and "self-stress" was calculated:

$$\sigma^{R} = E_b \varepsilon^{ED} = E_b (A + Bz - \varepsilon^{R}) \tag{3}$$

We can write the total stress as a sum of self-stress σ^R and easy to obtain linear elastic stress σ^E:

$$\sigma^{RT} = \sigma^R + \sigma^E \tag{4}$$

The steel reinforcement is stressed only in one direction. The material is represented by a bilinear model which may either be elastic - perfectly plastic or strain-hardening as shown in Fig. 2.

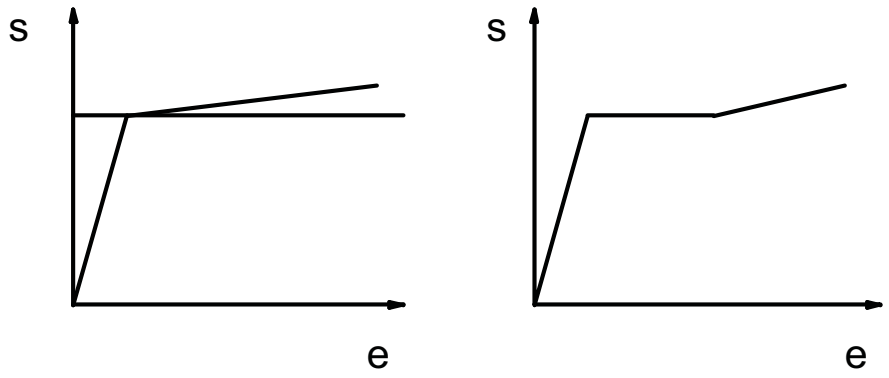

Fig. 2. Stress strain model for steel.

2. SELF-STRESS IN CONCRETE ELEMENT

The self-stress was calculated for bending concrete beam Fig. 3.

The course of residual strain was assumed as known and described:

$$\varepsilon^R = \begin{cases} -kz^6 & \text{for } z<0 \\ kz^6 & \text{for } z>0 \end{cases}, \tag{5}$$

where: $z = \sigma / R_{bk}$ for $\sigma<0$,

$z = \sigma / R_{bzk}$ for $\sigma>0$.

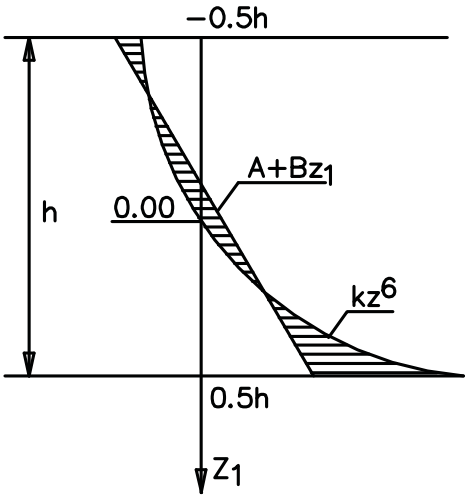

Fig. 3. Self-stress in concrete beam.

Using the equilibrium of forces and moments (Eq. 2) the constants A, B was calculated:

$$\int \sigma^R \, dF = \int \left[A + Bz_1 - \varepsilon^R(z_1) \right] b \, dz_1 = 0 \quad , \tag{6}$$

$$\int \sigma^R z_1 \, dF = \int \left[A + Bz_1 - \varepsilon^R(z_1) \right] b z_1 \, dz_1 = 0 \quad ,$$

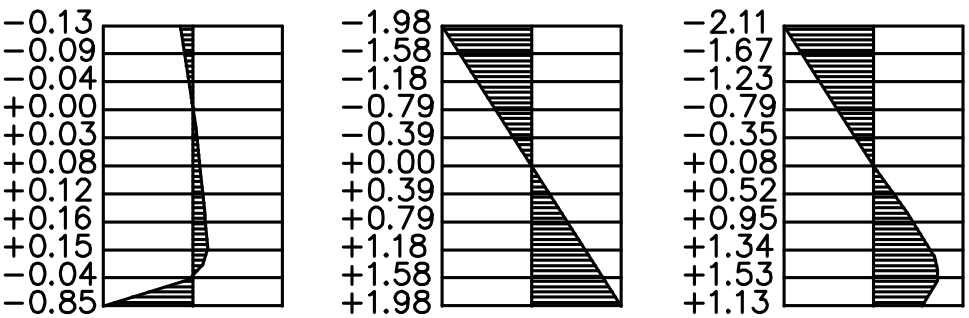

Fig. 4. Results of calculation the self-stress for concrete B-15 (f_c=15.0 Mpa, f_{ct}=1.40 Mpa, E_c=23.1*10^3MPa).

$$A = 1/F_b \int \varepsilon^R(z_1) b \, dz_1 \;\; ; F_b = bh \quad ,$$

$$B = 1/I_b \int \varepsilon^R(z_1) z_1 b \, dz_1 \;\; ; I_b = bh^3/12 \quad . \tag{7}$$

Some calculations for different concrete was done The results of calculations of self-stress, elastic stress and total stress are shown on Fig. 4.

3. SELF-STRESS IN REINFORCEMENT CONCRETE ELEMENT WITH CRACK

The self-stress in reinforcement concrete bending beam was calculate in the same way as in concrete element Fig. 5.

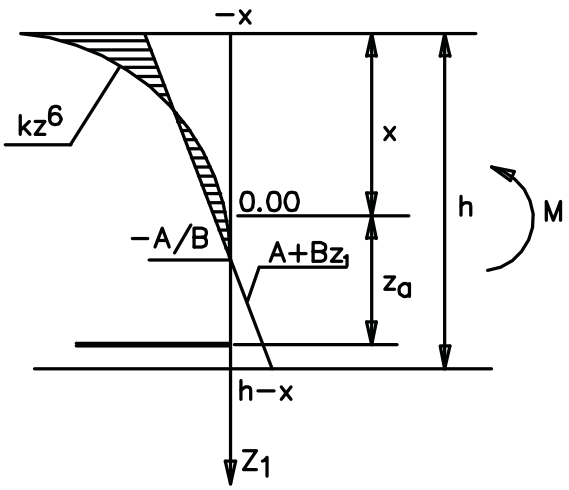

Fig. 5. Self-stress in reinforced concrete beam with crack.

The residual strain-stress relationship described the same equals (Eq. 4) like for concrete element. Using condition (2) the constants A, B was calculated:

$$E_b \int (A + Bz_1 - \varepsilon^R(z_1)) \, dF \; + \; E_a F_a (A + Bz_a - \varepsilon_a^R) = 0 \quad ,$$

$$E_b \int (A + Bz_1 - \varepsilon^R(z_1)) \, z_1 b \, dz_1 \; + \; E_a F_a (A + Bz_a - \varepsilon_a^R) z_a = 0 \quad , \tag{8}$$

where: ε_a^R - residual strain for steel.

Some numerical calculations for different causes were done. The results of these calculations are shown in Fig. 6.

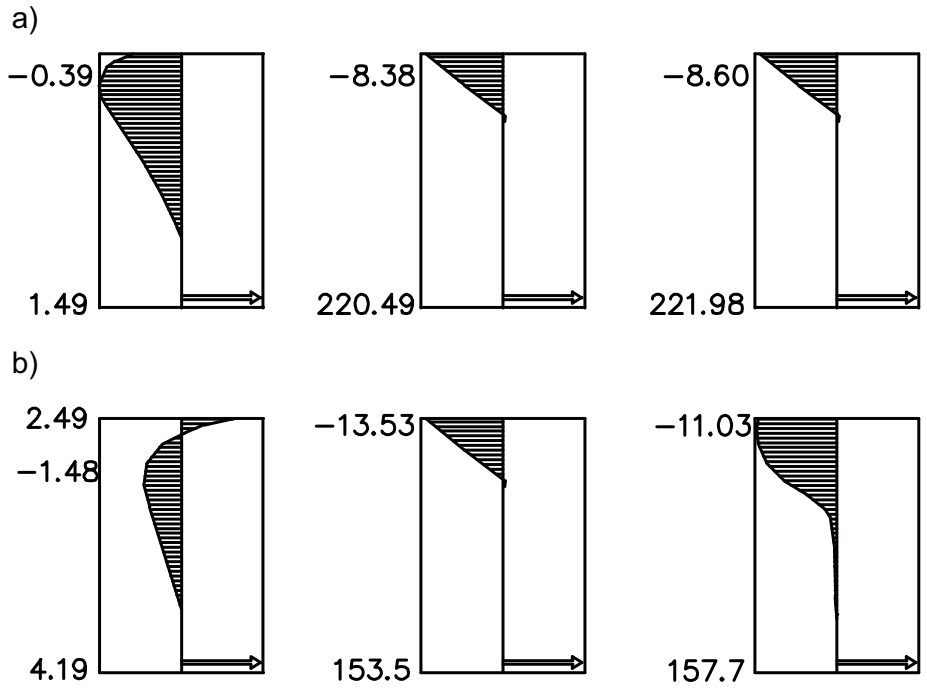

Fig. 6. Stresses in cracked concrete element, concrete B-15 (see Fig.4), steel f_y = 220 MPa. a) μ = 0.5%, M = 29 kNm, b) μ = 2%, M = 75 kNm

4. NON-LINEAR ANALYSIS USING F.E.M.

The Finite Elements Method was used to calculate the non-linear effects in reinforced concrete elements. The rectangular elements were used with stiffness matrix calculated by Rockey [5]. The first steep is taken as the linear solution using known relationship of F.E.M. [6]:

$$[K]\{\delta\}-\{R\}=0 \quad , \tag{9}$$

where: [K] - stiffness matrix,

{δ} - displacement,
{R} - external forces.

In Eq. 9 the linear behaviour of materials was assumed:

$$\{\sigma\}=[D](\{\varepsilon\})-\{\varepsilon o\})+\{\sigma o\} \ , \tag{10}$$

$$F(\{\sigma\},\{\varepsilon\})=0 \quad . \tag{11}$$

The non-linear effects were calculated using iteration and changing of the external forces {R}. The external forces were calculated on the basis of initial strain and initial stress which described the cracks or non-linear material behavior. This method needs no necessity of changing of the stiffness matrix. The reinforcement was described as linear elements which are added to the stiffness matrix. Before the cracks appear the concrete strain and the steel strain are equal. After cracking the steel elements take over the stresses from the concrete. This stresses are added to the external forces as initial stresses.

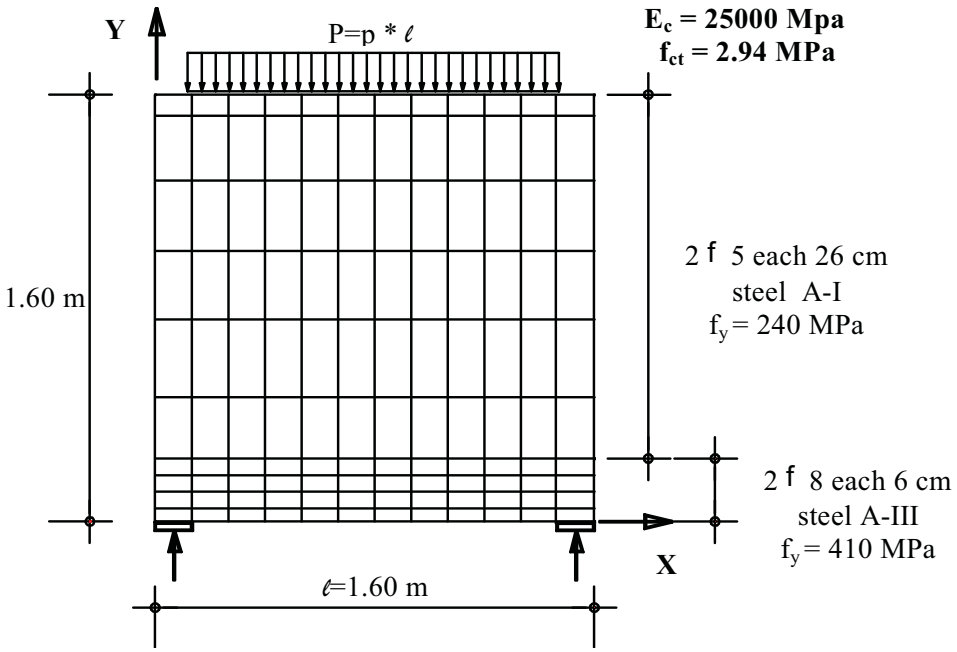

Fig. 7. The schema of calculated RC panel

5. ANALYSIS OF RC DISK WHICH WAS TESTED BY LEONHARDT AND WALTHER [7]

The purpose method was examined on calculations of the RC panel (Fig.7) tested by Leonhardt and Walther [7]. The same panel was calculated by Floegl [8], Buyukozturk [9] and Lewiñski [10]. So, there is the material to compare the results of analysis.

The results of numerical calculations are shown on Fig. 8-11. Figure 8 shows the propagation of cracks under different loading. The first cracks was observed for P=400 kN. In each level of the loading the number of cracks and the width of the cracks vary as shows the figure.

In Fig. 9 the relationship between loading and displacement of the panel as compared with other finding. The good compatibility was notice.

Fig. 10 and 11 show the comparison of stresses in steel bars calculated by authors with experimental findings and other calculations.

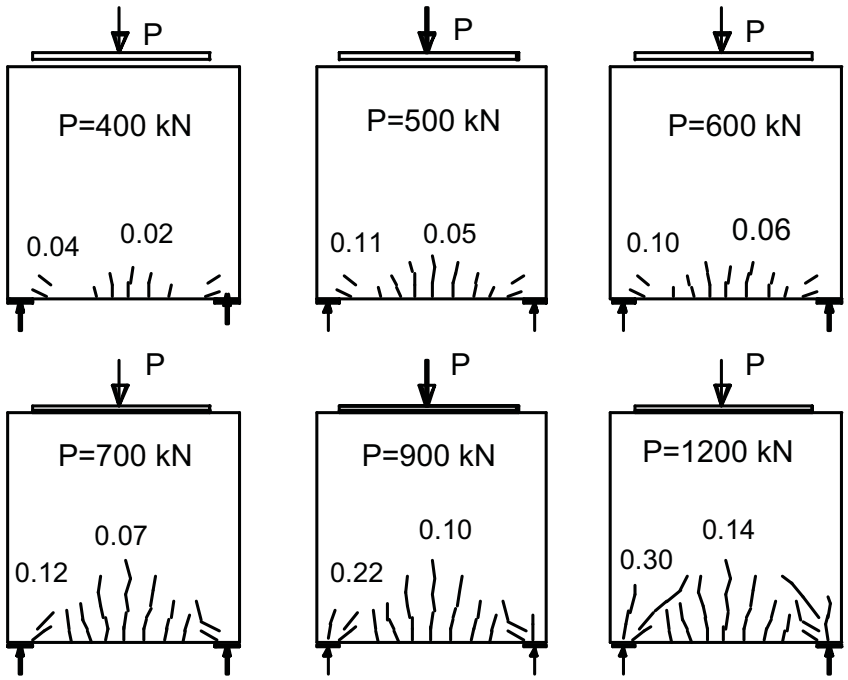

Fig. 8. The propagation of the cracks under different level of loading

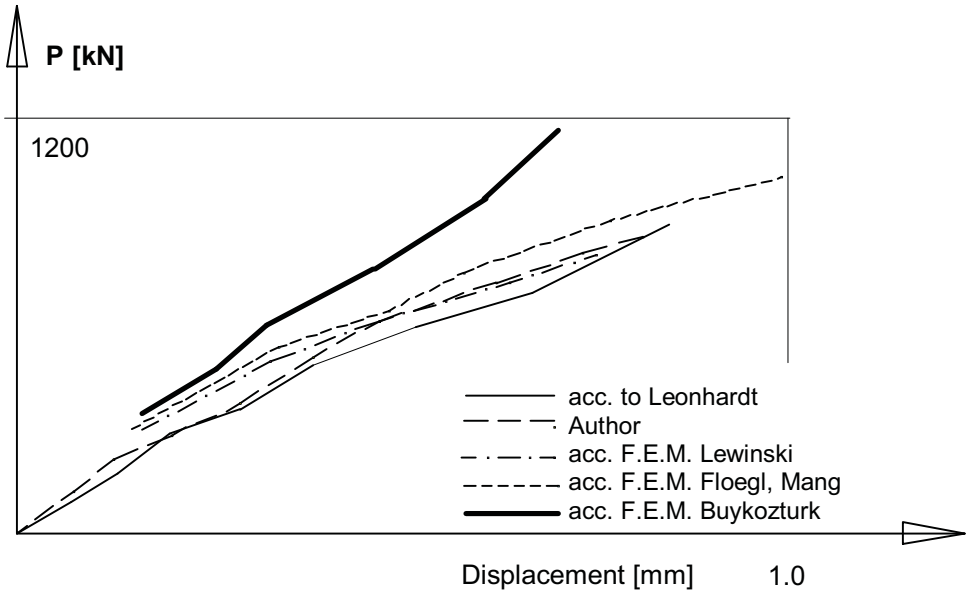

Fig. 9. The relationship between loading and displacement.

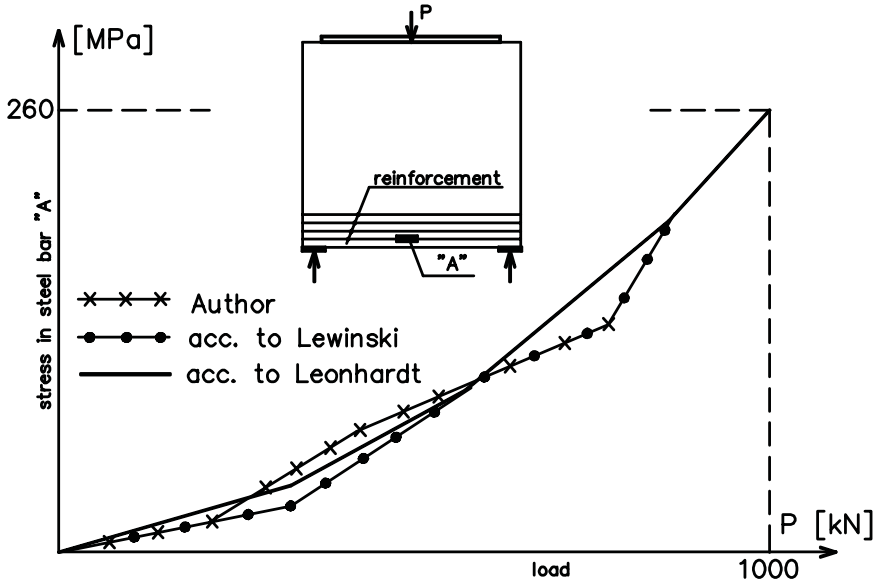

Fig. 10. Comparison of the stresses in reinforcement of the panel with other finding.

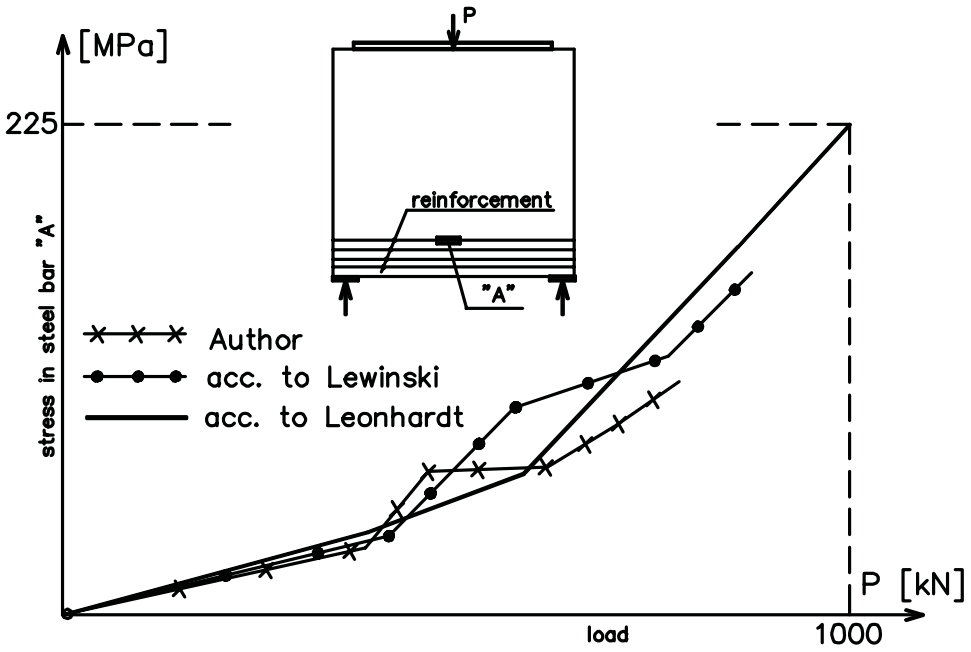

Fig. 11. Comparison of the stresses in reinforcement of the panel with other finding.

4. CONCLUSIONS

The mathematical idealization of cracked reinforced concrete structures is very difficult. The presented model of non-linear behavior of reinforced concrete can be used to numerical analysis with the finite element method. It may give relatively quick solution because of no necessity to change the stiffness matrix and solve equations several times. Descriptions of all non-linear behavior of materials, cracks, self-stresses treated as initial strains gives only different right sides of standard equals. Therefore the iteration of cracks and loads do not change the stiffness matrix. All that may preference finite element method to numerical analysis.

References

1. GODYCKI-ĆWIRKO, T. - *"Mechanika betonu"*, Arkady, Warszawa, 1982.
2. RUSCH, H. and JUNGWIRTH, D. - *"Skurcz i pełzanie w konstrukcjach betonowych"*, Arkady, Warszawa, 1979.
3. BORCZ, A. - W sprawie mechaniki konstrukcji betonowych, *Inżynieria i Budownictwo*, **4,5**, (1986).

4. BORCZ, A. - Teoria konstrukcji żelbetowych, wzbrane badania wrocławskie, *Skrypt Politechniki Wrocławskiej*, Wrocław, (1986).
5. ROCKEY, K.C. and EVANS, H.R. - *"The finite element method",* Crosby Lockwood Staples, London, 1975.
6. ZIENKIEWICZ, O.C. - *"Metoda elementów skończonych"*, Arkady, Warszawa, 1972.
7. LEONHARDT, and F., WALTHER, R. - *"Wandartige träger".* Deutscher Ausschuss für Stahlbeton, H. **178**, Verlag Wilhelm Ernst & Sohn, Berlin, 1966.
8. FLOEGL, H. and MANG, H. A. - On tension stiffening in cracked reinforced concrete slabs and shells considering geometric and physical nonlinearity., *Ing-Arch.,* **51**, 215-242 (1981)
9. BUYUKOZTURK, O. - Non-linear analysis of reinforced concrete structures, *Computers and Structures*, **7**, 149-156 (1977).
10. LEWIŃSKI, P.M. - Nieliniowa analiza płyt i tarcz żelbetowych metodą elementów skończonych, *Studia z zakresu inżynierii*, **29**, PWN Warszawa-Łódź, (1990).

"Computational Civil Engineering 2006", International Symposium
Iaşi, România, May 26, 2006

Numerical modelling for homogenization of masonry structures

Jerzy Szołomicki[1]

[1]*Departmen of Civil Engineering, Wrocław Universityof Technology, Wrocław, 50-370, Poland*

Summary

In the present study, equivalent elastic properties, strength envelope and different failure patterns of masonry material are homogenized by numerically simulating responses of a representative element under different stress conditions. The representative volume element provides a valuable dividing boundary between the discrete model and the continuum model. This paper presented a computational homogenization technique of masonry.

KEYWORDS: Masonry structures, homogenization, computational simulations

1. INTRODUCTION

In recent years growing attention has been paid by researches in structural mechanics to masonry structures with the intent to provide theoretical and numerical tools for better understanding the complex mechanical behavior of such structures. The complex mechanical behavior of masonry structures depends strongly on the composite nature of masonry material. Masonry is constituted by blocks of natural or artificial material jointed by dry or mortar joints; the latter are the weakness – areas of such a composite material and notably affect the overall response of the assembly with a number of kinematical modes at joints such as sliding, opening – closing and dilatancy. Generally, two different methods have been developed to perform linear and non-linear analyses of masonry structures (Szołomicki 1997). The macro-modelling approach intentionally makes no distinction between units and joints but smears the effect of joints presence through the formulation of a fictitious homogeneous and continuous material equivalent to the actual one which is discrete and composite. The alternative micro-modelling approach analyses the masonry material as a discontinuous assembly of blocks, connected each other by joints at their actual position, being simulated by appropriate constitutive models of interface (Zucchini 2002). Another direction, presented in this paper, is a method which resorts to homogenization technique. The homogenization method that would permit to establish constitutive relations in terms of averaged stresses and strains from the geometry and constitutive relations of the individual components would represent a major step forward in masonry modelling. In this paper, a typical unit of masonry is selected to serve as a

representative volume element. Both the bricks and mortar joints are idealised as isotropic material having their own properties such as stiffness, strength and damage characteristics. In the homogenization process, failure of the individual material in the unit is divided into three modes: tensile failure of mortar joint, shear failure of mortar joint and brick, and compressive failure of brick. A fracturing law is associated with the tensile failure of the mortar joint, while the shear failure accounts for the variations of shear strength as a function of normal stress.

2. FORMULATION OF REPRESENTATIVE VOLUME ELEMENT

The homogenized constitutive law is determined by studying the behaviour of the representative volume element (RVE) which is the cell of periodicity in the case of periodic media (Galvanetto 1997). Such a RVE plays in the mechanics of composite material the same role as the classical elementary volume of continuum mechanics, therefore in general a homogenized approach is successful if the size of the cell is small compared with that of the structure.

The representative volume element of masonry should include all the participant materials, constitute the entire structure by periodic and continuous distribution, and be minimum unit satisfying the first two conditions. Under conditions of an imposed macroscopically homogeneous stress or deformation field on the representative volume element, the average stress and strain fields are respectively:

$$\overline{\sigma}_{ij} = \frac{1}{V}\int_V \sigma_{ij} dV \tag{1}$$

$$\overline{\varepsilon}_{ij} = \frac{1}{V}\int_V \varepsilon_{ij} dV \tag{2}$$

where V is the volume of the representative volume element.

Based on the constitutive relations of the brick and the mortar materials, the equivalent stress-strain relations of the RVE are homogenised by applying various compatible displacement conditions on the RVE surfaces (Luciano 1997).

3. DAMAGE MODEL FOR MORTAR JOINT AND BRICK

3.1 Damage of mortar joint

Most of the non-linear deformation in brick masonry, until failure, occurs only in the joints. Establishing a reliable material model for the mortar joint is very important for analysing the masonry load-bearing and deformation capacity.

The degradation of tensile strength in mortar joint can be expressed by an exponential approximation as:

$$\sigma = E_n \varepsilon_n, \qquad \varepsilon_n \le \varepsilon_0 \tag{3}$$

$$\sigma = \sigma_0 e^{-\alpha_n (\varepsilon_n - \varepsilon_{n_0})/\varepsilon_{n_0}}, \qquad \varepsilon_n \ge \varepsilon_{n_0} \tag{4}$$

where: α_n is a material parameter, ε_{n0} – threshold strain that initiates tensile fracturing of the material, σ_0 is the elastic limit stress of the mortar joint.

The exponential decay leads to the following total fracture release energy:

$$G_f^I = \int_0^{+\infty} \sigma d\varepsilon_n . \tag{5}$$

The differential of fracture energy is obtained as:

$$dG^I = \frac{1}{2}\sigma d\varepsilon_n - \frac{1}{2} d\sigma \varepsilon_n . \tag{6}$$

Thus tensile damage can be defined as the ratio of released fracture energy to the total fracture release energy as:

$$D^I = \frac{\int_0^{\varepsilon_n} dG^I}{G_f^I} . \tag{7}$$

In the compression – shear region of mortar joints is reasonable to use the Mohr – Coulomb criterion, which can be expressed as:

$$F(\sigma, \tau) = |\tau| + \mu\sigma - c(G^{II}) = 0, \tag{8}$$

where: μ and c are frictional coefficient and cohesion, respectively; σ is a compressive stress; G^{II} is the dissipated plastic work that results from shear failure of mortar joint.

The incremental strain vector of mortar can be divided into elastic and plastic parts:

$$d\varepsilon = d\varepsilon^{e} + d\varepsilon^{p} \tag{9}$$

To avoid excessive plastic dilatancy, a non-associated flow rule is proposed. It is expressed as:

$$Q(\sigma,\tau) = \boldsymbol{\eta}(\tau) + \mu\sigma \tag{10}$$

where: η is parameter that scales the dilatancy.

The direction of plastic relative displacements is governed by the flow rule as:

$$d\varepsilon^{p} = d\lambda \frac{\partial Q}{\partial \sigma} \tag{11}$$

where dλ is the plastic multiplier.

According to the traditional plastic flow rule the complete elasto-plastic incremental stress-strain relationship is presented as:

$$d\sigma = E^{ep} d\varepsilon \tag{12}$$

where:

$$E^{ep} = E^{e} - \frac{E^{e} \dfrac{\partial Q}{\partial \sigma} \dfrac{\partial F}{\partial \sigma^{T}} E^{e}}{-A + \dfrac{\partial F}{\partial \sigma^{T}} E^{e} \dfrac{\partial Q}{\partial \sigma}} \tag{13}$$

and A is a hardening parameter.

The plastic work done by the shear stress τ depends on the lateral compression σ. When the combination of (τ, σ) on the strength surface is expressed as (8), the incremental plastic work is the following:

$$dG^{II} = (|\tau| + \mu\sigma) d\varepsilon_{t}^{p} = \begin{Bmatrix} |\tau| + \mu\sigma & 0 \end{Bmatrix} \begin{Bmatrix} d\varepsilon_{t}^{p} & 0 \end{Bmatrix}^{T}. \tag{14}$$

The damage value at compressive-shear region can be expressed as:

$$D^{II} = \frac{G^{II}}{G_f^{II}} \tag{15}$$

where:

$$G^{II} = \int_0^{+\infty} (|\tau| + \mu\sigma) d\varepsilon_t^p \tag{16}$$

The total dissipated energy due to friction can be calculated by the relationship of the shear stress and strain with no lateral compression on the surfaces. The relationship can be written as:

$$\tau = E_t \varepsilon_t \text{ when } \varepsilon_t \le \varepsilon_{t_0} \tag{17}$$

$$\tau = E_t \varepsilon_{t_0} e^{-\alpha_t (\varepsilon_t - \varepsilon_{t_0})/\varepsilon_{t_0}} \text{ when } \varepsilon_t \ge \varepsilon_{t_0} \tag{18}$$

where α_t is a material parameter and ε_{t0} is threshold shear strain of mortar joint without lateral compression. The cohesion c is expressed as:

$$c = \left(1 - \frac{G^I}{G_f^I}\right)\left(1 - \frac{G^{II}}{G_f^I}\right) c_0 = \left(1 - D^I\right)\left(1 - D^{II}\right) c_0 . \tag{19}$$

3.2 Damage of bricks

Damage of bricks is composed of compressive crushing and tensile splitting due to high compression. According to the isotropic damage theory, the secant constitutive tensor can be written as:

$$\Lambda_{ijkl}(D) = \Lambda_{0ijkl}(1 - D) \tag{20}$$

where: Λ_{0ijkl} is initial stiffness of material and D is a damage.

The damage scalar consists of two parts, namely D_t due to tensile damage and D_c due to compressive damage. It is evaluated by the combination of:

$$D = A_t D_t + A_c D_c, \ \dot{D} > 0 \tag{21}$$

where: A_t and A_c are the balancing coefficient characterizing tension and compression, respectively. Damage scalars D_t and D_c corresponding respectively

to damage measured in tension and compression can be expressed again in exponential approximation as:

$$D_t = 1 - e^{-\beta_t(\tilde{\varepsilon}^+ - \varepsilon_0^+)/\varepsilon_0^+} \tag{22}$$

$$D_c = 1 - e^{-\beta_c(\tilde{\varepsilon}^- - \varepsilon_0^-)/\varepsilon_0^-} \tag{23}$$

where $\tilde{\varepsilon}^+$ and $\tilde{\varepsilon}^-$ are the equivalent tensile and compressive strains.

4. FINITE ELEMENT IMPLEMENTATION

The material model proposed above is used into finite – difference program. The finite element analysis is based on this decoupling of the macroscopic and microscopic displacement fields. In the present analysis, the material is considered in elastic state before the directional strain of the mortar joint reaches the threshold strain. In post-failure state, the stress will decrease with increase of uniaxial strain. The material parameters of brick can also be determined by uniaxial tensile and compressive test data. The computational models of RVEs in the present numerical analysis are shown in Figure 1. The brick and mortar are discretized individually. The brick size is 250 x 65 x 120 mm and mortar thickness is 10 mm. In numerical simulation, vertical and horizontal displacements are applied to the RVE surfaces. The advantage of using displacement boundaries can not only avoid incompatible deformation between RVEs, but also makes it possible to obtain a complete monotonic stress-strain curve through the homogenization process.

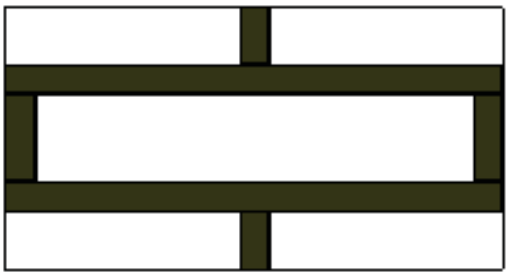

Figure 1. Representative volume element of masonry

5. NUMERICAL APPLICATION

The theory presented above has been used in the following example. The masonry panel schematically reported in Figure 2, subjected to pure shear loading is analyzed. This is characterized by the following geometrical parameters: H = 3000 mm, B = 2000 mm and material characteristics (Tab. 1,2). In Figure 3, the damage and the minimum principal stress maps for the prescribed displacement u = 5 mm is plotted for analyzed panel. It can be noted that the failure mechanism is characterized by the formation, growth and propagation of inclined damage bands, as it typically occurs in structures subjected to horizontal forces. Damaging process in analysed example is concentrated in a single band.

Table 1. Material parameters for brick

Material	E MPa	G MPa	ν -	σ_t MPa	σ_c MPa	ε_0^+ -	ε_0^- -
Brick	12000	4700	0,15	2	50	0,0002	0,0004

Table 2. Material parameters for mortar

Material	E_n MPa	E_t MPa	σ_0 MPa	c_0 MPa	μ -	ε_{n0} -	ε_{t0} -
Mortar	2,0	1,0	0,9	1,1	0,8	0,0004	0,001

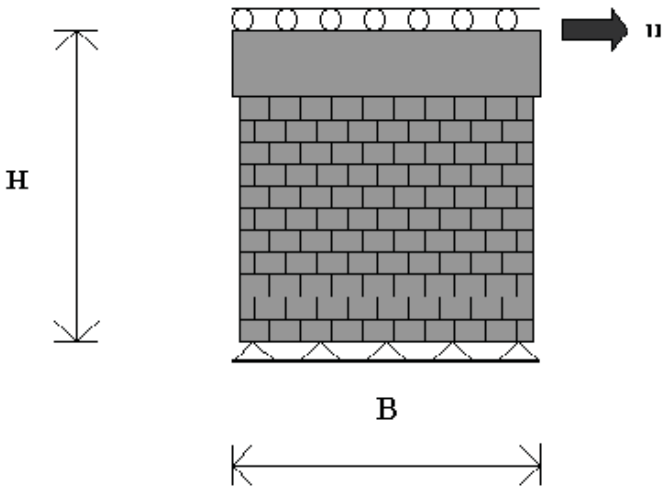

Figure 2. Analyzed masonry panel

It can be noted that the mechanical response of wall subjected to shear loading is characterized by:

- an initial elastic response,
- a first step softening branch due to the damage propagation concentrated in place where the maximum tensile strains occur,
- a hardening phase during which the plastic evolution process becomes more significant than the damage one.

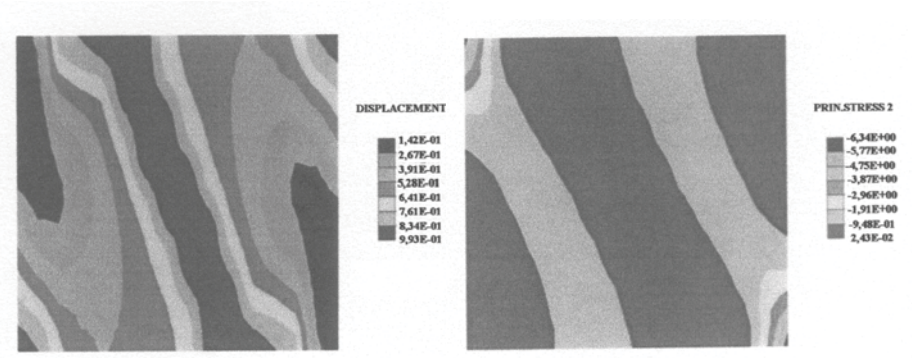

a) b)

Figure 3. Numerical analysis of masonry panel: a) damage distribution and b) minimum principal stress distribution for u = 5 mm

6. CONCLUSION

In this paper the authors presented a numerical homogenization technique of masonry. The strength behavior and damage behavior have been obtained by numerical analysis of the representative volume element responding to various boundary conditions. They have been implemented into a continuum plastic damage model. Failure of masonry can be described into three types: tensile failure due to mortar tensile damage, shear failure of brick and mortar and compressive failure of brick. It should be noticed that the RVE employed in a general homogenization process should be smaller than the whole masonry structure. Otherwise the edge effect will affect the macro-material properties significantly, and in that case the discrete element method is preferred.

References

1. Galvanetto, U., Ohmenhäuser, F. Schrefler, B.A. A homogenized constitutive law for periodic composite materials with elasto-plastic components. *Composite Structures*, vol. 39 (3-4): p. 263-271, 1997.
2. Luciano, R., Sacco, E. Homogenization technique and damage mode for masonry material. *International Journal of Solids and Structures*, vol. 34(24): p. 3191-3208, 1997.
3. Szołomicki, J.P. *Statical-strength analysis and computational modeling of masonry structures.* Wrocław University of Technology PhD. Thesis: p. 228, 1997 (in Polish).
4. Zucchini, A., Lourenço, P. A micro-mechanical model for homogenization of masonry. *International Journal of Solids and Structures*, vol. 39: p. 3233-3255, 2002.

"Computational Civil Engineering 2006", International Symposium
Iaşi, România, May 26, 2006

About some important changes in applied structural optimization

Jacek Boroń

Building Engineering Institute, Wroclaw University of Technology, Wroclaw, 50-370, Poland

Summary

Structural optimization is special domain of employment researching many and how different problems in the field of forming structure. In times of early computer science and computational technology, when the access to "computing time" of the machine was strongly regulated (from the point of view of considerable costs) some optimization problems were very strongly simplified, so their solution could be possible without mathematical programming methods and therefore cheaper.

In times of stormy development of informatization and almost free-for-all personal computers as well as specialized software, complication of structural optimization modeling has grown considerably.

In this paper being short recapitulation of achievements made by Division of Computational Methods in Engineering Design, it refers to these earliest problems and to these very modern both dealing with applied structural optimization, what is the domain of interest of our team from over 25 years.

KEYWORDS: structural optimization, scalar optimization problem, genetic algorithm, vector optimization problem

1. INTRODUCTION

As member of the Team for Computational Methods in Engineering and Design, I have started dealing with the applied structural optimization in the end of 70-ties in XX century. In the beginning it was research concerning steel bar structures (trusses and frames) and industrial buildings (concrete beams, silos and tanks). All of these early problems mentioned above were formulated and then solved as scalar optimization questions.

Next we started researching with vector optimization problems (steel frames and trusses) and genetic algorithms (thanks to cooperation with Carlos Coello Coello and Gregorio Toscano-Pulido).

In this paper I'm trying to bring you closer how deep were the differences between these first and last problems (exactly in this year was my personal 25th anniversary of optimization research).

2. SCALAR OPTIMIZATION PROBLEM

2.1 Simple example of the tank welded from steel

The first example of optimization I want to present (in this case example of scalar optimization, started and conducted in 1981) is a tank (the part of steel water tower), shown on the drawing below (Fig. 1).

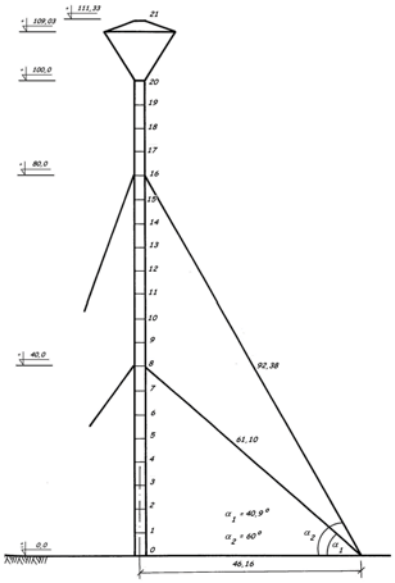

Fig. 1. Steel water tower

For optimization the following lump of the tank, made from two cut off cones and one internal cylinder, has been chosen. Surface plan it in places of intersections circled wreaths stiffening. Described has resulted from capacity form highly, allocations and easy installment available methods (so called "easy" or "heavy" one).

2.2 Scalar optimization model

As criterion of optimization accept minimum of expenditure of material preliminary. Become setting up average thickness of covering above-mentioned question fetch for determination of condition of occurrence of minimum of lateral surface. Besides, it accepts following foundation and simplification:

- dimension section - they mirror middle surface,
- thickness of covering is constant (and average),
- water fulfills only maximum bottom cone,

- we use only one design variable: corner of inclination of surface for vertical α in bottom cone (see Fig. 2),
- capacity of useful tank totals 600 m^3.

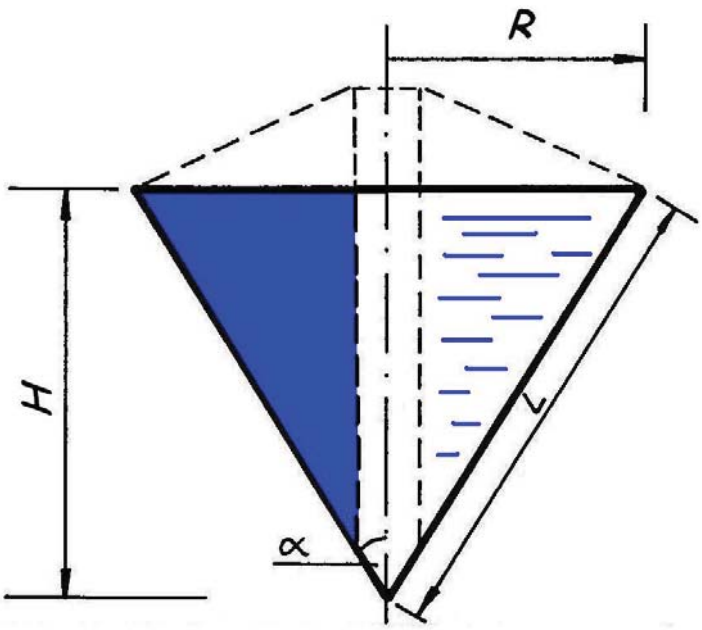

Fig. 2. Steel tank – lump and design variable α

It takes into consideration, in the farthest consideration, following geometric dependences:

$$R = H \bullet tg\,(\alpha)\,, \tag{1}$$

$$L = H / cos\,(\alpha)\,, \tag{2}$$

Field of the lateral surface:

$$F = \pi \bullet R \bullet L = H \bullet tg(\alpha) \bullet H / cos\,(\alpha) = H^2 \bullet tg(\alpha) / cos\,(\alpha), \tag{3}$$

Capacity of the cone:

$$V = 600 = 1/3\ \pi \bullet R^2 \bullet H = \ldots = 1/3\ \pi \bullet H^3 \bullet tg^2(\alpha), \tag{4}$$

Basing on (4) in the function of the corner α , next H was indicated:

$$H = [1800 / \pi \bullet tg2(\alpha)]^{1/3}\ , \tag{5}$$

and it put for (1)

$$F = A \bullet \sin^{-1}(\alpha) \bullet [tg^2(\alpha)]^{1/3},$$

$$\text{where } A = 1800 \bullet (\pi/1800)^{1/3} = \ldots = 216{,}72, \quad (6)$$

Task of minimization solve existence of minimum of function alternate one researching F(α).

$$\min F(\alpha) \leftrightarrow F'(\alpha) = 0, \quad (7)$$

Solution illustrate on the drawing (see Fig. 3). Next it verify „candidate for minimum" (α') calculating in this point value of second derivative function F''(α):

$$F''(\alpha') = \ldots = 1{,}833 > 0 \quad (8)$$

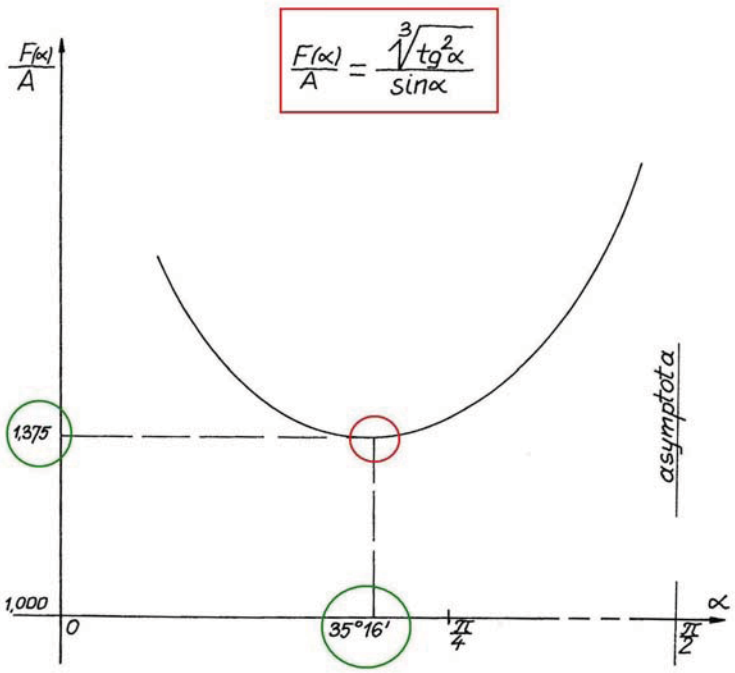

Fig. 3. Solution of question of simple scalar optimization

2.3 Recapitulation and final conclusions

It exert in the first approximation, that conical tank has minimal field of lateral surface (but what behind it go, grant demanded criterion: minimum of material), when it lateral is drooping for vertical under corner creating $\alpha = 35^{o}\ 16^{''}$.

Having the corner of creating inclination α and foundations or simplifications mentioned on admission of preamble, remained dimension of the tank have been calculated from simple geometric dependences.

Fundamental geometric dimensions of the tank accepted for the farthest technical and executive design, it present on following drawing (Fig.4).

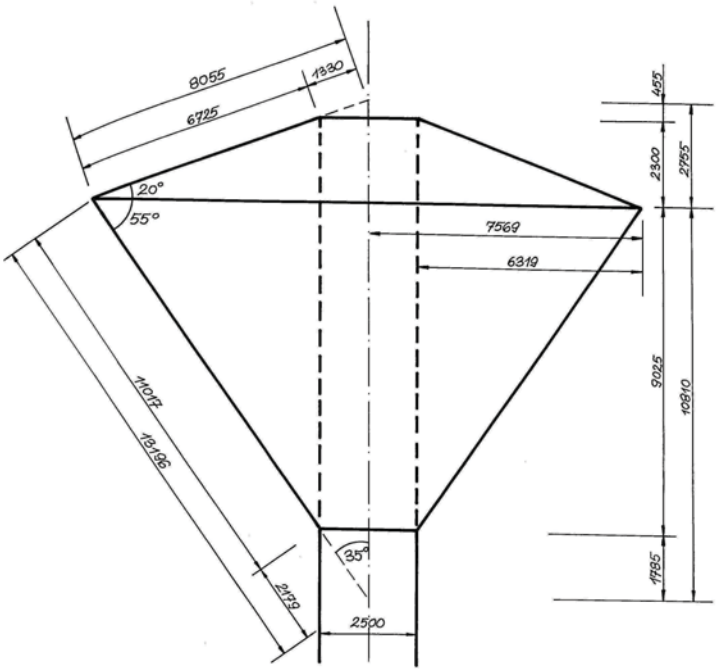

Fig. 4. Conical tank accepted for the farthest technical design

Assuring, as contact limit, the smallest surface of conical covering with aggressive environment (the water stored in this tank, so-called: industrial, with mineral small parts inclusive, about predefined temperature gone up with technological respects) we can prominently extend the constancy of maintenance of the building (water tower) in the best condition.

3. MICRO-GA AS AN EFFECTIVE SOLVER FOR MULTIOBJECTIVE OPTIMIZATION PROBLEMS

3.1 Genetic algorithms in multiobjective structural optimization

Genetic algorithms (GAs) have become very popular optimization techniques in structural optimization, but their use in multiobjective structural optimization has become less common. Additionally, only few researchers have emphasized the importance of efficiency when dealing with multiobjective optimization problems, despite the fact that its (potentially high) computational cost may become prohibitive in real-world applications. In this paper, we present a GA with a very small population size and a reinitialization process (a micro-GA) [1] which is used for multiobjective optimization of trusses.

3.2 The micro-GA

This micro-GA approach elaborated by Toscano-Pulido [3,5] works as follows (Fig.5). It starts with a random population, it uses two memories: a replaceable (that will change during the evolutionary process) and a non-replaceable (that will not change) portion. Micro-GA uses 3 types of elitism. The first is based on the notion that if we store the non-dominated vectors produced from each cycle of the micro-GA, we will not lose any valuable information obtained from the evolutionary process. The second is based on the idea that if we replace the population memory by the nominal solutions (i.e., the best solutions found when nominal convergence is reached), it will gradually converge, since crossover and mutation will have a higher probability of reaching the true Pareto front of the problem over time. The third type of elitism is applied at certain intervals (defined by a parameter called "replacement cycle"). It takes a certain number of points from all the regions of the Pareto front generated so far and it uses them to fill the replaceable memory. Depending on the size of the replaceable memory, it chooses as many points from the Pareto front as necessary to guarantee a uniform distribution. This process allows us to use the best solutions generated so far as the starting point for the micro-GA, so that we can improve them (either by getting closer to the true Pareto front or by getting a better distribution along it). To keep diversity in the Pareto front, it use an approach based on geographical location of individuals (in objective function space) similar to the adaptive grid proposed by Knowles & Corne [2]. This approach is used to decide which individuals will be stored in the external memory once it is full. Individuals in less populated regions of objective space will be preferred. In previous work, our micro-GA has performed well (in terms of distribution along the Pareto front, and speed of convergence to the global Pareto front) with respect to other recent evolutionary multiobjective (vector) optimization approaches, while requiring a lower computational cost [3].

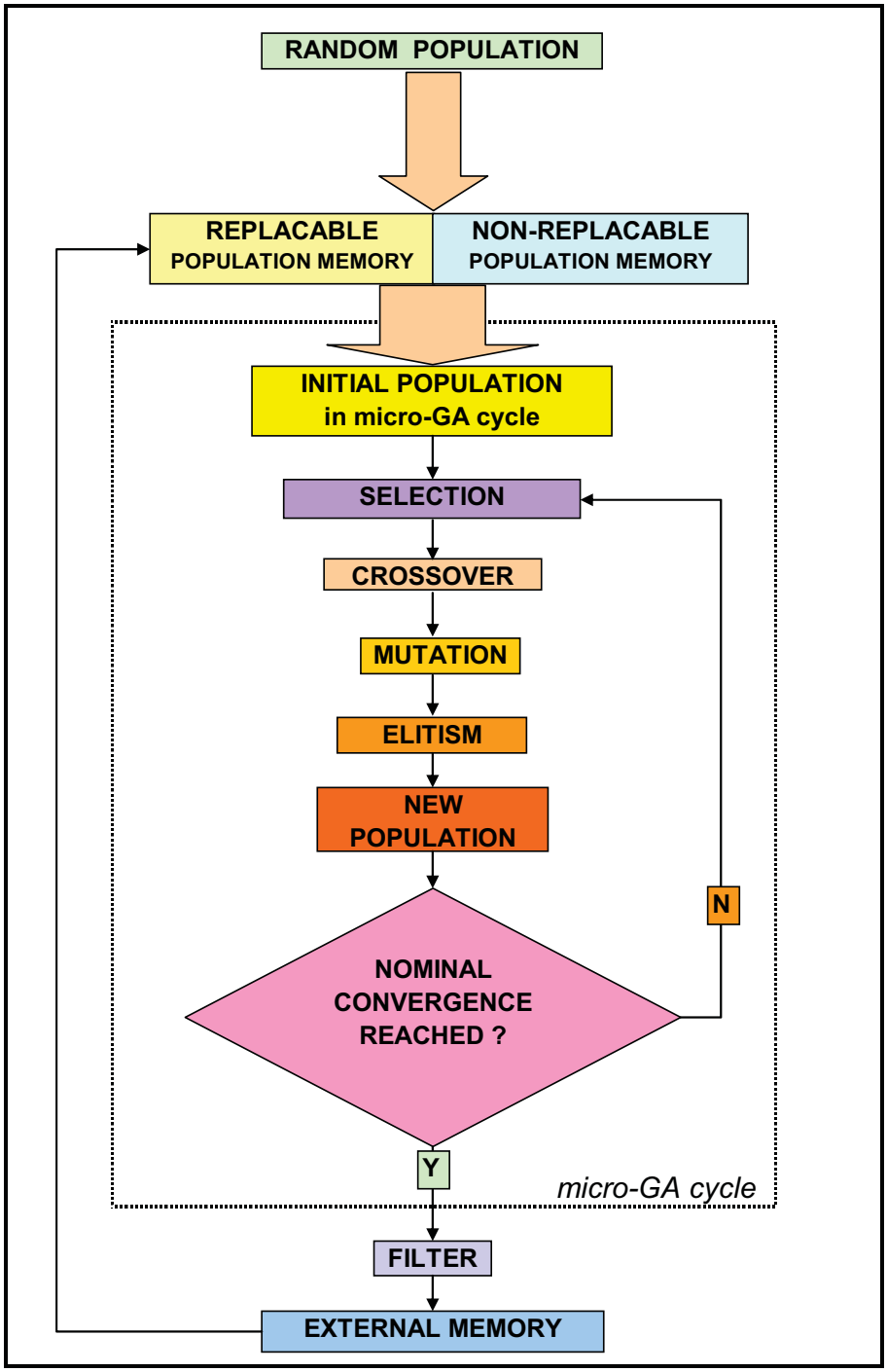

Figure 5 : Diagram of micro-GA

3.3 Illustrative example

The 4-bar plane truss shown in below (Fig.6) is used to illustrate this approach. Two objectives were considered in this case: minimize volume and minimize its joint displacement δ. Four decision variables are considered (for details of this problem, see [4]).

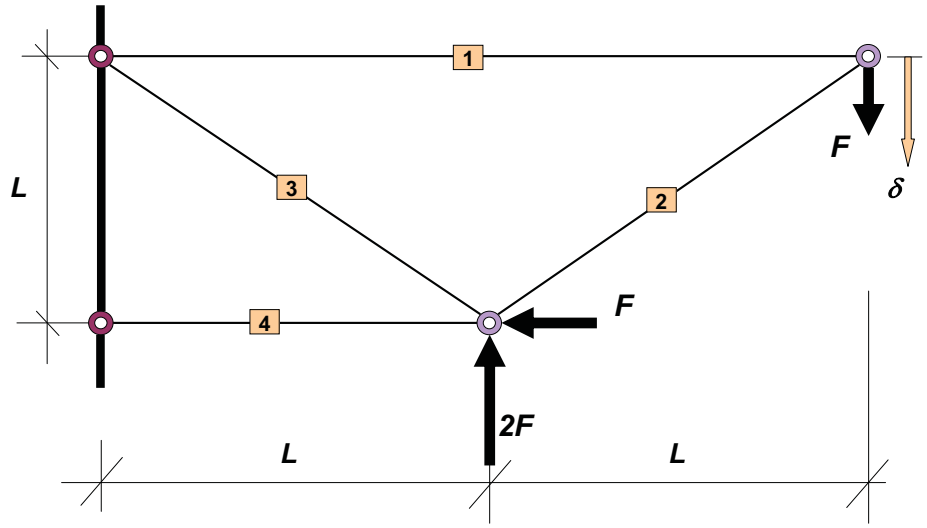

Figure 6 : Four-bar plane truss with one loading case

The Pareto front produced by micro-GA mentioned above, and its comparison against the global Pareto front (produced using an enumerative approach) is shown in the next figure (Fig. 7).

3. CONCLUSIONS

The task of structural optimization is to support the constructor in searching for the best possible design alternatives of specific structures. The "best possible" or in the other words "optimal" structure means that structure which mostly corresponds to the designer's objectives meeting of operational, manufacturing and application demands simultaneously. Compared with the "trial and error"- method mostly used in engineering practice (and based on an individual, intuitive, empirical approach) the seeking of optimal solutions by applying MOP (mathematical optimization procedures) is much more efficient and reliable. Nowadays in the time of market

economy also research has to be “market one”. In my opinion “to be market” is now the greatest challenge for applied optimization in Poland and everywhere [6].

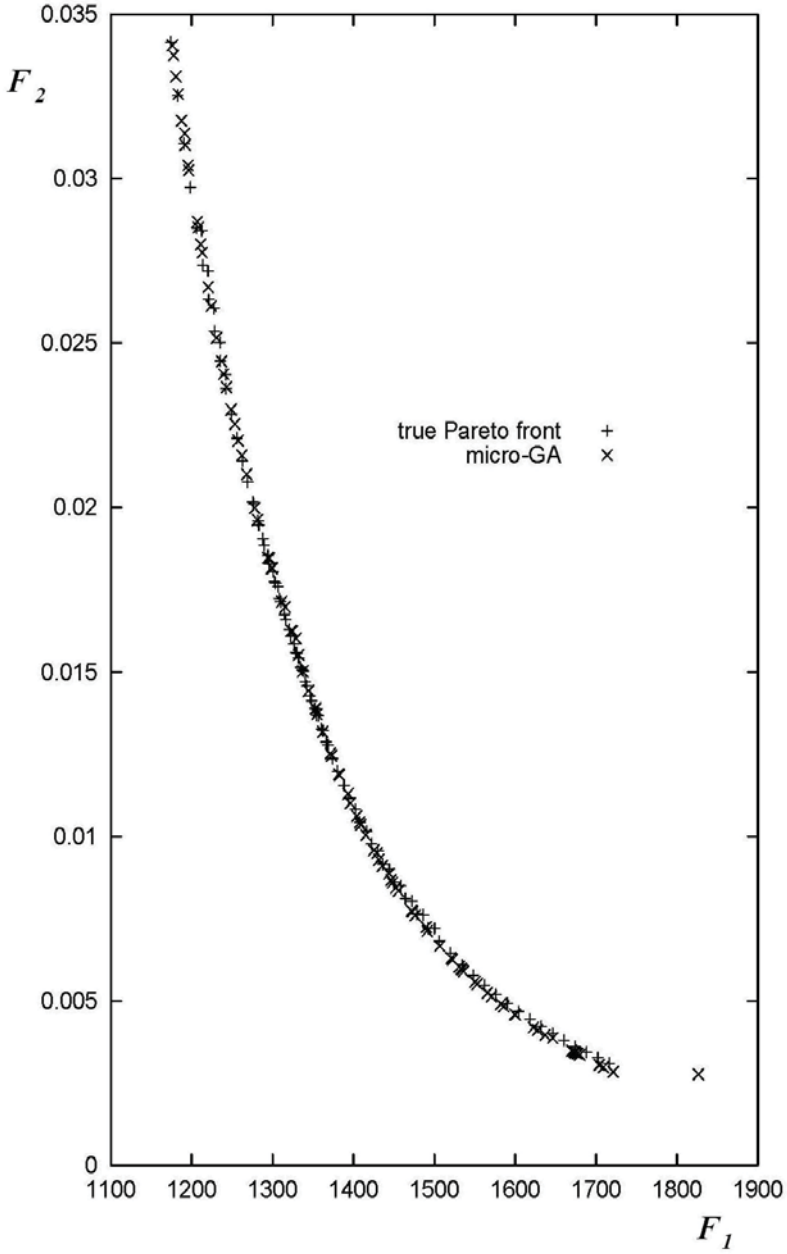

Fig. 7. True Pareto front vs. front obtained by micro-GA

References

1. Krishnakumar K., *Micro-genetic algorithm for stationary and non-stationary function optimization*, SPIE Proceedings: Intelligent Control and Adaptive Systems, Vol. 1196, pp. 289-296, 1989.
2. Knowles J.D. & Corne D.W. , Approximating the Nondominated Front Using the Pareto Archived Evolution Strategy, Evolutionary Computation, 8(2):149-172, 2000.
3. Coello Coello C.A. & Toscano-Pulido G., A Micro-Genetic Algorithm for Multiobjective Optimization, In Proceedings of the First International Conference on Evolutionary Multi-Criterion Optimization, Springer-Verlag, Lecture Notes in Computer Science No. 1993, pp. 126-140, March 2001.
4. Stadler W. & Dauer J., *Multicriteria optimization in engineering: A tutorial and survey*, in Structural Optimization: Status and Future, pp. 209-249, American Institute of Aeronautics and Astronautics, 1992.
5. Boroń J. & Coello Coello C.A. & Toscano-Pulido G., *Multiobjective optimization of trusses using a micro-genetic algorithm*, Politechnnika Koszalińska, Katedra Systemów Sterowania, Materiały XIX Ogólnopolskiej Konferencji Polioptymalizacja i Komputerowe Wspomaganie Projektowania, Mielno, 2001.
6. Boroń J., *Structural Optimization in polish terms of market economy; challenge or defeat?* European Congress on Computational Methods in Applied Sciences and Engineering ECOMAS 2000, Barcelona 11-14 September 2000.

"Computational Civil Engineering 2006", International Symposium
Iaşi, România, May 26, 2006

A database for elements' and structures' computation

Gabriela Ecaterina Proca

Department of Cadastre, Technical University Jassy

Summary

Analyzing Romanian regulations in constructions is sometimes difficult to understand calculation of elements or structures because of the great information's volume enclosed or the kind of expressing it.

For a better understanding, the author begins to create information's database for each kind of normative.

Present paper introduces a database for the computation of flexible catch for section walls made by easy concretes, enclosed in G 035-2000 Instructions.

KEYWORDS: computational database

1. INTRODUCTION

The instructions and other regulations in constructions are created by national research companies and are obligatory for all specialty designers.

Each instruction contains some important sections: "Domains of Use", "Terminology", "Constructive Solutions", "Computational Rules and Constructive Foresights", "Technical Performance", "Quality Requirements", "Rules for Receptions" and "Methods for Work's Safety".

"Domains of use" gives important information concerning where will be use the specific material or a technology, if other materials or technologies will be kept or replaced.

"Terminology" introduces the main materials or technologies used and their technical definition.

"Constructive Solutions" has more points, by example: rules to compile elements or systems indicating plans enclosed in the same normative; materials – which indicated all materials necessary for technical solution, other referring normative, or Romanian Standard Library, some practical indication during the performance of the main process.

"Computational Rules and Constructive Foresights" indicate: static plan, specifically loadings in constructions and formulas to evaluate sectional strains

(axial force, shear force, bending moment), diagrams, maximum principal stress, deformations, maximum values to respect, after case.

In order to create a logical database for computation, are interesting all chapters till the Reception's Rules.

2. CONTENT OF DATABASE

Each normative contains specifically information. By example, in a database can be included: geometrically characteristics of sections (length, height, and thickness), some typically cross sections; mechanically characteristics (elasticity modulus, Poisson coefficient); static plan, external loadings; efforts' diagrams. Can be included both specific details in performing.

Another important point is indications on computation's phases. Thus are indicated: the loadings' calculations phases and formulas after Romanian Standard Library; static plans; the main verifications for the most loaded sections, constructive solutions and stick figures.

The logic plan is the following:

Initial data » verifying sections or elements » sizing elements/ constructive details

The contribution of author consists in a systematic wording of Instructions' content. Similarly are indicated computation's phases. Belong these activities are used indications and references from actual formatives.

This kind of normative' interpretations can help engineers to understand without doubts the content of each normative and to design rapidly and correctly different elements or structures.

Next section presents a proposed database for GP 053-2000 Instructions.

3. EXAMPLE OF DATABASE FOR GP 053-2000 INSTRUCTIONS

Domain of use: nonstructural elements for separation walls made by lightly concrete plates, plaster plates, three layers panels with polystyrene middle;

Flexible catching – used for buildings (apartments, social-administrative destinations) having a flexible structure (reinforced concrete frame) or for other destinations, but having a flexible architecture;

Initial database

- *Material*: lightly concrete plates, plaster plates, three layers panels with polystyrene middle;
- *Mechanic and geometric characteristics*: length of panel (l), width of panel (b), thickness of panel (d), level's height (h_e); elasticity modulus (E_p); moment of inertia (I_p); bending rigidity (K) and it's formula $K = E_p \cdot I_p = \frac{bd^3}{12} E_p$
- *Catching elements*: steel plates havening 0.7...2 mm of thickness
- *Loadings*:

1. Concentrated force (P = 10; 30; 300 N) applied statically or dynamically in the middle of the panel at the height of 0.5 or 0.8 m;
2. Distributed force made by wind's action and evaluated after STAS 10101/20-90;

- Movements of catching elements at superior and inferior bearings $\delta_{st}^{r,i}$; $\delta_{st}^{r,s}$.Bending moments and deformation values are evaluated using Buildings' Static methods.

Verifications

a. Panels

a.1. *Verifying panels at loaded perpendicularly on their middle plan*

*carrying capacity for soft shock with impact energy of 240J: $M_{\max}^{d} \le M_{cap}^{panel}$

where,

$M_{\max}^{d}$ - bending moment generated by a concentrated force applied dynamically in the middle of the panel;

M_{cap}^{panel} - carrying moment generated by a concentrated force applied dynamically in the middle of the panel;

Ψ – dynamic coefficient for soft shock;

$M_{\max}^{st} = 0{,}8\frac{Pl}{4}$, bending moment generated by a concentrated force applied statically in the middle of the panel.

**carrying moment capacity for hard shock with impact energy of 100J: $M_{\max}^{d} = \Psi M_{\max}^{st}$.

a.2. *Verifying the maximum deformation made by a soft shock with energy of 120J*

P = 300 N and h = 0.80 m

- formula: $\Delta_{\max}^{d} = \psi \cdot \Delta_{\max}^{st}$,

where: Ψ is dynamic coefficient for shock; $\Delta_{\max}^{st}$ is calculated with formula: $\Delta_{\max}^{st} = 0{,}8\frac{Pl^3}{48K}$

a.3. *Verifying panel's deformations:*

General condition: $\Delta^d_{\max} \le \{H_e / 2500; 20mm\}$

Particular conditions:

- Shock's deformation – made by soft shock with impact energy of 30 J

– Formula: $\Delta^d_{\max} = \psi \cdot \Delta^{st}_{\max}$

- Control value: $\Delta^d_{\max} \le \{H_e / 5000; 5mm\}$

- Deformation made by wind's action (uniform loading made by internal wind's pressure)

-bending moment: $M_{\max} = \dfrac{p_n^n \cdot \gamma_F \cdot bl^2}{8} \le M_{cap}^{panel}$

- deformation's value: $\Delta_{\max} = \dfrac{5 p_n^n l^4}{384 K}$

- control value: $\Delta_{\max} \le \{H_e / 5000; 5mm\}$

b. *Sizing flexible catching*

It's imposed for thickness of steel panel **(t) =** de 0.7...2 mm; this way isn't admitted large deformations.

Formula: $W_{nec} \ge \dfrac{M^{st}}{R}$; and results that: $a_{nec} \ge \dfrac{6M^{st}}{Rt^2}$

Verifying flexible catching, formula : $\sigma^d_{\max} \le \sigma_a$;

Where, $\sigma^d_{\max} = \Psi \cdot \sigma^{st}_{\max}$ [$\sigma^{st}_{\max} = \dfrac{M^{st}}{W_{ef}}$] and M^{st} is evaluated using the static plan indicated in Instructions.

For all shown data bellow, can be created a plan (table 1).

Table 1

Initial data	Verifications		Control values
	Panels	Flexible catching	
Material Mechanic and geometric characteristics Loadings	**Carrying capacity** - soft shock with impact energy of 240J $M^d_{\max} \le M_{cap}^{panel}$ - hard shock with impact energy of 100J $M^d_{\max} = \Psi M^{st}_{\max}$	**Sizing** $a_{nec} \ge \dfrac{6M^{st}}{Rt^2}$ **Verifying** $\sigma^d_{\max} = \Psi \cdot \sigma^{st}_{\max}$	$\sigma_a = 10 N/mm^2$
	Deformation		

	- soft shock with energy of 120J $\Delta^d_{\max} = \psi \cdot \Delta^{st}_{\max}$ - soft shock with impact energy of 30 J $\Delta^d_{\max} = \psi \cdot \Delta^{st}_{\max}$ - shock by wind's action $\Delta_{\max} = \frac{5 p_n^n l^4}{384 K}$		$\Delta^d_{\max} \le \{H_e / 2500; 20mm\}$ $\Delta^d_{\max} \le \{H_e / 5000; 5mm\}$ $\Delta_{\max} \le \{H_e / 5000; 5mm\}$

Final results included in database are **c**onstructive solutions to perform are presented as details.

4. CONCLUSIONS

These kinds of databases will be distributed with the corresponding computation normative, next year; the author and the publisher editor believe to be helpful for specialty designers.

References

[1] Jerca, Şt., şa. Rezistența materialelor şi statica construcțiilor, Ed. U. T. Iaşi, 1982
[2] Vlad, Ioana Strength of Materials, Ed. Tehnopress, Iaşi, 2004
[3] * * * Ghid de proiectare şi execuție pentru prinderea elastică a pereților de compartimentare de structura de rezistență, indicativ GP053-2000

"Computational Civil Engineering 2006", International Symposium
Iaşi, România, May 26, 2006

Thermal composites design

Rodica Rotberg [1]

[1] *Civil Engineering, Technical University Iasi, Iasi, 700050, Romania*

Summary

The paper presents the results obtained by numerical simulation program for thermal calculus of hybrid structures. The thermal behaviors of hybrid structures have been evaluated using classical laminate theory. The detailed presentation of the algorithm will be followed by a case study using software developed. The case study refers to the thermal analysis of a plate hybrid structure

KEYWORDS: hybrid structures, thermal analysis, numerical simulation, classical laminate theory.

1. INTRODUCTION

On main objective of the thermal analysis is to control if a structure fulfils the thermal requirements and to supply temperature distribution as input for the thermo mechanical analysis.

Hybrid structures in service conditions rarely experience uniform temperature distributions throughout their service lives. Thermal stresses arising from thermal transients can built up and lead to high stresses that can sometimes be damaging to the structures. The thermal expansion behavior of the hybrid structures is an important thermal property that affects the build up of such stresses. Question often asked is: How far can I change the operating temperature until failure occurs? For each ply, thermal stress vector has to be calculated and taken into consideration in the failure criterion.

Simple structures like beams, tubes, plates can be calculated analytically using Classical Laminate Theory (CLT). The material input data needed for the CLT consist of the mechanical and physical properties of the laminate's plies. In general, material suppliers only provide data about their fibers or resins. With these data and micromechanical models it is possible to calculate the ply data. The algorithm for the thermal response of the laminated based on CLT is presented in paragraph 2. The thermal behavior simulation was conducted by means of a modular program that was written using the MATCAD facilities.

The paper examines the behavior of six hybrid's structures (table 1), made of timber lumbers and polymeric composite plates, under varying temperature.

2. THERMAL STRESSES

When materials are exposed a temperature change, they exhibit thermal strains $\{\varepsilon^T\}$ which are proportional to temperature changes ΔT. The thermal strain in material principal coordinates are then written:

$$\{\varepsilon^T\} = \{\alpha\}\{\Delta T\} \tag{1}$$

Where α is the coefficient of thermal expansion (CTE).

The equivalent thermal forces per unit length $\{N^T\}$ can be defined as:

$$\{N^T\} = \int_{-H}^{H} [\overline{Q}]^k \{\varepsilon^T\}^k dz = \int_{-H}^{H} [\overline{Q}]^k \{\alpha\}^k \{\Delta T\}^k dz \tag{2}$$

And the equivalent thermal moments per unit length $\{M^T\}$ as:

$$\{M^T\} = \int_{-H}^{H} [\overline{Q}]^k \{\varepsilon^T\}^k z_k dz = \int_{-H}^{H} [\overline{Q}]^k \{\alpha\}^k \{\Delta T\}^k z_k dz \tag{3}$$

Where: - 2H is the thickness of the laminates

- k is number ply ;
- z_k is the distance from the mid-plane of the laminate to the k layer ;
- $[Q]^k$ is the reduced stiffness matrix for the plane stresses state :

$$\overline{Q}^k = \begin{bmatrix} \overline{Q}_{11}^k & \overline{Q}_{12}^k & \overline{Q}_{16}^k \\ \overline{Q}_{21}^k & \overline{Q}_{22}^k & \overline{Q}_{26}^k \\ \overline{Q}_{61}^k & \overline{Q}_{62}^k & \overline{Q}_{66}^k \end{bmatrix} \tag{4}$$

The fundamental equation of lamination theory is:

$$\begin{Bmatrix} \varepsilon^O \\ \kappa \end{Bmatrix} = \begin{bmatrix} A & B \\ C & D \end{bmatrix}^{-1} \begin{Bmatrix} N^T \\ M^T \end{Bmatrix} \tag{5}$$

Where:- ε^o is the midplane strain ;

- κ is curvatures ;

- [A] = the extension stiffness matrix, $A_{ij} = \sum_{k=1}^{N} \left[\overline{Q} \right]^k (z_k - z_{k-1})$

- [B] = the coupling stiffness matrix, $B_{ij} = \frac{1}{2} \sum_{k=1}^{N} \left[\overline{Q} \right]^k (z^2{}_k - z^2{}_{k-1})$

- [D] = the bending stiffness matrix, $D_{ij} = \frac{1}{3} \sum_{k=1}^{N} \left[\overline{Q} \right]^k (z^3{}_k - z^3{}_{k-1})$

in which N is the total number of lamina

Using the notation $\{\varepsilon^o\}-\{\varepsilon^T\}^k = \{\varepsilon\}^k$ where $\{\varepsilon\}^k$ are the effective stress- inducing strains, the uniform stresses within the plies are calculated with formula:

$$\{\sigma\}^k = \left[Q \right]^k (\{\varepsilon\}^k + z_k \{\kappa\}) \tag{6}$$

3. THERMAL STRESSES IN A PLATE LAMINATE

Consider six hybrid structures based of unidirectional plies made of:

1. timber lumber (wood C14) ;
2. polymeric composites plates made of polyester resin reinforced with glass fibers ;
3. adhesive (sikadur 30).

Structures are presented in table 1.

The temperature change ΔT has been calculated with a FEA program, RDM5, for a variation : from 0 to 25 ^{o}C (fig. 1).

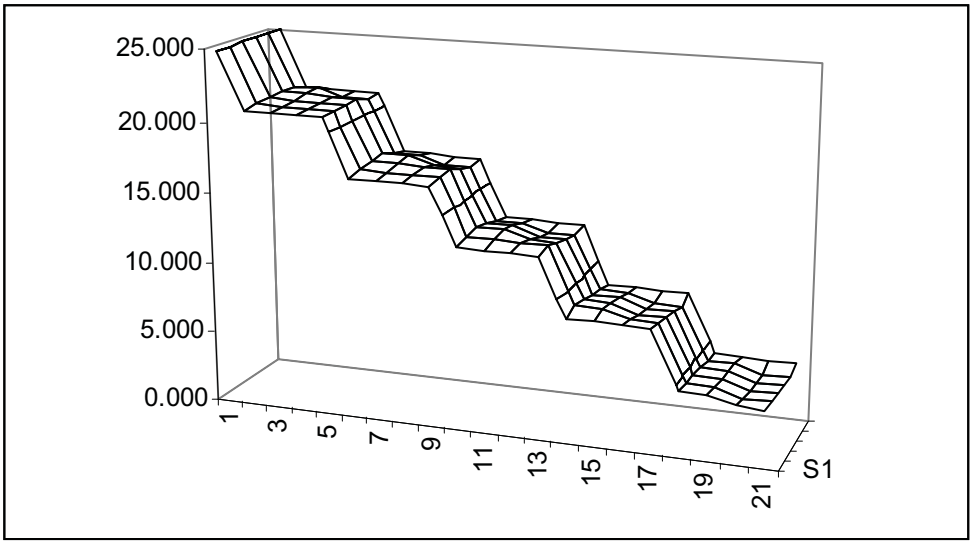

Fig. 1 The temperature variation (^{o}C) through the hybrid structures

Table 1 Hybrid structures made of timber lumbers and polymeric composites plates

No. Ply	Thickness (mm)	STRUCTURES					
		S1	S2	S3	S4	S5	S6
1	24.5	Wood	Wood	Wood	Wood	Wood	Wood
2	0.4	Sikadur	Sikadur	Sikadur	Sikadur	Sikadur	Sikadur
3	1.8	Polyester	Polyester	polyester	polyester	Polyester	sikadur
4	0.4	Sikadur	Sikadur	Sikadur	Sikadur	Sikadur	Sikadur
5	24.5	Wood	Wood	Wood	Wood	Wood	Wood
6	0.4	Sikadur	Sikadur	Sikadur	Sikadur	Sikadur	Sikadur
7	1.8	Sikadur	Polyester	Polyester	Polyester	Polyester	Sikadur
8	0.4	Sikadur	Sikadur	Sikadur	Sikadur	Sikadur	Sikadur
9	24.5	Wood	Wood	Wood	Wood	Wood	Wood
10	0.4	Sikadur	Sikadur	Sikadur	Sikadur	Sikadur	Sikadur
11	1.8	Sikadur	Sikadur	Polyester	Polyester	Polyester	Sikadur
12	0.4	Sikadur	Sikadur	Sikadur	Sikadur	Sikadur	Sikadur
13	24.5	Wood	Wood	Wood	Wood	Wood	Wood
14	0.4	Sikadur	Sikadur	Sikadur	Sikadur	Sikadur	Sikadur
15	1.8	Sikadur	Sikadur	Sikadur	Polyester	Polyester	Sikadur
16	0.4	Sikadur	Sikadur	Sikadur	Sikadur	Sikadur	Sikadur
17	24.5	Wood	Wood	Wood	Wood	Wood	Wood
18	0.4	Sikadur	Sikadur	Sikadur	Sikadur	Sikadur	Sikadur
19	1.8	Sikadur	Sikadur	Sikadur	Sikadur	Polyester	Sikadur
20	0.4	Sikadur	Sikadur	Sikadur	Sikadur	Sikadur	Sikadur
21	24.5	Wood	Wood	wood	wood	Wood	wood

Data for the ply are given in Table 2.

The values of reduced stiffness matrix for each lamina from Table 2 has been calculated with formula:

$$[\overline{Q}] = \begin{bmatrix} \frac{E_L}{1-\nu_m\nu_M} & \frac{\nu_M E_T}{1-\nu_m\nu_M} & 0 \\ \frac{\nu_M E_T}{1-\nu_m\nu_M} & \frac{E_T}{1-\nu_m\nu_M} & 0 \\ 0 & 0 & G_{LT} \end{bmatrix} \tag{6}$$

and are presented in table 3.

Table 2 Value of lamina characteristics

Lamina characteristics	Units	Value of lamina characteristics		
		Wood C14 Orthotropic mat.	Sikadur 30 isotropic mat.	Polyester with glass fiber orthotropic mat.
Longitudinal elastic modulus, E_L	N/m^2	7×10^9	4.481×10^9	5.4×10^{10}
Transverse elastic modulus, E_T	N/m^2	2.3×10^8	4.481×10^9	6.6×10^9
Shear Elastic modulus, G_{LT}	N/m^2	4.4×10^8	1.792×10^9	4.14×10^9
Poisson's ratio major coefficient, ν_M		0.37	0.22	0.205
Poisson's ratio minor coefficient, ν_m		0.15	0.22	0.105
Thermal expansion Coefficient α_1	/ ^oC	58.4×10^{-6}	18×10^{-6}	7.43×10^{-6}
Thermal expansion Coefficient α_2	/ ^oC	15.8×10^{-6}	18×10^{-6}	5.31×10^{-5}
Thermal expansion Coefficient α_3	/ ^oC	3.7×10^{-6}	18×10^{-6}	5.31×10^{-5}

Table 3 The values of reduced stiffness matrix

Value of reduced stiffness matrix		
Wood C14	Sikadur 30	Polyester with glass fiber
$\begin{bmatrix} 7.032x10^9 & 8.548x10^7 & 0 \\ 8.548x10^7 & 2.310x10^8 & 0 \\ 0 & 0 & 4.4x10^8 \end{bmatrix}$	$\begin{bmatrix} 4.7x10^9 & 1.03x10^9 & 0 \\ 1.03x10^9 & 4.7x10^9 & 0 \\ 0 & 0 & 1.79x10^9 \end{bmatrix}$	$\begin{bmatrix} 5.4x10^9 & 1.36x10^9 & 0 \\ 1.36x10^9 & 6.6x10^9 & 0 \\ 0 & 0 & 4.1x10^9 \end{bmatrix}$

The following assumptions are fundamental to lamination theory:

- the laminate consists of perfectly bonded layers (laminate);
- the basic ply constituent materials (matrix and fiber) are considered isotropic materials ;
- total strain in the laminate follow from the Kirchhoff assumptions on displacements ;
- each layer is in state of plane stress
- stiffness properties of the basic ply material are unaffected by temperature and the thermal expansion coefficient are constant ;

The thermal behavior simulation was conducted by means of a modular program that was written using the MATCAD facilities, on the basis of the equation presented in paragraph 2. The stress values for the basic plies are given in figure 2, 3, 4

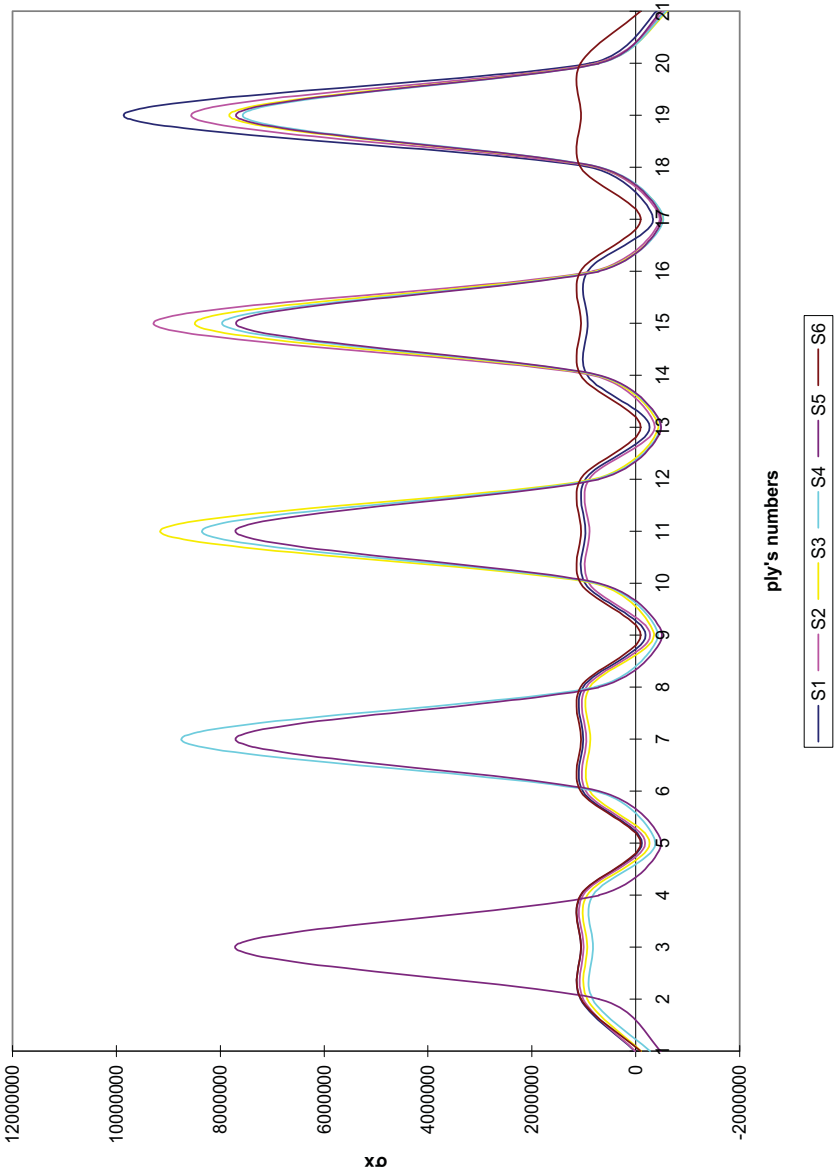

Fig. 2 Thermal stress σ_x

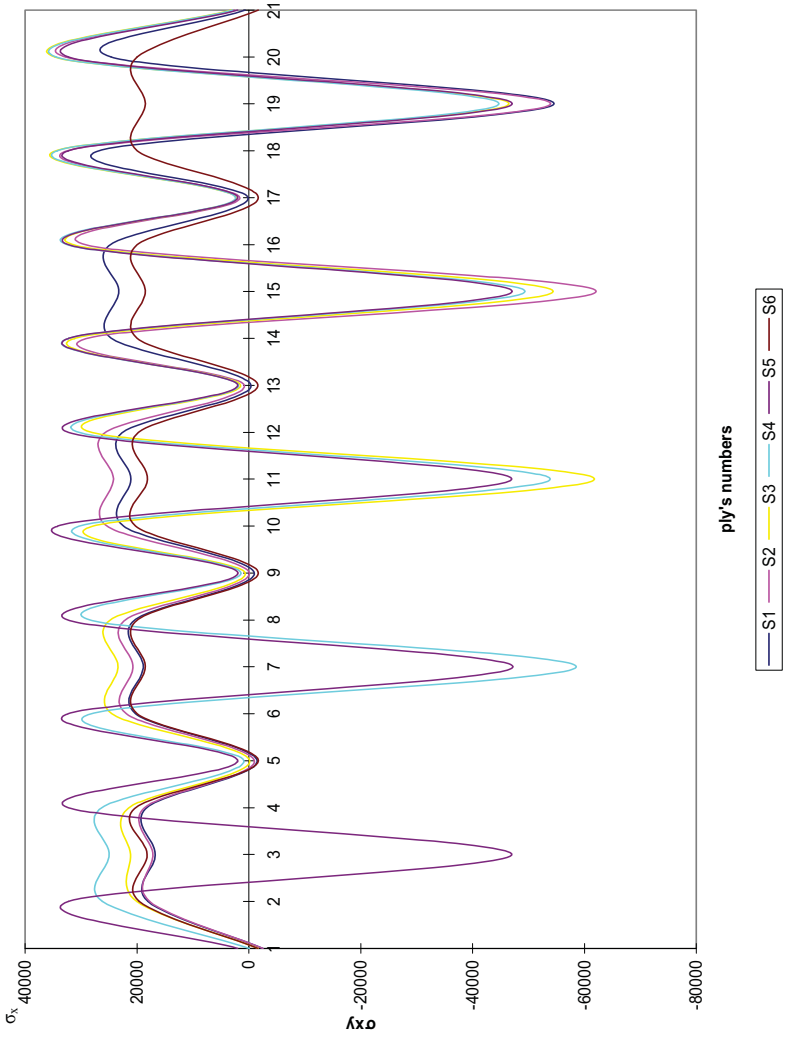

Fig. 3 Thermal stress σ_{xy}

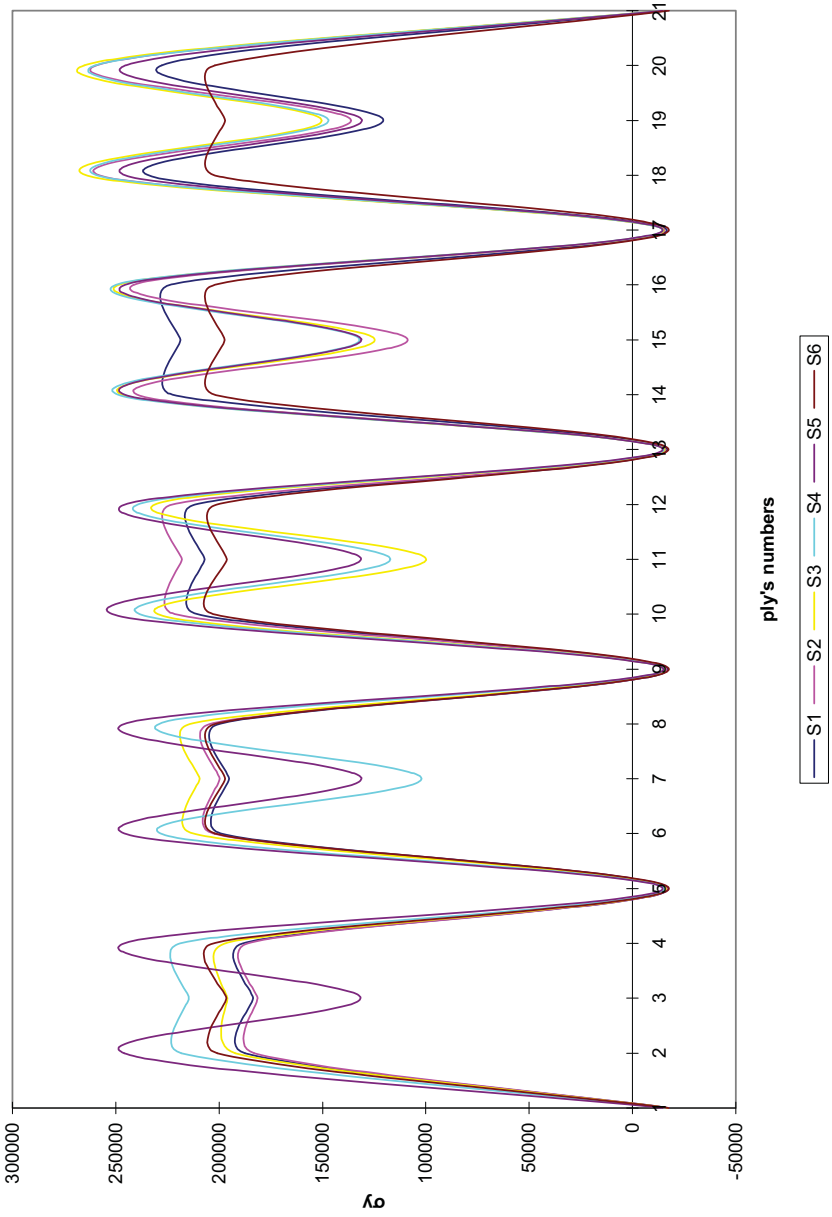

Fig. 4. Thermal stress σ_y

4. CONCLUSIONS

In this paper, the stress analysis of multilayered plates subject to thermal load is performed in the context of the theory of thermo elasticity. Temperature distributions varying linear through the thickness are considered. A procedure for the reliable modeling and the application is presented. Structures made with composite materials are more sensitive and vulnerable to temperature change than their isotropic counterpart. The reason is that the thermal expansion coefficient of different constituents of the material is usually dramatically different from each other resulting in high stresses due to temperature change. The analysis including thermal effects is much more involved than that for the isothermal conditions. All stress values depend on the lamina constituent material properties, the geometrical characteristics of the individual layers, and the stacking sequence.

A complete thermo-mechanical analysis was made to identify the most stressed individual layers and to prevent failure of a composite laminated structure under mechanical and thermal loadings.

References

1. Herakovich C.T., *Mechanics of Fibrous Composites*, University of Virginia, Charlottesville Printing office, 1996
2. Taranu N., Isopescu D. – *Structures Made of Composite Materials*, Ed. VESPER, Iasi, 1996
3. Gurdal Z. et co., *Design and Optimisation of Laminated Composite Materials*, John Wiley & Sons, Inc.,New York, 1998

"Computational Civil Engineering 2006", International Symposium
Iaşi, România, May 26, 2006

A generalization of the moments distribution method for the structure computation in the postelastic field

Constantin Amariei, Vasile Filip

Faculty of Civil Engineering, "Gh. Asachi" Technical University of Iasi

Summary

A generalized expression of the moment distribution method in the postelastic field, is presented where there are operating both with work quantities for balancing kinematic chains for nodes too, the balancing of the bars being canceled.

The possibility of calculus process automation is also eliminated, in the aim to perform computer aided solving.

KEYWORDS: structures, moment distribution, work quantitties postelastic design.

1. INTRODUCTION

In the case of frames with unparallel displaced nodes (fig. 1.a) it isn't adequate to work on the balance of the kinematic chains with moments, because of the difficulties concerning the determination and repartition of the unbalanced moments on the bars.

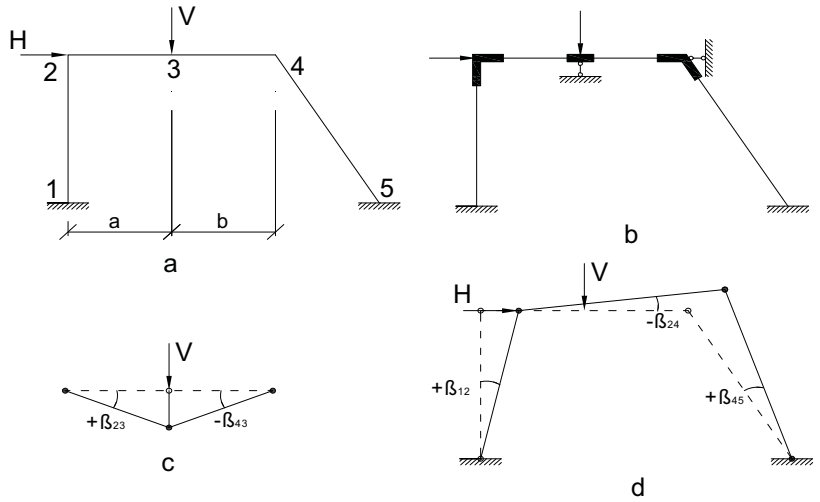

Fig.1

In the paper no.[3], Prof. A. Sesan has proposed to work with work quantities on the balance of the kinematic chains for the frames through the moment distribution method in the postelastic field.

The work is calculated as follows:

- the initial work (1st stage of the calculus):

$$W_A = \sum_A m_{ij}\beta_{ij} + \sum_A \overline{P_i}\,\overline{\delta_{i(A)}} \tag{1}$$

- the unbalanced work (intermediary stage of the calculus):

$$\Delta W_A = \sum_A \Delta m_{ij}\beta_{ij} \tag{2}$$

In this way the work is distributed on the bars and this operation can be done using repartition coefficients which depend only on the kinematic characteristics of the kinematic chains and which remain unchanged throughout the stages of the postelastic computation. So, for a (i-j) bar, which has a turning proportionality coefficient β_{ij} in a kinematic chain A, the repartition of the work coefficient has the following expression (fig. 1.c, 1.d):

$$\nu_{ij}^{''(A)} = \frac{\beta_{ij}}{\sum_A \beta_{ij}} \tag{3}$$

so the repartition of the chain work on the bars is done as follows:

$$W_{ij} = -\nu_{ij}^{''(A)} W_A \tag{4}$$

for the 1st stage of the computation and:

$$\Delta W_{ij} = -\nu_{ij}^{''(A)} \Delta W_A \tag{5}$$

for the current stage.

2. THE GENERALIZATION OF THE METHOD FOR A COMPLETE COMPUTATION WITH WORK

The calculus approach mode presented earlier can be generalized and summarized in order to use it for the rational and economic design of any structure type using a low amount of calculus operations.

Primarily, for the calculus simplification and unity, we will insert virtual nodes near the forces on the bars with loads on the opening, in this way the bars can be treated as kinematic chains. The important result of this operation is the fact that the stages of the calculus will only contain balancing of nodes and kinematic chains, the balancing of bars being eliminated from the usual method.

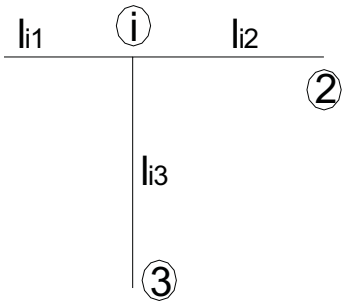

Fig.2

Secondly, we choose as operating values the work for balancing the kinematic chains, as well as the nodes. Obviously, in the balancing operations for the nodes the work will be affected, in this case by correction coefficients deduced from the condition of balancing regarding moments. So, for example, for a node in which three bar ends intersect (fig. 2), using the notations:

w_{ij} = work on the (i-j) bar;

β_{ij} = the rotation proportionality coefficient of the (i-j) bar in a certain kinematic chain,

the condition $\sum M_{ij} = 0$ becomes:

$$\frac{w_{i1}}{\beta_{i1}} + \frac{w_{i2}}{\beta_{i2}} + \frac{w_{i3}}{\beta_{i3}} = \frac{\beta_{i2}\beta_{i3}w_{i1} + \beta_{i1}\beta_{i3}w_{i2} + \beta_{i1}\beta_{i2}w_{i3}}{\beta_{i1}\beta_{i2}\beta_{i3}} \tag{6}$$

or:

$$\sum k_{ij}^{*} w_{ij} = 0 \tag{7}$$

where:

$$k_{ij}^{*} = \prod_{k=1}^{m} \beta_{ik} \, (k \neq j) \tag{8}$$

m being the number of bars that intersect in the (i) node and have rotations different from zero in the kinematic chains that they are a part of.
With these adjustments, the computation can be done using the following stages:

1. We determine the calculus elements : $\beta_{ij}, \nu_{ij}'', k_{ij}^{*}$.
2. We perform the first balancing of the kinematic chains which contains the following operations:

2.1 We determine the unbalanced work on the kinematic chain:

$$W_A = \sum \pm \left[m_{ij} \beta_{ij(A)} \right] + \sum \pm \left[\bar{\lambda}_i \bar{\delta}_{i(A)} \right] \tag{9}$$

where:

m_{ij} = moments of perfect fixed end;

λ_i = loading parameters;

$\delta_{i(A)}$ = displacements corresponding to the loading parameters, in the respective kinematic chain.

2.2 We distribute the unbalanced works on the bars of the kinematic chains:

$$W_{ij}^{(A)} = -\nu_{ij}''^{(A)} W_A \tag{10}$$

2.3 We distribute the works at the bar ends:

$$\bar{w}_{ij} = \eta_{ij} W_{ij}^{(A)} \tag{11}$$

$$\bar{w}_{ji} = \eta_{ji} W_{ij}^{(A)} \tag{12}$$

where η_{ij} and η_{ji} are set using the criteria shown previously regarding the distribution of the moments (without the criteria, we will use $\eta_{ij} = \eta_{ji} = 1/2$).

3. We perform the first balancing of the nodes, which for an (i) node means:

3.1 We determine the unbalanced work on the node:

$$\Delta w_i^{'} = \sum_i k_{ij}^{*} \overline{w}_{ij} \tag{13}$$

3.2 We balance the node by allocating the unbalanced work to one (usually) or more bars (i-k) appointed previously, in accordance with the computation method that we choose:

$$w_{ik}^{'} = -\mu_{ik} \frac{\Delta w_i^{'}}{k_{ik}^{*}} \tag{14}$$

where μ_{ik} is a distribution coefficient between the bars on which we make the allocation of the unbalanced moment. These coefficients are also set previously from the same reasons on which we chose η_{ij}.

On the other bars in the node, the work remains the same.

4. We perform alternative balancing of kinematic chains and nodes, until we reach the necessary precision.

So, in a certain stage (m) of kinematic chains balancing, the calculus operations for a chain (A) are:

a. The calculus of the unbalanced work:

$$\Delta W_A^{(m)} = \sum_A -\mu_{ik} \frac{\Delta w_{i(A)}^{(m-1)}}{k_{ik}^{*}} + \sum_A \Delta w_{ij(B)}^{(m-2)} \tag{15}$$

where:

$\Delta w_{i(A)}^{(m-1)}$ - the work on the node balanced in the previous stage;

μ_{ik}, k_{ik}^{*} - they have the same meaning as earlier and they refer to the (i-k) bars on which adjustments have been made in the (m-1) stage;

$\Delta w_{ij(B)}^{(m-2)}$ - the works on the (i-j) bars of the (A) kinematic chain in common with the ones of another chain (B); it's balancing has been performed in the (m-2) stage after the one of chain (A) [so, they are unbalanced works, remained from the (m-2) stage].

b. The distribution of the unbalanced work directly on the bar ends:

$$\Delta \overline{w}_{ji}^{(m)} = -\nu_{ij}'' \Delta W_A^{(m)} \tag{16}$$

(j-i) being the opposite ends of the (i-j) bars on which adjustments have been made in the previous node balancing stage (m-1).

For the other bar ends:

$$\Delta\overline{w}_{ij}^{(m)} = 0 \tag{17}$$

In a certain stage (n) of node balancing, the calculus operations for a node (i) are:

a. Determination of the unbalanced work in the node:

$$\Delta w_i^{(n)} = \sum k_{ij}^* \Delta\overline{w}_{ij}^{(n-1)} \tag{18}$$

b. The balancing of the node, by adjusting the work on the pre-established (i-k) bars (the same as in the 3.2 stage):

$$\Delta w_{ik}^{(n)} = -\mu_{ik} \frac{\Delta w_i^{(n)}}{k_{ik}^*} \tag{19}$$

For the other bars, the work remains the same, meaning:

$$\Delta w_{ij}^{(n)} = 0 \tag{20}$$

After performing the number of balancings imposed by the necessary calculus precision, we determine through addition the work on the bar ends w_{ij} and afterward we proceed to the moments on the bar ends:

$$m_{ij} = \frac{w_{ij}}{|\beta_{ij}|} \tag{21}$$

in which:

w_{ij} - the added work from all stages;

β_{ij} - the rotation proportionality coefficients of the bars in their respective kinematic chains.

After knowing the moments distribution, we will proceed to structure bars sizing.

3. CONCLUSIONS

a. Even if the successive approximations are not mechanized as in the elastic calculus, they can still be arranged and that's why we remove the somehow arbitrary adjustment operations from the regular moment distribution method in the postelastic field.

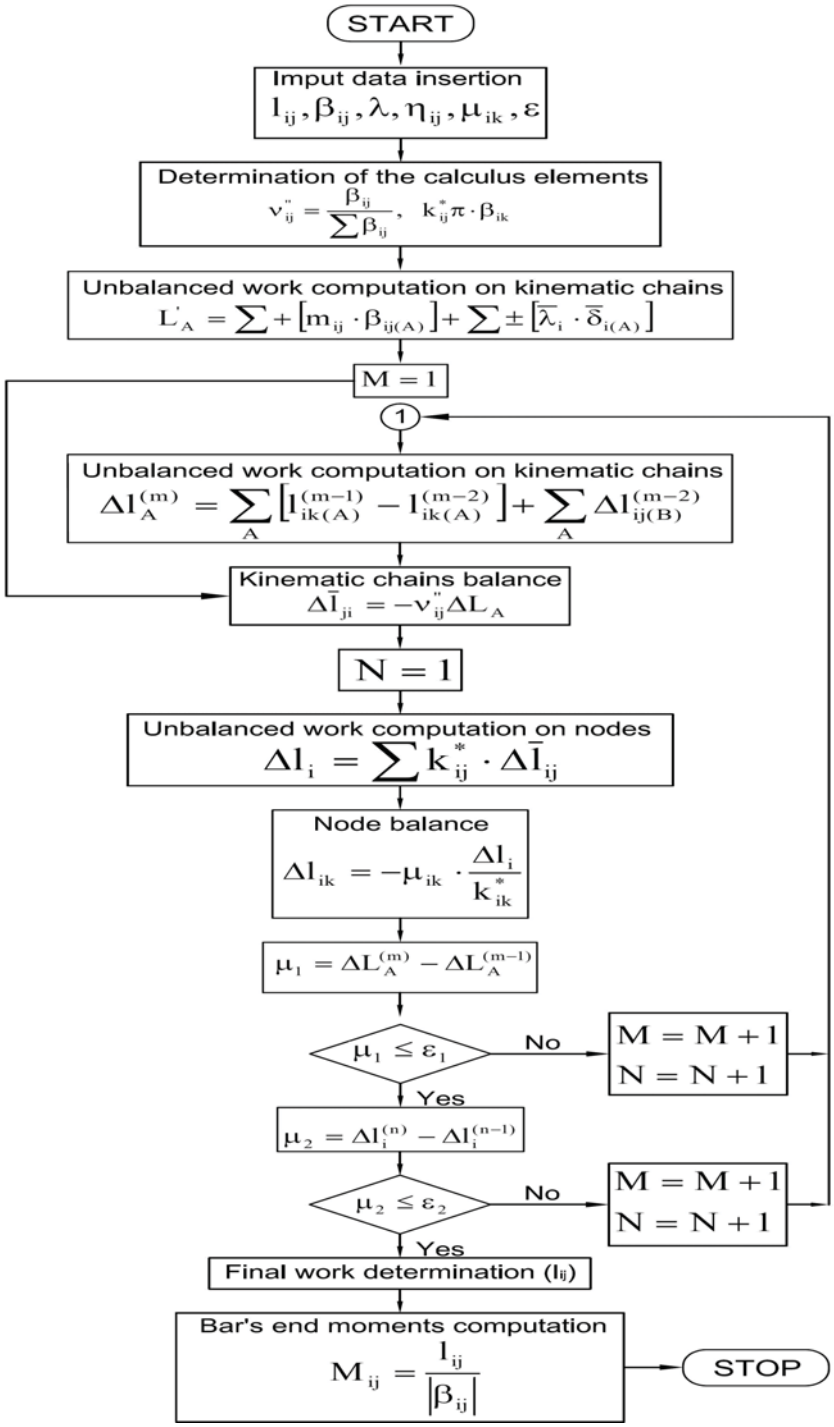
START
Imput data insertion
$l_{ij}, \beta_{ij}, \lambda, \eta_{ij}, \mu_{ik}, \varepsilon$
Determination of the calculus elements
$\nu''_{ij} = \frac{\beta_{ij}}{\sum \beta_{ij}}, \quad k^*_{ij}\pi \cdot \beta_{ik}$
Unbalanced work computation on kinematic chains
$L'_A = \sum + [m_{ij} \cdot \beta_{ij(A)}] + \sum \pm [\bar{\lambda}_i \cdot \bar{\delta}_{i(A)}]$
M = 1
1
Unbalanced work computation on kinematic chains
$\Delta l_A^{(m)} = \sum_A [l_{ik(A)}^{(m-1)} - l_{ik(A)}^{(m-2)}] + \sum_A \Delta l_{ij(B)}^{(m-2)}$
Kinematic chains balance
$\Delta \bar{l}_{ji} = -\nu''_{ij} \Delta L_A$
N = 1
Unbalanced work computation on nodes
$\Delta l_i = \sum k^*_{ij} \cdot \Delta \bar{l}_{ij}$
Node balance
$\Delta l_{ik} = -\mu_{ik} \cdot \frac{\Delta l_i}{k^*_{ik}}$
$\mu_1 = \Delta L_A^{(m)} - \Delta L_A^{(m-1)}$
$\mu_1 \le \varepsilon_1$
No
M = M + 1
N = N + 1
Yes
$\mu_2 = \Delta l_i^{(n)} - \Delta l_i^{(n-1)}$
$\mu_2 \le \varepsilon_2$
No
M = M + 1
N = N + 1
Yes
Final work determination (l_{ij})
Bar's end moments computation
$M_{ij} = \frac{l_{ij}}{|\beta_{ij}|}$
STOP

Fig.3

b. Now it's possible to apply this method for the automated calculus. In figure no.3 we have the block diagram for the calculus using the moments distribution method in the postelastic field, in the generalized form using work quantities for kinematic chains balancing as well as for node balancing.
c. By changing the group of bars on which we make adjustments on the node balancing, we can obtain various solutions, from which we choose the one that meets the economic condition, meaning the solution with the minimum weight.

References

1. Amariei, C. *Calculul structurilor in domeniul plastic*, I.P. Iasi, 1974
2. English J.M. *Design of Frames by Relaxation of Yield Hinges*, J. Asce, 1953,79
3. Sesan, A. *Generalizarea metodei distribuirii momentelorin calculul plastic la cadre oarecari*, Institutul Politehnic Iasi, 1958, IV (VIII), 1-2.

"Computational Civil Engineering 2006", International Symposium
Iaşi, România, May 26, 2006

Finite element model for composite steel-concrete column

Cristina Campian, Paul Pernes

Technical University of Cluj-Napoca, 400020 Cluj-Napoca, Romania

Summary

In Technical University of Cluj Laboratory, several tests according to ECCS loading procedure were carried out. The tested specimens were composite columns of fully encased type subject to a variable transverse load at one end while keeping a constant value of the axial compression force into them. The complex evolution of the hysteretic cyclic curves representing the transverse force versus the associated displacement up to a pronounced deterioration of the column bases leads to a analytical simulation in finite elements program. A comparison is made and several conclusions end the presentation.

KEYWORDS: composite columns, finite elements, monotonic behavior

1. INTRODUCTION

The experimental program was made for 12 columns with the same cross-section, rallied in three groups of four columns each called SI, SII and SIII according to their length. The testing procedure was the one recommended by ECCS for characterizing the behaviour of steel elements with respect to seismic action (ECCS-TWG 1.3, 1986).

2. TESTED SPECIMENS

The element were fabricated from a Romanian steel section I12 (which is quasi similar to IPN 120 section) fully covered with reinforced concrete including 4Φ10 longitudinal bars (shown in Figure 1). The mechanical model is a cantilever element subject to an axial force N in compression and to a transverse variable force H located at the free top.

To ensure a suitable full restraining at the column base, the elements were ended by a sudden cross-section enlargement acting as a foundation (the flexural stiffness ratio between the element and the so-realized foundation was about 1/5). The external dimensions of the composite cross-section were 170x200 in mm. The three column lengths were:

l = 2.00 m for the column series SI,

l = 2.50 m for the column series SII,

l = 3.00 m for the column series SIII.

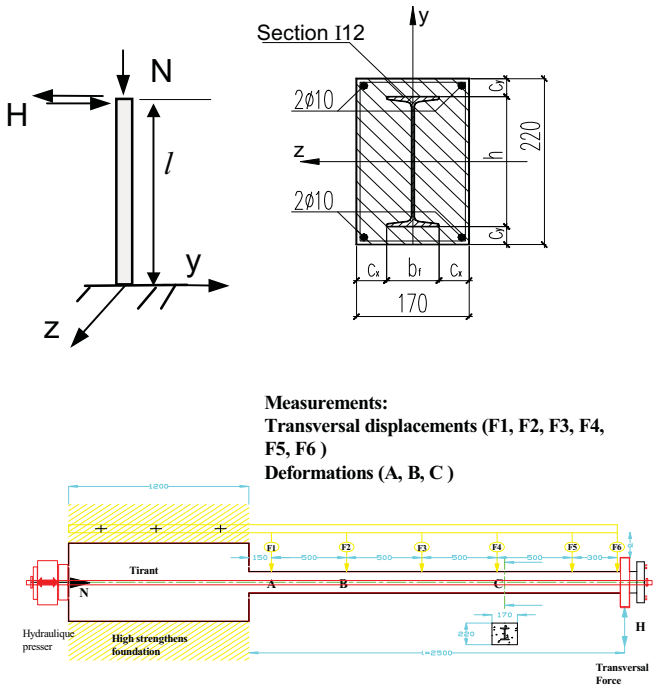

Figure 1. Mechanical model and composite cross-section of the elements

The used materials were:

- OL37 structural steel (which may be compared to S235 European grade) for the I12 section;
- PC52 reinforcing steel (which may be compared to S550 European grade);
- C20/25 concrete class, as defined in Eurocode (for example, see clause 3.1.2 in CEN-EUROCODE 4, 1992).

To satisfy the plastic rotation demand at the column base and to compensate for possible loss of resistance due to spalling of cover concrete, a transverse reinforcement for an efficient concrete confinement was ensured by closed rectangular stirrups of 10 mm diameter with a spacing s of 10 cm along the whole column length as well as the foundation.

It should be noted that this spacing is just a bit wider than the value s=7 cm within the critical length l_{cr} = 60 cm of the columns such as specified in Eurocode 8 (see clause 7.6.4 in CEN-EUROCODE 8, 2002) for belonging to class H of high ductility.

Moreover, checks confirmed that the longitudinal reinforcing bars were of high ductility (ε_{su}>5% and f_{su}/f_{sk}>1.08).

3. EXPERIMENTAL RESULTS

The columns were loaded in horizontal position, with the compression axial force N of constant intensity (100 kN or 200 kN) and the variable force H at the free end controlled by imposed displacements, as shown in photo of Figure 2 and Figure 3. Force N does not keep the same direction rigorously because it passes approximately through the base of the column (more exactly through the center of the external face of the foundation).

Figure 2. Testing installation

All the tests were conducted up to the maximum damage of concrete at the column bases; generally, at this stage, buckling of the longitudinal reinforcing bars occurred in the critical zone due to a quasi full deterioration of concrete encasement.

Table 1 collects the different types of test carried out and the maximum values of transverse force $H_u^{(exp)}$ reached under monotonic or cyclic loading.

Table 1

Tests	*l* (m)	Axial force N (kN)	Testing procedure	Maximal transverse force $H_u^{(exp)}$ (KN)
SI-1	2.00	200	Monotonic	28.1
SI-2	″	200	Cyclic	25.7
SI-3	″	200	(ECCS) with elastic limit 40	24.1
SI-4	″	100	mm	26.0
SII-1	2.50	200	Monotonic	20.0
SII-2	″	200	Cyclic	19.6
SII-3	″	200	(ECCS) with elastic limit 40	20.5
SII-4	″	100	mm	20.5
SIII-1	3.00	200	Monotonic	17.2
SIII-2	″	200	Cyclic	17.5
SIII-3	″	200	(ECCS) with elastic limit 40	16.5
SIII-4	″	100	mm	17.8

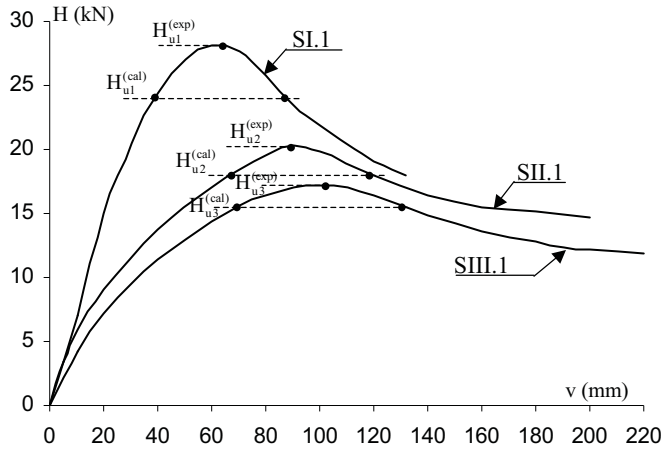

Figure 3. Curves of the monotonic tests

Figure 3 shows the transverse force H-displacement v curves registered for the three monotonic tests, each curve including a clear softing branch below $H_u^{(exp)}$ due to buckling.

4. NUMERICAL MODELLING USING DRAIN-2DX

4.1 Generalities

The DRAIN 2DX is an EF program developed by Berkley University of California. In this paper the 1.10 version is utilized.

The column has a fixed end and a free end. The realized grid is adapted to geometrical points on which we had measurements points.

The number of points on longitudinal direction x is given by table 2 , for each studied points

Table 2

Column	No of elements
SI.1	41
SII.1	51
SIII.1	61

For the modelisation we chose from the library of EF the « Fiber beam-column element 15 » an inelastic finite element.

This element is recommended for the behavior of elements made from different materials , subjected to compression and flexion.

The transversal cross section of the column is divided in fibers on the web direction.

The element is supposed to elastic in shear and the P-Δ effects can be taken into account

The calculus hypothesis are the next :

- The section remains plane after deformation
- The behavior in shear is supposed to be elastic.

This is a so called a 'low order' finite element, which give a more stable behavior.

The utilized analyze is that called "event by event". An event corresponds to a change of rigidity of the element, cause by traction, an inelastic uncharged, etc of a fiber. So, the rigidity of the structure is calculated each time, for each "event".

We adopted a behavior model for each material, concrete, steel and reinforcement.

For concrete, we used 5 characteristic points for compression and 2 characteristic points for tension.

For the uncharged part, we used a uncharged factor (FU) of 0.5 , who is very close to the real behavior of the utilized concrete.

For the steel, as tests were made in laboratory, we had the real curves for the behavior of the material. The introduced curves are very close to the ones really obtained

4.2 Modelisation in the cross section

In the cross section, the element was modulated by 30 fibers, fibers called CO1 for the concrete, SO2 for steel and SO1 for reinforcement.

So, on the width of the cross section, the fibers were defined by their surface and their coordinates from the gravity center of the cross section for each fiber.

The reinforcement was assimilated with a very thin layer of steel. The profile steel was assimilated with two flange-layers and many thin layers for the web, alternatively with layers of concrete.

The figure 4 shows the cross section modeling.

The charge was applied in two phases:

- A statically one (axial compression of constant value of 00KN),
- A « dynamic » one of transversal step by step growing force

The transversal forces correspond to forces values measured in the experimental test.

The experimental displacement- force curve allowed the making of a given force values folder, for the calculus with approximately 100 points.

A lot of tests were carried out to calibrate the model.

4.3.Results

For monotonic charge, the next figures give the displacements-forces curves obtained with DRAIN and those obtained by the experimental tests.

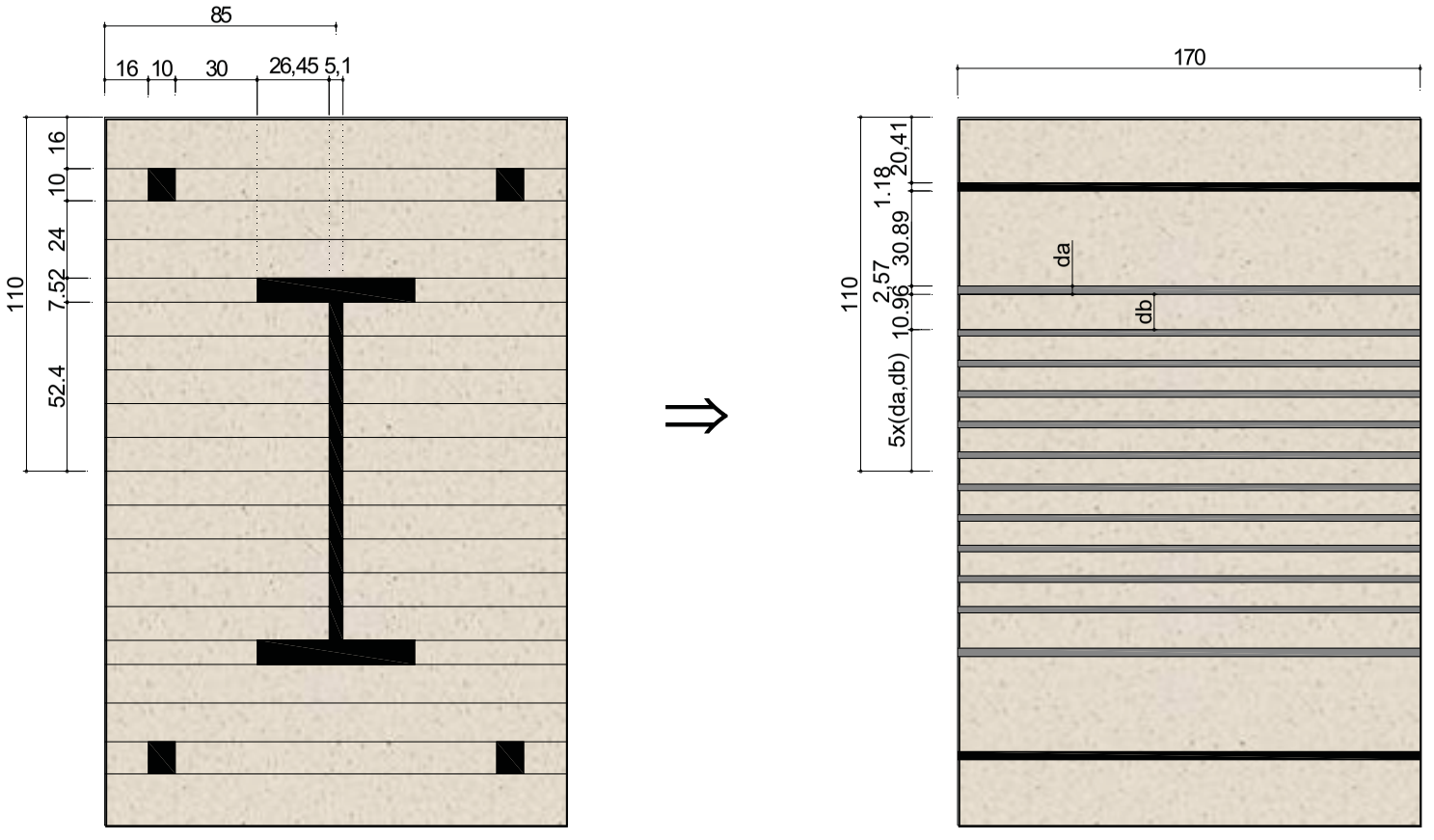

Figure 4. The assimilated cross section

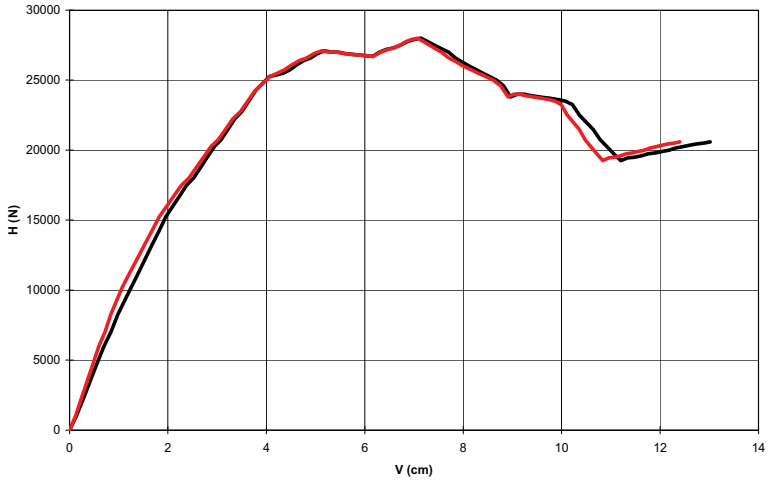

Figure 5. Comparation for the SI.1 column

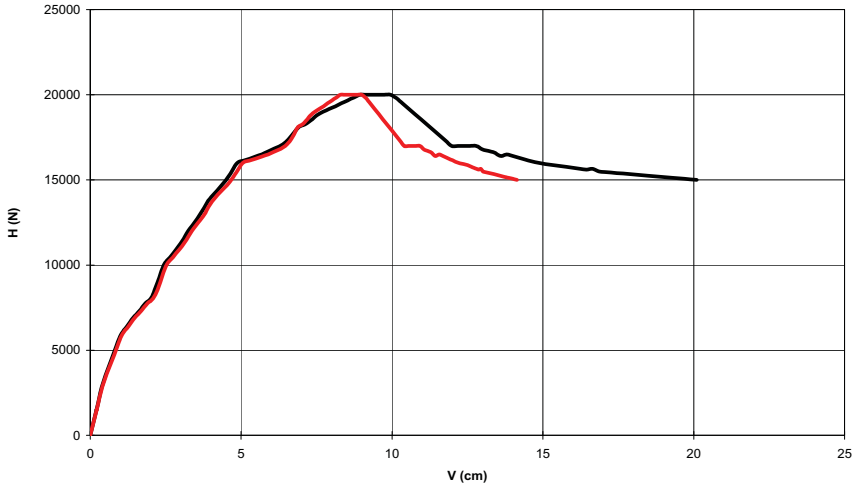

Figure 6. SII.1 Column

It can be observed that the differences in displacements are under the 5% in value of maximal force. The biggest difference appeared on the descending branch, until the considered collapse.

Bibliography

1. Campian Cr (2001), „*Contribution a l'etude du comportement rt au calcul de poteaux mixtes acie-beton (sous des charges transversals de variation monotone ou cyclique alternee* „ these de doctorat en co-tutelle, INSA Rennes and UT Cluj,
2. Aribert, J.M, Campian, Cr , Pacurar, V.(2003) „*Monotonic and cyclic behaviour of fully encased composite columns and dissipative interpretation for seismic design*". Swets&Zeitlinger B.V., Lise, The Netherlands, STESSA 2003, , ISBN 90-5809-577 0, pag 115-122
3. Aribert, J.M, Campian, Cr .(2004),„*Etude expérimentale et interpretation analytique du comportement statique et cyclique de poteaux mixtes acier flechis par une charge transversale"*. Revue de Construction Métallique n°4, p. 3-22, 2004.
4. CEN EUROCODE 4 Final Draft (2002): *Design of Composite Steel and Concrete Structures - Part 1.1: General Rules and Rules for Buildings*, August 2002.
5. CEN EUROCODE 4, ENV 1994-1-1 (1992): *Design of Composite Steel and Concrete Structures - Part 1.1: General Rules and Rules for Buildings*, October 2002.
6. ECCS (1986): *Recommended testing procedure for assessing the behaviour of structural steel elements under cyclic loads*, Doc. no 45 of European Convention for Constructional Steelwork, TWG 1.3, 1986.

"Computational Civil Engineering 2006", International Symposium
Iaşi, România, May 26, 2006

Determination of temperature course in concrete during hydration

Jiri Zach[1], Hana Kminova[2] and Ondrej Horky[3]

[1, 2, 3] *Department of Technology of Building Materials and Elements, University of Technology, Brno, 60200, Czech Republic*

Summary

Durability of the concrete responds very close with the microstructure - cement stone microstructure. Each crack in a concrete microstructure very strongly decreases mechanical properties and durability of final concrete structure. Determination of temperature course in concrete structure during hydration and estimation of possibility for cracks inception is possible through modeling.

Hydration heat liberation is dependent on type and amount of cement, additives, and chemical admixtures. For most of modern concretes, is used relatively high amount of chemical (plasticizing) admixtures for improvement of their properties and decreasing of binder amount. These admixtures significantly influence hydration heat course and from the point of view of determining temperature course in concrete during hydration, it is necessary to know co-reaction of binder and chemical admixtures.

On basis of prediction of concrete massive temperature, it is possible to change the material amount of a concrete mixture by carrying out the choice of optimum chemical admixture and amount of binder. By means of such a process, it is possible to reduce risks of crack creation for concrete structures efficiently and so that to increase final properties and their durability.

KEYWORDS: hydration, heat, concrete, cement, temperature, additives, admixtures, chemicals.

1. INTRODUCTION

If we want to predict temperature course in concrete solids during hydration, it is necessary to know thermal technical properties of hydrating concrete at first. One of basic thermal technical properties is dependency of intensity of hydration heat liberation in time and further value of heat transfer coefficient of concrete and heat capacity of hydrating concrete. The entire calculation procedure has been demonstrated below on the model example of real structure.

2. DETERMINATION OF HYDRATION HEAT LIBERATION

This relation can be usually assessed on binder itself by means of direct calorimetric methods. One of the possible methods is determination of hydration heat liberation of used binder with help of izoperibolic calorimeter. Measurement is to be carried out under required boundary conditions responding to those ones under which concreting of building structure will be carried out.

The measurement has been carried out on modified cement paste at temperature +20°C in the first stage. The composition of cement paste has been as follows:

- CEM I 42,5 R (factory – Radotin) – 390g,
- batch water – 165 g,
- superplasticizing admixture – 2,30g

The calculation of intensity of hydration heat liberation has been carried out on basis of temperature course of hydrating cement paste, thermal technical properties of calorimeter, and boundary conditions. The following graph shows the curve of intensity course of hydration heat $\dot{Q}_{hydr}$ v $W.kg^{-1}$ for modified cement paste (for composition see above) which hydrated in calorimeter at environment temperature + 20°C.

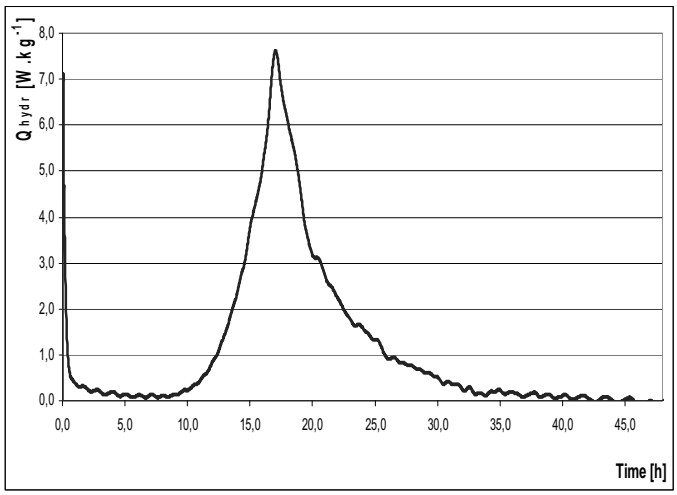

Figure 1: Course of intensity of hydration heat liberation for examined modified cement paste

As it is obvious from the Figure 1, maximum value of intensity of hydration heat liberation of given mixture has been equal to 7,5 $W.kg^{-1}$ and has been reached in time of 17.2 hours.

3. DETERMINATION OF HEAT TRANSFER COEFFICIENT

Determination of heat transfer coefficient has been carried out with samples of hydrated concrete by stationary method of plate by means of device Holometrix Lambda 2300. Value of heat transfer coefficient changes during hydration of concrete but with respect of the fact that this change of heat transfer coefficient is very difficult to be express, approximation relation is being used for calculations.

$$\lambda = \frac{(\lambda_b - \lambda_a)\,\tau}{0{,}3989\sqrt{2\pi\frac{\tau_{\max}}{3}}} e^{-\left(\frac{\tau-\tau_{\max}}{\frac{2\tau_{\max}^{\ 2}}{9}}\right)}. + \lambda_a \tag{1}$$

$$\lambda = \frac{(\lambda_b - \lambda_c)\,\tau}{0{,}3989\sqrt{2\pi\frac{\tau_{\max}}{2}}} e^{-\left(\frac{\tau-\tau_{\max}}{\frac{2\tau_{\max}^{\ 2}}{2}}\right)}. + \lambda_c \tag{2}$$

where: λ_a .. thermal conductivity in time 0 [$W.m^{-1}.K^{-1}$],

λ_b .. th. conductivity in time of max. hydration heat liberation [$W.m^{-1}.K^{-1}$],

$\lambda_{c\ ....}$ thermal conductivity of hydrated concrete [$W.m^{-1}.K^{-1}$],

τ .... time [s],

τ_{max} time of maximal hydration heat liberation [s],

As follows from above mentioned relation, value of heat transfer coefficient of fresh concrete varies within range 1.8 – 2.3 $W.m^{-1}.K^{-1}$ (regarding thermal technical properties of aggregates and concrete composition). Further, value of heat transfer coefficient increases and reaches its maximum value approximately in the same time when intensity of hydration heat liberation reaches its maximum. After that,

value of heat transfer coefficient of concrete gradually decreases to value of hydrated hardened concrete.

Results of measurement are listed in Tab.1:

Tab.1: Overview of measured values of heat transfer coefficient, volume mass, and compression strength in three selected concrete specimens

Specimen	Volume mass $kg.m^{-3}$	Heat transfer coefficient $W.m^{-1}.K^{-1}$
1	2442,0	1,750
2	2551,4	1,750
3	2295,4	1,768
Average	2429,6	1,710

Note: Values for hardened concrete after 28 days

4. CALCULATION OF TEMPERATURE COURSE IN CONCRETE STRUCTURE DURING HYDRATION

Calculation has been carried out on model of tunnel lining with wall thickness of 0.5 m. Concrete fragment with dimensions 0.4x1x1 m has been selected as a specific element and concrete properties has been selected consistent with measured values and table values as follows:

$\lambda_a = 2,0\ W.m^{-1}.K^{-1}$, :

$\lambda_b = 3,0\ W.m^{-1}.K^{-1}$,

$\lambda_c = 1,71\ W.m^{-1}.K^{-1}$,

$c_0 = 1124\ J.kg^{-1}.K^{-1}$,

$\rho = 2378\ kg.m^{-3}$.

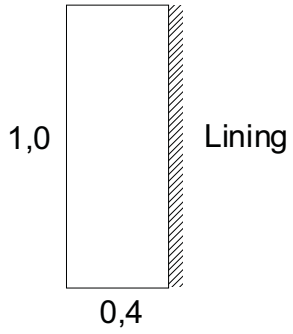

Figure 2: Scheme of calculated model fragment

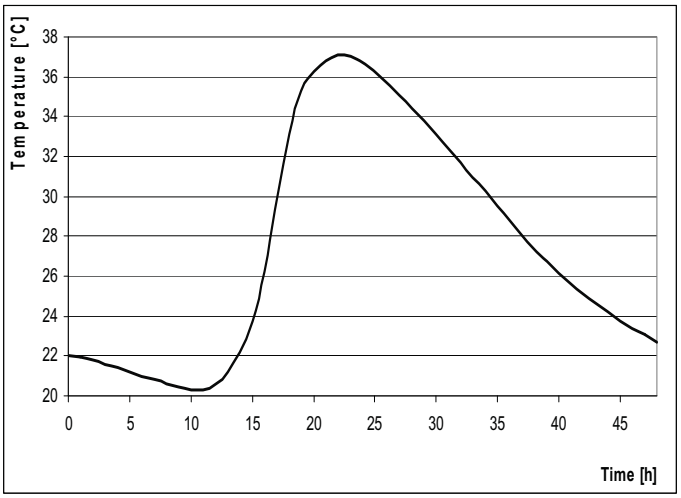

Figure 3: Temperature courses in centre of examined profile dependent on time:

The following has been considered for the calculation:

Temperature of laid mixture equal to + 22.0 °C,

Temperature of environment equal to + 20.0°C,

Temperature of sub-lining equal to + 16,0 °C.

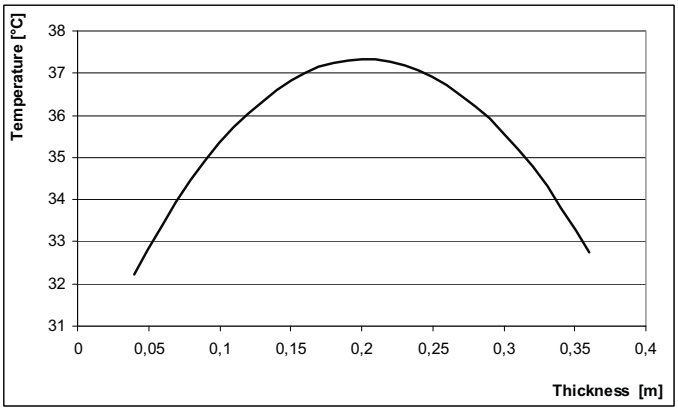

Figure 4: Thermal field distribution in lining profile after 22 hours of hydration

Note: Heat transfer coefficient of hydrating concrete reaches value approx. 50% higher than hardened concrete (see above).

The calculation has been carried out by means of finite element method with isometric meshing. The results of calculation are graphically displayed Figure 3.

As it is obvious from the graph, maximum temperature in the centre of profile is approximately + 37,3°C and it is reached after 22 hours.

The Figure 4 shows distribution of thermal field in lining profile in time of reaching the maximum temperature.

As it is obvious from the graph, temperature difference between centre and surface of lining is approximately 6 K.

5. CONCLUSION

As it has been demonstrated, it is possible to predict temperature course in concrete structure during hydration. As it has been elicit from calculation on the model of real structure, temperature inside the concrete profile should not exceed temperature 38.0°C during hydration process. Temperature of laid concrete during concreting equal to +22.0°C and temperature of environment equal to +20°C have been considered in the calculation. In case that temperature of concrete laid during concreting is higher, it is necessary to deal with acceleration of hydration process and with higher temperature increase in profile. We may assume that temperatures in profile even at higher temperatures or at higher temperature of laid concrete will not be critical due to relatively low thickness of structure.

In this manner, it is possible to estimate temperature course inside massive concrete structures during hydration of binder with sufficient accuracy and provide relevant arrangements in sufficient timing advance to prevent structural disruption due to unfavorable affects of stress from thermal gradients and volume changes during hydration.

This outcome has been achieved with the financial support of the Ministry of Education, Youth and Sports of the Czech Republic, project No. 1M6840770001, within activities of the CIDEAS research centre and research plan MSM 0021630511.

"Computational Civil Engineering 2006", International Symposium
Iaşi, România, May 26, 2006

High order beam elements for the stability and non-linear analysis of frame structures

Adam Dósa[1], Lucian Popa[1]

[1]*Department of civil engineering, "TRANSILVANIA" University, Braşov, 500152, Romania*

Summary

The Euler-Bernoulli beam elements presented in this paper are based on the improvement of the accuracy of the finite element solution by increasing the polynomial degree of the shape functions. This approach, called the p-version of the finite element method has become more and more attractive in the last two decades. It was shown in the literature, that the p-version for linear elliptic problems with smooth solutions converges exponentially in the energy norm. In the practical analyses, the p-version yields an accuracy which can hardly be obtained by the classical h-version, based on the refinement of the finite element mesh.

The elements studied in this paper show very high convergence in buckling and nonlinear analyses. The final result of the studies is a beam element with six degree polynomial shape functions, which yields engineering accuracy in the practical buckling and non-linear frame analyses with only one element per column. Although this type of element introduces three supplementary non-nodal degrees of freedom, the computational costs of the analyses are much lover than in the case of the classical beam elements based on cubic shape functions.

KEYWORDS: beam elements, p-version, buckling, non-linear analysis of frames.

1. INTRODUCTION

In this paper a family of Euler-Bernuolli beam elements are presented for stability and geometrically nonlinear structural analysis. In the nonlinear analysis the updated lagrangean formulation is used. The developement of the element equilibrium relations is based on the principle of virtual work. The element has six degrees of freedom at the nodes and a number of supplementary non-nodal displacements corresponding to higher order bending modes. In the current reference system, the diplacement and force vectors of the element are:

$$\begin{aligned}\mathbf{a} &= (a_1, a_2, \cdots, a_{nge})^T = (u_1, v_1, \theta_1, u_2, v_2, \theta_2, a_7, \cdots a_{nge})^T, \\ \mathbf{f} &= (f_1, f_2, \cdots, f_{nge})^T = (N_1, T_1, M_1, N_2, T_2, M_2, f_7, \cdots f_{nge})^T.\end{aligned} \tag{1}$$

where *nge* is the total number of degrees of freedom of the element. The incremental and virtual displacements will be noted by $\delta\mathbf{a}$ and $\delta\mathbf{a}_v$. It is advantageous to use a reduced set of displacement increments, removing the rigid body movement of the beam and using only strain-inducing displacements.

$$\delta\mathbf{a}_r = (\delta u_r, \delta\theta_{r1}, \delta\theta_{r2}, \delta a_7, \ldots \delta a_{nge})^T = (\delta u_r, \delta\mathbf{q}_r)^T. \tag{2}$$

Where $\delta\mathbf{q}_r = (\delta\theta_{r1}, \delta\theta_{r2}, \delta a_7, \ldots \delta a_{nge})^T$ are the bending displacements, $\delta u_r = \delta u_{21} = \delta u_2 - \delta u_{1r}$ is the extension of the beam and

$$\delta\theta_{r1} = \delta\theta_1 - \alpha, \quad \delta\theta_{r2} = \delta\theta_2 - \alpha, \tag{3}$$

are the reduced slopes $d\delta v/dx$. For small increments the rigid rotation of the beam, can be expressed as: $\alpha \cong \delta v_{21}/L = (\delta v_2 - \delta v_1)/L$ (figure 1).

Remark: Since the updated lagrangean formulation is used, on the current configuration only the bending displacements are nonzero.

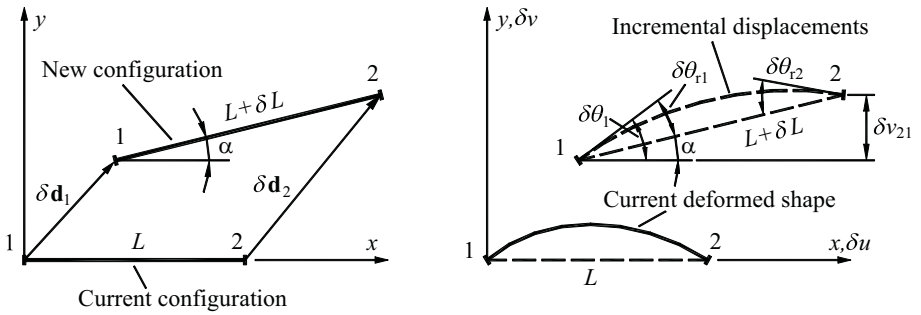

Figure 1. Incremental displacements of the beam

2. FORMULATION OF THE ELEMENTS

2.1 The shape functions

The transversal displacements of the beam are defined with the help of the shape functions. The first two functions are the conventional cubic shape functions (but with v_r=0 at the two ends). The next shape functions are hierarchical ones whitch give zero transversal displacements and slopes at the nodes of the beam.

$$v_r = \begin{Bmatrix} L/8(1-2\xi-4\xi^2+8\xi^3) \\ L/8(-1-2\xi+4\xi^2+8\xi^3) \\ (1-4\xi^2)^2 \\ L(1-4\xi^2)^2\xi \\ \vdots \\ L(1-4\xi^2)^2\xi^{nge-7} \end{Bmatrix}^T \begin{Bmatrix} \theta_{r1} \\ \theta_{r2} \\ a_7 \\ a_8 \\ \vdots \\ a_{nge} \end{Bmatrix} = \mathbf{n}\mathbf{q}_r. \tag{4}$$

Here $\xi = x/L - 1/2$. The polynomial order of these functions is up to $p = nge - 3$. The first derivative of (4) gives the slopes:

$$\theta = \frac{dv}{dx} = \frac{d\mathbf{n}}{dx}\mathbf{q}_r = \mathbf{s}\mathbf{q}_r. \tag{5}$$

Further derivation leads to the curvatures:

$$\chi = \frac{d\theta}{dx} = \frac{d\mathbf{s}}{dx}\mathbf{q}_r = \mathbf{b}\mathbf{q}_r. \tag{6}$$

The same relations will be used for the incremental and virtual quantities.

3. THE TANGENT STIFFNESS MATRIX

The equilibrium of the element in an incremental step can be expressed with the help of the principle of virtual work.

$$\delta V = \delta\mathbf{a}_v^T \mathbf{k}_t \delta\mathbf{a} - \delta\mathbf{a}_v^T \delta\mathbf{f} = 0., \tag{7}$$

where $\mathbf{k}_t$ is the tangent stiffness matrix of the beam.

3.1 The stretching stiffness

In the incremental step, the bending and the stretching of the element are coupled because, the shape of the beam in the current configuration is curved. Since θ_r is small and $\delta\theta_r << \theta_r$ (see figure 2.a), the axial length increment due to the bending of the beam can be approximated by:

$$\delta L^q = \int_0^L d\delta L^q \cong \int_0^L \theta_r \delta\theta_r dx = \mathbf{q}_r^T \int_0^L \mathbf{s}\mathbf{s}^T dx \delta\mathbf{q}_r = \mathbf{q}_r^T \mathbf{k}^* \delta\mathbf{q}_r. \tag{8}$$

The virtual work done by the total axial stretching is:

$$\delta V^s = \delta \mathbf{a}_{rv}^T \begin{bmatrix} 1 \\ \mathbf{k}^* \mathbf{q}_r \end{bmatrix} \frac{EA}{L} \begin{bmatrix} 1 & \mathbf{q}_r^T \mathbf{k}^* \end{bmatrix} \delta \mathbf{a}_r . \tag{9}$$

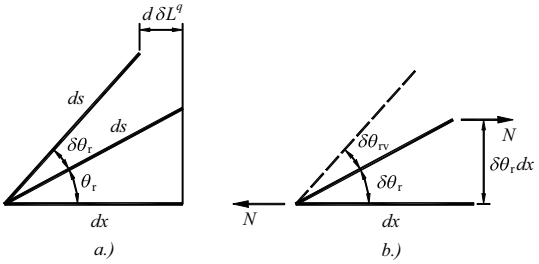

Figure 2. Higher order axial effects

3.2 The bending stiffness

The virtual work produced by the bending is composed by a term resulted from the moment-curvature part and a term given by the higher order effect of the axial force as the work done by the moment of N on the rotated infinitesimal element dx with the virtual rotation $\delta\theta_v$ (see figure 2.b).

$$\delta V^b = \int_0^L \delta\chi_v EI \delta\chi dx + \int_0^L \delta\theta_v N \delta\theta dx = \delta \mathbf{q}_{rv}^T (\mathbf{k}_r + N\mathbf{k}^*) \delta \mathbf{q} . \tag{10}$$

In relation (10)

$$\mathbf{k}_r = EI \int_0^L \mathbf{b}^T \mathbf{b} dx, \quad \mathbf{k}^* = \int_0^L \mathbf{s}^T \mathbf{s} dx. \tag{11}$$

Relation (11) can be evaluated symbolically. For example, for *nge*=9 (p=6) the following matrices result:

$$\mathbf{k}_{r(p6)} = \frac{EI}{L} \begin{bmatrix} 4 & 2 & 0 & 0 & 0 \\ 2 & 4 & 0 & 0 & 0 \\ 0 & 0 & 1024/5 & 0 & 256/35 \\ 0 & 0 & 0 & 256/7 & 0 \\ 0 & 0 & 256/35 & 0 & 192/35 \end{bmatrix}, \tag{12}$$

$$\mathbf{k}^{*}_{(p6)} = \frac{L}{30}\begin{bmatrix} 4 & -1 & 16 & 24/7 & 4/7 \\ -1 & 4 & -16 & -24/7 & -4/7 \\ 16 & -16 & 1024/7 & 0 & 0 \\ 24/7 & -24/7 & 0 & 256/21 & 0 \\ 4/7 & -4/7 & 0 & 0 & 64/77 \end{bmatrix}. \tag{13}$$

3.2 Transferring the current nodal forces to the new configuration

The nodal forces in the current configuration are (see figure 3):

$$\mathbf{f}_n = (N_1, T_1, M_1, N_2, T_2, M_2)^T = (-N, T, M_1, N, -T, M_2)^T. \tag{14}$$

The shear force $T=(M_1+M_2)/L$ results from the equilibrium of the beam. In the new configuration the forces N and T change their direction and the shear force has a new value $T'=T+\Delta T$. From the new moment equilibrium of the current forces, retaining only the first order terms results:

$$\Delta T = -\frac{T\delta L}{L+\delta L} \cong -\frac{M_1+M_2}{L^2}\delta u_{21}. \tag{15}$$

The variation of the nodal forces expressed in the current reference system becomes:

$$\begin{aligned} \Delta X &= N\cos\alpha + T'\sin\alpha - N \cong T\sin\alpha \cong \frac{M_1+M_2}{L^2}\delta v_{21}, \\ \Delta Y &= N\sin\alpha - T'\cos\alpha - T \cong N\sin\alpha - \Delta T \cong N\frac{\delta v_{21}}{L} + \frac{M_1+M_2}{L^2}\delta u_{21}. \end{aligned} \tag{16}$$

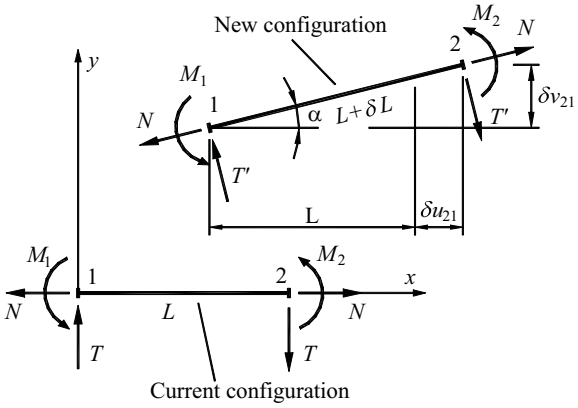

Figure 3. Transfer of the current nodal forces to the new configuration

The forces (16) and the virtual displacements of the nodes introduce a new virtual work term:

$$\delta V^t = \Delta X \delta u_{v21} + \Delta Y \delta v_{v21} = N \delta \mathbf{a}^T \mathbf{z}^T \mathbf{z} \delta \mathbf{a} + \frac{M_1 + M_2}{L^2} (\delta \mathbf{a}^T \mathbf{z}^T \mathbf{r} \delta \mathbf{a} + \delta \mathbf{a}^T \mathbf{r}^T \mathbf{z} \delta \mathbf{a}), \quad (17)$$

where $\mathbf{r} = (-1\ 0\ 0\ 1\ 0\ 0\ 0\ ...0)^T$ and $\mathbf{z} = (0\ -1\ 0\ 0\ 1\ 0\ 0\ ...\ 0)^T$, such that $\delta u_{21} = \mathbf{r}^T \delta \mathbf{a}$ and $\delta v_{21} = \mathbf{z}^T \delta \mathbf{a}$.

Using relations (7), (9), (10) and (17), the tangent stiffness matrix of the element can be written as:

$$\mathbf{k}_t = \mathbf{B}^T \begin{bmatrix} EA/L & \mathbf{0} \\ \mathbf{0} & k_r \end{bmatrix} \mathbf{B} + N \mathbf{B}^T \begin{bmatrix} 0 & \mathbf{0} \\ \mathbf{0} & k^* \end{bmatrix} \mathbf{B} + \frac{N}{L} \mathbf{z}^T \mathbf{z} + \frac{M_1 + M_2}{L^2} (\mathbf{r}^T \mathbf{z} + \mathbf{z}^T \mathbf{r}). \quad (18)$$

In relation (18)

$$\mathbf{B} = \begin{bmatrix} \mathbf{r}^T + \mathbf{q}_r^T \mathbf{k}^* \mathbf{A} \\ \mathbf{A} \end{bmatrix}, \quad (19)$$

with

$$\mathbf{A} = \begin{bmatrix} 0 & -1/L & 1 & 0 & 1/L & 0 & 0 & \cdots & 0 \\ 0 & -1/L & 0 & 0 & 1/L & 1 & 0 & \cdots & 0 \\ 0 & 0 & 0 & 0 & 0 & 0 & 1 & \cdots & 0 \\ \cdots & \cdots & \cdots & \cdots & \cdots & \cdots & \cdots & \cdots & \cdots \\ 0 & 0 & 0 & 0 & 0 & 0 & 0 & \cdots & 1 \end{bmatrix}, \quad (20)$$

such that $\delta \mathbf{q}_r = \mathbf{A} \delta \mathbf{a}$ extracts the reduced bending displacement set from the complete displacement vector of the element.

4. NUMERICAL EXPERIMENTS

4.1 Buckling of beams

Using the stiffness matrix (18) a convergence study was performed for the known cases of buckling of beams subjected to axial force. Both *h*- and *p*-refinements were used by dividing the beams and respectively increasing the polynomial degree of the elements. In the figure 4, the variation of the relative error $e_r = (N_{cr}^{approx} - N_{cr}^{exact}) / N_{cr}^{exact}$ of the buckling force for the worse case - the

clamped-hinged beam is presented. The parameters of the corresponding refinements are presented in the table 1.

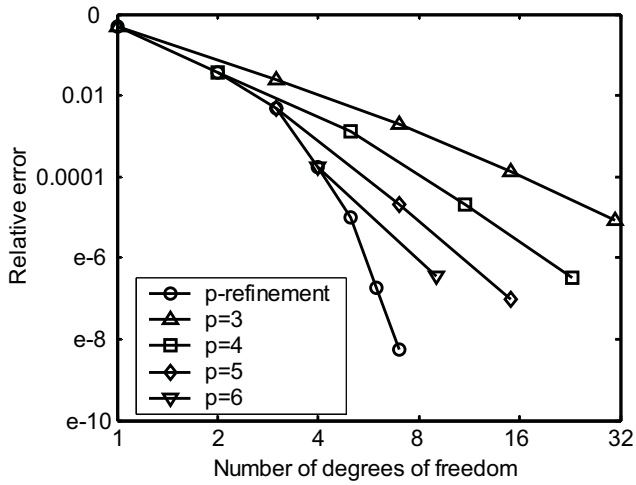

Figure 4. Convergence study for the buckling of a clamped-hinged beam

Table 1. Number of degrees of freedom for the beam buckling problem

Polynomial degree p	Number of divisions				
	1	2	4	8	16
3	1	3	7	15	31
4	2	5	11	23	
5	3	7	15		
6	4	9			
7	5				
8	6				
9	7				

It can be observed that in the case of the same number of degrees of freedom, the best results are obtained by the *p*-refinement.

4.2 Post-critical behavior of the Roorda frame

In the figure 5, the equilibrium paths are presented for six eccentric loadings of the Roorda's L-frame. This case is a classical example of asymmetric bifurcation, where for some small imperfections (introduced here by the eccentricity of the load) the post-critical limit load can be smaller than the corresponding critical load of the perfect system. For example for $e = -0.01L$, the limit load is $P_{max} = 0.899 P_{cr}$ [1]. The result for this case obtained by using only two $p6$ elements, without dividing the beams was $P_{max}^{1-p6} = 0.899 P_{cr}$.

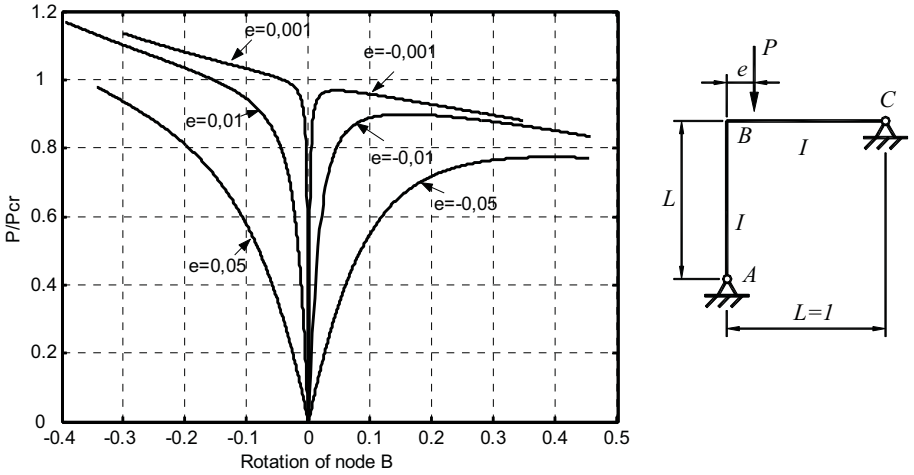

Figure 5. Equilibrium paths for the Roorda's L-frame

5. CONCLUSIONS

In this paper high order beam elements are presented for stability and geometrically nonlinear analysis of frames. The development of the elements uses non-nodal displacements and hierarchical shape functions with increasing polynomial degree for the bending of the elements. Numerical experiments show a very high accuracy of the results. In practical analyses, the element with polynomial degree six eliminates the necessity of dividing of beams and leads to engineering precision of results.

References

1. Bažant, Z.P., Cedolin, L. *Stability of structures: Elastic, Inelastic, Fracture and Damage Theories*, Dover Publications, 2003.
2. Bănuț, V. *Calculul neliniar al structurilor*, Editura tehnică, Bucureşti, 1981.
3. Caracostea, A.D., ş.a. *Manual pentru calculul construcțiilor*, Editura tehnică, Bucureşti, 1977.
4. Przemieniecki, J.S. *Theory of matrix structural analysis*, Dover Publications inc., New York, 1985.
5. Crisfield, M.A. *Non-linear Finite Element Analysis of Solids and Structures*, John Wiley & Sons, 1991.
6. Szabó, B., Babuška, I. *Finite Element Analysis*, John Wiley and Sons Inc, 1991.
7. Zienkiewicz, O.C., Taylor, R.L. *The Finite Element Method, Volume 2: Solid Mechanics*, Fifth Edition, Butterworth-Heinemann, 2000.

"Computational Civil Engineering 2006", International Symposium
Iaşi, România, May 26, 2006

The analysis of frame structures with non-prismatic beams

Lucian Popa[1]

[1]*Department of Civil Engineering, "TRANSILVANIA" University, Braşov, 500152, Romania*

Summary

This paper studies the static analysis of frame structures with non-prismatic beam elements. The flexibility coefficients of the non-prismatic elements are obtained by numerical integration of the equation of deflection of beams in bending The paper studies the possibility of approximation of the behavior of the non-prismatic beams by subdividing them in a minimal number of prismatic elements.

The results of this study are very useful in the practice, when special analysis software for non-prismatic beams is not available.

KEYWORDS: non-prismatic beam elements, frame structures.

1. INTRODUCTION

For a beam loaded only at the two ends, the end rotations can be computed with the help of the flexibility coefficients [1], [2]:

$$\begin{aligned} \varphi_1 &= \frac{l}{EI_0}(M_1 c_1 + M_2 c_3), \\ \varphi_2 &= \frac{l}{EI_0}(M_1 c_3 + M_2 c_2). \end{aligned} \tag{1}$$

The flexibility coefficients computed for unit end moments (figure 1.) are:

$$c_1 = \frac{I_0}{l}\int_0^l \frac{m_1^2}{I}dx; \quad c_2 = \frac{I_0}{l}\int_0^l \frac{m_2^2}{I}dx; \quad c_3 = \frac{I_0}{l}\int_0^l \frac{m_1 m_2}{I}dx; \tag{2}$$

2. THE EQUIVALENT BEAM

The idea is to replace the given variation $I(x)$ of the moment of inertia with two constant values I_1 and I_2 as it is shown in figure 2. In order to find these unknown values together with the non-dimensional length λ, the following notations are used:

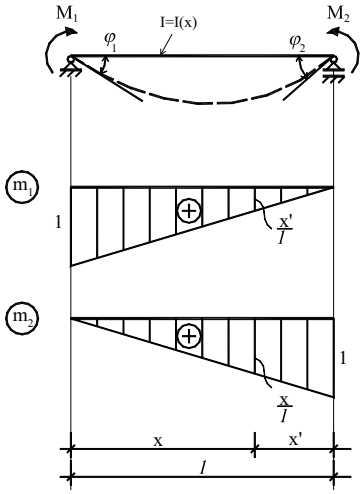

Figure 1. The deflection of the beam

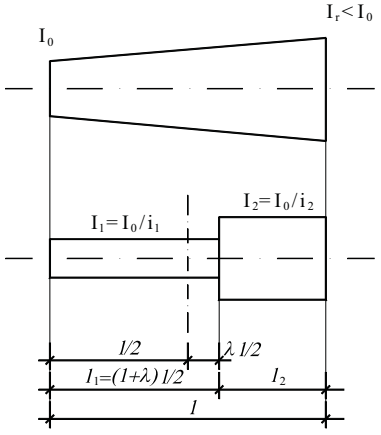

Figure 2. The equivalent beam

$$r_1 = \frac{I_0}{2}\int_{-1}^{1}\frac{\overline{m}_1^2}{I}d\xi = c_1 + c_2 + 2c_3;$$

$$r_2 = \frac{3I_0}{2}\int_{-1}^{1}\frac{\overline{m}_2^2}{I}d\xi = 3(c_1 + c_2 - 2c_3); \qquad (3)$$

$$r_3 = I_0\int_{-1}^{1}\frac{\overline{m}_1\overline{m}_2}{I}d\xi = 2(c_2 - c_1).$$

The bending moment diagrams $\overline{m}_1$ and $\overline{m}_2$ are given in figure 3.

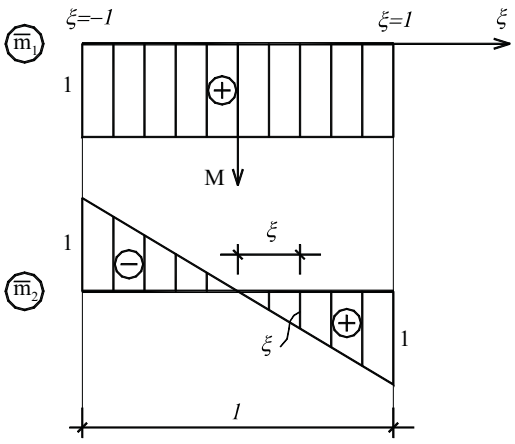

Figure 3. Bending moment diagrams $\overline{m}_1$ and $\overline{m}_2$

Introducing the step variation of the moment of inertia in relation (3) results a system of three equations:

$$\begin{cases} (1+\lambda)i_1 + (1-\lambda)i_2 = 2r_1 \\ (1+\lambda^3)i_1 + (1-\lambda^3)i_2 = 2r_2 \\ (-1+\lambda^2)i_1 + (1-\lambda^2)i_2 = 2r_3 \end{cases} \tag{4}$$

Here $i_1 = I_0 / I_1$ and $i_2 = I_0 / I_2$.

The solution of the system (4) is:

$$\begin{aligned} \lambda &= \frac{r_2 - r_1}{r_3}; \\ i_1 &= r_1 - \frac{r_3}{\lambda + 1}; \\ i_2 &= r_1 - \frac{r_3}{\lambda - 1}. \end{aligned} \tag{5}$$

3. NUMERICAL EXAMPLE

In the figure 4 a beam with I cross section is presented. The height of the beam has a linear variation. The equivalent beam gives exact results if the beam is loaded only at its ends.

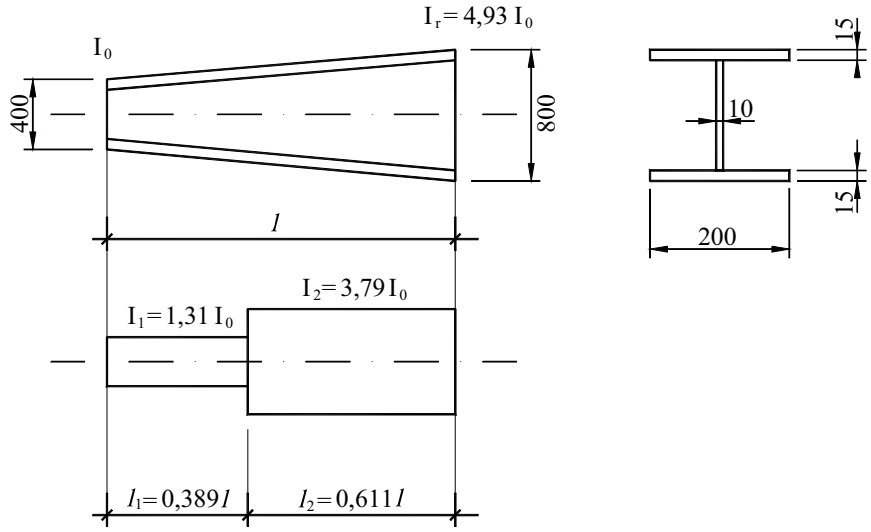

Figure 4. Numerical example

4. CONCLUSIONS

This paper introduces a very efficient way to treat the structures with non-prismatic beams. The given relations are based on the usual flexibility coefficients available in the literature or easy computable by numerical integration of the equation of deflection of the beams and permit to create simple structural models even when special software for non-prismatic beams is not available.

References

1. Avram, C.N. *Grinzi continue*, Editura tehnică, Bucureşti, 1981.
2. Caracostea, A.D., ş.a. *Manual pentru calculul construcţiilor*, Editura tehnică, Bucureşti, 1977, pag. 646-681.
3. Dósa, A. *Proiectare asistată de calculator*, îndrumător de lucrări, Reprografia Universităţii Transilvania din Braşov, 1999.

"Computational Civil Engineering 2006", International Symposium
Iaşi, România, May 26, 2006

Computer aided tool for personal protection equipment generation

Mária Kozlovská, Kozák Peter

Technical University of Kosice, Faculty of Civil Engineering, Slovakia

Summary

The worldwide trend in the hazard elimination of building works through equipments of the personal protection, prevents to the active access to them generation. This active approach forms assumes for the hazards appreciation, their effects analysis and their awareness elimination through awareness using of the personal protection equipment.

The paper presents computer model for generation of asking outputs in the area of selection and exploitation the necessary personal protection equipment on the specific building site in dependence from the specific conditions and hazards, coupling with the building processes performance on it.

KEYWORDS: occupational health and safety (OHS), personal protection equipment (PPE), building industry, computational

1. INTRODUCTION

One of the specific building production characters are big safety hazards, which result not only from building processes, but mainly from conditions, in which are performed.

The occupational health and safety (OHS) has got in building industry, as well as in building production long tradition. Back in period of "planned economy" all (national) building companies had adapted and applied occupational health and safety systems, which more or less had flown only from obligatory legislation. But the market economy period relayed formation of many especially small building companies, which mainly because of dates running or costs "economizing", do not follow neither obligatory legislation. The absence of this field in company system management is often reasoned by them as the finance defect for such "non-productive" activities assurance. Creation of an effective occupational health and safety system brings to companies not only staff satisfaction - as internal customers, but also its effects and production rate increasing, because only satisfied worker, who is not exposed to hazards (suspecting employer responsibility for its occupational safety) can satisfy an external customer - investor.

From system approach point, in western countries OHS system is in companies built as the first, unlike the actual trend in Slovak Republic, where is quality management system established as the first (often only formally, because of order receiving). The environmental management system is in companies established as the second. Only as the last, or as the component of integrated management system, is established the occupational health and safety management system. Whereas just in this field exist many obligatory legislation, which demand performance and application of various tools, at company level, or also in level of particular activities performance directly at building site.

2. THE BUILDING INDUSTRY SAFETY – ALL THE EUROPE PROBLEM

The building industry is ranked among national economy sector, where is fatal injury occurrence according to European agency for occupational health and safety bigger than in other sectors. But also accident hazard is by much bigger, as average in EU is. After statistics is two-timed more possible, that building industry staff receive an accident, which is not fatal, that average worker in other industries.

The survey, which was held in Great Britain attained into estimation that costs connected with occupational accidents and with bad health state in building industry sector – including costs for lost times, absence at the workplace and charges connected with health and insurance - presented 8, 5% of the project costs.

Because of lack of financial and organizational resources, many small and medium companies have got only limited knowledge and capacity pertinent to occupational health and safety covering. Therefore the agency evolves intensive activities in so called good practice field.

Information about good practice should help to companies act in accordance with existing legislation. In many cases are regular requirements clear, but sometimes, although law refers, what is necessary for its fulfilling, does not refer how to achieve or assure it in practice. The law often does not refer about that, which forms, equipments or tolls is possible to use, in order to its appointments were effectively transmitted just there, where have to affect and especially, in order to be clear to people, for which is dedicated and who have to observe it.

One of such field, which markedly contributes to safety prevention directly at building works, is the field of planning and applying of personal protection equipment.

3. ACTIVE APROACH TO PERSONAL PROTECTION EQUIPMENT (PPE) SUPPLYING ON BUILDING SITE

After legislation regulations the building contractor is compulsory to provide to persons, who arrive on building site (workplace) with his mind, personal protection equipment corresponding with their hazards. This obligation is in detail appointed by government direction about conditions of personal protection equipment providing.

By this regulation is essentially changed the approach into personal protection equipment (PPE) providing. Instead of simple and directive instruction for protection resources using, as it was in history, every employer has to identify severally all hazards, resulting from actual activities as well as conditions, in which they are realized. The sector lists elaborated in history by ministries, had not responded to requirements of individual employee protection in specific conditions.

The present regulations directly place duty on employer to elaborate "tailor-made" list of provided PPE, according to real hazards and risk amount. Every employer has to actively approach in this manner into generation of self list of PPE, following appraisal and valuation of hazards in every activity, which his employees perform. Then he has to examine the lists and propose how to avoid risks, advise his employees with this, create the list for PPE providing and ensure their providing and application control.

This active approach into PPE generation makes suppositions for:

- appreciation of safety hazards according to specific conditions at workplace and realized activities character,
- reviewing of amount and possible hazards effects,
- conscious elimination of all aspects, which an accident can cause,
- conscious application of PPE by all employers at the workplace.

In the sense of law about work inspection, inspectors have powers to verify practices for hazards appraisal by employer. Besides control of PPE application directly on building site may demand also demonstration of following documentation:

- list of PPE
- documentation interpreting hazard appraisal practice (system description)
- documentation of employees information about hazards, risks and dangers, for which are PPE intended
- employees information how to protect against the danger, hazards and risks (details of trainings and trainings records)

4. THE ALGORITHM OF PERSONAL PROTECTION EQUIPMENT (PPE) FOR BUILDING WORKS DOCUMENTATION GENERATION PROPOSAL

One of the legislation regulations „defects" is, that they order what is prohibited or what has to be done, but they does not offer any system of how to cover practically these commands or prohibitions. That is why the article authors had created an algorithm and consequently an software tool, which permits to building companies employers by simple and especially system method prepare all the government instruction requirements about personal protection equipment providing conditions.

In creation of the tool for documentation of PPE for employees' generation, we were appeared from following anticipations:

- ✓ fulfilment of general government regulations requirements in conditions of personal protection equipment providing, by adapting for building industry specifics
- ✓ simply manageable tool for required outputs generation
- ✓ generally available (standard) software
- ✓ possibility of final documentations various combinations depending on necessity and purpose place
- ✓ documentation directness for particular buildings (workplaces)
- ✓ possibility of already executed analysis (buildings, actions) archiving
- ✓ possibility of fast generation following archived analysis
- ✓ possibility of revaluation (actualization) especially in changed working conditions

From follow analysis of law regulations, employer responsibilities and especially requirements of government regulations about personal protection equipment providing conditions were defined inputs and required outputs.

4.1 The inputs definition

Among main inputs were arranged the regulations appendices, worked into databases. The appendix which involved works list, in which PPE have to be offered (in division also for concrete body part protection), has been chosen as "jumping-off" for the model and consequently has been selected according to building works specifics.

Input databases (created following government regulations appendices)		
D1	Appendix nr.2	**PPE list –** PPE groups structured for concrete body parts or body member protection: head, ears, eyes and face, breathing apparatus, limbs, legs, trunk and belly, all body, skin and other.
D2	Appendix nr.3	**Hazards list** - 4 main groups: physical, chemical, biological and other dangers, while for building works are specific mainly physical dangers (workplace position in regard to earth top, bad surface of floors and communications, press, stroke, section, slash, lash, chafing, reeling, unfolding and falling objects, deficient image, noise, judder, …)
D3	Appendix nr.4	**Operations list** Operations in which PPE have to be offered, structured following concrete body parts and members protection.
„jumping-off“ see picture1		
D4	Appendix nr.5	**List of criteria for PPE selection -** Hazards reasons and types, against which concrete PPE should protect.

4.2 The outputs definition

The outputs according to government regulations about personal protection equipment providing conditions, reproduce required documentation. In form of indirect outcomes permit fulfilment of next regulations conditions, which are information offer about dangers and allowance of their systematic revaluation

Required outputs (according to government regulations)	
V1	Hazards analysis
V2	PPE character (against what protects)
V3	Specific types of PPE
V4	Application conditions (especially application time – PPE durability)
V5	PPE list
Indirect outputs:	
Vn6	Apprising of dangers – information about dangers
Vn7	Hazard revaluation (in building site conditions changes)

Considering the required outputs, were connected also next two new databases, which permit to choice also specific types of PPE, available on market, were can be inserted data concerning PPE application, PPE keeping up, but also data about concrete contractor. (Db5). Next database (Db6) is PPE application time (durability), which is unlike history defined by employer, regarding conditions and intensity of operations realized it means PPE abrasion. The database is directly from the software available for number data modification. From input and output parameters was consequently created the model with work name **GENOPSTAV** (PPE for building works generation).

4.3 The algorithm for PPE generation

The hearth of the system is operations list from government regulations appendix, where are inscribed operations, in which in generality have to be offered PPE to all employees. For PPE specifically for building works generation needs, was needed the list redistribute into three sub lists. So condition for simpler "listing" among processes was created.

Sub list 1	**list of operations typical for building industry** (earth works, scaffold works, formwork installation and dismounting, ...)
Sub list 2	**list of operations expressive working conditions** (works in heights, work in cuttings, work in noise, work in winter and cool, …)
Sub list 3	**list of other special and another operations**, only sporadical works on building site

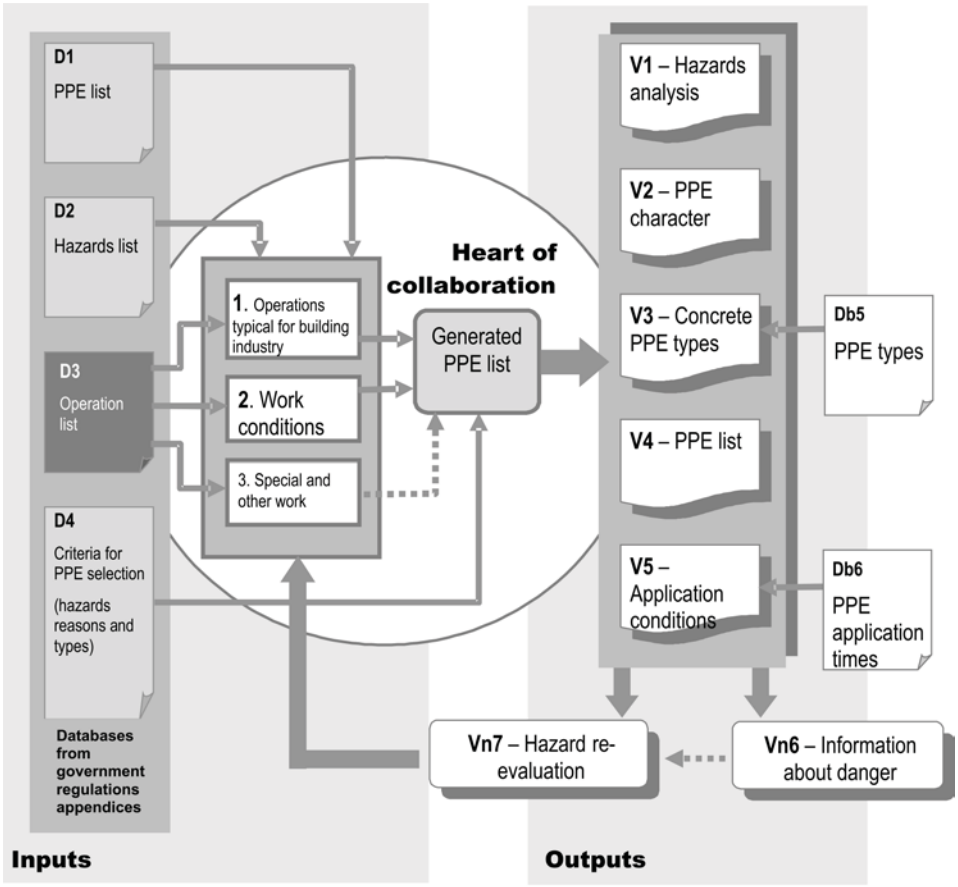

Picture 1. Algorithm of the model GENOPSTAV for PPE generation

The heart of the system is the heart of bearing collaborative relations (Picture 1). On presented sub lists are automatically tied, as well as particular dangers, which impend in existing operation, as needed PPE, by which should be these dangers minimized. On so generated list of PPE is then automatically connected next database, which identify dangers reasons and types, against which should involved PPE protect. This connection is important for these outputs, by which employer should inform their employees about dangers, which impend them in particular works performance.

5. CREATION OF THE SOFTWARE ENVIRONS FOR THE TOOL OF PPE GENERATION

As it results from the model algorithm, the software for particular inputs into required outputs transformation has to be data basely oriented. In this cause, and in cause of general availability, in the model processing was applied software **MS Access**, which is the part of MS Office Professional packet. It is data basely oriented software, supporting creation, processing and consequent transformation of the inputs into required outputs. By this manner ensued the software architecture of the tool for personal protection equipment generation (picture 2), which is structured into three bearing parts (tabs, forms and output reports).

Particular input databases of the model were executed into software environs by tabs, which were each other connected by mentioned relations. Next was needed to offer and create particular forms for import of inputs and outputs forms and ensure collaboration (cooperation following date) among tabs. The output of the software model is in reports version – so in output printing formations. These reports are beforehand presented, divided according to offered data type.

After particular form filling by data, by tool Microsoft Visual Basic was created code for total database action assign.

The outputs can be modified by many methods, according to final user requirements. In this manner different structures of output formations can be achieved:

- risk processes list on existing building site
- risk processes list on existing building site including PPE
- PPE list on existing building site
- list including PPE and all at once hazards, which flow from existing work and against which should PPE protect etc.

The model and its outputs provide bases for next, by government regulations required activities, among which belong information of employees with possible hazards and in cause of working conditions on building site changes, the model permit fast and simple hazards re-evaluation.

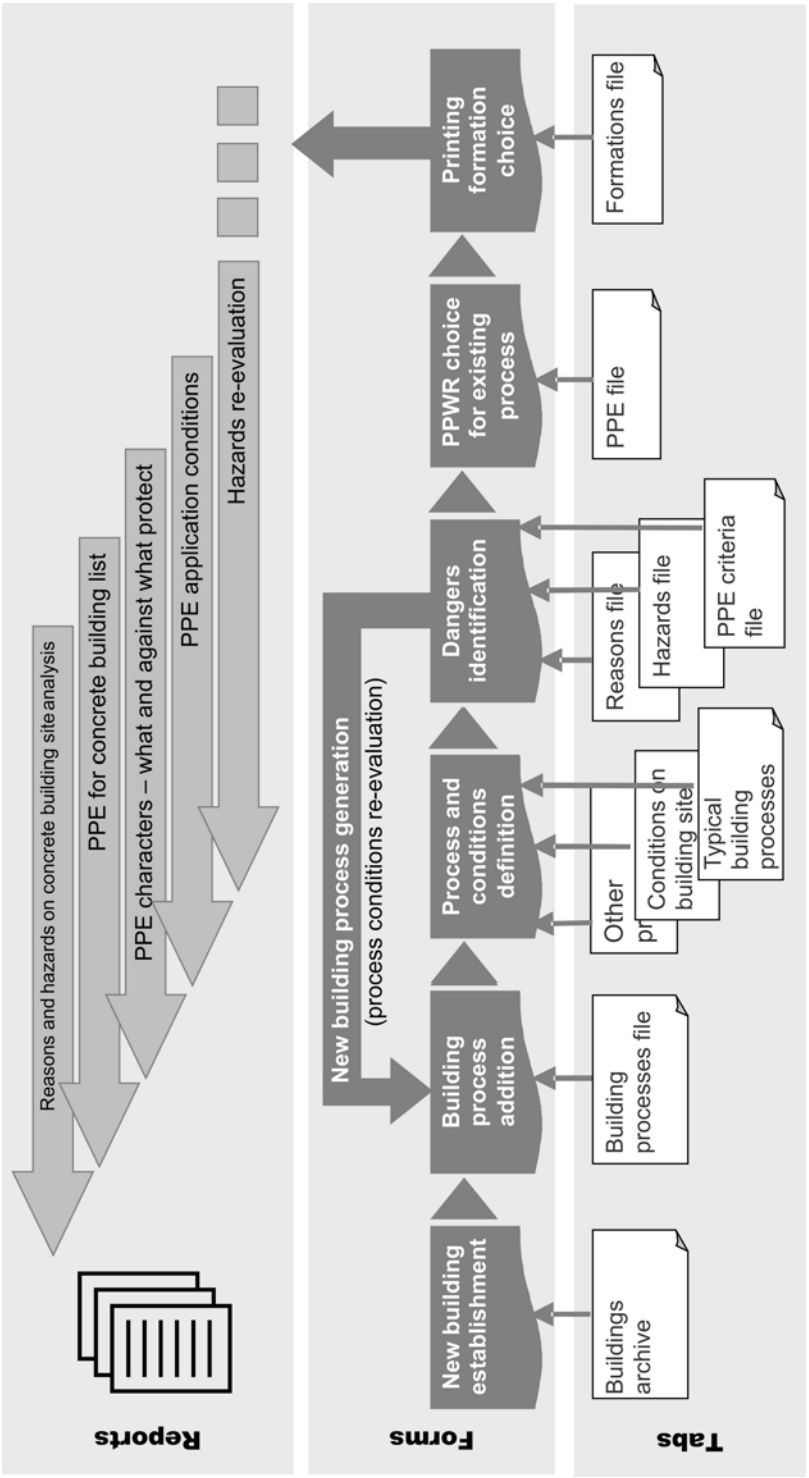

Picture 2 Software architecture of the model GENOPSTAV

Example of specific project outputs for concrete construction and concrete building site

CAUSE AND DANGER ANALYSIS AND THE RELEVANT PPE			
Structure Code:	000-000-003	**Processed by:**	Ing. Peter Kozak
Structure Name:	Extension of Cobalt X-ray Cover, Košice	**Analysis ordered by:**	StavaIP Košice
Structure Place:	Košice	**Structure made by:**	StavaIP
Date of work:	18.1.2005		

Brickwork demolition

WORK, CONDITIONS	CAUSE OF DANGER	PPE
construction work	falling things/items	safety helmet
building and structure demolition	items falling at front site of foot	safety shoe with resistant sole against sticking and pruning
work with pneumatic tools	continual noise, impulsive noise	ear muff
fragments splinters raised from work	particles with high energy as glass	safety goggles
high dustiness tools	solid and liquid matter contaminating air	respirator

Delivery and assembly of roof LEXAN

WORK, CONDITIONS	CAUSE OF DANGER	PPE
construction work	blow, hit	safety helmet
handling with sharp edge tools	rough, sharp and pointed tools	safety gloves
assembly work	blow, hit	safety helmet
work on roofs	step on sharp, pointed tools	safety shoe with resistant sole against sticking and pruning
near crane work	site grip	safety helmet
work in high	fall from high, or fall to deep	safety tool against fall, safety rope
work in high	blow, hit	safety helmet
work outside at rainy and cold weather	hot or cold materials, site temperature	clothing against unfriendly weather

6. CONCLUSIONS

The article is a contribution into risks reduction and information increasing about safety prevention in building industry. The article presents the model for required outputs execution in field of personal protection equipment providing in building practice conditions, which permitted elaboration of the effective software tool for all needed documentations for their effective management generation.

The aim of the article is also to mention the possibilities of usual software tools application in concrete building practice tasks solution. It is possible to facilitate many administration works and help to concerned workers in needed activities performance by creation of such tools.

The article is the part of the project ***VEGA Nr.1/1221/04 Integrated Building Management System*** *solution*

References

[1] http://www.build.gov.sk/ Information - Year 2004, year of occupational health and safety in building industry

[2] http://ew2004.osha.eu.int European week of occupational health and safety. The building industry safety.

[3] http://agency.osha.eu.int/publications/factsheets/ Health and safety on small construction sites

[4] Health and Safety Executive, Great Britain, The costs of accidents at work, HSG96, 1997

[5] KOZLOVSKÁ M., KOZÁK P.: Satisfied and healthy worker – condition of building company effects. In: Building market, year VII, nr.3, pages 26-29, MC SR: 2150/99

"Computational Civil Engineering 2006", International Symposium
Iaşi, România, May 26, 2006

Computational modeling of building process time behaviour

Renáta Bašková

Faculty of Civil Engineering, Technical University of Kosice, e-mail: renata.baskova@tuke.sk , SLOVAKIA

Summary

The network analysis methods present the main tool for building schedule execution by computer. The principal element of network, which is the building time behaviour model, is the building process at various aggregating level. The networks topology models technological and organizational relativities of the building processes.

The classical network analysis methods mostly perceive an activity as one network element, with two events namely start and finish, not allowing the fact, that each building process has got its internal time structure, which is relatively complicated.

In the paper is in detail executed division of building processes and their time parameters. The internal time structure is explained by various graphical models and mathematically are defined the interaction continuities among internal events of one building process. The time structure of one building process, defined in this manner, consequently permit define mathematically the conditional ties - relations among processes so that the final mathematical model will represent the real building time structure.

KEYWORDS: building process, activity, milestone, dummy process, real process, aggregated process, summary process, network analysis, network, network topology, arc, node, earliest start, earliest finish, latest start, latest finish, process duration, date of an event, resource

1. INTRODUCTION

Most building companies aim at integrated information management system, processing by computers in its every side. The main principle of such integration is saving of all primary and also processing data about particular building objects into properly ordered data bases and permanent reflection of these data into calendar time. Determining element of building management scheme, which allow modelling of data in time, is building schedule. Therefore is necessary to have a building schedule computational processing as at full just model of factual building processes behaviour model.

Network analysis methods present the main tool for the building schedules execution by computer. Particular methods allow mathematical modelling of the projects by networks. The holder of building production in network is operation, i.e. building process on various aggregating level. The network topology describes activities relative connection method in the model. Classical network analysis methods have general application, but in them using for building process mathematical modelling rise inaccuracies, which markedly reduce the final model quality, i.e. building schedule quality.

The processes relativities have got their particularities in building industry. The network building model topology should represent real technological and organizational relativities of particular building processes. In application of concrete network analysis method for building time behaviour modelling by computer is possible define in network topology only such relations among processes, which actual method, applied for computer programme can mathematically define. Also modelling of the building process internal time, technological and spatial structure is possible only in dimension, which actual computer programme affords to its user.

2. COMPUTATIONAL MODELING OF BUILDING PROCESS TIME BEHAVIOUR

The network analysis methods present the base of computer programmes for projects behaviour mathematical modelling creation. The network analysis methods intended for mathematical modelling of building schedule should respect particularities of building process internal structure, as well as particularities of their interaction relativities. For suitable mathematical definition of relations between events, exact analysis of building processes and knowledge about their internal time structure is necessary.

2.1 The building processes division

The building process is process of production**,** whose final product is a building construction, a building object or a building (operation, activity, partial stage, object, complex process). Time of the process duration is the function of the production amount (content in financial or physical measure units) and of work force load. It has requirements on resources (operation articles and working means). It is possible to factorise the building process in term of time and resource assessment into real process and to him pertaining internal and external dummy processes. Complexity of the building process internal time structure depends on amount and mutual relativities of processes, which are aggregated in the process.

It is possible to divide building processes in term of time and resource assessment in network into:

- **real process** – the building process part**,** which has requirements on resources, for all that the resources requirements are fragmented (calculated) equally for all its duration time,
- **dummy process –** it can not exist independently, it always connects on an event (start or finish) of other activity, process, process set up or milestone. It has not requirements on resources (it is not resource appreciated). Its time assessment is derived from the building process technological structure, whose component it is, or from technological and time structure of the process set up, on which it is fixed. Among dummy processes belong for example the process development, settlement and reduction, deferments and technological intervals between processes, next time determination of the processes set up or its parts time duration (summary process) etc.
  Note: in arc-defined networks of the processes set ups is term dummy activity used for designation of not only dummy processes, but also for designation of knot of two activities events, such designation is not accurate and do not satisfy with actuality. In such denotation it means an "activity relation". Also between events of two dummy processes can be time relativity, i.e. their events can be each other relative by the relation.

  Next it is possible to divide **dummy processes** into:
  - **internal dummy processes** (development, settlement, reduction), by change of their time assessment does not come directly about change of earliest and latest terms of the real process start and finish, into which are allocated, but they can influence time weight of relations on previous or following processes events.
  - **external dummy processes** (deferments and technological intervals – i.e. necessary intervals before start and after finish of the real process or its part). Their events terms are defined by relativity towards other building processes. By the change of their time assessment and their events terms is possible to come about change of earliest and latest terms of the real process start and finish, into which they are allocated.
  - **summary processes –** (also term process heading and the process set ups heading is used) indicate time interval from the start of the first to the end of the last from grouped processes. The terms of the summary process events vary only in dependence on events terms changes in the grouped processes set up.
    Note: in some literature is for summary process applied term "aggregated process", what is suitable only for cases of time-evaluated processes net models without their resource evaluation. If the processes net model

elements have requirements on resource, it is necessary to distinguish between summary and aggregated process.

- **aggregated process –** it arises by integration of several activities or building processes into one process. It involves time and resource evaluated real process and time evaluated dummy processes (while time evaluation of dummy processes can be nought). Its time and resource evaluation is derived from the process set up parameters, which are in this process aggregated, while requirements on resources are in its real process fragmented (calculated) equally for all its duration term.
  Note: Resources requirements are in aggregated process fragmented (calculated) equally for all its duration term. If it means only formal aggregation of the processes into one title, in such term arose summary process has got characters or dummy process, has got its own time evaluation, derived from grouped processes events terms, but has not got own resources requirements. Resources requirements are calculated from grouped processes requirements and therefore they can be unevenly distributed during the summary process duration term. The summary process and the aggregated process have got different parameters, therefore should not be these terms each other replaced.
- **milestone –** is created by one event, which indicates important project state, or its part, it has not got resource evaluation and has got nought duration term. Such event can but must not have in advance defined earliest, latest or stabile date.

2.2. Time parameters of the building process

Among time parameters of the building process belong:

- operation process duration (in elected measure units)
- process development date
- process reduction date
- process settlement date
- time deferment (in time units or in work amount %)
- technological interval (in time units)
- terms (non-calendar or calendar) starts or finishes of the process or its part (earliest, latest, bound earliest, bound latest or stabile term).

The time parameters of the building process can be defined by constant (by account, by calculi, stochastically, deterministically), or as variable, in dependability on other parameters of the process or other processes values.

2.3 Models of the building process time structure

The are many abstract models for formulation of the building process time structure:

- verbal (time structure is stated by definition of parameters and their time evaluations),
- mathematic (time structure is stated by mathematical substances),
- graphical models (time structure is stated by graphical presentation).

For better visualise, better information relative density are all three types of the model normally applied together.

The building processes and their set ups network analysis, which is in its reality the complex of mathematical methods of the project modelling by networks, uses the combination of all three types of abstract models. The base is created by the network, which is supplemented by radical or computed values of time parameters, eventually by definition of the process and by particular mathematical apparatus, which serves for network elements parameters evaluation (arcs and nodes).

For mathematical and graphical formulation of relativities among particular time parameters of the building process or building process set up are applied such identifications:

i, j, k, ... – indexes for general identification of the process,
a, b, c, ... – indexes for identification of the partial processes,
A,B,C ... – indexes for identification of the aggregated processes,
(i+0), (k+0) till *(i+7), (k+7), ...* - indexes of the building process *I, k* events arcs,
t_i - process *i* duration term,
T_i - general identification of the process *i* event term,
U_i - general identification of the process *i* event,
Z_i - start of the process *i*,
K_i - finish of the process *i*,
Ro_i - development of the process *i*,
Us_i - settlement of the process *i*,
Zu_i - reduction of the process *i*,
Pr_i - technological interval of the process *i*,
Od_i - deferment of the process *i*,
tRo_i - development date of the process *i*,
tUs_i - settlement date of the process *i*,
tZu_i - reduction date of the process *i*,
tPr_i - technological interval duration date of the process *i*,
tOd_i - deferment of the process *i* duration date,
TZ_i - date of the process *i* start,
TK_i - date of the process *i* finish,
TRo_i - date of the process *i* development finish (settlement start),
TZu_i - date of the process *i* reduction start (settlement finish),

T_1Pr_i - date of technological interval finish after process *i* development,
T_2Pr_i - date of technological interval duration finish after process *i* finish,
T_1Od_i - date of deferment duration start before process *i* start,
T_2Od_i - date of deferment duration start before process *i* reduction start.

For mathematical and graphical expression of relativities between parameters of the processes and the relations among processes in network of the process set up (for solution by network analysis), are applied following identifications:

NT - bound date (taken by real or relative calendar date),
TM - earliest event date, taken "by computation ahead",
TP - latest event date, taken "by computation aback",
ZM_i - earliest start of the activity *i* date,
KM_i - earliest finish of the activity *i* date,
ZP_i - latest start of the activity *i* date,
KP_i - latest finish of the activity *i* date,
ε_{ij} - time evaluation of the relation between events U_i and U_j

On the picture nr.1 is in time-spatial diagram image behaviour of the building

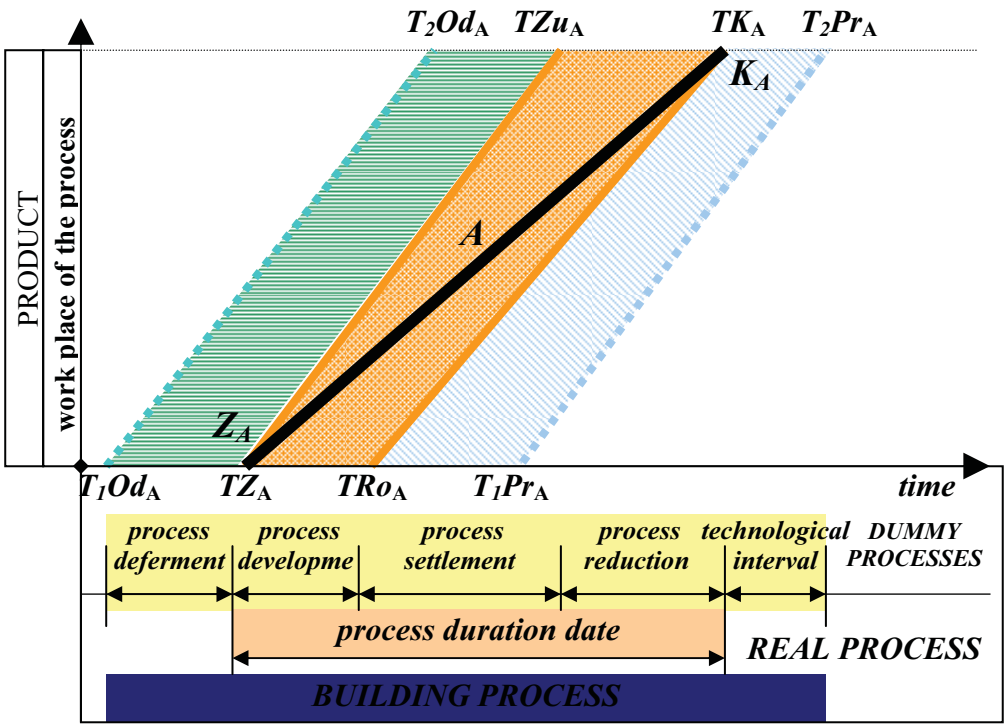

Picture 1. In time-spatial diagram presented behaviour of the process ***A*** and to it pertaining dummy processes: deferment, technological interval, development, settlement and reduction of the process

On the picture nr.2 is the same process presented in line schedule, where are equally graphically distinguished its real part and dummy processes: deferment, technological interval and development, settlement and reduction of the process.

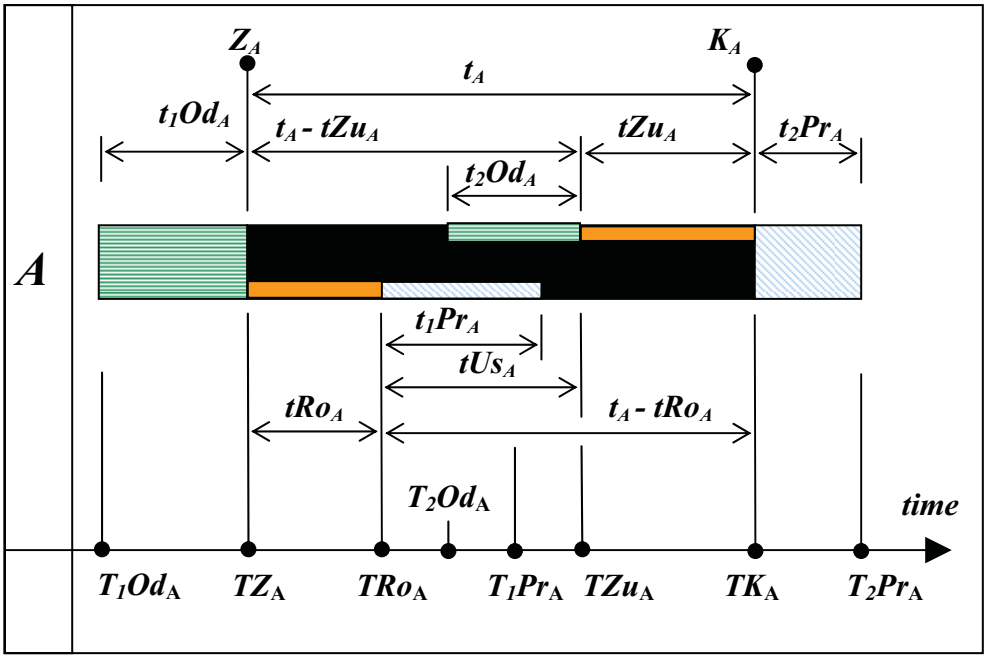

Picture 2. Presentation of the process ***A*** and its real and dummy processes in line schedule

In case, that dummy processes, i.e. development, reduction and external dummy processes have got nought time evaluation and the process settlement date is the same as the process duration date, graphical presentation of the process *A* is in diagrams reduced into vector (Z_A, K_A).

In arc-defined network, which serves as a basis for mathematical building process model, one node of the net responds mostly to one building process. For specification of particular building process time parameters mostly only definition of parameters with their computed or taken time evaluation situated directly in the process node is applied.

Mathematical schemes for the terms of the building process (its real and dummy processes) events computation (earliest and latest), defined by actual network analysis methods, are fixed into verbal definition of the net elements and are not directly image of their graphical description. On the picture nr.3 is described the node, which presents the process *A*, where are in node presented the process time parameters evaluations (its real and dummy processes) and their events terms *TM* and *TP*.

<table>
<tr><td rowspan="2">i</td><td>ZM_A</td><td>KM_A</td><td>tRo_A</td><td>TM_{Ro}</td><td>TP_{Ro}</td></tr>
<tr><td rowspan="4">A</td><td></td><td>tZu_A</td><td>TM_{Zu}</td><td>TP_{Zu}</td></tr>
<tr><td rowspan="3">t_A</td><td>t₁Pr_A</td><td>TM_{Pr1}</td><td>TP_{Pr1}</td></tr>
<tr><td>t₂Pr_A</td><td>TM_{Pr2}</td><td>TP_{Pr2}</td></tr>
<tr><td>t₁Od_A</td><td>TM_{Od1}</td><td>TP_{Od1}</td></tr>
<tr><td>ZP_A</td><td>KP_A</td><td>t₂Od_A</td><td>TM_{Od2}</td><td>TP_{Od2}</td></tr>
</table>

Picture 3. The node of node-defined network, which presents the building process ***A***, where are by definition presented time parameters and events terms of real and dummy processes of the process ***A***

Such node is then one element (node), which is in node-defined diagram consequently interconnected by arcs presenting technological and organizational knots among processes. Definition of these arcs consists of relation type identification and its time evaluation. Methods of description and definition of relations among processes have got particular network analysis methods different, but in principle all the methods have got for certain processes relativities styles defined concrete mathematical algorithms for underlying processes events terms determination.

Note: In computer processing and accounts in processes net is necessary identify (by constant or by account in dependability on other process parameters values) for particular processes (net nodes) only duration dates of their real and dummy processes and relation type between processes. Time evaluation of the terms is accounted automatically following defined mathematical algorithms for method relations, which is used by software. The outputs are then mostly processed in line schedule or in time-spatial diagram.

If is necessary directly graphically express mathematical relativity between events terms of one building process, as well as among events terms of all process set up, it is suitable to describe network as arc-evaluated. The number of the net model elements is on the one hand several fold enlarged, because one net node responds to every process event, which must be tied in the network by one or by several arcs with different event of one or several processes. On the other hand right formed, described and evaluated arc-defined diagram enables to define correctly the mathematical relations among particular real and dummy processes events.

Note: In computer processing and accounts in processes net is not necessary to draw the network topology. The processes parameters processes, as well as processes relativities can be taken for example column ally. The network analysis and its mathematical apparatus is the toll, which enables from like that taken data

to form a flexible building model and to show the outputs for example by line schedule form.

2.4 Description of events and building process behaviour by arc-defined network

For the building process description (its internal technological structure, i.e. real process events relation and into him pertaining dummy processes) by arc-defined network (see picture nr.4), seven time evaluated arcs with following evaluation are necessary:

t_A - process A duration date – (real process, which is resource evaluated)
tRo_A - process A development date,
tZu_A - process A reduction date,
t_1Pr_A - technological interval after process A development duration date,
t_2Pr_A - technological interval after process A finish duration date,
t_1Od_A - deferment before process A start duration date,
t_2Od_A - deferment before process A reduction start duration date.

The settlement date tUs_A of the process A has not any own arc, it is only time interval between events TRo_A and TZu_A and can acquire plus, nought and minus value (description of arc for the process settlement is not necessary, it does not extend to terms accounts in the process inside).

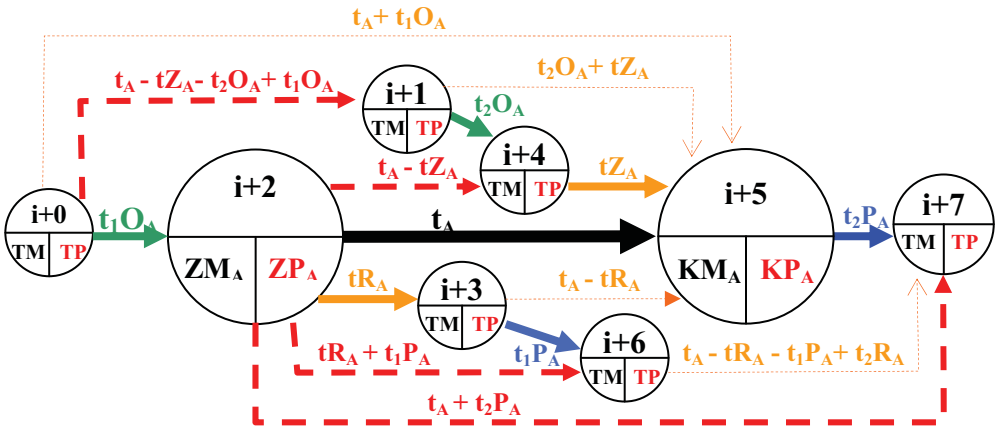

Picture 4. Arc-defined network of the process A with description and time evaluation of the arcs (relations and behaviour) and nodes (events) of real process and dummy processes

Dummy process can not exist independently, it is always tied to event (presented by node) of other process (real or dummy), with which has got same time evaluation at least in one node, i.e. has got at least one generic node with other process. For six dummy processes of the process A events description, only six other nodes are therefore necessary.

2.5 The arcs evaluation in arc-defined network of one building process

On the picture nr.4 is described arc-defined network of one building process.

By fat continual line is arc of the real process described, dummy processes are described by thinner continual line. Orientation of the arcs is presented by arrows. By linear fat line are described assistant arcs, which are used in mathematical account of *TM* and by linear thin line are described assistant arcs, which are used in mathematical account of *TP*.

The arcs evaluation in arc-defined network of one building process is inscribed on the picture nr.4. The assistant arcs evaluation is mathematically derived from the real process *A* and its dummy processes time evaluation.

2.6 Account of the events terms of one building process TM and

Each arc-defined network must verify one formal condition: „ the net has to have one input and one output node". Completion of the condition is necessary for the net numbering and for mathematical account of the events terms by "method ahead" and also by "method aback". From counted values *TM* and *TP* is possible to define critical path behaviour in the net model. Regards of relativity, i.e. relations among particular events of the building process *A* real process and dummy processes can not create a cycle. The algorithm of the terms account by "method ahead" by "method aback" inside the process is the same as in classical method CPM. The difference is only in net arcs perception. The net arcs create not only real process and dummy processes, but also relations among particular events within the process.

Numbering of one building process network nodes is derived from number *(i+0)* of entry process node. While nodes events *(i+1)* till *(i+7)* respond to events described on the pictures 1 and 2 as follows:

node *(i+0)* - $\boldsymbol{T_1Od_A}$ - date of deferment before process *A* start duration start,
node *(i+1)* - $\boldsymbol{T_2Od_A}$ - date of deferment before process *A* reduction start duration start,
node *(i+2)* - $\boldsymbol{TZ_A}$ - date of the process *A* start,
node *(i+3)* - $\boldsymbol{TRo_A}$ - date of the process *A* development finish (settlement start),
node *(i+4)* - $\boldsymbol{TZu_A}$ - date of the process *A* reduction start (settlement finish),
node *(i+5)* - $\boldsymbol{TK_A}$ - date of the process A finish,
node *(i+6)* - $\boldsymbol{T_1Pr_A}$ - date of the technological interval after process *A* development finish,
node *(i+7)* - $\boldsymbol{T_2Pr_A}$ - date of the technological interval after process *A* finish duration finish.

By mathematical account by „method ahead", which runs following arcs orientations, i.e. following described arrows, are in particular nodes defined values of *TM*. The node *(i+0)* is beginning node with known value *TM*, if $t_1O_A=0$ and

$t_2O_A=0$, then beginning node is the node with index $(i+2)$ and with value ZM_A. From arcs evaluation and from value $TM_{(i+0)}$ are counted values $TM_{(i+1)}$ and ZM_A, consequently from value ZM_A are counted values TM in nodes $(i+3)$, $(i+4)$, $(i+5)$, $(i+6)$ and $(i+7)$.

Account by „method aback" runs non-following the arcs orientation. Account begins in node with index $(i+7)$ and value $TP_{(i+7)}$, if $t_1P_A=0$ and $t_2P_A=0$, then begins in node with index $(i+5)$ and with value KP_A. From the value $TP_{(i+7)}$ is counted value $TP_{(i+6)}$ and value KP_A in node with index $(i+5)$. Consequently from the value KP_A are counted values TP in nodes $(i+4)$, $(i+3)$, $(i+2)$, $(i+1)$ and $(i+0)$.

Accounts of one process events dates are in the process set up tied by relations to dates of technologically or organizationally related processes. It depends on actual network analysis method possibilities, which relations among process events defines, into what volume is possible by relations in network model serious technological and organizational relativities of the building processes, i.e. into what volume can relations allow internal complexity of the building processes and their structures. It is not eligible in praxis to draw complicated networks. The network of one building process presents in principle only one element in processes set up network. In node-evaluated network the building process can be presented only by one net node and for example in schedule only by vector. The analysis of one process internal structure is the bases for mathematical definition of such relations among processes, which enable in processes models creation by network analysis method, allow the building industry particularities.

3. CONCLUSIONS

Unlike activities in other economic sector, the building process has got relatively complicated its own internal time structure. Classical network analysis methods mostly apprehend the activity as one network element, with two events namely start and finish. Besides simplified perception of the building process, some classical network analysis methods have got limited number of mathematically defined mutual relations among processes events (start and finish), what is the problem in the building process technological relativity definition in creation and especially in tuning of building time behaviour mathematical model.

In the article the output of one building process time structure internal analysis is description of its arc-defined net model. In one process network are defined arcs, i.e. events relating to one process and arc, which each other interconnect the process events. Mathematical evaluation of the arcs is derived from duration date of building process real process and dummy processes. One building process values events dates are mathematically derived from input and output net node values.

Perception of the building process through its internal structure consequently enables definition within concrete network analysis method such relations among processes events, which enable model the building process with its special technological and organizational relativities of the processes. In each computer programme for building time planning lays an actual network analysis method. The program ability to discharge its user requirements, which rise in creation and tuning of building time plan model in pre-production, production and realization stage of the capital project, depends on its mathematical apparatus.

The article is the part of the project ***VEGA nr. 1/1221/04 Integrated building management system*** *solution*

References

1. BAŠKOVÁ, R.: Building Processes Modelling: Economic-mathematical Methods – part I. (Linear Optimization and Network Analysis). 1. Edition. Košice: TU in Košice - SvF, October 2004. 150 pages ISBN 80-8073-188-8.
2. BAŠKOVÁ, R.: Models Management in Building Project. In: KIP- Quality-Innovation-Prosperity VII/2, Q-Project PLUS Ltd., Košice, 2003. Pages 1-11. ISSN 1335-1745.
3. TRÁVNIK, I. a VLACH, J.: Network Analysis. 1. Edition. Bratislava: Alfa, 1974. ISBN 63-057-74
4. CA-SuperProject 3.0 - Referenčná príručka. Bratislava: Data System Soft, s.r.o., 2003
5. Jarský, Č.: Automatizovaná příprava a řízení realizace staveb. CONTEC, Kralupy nad Vltavou, 2000

"Computational Civil Engineering 2006", International Symposium
Iaşi, România, May 26, 2006

Electronic portal for occupational health and safety management on building site

Zuzana Struková

Faculty of Civil Engineering, Technical University of Košice, Košice, 040 02, Slovak Republic

Summary

In the paper is presented an internet information application, which is intended mainly to construction managers in order to support and help in health and safety on building site problems performing. The portal provides to its user the survey of health and safety management on building site centre fields main terminology, survey of obligatory legislation, but mainly survey of particular procession steps destined into right managing of these fields, as well as survey of obligatory health and safety documentation, what can help to construction manager in everyday work on building site in managing, controlling and surveying the health and safety state on building site. The portal also presents the communicational channel interposing the transfer of health and safety management outputs from building contractor company level into building environs in documentation form of real construction offer.

KEYWORDS: occupational health and safety management, portal, building site, construction, company, construction manager, tool

1. INTRODUCTION

The building industry belongs surely to traditionally high risk sectors from the point of work injuries statistics. In case of small and medium building companies is even accident rate in Slovak republic few ten percents bigger as the average in other European Union states is. It is concerned exactly the companies, in which occupational health and safety (OHS) field is not managed completion ally, it means, that for ensuring of employees safety and health protection are mostly performed only some activities, most often only work accidents investigation and trainings.

The purpose of the thesis, of which one of the outputs is presented in the article, was rivet into occupational health and safety management system especially in small and medium building industries, those amounts is the biggest in business subjects of this field in Slovak republic.

2. PURPOSE AND ROLE OF THE ELECTRONIC WORK PORTAL

The electronic work portal is an internet application, which is dedicated mainly to construction managers and foremen, as building contractor representatives, for support and help in health and safety tasks during building realization performance and secondly to safety coordinator, person which is entrusted by the project investor, the person who should also insure, manage and control occupational health and safety on building site.

The portal uses especially as:

- **communication channel -** for transfer and interposition of information and outputs from occupational health and safety management at the company level into building site environs;
- **working tool -** for construction manager and foreman directly on factual building;
- **feedback -** completed agenda on the building site offers information about real state of occupational health and safety on building site.

Information, which portal consists and offers make easier to manager on building site work with occupational health and safety agenda completing and management and permits him simplification of control and survey state of OHS on building site.

To building contractor employees, it means to building workers, can the portal serve as very good aid for better understanding of tenets and principles of safety conduct on building site, where they daily perform their works.

3. THE ELECTRONIC WORK PORTAL STRUCTURE

The web site net is divided into following seven main contextual sections depending on seven chosen **central fields of occupational health and safety management on building site**, which were specified following the analysis of OHS state in building industry of Slovak republic and European Union:

1. Trainings
2. Safety coordination
3. Personal protection work resources
4. Accidents
5. Machines and equipments
6. Noise
7. Hazardous substances

Each of these contextual sections is divided into following five rubrics:

1. Terms
2. Legislation
3. Main activities
4. Documents
5. Agenda

Content of particular rubrics:

- **Terms**
  - Explaining of important terms understanding – necessary for right use of other information from the portal content.
  - Resource for applied terms is terminology undertaken from at the present actual legislation, from European regulations and from Slovak technical norms pertinent to given problems.
- **Legislation**
  - Survey of at the present actual legislation Slovak regulations, statutes and instructions, eventually technical norms, which deal with OHS problems from the point of specified central fields of occupational health and safety management on building site.
  - The portal includes also full texts of obligatory legislation regulations with their assigning into particular fields of OHS management on building site.
- **Main activities**
  - Survey of main tasks and requirements flowing mainly from obligatory legislation, from internal company instructions in given OHS management fields; let us say generally recommended activities insuring safe performance on building site. Denominated key tasks and requirements are further explained with mention on responsibilities for their accomplishment delegation to particular persons attending the building realization.
- **Documents**
  - Survey and brief explanation of particular documents necessary for OHS on building site system management, which are elaborated mainly at the building contractor company level and have to be physically available on building site because of their effective transformation and application in daily practice during building works performance.
  - There are mainly documents, which provide information about remains risks on building site, about operation procedures and technologies, about right application of machines and equipments during building realization etc.
- **Agenda**
  - Survey and brief explanation of documents, which construction manager has to complete and manage on building site in the building realization

phase. Primarily there are records and reviews important for OHS management on building site indication in case of controls from public authority carrying out check on OHS in companies. Secondly it is documentation, which serves as a feedback, if you like response on OHS management at the company level, because records safety state and building work environs level.

- There are some forms and record application forms, for example for evidence keeping and registration of work accidents and other unwanted incidents occurrence on building site, about trainings taking place directly on workplace, about provided personal protection work resources, records from testimonies after work accident etc.
- The practical advantage of electronic work portal is, that permits direct completion of particular available forms and application forms and their printing after completion.

4. THE ELECTRONIC WORK PORTAL OPERATION

As it is an interactive web site, the portal users come into system through internet. By this the system flexibility and possibility of its service from whichever computer on whichever place using is covered.

On left side of the monitor are situated hyperlinks of seven central fields of OHS on building site management, from which the user can select this one, in which is he interesting. Consequently on the monitor right side arise hyperlinks of upper mentioned rubrics within the fields (terms, legislation, main activities, documents and agenda). The user click to the rubric, of which information wants to apply or with which wants to work and next on the monitor arise all available information, if you like hyperlinks of other information, which are related with given OHS management field within taken rubric.

Full texts of legislation regulations and forms or application forms, which the portal includes, upraise after click on relevant hyperlink in new individual sight.

The user can whenever go back or ready open some another management field. Information from the portal is possible to print or remove into another text editor and so can be more applied.

Pictorial samples from the electronic work portal content are presented next:

Figure 1. Content of the rubric „Terms" within „Accidents" field.

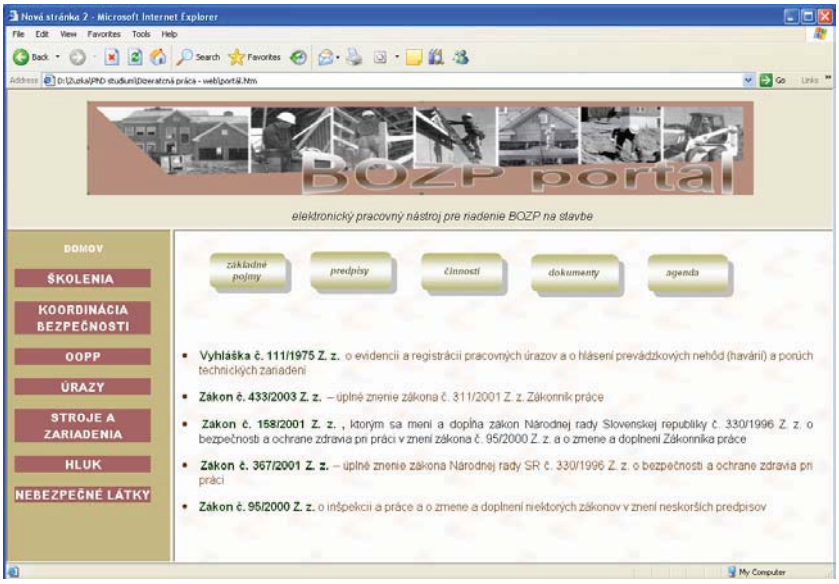

Figure 2. Content of the rubric „Legislation" within „Accidents" field

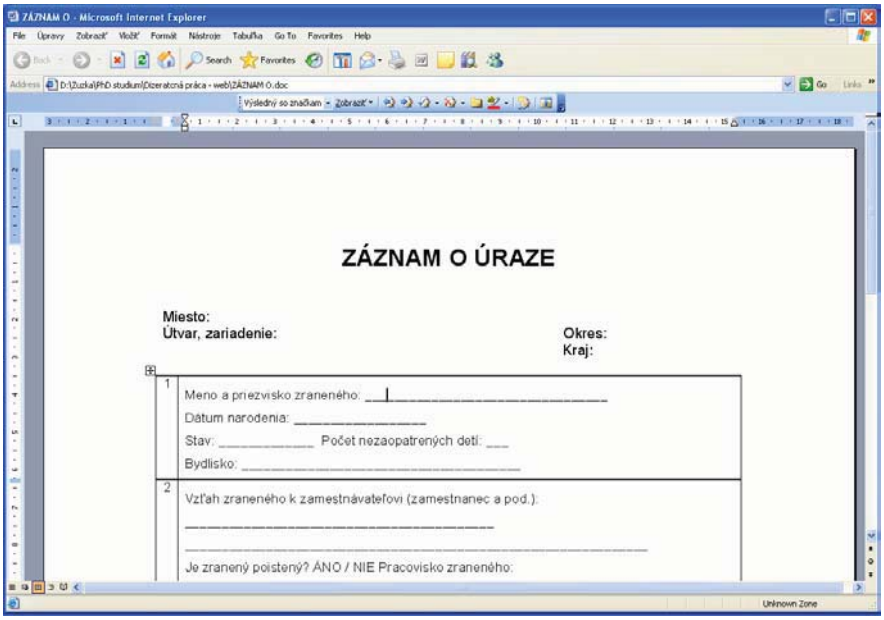

Figure 3. Application form for record of an accident completion situating in rubric „Agenda" within „Accidents" field

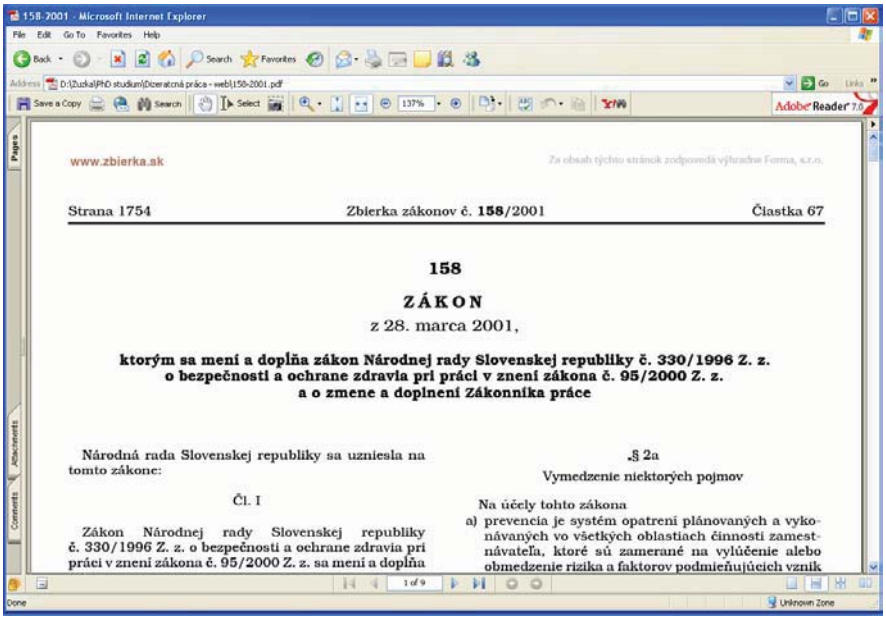

Figure 4. Full text of the regulation situated in rubric „Legislation" within „Accidents" field

5. CONCLUSIONS

Establishment of occupational health and safety management system is only the first but certainly not satisfactory step, which company leading should perform on behalf of OHS state increasing. Only management system establishment is not guaranty, that it will be function system and that the system brings effect of OHS state and work conditions improvement, if its implementation into daily practice on company workplaces is not made. That is why is important along with OHS management system on company level establishment, keeping and improvement pay bigger attention to generation and creation of effective tools, which insure building realization management in terms of established OHS management system in company, what brings reduction of work accidents or other unwanted incidents amount on building sites.

The article is the part of the project ***VEGA nr.1/1221/04 Integrated building management system*** *solution*

References

1. http://www.sme-safesite.com/good practice examples.php Good practice for the prevention of work accidents in the building and construction industry. A collection of examples for small amd medium – sized enterprises.
2. **STRUKOVÁ, Z.**: The Occupational Health and Safety Management System in Building Companies: Thesis. Košice 2005. 140 pages.
3. Relevant legislation

"Computational Civil Engineering 2006", International Symposium
Iaşi, România, May 26, 2006

Non-linear constitutive model for mortar

Jiri Brozovsky jr.[1], Ivan Kolos[2] and Alois Materna[3]

[1]*Department of Structural Mechanics, VSB - Technical University of Ostrava, Ostrava, CZ70833, Czech Republic*
[2]*Department of Structural Mechanics, VSB - Technical University of Ostrava, Ostrava, CZ70833, Czech Republic*
[3]*Department of Building Structures, VSB - Technical University of Ostrava, Ostrava, CZ70833, Czech Republic*

Summary

The non-linear constitutive model of a mortar is presented in the paper. The model is based on the equivalent one-dimensional stress-strain relation and on the smeared crack model. The limits of the one-dimensional relation are computed from the 2D state of stress with the help of the Kupfer failure condition. The smeared crack model is used for the modeling of tension crack propagation and the elasto-plastic behavior is assumed for the compression. It is assumed that concrete ca include up to two perpendicular crack direction. This model is similar to the ones that are used for a non-linear modeling of concrete.

KEYWORDS: constitutive models, finite element method, masonry, plasticity condition, smeared crack model, equivalent one-dimensional stress-strain relation.

1. INTRODUCTION

The masonry structures have been used for a very long time. In the present time it is often necessary to do a repair or reconstruction of many historical masonry buildings and engineering structures (bridges, for example). For this task, it is usually necessary to conduct a numerical analysis of the structure to understand its behavior and its carrying capabilities. The problem is that current technical standards (e.g. Eurocodes) don't provide instruction for assessment of existing structures (they have been created for a design and an assessment of new structures). Additionally, current technical standards don't allow to use masonry for complicated states of stress (and especially for masonry loaded by tension loads) but it is often necessary to respect that historic structures may (in some cases) work also in tension or bending. Also, numerical analysis according to the Eurocodes should be done with the linear elastic model of material but masonry has highly non-linear behavior.

The masonry consists of two main components with very different properties - a mortar (which is quasi-brittle) and bricks or stones (they are brittle). The resulting

material has complicated non-linear behavior with radically different properties in a tension and in a compression.

The paper presents only the non-linear model for the mortar. Its properties are very similar to a concrete. For this reason we use a constitutive model that is very similar to some constitutive models of concrete [9].

2. CONSTITUTIVE MODEL

2.1 Model overview

The model is based on the one-dimensional equivalent stress-strain relation (Figure 1). The relation uses so-called equivalent stress and strains that are defined (in this case) as a stresses and strains in the principal stress direction. We assume the initial linear behavior with softening (linear or non-linear) after the peak stress in tension. In a compression we assume the curvilinear behavior before the peak stress and a linear softening after the peak.

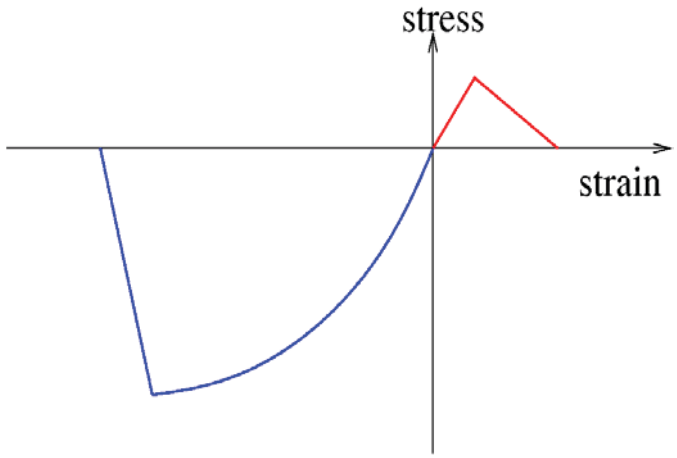

Figure 1. Equivalent one-dimensional relation (stress-strain diagram)

The limits of the equivalent one-dimensional relation (the tension and compression peak stresses and their related strains and also a strain limits) are obtained from two-dimensional (or three-dimensional) state of stress. The Kupfer or, alternatively, Chen-Chen failure condition is used for the computation of the limits. The Kupfer [2] condition is more proven for this type of the analysis [1] but the Chen-Chen [3] relation is more universal and is designed to be used both for the 2D and the 3D. The Kupfer condition is defined only for 2D. This type of the

model is often used for the concrete and is known to be very useful. For example, similar model is used in the successful commercial finite element code ATENA[4].

The behavior in unloading is assumed to be linear, with the initial Young modulus. It means that there is elastic and an inelastic part of deformation. Numerous authors use elastic unloading without inelastic part of deformations here [1] but the inelastic deformation is known to occur in the real material and this fact have to be respected in the model.

2.2 Modeling of behavior in tension

There is a problem related to this type of constitutive model and to its combination with finite element method: if peak stress occurs and behavior of model has to simulate the crack propagation, it is obvious that Young modulus have to be changed. But the size of the area of changing modulus is related to the size of the finite element on which the peak stress was detected. It means the behavior in a tension depends on the size of finite elements. It can be tested that very fine mesh (with very small finite elements) can lead to absolutely useless results (the model is very soft and fails very fast). There is also second problem - the peak criteria depends on the stress but with finite element analysis the extreme stresses can be lower for meshes with large finite elements due to averaging of results. So a model with a fine mesh can also reach the peak stress faster than a model with less fine mesh. But the later problem is minor a less difficult than the first one.

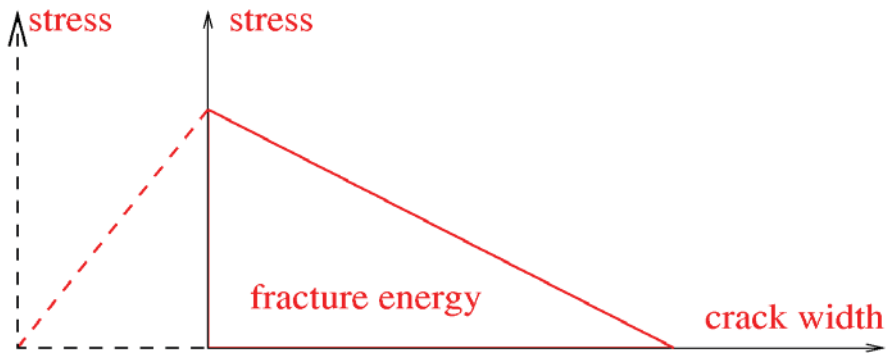

Figure 2. Relation between crack width and stress

Bazant [5] calls the problem a size-effect and offers a solution. The energy that is dissipated during the crack propagation can be measured and is can be used as a material property (but it also may vary and there is several definition of it that results to different sizes of this property - see [6] for details). It is usually referred as fracture energy. Because the fracture energy is related to the crack width and the widht of a cracking area (in our case it is a finite element width - see Figure 2), it is

possible to use it to modify the parameters of the tension part of the equivalent one-dimensional stress-strain relation (Figure 1).

3. NUMERICAL EXAMPLE

To illustrate the described constitutive model we provide a very simple numerical example. The computations were done in the uFEM finite element method software [7]. The example was conducted to show the behaviour of the constitutive model in the tension.

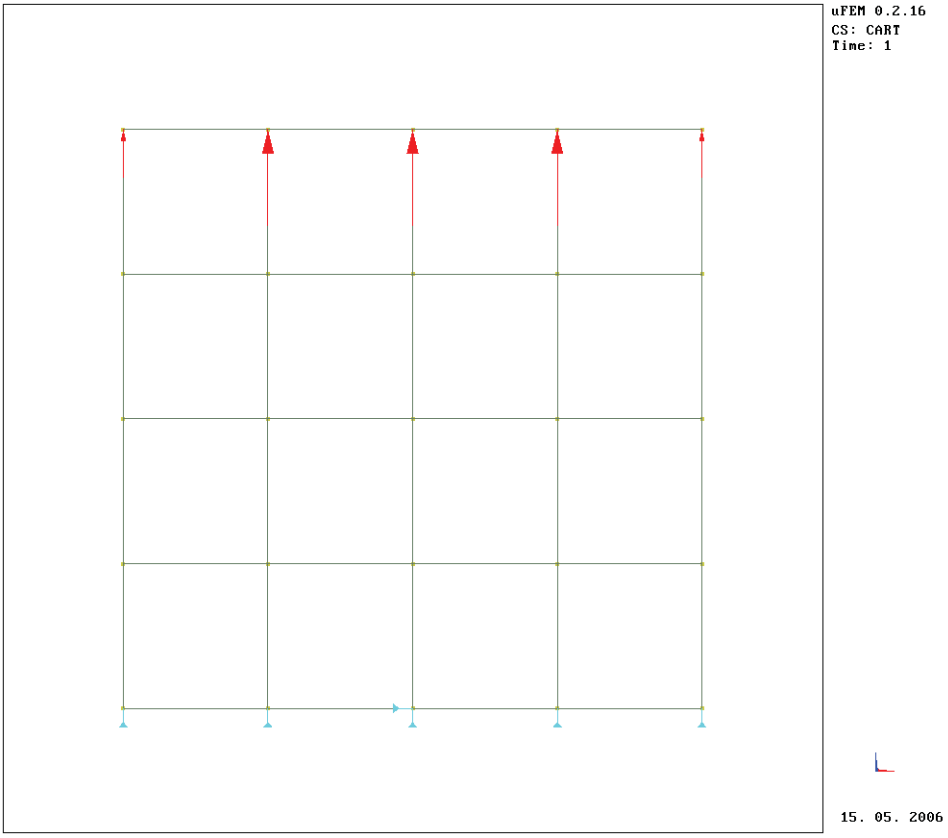

Figure 3. Finite element model of the illustrative example

The structure size is 0,4x0,4m and the width is 0,2m. The Young's modulus is 20 GPa, compression strength is 10,0 MPa and tension strength is 1,0 MPa. The forces represents the continuous load of a size of 5,2 kN/m.

The structure was analyzed in 2D as a plane stress problem with help of the Finite Element Method with the four-node isoparametric finite elements (well-known serendipity family elements).

The Newton-Raphson method was used for the control of the non-linear computational process. The solution consisted from 20 substeps. A total about 150 iterations were done.

The computational time for this solution was only few minutes on a 250 MHz workstation and under one minute on a modern computer (Sun Ultra 20 with Opteron 1,8 GHz processor).

The resulting load-displacement curve is shown in the Figure 4. The displacements were measured at the center of the structure. The load size shown in the Figure 4 is a relative (e.g. load size 1 is equal to 5,2 kN/m as mentioned above).

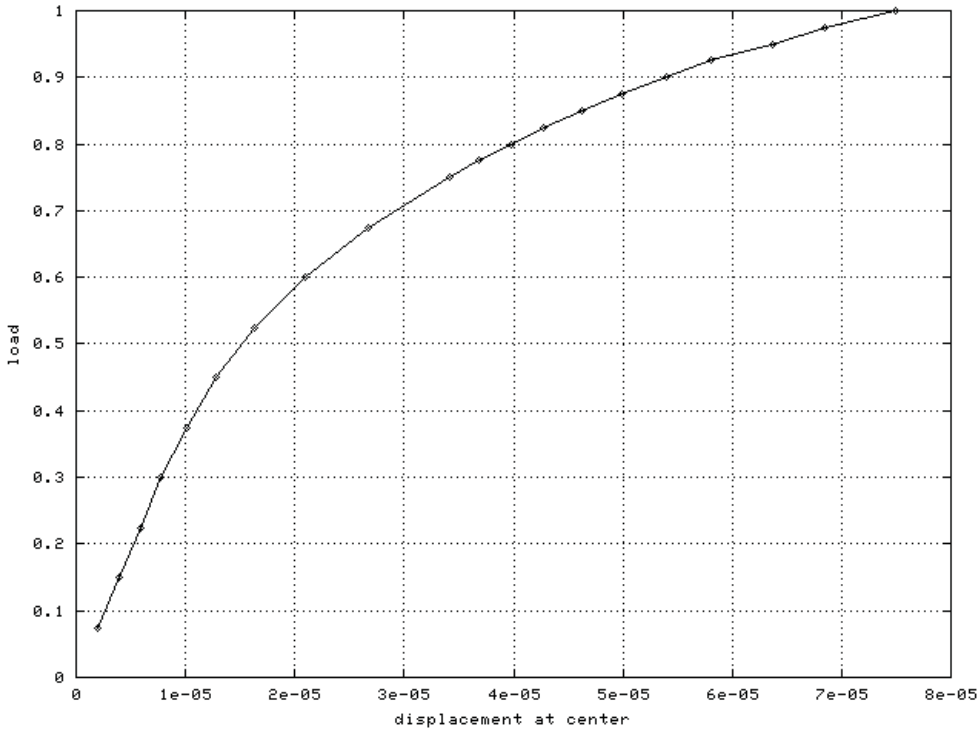

Figure 4. Load-displacement diagram for the illustrative example.

It is visible that behavior of the presented constitutive model is highly non-linear. The results presented here are only illustrative; however it is visible that the given approach can be used for modeling of mortar.

4. CONCLUSIONS

The article presents a non-linear constitutive model for mortar. This model is similar to ones that have been successfully used for modeling of a concrete because of high level of similarity of these material. The example solution that uses the model is also presented.

During further works we will concentrate on the verifying of the model and comparison with results of experimental laboratory tests.

We also work on the integration of this model with constitutive model for brittle materials that will simulate behavior of bricks and stones.

ACKNOWLEDGEMENT

The works have been supported from Czech state budget through Czech Science Foundation. The registration number of the project is 103/06/P389.

References

1. Cervenka, V. Constitutive Model for Cracked Reinforced Concrete, *ACI Journal*, Titl.82-82, 1985.
2. Kupfer H., Hilsdorf H.,K., Rüsch H.: Behaviour of Concrete Under Biaxial Stress, *Journal ACI*, Proc. V.66, no. 8, 1969
3. Chen, A. C. T., Chen, W. F. Constitutive Relations for Concrete, *Journal of the Engineering Mechanics Division* ASCE, 1975.
4. *ATENA Theory Guide*, Cervenka Consulting, Prague, 2005.
5. Bazant, Z. P., Planas J. *Fracture and Size Effect in Concrete and Other Quasib-rittle Materials*, CRC Press, Boca Raton, 1998.
6. Karihaloo, B. L. *Fracture Mechanics and Structural Concrete*, Longman Group Limited, Essex, 1995
7. uFEM software home page: http://www.penguin.cz/~jirka
8. Majewski, S., Szojda, L., Wandzik, G. *MWW3: modifkacja powierzchni granicznej trojparametrowego modelu Willama-Warnke*, Conference New Trends in Statics and Dynamics of Buildings, STU, Bratislava, 2002
9. Kralik, J. *Nonlinear Analysis of Resistance and Reconstruction Project of Emergency Water Storage tank on NPP with VVER 440*, 12th ANSYS User's Meeting, Brno, 2004

"Computational Civil Engineering 2006", International Symposium
Iaşi, România, May 26, 2006

Implementation of computational methods in Physics learning

Irina Radinschi and Brindusa Ciobanu

Department of Physics, "Gh. Asachi" Technical University, Iasi, 700050, Romania

Summary

Recently Physics learning studies have pointed out that implementation of computational methods can has a significant impact on students' skill development. Also, to solve problems in the traditional way it is not the most indicated way for understand the whole material of our Physics course and seminars. We point out that many students' poor math skills is a problem that we face at our institution and has a significant impact on understanding and applying the content of our Physics course. We want to find a way to improve the students' knowledge in spite of these math deficiencies. We want them to understand the Physics phenomena and their applications. Also, we want them to make progresses and to make these progresses rapidly. In this paper we describe our computational methods designated to Physics learning and how they have been integrated in our lecture courses of Physics in powerful ways.

Our experience demonstrates that these methods appear to be some of the most preferred modes of instruction. They are designed to remedy some of the students' skill deficiencies and guide study time towards an efficient learning of Physics. These computational tools are some "teaching-while quizzing" tests destined to the work at Physics course and seminars. The topics within the quizzes are restricted to the chapters of our Physics course and make them an efficient tool. Because of the multiple topics and difficulty levels, which are connected to the content of our Physics course, the "teaching-while quizzing" tests make the students to learn the material as a whole. In the context of implementation of computational methods in Physics learning, our computational tools are likely to be effective.

KEYWORDS: computational methods, Physics learning, "teaching-while quizzing" tests, computational tools

1. INTRODUCTION

Our experience in Physics teaching [2]-[6] has demonstrated that for students, to have good math skills and, also, to be a good problem-solver is a difficult task. From our experience we have concluded that students have a "little fear of Physics" and of what is behind the equations that describe the Physics phenomena.

Also, from high schools they have an established view of both the physical world and learning. On the other hand, physics relies heavily on mathematics.

When solving a problem involving physics students need to convert words and events into mathematical concepts, and this conversion results in an equation. They couldn't avoid applying the mathematics to solve physics problems but they couldn't do this without a good understanding of physics phenomena. In this way an interesting question arises: what are more important, converting words and events into mathematical concepts or have a good understanding of physics phenomena? We think both of them are important and strongly connected one to other. Also, of great importance is firstly to become familiar to the physics phenomena and, after this, to apply the mathematics for solving problems. And certainly, processing data using the computational methods help students to learn the entire material presented at the course and to all degrees.

Physics education research has shown that students' poor math skills is a problem that we face at our institution and it can have a significant impact on understanding and applying the content of our Physics courses. Also, simply collecting the data without using computer tools for processing them is not a good motivation for obtaining performance in the learning process in our Physics laboratory. To solve problems in the traditional way it is not a rapid way for understand and learn the whole material of our Physics courses. For this reason we decide to use some "teaching-while quizzing" tests destined to the work at Physics course and seminars. Because of the multiple topics and difficulty levels, which are connected to the content of our Physics course, the "teaching-while quizzing" tests make the students to learn the material as a whole. These "teaching-while quizzing" tools are implemented in our course of Physics and seminars like a computational method of Physics learning.

2. COMPUTATIONAL METHODS IMPLEMENTED IN PHYSICS LEARNING

From year to year the traditional methods [1] become less acceptable tools for diagnosing students' knowledge. Educators have often pinned their hopes of better instruction on technology. Yet teaching with technology, without a sound pedagogy, can yield no significant educational gain. An interactive pedagogy constructed around current internet technologies, is one of the few approaches that has been shown to produce positive cognitive gains. Also, our experience in the field demonstrated that "testing Physics" and computational methods are good tools for diagnosing the content and structure of students' knowledge of Physics.

Traditional ways, without including some "teaching-while quizzing" tests and without using computational methods are inefficient and ineffective for promoting

true Physics expertise. To solve a "mountain" of homework problems can be boring mostly if students do this without a good understanding of the Physics course, simply applying some equations and making calculations. The discussion of the content of Physics course and making some practice applying the "teaching-while quizzing" tests can be an easy way to learn Physics. Students have an established view of both the physical world and learning, formed from prior experience and learning. They filter all new observations and experiences. Also, they are attached to their world views and must expend much effort to revise and enriched their world views.

Construction of knowledge requires a well defined activity. Because of these, we permanently improve our Physics content knowledge and we focus our attention to the acquisition of new computational programs. In this way, we are endowed with a powerful teaching methodology for developing students' abilities to understand scientific claims and use these computational programs that describe, evaluate, design and simulate physical phenomena. In Physics laboratory the students use the computers as scientific tools for collecting, analyzing, visualizing and modeling real data. We hope that in this way, we succeed in attracting students' attention and they become more active. So, the students will not learn only a part of the material presented at the course and only to some degree because these serve them poorly and are not well matched to our goals. We desire our students to make important progress in Physics learning and, also, to make this progress rapidly. We want them to develop their ability to apply Physics concepts to physical situations and reason with them. For students it is important to handle with the content of the Physics courses and with some computational programs.

At the end of the course, seminars and Physics laboratory we want our students to understand the physical phenomena and to transfer the ideas and skills. To improve the Physics learning we propose the "teaching-while-quizzing" test [2] that can improve the instruction and, also, develops the students' abilities. The questions and exercises have been written for topics from introductory to advanced Physics and are limited to the chapters of our Physics course.

We are currently developing conceptual, traditional and non-traditional questions and exercises students. Also, we are currently developing conceptual tests and problems that bridge the gap between introductory Physics more advanced Physics levels and which have been greatly extended to improve the way we can present advanced curricular material to students. Over the past year the functionality of the "teaching-while-quizzing" test has been greatly extended to our students and we obtain good results. This test is given after a half of course and as a post-test surrounding the Physics course and evaluates the improvement in their conceptual understanding. We observe a good improvement in students' knowledge of Physics. Also, the students can receive a part of the "teaching-while-quizzing" tools through internet or on diskettes and have the possibility to handle with them.

The questions, exercises, demonstrations and tools have been developed to stress the visualization of Physics concepts. The exercises are geared to address the conceptual difficulties encountered by many students, with the goal of achieving better student understanding of these concepts.

A major objective of this project is the enhancement of student preparation for class and the improvement of their in-class experiences. We have assessed students' understanding after instruction, and actively engaged students are better prepared for class, are better motivated to learn the material. Also, in this way they have the possibility to apply their skills at the Physics seminars and laboratory. When the "teaching-while-quizzing" test is given after a half of course and as a post-test surrounding the Physics course and evaluates the improvement in the conceptual understanding of students, they can select Physics ideas from their entire Physics repertoire and give the good answer. In this way we replace the traditional way of giving the good answer by the way of pick up the good answer from a plethora of Physics world situations, many of them wrong.

Students are engaged in an activity of building and organizing their knowledge. They analyze the exercises, seek and weigh the solutions, compare the alternatives with more familiar they learned and monitor them and select the good answer. On the other hand, they must do these in a short time, they have allocated a few minutes for giving the good answer at every question. They can organize their knowledge to be useful. This method was successfully implemented in our Physics course, seminars and laboratory and enables the students to transfer knowledge and skills to new contexts as they are encountered. The "teaching-while-quizzing" tests have been implemented like a computational method in the process of Physics learning.

A powerful computational program has to satisfy some requirements which make it an efficient tool, so it has to be a good computational tool and this implies to works fast enough, gives the possibility to be applied for a large number of applications and facilitates to make predictions and analogies between different situations. The web-design and database are elaborated using PHP.Triad and MySQL programs. MySQL is recognized for superior ease of use, performance, and reliability.

For using the "teaching-while-quizzing" tools students have to register firstly and give a password. The students are asked to pick up the right answer at the questions of the "teaching-while-quizzing" test rapidly and to mark it into a dialog box. To do this they have an allotted time and, also, if they fail, we indicate them the correct answers. Also, if the students do not know the right answer at a quiz they can move on to the next quiz, but finally they have to indicate an answer to each quiz.

When they give all the answers they have the possibility to view their score. For the perfect score which means they give the right answer to all the quizzes the students obtain the mark 10. All the other marks are calculated proportional to the

number of the right answers. In the Figure 1 we present the web page for the "teaching-while-quizzing" tools.

Figure 1. Web page for "teaching-while-quizzing" tools

3. CONCLUSIONS

In the last years the rapid development of the Internet and new computational technologies has had a great impact on the implementation of the new computational methods in engineering education. We want to provide a framework for the integration of new computational tools attached to our Physics course and seminars in Physics learning. Good teaching is good communication and we believe that teachers should find a way to break out of the cycle of giving exams only in the traditional ways. Also, it is good for students to use the computational methods for evaluating themselves their knowledge and to learn how to handle with the content of Physics course and seminars.

The "teaching-while-quizzing" tests that we proposed for improving the Physics learning are already used by our students. Also, this computational method has improved the instruction and developed the students' abilities. They learned how to use with maximum efficacy the time designated for giving the good answer. The

multiple topics and difficulty levels, which are connected to the content of the Physics courses, make the students to learn the material as a whole.

The web-design and database are elaborated using PHP.Triad and MySQL programs. These programs are powerful computational tools and, also, the students can easily handle the on-line test. We use the "teaching-while-quizzing" tests for estimating the level of students' knowledge of our Physics course and we give to the students the possibility to improve their marks. In this way we add to the traditional methods of testing Physics a computer-based tool. Also, the students can receive a part of the "teaching-while-quizzing" tools through internet or on diskettes and have the possibility to handle with them. They improve their skills and develop their ability to apply Physics concepts to physical situations and reason with them.

The "teaching-while-quizzing" test is a reliable tool for the content and structure of students' knowledge of Physics. Authors are indebted to Luminita Scripcariu and Mircea Frunza for editing the TEST ONLINE.

References

1. Gerace, W. J., Beatty, I. D., Teaching vs. learning: Changing perspectives on problem solving in Physics instruction, An invited talk at the 9th Common Conference of the Cyprus Physics Association and Greek Physics Association: Developments and Perspectives in Physics--New Technologies and Teaching of Science, Nicosia, Cyprus, Feb 4-6 2005; Toback, D., Mershin, A., Novokova, I., A Program for Integrating Math and Physics Internet-Based Teaching Tools into Large University Physics Courses, Physics/0505026, submitted to the Physics Teacher; Toback, D., Mershin, A., Novokova, I., New Pedagogy for Using Internet-Based Teaching Tools in Physics Course, Physics/0408034; http://www.webct.com
2. Radinschi I., Ciobanu B., Teste de Fizica, Editura Junimea Iasi, 2006, ISBN (10)973-37-1166-7, ISBN (13)978-973-37-1166-7; Radinschi I., Ciobanu B., Fizica pentru ingineri, Editura Junimea Iasi, 2006, ISBN (10)973-37-1167-5, ISBN (13)978-973-37-1167-4
3. Ciobanu B., Radinschi I., Implementation of Physics Teaching in Engineering Education, The 6-th International Balkan Workshop on Applied Physics, July 5-7, 2005, Constanta, Romania.
4. Ciobanu B., Radinschi I., Computational Method for Study of Hall Effect in Physics Laboratory, The 6-th International Balkan Workshop on Applied Physics, July 5-7, 2005, Constanta, Romania
5. Ciobanu B., Radinschi I., One Computational Algorithm for Physics Modeling, Proceedings of 5th International Conference on Electromechanical and Power Systems, SIELMEN, October 6-8, 2005-Chisinau, Rep. Moldova.
6. Ciobanu B., Radinschi I., Implementation of some teaching tools in Physics education, Proceedings of International Symposium Present and Perspective in Textile Engineering, November 10-12, 2005, Iaşi, Romania, p. 607-611, ISBN 2973-730-120-X

"Computational Civil Engineering 2006", International Symposium
Iaşi, România, May 26, 2006

Indoor climate in contemporary buildings

Lenka Másilková

Department of Micro environmental and Building Services Engineering, Faculty of Civil Engineering, Czech Technical University in Prague, 166 29, Czech Republic.

Summary

Microclimate in contemporary residential buildings is nonconforming, because packaging constructions are too tight. In the aspect of presence of people is the most important thermal-moisture microclimate.

To guarantee optimal temperature in an interior can be quite simple, but to achieve optimal relative humidity can be problematic. But mildew emerges from higher relative humidity. It is important to guarantee sufficiency of ventilation air in the rooms, especially in winter period. Winter is the highest-risk period for increasing the relative humidity and following arise of the mildew.

This entry is comparing results of intensity of natural ventilation in various types of contemporary buildings.

KEYWORDS: indoor climate, contemporary buildings, relative humidity, natural ventilation, exfiltration, infiltration

1. INTRODUCTION

This entry intends to verify the authenticity methodology of computation of buildings ventilation. It especially determines more accurately interdependence parameters of leakage window chink of ventilated room size in the case of meeting existing hygienic requirements and conditions for protecting engineering construction (such requirement is for example moisture outlet).

At computations air change rate was not taken into account effect of under pressure ventilation bathroom and toilet to other rooms. Considering limited range of this article it is impossible to describe all the computations, which we have made. To make the computations more understandable I added a table to the last part of each of them.

Below in the text I am using a help term „diagonally ventilated flat". Diagonally ventilated flat is a flat, which windows are situated on the opposite sides of building facades. On the contrary not diagonally ventilated flat has windows only on one facade.

As basis of computations all three examples of natural ventilated rooms are taken into account flat 3+1. Disposition of this flat in a panel house has total volume of all the rooms 160m3.

2. VENTILATION IN CONTEMPORARY BUILDINGS

2.1 Problems of heat consumption for ventilation

Almost 4 million people in the Czech Republic live in panel houses. Majority of older panel houses are not corresponding to the standard ČSN 73 05 40 (thermal buildings protection) nowadays. Expensive reconstructions of panel building are passing through – heat cladding facades, changing original wooden windows to plastic, glazzing loggia as well. We are packing flats to save money for energy.

But how big is the importance of these changes to the flat natural ventilation? Well, all the buildings are so tight now that the infiltration rate is so minimal – the air supply by the chink in construction's blocking.

Nevertheless each household is producing moisture – by evaporating from the flowers, by cooking, by bathing etc. As far as the draining away of this moisture is not solved, due to it can be inception of moisture and degradation of engineering construction (rot). There is only one possible solution how to reduce relative humidity. It is ventilation, which at the same time ventilates others injurants from the interior (CO2, formaldehyde etc.) and ensures the supply fresh air into the flat.

Is it possible to count only on infiltration by window chink in so tight objects?

Does not mean heat cladding facade, new tighter windows, possibly glazed loggia periodical opening the windows for ventilation, so that to ventilate the room actually?

Will not be necessary to wake up each 1,5 hour and perfectly air all the room?

In this entry author presents how much energy do we use up for prescribed necessary hygienic need on air change rate in the room. How does differ from each other the heat consumption for ventilation by infiltration, exfiltration or standard 0,5times air change rate per hour for definite flat in the panel house?

2.2 Ventilation by wind with its different speed during the year – INFILTRATION

The main part of the wind effect ventilation in the flat takes not only the wind speed, but the flat position too. We consider a wind speed in variants of 2,5m/s; 5m/s; 10m/s.

The air change rate in the flat grows according to the velocity of wind. Flats in the ground floor of the buildings are mildly ventilated by wind in comparison with the flats in the upper floors, which are ventilated intensively.

It is valid the rule of wind influence to the buildings. Wind speed is increasing with the building height. And that is why the flat in the eight floor is more ventilated then the flat situated in the first above-ground floor.

Of course we consider flat position in the computations. We choose different coefficient leakage window chink and variants closed or opened interior doors in the flat in computations as well.

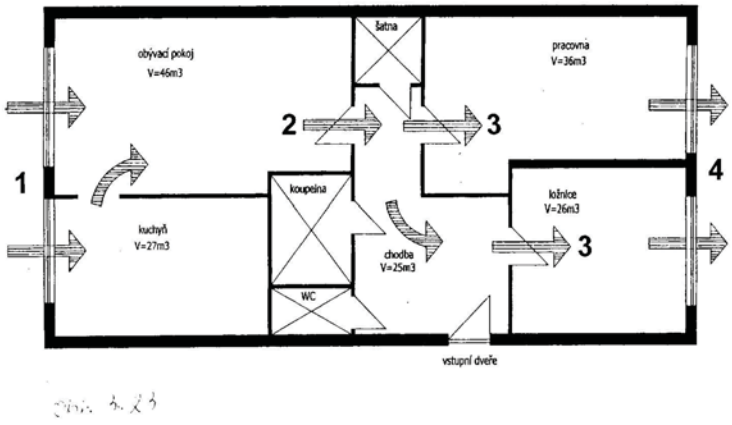

Figure 1. Ground plan of the flat – wind effect ventilation - INFILTRATION

2.3 Ventilation by static pressure effect in the stair's shaft – EXFILTRATION

Lower flats are intensively ventilated, namely at not tight openings and chinks in the upper part of stair's shaft. When the inner stair's shaft is connected through the flats on exterior the ventilating air from the lower flats can get into the upper flats namely when

- Entry flat's door is not tight
- Lower flat's windows are not tight or opened

For ventilation by static pressure effect in the stair's shaft is important that

- Upper flats are practically not ventilated from the exterior. But air is pressed from lower flats to upper flats through the stair's shaft (by inner stair's shaft).

- On the contrary lower flats are intensively ventilated by exterior air, the air is sucked up to them under pressure through the stair's shaft.

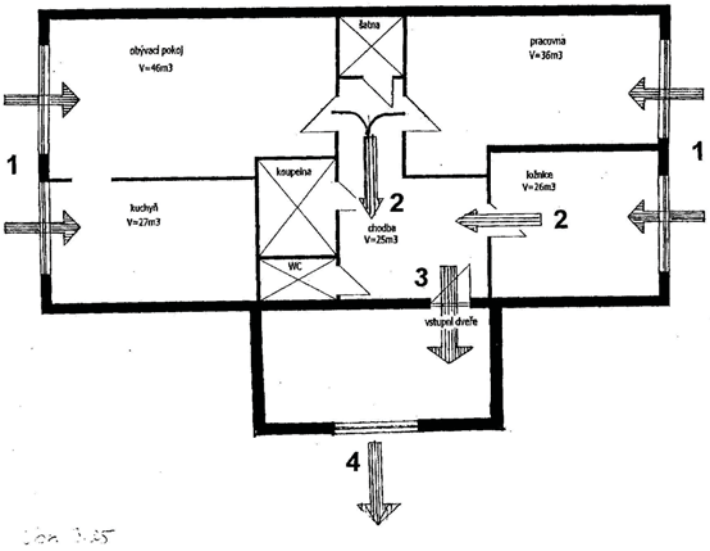

Figure 2. Ground plan of the flat – ventilation by static pressure effect in the stair's shaft - EXFILTRATION

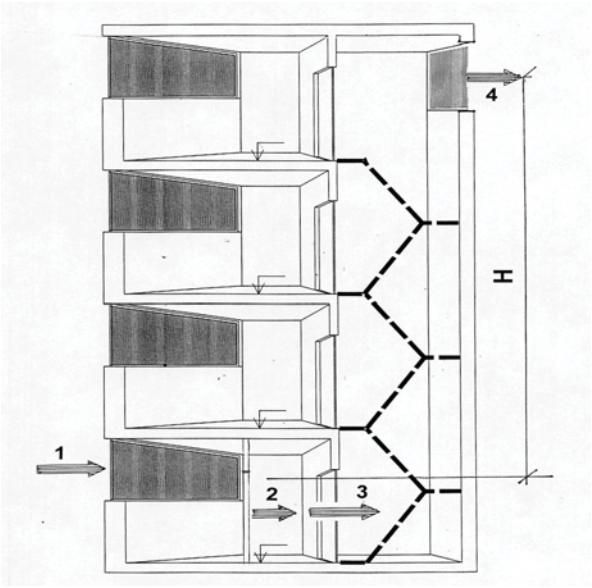

Figure 3. Section across the building – ventilation by static pressure effect in the stair's shaft - EXFILTRATION

2.4 Ventilation by combination of wind effect and stair's shaft effect

Combination of wind effect and stair's shaft effect compensates fair extremes in upper and lower flats (we do not include this combination in computations)

- Low – small wind effect and up – meaningful stair's shaft effect.
- Up – meaningful wind effect and low – small stair's shaft effect (under pressure against to excess pressure from the wind).

2.5 Ventilation by standard 0,5times air change rate per hour

Hygienic requirement for ventilation by standard 0,5times air change rate per hour lets

- By relatively small total volume of the room and small length window's chink, for example in panel building bigger infiltration coefficient i_{LV} (classic value coefficient leakage for original wooden windows is 1,4*10-4 m-2 s-1 Pa-n). From the energetic point of view in panel buildings is not necessary to plant tight windows.
- By relative large total volume of the room in old buildings (high room's headroom) and large length window's chink could be smaller infiltration coefficient i_{LV} (tightly windows).

3. AIR CHANGE RATE – COMPUTATIONS

End computation conditions: we consider a flat with a total volume of 160 m3 (area with 64m2 and height of 2,5m).

Rooms are ventilated by natural infiltration or exfiltration effect. MS Excel makes all the computations.

Entry value, inter computations and results are elaborated in well-arranged tables with particular descriptions of quantities, formulas and at the end comparing end values with standard values.

4. HEAT CONSUMPTION FOR VENTILATION - COMPUTATIONS

Computations about heat consumption for ventilation are elaborated in three variants air change rate in the flat.

4.1. Heat consumption for ventilation by wind effect – INFILTRATION

When wind speed is higher, than heat consumption need is higher too, we have higher heat consumption to secure the loss during the ventilation.

With the wind speed of 10m/s is used up to 47% heat consumption quantity from total heat quantity.

Table 1. Ventilation by wind effect force with different wind speed during the year

	wind speed	percentage share	hour number	exterior temperature	interior temperature	ventilation air volume	$(t_i-t_e)*0,36$	power	heat quantity
	c	**x**	**h**	**t_{em}**	**t_i**	**Vv**		**Q**	**Q_c**
	m/s	%	h	(°C)	(°C)	m^3/h		W	kWh
1	2,5	30	1800	4	20	20,36	5,76	117,27	211,09
2	5	15	900	4	20	81,46	5,76	469,21	422,29
3	10	5	300	4	20	325,84	5,76	1876,84	563,05
		50% =	3000 hours from 6000 hours in heating period						1196,43

4.2. Heat consumption for ventilation by static pressure effect in the stair's shaft – EXFILTRATION

- To secure the loss during the ventilation is needed the biggest heat quantity, when the exterior temperature is -2,2 °C. It is 55 %.
- At the same time this maximum is raised by the fact that the temperature of -2,2 °C secures 118 days from 240 days in heating period.
- It is 50% of days in the heating period.

Table 2. Ventilation by static pressure effect in the stair´s shaft

interior air density	exterior temperature	day number	$(273+t_e)$	$\frac{273}{(273+t_e)}$	$\frac{1,293*273}{(273+t_e)}$	shaft´s high	$(\rho_e-\rho i)$	static pressure	ventilation air volume	power	heat quantity
ρ_i(20°C)	**t**	**x**			**ρ_e(při x°C)**	**H**		**p_H**	**Vv**	**Q**	**Q_c**
kg/m^3	(°C)				kg/m^3	m		Pa	m^3/h	W	kWh
1,205	-15	6	258	1,058	1,368	15	0,163	24,476	31,53	397,28	57,21
1,205	-9,4	19	263,6	1,036	1,339	15	0,134	20,116	25,77	272,75	124,37
1,205	-2,2	118	270,8	1,008	1,304	15	0,099	14,776	18,84	150,57	426,41
1,205	1,8	52	274,8	0,993	1,285	15	0,080	11,930	15,19	99,52	124,21
1,205	7,4	37	280,4	0,974	1,259	15	0,054	8,081	10,19	46,22	41,04
1,205	11,2	18	284,2	0,961	1,242	15	0,037	5,557	7,11	22,52	9,73
	day sum =	**250**							total heat quantity	**Q_{SUMA} =**	782,98

4.3.Heat consumption for ventilation by standard 0,5times air change rate per hour

- Results are percently agreeing with example 4.2
- To secure the loss during the ventilation is needed the biggest heat quantity, when the exterior temperature is -2,2 °C. It is 54 %.
- At the same time this maximum is raised by the fact that the temperature of -2,2 °C secures 118 days from 240 days in heating period.
- It is 50% of days in the heating period.

Table 3. Ventilation by standard 0,5times air change rate per hour

exterior temperature	day number	interior temperature	air change rate	flat volume	ventilation air volume	$n*V_v*0,36$	temperature difference	power	heat quantity
t	**x**	**t_i**	**n**	**V**	**Vv**		**t_i-t_e**	**Q**	**Q_c**
(°C)		(°C)	h^{-1}	m^3	m^3/h		(°C)	W	kWh
-15	6	20	0,5	160	80	28,8	35	1008,00	145,15
-9,4	19	20	0,5	160	80	28,8	29,4	846,72	386,10
-2,2	118	20	0,5	160	80	28,8	22,2	639,36	1810,67
1,8	52	20	0,5	160	80	28,8	18,2	524,16	654,15
7,4	37	20	0,5	160	80	28,8	12,6	362,88	322,24
11,2	18	20	0,5	160	80	28,8	8,8	253,44	109,49
day sum =	**250**						total heat quantity Q_{SUMA} =		3427,80

5. CONCLUSIONS

- The highest heat consumption provides ventilation by standard 0,5 times air change rate per hour
- At the same time maximal heat quantity is value, which is needed for perfect flat airing, it means to hold the norm standard 0,5 times air change rate per hour
- Airing by INFILTRATION, with the same entry conditions, air change rate is only 0,175 times per hour
- Airing by EXFILTRATION, the flat is ventilating only 0,115 times

Table 4. Results comparing – computations heat consumption for ventilation

	heat quantity	percentage share	air change rate
	Q_c	heat	**n**
	kWh	quantity	h^{-1}
INFILTRATION	1196	35%	0,175
EXFILTRATION	783	23%	0,115
n = 0,5per hour	3428	100%	0,5
		maximum	

After comparing the results of total heat consumption we are satisfied that maximal heat quantity (that is 55% from total heat consumption) is important to supply when the exterior temperature is -2,2 °C.

This percentage share completely corresponds with percentage share day number during heating period while different exterior temperatures. Day number during heating period while exterior temperature is -2,2 °C, it is to 50%. And it is the same in the case of stair's shift effect and standard 0,5times air change rate per hour too. In both cases is used about 55% from total heat consumption.

We are satisfied that room's ventilation by standard 0,5times air change rate per hour is the most energetic expensive.

Total heat consumption for ventilation by standard 0,5 times air change rate per hour is 100%. This energy cost we could theoretically decrease by calculated heating loss by infiltration (35%) and exfiltration (23%). We can decrease total heat quantity by heat quantity from wind effect (infiltration) and stair's shaft effect (exfiltration). Percentage share 58% (35% + 23%) is more than a half needed heat quantity. This result we cannot neglect.

Total air change rate can we compute by this equation (1). Air change rate 0,79times per hour in this case is much more than hygienic requirement presents.

$$n_{0,5} + n_{INFIL.} + n_{EXFIL.} = n_{TOTAL}\ [h^{-1}] \quad (1)$$

$$0,5\ h^{-1} + 0,175\ h^{-1} + 0,115\ h^{-1} = 0,79\ h^{-1}$$

Because natural ventilation is passing through all the time in parallel with controlled standard 0,5 times air change rate per hour. If we do not accept natural ventilation, the room will be ventilated more than hygienic minimum.

Controlled standard 0,5 times air change rate per hour is the most energy consuming. We can decrease total heat quantity by heat quantity from wind effect (infiltration) and stair's shaft effect (exfiltration). It is computed in second equation (2).

$$Qn_{0,5} - Qn_{INFIL.} - Qn_{EXFIL.} = Qn_{TOTAL}\ [kWh^{-1}] \quad (2)$$

$$100\% - 35\% - 23\% = 42\%$$

We are satisfied that total heat quantity can bee decreased more than to half.

ACKNOWLEDGEMENTS

This research has been supported by MŠMT grant No. MSM 6840770005.

References

1. JELÍNEK, V., Micro environmental and building services engineering, 2nd ed. Prague: University press ČVUT, 2004. 158 s. ISBN 80-01-02887-9.
2. Norm Thermal building protection – ČSN 73 05 40

"Computational Civil Engineering 2006", International Symposium
Iaşi, România, May 26, 2006

Correlations of earthquake ground motion and energy distributions in one-story irregular building structures

Mihail Iancovici[1,2]

[1]*Department of Mechanics, Statics and Dynamics of Structures, Technical University of Civil Engineering (UTCB), Bucharest, 020396, Romania*
[2] *National Center for Seismic Risk Reduction (NCSRR), Bucharest, 021652, Romania*

Summary

Seismic vulnerability evaluation of one-story irregular buildings is important, especially in the case of existing structures, designed in the "pre-seismic design codes era". Ideally, a structural system must have equal performance to earthquake ground motions (EQGM) from all possible directions, resulting uniformly exposed to risk structures. Since the structural performance is mainly controlled by the mechanism of how the structure supplies the energy received from the ground motion, the energy balance-based analysis has the potential to synthetically and more efficiently describe such mechanism.

The paper investigates the plan stiffness irregularity effect on the time-history and peaks of seismic energy distribution in one-story linear-elastic buildings, subjected to bi-directional ground motion, applied under a 10^o rosette from the main stiffness axes of the model. Through a linear energy balance-based analysis, modal and total energies are computed and the input energy distribution coefficients are obtained in order to assess the structural damage exposure of irregular structures and the associated critical directions of motion. The framework may be successfully extended to multistory buildings having complex plan and elevation shapes.

KEYWORDS: earthquake ground motion, structural performance, irregular structures, energy balance-based analysis, input energy, damage exposure

1. INTRODUCTION

Uncertainties in the ground motion characterization and structural mass, stiffness and strength distribution may be pointed out as sources of discrepancies between analysis and observed behavior, during relatively recent earthquakes 1989 Loma Prieta (U.S.), 1994 Northridge (U.S.) and 1995 Kobe (Japan).

For regular structures usually, only the plan orthogonal translational components of ground motion are considered in analyses. While the vertical component may be

neglected for many of cases, the rotational component might produce significant effects even in perfectly plan symmetric systems (Wen, Chopra, 2002), as recorded during past seismic events.

Ideally, a structural system must have equal performance to earthquake ground motions from all possible directions, resulting uniformly exposed to risk structures. Currently, the seismic design is based on static equivalent seismic loads obtained from acceleration response spectra. The major overcome of this approach is that does not account directly for the ground motion total duration nor for the hysteretic properties of structural elements. The peaks of resultant seismic effects (e.g. shears) in a certain structural member are computed using several combination rules of peak effects under the main stiffness axes of building (e.g. SRSS, CQC etc.). Recently, the CQC3 method for the combination of the orthogonal spectrum effects was derived (Menun and Der Kiureghian, 1998). This approach does produce significant differences between different structural members.

Alternatively, a large number of dynamic analyses at various angles of ground motion in order to check all points for the critical earthquake directions can be performed. Such an elaborate study could conceivably produce a different critical input direction for each stress evaluated. While, the cost of such a study for complex structures could be prohibitive, the actual hardware performance allows performing such analyses. Moreover, for structures having complex plan shape, the principal directions of motion are not apparent.

For regular structures, having uniform mass and stiffness distribution, the building response in each direction can be studied separately without the consideration of cross-correlation of ground accelerations acting in different directions. However, structural systems having non-coincident centers of mass and stiffness, or both, may experience coupled seismic responses. Furthermore, frequencies in the fundamental modes of vibration in three primary directions may be closely spaced. These situations warrant a 3D coupled response analysis framework that take into account the cross-correlation of ground motion acting in different directions and the inter-modal coupling of modal responses. Additionally, the irregularity due to strength distribution in the case of inelastic behavior might produce important effects.

The structural performance is mainly controlled by the mechanism of how the structure supplies the energy received from the ground motion. The energy balance-based analysis has some advantages over the current analysis procedures: (1) assess more efficiently the earthquake ground motion destructive potential, through the input energy induced into a structural system, (2) fully accounts for the total duration of the earthquake ground motion and (3) has the potential to synthetically and more efficiently describes such mechanism.

The input energy induced by the earthquake ground motion into a structural system represents a more complete parameter to estimate its destructive potential

(Akiyama, 1985). It includes both, the ground motion characteristics and the structural properties. While for perfectly plan symmetric systems, the earthquake ground motion in one direction produces effects only in that direction, in the case of non-symmetric systems, the ground motion in one direction may transfer energy in the other direction, eventually contributing to the overall structural damage. Obviously, eccentric systems could be more exposed to damage than symmetric systems, even if the rotational component of EQGM is neglected.

In the present paper, the effects of plan stiffness on the seismic energy distribution are studied using a one-story linear-elastic system, subjected to bi-directional ground motion.

2. ENERGY-BASED CHARACTERIZATION OF EARTHQUAKE GROUND MOTION

The energy content of an EQGM accelerogram can be expressed in both, *time* and *frequency* domain through energy-associated parameters: the cumulative energy function and power spectral density function (*PSD*), respectively. While one describes the intensity distribution of the accelerogram over the *time* domain, the other describes the *frequency* decomposition of the signal's energy. The total power can be consequently obtained by integrating the *PSD* function over the frequency domain, its value yielding the mean square value of the accelerogram.

The cumulative energy of an accelerogram $a_g(t)$ is expressed by

$$E_{cum}(t) = \int_0^t a_g^2(\tau) d\tau \tag{1}$$

One of the frequency content descriptor of an accelerogram is the dimensionless factor $\boldsymbol{\varepsilon}$ (Cartwright&Longuet-Higgins)

$$\varepsilon = \sqrt{1 - \frac{\lambda_2^2}{\lambda_0 \lambda_4}} \in [0,1] \tag{2}$$

where,

$$\lambda_i = \int_{-\infty}^{\infty} \omega^i S_x(\omega) d\omega \tag{3}$$

is the i^{th} spectral moment about the mean and $S_x(\omega)$ is the *PSD* function of the accelerogram (Kramer, 1996).

For illustration purposes, a representative EQGM is analyzed. The orthogonal accelerograms components of El Centro (U.S.) EQGM - May 19, 1940 (USGS 117 Station, PGA_{180} = 0.31g, PGA_{270} = 0.21g) are presented here.

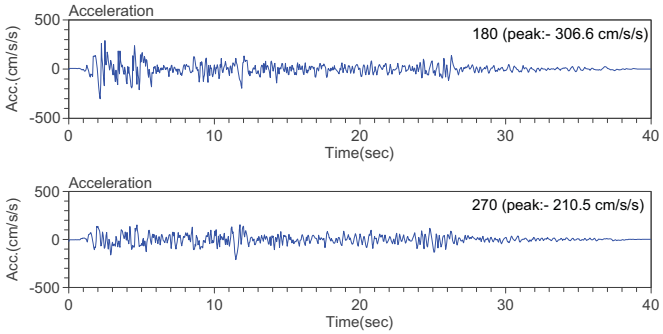

Figure 1. Orthogonal acceleration records, El Centro, May 19, 1940

Time and *frequency* domain energy-associated parameters distributions are shown in fig.2.

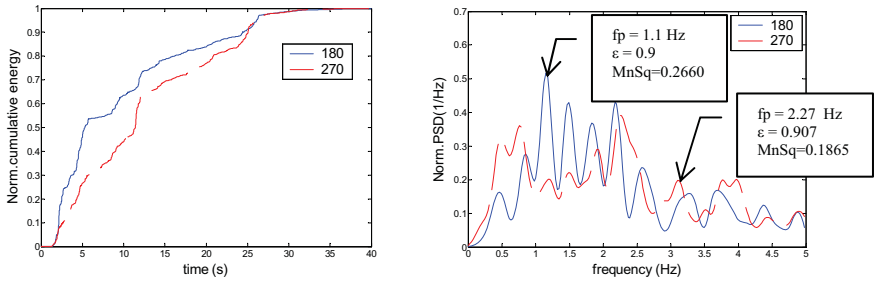

Figure 2. Normalized cumulative energy functions and normalized power spectral density functions

The near-field type ground motion records are characterized by large frequency bandwidths and high predominant frequencies, in the range of low-rise building structures. The energy distributions are rather uniform in the range of 0.5-3 Hz, the total power ratio yielding 1.37.

Such energy content patterns are to be taken into account, in order to assess the destructive potential of an EQGM, especially in the case of flexible structures (Iancovici, 2005).

3. ENERGY BALANCE-BASED ANALYSIS. CORRELATION OF BI-DIRECTIONAL EQGM AND STRUCTURAL ENERGY DISTRIBUTION.

3.1 Structural model description and analysis

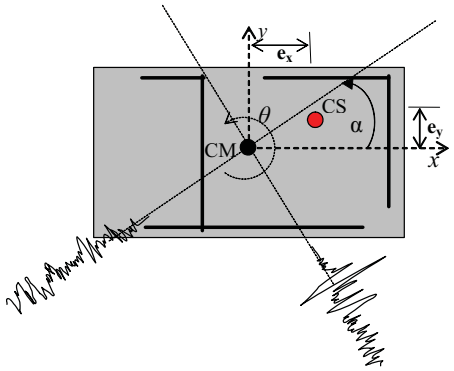

Figure 3. Floor plan and ground motion directivity

The structural model is a one-story building system, with uniform mass distribution and typical floor plan as presented in fig. 3 (CM – center of mass, CS – center of stiffness).

The input ground motion consists of two orthogonal ground accelerations, acting under the α directivity angle. Four cases of equal eccentricity ratios (e_x=e_y) are considered: *0%* (symmetric system, referred as *standard system*), 0.01 *r* (1%), 0.05 *r* (5%) and 0.1 *r* (10%), where *r* is the radius of gyration.

The 3*DOF* system of equations of motion, subjected to ground acceleration is given by

$$M\ddot{u}(t) + C\dot{u}(t) + Ku(t) = -Mia_g(t) \tag{4}$$

where *M*, *C* and *K* are the mass, damping and stiffness matrices, *i* is the influence matrix and a_g is the ground acceleration vector, comprising of *x, y* and θ-direction (rotational component) acceleration. While the rotational component for regular one-story buildings can be neglected, the *x* and *y* – direction accelerations are obtained by composing the two orthogonal components (fig.3).

Following equation (4), time-history energy balance equation yields

$$\int_0^t \ddot{u}^T(\tau)M\dot{u}(\tau)d\tau + \int_0^t \dot{u}^T(\tau)C\dot{u}(\tau)d\tau + \int_0^t u^T(\tau)K\dot{u}(\tau)d\tau = -\int_0^t M\cdot i\cdot a_g(\tau)\cdot\dot{u}(\tau)d\tau \tag{5}$$

where the components are the kinetic energy $E_k(t)$, viscous damping energy $E_d(t)$, potential energy $E_p(t)$ and input energy $E_i(t)$, respectively. The potential energy consists of elastic-strain energy $E_s(t)$ and hysteretic energy $E_h(t)$.

From the point of view of investigating the damage exposure, of primary importance is to study the amount of energy input attributable to potential damage (elastic vibration energy, E_k+E_s), by using a linear energy balance-based analysis (Iancovici, 2005).

Equation (5) may be either solved by direct integration or using modal superposition method. Modal superposition has the advantage over the direct integration that estimates the contribution of each modes of vibration to the total energy distribution.

The energy-balance modal equation corresponding to the j^{th} vibration mode is thus

$$\int_0^t M_j \ddot{\varsigma}_j(\tau)\dot{\varsigma}_j(\tau)d\tau + \int_0^t C_j \dot{\varsigma}_j^2(\tau)d\tau + \int_0^t K_j \varsigma_j(\tau)\dot{\varsigma}_j(\tau)d\tau = -P_j \int_0^t a_g(\tau)\cdot\dot{\varsigma}_j(\tau)d\tau \quad (6)$$

where M_j, C_j and K_j are the generalized mass, damping and stiffness of the j^{th} mode, ς_j is the generalized coordinate and P_j is the modal participation factors vector.

The components of equation (6) are the generalized kinetic energy $E_{k,j}(t)$, generalized viscous damping energy $E_{d,j}(t)$, generalized potential energy $E_{p,j}(t)$ and generalized input energy $E_{i,j}(t)$, respectively.

In terms of generalized energies, the ratio of the input energy attributable to potential damage to the input energy, has the means of time-instant modal damage exposure coefficient, corresponding to the j^{th} vibration mode:

$$d_{i,j}^{dam}(t) = \frac{E_{k,j}(t) + E_{s,j}(t)}{E_{i,j}(t)} \quad (7)$$

The peaks ratio hence is a useful measure to comprehensively asses, through modal responses, the damage exposure of a structure (Iancovici, 2005):

$$d_{i,j}^{dam} = \frac{\left|E_{k,j}(t) + E_{s,j}(t)\right|_{\max}}{\left|E_{i,j}(t)\right|_{\max}} \quad (8)$$

In order to evaluate the correlation between ground motion energy-associated parameters and structural energy distribution, both components needs to be analyzed.

Thus, the total power of the resultant ground motion accelerations, in x and y-direction are given in fig. 4, in terms of directivity:

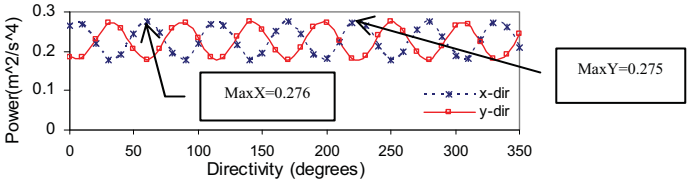

Figure 4. Total power of ground accelerations, in *x* and *y*-direction

The modal properties of the system, in terms of eccentricity ratio are given in Table 1. 5% damping ratios were assumed for all modes of vibration.

The vibration modes correlation coefficients were computed by using Der Kiureghian's equation (Der Kiureghian, 1980)

$$\rho_{jk} = \frac{8\sqrt{\xi_j \xi_k}\,(\beta_{jk}\xi_j + \xi_k)\beta_{jk}^{3/2}}{(1-\beta_{jk}^2)^2 + 4\xi_j\xi_k\beta_{jk}(1+\beta_{jk}^2) + 4(\xi_j^2 + \xi_k^2)\beta_{jk}^2} \tag{9}$$

where ξ_j, ξ_k are the damping ratios corresponding to mode j and k. β_{jk} is the ratio of j and k natural circular frequencies of vibration. The vibration modes correlation coefficients, as computed by equation (9), are given in Table 1, for those 4 cases of eccentricity ratios.

Table 1. Vibration modes correlation coefficients

e_x, e_y (*r)	Mode	1	2	3	ω_n, rad/s
0	**1**	1.000	1.000	0.038	16.28
(standard system)	**2**	1.000	1.000	0.038	16.28
	3	0.038	0.038	1.000	28.19
1%	**1**	1.000	0.989	0.036	15.22
	2	0.989	1.000	0.037	15.38
	3	0.036	0.037	1.000	26.74
5%	**1**	1.000	0.103	0.012	9.61
	2	0.103	1.000	0.029	12.87
	3	0.012	0.029	1.000	23.87
10%	**1**	1.000	0.018	0.004	5.94
	2	0.018	1.000	0.025	12.02
	3	0.004	0.025	1.000	23.30

As the eccentricity ratio increases, the natural circular frequency decreases, as well as the correlation between vibration modes decreases. The largest decay may be observed for the 1st and 2nd mode and for the 1st and 3rd mode. In the 2nd mode of

vibration, no influence of eccentricity and no rotation occurs (not represented here).

In the followings, time-histories and peaks of generalized and total energy distributions for 36 directions, corresponding to those 4 cases of eccentricity ratios, are studied. Statistical correlation of loads and the vibration modes correlation is studied in order to completely characterize the energy distribution.

3.2. Generalized seismic energy distribution

The correlation coefficient of modal responses depends not only on the modal frequencies and damping ratios, but also on the correlation/coherence of the associated generalized loads (Der Kiureghian, 1980). The statistical correlation of generalized seismic loads in terms of eccentricity ratios is represented in fig. 5.

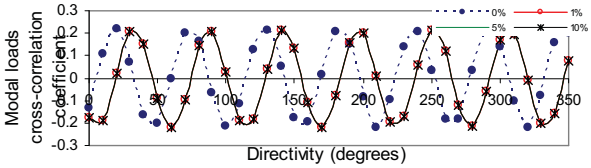

Figure 5. Cross-correlation coefficients of generalized loads

For illustration purposes, time-histories of generalized energies for 60° directivity are given in the fig. 6 and 7.

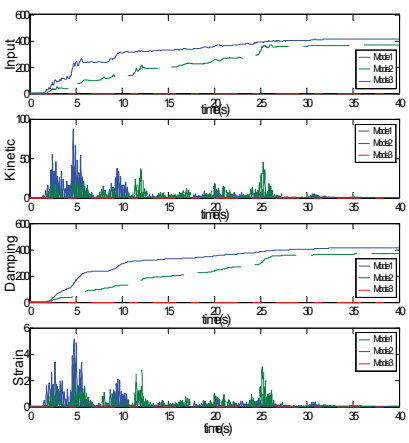

Figure 6. Generalized energies, $e_x=e_y=0$, 60° directivity (kNm, kNmrad^2)

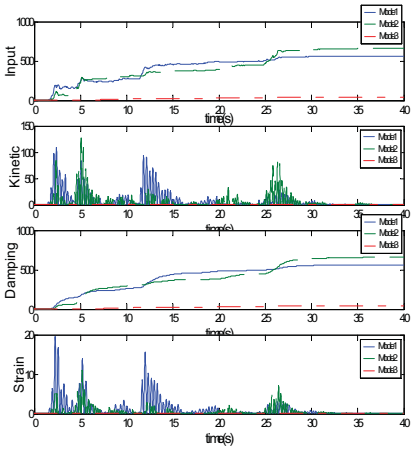

Figure 7. Generalized energies, $e_x=e_y=0.1r$, 60° directivity (kNm, kNmrad^2)

The correlation between the generalized loads is little influenced by eccentricity. The eccentricity effect on modal energy distribution can be briefly observed in the

occurrence of larger values and rotational component of energies. The 36 directions rosettes of peaks modal (generalized) energies are represented below (1-means 0^o).

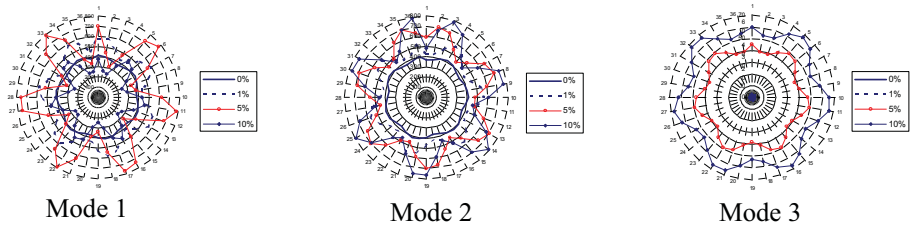

Figure 8. Maximum generalized input energy (kNm, $kNmrad^2$)

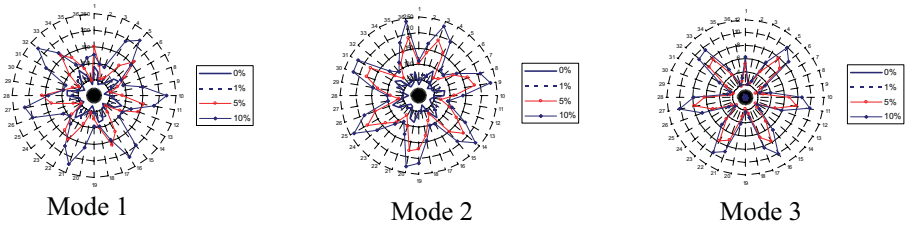

Figure 9. Maximum generalized kinetic energy (kNm, $kNmrad^2$)

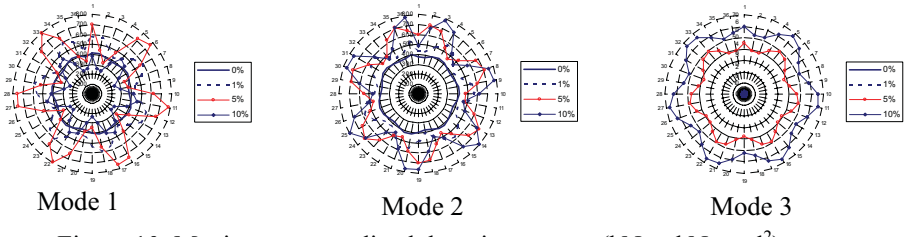

Figure 10. Maximum generalized damping energy (kNm, $kNmrad^2$)

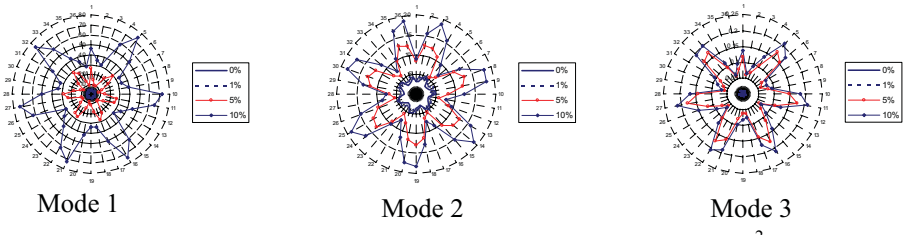

Figure 11. Maximum generalized strain energy (kNm, $kNmrad^2$)

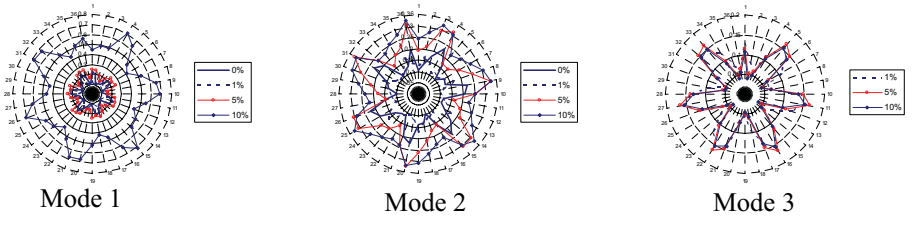

Figure 12. Generalized damage exposure coefficients

3.3. Total seismic energy distribution

The statistical correlation of ground accelerations in *x* and *y*-direction, shows a maximum value corresponding to 210° directivity and nearly 0 correlation for 60° directivity (fig.13).

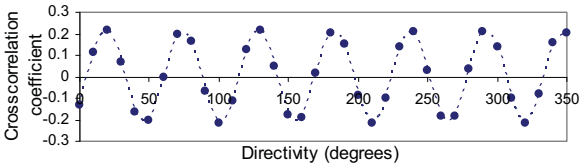

Figure 13. Cross-correlation coefficients of ground accelerations, in *x* and *y*-direction

Time-histories of seismic energies for 60° directivity are given in the fig. 14 and 15.

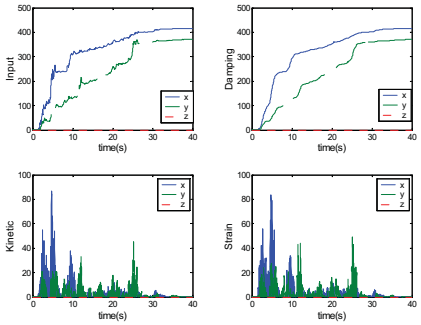

Figure 14. Total energies, $e_x=e_y=0$, 60° directivity (kNm, kNmrad^2)

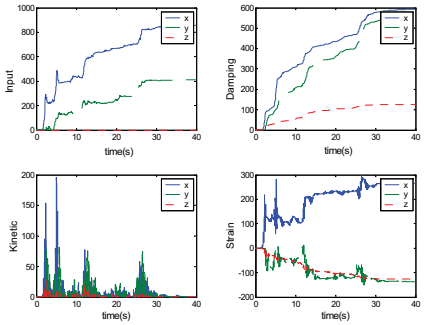

Figure 15. Total energies, $e_x=e_y=0.1r$, 60° directivity (kNm, kNmrad^2)

For convenience, energies may be converted into equivalent velocities, as defined by Housner (1956) and Akiyama (1985). The ratio of equivalent velocities is equal to the squared ratio of energies. Peaks of total input and strain energy are plotted below (1-means 0°).

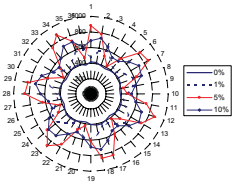

x – direction, kNm

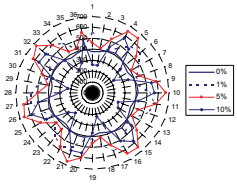

y – direction, kNm

Figure 16. Maximum input energies

While in the case of *standard system*, no torsional effects on strain energy are observed, for irregular structures case the ground motion induces effects on the strain energy, even if the rotational component of ground motion are negligibly small (fig. 17).

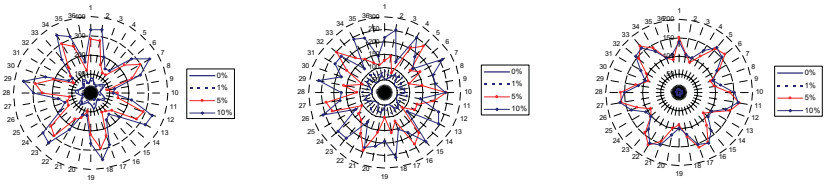

x – direction, kNm y – direction, kNm θ – direction, kNmrad^2

Figure 17. Maximum strain energies

Rotational strain energy is less influenced at smaller eccentricity ratios (e.g. accidental eccentricity) but it is larger for higher values of those.

4. CONCLUSIONS

The increase of eccentricity ratio induces basically the growth of seismic energy value. For instance in the case of the 1st mode generalized input energy, the ratio of peaks corresponding to 5% and 0% eccentricity ratio, for 60^o directivity, is about 2.

The eccentricity effect on the generalized energies is especially observed in the case of third mode of vibration, where the ratio of input energy for instance, is about 25, corresponding to 10% and 5% eccentricity ratios. The corresponding ratio of equivalent velocities is therefore 5.

In the case of *standard system* the directions of maximum earthquake ground motion power coincides with those of maximum energies (60^o and 250^o, respectively), in the case of irregular structures, those directions are considerably influenced by the vibration mode coupling.

The damage exposure coefficient plots permit to estimate the directions of motion that creates maximum modal effects. The plots show that as the eccentricity increases, the exposure to damage increases. For instance, the ratio of these coefficients peaks for the 1st vibration mode, corresponding to 10% and 0% eccentricity ratio, in the *x*-direction, is about 3.5.

By performing energy balance-based analyses at various directivity angles of orthogonal ground motions, more reliable and more economical building structures may be obtained, by adopting an integrated dynamic analysis framework. This can

be successfully extended to multistory buildings having complex plan and elevation shapes.

References

1. Akiyama, H., *Earthquake-resistant limit-state design for building*, the *University* of Tokyo Press, Tokyo, Japan, 1985
2. Housner, G., W., *Limit Design of Structures to Resist Earthquakes*, Proc. 1st World Conf. Earthquake Engineering, 5-1 to 5-13, Berkeley, CA, 1956
3. Iancovici, M*., Evaluarea performantei structurale a cladirilor de beton armat.*. Ph.D. Thesis. Technical University of Civil Engineering Bucharest, 2005 (in Romanian)
4. Kramer, Steven, L., *Geotechnical Earthquake Engineering*, Prentice Hall, Inc., NJ 1996
5. Menun, C., Der Kiureghian, A., *A Replacement for the 30 % Rule for Multi-component Excitation*, Earthquake Spectra, Vol. 13, Number 1, February 1998
6. Wen, H.,L., Chopra, A., *Accidental torsion in buildings: analysis versus earthquake motions*, Earthquake Engineering Research Center University of California, Berkeley, Report no. 01, 2002

"Computational Civil Engineering 2006", International Symposium
Iaşi, România, May 26, 2006

Building system loads and its climatic data

Roman Musil

CTU in Prague, Department of Microenvironmental and Building Services Engineering, Thákurova 7, 169 34 Prague 6, e-mail: roman.musil@fsv.cvut.cz

Summary

This paper is considering application of stochastic models on human factor. It describes energy and environmental loads of buildings and types of data needed to be obtained in practice.

KEYWORDS: Water and electricity consumption, waste production, building occupation, climate dates and its formats.

1. TYPE OF ENERGY AND ENVIRONMENTAL BUILDING SYSTEM LOADS

1.1 Water consumption

Consumption of water depends on the type of building and its occupancy during operation. It is necessary to have a respect to behavior of users, to respect their needs, regional practice or hygienic consumer habits by assessment water consumption. It isn't important only total water consumption, but we want to know distribution of fractional water consumption in the time period. On the basis of improvement curves of water consumption for particular types of buildings is possible to design smaller reservoir for warm water and in consequence smaller heat sources. Subsequently it leads to reduction of flow warm water in circulatory pipe and it leads to lowing energy intensity of heating water.

Model of water consumption depends on these characteristics:

- type of building and its purpose
- number of people in the building
- direct water using (for toilet, shower, cooking, garden watering, swimming pool…)
- using water for technical equipment (production processes)

Work objective:

It is necessary to develop models which will correspond with real consumption profile. We have to obtain for practice two formats of data:

- average yearly values (for overall summary of water consumption)
- water consumption distribution to time period (for precise design of heating water)

1.2 Waste water production

Waste water production is directly linked with consumption of water in most of cases. For most cases flow waste water is equal to consumption of water which means that the sum of warm and cold water consumption in time period is equal to flow waste water in the period. In some cases the water doesn't outflow (for example garden watering) or it outflows with some time-current delay (filling swimming pool, washing up or tidying up). This delay isn't important for us because it is only drainage of waste water from the building. It is important for us to know total production waste water and its quality which can be very different and again it depends on the user.

Waste water is divided on 3 types:

- waste water from toilets which are contaminated and needs biological cleaning
- waste water from wash-basins, baths, showers, roofs,…which is possible considered as almost clean and it is appropriate for recycling and reuse.
- waste water with fat, oil or petrol which needs special wastewater pretreatment.

Recycling possibilities depend on resource of waste water and on using of recycled waste water in building.

Work objective:

We need similar data as like as water consumption

1.3 Production of solid waste

Daily profiles these waste aren't interesting because these waste collection is realized in regulated interval, for example two times a week for household waste or one times a month collection of paper and its following recycling. Average values of waste depend on the type of building, for example in the offices. There is massing more wastepaper than in other buildings over big quantity of computation techniques. It is the most important by this waste their sorting which increases

efficiency liquidation of this waste and reduces energy intensity of proper liquidation.

Work objective:

We need average values waste production of solid fabric (paper, special waste, biologically liquidated waste and type of building). These values serve for design temporary storage spaces and collectors equipments.

1.4 Electricity consumption

Consumption of electricity depends on occupancy and use of building. User behavior is in this case again the key factor, next key factor is using of control systems which are setup in building service (for example automatic switch of lighting during person absence in interior) or economic running equipment (PC, printers, copiers, …). This precaution has influence on total consumption of electricity. When lighting is switch off during user's absence or offices equipment is running in economic mode so total profile will be very different from the profile, when real occupation in the building wasn't taken into calculation.

The model should be made from independent part of each specific electricity use:

- lighting
- heating and cooling including additional equipment (circulatory pumps, humidification and cooling boxes
- ventilation
- computers and other office equipment
- domestic electrical appliances (television, stereo, cleaning equipment, cooking, fridge, freezer)

Work objective:

Created model should copy real energy consumption and should have included all control systems.

2. LOADS MODELING

2.1 Building occupation

Occupation has very significant effect on energy flows in buildings.

- Directly production, for example heat production of person (in usual situations one person products around 100 watt heat which can represent significant part of need for heating of very good insulated buildings).

Direct heat consumption depends on number of person in the building and their activity.

- Indirectly consumption of sources (water, electricity, energy) and production of waste linked with people behavior (for example: opening windows, using water on toilet, switching on electric equipment and lighting). It depends on number of person in the building and probably people behavior in the building.
- Indirectly consumption of sources for associate operation equipment of building (circulatory pumps, sanitation pumps, ventilators, air conditions units,…) and emergency equipments, for example lighting. This consumption depends mainly on time of running equipment.

Building or room occupation is independent parameter, user's profile of one need is usually independent on other variables (for example: energy consumption doesn't depend on waste water production). User's profile strongly depends on occupancy and time-current interval.

2.2 Models type of people behavior in the building

- fixed profile which depends on time: day, weekday, month (we are taking into consideration leave and arrival time, weekdays plan and holidays)
- stochastic models based on Markov chains, which are giving probably transition from one state to another, are processed on real dates in similar building type.
- empiric models based on obtaining information from real dates of occupancy in similar building.

2.3 Description principles of building loads:

Buildings loads which depended on human factor we call stochastic processes. Stochastic processes are such process where are physical laws supplying laws of probability which are showing for random time interval probability values. The processes are developing randomly from one to second state and future these states is possible to determine only on the basis probability. For description these states are using markov chains which are stochastic processes with final number of states where is time divided on individual time intervals. Markov chains are possible to use only when it discharge following condition: "Future development of process depends only on existent process state and no on its history.

2.4 How do we use Markov chains?

Mainly idea this method is building matrixes (Markov matrix) which expressive probability of process in time interval which is going from the one state to another state during next time step. Every element $P_{ij}(t)$ represent probability of change process from state i in time t to state j in the future time step t+1, which we call "change probability" state i to state j. Theory of Markov chain give information to us about probability behavior of process and calculation "static vector of probability". This vector gives probability apparition each state in long-time interval.

2.5 Model

It is necessary to have enough dates in acceptably period which will designate and probability of use. We have to determinate time step about which we interest and we have to be sure that it is possible to obtain data with time results. Because this method use union of discreet states, we need again to group parameters values to final number intervals where every interval is termed represent values (often it is maximum, minimum, or average value from the interval) We can use dates for derivation to transition probability as per cent of incident which we interest and total number of events. Now we have "catalogue" of transition probability from one state to other. Next it is possible use this information for simulation behavior of parameters by simple method which is calling reverse method.

3. CLIMATIC DATES, THEIR FORMATS AND USE IN THE SIMULATION COMPUTER PROGRAM

Except people behavior in the building, exterior climatic conditions influence energy and environmental building systems loads modeling. It influences consumption of energy for heating and cooling by these exterior conditions. Climatic conditions are simultaneously impulse for user which for example in summer, when it is hot, switches on air-conditioning or ventilator. I winter user can increase temperature on term regulator in required room or heating sources output. Public notice 152/2001Sb. establishes rules for heating and assessment consumption of energy. This notice fixes start (1. September) and end (31. May) of heating period. Heat supply starts in heating period, when average daily temperature of exterior air goes down below 13°C in two tandems following days and cannot expect increasing this temperature above 13°C for following day. Heat consumption is currently assessing by day-degrees method where we know number of days and average exterior temperature in heating period for every locality.

$$Q_{VYT,r} = \frac{24 Q_c \bullet \varepsilon \bullet D}{t_{is} - t_e} [Wh / rok] \qquad (1)$$

where:

$Q_{VYT,r}$ - yearly need of heat [Wh/rok]

Q_c - heat loss of building [W]

ε - correction factor

D - number of day-degrees [d.K]

t_{is} - average interior temperature [°C]

t_e - calculating exterior temperature (it is assigned according to locality). [°C]

$$D = (t_{is}-t_{es})\cdot d \tag{2}$$

where:

t_{es} - average exterior temperature in heating period [°C]

d - number of days in heating period [-].

A Day-degrees pattern shows that it is two-times influenced by climatic dates. Firstly, average exterior temperature and than number of days in heating period are influenced. Number of days in heating period is possible to determine returnly for each heating period.

Nowadays average daily exterior temperature is assessed as:

$$t_{ed} = \frac{t_7 + t_{14} + 2 \bullet t_{21}}{4} \tag{3}$$

Nowadays, when it is going to building-up development from thermal properties aspect of building, this assessment way is unsatisfactory. Using existing average exterior temperature by very good insulated building leads to deviation of calculated and real values. Today, it is setup in some meteorological stations automatic monitoring and writing climatic dates. By using existing thermal average, it is necessary to make a difference between average daily temperatures, average monthly temperatures and thermal average of individual years. The long-term average values show smaller fluctuations of temperatures. The daily average exterior temperature is assessed from measured values:

$$t_{ed} = \frac{\sum_{e=1}^{e=24} t_e}{24} \tag{4}$$

We can obtain average exterior temperature in heating period t_{es} from this assessment daily average exterior temperature

$$t_{es} = \frac{\sum_{d=1}^{d=n} t_{ed}}{d} \tag{5}$$

where *d* is number of days in heating period.

Using average daily exterior temperature is by using spreadsheet program possible and calculated value of energy consumption is most approached to real energy consumption. Use of average hourly temperatures is possibility of next improvement of energy consumption. The average hourly temperatures for heating period are used in simulating programs with using climatic databases due to big number of this values (for example: TMY, IWEC, WEA,…etc.)

4. TYPICAL METEOROLOGICAL YEAR

It is most significant format of climatic dates. It is a group of meteorological dates with values for typical year which is making from selection month of separate years (long-time measured during 30 or 50 years). Individual selections are linked to typical meteorological year format. Typical meteorological year has two format types: TMY and TMY2. In this formats are including hourly and monthly dates. Every file have to obtain head with title of measured station, WBAN number (this is identification number of station), town, state, time zone, latitude, longitude and camber. For get date it is necessary to know its position in the column, type of date and range their values. Measured dates are divided to groups. A-D is calibration measured dates, E-I is data which isn't directly measured, but it are generating by other inputs or are obtaining from prediction models. Further are data divided to groups (1-9) according to uncertainly of measured or generation where the group 1 has smallest % uncertainly.

Mainly dates of meteorological year:

- dry-bulb temperature
- dew point temperature
- relative humidity
- static pressure
- direct solar radiation
- diffusion solar radiation
- global solar radiation
- wind direction
- wind speed

- precipitation
- cloudiness

TMY and TMY2 has different time format and units hence isn't possible change it. Sometimes is directly and complex data hard to obtain or it is available in other format which we need. In this case we have to use for example Weather manager which can analysis and conversation to other dates formats. Among most supported dates formats is:

- TMY Climate Data (TMY)
- TMY2 Climate Data (TMY2)
- Energy plus weather files (EPW)
- Weather data file (WEA)

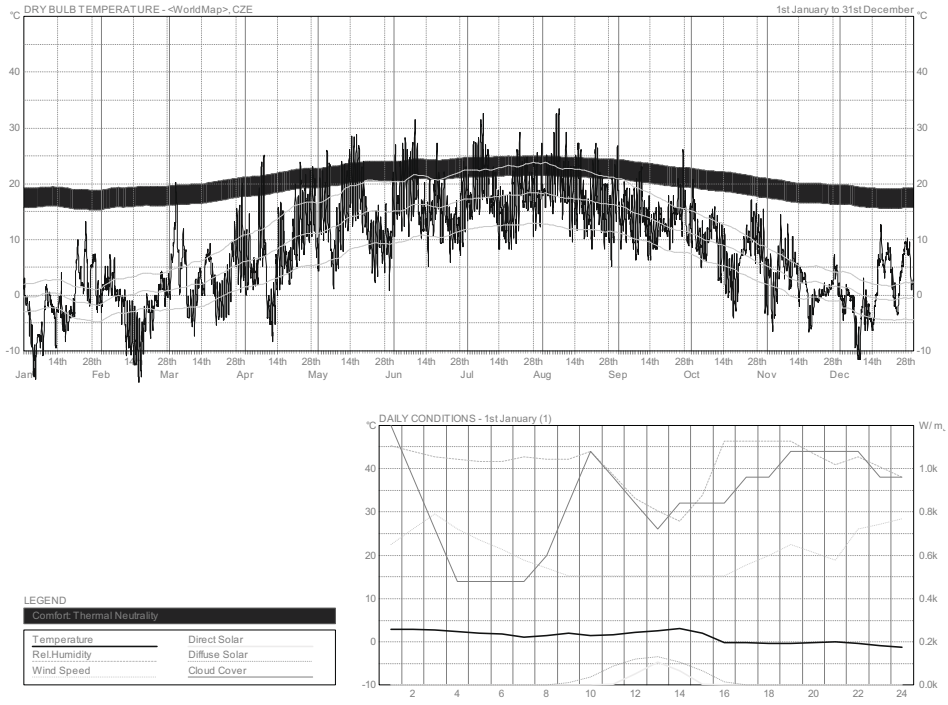

Figure 1 Example of graphic representation TMY which is generation from the Weather data manager.

5. CONCLUSION

Using input data in simulation calculations is one from dominates element which determines result quality and its application for practice. Building face, its structural solution or acquisition costs, aren’t only important by new projects realization. Nowadays, when continually grow energy costs and environmental importance increases, we are essentially more interested in real building service during its lifetime. It is important to consider building working state, already at projection documentation. Simulating programs are used for expectant building behavior. Every simulating program is as good as good are used input data. This paper shows overview of input data which are necessary to compile for characteristic building types.

Acknowledgements

This paper presented results supported by Research Plan CEZ MSM 6840770003.

References

1. SunTool Report - Apríl
2. Notice 151/2001sb.
3. User's Manual for TMY2
4. KABELE,K; MUSIL, R., Analysis Consumption of Water in Residential building, Czech Plumber, 2006, CTU in Prague , ISSN 1210-695X.
5. MUSIL, R, Climatic Dates for Simulation Internal Environment, Proceedings Indoor Clima of Building 2005 , Bratislava ISBN 80-89216-05-6.

"Computational Civil Engineering 2006", International Symposium
Iaşi, România, May 26, 2006

Utilization of the Statistical Method of Planned Experiment (PLANEX) for research of building materials properties

Radomir Sokolar

Department of Technology of Building Materials and Components, Faculty of Civil Engineering, Brno University of Technology, City, Veveri 331/95, 602 00 Brno, Czech Republic

Summary

The mathematical (statistical) Method of planned experiment (PLANEX) enable creation of mathematical models of choice for example building materials properties functionality (e.g. water absorption, strength) on selected independents of variables (for example value of firing temperature, quantity of cement) in selected intervals by force of statistically rated multinominals. All calculations are performed in MS Excel software. The paper describe particular example of PLANEX utilization in development of new ceramic bodies – ceramic tiles.

KEYWORDS: Method of planned experiment (PLANEX), properties of building materials.

1. INTRODUCTION

The aim of the experimental laboratory work was to examine the fine fly ash from black coal as a basic raw material for the production of ceramic tiles and thus determine the properties of fired fly ash body at firing temperature interval from 1100 till 1200 °C prepared according to the standard requirements and processing of dry pressed ceramic tiles (wall and floor) – group B according EN 14411.

Table 1 – Choice requisite properties of ceramic tiles (group B).

Properties		BIa	BIb	BIIa	BIIb	BIII
Water absorption [%]	average individually	≤ 0,5 Max. 0,6	0,5 - 3 Max. 3,3	3 - 6 Max. 6,5	6 - 10 Max. 11	> 10 Min. 9
Bending strength [MPa]	average individully	≥ 35 Min. 32	≥ 30 Min. 27	≥ 22 Min. 20	≥ 18 Min. 16	≥ 15[1)]

[1)] for body thickness over 7,5 mm

2. EXPERIMENTS

The Method of planned experiment (PLANEX) was used, which enables the creation of mathematical models of choice fly ash body properties functionality

(e.g. water absorption, bending strength) on selected independents of variables in selected intervals by force of statistically rated multinominals (table 2).

Table 2 – Selected intervals of independent variables in terms of PLANEX

Variables		middle (0)	interval of change	High mark (+)	Low mark (-)
X_1	Pressing pressure [MPa]	35	10	45	25
X_2	Firing temperature [°C]	1150	50	1200	1100
X_3	Soaking time [min]	20	10	30	10

PLANEX imposed composition of test mixtures 1 – 17 (table 3). In the table 3 there are showed determine properties of prepared test mixtures 1 -17 – firing shrinkage, bending strength, water absorption and bulk density. Software PLANEX computed mathematical models as polynomial functionality.

Table 3 – Test specimens and their properties by PLANEX

Type and number of mixture					**Firing shrinkage (FS)**	**Bending strength (R)**	**Water absorption (E)**	**Bulk density (B)**
No.	**Mixture type**	**X_1**	**X_2**	**X_3**	**[%]**	**[MPa]**	**[%]**	**[kg.m^{-3}]**
1	+++	45	1200	30	11,8	35,0	0,5	2135
2	++-	45	1200	10	11,1	32,2	2,0	2150
3	+-+	45	1100	30	4,7	13,6	19,5	1690
4	+--	45	1100	10	4,0	12,3	19,7	1685
5	-++	25	1200	30	13,3	33,1	0,5	2150
6	-+-	25	1200	10	10,6	31,5	1,0	2185
7	--+	25	1100	30	4,3	13,1	20,9	1660
8	---	25	1100	10	3,5	12,3	21,1	1650
9	+00	45	1150	20	7,0	23,1	15,4	1820
10	0+0	35	1200	20	12,4	38,4	0,7	2165
11	00+	35	1150	30	6,6	17,9	14,1	1810
12	-00	25	1150	20	7,0	17,1	17,0	1760
13	0-0	35	1100	20	3,5	14,3	18,9	1675
14	00-	35	1150	10	4,8	22,5	16,9	1765
15	000	35	1150	20	5,7	20,1	16,5	1790
16	000	35	1150	20	5,6	20,0	15,7	1815
17	000	35	1150	20	5,5	20,2	16,5	1795

2.1. Firing shrinkage

$$FS = 837{,}27946 + 0{,}014992x_1 - 1{,}522375x_2 - 0{,}211326x_3 + \\ + 0{,}007964x_1^2 + 0{,}000699x_2^2 - 0{,}005036x_3^2 - 0{,}00045x_1x_2 + 0{,}0005x_2x_3 [\%] \quad (2)$$

Firing shrinkage of fly ash bodies is increased with increasing the firing temperature first of all (it is exposure to the sintering process). Firing shrinkage is not influenced very much by the pressing pressure. Also less expressive is the influence of final temperature soaking time duration (figure 1). Drying shrinkage reaches minimal values, and that explains why general shrinkage of firing fly ash ceramic body consists only of firing shrinkage.

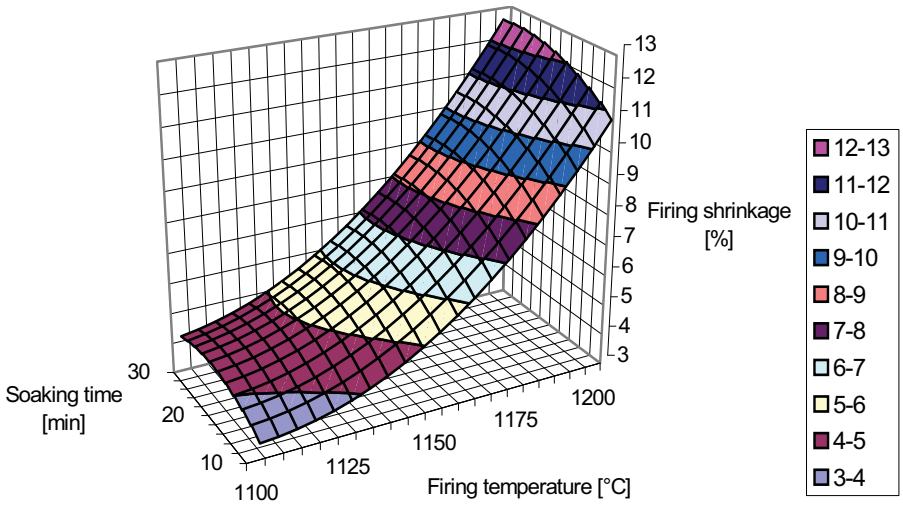

Figure 1. Firing shrinkage – constant pressing pressure 35 MPa.

2.2. Water absorption

$$E = -2838{,}588989 - 1{,}629193\ x_1 + 5{,}207783\ x_2 - 0{,}0511\ x_3 \\ + 0{,}007467\ x_1^2 - 0{,}002361\ x_2^2 + 0{,}000928\ x_1x_2 [\%] \quad (3)$$

Water absorption (according to EN ISO 10545-3 by boiling method) also depends on sintering level of body, and thus corresponds to the shrinkage of fired fly ash body. Here again features height firing temperature, smaller influence on water absorption has the duration of final temperature holding time, however the influence of the pressing pressure is unconvincing. Fly ash bodies, without any admixtures (only water), fired at a temperature of 1200 °C with a soaking time of 30 minutes run to water absorption in wheel diameter 0,5 % (abstractedly from

pressing pressure), which is the limited value for so-called highly sintered tiles of type Gres Porcellanato (group BIa). Division qualities of fly ash body is stated in the table according to EN 14411 dependent on temperature slops and duration of soaking time in figure 2. It is evident that intensive sintering happens only after an overrun of firing temperature 1150 °C.

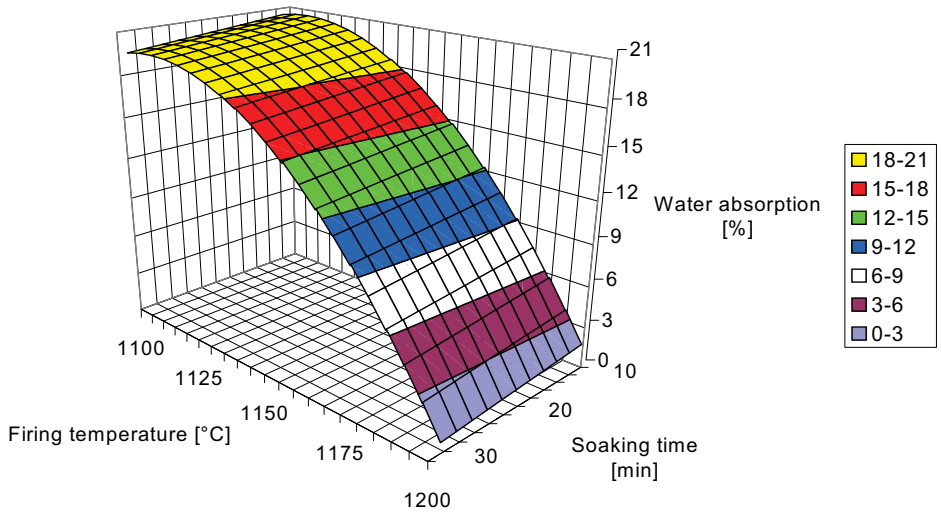

Figure 2. Water absorption - constant pressing pressure 35 MPa

2.3. Bending strength

$$R = 2343{,}18044 + 0{,}441102\,x_1 - 4{,}261184\,x_2 - 0{,}187281\,x_3 + 0{,}014234\,x_1^2 + 0{,}001931\,x_2^2 - 0{,}013234\,x_3^2 + 0{,}000525\,x_1x_2 + 0{,}002125\,x_1x_3 + 0{,}000575\,x_2x_3 \left[MPa\right] \quad (4)$$

Bending strength (according CSN EN ISO 10545-4) generally corresponds to the water absorption of firing body. It is important the fact that the bending strength corresponds to the standard requirements for qualitative groups of ceramic tiles body according to table 1. Mild bending strength decreases in firing bodies, which have been pressed at a pressure of 45 MPa and firing at a maximal firing temperature (1200 °C) with the longest soaking time (30 min.) is necessary adjudicate for the rising of secondary closed porosity in body.

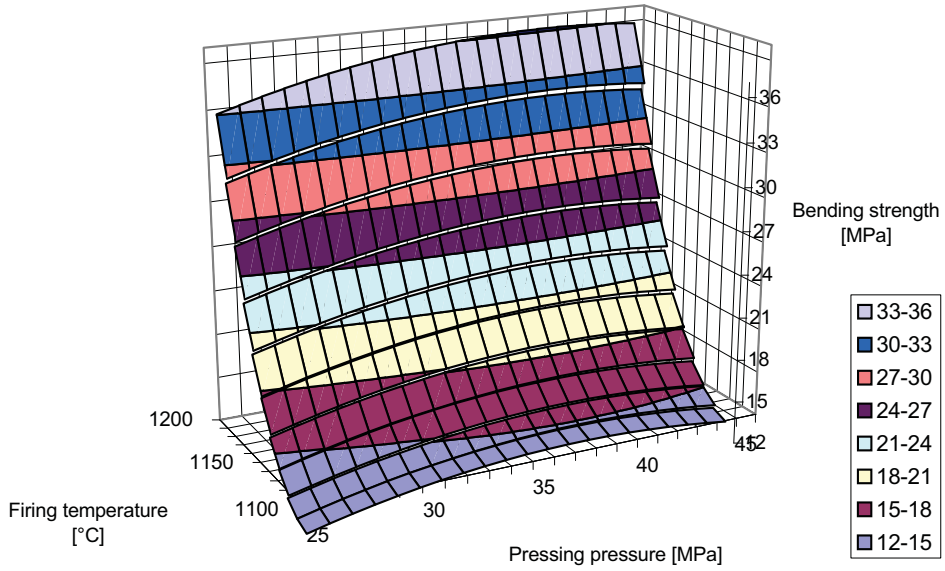

Figure 3. Bending strength – constant soaking time 30 min.

2.4. Bulk Density

$$B = 59595{,}1845 + 33{,}8125\,x_1 - 106{,}75347\,x_2 + 18{,}6875\,x_3 + 0{,}049106\,x_2^2 - 0{,}02875\,x_1x_2 - 0{,}01625\,x_2x_3\left[kg.m^{-3}\right] \quad (1)$$

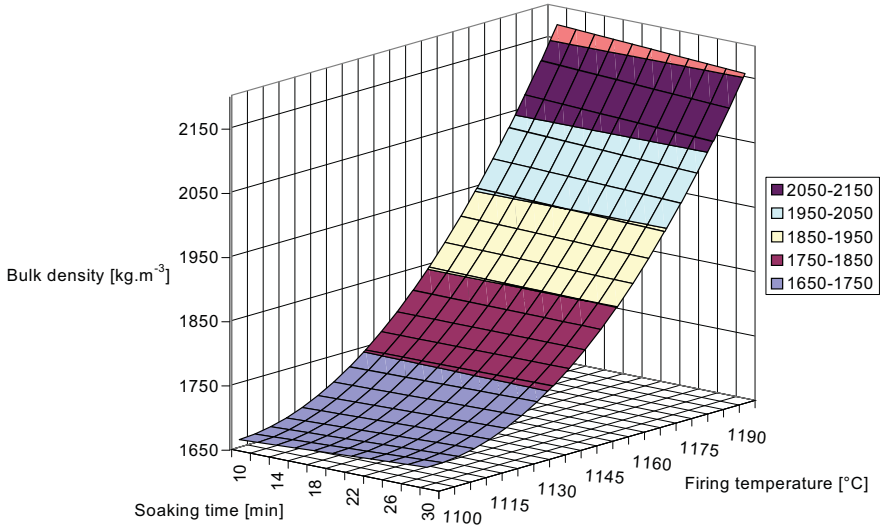

Figure 4. Bulk density – constant pressing pressure 35 MPa

3. CONCLUSIONS

The paper showed a case study of Method of planned experiment (PLANEX), which enables to determine the regularity of the different variables influence (in this case for instance the value of pressing pressure, firing temperature etc.) on selected properties of the ceramic body (water absorption, strength etc.) with utilization of the planned experiment method and in view of the optimization of demanded properties of the ceramic body by evaluation of results with methods of mathematical statistics.

Under the term mathematical description of process properties (in this case the properties of the ceramic body) we understand the system of polynomial equations connecting the dependent variable with acting (affecting) variables. The dependent variables we call in the theory of experiment planning the variables characterizing the properties or the process. The acting variables in the examined process can express in arranged units the quality (type of opening material, fluxing agent etc.) or the quantity (mass of the individual admixture).

Acknowlegements

This Research project was financed with MSM 0021630511 „Progressive Building Materials with Utilization of Secondary Raw Materials and their Impact on Structures Durability"

References

1. PYTLÍK, P., SOKOLÁŘ, R.: Building ceramics: Technology, properties and utilization. CERM Brno 2002, ISBN 80-7204-234-3 (in Czech).

"Computational Civil Engineering 2006", International Symposium
Iaşi, România, May 26, 2006

Soil improvement in the design of the foundation rehabilitation

Irina Lungu[1)], Nicolae Boți[2)]

[1] *Department of Roads, Railways, Bridges and Foundations, Technical University "Gh. Asachi", Iaşi, 700050, Romania*
[2] *Department of Roads, Railways, Bridges and Foundations, Technical University "Gh. Asachi", Iaşi, 700050, Romania*

Summary

Rehabilitation of the building infrastructures has various particularities and solutions depending on both the type of structure and the degradation assessment, and the foundation soil.

The alterations induced into the foundation soil due to various causes and the time dependency underground water evolution can be responsible of the decrease of both bearing capacity and compressibility.

Soil improvement techniques are focused onto the increase of the soil mechanical properties to face rehabilitation of the damaged foundation systems.

The paper presents evaluations of the foundation consolidation solutions interacting with the soil improvement related to the active zone.

KEYWORDS: rehabilitation, foundations, soil improvement, bearing capacity, degradation assessment.

1. INTRODUCTION

Damages of building infrastructure are usually perceived at a later stage than their occurrence, when being propagated and consequently reflected into structural degradations. Intervention works are established after a careful assessment of the degradation state of the foundation and a geotechnical report related to active zone within the subsoil.

Typical degradations of foundations for old buildings are considered to be the followings [1]:

- erosion of the foundation made of stones - the strength and durability of rocks are determined by the amount and distribution of the soft mineral included in the mineralogical composition and when this is destroyed and removed by mechanical alteration and dissolution, the hard mineral groups remain with almost no connections among them; this degradation process, which is present in the

natural stone foundations, is accelerated by the succession of the freezing – thawing phenomena and by the presence of salts in the gravitational water.

- partial crumbling of foundations made of brickworks - brick is the most porous foundation material and consequently moisture leads to damages due to the frost-thaw successions, which materialize in exfoliation or splitting of the surface parallel to the external side with no waterproofing; large continuous cracks can completely destroy the bricks.

- rot of wood foundations - raft and pile foundations are frequently subjected to attack by fungus rot when the water table sinks below the top of the foundations. Wood infrastructures damaged by fungus rot are the most vulnerable to the wood-boring insect attacks that destroy the wooden mass, accelerating the decrease in their strength and durability.

- moisture damage on stone and brick infrastructures where lime and clay as mortar - brick walls where lime and clay are used as a mortar often absorb moisture. In this situation problems show, after a while only to walls that have been covered, especially with cement mortar, disturbing the moisture balance in the wall, and blocking the air escape. Moisture can thus penetrate further up into the wall before it finds a zone where the fluid exchanges with the exterior are no longer blocked. These situations are recorded on old buildings because the original ground level increases by: modernization of the urban planning in the built area, asphalt works, arrangement of the ground for a fast exhaustion of the run off waters near the building etc.

- fissures, cracks, fractures into the foundation elements due to uneven settlements developed within the soil underneath. Situations responsible for such degradations are created by artificial lowering of the water table, or on the contrary, in some cases by the level increase of the underground water, deep excavation works closely located to the building and inadequately supported by bracings, irregular soil profile unknown by a routine geotechnical investigation at an earlier stage.

Consolidation works are either restricted to the foundation system or include also interventions within the soil into the active zone of foundations.

2. THE UNDERPINNING EFFECT OVER THE BEARING CAPACITY OF THE FOUNDATION SOIL

When deciding over the most cost effective solution in consolidating the damaged infrastructure one has to consider that the bearing capacity and settlement of the foundation soil is influenced by both foundation dimensions and soil characteristics.

The plastic pressure (p_{pl}) is considered the reference pressure in the deformation limit state accompanying the settlement prediction in the process of dimensioning shallow foundations. When regarding the definition of the plastic pressure, the development of the plastic zones ($\tau = \tau_f$) is set to a depth depending on the foundation width (figure 1).

The relevant factors dictating the final value of the plastic pressure applied not only for the initial design stage but also for the consolidation solutions as underpinning are included in the design codes as (1):

$$p_{pl} = m_l\left(\gamma \cdot B \cdot N_1 + q \cdot N_2 + c \cdot N_3\right) \quad (1)$$

where : m_l – is the working coefficient; γ – weighted mean value of the unit weight of the soil within a B/4 depth from the footing; B – the footing width; q – geological pressure at the foundation depth; c – the design value of the soil cohesion underneath the footing; N_1 , N_2 , N_3 – dimensionless coefficients, depending on the design value of the internal friction angle of the soil underneath the footing.

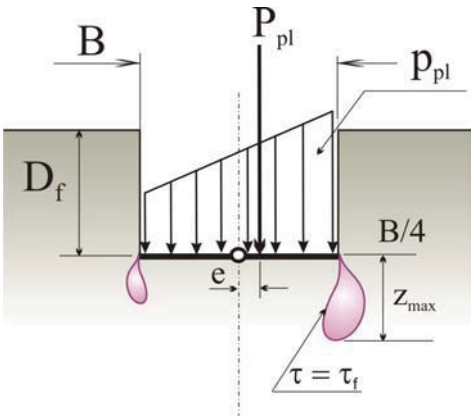

Figure 1. The development of the plastic zones within the foundation soil

The alteration of the foundation dimensions by underpinning increases the overall value of the plastic pressure and consequently complies with the load increase transmitted to the foundation by the covering techniques applied to the structural elements.

Figure 2 presents the direct effects of the dimensions increase for the plastic pressure value in case of underpinning. One-side covering does not increase the plastic pressure (figure 2a) and is recommended in case of continuous footings where the mechanical alteration (erosion or dissolution of the mortar) is propagated from the outside and consequently the intervention is restricted to the outer face of the foundation. Figure 2b refers to situations where the continuous footings are damaged over the entire width and the covering is consistent on both sides. In this

case one may consider a significant increase of the plastic pressure that supports the possibility of introducing additional floors in the structure.

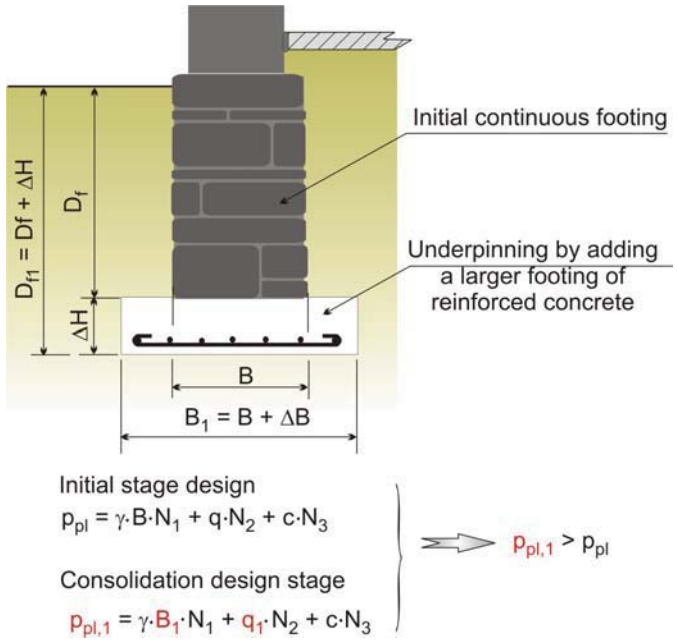

Figure 2. Increase of the soil plastic pressure with the underpinning

Figure 2c reflects less a consolidation of the foundation but mainly a significant increase of the foundation width in order to decrease the pressure delivered by the shear walls and at the same to increase the plastic pressure. Such situations complies with a load increase within the structure in consequence of introducing additional floors, changes of the building destination and consequently an increase of the service load, or by severe consolidation techniques within the structure.

3. JET GROUTING IN INFRASTRUCTURE REHABILITATION

The jet grouting applied to the foundation soil simultaneously with the building rehabilitation involves the following aspects [2]: an increase of the soil bearing capacity and compressibility, and a potential increase of the impermeability of the ground.

The ground injection is performed by introducing a substance that bonds the particles and fills in the voids with a gel that strengthens in time, obtaining an increase of the resistance and the impermeability. This procedure is applied to: soils with reduced cohesion, cohesionless soils, soils with high permeability – with large voids or cracks.

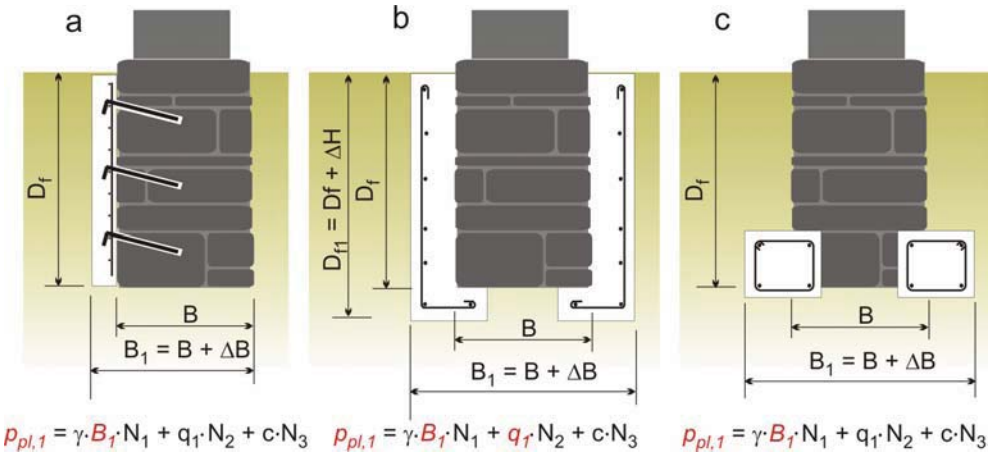

Figure 3. Consolidation procedures of continuous footings: a. one side covering, b. two sides covering, c. introducing of adjacent foundations

Introducing the solutions into the soil is performed with injectors and to ensure a uniform solution penetration, the injectors are successively pushed.

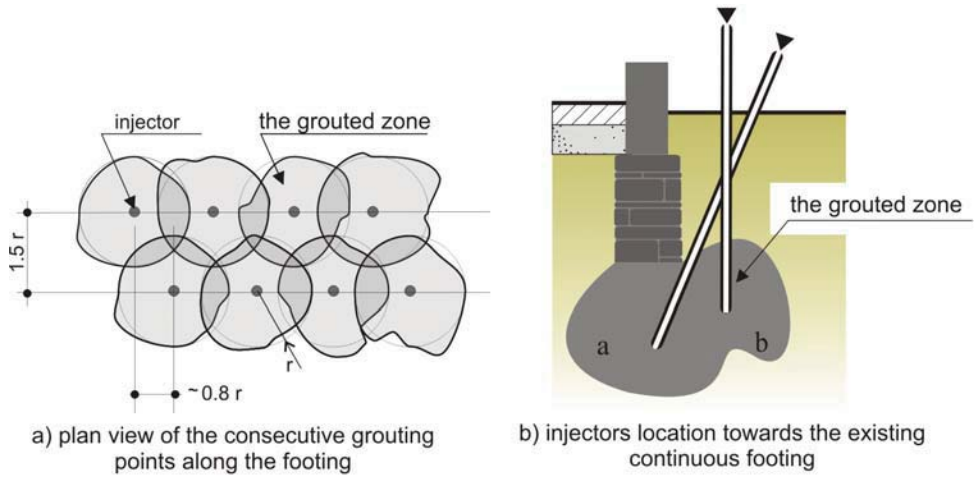

Figure 4. Typical view of a jet grouting technique

Many cases of jet grouting are working effectively in improving soil characteristics for loess and loessy soils. Constant increase of the underground water table in

subsoil consisting in 8-12m thickness of sandy and silty loess had a strong effect on the increase of the differential settlements at the footing level due to the supplementary settlement induced by the soil saturation.

Only intervention works at the continuous footings do not prevent future degradation as long as the foundation soil is still sensitive to moistening.

Silication and jet grouting are convenient techniques to induce the soil improvement by filling the voids within the soil structure with materials that not only strengthen in time but increase the inner bonds among the soil particles reflected into a higher cohesion.

The cementation effect changes the cohesion from being only electro-molecular (c_w) type into being mainly cementation type (c_c). This effect reflects also into an increase of the internal friction angle. The overall effect is a significant higher value of the resulted plastic pressure and a reduction of the sensitivity to moistening (figure 4).

Research over the soil improvement results during electrosilication of loess and loessy soils reported a 6 times increase in terms of cohesion and 3 times increase of the plastic pressure [3].

4. CONCLUSIONS

Infrastructure rehabilitation is a costly intervention and with technological difficulties in comparison to structural intervention works. Most of the situations include both foundation consolidation and soil improvement works. Historical monuments are constructions with the highest restrictions during rehabilitation, related to safety during a very long term service. Changes in the building rigidity by various consolidation techniques should be always accompanied by an increase of the foundation rigidity within the limits of the soil plastic pressure and allowable average and differential settlement.

References

1. Budescu, M., et all *Building Rehabilitation*, Matei-Teiu Botez Academic Society Publishing House, Iaşi, România, 2003
2. Van Impe, W.F., *Soil Improvement*, Ed. A.A. Balkema, Rotterdam, The Netherlands, 1995
3. Răileanu, P., Muşat, V., Lungu, I., *Foundation Soil Improvement by electrosilication*, Proceedings of the 10th Danube-European Conference on Soil Mechanics and Foundation Engineering, Mamaia, România, 1996

"Computational Civil Engineering 2006", International Symposium
Iaşi, România, May 26, 2006

Evaluation of the geotechnical risk in the hilly zones within the city of Iaşi

Nicolae Boţi[1)], Irina Lungu[1)], Ioan Boţi[2)]

[1] *Department of Roads, Railways, Bridges and Foundations, Technical University "Gh. Asachi", Iaşi, 700050, Romania*
[2] *Department of Geotechnics and Foundations, Technical University of Civil Engineering, Bucureşti, 020396, Romania*

Summary

The geotechnical investigation works performed for the design of new constructions on urban slopes, the identification of the layer successions, types, and both physical and mechanical characteristics restricted into the foundation soil within the influence zone of the constructions can be included in a safety evaluation against landsliding.

The paper presents the geotechnical risk evaluation for the construction site located in the Fagului Street for a building assemble, 4 units with variable height: semi-basement, groundfloor, and 3/4/5 (partial) storeys.

The ground conditions locate the investigated site in group C – difficult foundation soils: natural slopes with landslide potential and the recommended foundation solutions are deep foundation systems.

KEYWORDS: geotechnical risk evaluation, urban slopes, landsliding, safety evaluation, building assemble.

1. INTRODUCTION

The geotechnical investigation made for the design stage, completed with a geotechnical report, is compulsory for any building that is performed based on a specific project, in compliance with the provisions of art.38 line 2 of the Romanian law 10/1995 regarding the quality of construction works and art.6 line 2 of the Romanian law 50/1991 regarding building licensing, with the prior amendments and completions made by the law 453/2001.

The construction site of interest is located in Iasi, on Fagului street, in Copou district, with the following neighbors: a military unit to the East, state land, Iasi City Police, Landslide Consolidation Site, to the North-East, and Fagului street to the South.

1.1 Survey purpose and volume

The geotechnical survey of the foundation soil aims to obtain the geotechnical data, the geological, hydrological, seismic elements, and the precedents of the construction site, for the description of the major characteristics of the ground and involves the followings:

- identification of the succession, type, condition and the physical and mechanical characteristics of the soil layers included into the influence area of the building or where hazards may occur (active area);
- processing and presentation of the laboratory and in situ test results;
- bearing capacity of the foundation soil;
- prediction on the potential time effects of the underground water on the foundation soil, foundation system, and implicitly on the new buildings;
- actions to proceed in providing land/natural slope stability.

The investigated site belongs to the C group of soil conditions – difficult soils: slopes with sliding potential.

In order to provide the detailed investigations onto the construction site three boreholes (F1, F2 and F3), at 25m depth and of 10,75" diameter, and three in situ tests – Standard Penetration Tests (SPT) were performed.

1.2 Building characteristics

The site investigation is related to the geotechnical conditions of strength and stability for a building assemble, 4 units with variable height: semi-basement, groundfloor, and 3/4/5 (partial) storeys.

The unit structure is made of either shear walls of brick masonry or of cast-in-place reinforced concrete frames. The foundation system is potentially a deep foundation – large diameter bored piles, Benetto type, of 1080 mm, embedded into the marly clay.

According to the Romanian Norm P100-1/2004, these buildings are included into the 3rd importance class – building of normal importance.

In respect to the settlement restrictions, these buildings are not sensitive to settlements (Romanian Standard 3300/2-85) and the maximum allowable values are 8cm for the brick masonry structure and 15cm for the reinforced concrete frames.

During service, these buildings have no operational restrictions – moist, chemical, thermal or dynamic processes that might influence the foundation soil.

2. SITE CONDITIONS

2.1 Geological and hydrological conditions

From a geological perspective, the investigated area belongs to the Moldavian Floor, characterized by the occurrence in the adjacent areas under the Quaternary strata of the Neocen deposits (Bassarabian) [1].

The area of the site is characterized by the presence of Sarmatian and Quaternary strata. The Sarmatian is the bedrock of the region, represented by the violet-blue, grey marly clay at 15m depth from the ground surface.

The Quaternary is presented in the recent deposits covering the bedrock as:

- top soil and unconsolidated recent fillings of 7 m thickness,
- silty clay, with intercalation of clay and clayey silt.

The underground water within the investigated area is distributed in an extremely uneven way, both on the horizontal and on the vertical, with wide oscillations in between 0 to 2,50m. The current underground water table is -1,50m deep from the ground surface and dewatering works are expected with no risk of degradation of the neighboring buildings.

2.2 Previous geotechnical conditions on the site

The geological profiles of the Copou hill favors the occurrence of the landsliding mechanisms that display the character of detrusive slides in the upper part, where by the moisture increase of the lower part of the loess layer, slices of terrace material fail creating some sliding surfaces.

These landslides affect the underground water system that once again increase the moisture content at the base of the terrace till saturation and thus creating conditions for stability loss falling into the category of delapsive slides [2]. The alteration of these phenomena induces a general movement of the entire material of the slope and new local failures/slides on top of the hill.

The landslide classification according to the maximum depth of the sliding surface is conventional and the investigated site includes a slide type – deep, with the depth of the sliding surface in between 5 to 20m from the ground surface.

Earlier investigations required drainage works that have been performed by the city hall authority and are currently working only partially and that are connected to the city sewage system of Fagului street.

2.3 Current geotechnical condition on the site

The site was visually investigated on the area in between Dr.Vicol street and Fagului street and photos have been taken to display the current state in the open of the ground surface.

In the upper part, immediately below the sports field level, the phenomenon of "drunkard forest" is conclusive to former ground movements – photo 1 and propagated downhill – photo 2.

Photo 1. Landsliding phenomena at the upper side of the sport field

Photo 2. The "drunkard" forest effect downhill the sport field

Another significant visual fact is the water bogging that counts for the alteration of the impervious soil layers location into the geological profile of the site due to soil mass movements – photo 3. Furthermore, there is a large diameter plastic pipework that instead of draining the water away from the site, discharges water in the area – photo 4.

Photo 3. The water bogging along the slope due to the soil mass movement

Photo 4. Malfunctioning of the drainage pipeworks due to the mass movement

3. GEOTECHNICAL TESTS

Within the limits of the site, 3 boreholes and 3 Standard Penetration Tests (SPTs) were performed. Two of the boreholes begin with recent construction waste deposits of variable thicknesses 0.60-1.70m followed by silty clays and clays, plastic hard to stiff and the third borehole display a top soil layer first of 0.60m thickness and then the layers formerly presented.

The SPTs displayed the existence of a layer with compressibility characteristics lower in the upper half of the layer of silty clay and especially the existence of a potential deep plan of lansliding located at the interface of the brownish clay with the violet-blue one [3].

The laboratory investigation consisted in soil tests to provide both physical and mechanical characteristics. Oedometer tests were performed in agreement with the nature of the analyzed soil types, to emphasize their behaviour related to water variation. Soils displayed a high compressibility ($M_{200\text{-}300}$ = 7000 – 12000 kPa) and the clayey layers exhibit no significant swelling pressure during saturation. Shear strength parameters were calculated based on UU triaxial test, and consequently the internal friction angle displayed small values as long as cohesion registered values of tens of kPa.

4. SLOPE STABILITY ANALYSIS

Risk analysis against landsliding was performed on a design soil profile based on the following structure – table 1:

Table 1. The soil characteristics for the slope stability analysis

Layers	Soil nature	Unit weight	Internal friction angle	Cohesion
Layer 1	Yellowish silty clay	20 kN/m^3	18^0	10 kPa
Layer 2	Brownish clay, stiff, with greyish inclusions	10 kN/m^3	14^0	20 kPa
Layer 3	Violet-blue clay, plastic hard, with brownish inclusions	20 kN/m^3	3^0	34 kPa
Layer 4	Violet-blue clay	20 kN/m^3	17^0	27 kPa

A safety factor was calculated for the design soil profile by running a computer programme for each of the situations:

- case 1 – a slope stability analysis prior to the building assemble construction, that resulted in a minimum safety factor Fs = 2.7 – figure 1;
- case 2 – a slope stability analysis of the investigated site during an earthquake, but prior to the building assemble construction, resulting with a minimum safety factor Fs = 0,9 – figure 2;

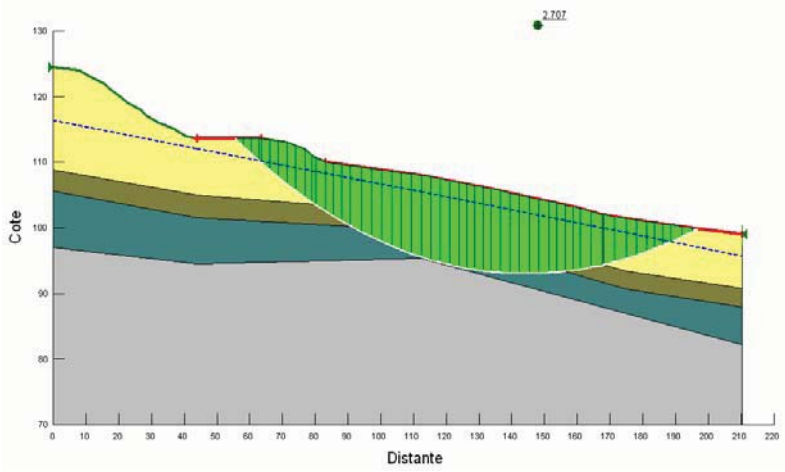

Figure 1. The potential sliding mass and safety factor according to case 1

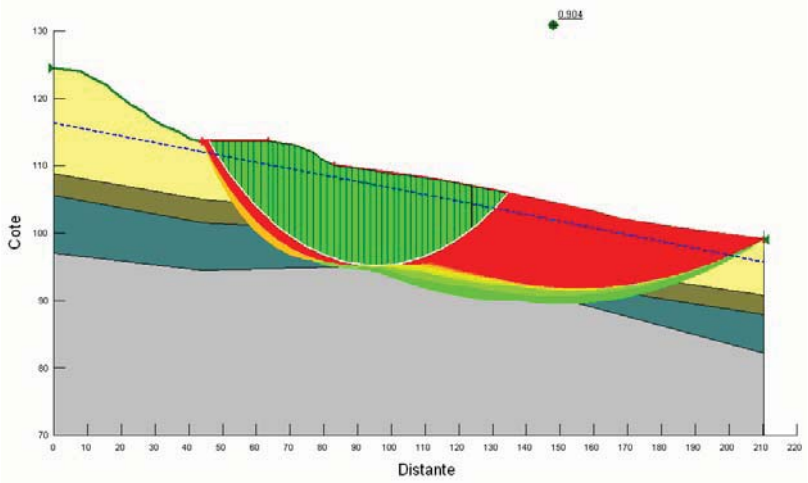

Figure 2. The potential sliding mass and safety factor according to case 2

- case 3 – a slope stability analysis with the building assemble on the designated location that resulted in a minimum safety factor Fs = 1,1 – figure 3;

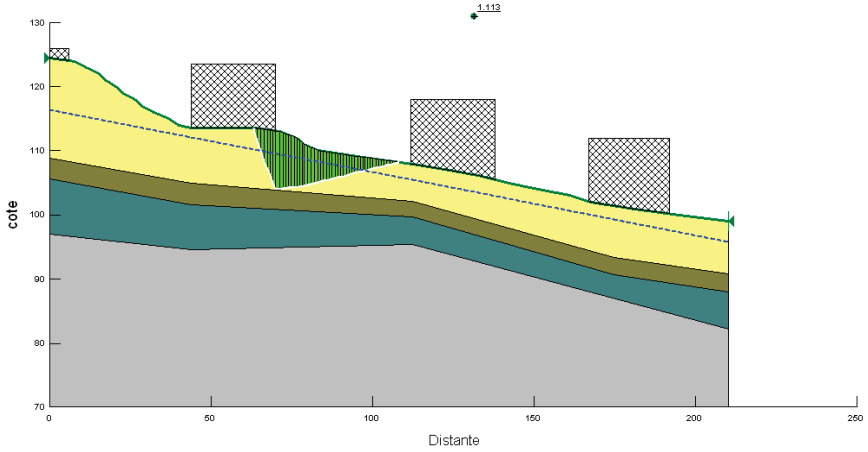

Figure 3. The potential sliding mass and safety factor according to case 3

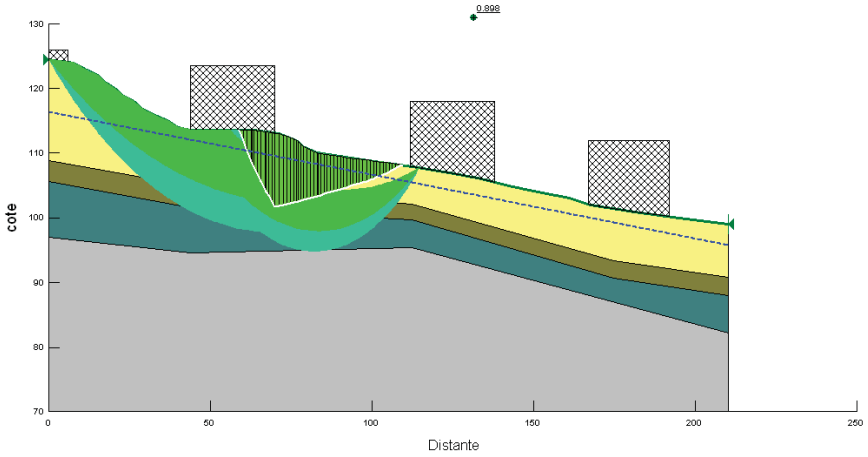

Figure 4. The potential sliding mass and safety factor according to case 4

- case 4 – a slope stability analysis considering the building assemble on the designated location, during an earthquake, that concluded in a minimum safety factor Fs = 0,898 – figure 4.

Based on the results and corresponding drawings, the concluding remarks related to the slope stability of the investigated site were the followings:

- the current slope has the local stability provided to the limit given the current circumstances;
- the potential sliding surface may start in an upper zone (Dr.Vicol street) and affect the investigated site (there are already some cracks into the pavement structure and the waste storage in the upper part of the slope enhances the sliding);
- an earthquake of 0.20 the corner period is definitely affecting the entire area;
- in case the building assemble is performed, the entire slope becomes unstable even without the earthquake effect;
- the potential sliding surfaces are at approximatively 10m depth (by means of the SPT results).

5. FOUNDATIONS OF THE BUILDING ASSEMBLE

The general stability of the entire soil mass was not the object on the investigated site and the local stability has a local stability provided to the limit prior to any construction in the area.

Considering the geological and the geotechnical profile of the site, the results of the basic classification regarding the physical and mechanical geotechnical indices within the boreholes records, and the slope analysis performed according to the cases presented above, the foundation system appropriate for each unit of the building assemble is considered a pile foundation involving large diameter bored piles – Benotto technology, embedded into the marly clay, of 25-35m long and 1080 mm diameter.

6. CONCLUSIONS

The complexity of the site conditions, difficult circumstances as the underground water table located close to the surface, the alteration of the stress state within the soil mass as a result of simultaneous action from both natural and human factors are in most cases responsible for activating prior landslide zones.

A detailed geotechnical investigation provided by both in situ and laboratory soil tests is the only one able to provide the necessary input data to run computer programs for a sound slope stability analysis of major factors involved and consequently decide over the appropriate foundation system of the construction, reflected on its safety during service, the building up and protection of the environment.

References

1. Boți, N., Stanciu, A., Lungu, I., Boți, I., Pleşu, Gh. *Consideraţii privind consolidarea zidului de sprijin – Râpa Galbenă – Iaşi*, Proceedings of the IXth Edition of the National Symposium Efficient Infrastructures for Land Transportation, Timişoara, România, 2005
2. Lungu, I., Stanciu, A., Boți, N. *Probleme Speciale de Geotehnică şi Fundaţii*, Junimea, Iaşi, România, 2002
3. Boți, I., *Field investigation results as an important way to railway rational design*, Proceedings of the IIIrd iYGEC International Young Geotechnical Engineers Conference, Osaka, Japan, 2005

"Computational Civil Engineering 2006", International Symposium
Iaşi, România, May 26, 2006

Present trends and potentialities in designing of log-houses external walls

Hana Brandejsová, Miloslav Novotný

Department of Building Structures, Brno University of Technology, Brno, 662 37, Czech Republic

Summary

The paper deals with designing of log-houses external walls with the viewpoint of thermal material characteristics. Timber is the natural material with the specific properties such as volumetric changes caused by drying-out. That fact has to be taken in account already during the design period. Window, door and stairs claim the correct and elaborated details of horizontal log joints.

One of the chapters refers to the incorrect solved details of log house.

In the contemporary building classification, according to LCA (Life Cycle Assessment), the log houses are ranked in very high position. Energy intensity of the construction life is calculated since the building material production, through the service till the demolition and removal.

The report deals with present trends in designing of the external walls of log houses.

KEYWORDS: Log houses, external walls, thermal material properties, volumetric changes, round timbers

1. INTRODUCTION

Recently, building of the classic log-houses becomes to be famous. This type of construction is typical especially for Scandinavia and Canada, where roughly 85 % of buildings are built from wood or wooden basis materials. In former times, the wooden houses were fully occurring in the area of Czech Republic but later on, wood had been jostled away by new materials, e. g. steel, concrete, glass. Within the years of wood declining, the original traditions and continuity of for centuries forwarding information had been broken and so we can say, building of long-houses is quite new in our regions nowadays.

That is why the research and progress in designing of problematic details and edification of log-house producers and lay public is so important. Many failures that can occur within the log-house service period are caused by specific wooden characteristics neglected when the structure have been constructing.

Timber is as a natural material sensitive to biotic and abiotic damages. These disadvantages are overcharged by relative source availability of sustainable material source, workability, by pleasant feature, and last but not least, by easy way how to dispose.

Lately, there are all over the world increasing demands for usage of environmental friendly and permanent available materials. Just timber is a material that satisfies these requirements.

2. EXAMPLES OF INCORRECT DETAILS

Figure 1. Left –Incorrect construction and insulation of gable; Right –Incorrect placing of vertical element (an adjusting screw is missing)

Figure 2. Incorrect corner structure (roughly encircled shapes)

3. DESIGNING OF THE LATERAL GROOVES

3.1 Termal-technical requirements

Recently, still increasing values of thermally technical construction requirements are heavily discussed among the construction specialist. Light framework constructions can be easily insulated by required thickness of insulator. The log-houses have different behavior – timber has a specific ability to accept and eliminate the moisture content in dependence with interior air relative humidity. Against that, totally insulated and closed buildings require to be furnished by forced ventilation system that ensures regular interior air changing and clear the interior air to anticipate the condensation and mould rises at the sensitive places.

Log walls are built up from logs of diameter 350 – 400 mm to meet standard ČSN 730540. The thermal resistance of wall is defined by the log diameter and tree species. However, the lateral grooves are staying the problematic details.

3.2 Insulation material

The lateral joint of two logs has to be designed in such a way to ensure as tight and stable barrier between interior and exterior as possible. The material used for jointing of lateral grooves has to guarantee to thermal-technical properties from the point of view of both thermal resistant and air infiltration. At once, the material has to show shape recovery that means it has to be able to follow the working of wood (swelling and shrinkage). Each log that is inbuilt with moisture content higher than 19 % has to be provided by longitudinal kerf. These kerfs cut on the top of logs show an effective way to control the location of checks as green logs dry. The depth of the kerf shall be at least one-quarter of the log diameter, and shall be no deeper than one half of the diameter.

Primarily, PUR foam was using for sealing of the grooves and notches. This material is shape stable when hardening that means it cannot respond to the woodworking, consequently cracks appear and need to be repair time to time. That is why this material is no more used. Today, two-level insulating is common used; it can be seen on the picture nr.1 - left. The mineral wool is embedded into the continuous lateral groove and protected by joint sealing tapes from both sides. The tapes are made from permanent elastic material on the base of modified rubber foam, which is impregnated to resist UV radiation and eliminate an absorbing power. Such a gasket shall also restrict the water, air and insect infiltration.

Recently, usage of fleece instead of mineral wool is considering in Czech Republic. This natural material has to be necessarily proofed in insect resistance. The subject of further research is a fleece availability and effectiveness within the gaskets problematic.

For comparison, the incorrect type of groove is shown on the picture nr. 1- right, there is neither notch nor insulation in the groove.

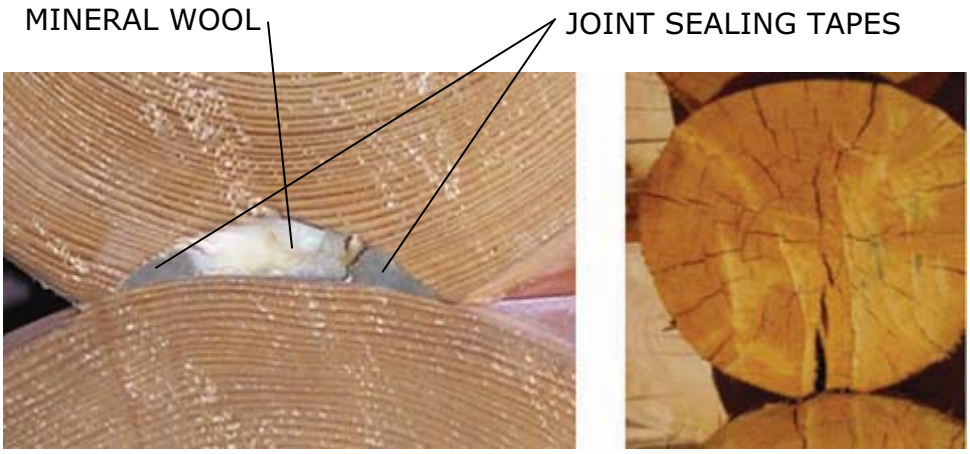

Figure 3. Examples of correct and incorrect groove type

4. MEASUREMENT

To obtain enter values necessary for further design analysis, the thermo vision measurement and surface temperatures measurements of log walls were realized. Shown outputs are from the log wall, where only the pairs of joint sealing tapes protect the grooves. There is no thermal insulation.

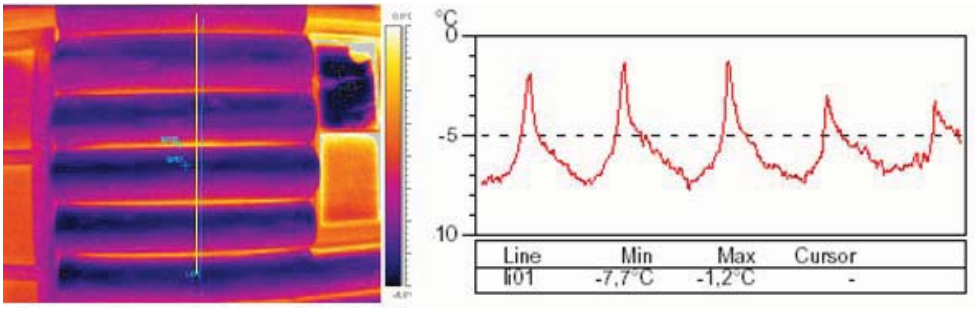

Figure 4. Thermo camera outputs – outside view

From the upper two graphs, the obvious difference between the log surface and groove temperature can be seen.

The subject of further research is an optimization of groove design with the point of view in thermal engineering.

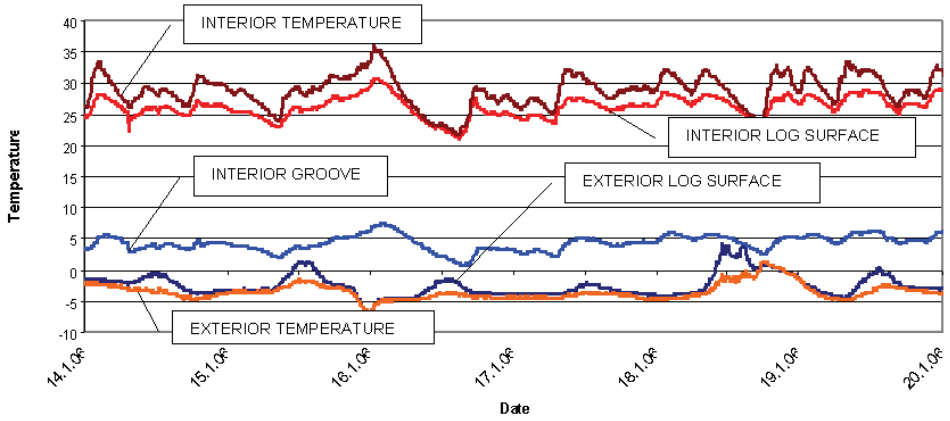

Figure 5. Surface temperature measurement outputs

5. ENVIRONMENTAL CLASSIFICATION

Recently, general attitude towards the environment is changing and also the civil engineering sphere is looking towards to original material base comeback. Also within the construction materials and elements classification, the environmental aspects have rising importance beside the technical and economical aspects. Effects on environment caused by usage of definite material have to be considered during the whole life element period.

The international reputable system for material and buildings classification is so called Life Cycle Assessment – LCA. To be the project certificated as an ISO suitable, the requirements of series ISO 14040 should not be omitted. Standards describe methods needed for Life Cycle Assessment generation. These are especially ISO 14040 Goal and scope, ISO 14041 Life Cycle Inventory Analysis, ISO 14042 Life Cycle Impact Assessment and ISO 14043 Life Cycle Interpretation. In practice this means that the fossil energy consumption used in building constructions should be reduced. The total fossil energy consumption does not only compose of coal and gas but this is a complex question of choice of particular material types, which had been produced with the aid of fossil energy. For that reason, as much renewable sources should be used for the constructing as possible. Wood is undoubtedly ranked among these low energy renewable materials.

6. CONCLUSIONS

From the point of view of recently LCA classification, the log houses are ranked among the energy modest construction. That is because wood is an easy available and renewable material, log houses production is easy while the construction details are finished in correct way, their operation is also quite unpretending and last but not least, they cause minimal environment pollution. Wood is a renewable natural source and that is why is so contradistinguished from other construction materials.

References

1. Houdek, D., Koudelka, O., *Srubové domy z kulatin*, ERA group spol.s r.o., Brno 2004. (in Czech Republic)
2. Novotný M., *Expert's report 53-09/05 About current state of carcassing of family house* , Brno 2005. (in Czech Republic)
3. Přeček, L., *Doctoral thesis – Podpora pro navrhování vícepodlažních dřevostaveb*, ČVUT Praha 2005 (in Czech Republic)
4. Houdek, D., *Conference proceedings - Dřevostavby*, VOŠ a SPŠ Volyně 2005 (in Czech Republic)

"Computational Civil Engineering 2006", International Symposium
Iaşi, România, May 26, 2006

Technical, environmental and security criteria of new building materials parameters evaluation

Tomáš Fojtík, Tomáš Vymazal, Nikol Žižková, Vít Petránek

Faculty of Civil Engineering, Brno University of technology, Veveří 95, 602 00 Brno, The Czech Republic

Summary

The success of new building materials in the market consists in the fulfillment of basic technical, environmental, security and economical demands. It is possible to minimize by means of the preventive FMEA method (Failure Mode and Effects Analysis) already during the development of new materials the risk of qualitative, environmental and security faults, risks and hazards.

The paper discusses the preventive FMEA method applied in the design and development of progressive building materials with utilization of secondary raw materials.

This method can in a basic way assist in the examination of physico-mechanical properties of these materials, in the formation of technical and security certificates and in this way it can eliminate the problems with the material application into structures, caused by users distrust to the secondary raw materials from the point of view of their technical, ecological and precautionary safety.

KEYWORDS: FMEA - Failure Mode and Effects Analysis.

1. INTRODUCTION

The FMEA method is ranked among the basic preventive methods of quality management and it is an important part of the design examination. It is based on the team analysis of possible faults of the examined design, concerning its evaluation, its risks and the realization of measures which lead to the improvement of the design quality.

The experience shows that it is possible by means of this method to detect 70% until 90% of possible disagreements [1].

The use of the FMEA method presents a systematic approach to the prevention of bad quality and it leads to the decrease of losses caused by the poor quality of products, to shortening of the solution period of the development work, to the

decrease of changes in the realization phase and to purposeful utilization of sources.

The results of the FMEA method application form a very valuable information data base about the product which can be utilized also for similar products and these results are a significant base for the elaboration or specification of quality plans and an important part of the control system in the area of design formation [2].

The method itself is realized in five steps:

1st step – *Determination of system elements and of system structure*

The system is composed of system elements (SE), which serve for the description and classification of the hardware conception and are arranged in the system structure. The system structure arranges the individual system elements from up to down on different hierarchical levels. Apart from it, it is necessary to describe the present interconnection of individual system elements as the interface to other system elements.

2nd step – *Representation of functions and of the functional structure*

The system elements have different functions or tasks in the system. The joint effect of more system elements functions can be demonstrated as the functional structure (the tree of functions/network of functions). For the determination of functional structures we have to monitor the input functions and the internal functions.

3th step – *Execution of faults analysis*

We must carry out the faults analysis for each observed element described in the system. The possible faults (F) of this system element are derived from the known function defined in the 2nd step and they describe the faulty functions.

The possible effect of each fault has to be determined and it will be evaluated (quantified) by means of the ten points scale from the point of view of its importance (B). The possible reasons of faults will be classified owing to the imperfect function of the subordinated system elements by means of the interface to the system element. The probability of fault occurrence (A) will be estimated for each reason by means of the ten points scale.

The analysis is determined by the specification of existing preventive measures (precautions to prevent the fault formation) and by the introduction of control measures. The probability of fault sources (mechanism) detection (E) is evaluated in the case of this measures application and it is quantified by the help of the ten points scale.

4th step – *The evaluation of the risk size*

The risk size (RPZ) is the product of the point evaluation: B – the importance of the fault effect, A- the probability of fault reason occurrence and E – the probability of the fault reason detection.

5th step – *The introduction of optimization*

It begins with the highest values of RPZ by definition of precaution/preventive measures. These measures have deadlines and they must be taken by appointed persons in charge. The optimization is necessary for high values of the risk factor (RPZ) or high values of B, A and E. The optimization is realized following this order of importance:

- Change of conception – in order to eliminate the reason of fault or in order to reduce the fault significance.
- The increase of conception reliability – for minimization of the fault reason occurrence probability.
- The effective detection of the fault reason (if possible without additionally tests).

The additionally measures for the risk minimization should be described and the responsibility for the realization of these measures must be clearly determined. It is necessary to realize all five steps of the system FMEA for the respective areas in the case of a deciding change of conception.

2. RISK FACTORS ANALYSIS BY MEANS OF FMEA

2.1 Preparation of FMEA – T

The subject of analysis should be determined and the members of the team selected, with respect to the effectiveness, before the beginning of the FMEA methodic application.

The selection of the team members should be made with regard to their activities in the FMEA teams following the criteria:

- FMEA- K (construction FMEA),
- FMEA- T (technological FMEA).

Further the data concerning the process description (the technological procedure), the flow chart with marked checking operations/control of the process (SPC) and information about all former (also only possible) problems with the

product/task/process and its solution should be collected. This information should be divided into three categories from the point of view of:

- significance of the fault (the consequences for the client),
- reason of the fault,
- checking or controlling measures (SPC).

2.2 Technical and qualitative demands

The technical and qualitative demands should contain especially the wishes of the client, juristic and other demands and the demands of other interested parties.

2.3 Environmental and ecological demands

The prevention of negative environmental aspects which can occur in the FMEA-T or FMEA-K and in the phase of product utilization or its post-action disposal is in particular the demand of the environmental area. This concern especially the areas connected with the:

- Atmosphere protection,
- Handling with hazardous chemical substances and wastes,
- Water resources management and water protection,
- Wholesome environment (e.g. noise and dust protection),
- Consumption of natural resources (utilization of waste materials – saving of natural sources, utilization of recycled materials),
- Energy saving (heat, electric power).

2.4 Safety requirements

The requirements which follow from the legislation and from demands of labour and health protection - it concerns especially the:

- Identification of hazards, risks and so called accidents.
- Fire safety.
- Hygiene.
- Health protection.
- Users safety.

3. REALIZATION OF FMEA IN THE DESIGN AND DEVELOPMENT OF CONCRETE

3.1 The team composition

Research teams of the research project No.: MSM 0021630511, called "Progressive Building Materials with Utilization of Secondary Raw Materials and their Effect on the Service Life of Structures" are participating on the proposal and development with the FMEA application, by partial subject matters:

- Research and Development of New Types of Concrete, coordinator is Doc. Dipl. Ing. Rudolf Hela, CSc.
- Securing of Concrete Durability, coordinator Doc. Dipl. Ing. Jiří Brožovský, CSc.
- Research of New Surface Treatments, coordinator Prof. Dipl. Ing. Rostislav Drochytka, CSc.
- Testing of Materials and Environmental Management, coordinator Prof. Dipl. Ing. Jiří Adámek, CSc.

3.2 The selection of concrete

One of most widespread building materials in the time being is the concrete, which is in the modern form produced already more than 100 years. The concrete technology has made significant steps ahead in the last decades. The raw materials used for the concrete manufacture used today we could mark as "hazardous waste" only some years ago. We would be obliged to dispose this waste under increased safety conditions and with financial costs.

These "new" raw material sources can with their physico-chemical properties lower the dement dose for 1 m3 of concrete and after mixing it into the concrete and its hardening these components can take part on the increase of some physico-mechanical concrete parameters and in some case even on the increase of the concrete durability. Such raw materials are for instance the power plant fly ashes, slag, waste ferrous dust etc. These materials must fulfill the given chemical and physico-mechanical and physico-chemical parameters.

Considering the fact that it concerns mostly the so called "secondary raw materials", i.e. raw materials which are formed as a by-product during the production of another product (material) this by- products don´t have in most cases constant properties. In this way the use of these materials for the concrete production can mean an increased risk.

The analysis and the evaluation of the usability and the risk elimination was tested on three selected types of concrete (common concrete, self compacting concrete

and reactive powder concrete). These three types of concrete were produced with the addition of a certain fly ash dose from the power plant Dětmarovice.

3.3 Decomposition and the risk analysis of input raw materials and of the resulting Product

Technical and qualitative demands

This concerns especially:

- The evaluation of input raw material considering the intended use
  - Physico-mechanical and physico-chemical properties
- The properties of fresh concrete
  - Consistency, volume mass, air content etc.
- The properties of hardened concrete
  - Volume mass, strength characteristics, concrete resistance against outer stress, appearance etc.
- The durability of concrete

Environmental and economic demands

These concerns especially the areas connected with the:

- Protection of the atmosphere
- Water resources management and water protection
- Handling with wastes
- Handling with hazardous chemical substances (NCHL)
- Wholesome living conditions (for instance noise and dust protection)
- Utilization of natural sources (utilization of secondary raw materials – savings of natural resources, utilization of recycled materials).
- Savings of energy (heat, electric energy)

Safety requirements

The safety requirements are connected with the utilization of secondary raw materials types which are as safe as possible of with respect to:

- Physico- mechanical and physico- chemical properties
- Storing and transport security
- Possible industrial accidents and professional disease
- Safety of the production technology
- Safety of application into the building structures
- Prevention of undesirable events, accidents and hazards

- Notification and announcement duty according to the legislation of the Czech Republic

4. CONCLUSION

It holds generally, the sooner in the service life period we succeed to disclose the risk of the improper product occurrence, the lower are the financial losses.

Some practical experience shows, that the costs for the elimination of disagreement in the phase of design can be hundred times lower than the costs for the elimination of disagreement determined for the expedition and thousand times lower, than the costs for the elimination of the disagreement which comes to the client.

It is still a very often event that "it is not enough money or time" to elaborate sufficiently the design and afterwards it must be enough money and time for much more expensive elimination of problems which come into being in the phase of realization [1].

It was in the area of technical requirements determined by the FMEA that in the case of of power plant fly ashes application in the production of SCC the pozzuolana reaction of the fly ash comes to light till after 180-days of the concrete age.

Since this time the increase of concrete characteristics took place in comparison with the self compacting concrete, manufactured without the utilization of the power plant fly ash. This showed itself significantly also on the resistance of SCC against individual, selected chemically aggressive media, to which the concrete was exposed.

As the most serious risks and hazards in the field of the environment and safety were identified those potential faults, which are connected with the utilization of fly ashes as the input raw material in the manufacture of SCC.

These risks and hazards are connected specially with the physico-mechanical properties of the fly ash, for instance with the inhomogenous chemical composition, with the specific surface, with the index of efficiency, with specific activity 226Ra etc.

Acknowledgments

The paper was elaborated with the support of the research project No.: MSM 0021630511: "Progressive Building Materials with the Utilization of Secondary Raw Materials and their Effect on the Durability of Structures"

References

[1] Plura, J. *The FMEA method*, Dům techniky Ostrava, Ostrava (in Czech)
[2] VDA 4.2 : *Quality control before the batch production*. System FMEA. *Česká společnost pro jakost,*Praha, 1997, ISBN 80-02-01188-0 (in Czech)
[3] ČSN IEC 812, *Methods of System Reliability Analysis, Procedure of faults and their consequences analysis*, ČNI, Praha, 1992.(in Czech)
[4] *Publication of the Ministry of Environment of the Czech Republic and of the Minstry of Health*, *concerning the evaluation of hazardous properties*, Vyhláška č.376/2001Sb, MŽP,Praha,2001 (in Czech)

"Computational Civil Engineering 2006", International Symposium
Iaşi, România, May 26, 2006

Selection of theoretical method for lateral load analysis of brick shear walls structures

Magda Brosteanu[1], Teodor Brosteanu[2]

[1]*CCI Department, Faculty of Civil Engineering and Installations, Technical University of Iasi, Romania*
[1]*CFDP Department, Faculty of Civil Engineering and Installations, Technical University of Iasi, Romania*

Abstract

This article refers to the basic data for structural design of masonry building structures and it has been based on a study of different patterns. On recommends the equivalent rigid frame pattern for simplified design and for the best approximation to the specimen experimental behavior, and for actual brick shear walls structure, as well.

KEYWORDS: buildings, brick shear walls, lateral loading, patterns, static analysis methods.

1. INTRODUCTION

There is a sustainable activity to unify the European Design Codes for an available joint set of Code of Practice.

The European pre-standard ENV 1996-1-3-Eurocode EC6 "Design of Masonry Structure" was realized by subcommittee B/525/6-Use of Masonry for a few keywords: buildings, construction, masonry works, IT, codes, details, and loads. The boxed values will be set by CEN Members (Comité Européen de Normalisation) function of each country requirements.

The rules of the Eurocode EC6 "Design of Masonry Structure, General Rules for Buildings, Rules for Reinforced Masonry" /1/ are the same with a few rules given by the Romanian STAS 10109:1982, P2:1985, STAS 10107-0:1992, P100:1992:1996:2004, and MP001:1996, and by British Standard BS5628-1:1992, except that the reinforced and pre-stressed masonry members are rarely used in the Romania.

A special attention has been devoted to the lateral load analysis of masonry walls and the design for accidental loading, others than earthquake load according to EC8.

2. WALLS LAYOUT

The functional requirement starts with the selection of walls layout since some arrangements for multistoried masonry buildings such as blocks of flats, students' hostels, hotels, and other residential buildings with cross-walls structures, for ensuring the robustness of building to accidental damage.

There are a few arrangements of cross-walls for masonry buildings with typified recurrent functional layouts:

(i) cellular walls system,

(ii) simple or double cross-walls system i.e. cross-walls without or with longitudinal walls,

(iii) complex arrangements,

(iv) a system made by frames and cross-walls, with a central core, or end diaphragms, or a flexible ground floor.

Note that the simple cross-walls system is liable to its longer axis.

On the other hand there is a torsion(al) induced effect on plane floor as a result of the application of level horizontal earthquake load with respect to the centre of mass "e" apart from the centre of stiffness.

3. THEORETICAL METHODS FOR LATERAL LOAD ANALYSIS

Because of bonding technological system with mortar joints and the concrete connections between elements have been used in masonry structures, it should be assumed that the 3D analytical structural analysis is not validated to on site masonry structure behavior to any lateral force.

There are shear walls and coupled shear walls. The pattern of each coupled shear wall consists of a diaphragm with "n" rows of gaps, and "n+1"posts, and "n" lintels distributed on elevation, distance apart to storey height. The deformations due to bending moments plus axial and shearing deformations of posts will be considered in the case of one row gap pattern having big breadths posts. In the case of "n" rows of gaps pattern, the deformations due to bending moments plus axial and shearing deformations of the first and the last posts will be only considered.

The diaphragms are classified by "α" monolith coefficient with regard to the gaps influence in the brick shear walls behavior for lateral loading. The assumption of the same rotation of posts on storey at the lintels level, and zero value of bending moment in the internal hinge at the mid-span of each lintel are considered for a small gaps diaphragm ($\alpha \geq 10$) or a middle gaps one ($1 < \alpha < 10$).

In the case of big gaps diaphragms ($\alpha \leq 1$), the lintels will be as pendulum connections between the cantilever walls having the same displacement.

The design of coupled shear walls with small gaps ($\alpha \geq 10$) and/or big ones ($\alpha \leq 1$) is the same with the design of shear walls. It is suggested that for small gaps diaphragm design, the computation of shear forces and bending moments in double fixed props of lintel is adequately. No computation in pendulum connections of big gaps diaphragms. There are supplementary assumptions for middle gaps diaphragms design.

Static analysis of a rigid structure made by coupled shear walls with "n" degrees of freedom of joint translation is shown. Interconnecting infinitely rigid diaphragms at floors are assumed. Five simplified methods derived from Displacement Method of 2D static analysis of multistoried monotone coupled shear walls concerning loading effects and nodal displacements computation for lateral loading applied on the following patterns are considered:

(i) individual simple cantilever,

(ii) equivalent rigid frame,

(iii) wide column frame,

(iv) shear continuum wall,

(v) 2D-FEM wall.

Pattern (i) is applied to big gaps diaphragms computation. Loading on each post is proportional to its moment of inertia. Post displacements will be computed by imposed deformations procedure.

Pattern (ii) is applied to middle gaps diaphragms computation. The frame columns will substitute the posts spanning between posts centroidal axes. The slabs will substitute the lintels.

To aid a better understanding of the assumptions of basic input system about, a comparison of two distinct design methods is made. The distortion method will be applied on the basic input system simplified by prevented rotations (slopes) and free translations (deflections) of nodes face to the displacement method on the basic input system simplified by prevented both rotations and translations of nodes.

To be noted that the pattern (iii) is applied to "1…n" rows of middle gaps diaphragms, in the substitute steps:

1 To apply the pattern (ii) of equivalent rigid frame.

2 To consider a semi-wide column frame with a single row of gaps symmetrically taken.

The columns gross areas of cross-sections and/or the second moments of gross areas, i.e. the moments of inertia, will be computed by summing up the same features of posts.

The slabs double fixed props will be considered at the fixed edges of its spans, no matter what the columns centroidal axes are, because the lintels having moments of inertia "Ir" will only strain on its spans.

The slabs will not strain beyond the lintels fixed edges and having moments of inertia "Ir=∞" up to the columns centroidal axes. The slabs gross areas of cross-sections "Ar" and/or the second moments of gross areas "Ir" will be computed by summing up the same features of lintels.

3 To compute bending moments of posts proportional with its moments of inertia. Bending moments of lintels will be computed from nodes equilibrium Eqs.

Pattern (iv) of shear continuum wall with continuum connections and shear loading effects distributed on posts heights is applied to "1…n" rows of middle gaps diaphragms computation.

Three distinct design approaches are considered for lateral displacements computation of middle gaps diaphragms: using pattern (i), or pattern (iii), or pattern (iv).

Pattern (v) applied on all types of diaphragms only implied an IT approach.

4. SELECTION OF THEORETICAL METHOD

All patterns and design methods selected can be developed for the estimation of loading effects for the claimed input data.

A rational approach on the best pattern will be validated by comparison of design and experimental results obtained by lateral loading applied on the same model, either mathematical model or a specimen at a real scale.

Considering a case-study by /2/ on a building specimen at a real scale, as a double cross-walls rigid structure having P+4E and a layout of a square plane shape of 6.25 m x 6.25 m of 4 rooms and a central longitudinal hall, subjected to a lateral loading applied by 3 hydraulic jacks that simulate an equivalent uniformly distributed load of 894 N/mm^2 applied on façade.

Structural performance requirements criteria were the deformation state and stress-strain relation. Performance levels, either designed or effective ones were the lateral displacements and the distribution of compressive stress and the tensile stress at the specimen basement section.

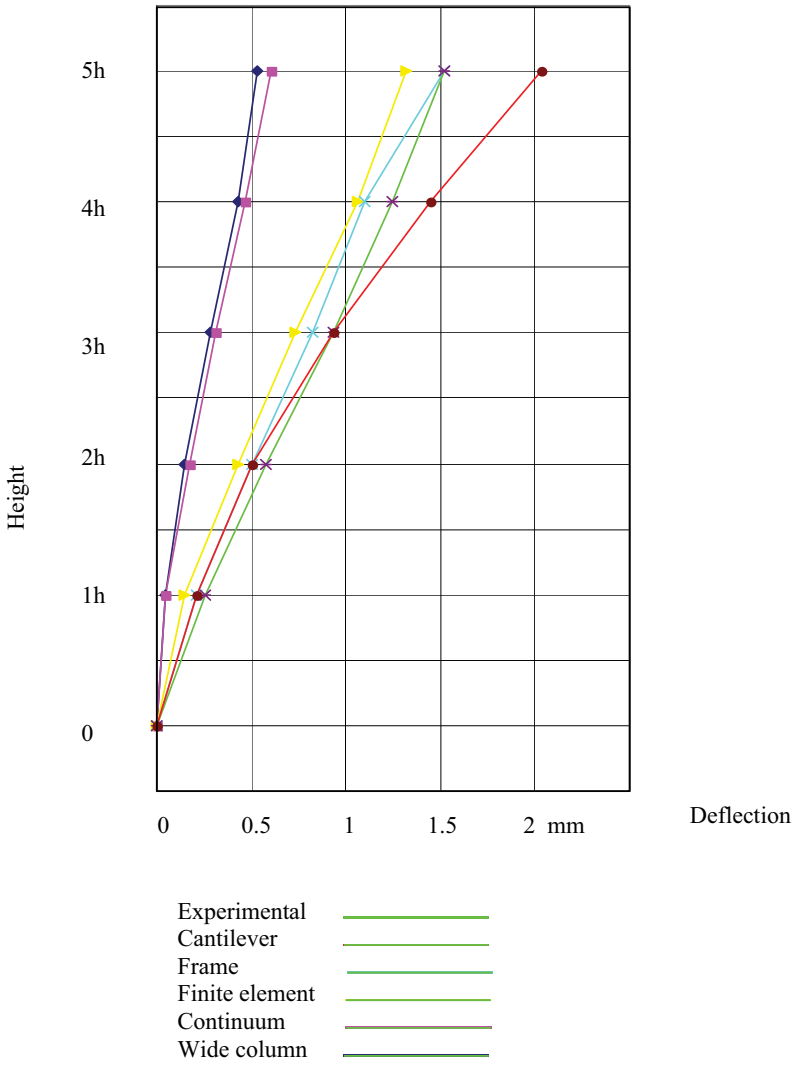

Fig.1. Level Lateral Displacements on Design Models

Theoretical and experimental displacements are compared in the Fig.1. The distribution of compressive and tensile stresses on a half of structure is compared in the Fig.2.

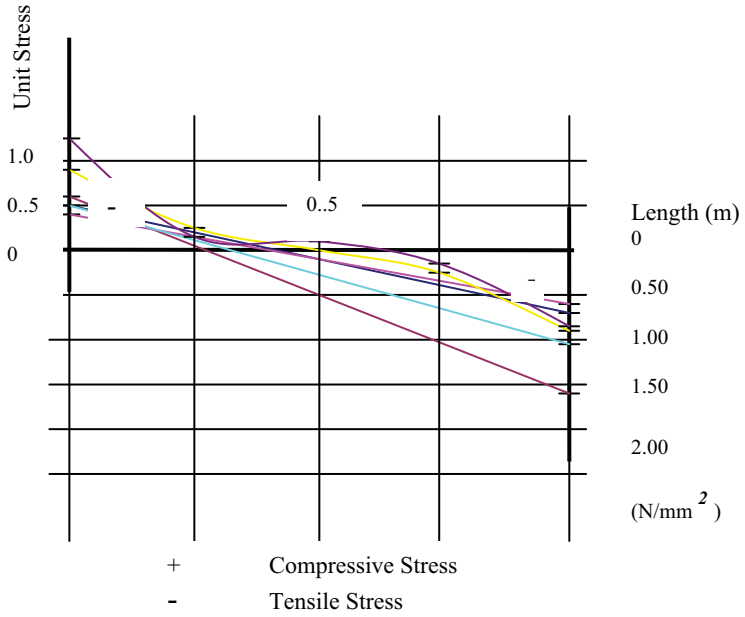

Fig. 2. Unit Stresses Distribution on a Half of Specimen

Note that there is a nonlinear distribution "σ" by Finite Element Method and experimental method, and a linear distribution "σ" by other applied methods.

5. CONCLUSIONS

Individual simple cantilever pattern (i) is suggested for predesign.

2D-FEM wall pattern (v) is suggested for research.

On recommends the equivalent rigid frame pattern (ii) for simplified design and for the best approximation to the specimen experimental behavior in the Fig.3., and for actual brick shear walls structure design, as well.

The equivalent rigid frame consists of columns with the same features as posts, and slabs with the same features as lintels. The frame columns will substitute the posts spanning between posts centroids. The slabs will substitute the lintels on the entire span of columns centroids.

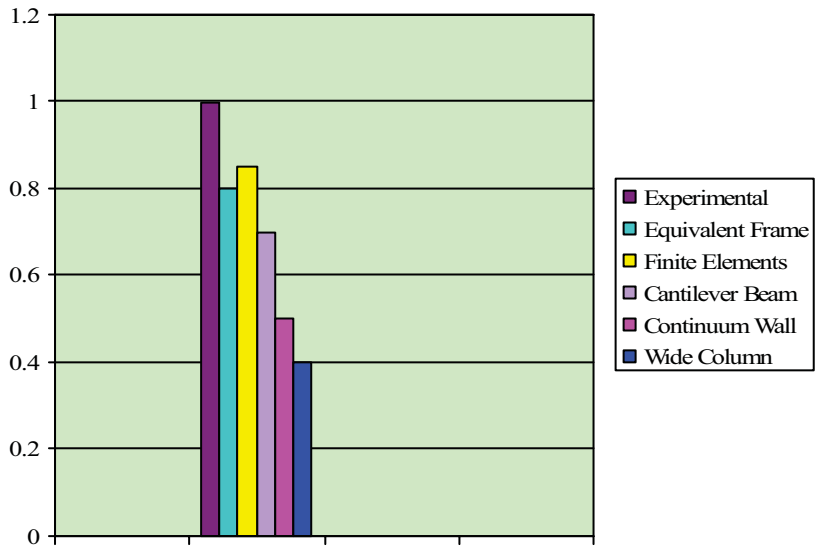

Fig.3. Accuracy of Design Patterns

References

1 xxx The European Pre-standard ENV 1996-1-3 Eurocode EC6 *"Design of Masonry Structure. General Rules for Buildings. Rules for Reinforced Masonry"*.

2 Hendry, A.W., Sinha, B.P., Davies, S.R.- *Design of Masonry Structures*, Third edition of Load Bearing Brickwork Design, E& FN Spon Publishing House, An Imprint of Chapman & Hall, London, Weinheim, New York, Tokyo, Melbourne, Madras, 1997, ISBN0419215603.

"Computational Civil Engineering 2006", International Symposium
Iaşi, România, May 26, 2006

Using computer technology for laboratory results (data) evaluation

Lenka Nevrivova

University of technology, Faculty of Civil Engineering,
Institute of Technology of Building Materials and Components, Brno, 602 00, Czech Republic

Summary

The article is focused on topics dealing with methods of processing a large data volume, applied in civil engineering. Evaluation of a large data volume retrieved during laboratory tests on laboratory samples pieces can be efficiently evaluated only using automated methods and computers. The article describes process of evaluation of output data, resulting from tests of thermo insulation chamotte (fire brick) samples that were prepared using waste raw materials, cenospheres, ash and slag. In particular, it describes using Microsoft Excel environment with a Visual Basic routine application.

KEYWORDS: insulating, fire brick, fly ash, waste raw material, Visual Basic, Microsoft Excel

1. INTRODUCTION

During finding new possibilities how to produce lightweight heat insulating fire brick material on basis of waste products, a large variety of new material compositions is being designed and large amount of testing samples tested in wide range of laboratory tests, is carried out. Large amount of measured values to be further processed and evaluated as the result of experimental works carried out on testing bodies is getting

The paper is divided into two main parts.

The first part of the paper describes the results of research performed to maximize utilization of waste materials in light-weight heat insulating fire brick. Waste from thermal power stations – ash, slag, and cenospheres – has been judged.

The second part of the paper deals with possibilities how to process measured data, how to think of the data, how to define data measured inaccurately, or how to define samples with extremely high (good) properties or data with extremely low (bad) properties. This part of the paper indicates and describes programme algorithm processed in VB software which significantly improves and makes easier evaluation of the measured values.

2. WASTE MATERIALS IN INSULATING FIRE BRICK

Light-weight refractory products may be light-weighted in various ways – using burning out additives, volatile substances, by foaming, using light-weight opening materials, etc. Using of volatile additives, sawdust, provides unpretentious production equipment and simple production process, the disadvantage is low dimension product accuracy of and need of the following calibration.

The aim of experimental works has been reviewing of possibility for using waste products from thermal power stations as a light-weight medium in a fire brick material which was not produced by drawing from a plastic body on a screw press but from a wetted body (crumbs) by pressing on a hydraulic press. The presswork from semi-dry mixture has many advantages. From the ecological point of view, this technology is profitable because a waste material is being processed and also when using non-burning out light-weight medium (ash, slag, cenospheres), harmful emission content produced during burning process of shaped products is significantly lower. From economical point of view, using waste product in a material content significantly reduces material costs in production and heat energy savings during product drying when amount of dried out water is two thirds lower than during production from plastic body which is not negligible as well.

2.1 Used raw materials

Kaolinitic clay has been used for a production of testing samples as a binder. **Ash, slag, and cenospheres,** and referential **keramzit** were used as light-weight medium (opening material).

Ash originates as a waste product from coal burning. From chemical point of view, it is an inert material composing mainly of particles of SiO_2 and Al_2O_3. Its granulometry is 0 – 1000 μm, powder density 750 – 1100 $kg \cdot m^{-3}$ and firing loss content max. 1% of mass. Price 40 CZK (circa 1.4 EUR) per ton.

Slag (from electric power stations) originates as a waste product during coal burning in thermal power stations. From chemical point of view, it composes mainly of particles of SiO_2 and Al_2O_3 and contents 15 – 45 % of water of its mass. Powder density of a dry slag is 600 – 800 $kg \cdot m^{-3}$, of a wet one 900 – 1000 $kg \cdot m^{-3}$, price 26 CZK (circa 1 EUR) per ton.

Cenospheres are aluminate-silicates hollow particles of a spherical shape originating during coal burning. They can be obtained either by ash washing or they are industrially produced. The mineralogical content of cenospheres is mostly mullite and β-cristobalite, powder density is about 420 $kg \cdot m^{-3}$. It is a secondary waste product which corresponds with the price of 12 000 CZK (circa 430 EUR) per ton.

Keramzit (trade name) is a ceramic granulation product originating during clay burning in rotary kilns under 1160 to 1200 °C which forms characteristic spherical

shape of porous hollow grains, powder density is 650 (500) kg·m^{-3} and water absorptive capacity max. 5%, price 1295 CZK per m^3.

2.2 Testing samples

The testing samples may be divided according to used light-weight medium to four basic groups. Material compositions 1 to 3 are only with cenospheres, material compositions 4-6 use keramzit as a light-weight medium, 7-9 use slag, and 10 to 12 use ash.

Table 1. Material compositions

Material composition	1	2	3	4	5	6	7	8	9	10	11	12
Chamotte opening material 0.5-1mm		10	20									
Chamotte opening material 1-3mm	30	30	30									
Keramzit 0-1mm					10	20						
Keramzit 0-4mm				45	45	45						
Slag							45	55	65			
Ash										25	35	45
Cenospheres	45	35	25	30	20	10	30	20	10	50	40	30

2.3 Assessment of utility properties and description of microstructure

Three testing samples were pressed for each material composition, each of them was fired in a tunnel kiln under a fire temperature 1050 °C, 1100°C, and 1250 °C.

Figure 1. Images of fired samples

The testing samples were tested in a wide range of laboratory tests. Macroscopic and microscopic descriptions were made (Fig. 1). Shrinkage by drying, firing and overall material shrinkage were assessed. Mass density, apparent porosity, absorptive capacity, and apparent density by hydrostatic weighting were measured, further coefficient of heat conductivity λ, strength in pressure in a cold state were assessed, mineralogical composition of material by RTG diffractive analysis was found out, and theoretical chemical composition of the material was calculated from chemical composition of a material. REM (Raster Electron Microscopy) test

serving for more detailed description of material microstructure was carried out as a complementary test (Fig. 2).

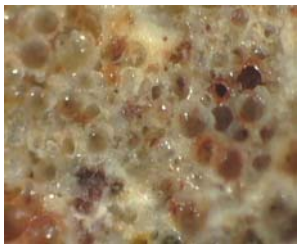

Optical microscope, enlarged 160times

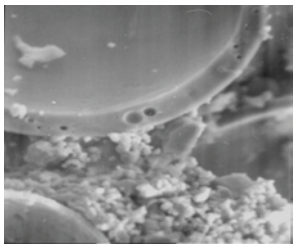

REM, enlarged 1000times

Figure 2. Characteristic microstructure of samples with cenospheres

The output of a whole experiment, observation, and measurement is a large amount of data (over 400 measured values) even the fact that only twelve material compositions were tested. Possibilities, how to process measured data, are listed in the next chapter, see Chapter 3.

2.3. Discussion of results

Usage of sawdust as a burning out light-weight substance is recessed due to both ecological and technological reasons. Overall material shrinkage during production of plastic body when using sawdust is up to 15%.

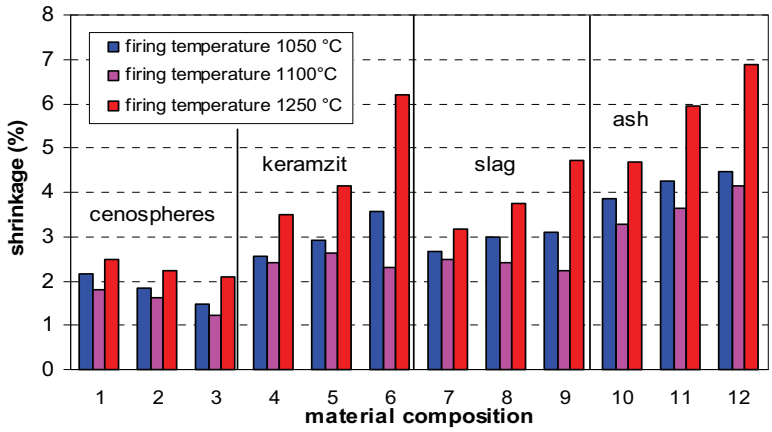

Figure 3. Shrinkage by drying and firing

When using our chosen light-weight substance, the overall material shrinkage is between 2-7%. Very good results were reached when using cenospheres and slag. Material shrinkage increases with firing temperature, Fig. 3.

Coefficient of heat conductivity λ is very important characteristics of heat insulating shaped bricks. As you can see on the following figure (Fig. 4), the influence of firing temperature on this characteristic is not significant, only direct dependence between bulk density and heat conductivity which is generally known was confirmed. Values of coefficient of heat conductivity were in a range from 0.2 to 0.43 $W.m^{-1}.K^{-1}$. Strength in pressure is a decisive criterion for light-weight insulating materials only if we want to use them as structural materials. Sufficient handling strength was confirmed for all the testing samples (Fig. 5).

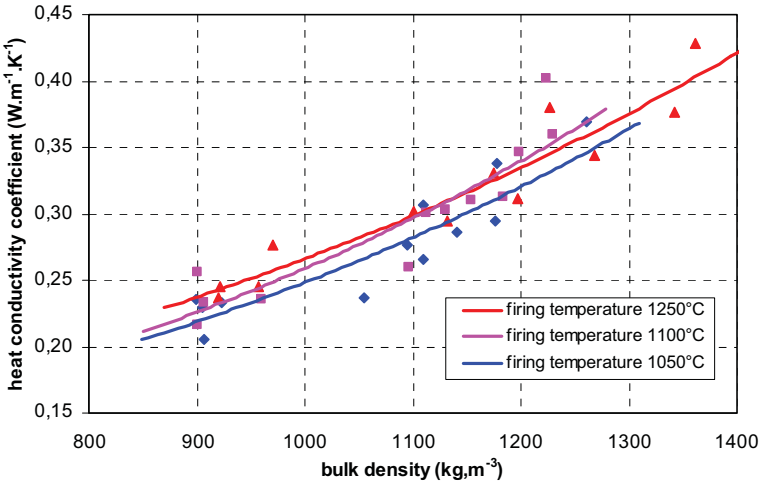

Figure 4. Effect of firing on heat conductivity

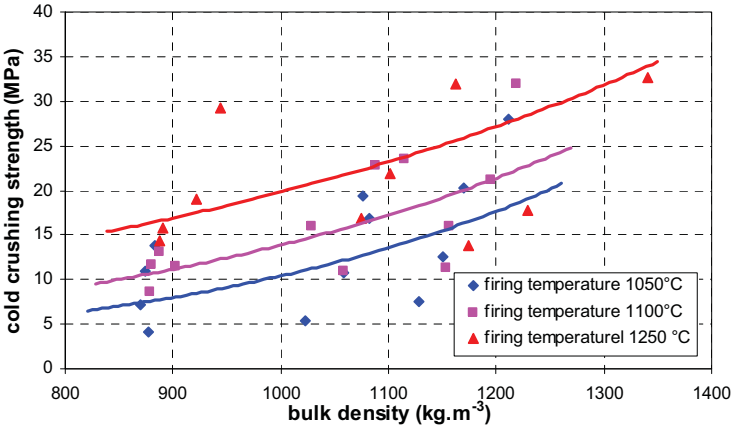

Figure 5. Effect of firing on strength

Bulk density of the samples prepared according our designed material compositions ranged on the upper limit of bulk densites for heat insulating

materials; value 1350 kg.m^{-3} cannot practically be reckoned for heat insulating material but structural insulating material.

With respect to low values of overall linear material shrinkage (3% on the average), it is possible to produce shaped bricks with sufficient accuracy even without consequent calibration which reduces production cost of the material. Material costs are lower as well – use of waste product in a material composition, and negligible is not financial savings during drying of shaped bricks, either.

Study has unambiguously approved that it is possible to produce insulating fire brick on basis of waste products from crumbs and that characteristics of such a material are comparable with the material which is industrially produced and supplied to domestic market.

3. USE OF COMPUTATIONAL ENGINEERING FOR PROCESSING OF LARGE AMOUNT OF MEASURED VALUES

3.1. Microsoft Excel

Big advantage during analysis of measured values is using table editor Excel which is very obviously used at present. This programme enables quick data processing; its output may be various types of graphs. However, if volume of measured values is too large, the work with editor Microsoft Excel does not provide an easy survey that leads to unnecessary mistakes during result processing.

3.2. Reasons and goals of VB software

Very frequent operation carried out during evaluation of measurement results is finding out the dependence rate of observed (measured) quantities. The dependence rate is being expressed by reliability coefficient R^2 ranging within the interval <0,1>.

In case that reliability coefficient has been assessed for all observed samples, this value will be surely much lower than if it was assessed only for selected samples; minimum amount of chosen samples must be defined by user. For samples excluded from a selection, it is necessary to find the reason of their exclusion from an observed data file. Several basic cases may happen here:

- Bad sample preparation, technology failure, low-class sample
- Exceptionally good, quality sample
- Laboratory test carried out badly

The outputs of software set up in VB are:

- Uniquely defined samples which significantly deviate from statistic file, a task for a user is to reversely find out why the given deviation happened.

- Graphically processed results for optimum combination of measured samples

3.2. Software algorithm for optimization of values of reliability coefficient

Detailed protocol about measurement history is carried out by a user during preparation of testing samples and during execution of laboratory tests. After result evaluation, a matrix [m,n] of a "measurement area" is set up which is further used by a programme.

Algorithm

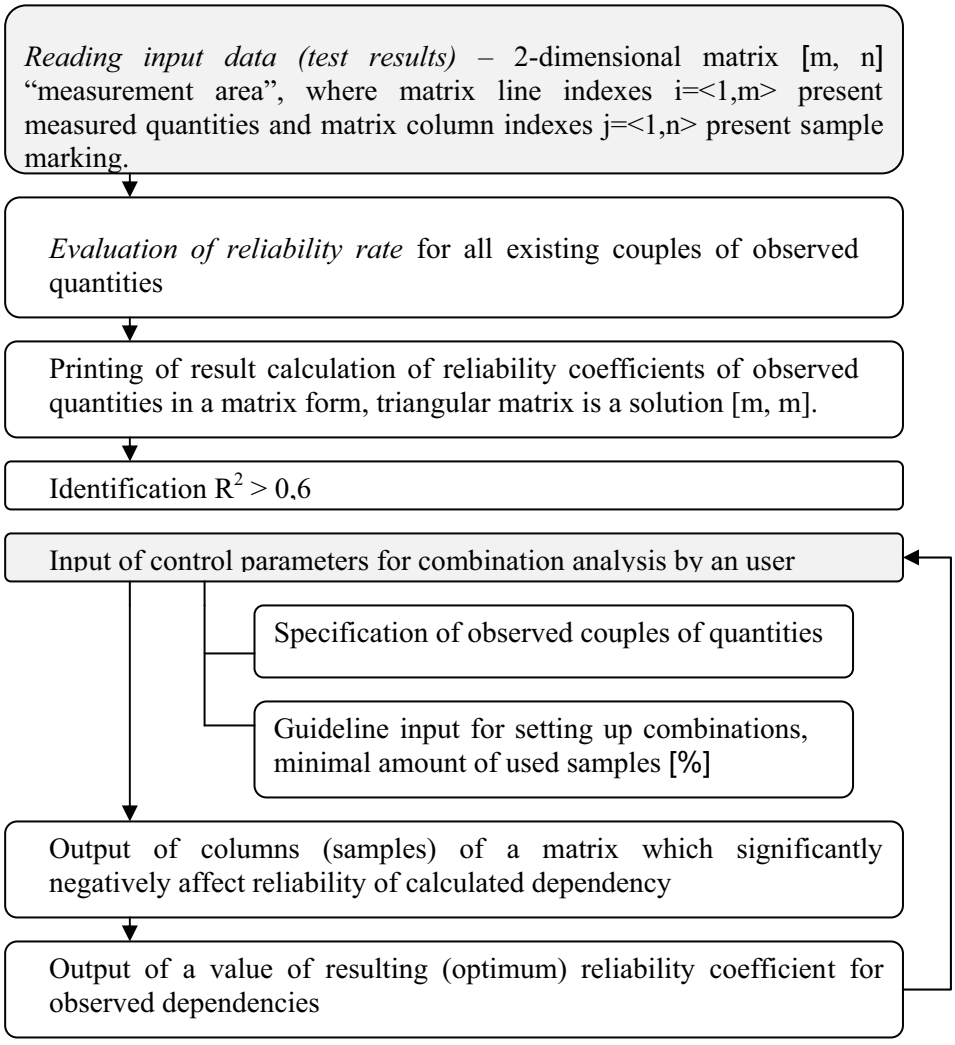

4. CONCLUSIONS

The results of carried out experimental work showed a possibility of using waste products in a material composition of heat insulating fire brick.

For processing of measured values, programme Microsoft Excel has been used, because it makes work with measured data easier. All existing dependencies of measured values on all the testing bodies were tested; the number of testing samples has not been optimized due to large volume of measured samples. The output of software suggested by us is graphical dependencies with coefficient value higher than 0.6, some of which are mentioned in the article.

Optimization of number of samples included in calculated dependency and mostly determination of samples which does not comply with the given dependency, is important for user from the point of view of feedback on such an abnormality (substandard behaviour) of a defined sample for mistake removal in a technology of sample preparation or, on the contrary, for selection of convenient change (technology, raw material, etc.) leading to improve utilization properties of a material.

This outcome has been achieved with the financial support of the research plan MSM 0021630511.

References

1. Kutzendörfer J., Máša Z. *Refractory heat insulating materials*, Informatorium, Praha 1991
2. Hanykýř V., Kutzendörfer J. *Technology of ceramics,* Vega 2000
3. Lang K. *Shaped insulating materials from point of view of standards ASTM and EN*, Conference Proceedings of XIII. International conference about refractories, Praha 2000; p. 22-28
4. Nevřivová, L., Kovář, P. *New possibilities for fire brick light-weighting*. Ceramic journal 2005-1, ISSN 1210-2520, p.10-14
5. Pytlík, P., Sokolář, R. *Building ceramic, technology, properties, and use*, Brno 2002, ISBN 80-7204-234-3

"Computational Civil Engineering 2006", International Symposium
Iaşi, România, May 26, 2006

A computer program for advanced analysis of semi-rigid steel space frames

Cosmin G. Chiorean

Faculty of Civil Engineering, Technical University of Cluj-Napoca, Cluj-Napoca, 400020, Romania

Summary

This paper presents an efficient computer-based analysis method for advanced analysis of semi-rigid steel space frames. The behavior model accounts for material inelasticity due to combined bi-axial bending and axial force, and provides the ability to monitor progressive plastification across the cross-sections of frame elements using only one element per member, which reduces the number of degree of freedom involved and the computational time. The flexibility approach is used in developing the inelastic stiffness matrix of beam-column elements in which element second-order effects is also accounted for. The analytical method described in this paper can be used to analyze 3D frameworks with or without a rigid floor diaphragm. The combined effects of material, geometric and connection behavior nonlinearity sources have been implemented in a general-nonlinear static purpose computer program NEFCAD. Several computational examples are given to validate the effectiveness of the proposed method and the reliability of the code.

KEYWORDS: advanced analysis; semi-rigid frameworks; plastic zone analysis; large deflections.

1. INTRODUCTION

Nowadays, a new approach for analysis and design of steel structures, called advanced analysis is proposed [3-4]. As advanced analysis is considered any analysis method that can satisfactory describe the strength and stability behavior of structure such that separate specification member capacity checks are not required [3]. Such analysis has to model as accurate as possible the real behavior of the structure, taking into account all significant factors: nonlinear elasto-plastic material behavior until the ultimate limit state of the structure, local and global second order effects, nonlinear behavior of semi-rigid connections, initial geometrical, local and global, and mechanical (residual stresses) imperfections. In general, the elasto-plastic behavior is modeled in two main types: (1) plastic zone, when it is modeled accounting for spread-of-plasticity effects in sections and along the beam-column element and (2) plastic hinge, when inelastic behavior is concentrated at plastic hinge locations. The plastic zone analysis can predict

accurately the inelastic response of the structure and is generally considered an exact method of analysis, but because of its complexity and cost has not yet found application in ordinary design practice. The spread of plasticity for various advanced analysis methods are illustrated in Fig.1

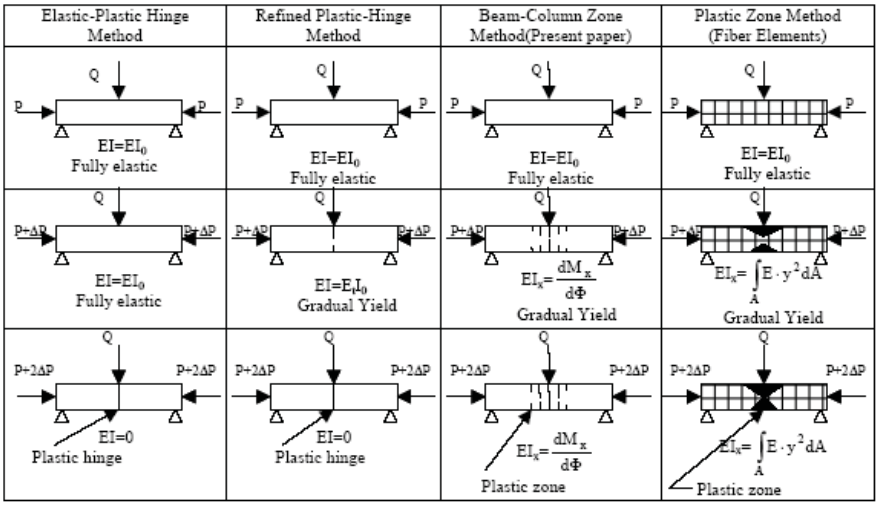

Fig.1 Concept of spread of plasticity for various advanced analysis methods

However, the rapid development of computer technology in recent years has enabled the plastic zone theory in which the spreading of plastic zones in members is taken into account to be developed. A number of computer programs have been developed, on this theory, in recent years, by researchers [7]. Unfortunately, the currently available methods for second-order spread of plasticity analysis and advanced analysis are not user friendly for practical applications. These methods ignore many important characteristics and requirements for practical design, consistency between the linear and nonlinear models due to the need to use several elements per member to model the distributed loads and spread of plasticity along the member length and enhances the computational effort.

The approach presented in this paper is intended to overcome these inconveniences and represents an efficient computer method for large displacement elasto-plastic analysis of 3D semi-rigid steel frames, fulfilling the practical and advanced analysis requirements. The method is based on the most refined type of second order inelastic analysis, the spread-of-plasticity analysis.

Gradual plastification through the cross-section is handled by smooth force-strain curves numerically calibrated. In this way, inelastic behavior in the member is modelled in terms of member forces instead of the detailed level of stresses and strains, with favourable effects on the computational effort. The inelastic cross-

section model is then used to obtain flexibility coefficients for the full member by numerical integrations along its length.

The geometrical nonlinear local effects are taken into account in analysis, for each element, by the use of stability stiffness functions in a beam-column approach. Using an updated Lagrangian formulation (UL) the nonlinear geometrical effects are considered updating the element forces and geometry configurations at each load increment.

The structural response of a steel frame is closely related with the behaviour of its beam to column connections. Most beam-columns connections of steel frames are flexible, ranging in stiffness from almost rigid to nearly pinned conditions. The realistic modelling of a steel frame, therefore, requires the use of realistic connection modelling if an accurate response of the frame is to be obtained. In the present approach, the effects of semi-rigid connections are included in the second-order elasto-plastic analysis using a new hybrid beam element method.

To incorporate the effect of the connection flexibility into the element tangent stiffness matrix, the connections are modelled as springs with the non-linear moment-rotation relationship described by Kishi-Chen power model [6].

The analytical method described in this paper can be used to analyze 3D frameworks with or without a rigid floor diaphragm. The combined effects of material, geometric and connection behaviour non-linearity sources have been implemented in a general-nonlinear static purpose computer program, NEFCAD-3D. A computational example is given to demonstrate the validity of the method and the reliability of the code.

2. FORMULATION

In this paper, the following assumptions are adopted in the formulation of analytical model: (1) Plane section remain plane after flexural deformation; warping and cross-section distorsion are not considered; (2) torsional buckling do not occur; (3) small strain but arbitrarily large displacements and rotations are considered; (4) nonlinearity is due to flexural joint flexibility, material inelasticity, local and global geometrical change; (5) the connection element is of zero length. The elastic unloading effect is included in analysis, but hysteretic and softening effects associated to damage in building frames under severe loadings are not taken into account.

The proposed approach is based on the most refined type of second order inelastic analysis, the plastic zone analysis, and employs modelling of structures with only one element per member, which reduces the number of degree of freedom involved and the computational time.

2.1. Elasto-plastic tangent stiffness matrix

Flexibility-based method is used to formulate the distributed plasticity model of a 3D beam-column element with 12 DOFs [1]. An element is represented by several cross-sections (i.e. stations) that are located at the numerical integration scheme points. The bending moments in these stations are computed through a second-order transfer matrix as functions of the nodal element forces following a detailed procedure given in [1]. The spread of inelastic zones within an element is captured considering the variable section flexural EI_y and EI_z and axial EA rigidity along the member length, depending on the bending moments and axial force level. Thus the nonlinear response of a beam-column element can be computed as a weighted sum of the response of a discrete number of cross-sections. Gradual plastification through the cross-section is modelled using the inelastic Ramberg-Osgood force strain relationships in conjunction with Orbisons's failure surface (Fig.2), and then, tangent stiffness properties of the cross sections are integrated along the member length to yield the member stiffness coefficients [1].

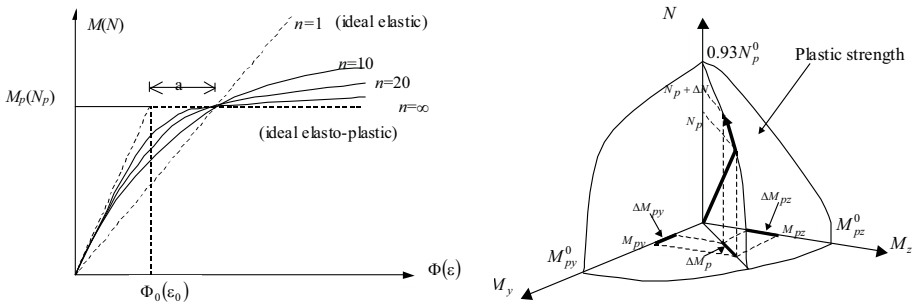

Fig.2. (a) Ramberg-Osgood force strain relationships; (b) Orbison's failure surface

2.2. The second-order effects on tangent stiffness matrix

The geometrical nonlinear effects for each element are taken into account in the present analysis, in a beam column approach, by the use of the inelastic stability stiffness functions and updating at each load increment the length, axial force and the flexural rigidity about of each principal axes of the element. This way minimizes modelling and solution time, generally only one or two elements are needed per member [1]. The effect of axial force on torsional stiffness is ignored in the present formulation.

2.3. Formulation of the tangent stiffness matrix with semi-rigid connections

The effects of semi-rigid connections are included in the analysis adopting the model presented in Fig.3 [2]. The behaviour of the connection element in each

principal bending direction (major and minor axis flexibility) is represented by a rotational spring, as shown in Fig.3 (a). We assume no coupling between different rotational degree of freedom at the connection. Assuming that axial, shearing and torsion deformations of the connections are negligible, the tangent stiffness relation of a connection element can be written as [2]:

$$\begin{bmatrix} M_{iy} \\ M_{jy} \\ M_{iz} \\ M_{jz} \end{bmatrix} = \begin{bmatrix} R_{iy} - \frac{R_{iy}^2}{\beta_y}\left(R_{jy} + k_{jjy}\right) & \frac{k_{ijy}}{\beta_y} R_{iy} R_{jy} & 0 & 0 \\ \frac{k_{ijy}}{\beta_y} R_{iy} R_{jy} & R_{jy} - \frac{R_{jy}^2}{\beta_y}\left(R_{iy} + k_{iiy}\right) & 0 & 0 \\ 0 & 0 & R_{iz} - \frac{R_{iz}^2}{\beta_z}\left(R_{jz} + k_{jjz}\right) & \frac{k_{ijz}}{\beta_z} R_{iz} R_{jz} \\ 0 & 0 & \frac{k_{ijz}}{\beta_z} R_{iz} R_{jz} & R_{jz} - \frac{R_{jz}^2}{\beta_z}\left(R_{iz} + k_{iiz}\right) \end{bmatrix} \begin{bmatrix} \theta_{niy} \\ \theta_{njy} \\ \theta_{niz} \\ \theta_{njz} \end{bmatrix} \tag{1}$$

$$\beta_y = \det\begin{bmatrix} k_{ii,y} + R_{i,y} & k_{ij,y} \\ k_{ij,y} & k_{jj,y} + R_{j,y} \end{bmatrix}; \beta_z = \det\begin{bmatrix} k_{ii,z} + R_{i,z} & k_{ij,z} \\ k_{ij,z} & k_{jj,z} + R_{j,z} \end{bmatrix} \tag{2}$$

where M_i, M_j are the applied moments at the element nodes i and j, θ_n and θ_b are the node, respective end element rotation, $\theta_r=\theta_n-\theta_b$ is the relative rotational angle, R_i, R_j the initial connection stiffness. From (1) and (2) the components of stiffness matrix, considering the effects of flexible connections can be determined. If the connection have a linear-elastic behaviour, then the connection rigidities R_i, and R_j are constants. If the connection behaviour is nonlinear, the following connection model is adopted in accordance with experimental model proposed in [4]:

$$\frac{M}{M_u} = \frac{\theta_r / \theta_0}{\left[1 + \left(\theta_r / \theta_0\right)^n\right]^{1/n}} \tag{3}$$

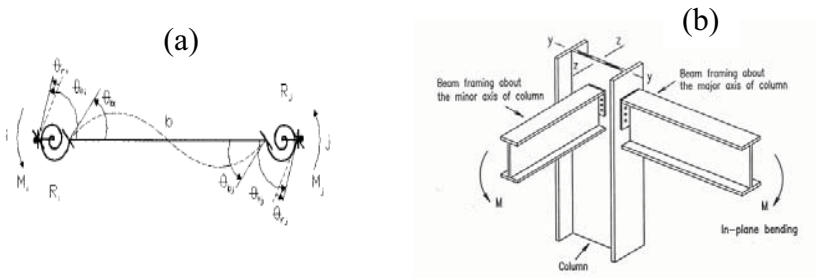

Fig.3. Semi-rigid connections (a) Beam-column element with semi-rigid connections (*X-Y* plane); (b) Beam-to-column connections

where M is the applied moment, M_u is ultimate moment capacity of the connection, n is the shape parameter, θ_0 is the reference plastic rotation defined as M_u/R_{i0}, and R_{i0} is the initial connection stiffness. The present formulation can model both major

and minor axis flexibility. However, in this study, only the relative rotations about the major-axis of the beam section are allowed at the semi-rigid connections. This is due to two reasons: (1) at present there is little experimental information on the torsional and out-of-plane behaviours of a semi-rigid connection, and (2) for typical framed structures with rigid floor diaphragms, the torsional and out-of-plane effects of semi-rigid connections are not significant.

2.4. Equivalent fixed-end forces

To perform the nonlinear analysis of frame structures, in the majority of previous publications, the loads are assumed to apply only at the nodes. In the present investigation, the loading due to the member lateral loads and transferred to the nodes are allowed and included automatically in the analysis. This leads to a significant saving in inputing the member loads, without the need to divide a member into several elements for simulation of these loads.

The elasto-plastic equivalent nodal forces transferred to the nodes, from the member loads, will not be constant during the analysis, and will be dependent on the variable flexural rigidity along the member according with the process of gradual formation of plastic zones. The equivalent nodal forces will be computed in order to accommodate member lateral loads, local geometrical imperfections and the plastic strength surface requirements [1]. The second-order and flexible joints effects on fixed-end forces and moments due to transverse loads, are taken into account, as well [2].

2.5 Geometry updating and force recovery

Using an updated Lagrangian formulation (UL) the nonlinear geometrical effects are considered updating the element forces and geometry configurations at each load increment. The natural deformation approach (NDA) in conjunction with the geometrical "rigid body qualified" stiffness matrix [5] is adopted for the element force recovery and the web plane vector approach is effectively used to update the frame element coordinates [1]. The element incremental displacements can be conceptually decomposed into two parts: the rigid body displacements and the natural deformations.

The rigid body displacements serve to rotate the initial forces acting on the element from the previous configuration to the current configuration, whereas the natural deformations constitute the only source for generating the incremental forces. The element forces at the current configuration can be calculated as the summation of the incremental forces and the forces at the previous configuration.

2.6. Diaphragm action

For normal building frameworks, a floor slab may be modelled as a rigid diaphragm, which is assumed to provide infinite in-plane stiffness and without any

out of plane stiffness. The lateral response of the floor slab is characterized by two translational and one rotational degrees of freedom located at the floor master node. The multi-freedom constraints, required by the rigid body floor model, are imposed by augmenting the finite element model just described, with the penalty elements. The main advantages of this technique with respect to the traditional master-slave elimination technique are its lack of sensitivity with respect to whether constraints are linearly dependent and its straightforward computer implementation.

Considering the homogenous constraints $\mathbf{Au}=0$ the penalty augmented system can be written compactly as:

$$\left(\mathbf{K}_T + \mathbf{A}^T\mathbf{W}\mathbf{A}\right)\Delta\mathbf{U} = \Delta\mathbf{F} \tag{4}$$

where $\mathbf{W}$ is a diagonal matrix of penalty weights, $\mathbf{A}$ is the unscaled matrix of the penalty elements, $\mathbf{K}_T$ is the global tangent stiffness matrix, $\Delta\mathbf{U}$ and $\Delta\mathbf{F}$ are the incremental displacement and force vector, respectively.

3. ANALYSIS ALGORITHM AND COMPUTER PROGRAM

In order to trace the equilibrium path, for proportionally and non-proportionally applied loads, the proposed model has been implemented in a simple incremental and incremental- iterative matrix structural-analysis program. In the simple incremental method, the simple Euler stepping algorithm is used in conjunction with constant work-load increments, whereas in the incremental-iterative approach, at each load increment a modified constant arc-length method is applied to compute the complete nonlinear load-deformation path [1].

Convergence of the iterative process is said to have occurred when within certain tolerances, moments at the element nodes and stations nowhere exceeds their limiting plastic values and the internal actions are in equilibrium with the applied external loads.

Based on the analysis algorithm just described, an object-oriented computer program, NEFCAD 3D, has been developed to study the combined effects of material, geometric and connection nonlinear behavior on the load-versus-deflection response for spatial framed structures. It combines the structural analysis routine with a graphic routine to display the final results [8].

The graphical interface allows for easy generation of data files, graphical representation of the data, and plotting of the deflected shape, bending moments, shear force and axial force diagrams, load-deflection curves for selected nodes, etc.

4. COMPUTATIONAL EXAMPLE

Although there are wide benchmark solutions available for rigid steel space frames and semi-rigid steel plane frames [8,10], in the open literature, no available benchmark problems of semi-rigid space frames subjected to combined action of gravity and lateral forces are available for verification study.

The Orbison's six story rigid space frame, studied previously by other researchers [9,10] was used in the verification study. The effects of rigid and semi-rigid connections, with either linear or nonlinear behaviour, of the space frame have been investigated.

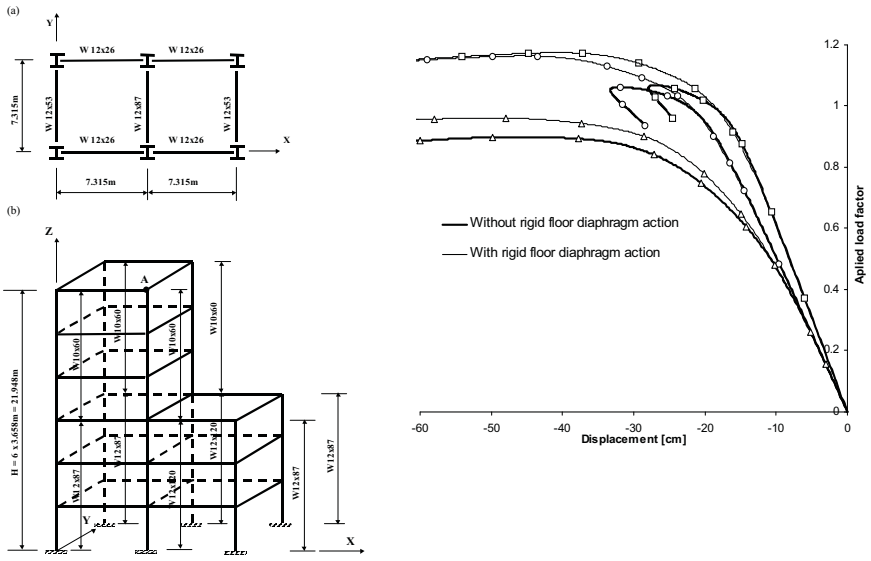

Fig. 4. Six-story space frame: (a) plan view; (b) perspective view; (c) Load-displacement curves at *Y* dirrection for node *A*

Further, in this study, the effect of rigid floor diaphragm action is investigated, as well. In the case of semi-rigid beam-columns connections, the beam connections were top and seat angles having the following characteristics:

(1) at the beam framing about the major-axis of column (see Fig.3b), the fixity factor g=0.86, ultimate moment M_u=300kNm, shape parameter n=1.57,

(2) at the beam framing about the minor-axis of column, the fixity factor g=0.86, ultimate moment M_u=200 kNm, shape parameter n=0.86.

The yield strength of all members is 250 MPa, Young´s modulus is E=206850 MPa and shear modulus G=79293 MPa. The frame is subjected to the combined action of gravity and lateral loads acting in the *Y*-direction.

Uniform floor pressure is 9.6 kN/m^2 and the wind loads are simulated by point loads of 53.376 kN in the *Y* direction at every beam-column joints.

One element with seven integration points (*NG*=7) has been used to model each column and beam; gradual plastification through the cross-section is modelled using the inelastic Ramberg-Osgood force strain relationships with the shape parameters *a*=1 and *n*=35 [1].

The load displacement curves of rigid and semi-rigid connections (with linear or nonlinear behaviour), and with or without the effect of rigid floor diaphragm action are compared in Fig. 4(c).

The ultimate load factors are depicted in Fig. 4(c), as well. As it can be seen, semi-rigid connection is a very crucial element, and must be considered in a valuable advanced analysis method.

Analyses carried out, indicate that the ultimate load factor of the framework can be increased up to 12% if the effect of rigid floor diaphragm action is considered in the analysis.

5. CONCLUSIONS

A reliable and robust nonlinear inelastic analysis of semi-rigid space frames has been developed. The proposed analysis can practically account for all key factors influencing steel space frame behavior: gradual yielding associated with biaxial bending and axial force, shear deformations, local and global second order effects, rigid diaphragm action, and nonlinear behavior of semi-rigid connections, with computational efficiency, and the necessary degree of accuracy, usually only one element per member is necessary to analyze.

Furthermore, distributed loads acting along the member length and local geometrical imperfections can be directly input into the analysis without the need to divide a member into several elements for simulation of these factors leading to a consistency in the linear and the nonlinear structural models.

The recent studies of the author [1] concerning the nonlinear inelastic analysis of 3D rigid space frames shows that the proposed method can be used in lieu of the costly plastic zone analysis methods.

References

1. Chiorean, C.G., Bârsan, G.M., - Large deflection distributed plasticity analysis of 3D steel frameworks, *Int. J. Comput. & Struct*., 83 (19-20), 2005.
2. Bârsan, G.M., Chiorean, C.G., - Computer program for large deflection elasto-plastic analysis of semi-rigid steel frameworks, *Int. J. Comput. & Struct*., 72, p. 699-711, 1999.

3. Chen, W.F., Toma, S., Advanced analysis of steel frames, CRC Press, US, 1994.
4. Chen, W.F., Kim S.E., LRFD steel design using advanced analysis, Boca Raton, FL., CRC Press, 1997.
5. Yang, Y.B., Yau, J.D., Leu, L.J., - Recent developments in geometrically nonlinear and postbuckling analysis of framed structures, *Appl. Mech. Rev*., 56(4), p.431-49, 2003.
6. Kishi, N., Chen, W.F., - Moment-rotation relations of semi-rigid connections with angles*, J. Struct. Engng*., 116(7), 1813-34, 1990.
7. Liew, J.Y.R., Chen, W.F., Chen, H., - Advanced inelastic analysis of frame structures*, J. Construct. Steel Res*., 55, p. 245-65, 2000.
8. Chiorean, C.G., - NEFCAD: Computer program for nonlinear inelastic analysis of 3D frame structures, Online documentation, https://users.utcluj.ro/~ccosmin
9. Kim, S.E., Choi, S.H., - Practical advanced analysis for semi-rigid space frames*, Int.J. Solids Struct*., 38, 9111-131, 2001.
10. Jiang, X.M, Chen, H., Liew, JYR, - Spread of plasticity analysis of three-dimensional steel frames, *J. Construct. Steel Res*., 58, 193-212, 2002.

"Computational Civil Engineering 2006", International Symposium
Iaşi, România, May 26, 2006

A computer program for *M-N-*Φ and *N-M-M* analysis of reinforced concrete sections

Cosmin G. Chiorean

Faculty of Civil Engineering, Technical University of Cluj-Napoca, Cluj-Napoca, 400020, Romania

Summary

A computer method for inelastic analysis of reinforced and composite concrete cross-sections of arbitrary shape subjected to axial force and biaxial bending moments is presented. The method can be applied to complex cross-sections of arbitrary shape and curved edges, with or without openings and consisting of various materials. An incremental-iterative procedure based on arc-length constraint equation is proposed in order to determine the M-N-Φ and N-M-M diagrams of arbitrary cross-sections.

This procedure adopts a tangent stiffness strategy for the solution of the non-linear equilibrium equations thus resulting in a high rate of convergence. The cross-section tangent stiffness derived here insures the convergence of the solution for the equilibrium equations in any load case. Based on Green's theorem, the domain integrals appearing in the definition of stress resultants and tangent stiffness are evaluated in terms of boundary integrals when the section boundary is rectilinear or circular. Various effects such as concrete confinement, strain hardening of the reinforcement bars, etc. may be taken into account. An object oriented computer program with full graphical interface, to obtain the ultimate strength of reinforced and composite concrete cross-sections under combined biaxial bending and axial load was developed.

In order to illustrate the proposed method and its accuracy and efficiency, this program was used to study several representative examples, which have been studied previously by other researchers using independent fibber element solutions. Examples run and comparisons made have proved the effectiveness and time saving of the proposed method of analysis.

KEYWORDS: Non-linear analysis; Reinforced concrete; stress integration; Cross-section analysis; Biaxial bending

1. INTRODUCTION

In recent years, some methods have been presented for the ultimate strength analysis of various concrete and composite steel-concrete sections such as

rectangular, L and T -shape, and polygonal, under biaxial moments and axial loads [2-9].

Among several existing techniques, two are the most common; the first consists of a direct search procedure to obtain either the strain equilibrium plane or the location and inclination of the neutral axis. This method can be used under any loading mode, but is rather time-consuming.

The second approach is based upon the solution of the non-linear equilibrium equations according to the classical Newton's scheme consisting of an iterative sequence of linear predictions and non-linear corrections. In general, this method gives fast solutions but some problems in convergence may arise, particularly when the initial or starting values of variables are not selected properly [8].

A further complication is represented by the non-linear constitutive law that is usually assumed for concrete in compression. Most existing methods for the analysis of cross sections under axial load and biaxial bending rely on the numerical integration of stress resultants using the well known "fibber decomposition method" where the cross-section is decomposed in filaments analysing the section response by composing the uniaxial behaviour of each filament [9].

This technique is not numerically efficient, due to the large amount of information needed to characterise the section and the high number of operations required implementing the stress integration with an allowable error level [9]. Rodriguez and Ochoa [3] presented a method to determine the biaxial interaction diagrams for any orientation of the neutral axis of RC short columns with any geometry, obtaining analytical closed form integral expressions for internal forces. Recently, Sfakianakis [7] developed an alternative method based of fibber decomposition approach that employs computer graphics as a computational tool for the integration of normal stresses over the section area. Based on Green's theorem Rotter [4] and then Fafitis [5] developed numerical procedures for numerical integration of concrete in compression, but these formulations are limited to fully confined concrete (i.e. the descending curve of the concrete is not included) and to polygonal cross-sections only.

Based on the secant stiffness strategy for the solution of non-linear equilibrium equations De Vivo and Rosati [6] developed two algorithms for evaluating the ultimate strength capacity of polygonal RC cross-sections, and an original boundary integration formula is presented.

The main objective of the present paper is to present a new formulation by which the biaxial interaction diagrams of an arbitrary composite steel-concrete cross-section can be determined. An incremental-iterative procedure based on arc-length constraint equations is proposed in order to determine the biaxial strength of an arbitrary cross-section for a given bending moment's ratio. A particularly

important feature of the present method is based on Green's integration formula according to which the domain integrals appearing in the evaluation of internal resultant efforts and tangent stiffness matrix coefficients of the section can be evaluated in terms of boundary integrals. Then the boundary integrals can be evaluated analytically or numerically.

To perform the analysis of circular cross section or sections with circular openings, in the majority of the previous publications a polygonal approximation is required. In the present approach, this approximation is eliminated. In this way, inelastic behaviour can be accurately computed with favourable effects on the computational and computer storage effort. The algorithm presented in the current paper is general and complete, and, of great importance, it is fast and assures convergence for any load case.

2. MATHEMATICAL FORMULATION

Consider the cross-section subjected to the action of the external bending moments about each global axes and axial force as shown in Figure 1. It is assumed that plane section remains plane after deformation and perfect bond and lack of shear postulates are implicit. Thus resultant strain distribution corresponding to the curvatures about global axes $\mathbf{\Phi}=\{\Phi_x, \Phi_y\}$ and the axial compressive strain ε_0 can be expressed in point $r = \{x, y\}$ in a linear form as:

$$\varepsilon = \varepsilon_0 + \Phi_x y + \Phi_y x = \varepsilon_0 + \mathbf{\Phi r}^T \tag{1}$$

Equilibrium is satisfied when the external forces are equal to the internal forces. The basic equations of equilibrium for the axial load N and the biaxial bending moments $\lambda M_{x,ref}$, $\lambda M_{y,ref}$ are given in terms of the stress resultants as:

$$\begin{aligned} &\int_A \sigma(\varepsilon_0, \Phi_x, \Phi_y) dA - N_{ext} = 0 \\ &\int_A \sigma(\varepsilon_0, \Phi_x, \Phi_y) y dA - \lambda M_{x,ref} = 0 \\ &\int_A \sigma(\varepsilon_0, \Phi_x, \Phi_y) x dA - \lambda M_{y,ref} = 0 \end{aligned} \tag{2}$$

The problem of the ultimate strength analysis of cross-sections can be formulated as [6]: Find the maximum values of loading parameter λ so as to fulfil at least one of the following conditions:

$$\max_{r \in A_c^*} \left\{ \Phi^* \mathbf{r}^T + \varepsilon_0^* \right\} = \varepsilon_{cu} \tag{3.1}$$

$$\max_{i \in \{1..N_a\}} \left\{ \Phi^* \mathbf{r}^T + \varepsilon_0^* \right\} = \varepsilon_{su} \tag{3.2}$$

where Φ^* and ε0 are the components of a generalised deformation vector **d**={Φx,Φy ε0} solution of the non-linear system (2), and Ac is the effective concrete section in compression:

$$A_c^* = \left\{ r \in A_c : \Phi \mathbf{r}^T + \varepsilon_0 \le 0 \right\} \tag{4}$$

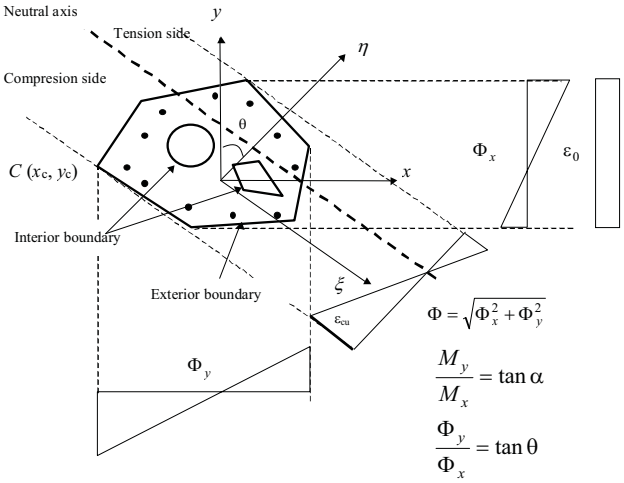

Figure 1. Model of Arbitrary Composite Cross-Section

2.1 Method of solution

An incremental-iterative procedure based on arc-length constraint equation is proposed in order to determine the biaxial strength of an arbitrary composite steel-concrete cross section for a given bending moment's ratio. The failure surface corresponds only to strains of the outer compressed point of the concrete section, consequently the relation (3.2) is omitted in the following discussion for simplicity. Consider an irregular composite section as shown in Figure 1. The global x, y -axes of the cross section could have their origin either in elastic or plastic centroid of the cross-section. For each inclination of the neutral axis defined by the parameters Φx and Φy the farthest point on the compression side is determined (i.e. the point on the exterior boundary with co-ordinates xc, yc). We assume that at this point the condition (3.1) is met:

$$\varepsilon_{cu} = \varepsilon_0 + \Phi_x y_c + \Phi_y x_c \tag{5}$$

Hence, the axial compressive strain ε_0 can be expressed as:

$$\varepsilon_0 = \varepsilon_u - \left(\Phi_x y_c + \Phi_y x_c\right) \tag{6}$$

Thus, resultant strain distribution corresponding to the curvatures Φ_x and Φ_y can be expressed in linear form as:

$$\varepsilon\left(\Phi_x, \Phi_y\right) = \varepsilon_u + \Phi_x\left(y - y_c\right) + \Phi_y\left(x - x_c\right) \tag{7}$$

In this way, the non-linear problem (2) with restriction (3.1) is reduced to the following non-linear system of equations, where the curvatures Φ_x and Φ_y and the load amplifier factor λ represents the unknowns:

$$\begin{aligned} &\int_A \sigma\left(\varepsilon\left(\Phi_x, \Phi_y\right)\right) y dA - \lambda M_{x,ext} = 0 \\ &\int_A \sigma\left(\varepsilon\left(\Phi_x, \Phi_y\right)\right) x dA - \lambda M_{y,ext} = 0 \end{aligned} \tag{8}$$

This can be rewritten in terms of non-linear system of equations in the following general form:

$$\mathbf{F}\left(\lambda, \Phi\right) = \mathbf{f}^{\text{int}} - \lambda \mathbf{f}^{ext} = 0 \tag{9}$$

In an arc-length incremental/iterative solution methods these equations are solved in a series of steps or increments, usually starting from the unloaded state ($\lambda = 0$), using an auxiliary constraint equation that is different for each algorithm [10]:

$$g\left(\lambda, \Phi\right) = 0 \tag{10}$$

The solution to (9) is referred to as equilibrium path and is given by solving the equilibrium equation (9) together with the auxiliary constraint equation (10). Assuming that a point ($^{\tau}\Phi$, $^{\tau}\lambda$) of the equilibrium path has been reached, the next point ($^{\tau+1}\Phi$, $^{\tau+1}\lambda$) of the equilibrium path is then computed by solving the equations (9) and (10), through Newton-Raphson procedure:

$$\begin{Bmatrix} {}^{\tau+\Delta\tau}\Phi \\ \Delta\lambda \end{Bmatrix}^{k+1} = \begin{Bmatrix} {}^{\tau+\Delta\tau}\Phi \\ \Delta\lambda \end{Bmatrix}^{k} - \begin{bmatrix} \dfrac{\partial \mathbf{F}}{\partial \Phi} & \dfrac{\partial \mathbf{F}}{\partial \lambda} \\ \dfrac{\partial g}{\partial \Phi} & \dfrac{\partial g}{\partial \lambda} \end{bmatrix}^{-1} \begin{bmatrix} \mathbf{F}\left(\lambda, \Phi\right)^k \\ g\left(\lambda, \Phi\right)^k \end{bmatrix} \tag{11}$$

where k represents the iteration number and the jacobian and tangent stiffness matrix of the cross-section is of the form:

$$\mathbf{J}=\begin{bmatrix}\mathbf{K}_T & -\mathbf{f}_{ext}\\ \dfrac{\partial g}{\partial \Phi} & \dfrac{\partial g}{\partial \lambda}\end{bmatrix} \qquad \mathbf{K}_T=\left(\frac{\partial F}{\partial \Phi}\right)=\begin{bmatrix}\dfrac{\partial M_{x,\mathrm{int}}}{\partial \Phi_x} & \dfrac{\partial M_{x,\mathrm{int}}}{\partial \Phi_y}\\ \dfrac{\partial M_{y,\mathrm{int}}}{\partial \Phi_x} & \dfrac{\partial M_{y,\mathrm{int}}}{\partial \Phi_x}\end{bmatrix} \tag{12}$$

The partial derivatives are with respect to the state of τ. The coefficients of the stiffness matrix can be symbolically evaluated as:

$$\begin{aligned}
k_{11} &= \frac{\partial M_{x,\mathrm{int}}}{\partial \Phi_x}=\frac{\partial}{\partial \Phi_x}\int_A \sigma\left(\varepsilon\left(\Phi_x,\Phi_y\right)\right)ydA=\\
&=\int_A \frac{\partial \sigma}{\partial \varepsilon}\frac{\partial \varepsilon}{\partial \Phi_x}ydA=\int_A E_T y\left(y-y_c\right)dA\\
k_{12} &= \frac{\partial M_{x,\mathrm{int}}}{\partial \Phi_y}=\int_A E_T y\left(x-x_c\right)dA\\
k_{21} &= \frac{\partial M_{y,\mathrm{int}}}{\partial \Phi_x}=\int_A E_T x\left(y-y_c\right)dA\\
k_{22} &= \frac{\partial M_{y,\mathrm{int}}}{\partial \Phi_y}=\int_A E_T x\left(x-x_c\right)dA
\end{aligned} \tag{13}$$

where the coefficients k_{ij} are expressed in terms of the tangent modulus of elasticity E_{T}. Procedure (11) is iterated until convergence upon a suitable norm is attained. The loading factor is then updated as:

$$^{\tau+\Delta\tau}\lambda = {}^{\tau}\lambda + \Delta\lambda \tag{14}$$

In the present approach, the interaction curves are obtained for a given bending moments ratio. This technique generates plane interaction curves for cross-sections under biaxial bending which are much easier to plot and use in actual design.

The failure surface in the *N-Mx-My* space can be defined as the geometrical locus of points (*N*, *Mx*, *My*) which correspond to the ultimate strength of the section.

The axial force N* is computed based on the resultant strain distribution corresponding to the curvatures Φx and Φy solutions of the non-linear system (9), and the ultimate bending moments, Mx and My, are obtained scaling the reference external moments Mx,ref and My,ref through loading factor λ^* given by Equation (14). Graphical representation of the present method according to equation (9) is depicted in Figure 2. It is important to note that, the stiffness matrix of cross-section K_T given by the Equation (12), becomes singular beyond the balance point

(see Figure 2), therefore the above procedure based on arc-length constraint equation is essential to overcomes these difficulties. In the present method the extra constraint equation is given by:

$$g\left(\Delta\Phi,\Delta\lambda\right)=\left({}^{\tau+\Delta\tau}\Phi-{}^{\tau}\Phi\right)^{T}\left({}^{\tau+\Delta\tau}\Phi-{}^{\tau}\Phi\right)+ \\ +\Psi\Delta\lambda^{2}f_{ext}^{T}f_{ext}-\Delta l^{2}=0 \tag{15}$$

where the scaling parameter ψ has a little influence in the results and is usually taken ψ=0, and Δl is the specified arc length for current increment.

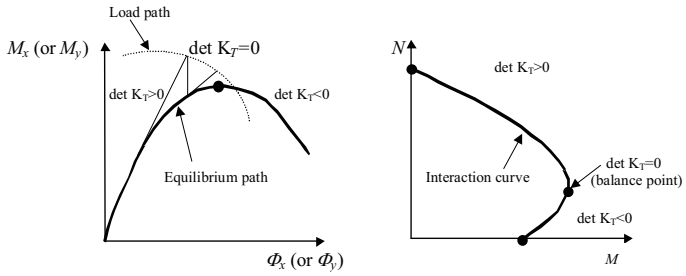

Figure 2. Geometrical representation of the present method.

2.3 Evaluation of tangent stiffness and stress resultant

Based on Green's theorem, the integration of the stress resultant and stiffness coefficients given by the Equation (13) over the cross-section will be transformed into line integrals along the compressive perimeter of this region.

For this purpose, is necessary to transform the variables first, so that the stress field is uniform in a particular direction, given by the current position of the neutral axis [1]. This is achieved by rotating the reference axes to ξ, η oriented parallel to and perpendicular to the neutral axis, respectively (Figure 1) such that:

$$\begin{cases} x=\xi\cos\theta+\eta\sin\theta \\ y=-\xi\sin\theta+\eta\cos\theta \end{cases} \tag{16}$$

where $\tan\theta=\Phi_y/\Phi_x$. Thus, the stress field is uniform in direction parallel with the neutral axis: $\sigma\left(\xi,\eta\right)=\sigma\left(\eta\right);\ E_T\left(\xi,\eta\right)=E_T\left(\eta\right)$.

Based on this transformation, the internal forces carried on by the compressive concrete section can be obtained by the expressions:

$$
\begin{aligned}
N_{\text{int}} &= \iint \sigma(x,y)dxdy = \iint \sigma(\eta)d\xi d\eta \\
M_{x,\text{int}} &= \iint \sigma(x,y)ydxdy = \\
&= \iint \sigma(\eta)(-\xi \sin\theta + \eta\cos\theta)d\xi d\eta \\
&= M_{\xi,\text{int}} \cos\theta - M_{\eta,\text{int}} \sin\theta \\
M_{y,\text{int}} &= \iint \sigma(x,y)xdxdy = \\
&= \iint \sigma(\eta)(\xi \cos + \eta \sin\theta)d\xi d\eta \\
&= M_{\xi,\text{int}} \sin\theta - M_{\eta,\text{int}} \cos\theta
\end{aligned}
\tag{17}
$$

where N_{int}, $M_{\xi,int}$ and $M_{\eta,int}$ are the internal axial force and bending moments about the ξ and η axis respectively and can be obtained by the following expressions:

$$
\begin{aligned}
M_{\xi,\text{int}} &= \iint \sigma(\eta)\eta d\xi d\eta = \oint \sigma(\eta)\xi\eta d\eta \\
M_{\eta,\text{int}} &= \iint \sigma(\eta)\xi d\xi d\eta = \frac{1}{2}\oint \sigma(\eta)\xi^2 d\eta \\
N_{\text{int}} &= \iint \sigma(\eta)d\xi d\eta = \oint \sigma(\eta)\xi d\xi d\eta
\end{aligned}
\tag{18}
$$

Using the following notations:

$$
\begin{aligned}
s_1 &= \iint E_T(\eta)\eta^2 d\xi d\eta = \oint E_T(\eta)\eta^2\xi d\eta \\
s_2 &= \iint E_T(\eta)\xi^2 d\xi d\eta = \frac{1}{3}\oint E_T(\eta)\xi^3 d\eta \\
s_3 &= \iint E_T(\eta)\xi\eta d\xi d\eta = \frac{1}{2}\oint E_T(\eta)\xi^2\eta d\eta \\
s_4 &= \iint E_T(\eta)\eta d\xi d\eta = \oint E_T(\eta)\xi\eta d\eta \\
s_5 &= \iint E_T(\eta)\xi d\xi d\eta = \frac{1}{2}\oint E_T(\eta)\xi^2 d\eta
\end{aligned}
\tag{19}
$$

the elements of the tangent stiffness matrix of the section can also be obtained:

$$
\begin{aligned}
k_{11} &= S_1 - y_c S_4 \\
k_{12} &= S_3 - x_c S_4 \\
k_{21} &= S_3 - y_c S_5 \\
k_{22} &= S_2 - x_c S_5
\end{aligned}
\tag{20}
$$

$$\begin{Bmatrix} S_1 \\ S_2 \\ S_3 \\ S_4 \\ S_5 \end{Bmatrix} = \begin{bmatrix} c & -s & & & \\ s & c & & & \\ & & -2sc & c^2 & s^2 \\ & & c^2 - s^2 & sc & -sc \\ & & 2sc & s^2 & c^2 \end{bmatrix} \begin{Bmatrix} s_1 \\ s_2 \\ s_3 \\ s_4 \\ s_5 \end{Bmatrix} \tag{21}$$

where $c = \cos\theta$, $s = \sin\theta$ and A_c is the compressed region of the concrete, L is the compressive perimeter of this region, $\sigma(\eta)$ and $E_T(\eta)$ is the concrete stress and tangent elasticity modulus of deformation of the fibber η respectively.

In order to perform the integral of a determined side of the contour of the integration area (L_i) the Gauss-Lobatto method is used. Though this rule has lower order of accuracy than customary Gauss-Legendre rule, it has integration points at each ends of interval, and hence performs better in detecting yielding.

However, because the stress filed is defined by a step function (i.e. a second-degree parabola, for ascending part, and a straight line for descending part) and there is no continuity in the derivative, the polynomial interpolation can produce important integration errors. In this case, it is better to subdivide the integration area into thick layers parallel to the neutral axis [9].

The contribution of the steel reinforcement bars does not present computational difficulties. The steel bars are assumed discrete points with area A_{sj}, co-ordinates x_{sj}, y_{sj} and stress f_{sj}. The total steel axial force and bending moment resultants are:

$$\begin{aligned} N_s &= \sum_{i=1}^{N_b} A_{sj} f_{sj} \\ M_{xs} &= \sum_{i=1}^{N_b} y_{sj} A_{sj} f_{sj} \\ M_{ys} &= \sum_{i=1}^{N_b} x_{sj} A_{sj} f_{sj} \end{aligned} \tag{22}$$

To avoid double counting of the concrete area that is displaced by the steel bars, the force $A_{sj} f_{cj}$ is subtracted from the bar force $A_{sj} f_{sj}$, where $A_{sj} f_{cj}$ being the concrete compressive stress at the centroid of the bar.

3. NUMERICAL EXAMPLES

Based on the analysis algorithm just described, a computer program, **ASEP** has been developed to study the biaxial strength behaviour of arbitrary RC cross sections. It combines the analysis routine with a graphic routine to display the final results (Figure 3).

The computational engine was written in Turbo Pascal/C++. The graphical interface was created using Microsoft Visual Basic 6. Dynamic Link Libraries (DLL) are used to communicate between the interface and engine. Many options are included in order to be a user friendly computer program.

The graphical interface allows for easy generation of cross-sectional shapes and reinforcement bars, graphical representation of the data, and plotting of the complete stress field over the cross-section, instantaneous position of neutral axis and interaction diagrams N-M_x-M_y. **ASEP** has a library of standard cross-sectional shapes and profiles in an easy to use interactive template.

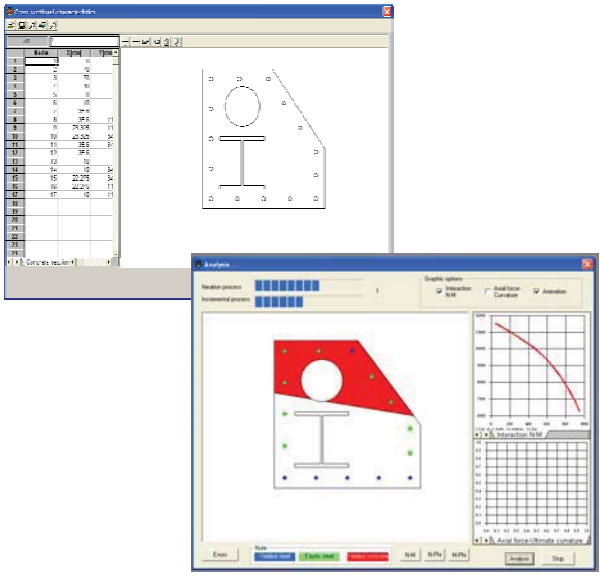

Figure 3. ASEP screen-shots.

The material model is automatically set to the proper strength and ductility levels based the geometry and the input parameters from the template. Input data in the section template can each be changed and then automatically, a sketch of the section is drawn. As material is added, everything is shown on the section colour coded to verify proper input and to see that everything looks correct. **ASEP** offers six material models: EC2 models for unconfined and confined concrete; bilinear steel, bilinear with linear strain hardening, Ramberg-Osgood, and user defined

models. Material parameters can be input very quickly and stress-strain curves can be viewed for correctness.

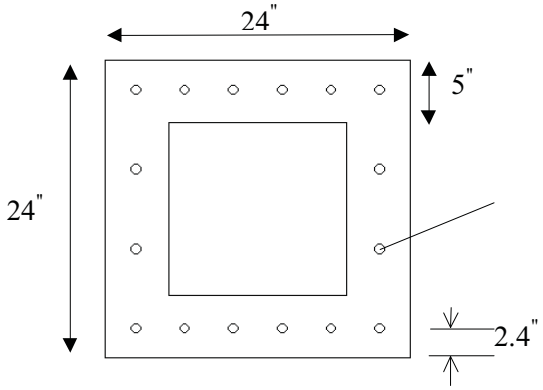

Figure 4. Example 3. Box cross-section with reinforcement arrangement.

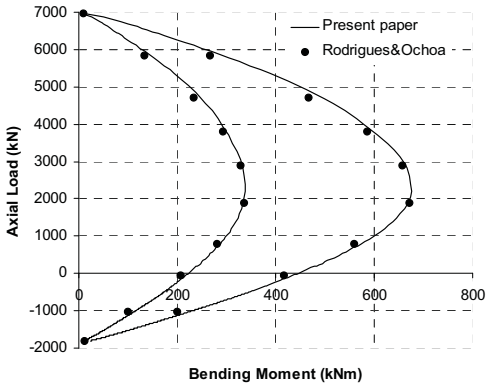

Figure 5. Example 3. Biaxial Interaction Curves.

The accuracy of the analytic procedure developed here has been evaluated using two selected benchmark problems analysed previously by other researchers using independent solutions.

In all computational examples, the stress-strain curve of the concrete under compression is represented by a combination of a second- degree parabola (for ascending part) and a straight-line (for descending part) [2].

The concrete tensile strength is neglected. A bi-linear elasto-plastic stress-strain relationship for the reinforcement bars, both in tension and in compression is assumed.

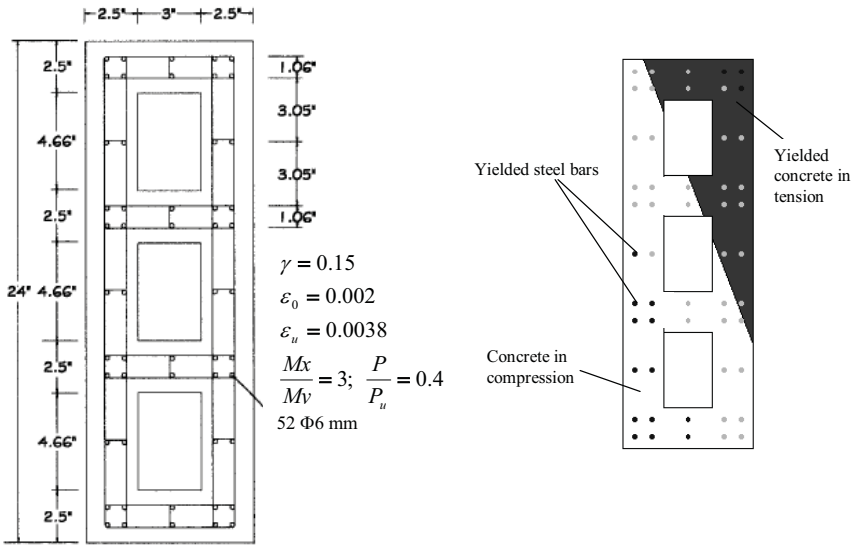

Figure 6. Rectangular RC Hollow Pillar. (a) Cross Sectional Properties and Reinforcement Arrangement; (b) Plastic status at ε_u=0.004.

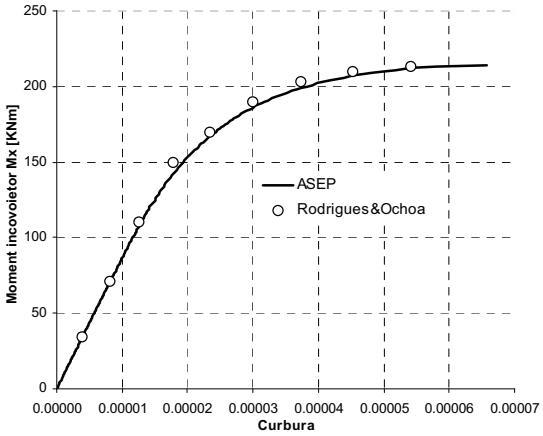

Figure 7 (a) *M-N-*Φ Diagrams in *X* direction

3.1. Example 1. Biaxial interaction diagrams for box section

Determine the biaxial interaction curves for the box cross-section using the centroidal axes as shown in Figure 4 and for $\alpha = 26.57^0$. Assume that $f_c^{'}$=27.58 Mpa, f_y=413.69 Mpa, ε_0=0.002, ε_u=0.0038, γ=0.15, and $f_c^{''}$=0.85 $f_c^{'}$. This problem was also solved by Rodrigues and Aristizabal-Ochoa (Rodrigues & Ochoa, 1999).

Figure 5 shows the corresponding interaction curves for both M_x and M_y of this section. As it can be seen the proposed interaction diagrams are in good agreement with that of Rodrigues & Ochoa [3].

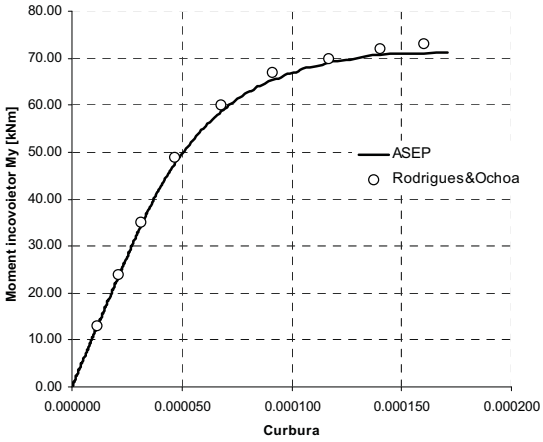

Figure 7 (b) *M-N-*Φ Diagrams in *Y* dirrection

4. CONCLUSIONS

A new computer method based on incremental-iterative arc-length technique has been presented for the ultimate strength analysis of composite steel-concrete cross-sections subjected to axial force and biaxial bending. Various effects such as concrete confinement, strain hardening of the reinforcement etc. may be taken into account. An object oriented computer program with full graphical interface, to obtain the ultimate strength of composite cross-sections under combined biaxial bending and axial load was developed. The method has been verified by comparing the predicted results with the established results available from the literature. The studies show that the proposed method is in general fast, stable, accurate and assures convergence for any load case.

References

1. Chiorean, C.G. 2004, A fast incremental-iterative procedure for inelastic analysis of RC cross-sections of arbitrary shape, *Acta Technica Napocensis*, 47: 85-98.
2. Rodrigues, J.A. & Aristizabal-Ochoa, J.D. 1999 M-P-Φ diagrams for reinforced, partially, and fully prestressed concrete sections under biaxaial bending and axial load, *Journal of Structural Engineering*, ASCE, 127(7): 763-773.

3. Rodrigues, J.A. & Aristizabal-Ochoa, J.D. 1999 Biaxial interaction diagrams for short RC columns of any cross section, *Journal of Structural Engineering*, ASCE, 125(6): 672-683.
4. Rotter, J.M. 1985, Rapid exact inelastic biaxial bending analysis, *Journal of Structural Engineering*, ASCE, 111(12):2659-2673.
5. Fafitis A. 2001, Interaction surfaces of reinforced-concrete sections in biaxial bending, *Journal of Structural Engineering*, ASCE, 127(7): 840-846.
6. De Vivo, L. & Rosati, L. 1998, Ultimate strength analysis of reinforced concrete sections subject to axial force and biaxial bending, *Computer Methods in Applied Mechanics and Engineering*, 166:261-287.
7. Sfakianakis, M.F. 2002, Biaxial bending with axial force of reinforced, composite and repaired concrete cross sections of arbitrary shape by fibber model and computer graphics, *Advances in Engineering Software*, 33: 227-242.
8. Chen S.F., Teng J.G. & Chan S.L. 2001 Design of biaxially loaded short composite columns of arbitrary section, *Journal of Structural Engineering*, ASCE, 127(6), 678-685.
9. Bonet, J.L., Romero, M.L., Miguel, P.F. & Fernandez M.A. 2004 A fast stress integration algorithm for reinforced concrete sections with axial loads and biaxial bending, *Computers and Structures*, 82:213-225.
10. Crisfield, M.A. 1991, Non linear finite element analysis of solids and structures, Wiley, Chichester.

"Computational Civil Engineering 2006", International Symposium
Iaşi, România, May 26, 2006

CFD simulation of indoor climate

Ondřej Šikula

Institute of Building Services, Brno University of Technology, Brno, 602 00, Czech Republic

Summary

The paper presents the experience acquired by the CFD (Computational Fluid Dynamics) simulation of indoor climate in a room heated by a gas space heater. The vertical air temperature difference in room is one of the indoor climate parameters. The simulation presents the non-stationary airflow and the distribution of temperatures in a dwelling room. The main goal of the paper is to identify factors which make a great vertical air temperature difference. Especially in a room which is heated up with high temperature of air. The paper compares results of CFD simulation with the measuring of temperatures and velocities in this room. The results can be considered trustworthy only if proper models of turbulence and radiation are used. The next goal is finding out appropriate turbulence and radiation models which could describe both heat transfer mechanisms in the room. The simulation is solved in the computer program FLUENT.

KEYWORDS: CFD simulations, indoor climate, dwelling room

1. INTRODUCTION

1.1 Indoor climate

The main goal in the field of environmental engineering is to ensure optimal conditions for work, relaxation and residence of people in buildings. Optimal conditions are created artificially by means of heating, ventilation and air-conditioning systems. In this connection we speak about creation of the indoor climate in buildings which can be distinguished as thermal-technical, lighting, acoustic, etc. The substantial part of HVAC designer's work constitutes the ensuring of the proper thermal and moisture microclimate in buildings. During winter and transition periods this problematics is ensured by the field dealing with heating systems. The humidity factor is in practice often omitted, therefore only the thermal component of indoor climate is observed. For simplification the problematics of the indoor climate creation during winter and transition period is focused on residential buildings. Factors creating the thermal microclimate within the room are especially temperature, intensity of thermal radiation and air turbulence level. The characteristic feature of all these factors is their distinctive time and spatial variability. These physical factors are present in all parts of the

room and form the indoor climate of the room. By means of computer simulations and practical measurements can be proven and shown that the state of indoor climate generally varies at individual points of the room and different time periods as well.

Practically it is important to observe the thermal microclimate within spaces occupied by people. This area is designated as the inhabitant's zone.

1.2 Vertical distribution of temperatures as a thermal comfort factor

One of the factors influencing the quality of indoor climate in a dwelling room is the vertical distribution of temperatures. From now on the article deals with this factor. Already the old literature gives attention to this topic. For example [1] recommends the maximal temperature difference between the position of a head (t1,7) and an ankle (t0,1) to be 2,0 K for standing person and 1,5 K for sitting person from the point of view of thermal comfort. At Tab. 1 are stated the ascertained vertical temperature differences for various types of heating according to [1]. The legal regulation for working environment requires the maximal vertical temperature difference to be 3 K, see [5].

Table 1. Maximal vertical temperature difference for standing person

Type of heating	Temp. difference between t1,7 a t0,1
Hot water heating – sectional heating element	1,5
Hot water heating – convector	2,7
Local heating – tiled stove	3,8
Warm-air heating	5,5

The requirement for thermal uniformity is easy to satisfy in case of floor heating, well-designed warm-air hating, etc. Generally we can say that the requirement on vertical temperature distribution is easily reachable when the temperature of the heating surface is not too much higher than the temperature of air. Problematic situations occur by heating systems which produce high temperature in the vicinity of the heating surface. Around very hot heating surfaces (approximately > 90 °C) occurs intensive flow of high air temperature caused by the thermic lifting force. Consequently the vertical temperature difference in the room is greater. Similar situation happens while heating with warm-air heating systems.

2. DESCRIPTION OF THE PROBLEM AND SOLUTION

This article deals with the theoretical and experimental assessment of vertical temperature distribution in a room. We investigate the influence of the heating system with large heating surfaces and high temperatures on the vertical

temperature distribution. The problem was solved theoretically and experimentally on a model room in a brick house heated by a gas space heater. The goal is to find out if the requirement on maximal vertical temperature difference according to [1] between the position of a head and an ankle can be satisfied especially at non-stationary conditions.

Numerical simulation of the airflow and the heat transfer is carried out in the computer software FLUENT on a simplified three-dimensional model of the room.

Theoretical solution

Theoretical solution is based on CFD simulation of the room created in the software Fluent. The calculation is solved for non-stationary conditions and three-dimensional case. The temperature boundary conditions of the model correspond to the condition of the day when the experimental measurement was done. For turbulence calculations the RNG k – e model was used. The heat transfer by long-wave radiation was solved by DO (Discrete ordinates) model.

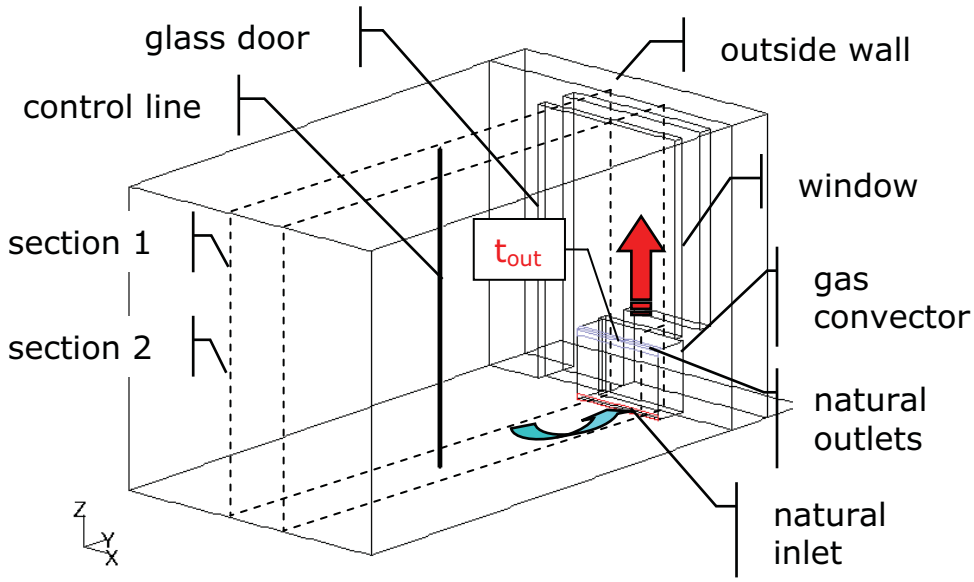

Figure 1. Geometry

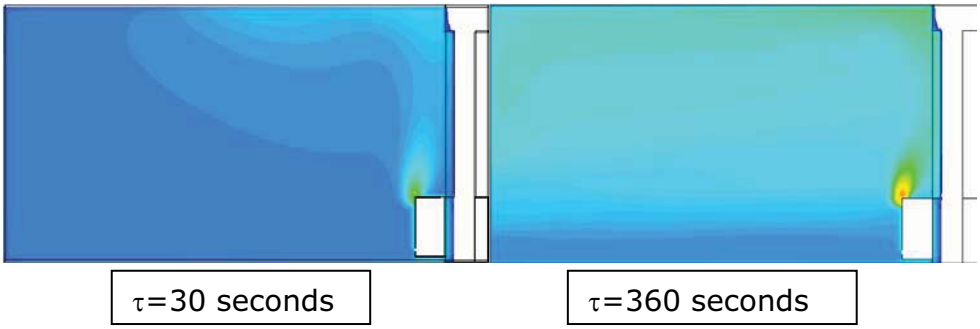

Figure 2. Unsteady temperature fields

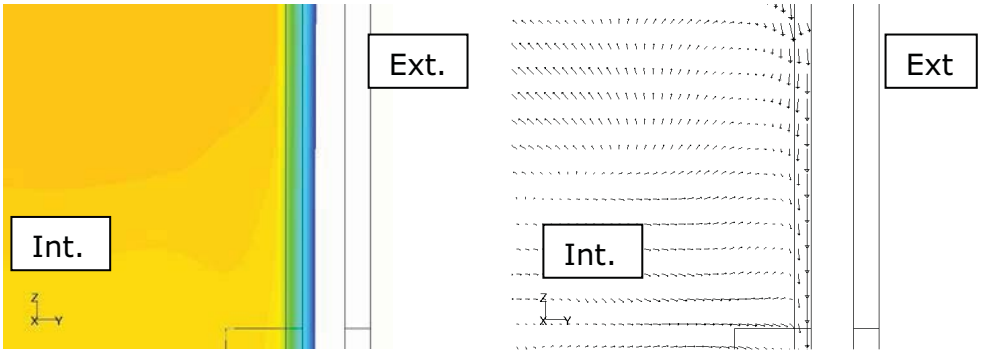

Figure 3. The creation of dropping airflow - section Nr. 1

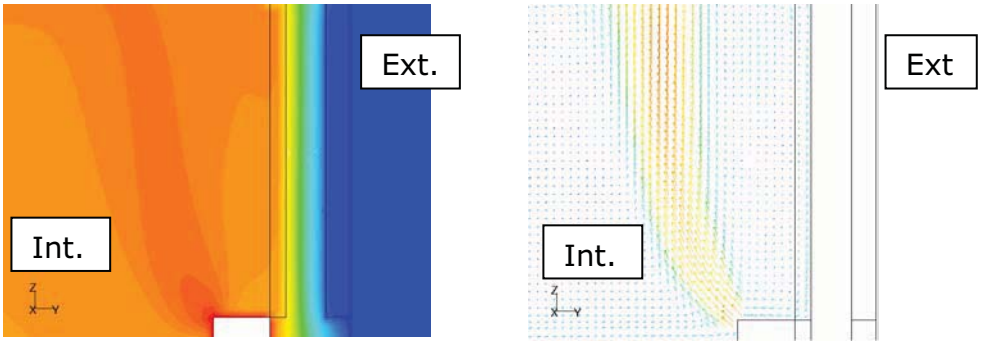

Figure 4. The shading out of dropping airflow - section Nr. 2

Simulation solution enables the illustration of temperature and velocity fields in the analyzed model room.

3. EXPERIMENT

Methods

The experimental measurement was taken in the winter period of 2005/2006 and was divided in two parts. First of all were measured vertical temperatures in eight height points in the symmetry plane of the room. At the same time the velocity and temperature of air coming out of the gas space heater was measured and recorded. Further the monitoring of temperature fields of building structure surfaces was performed by the digital thermal-vision camera IR FLEXCAM. The aim of the temperature, velocity and thermal-vision measurements was the identification of some indoor climate parameters and partially the verification of the numerical simulation results. The measurements proceeded as follows. First the model room was pre-heated (see the first temperature wave at Fig. 5). By this pre-heating the "start" temperature profile of the room was obtained (see the black vertical temperature distribution profile at Fig. 6). By gradual heating the maximal temperature profile was obtained (see the black vertical temperature distribution profile at Fig. 7). After shutdown of the gas space heater the temperatures decreased (see the left vertical temperature distribution profile at Fig. 7). Also the temperature and velocity of the air coming out of the gas space heater and the interior air temperature were continuously measured. The output temperature on the gas space heater reaches its maximal values up to 120 °C. From the measurement follows that the requirement on the vertical temperature difference between the position of a head and an ankle for standing person was just satisfied at the "start" temperature profile. In all remaining phases the requirement was substantially over-ranged.

At Fig. 9 is shown the dependency of the air velocity coming out of the gas space heater on the difference of air temperatures coming out of the gas space heater t_{out} and the interior air temperature t_i. Fig. 8 illustrates the process of pre-heating and cooling of the interior air temperature t_i and its dependency on the air temperature coming out of the gas space heater t_{out}.

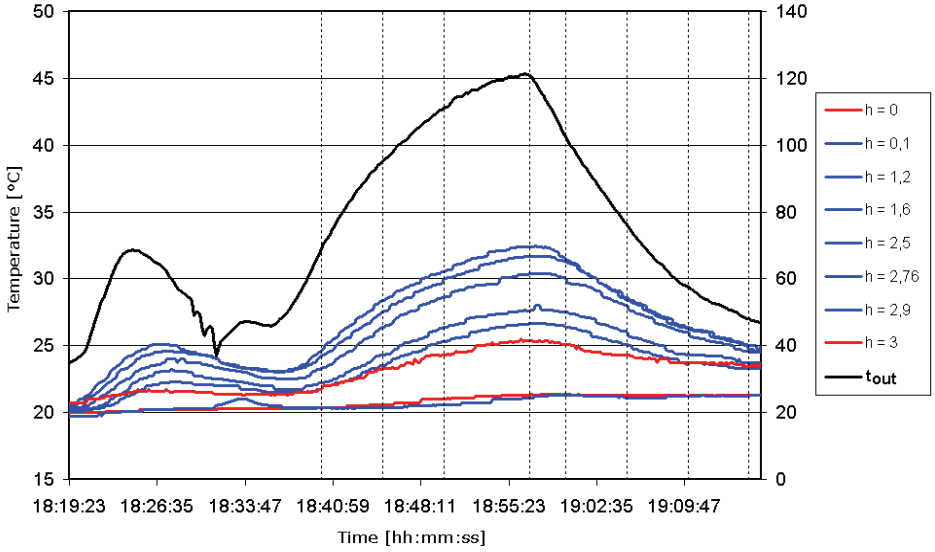

Figure 5. Time flow of the experiment

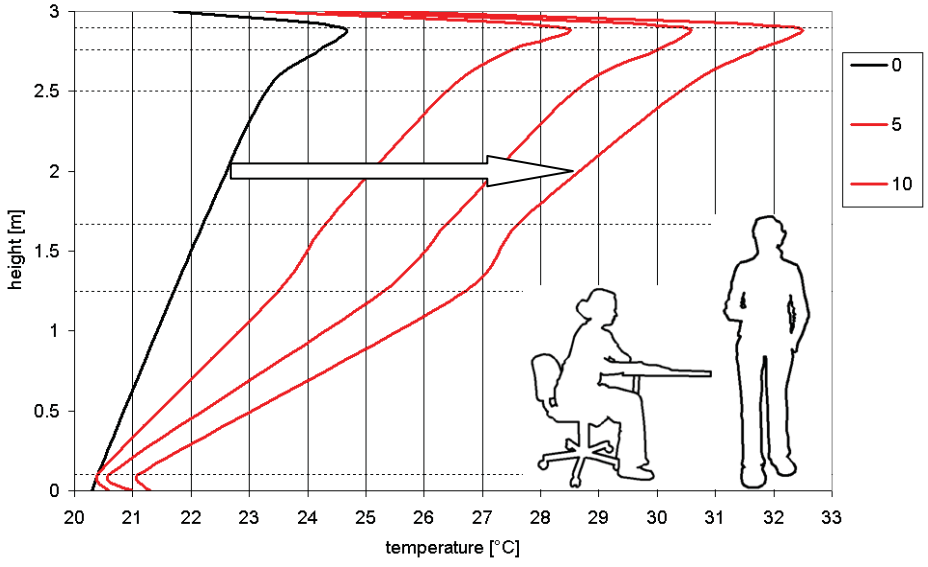

Figure 6. The vertical air temperature difference; warming-up

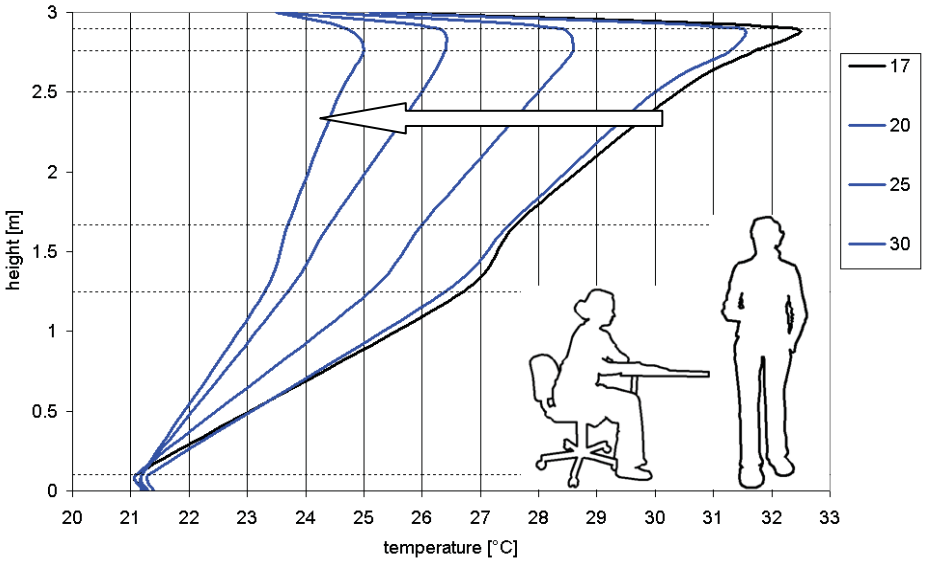

Figure 7. The vertical air temperature difference; cooling

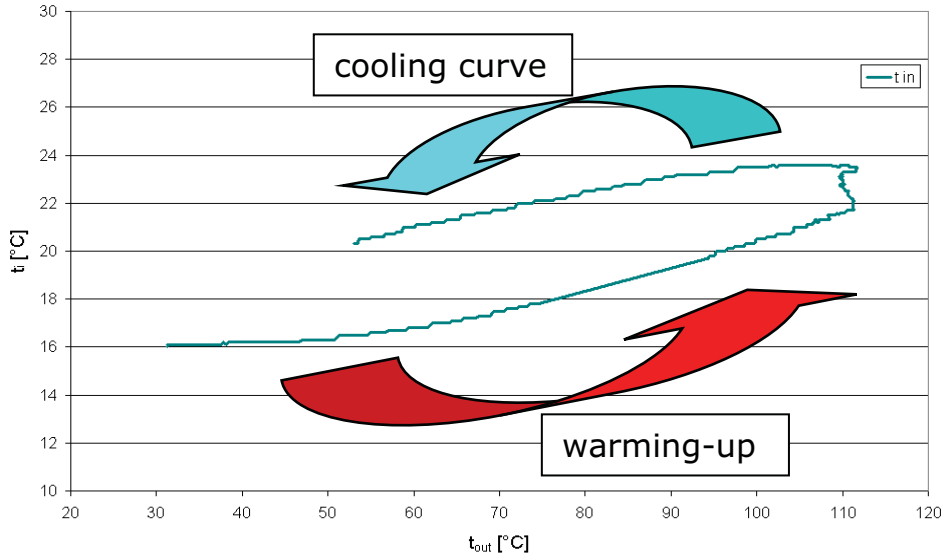

Figure 8. Warming-up and cooling of the interior air temperature t_i and its dependency on the air temperature coming out of the gas space heater t_{out}

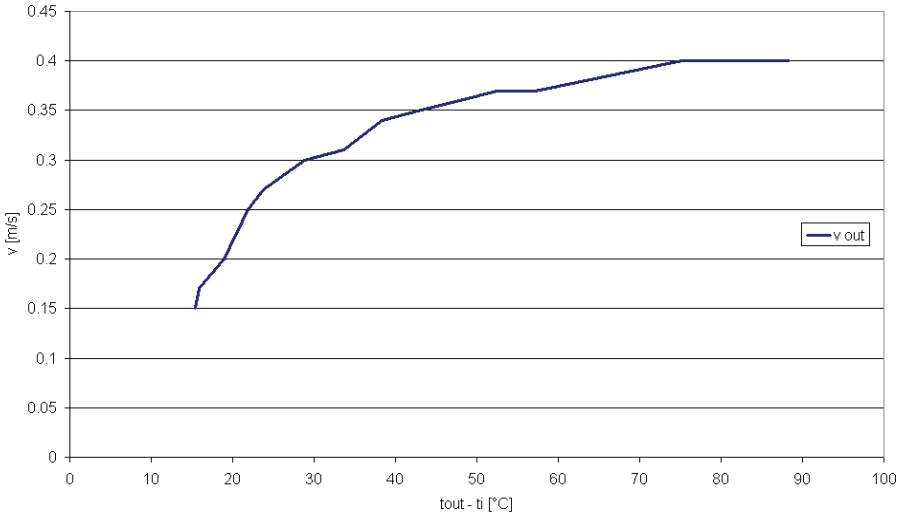

Figure 9. The dependency of the air velocity coming out of the gas space heater on the difference of air temperatures coming out of the gas space heater t_{out} and the interior air temperature t_i

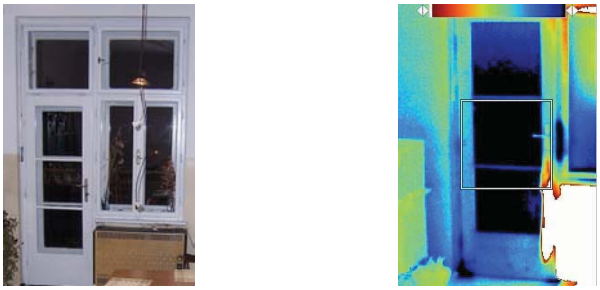

Figure 10. Surface temperatures

4. CONCLUSIONS, DISCUSSION OF RESULTS

Above mentioned and described results prove the unfavorable influence of heating systems with high heating surface temperatures on the state of thermal indoor climate in residential rooms.

Reasons of great vertical temperature difference in the room are following:

- The formation of dropping airflows at the vicinity of cool surfaces (Fig. 10) as a result of insufficient thermal insulation properties of the envelope constructions and high air infiltration of the window and door joints
- Insufficient or no shading out of the dropping cool airflows (Fig. 3 and 4)
- High temperature (Fig. 5) and velocity (Fig. 9) of the air coming out of the gas space heater (t_{out}).

It is not easy to satisfy the requirement on vertical temperature distribution in the room in cases as the one described here. Experimental measurement proves that the worst situation from the point of view of temperature distribution is while dynamic changes of heating system, particularly while heating of the room (Fig. 6 and 7). The results of non-stationary numerical simulation do not correspond precisely to results of the experimental measurements. Nevertheless in principal the simulation results correspond to the measurements and so they give us objective image of thermal processes which take place in the observed model room.

Acknowledgments

Numerical calculation in the Fluent software was performed in conjunction with the company Sobriety Ltd.

References

1. Cihelka, J. *Vytápění a větrání*, Praha: SNTL, 1969. 610 s.
2. Šikula O., Ponweiser. K. *Modelling of heat transfer in the field of technical facility equipment and calculation using modern techniques*, Civil Engineering Journal Stavební obzor 4/2006, pages 6, Prague, Czech Republic, March 2006.
3. Jokl, M. *Teorie vnitřního prostředí budov*, ES ČVUT, Praha 1993.
4. FLUENT *User's Guide*, February 2003.
5. Regulation No. 6/2002 Sb.

"Computational Civil Engineering 2006", International Symposium
Iaşi, România, May 26, 2006

Remarks on the geometrical non-linear analysis of cyclic symmetrical structures

Andrei Vasilescu

Department of Mechanics, Statics and Dynamics of Structures, Technical University of Civil Enginneering, Bucharest, 020396, Romania

Summary

The symmetry of a state of a structural system is an intrinsic property that is independent from the external loading or from the analysis type: linear or non-linear, static or dynamic, etc. However, specific methods have been developed and implemented in FEM programs only in the linear elastic and modal analysis. The aim of this approach is to survey one direction possible in using the initial cyclic symmetrical configuration in a geometrical non-linear analysis of structures .

KEYWORDS: symmetry, geometrical non-linear analysis, mNR method.

1. INTRODUCTION

A possible challenge in the work of a researcher or designer is when a structure with cyclic period geometry appears. This type of symmetry remains on-going subject in the theoretical and practical fields of engineering. Cyclic symmetry is present in many civil engineering structures (domes, cooling towers, chimneys, etc.) and in mechanical engineering (milling cutters, turbine bladed disks, gears, fan or pump impellers, etc.).

Such a structure may be considered as a domain composed of identical, coupled subdomains positioned symmetrically with respect to an axis. Analysis of one of the subdomains, namelly the fundamental, and its high degree of repetition, represents the key to obtaining major savings in calculus. It is relevant to present the overall stiffness matrix **K** for a cyclically symmetric structure and it is essential to the development of the theory that the reference system of co-ordinates should itself be cyclically symmetric: the axes attached to a subdomain are carried into those of the next similar subdomain when the whole domain (the structure) is rotated through an angle of $2\pi/N$ (fig. 1,2). N is the number of identical subdomains and it represents the order of cyclic symmetry. In this way the overall stiffness matrix has a special form: it is block circulant.

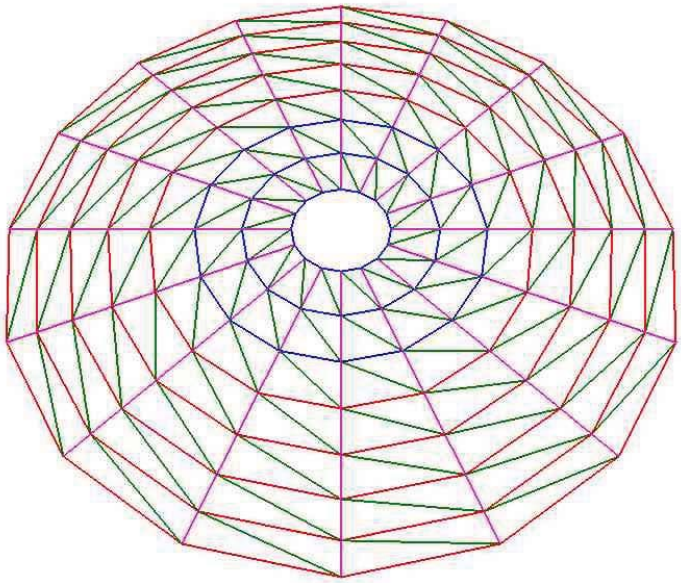

Figure 1. Cyclic symmetrical dome (order $N = 16$)

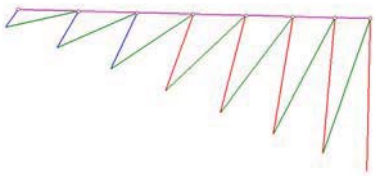

Figure 2. Fundamental subdomain of the structure

The theory of circulant and block circulant matrices shows that **K** is similar to a matrix with diagonal blocks [1]. The consequence is that the system of equations for the structure:

$$\mathbf{K} \cdot \mathbf{U} = \mathbf{P} \tag{1}$$

can be split into N decoupled hermitic systems [2]

$$\mathbf{K}_n \cdot \mathbf{D}_n = \mathbf{F}_n \tag{2}$$

solved for each harmonic, n = 0,1,2,...,Int(N/2), where the elements of the vector $\mathbf{F}_n$ are obtained by the Inverse Discrete Fourier Transform (**IDFT**) of the force acting in the k-th degree of freedom (d.o.f.) of the j-th segment:

$$f_{nk} = \frac{1}{N}\sum_{j=1}^{N} p_{jk} e^{i(j-1)\psi} \tag{3}$$

Since all forces acting on adjacent segments are related by the same phase constant, $e^{-i\psi}$, the deflections on adjacent segments should be connected in the same way, using Discrete Fourier Transform (**DFT**):

$$u_{jk} = \sum_{n=1}^{N} d_{nk} e^{-i(j-1)\psi} \tag{4}$$

where $\psi = 2\pi n / N$. In conclusion, the analysis of cyclic structures by means of the theory of cyclic symmetry is not an approximation technique (as in Fourier analysis of axi-symmetric systems), but is an effective and exact way to express the cyclicity conditions and thereby to form a decoupled system of equations. Numerical examples are presented in [3].

2. GEOMETRICAL NON-LINEAR ANALYSIS

2.1 Preliminaries

In linear structural analysis, it is assumed that the joint displacements of the structure under the applied loads are negligible with respect to the original joint coordinates. Thus, the geometric changes in the structure can be ignored and the overall stiffness of the structure in the deformed shape can be assumed to equal the stiffness of the undeformed structure. However, in the space truss structures like domes, significant changes in the initial geometry can occur. In such cases, the stiffness of the dome in the deformed shape should be computed from the new geometry of the structure. That means formulating the condition of equilibrium in the deformed configuration, since the truss members of the dome are assumed to have linear stress-strain relationships.

The problem to be solved in the static geometric non-linear structural system, is the determination of the displacements, **U**, corresponding to some load, **P**, since the stiffness matrix, **K**, in the equilibrium equation is a function of the joint displacements' **U**, which are yet unknown. The analysis will typically proceed in two phases: the first is a solution that may be termed the incremental phase; the second is a corrective procedure applied to the first in an attempt to obtain the

solution close to the equilibrium path. The reference configuration for the incremental analysis is thus no longer cyclic and the genuine tangent matrices are not block circulant. As a consequance, the theory for cyclically symmetrical structures is not applicable to non-linear analysis.

The way to preserve the advantage induced from the initial cyclic symmetry of the structure is to choose the modified Newton-Raphson method (mNR), in which the same matrix $\mathbf{K}_{(0)}$ is used for all the iterations. $\mathbf{K}_{(0)}$ is the stiffness matrix from the linear analysis, named also the tangent stiffness matrix. This matrix is computed at the beginning, and has a circulant or block circulant form [5].

2.2 Modified Newton-Raphson procedure

Equilibrium condition for the initial position is denoted by the linear system of equations:

$$\mathbf{K}_{(0)}\mathbf{U}_{(0)} = \mathbf{P} \tag{5}$$

Let $\mathbf{U}_{(0)}$ the diplacements resulted from (5). The updated stiffness matrix is

$$\mathbf{K}_{(1)} = \mathbf{K}(\mathbf{U}_{(0)}) = \mathbf{K}_{(0)} + \Delta\mathbf{K}_{(0)}\,. \tag{6}$$

The equilibrium condition must be satisfied in the new configuration, for the same level of loading **P**:

$$\mathbf{K}_{(1)}\mathbf{U}_{(1)} = \mathbf{P}\,. \tag{7}$$

The new displacements $\mathbf{U}_{(1)}$ are expressed function of initials displacements $\mathbf{U}_{(0)}$

$$\mathbf{U}_{(1)} = \mathbf{U}_{(0)} + \Delta\mathbf{U}_{(0)} \tag{8}$$

Conditions (6), (8) can be introduced in (7):

$$(\mathbf{K}_{(0)} + \Delta\mathbf{K}_{(0)})(\mathbf{U}_{(0)} + \Delta\mathbf{U}_{(0)}) = \mathbf{P} \tag{9}$$

If we consider $\Delta\mathbf{K}_{(0)}\Delta\mathbf{U}_{(0)} \approx 0$, equation (9) can be write

$$\mathbf{K}_{(0)}\Delta\mathbf{U}_{(0)} = \mathbf{P} - \mathbf{K}_{(1)}\mathbf{U}_{(0)} \tag{10}$$

The right hand side of equation (10) has a meaning of a unbalanced force $\mathbf{P}_{(1)}$ in the global axes system:

$$\mathbf{P}_{(1)} = \mathbf{P} - \mathbf{K}_{(1)}\mathbf{U}_{(0)} \tag{11}$$

Then we have $\Delta\mathbf{U}_{(0)}$

$$\Delta\mathbf{U}_{(0)} = \mathbf{K}_{(0)}^{-1}\mathbf{P}_{(1)} \tag{12}$$

and the first iteration is finished with the update of $\mathbf{U}_{(1)}$ displacements:

$$\mathbf{U}_{(1)} = \mathbf{U}_{(0)} + \Delta\mathbf{U}_{(0)} \tag{13}$$

For the *n*-th iteration, the displacements are computed with

$$\mathbf{U}_{(n)} = \mathbf{U}_{(n-1)} + \Delta\mathbf{U}_{(n-1)} \tag{14}$$

and the equilibrium condition will be

$$\mathbf{K}_{(n)}\mathbf{U}_{(n-1)} + \mathbf{K}_{(n)}\Delta\mathbf{U}_{(n-1)} = \mathbf{P} \tag{15}$$

or

$$\mathbf{K}_{(n)}\Delta\mathbf{U}_{(n-1)} = \mathbf{P} - \mathbf{K}_{(n)}\mathbf{U}_{(n-1)} \tag{16}$$

Keeping the notation $\mathbf{P}_{(n)}$ for the unbalanced forces from the right hand side of (15), since the left hand side can be approximated

$$\begin{aligned}\mathbf{K}_{(n)}\Delta\mathbf{U}_{(n-1)} &= (\mathbf{K}_{(0)} + \Delta\mathbf{K}_{(0)} + \Delta\mathbf{K}_{(1)}\cdots \\ &\cdots + \Delta\mathbf{K}_{(n-1)})\Delta\mathbf{U}_{(n-1)} \approx \mathbf{K}_{(0)}\Delta\mathbf{U}_{(n-1)}\end{aligned} \tag{17}$$

The equation system is obtained from (16)

$$\mathbf{K}_{(0)}\Delta\mathbf{U}_{(n-1)} = \mathbf{P}_{(n)} \tag{18}$$

resulting $\Delta\mathbf{U}_{(n-1)}$ and so, the total displacements $\mathbf{U}_{(n)}$ with (14).

2.3 Implementation

1. Initialization and input parameters such as geometric and material properties, connections, boundary conditions, and reference loads.
2. Initial step: solve $\mathbf{K}_{(0)}\,\mathbf{U}_{(0)} = \mathbf{P} \Rightarrow$ get $\mathbf{U}_{(0)}$
3. Compute initial member end forces in global co-ordinates.
4. For each iteration (*n*)
  4.1. For each element, form its stiffness matrix in local, and then, in global co-ordinates $\mathbf{k}_{(n)} = \mathbf{k}(\mathrm{U}_{(n-1)})$.
  4.2. Compute unbalanced joint loads in global coordinate system
    $\mathbf{P}_{(n)} = \mathbf{P} - \mathbf{K}_{(n)}\,\mathbf{U}_{(n-1)}$

4.3. Solve $\mathbf{K}_{(0)} \Delta\mathbf{U} = \mathbf{P}_{(n)} \Rightarrow$ get $\Delta\mathbf{U}$
4.4. Update joint coordinates $\mathbf{U}_{(n)} = \mathbf{U}_{(n-1)} + \Delta\mathbf{U}$
4.5. Check convergence by considering force norm. If no convergence and $n <$ max. number of iterations GO TO Step 4.1.
5. Print on files final results.
6. Stop.

Apparently, we must assemble the overall tangent stiffness matrix of the structure to calculate in each iteration the unbalanced forces (see Step 4.2). This would compromise the present method as it is extremely expensive in the memory allocation and CPU time. In fact, we need to process only the new element stiffness in local, and then in global co-ordinates. The unbalanced forces in the global co-ordinate system are established by the contribution of each element. Therefore, there is no need to assemble the overall tangent stiffness matrix of the structure [4].

3. CONCLUSIONS

A solution strategy for the geometrical non-linear analysis of elastic cyclically symmetric structures like domes has been presented. The modified Newton-Raphson method (mNR) has been adopted for the formulation, to take full advantage of cyclic symmetry of the structure. We remember that in non-linear analysis, solution algorithms are problem dependent. It is well known, however, that the convergence of the mNR method is linear and may run into serious difficulties if the loading level produces large changes in displacements. A simple method of preventing this is to scale back the loads. At this stage, it is necessary to underline the limits of the mNR method in the cyclically symmetric context: it only works on mild geometrical non-linear structures like domes. Strong non-linear cyclic structures are not to be solved by the technique developed above and they constitute the reason for a future research in this field.

References

1. Davis, P.J. *Circulant Matrices*, John Wiley & Sons, 1979.
2. Thomas, D. L. Dynamics of rotationally periodic structures, *Int. J. Numer. Methods Eng*., vol. 14, pp. 81-102, 1979.
3. Vasilescu, A. Discrete Fourier transform application to analyse cyclic symmetric structures, *Buletinul Ştiintific al Universității Tehnice de Construcții Bucureşti*, **1**, 51-62, 1997.
4. Vasilescu, A. Cyclic Symmetry in Geometrical Non-linear Analysis of Structures, *Domain Decomposition Press Bergen*, 843 - 849, 1997.
5. Vasilescu, A. Particularități privind analiza statică la structurile cu simetrie ciclică, *SIMEC 2006*, Universitatea Tehnică de Construcții Bucureşti, Ed CONSPRESS Bucureşti, 213-218, 2006. (in Romanian)

"Computational Civil Engineering 2006", International Symposium
Iaşi, România, May 26, 2006

Computer modelling and simulation of carbon dioxide indoor concentration

Hana Doležílková[1]

[1]*Department of Microenvironmental and Building Services Engineering, Czech Technical University in Prague, Prague, 166 29, Czech Republic*

Summary

Indoor pollutant concentration is more significant for human health than the outdoor atmosphere because people spend most of their time in buildings. There is pollutant concentration enhancement, relative humidity, mould reproduction and rise of environment not corresponding to human organism needs because of insufficient ventilation. Indoor air quality depends on many factors. Carbon dioxide is the most important indoor pollutant whether the pollutant source is presented only by people. There is overview of software enabling carbon dioxide modelling and simulation and also program CONTAM 2.4 using in my paper. It means multizone modelling where at the single zone is obtained carbon dioxide concentration thanks to geometry, openings, ventilation and pollutant sources interpolation. There were chosen three spaces for simulation of occupied flat. The results show, that CO2 concentration run is similar to interior occupation, increasing time of concentration to constant value and decreasing time of concentration to ventilation air concentration depend on room volume.

KEYWORDS: Indoor Air Quality, Computer Modelling and Simulation, Carbon Dioxide

1. INTRODUCTION

The aim for thermal losses lowing directed to limiting natural ventilation by windows. Tight windows have insufficient infiltration, they are unsuitable from the hygienic point of view. It leads to pollutant concentration enhancement relative humidity, mould reproduction and rise of environment not corresponding to human organism. So it is necessary to ensure sufficient mechanical ventilation. In spite of minimal ventilation, the poor window sealing of old windows ensured sufficient ventilation rate, but it led to higher thermal losses. The residential space ventilation should ensure taking away of the depleted air, pollutants, moisture and smell to ensure the pleasant microclimate in rooms. Sufficient ventilation is important for a construction itself as well. High relative humidity can in colder places – thermal bridges – causes water vapour condensation and thereby increase mould rise risk.

2. ANALYSIS

2.1 Indoor air quality

Indoor air quality depends on many factors, especially on: outdoor air quality, air amount per person or ventilation rate, ventilation plant, amount of air pollutants, that sources are: inhabitants and their metabolism, inhabitants‘ activities, construction materials, social settlement, flat cleaning and housekeeping. Pollutants influencing indoor air quality are: carbon dioxide CO2, carbon monooxide CO, nitrogen oxides NOx, sulfur oxides SOx, formaldehyd, VOC, asbestos, dust, ozone, hydrocarbones, odours, radon, relative humidity, acarides and microorganisms. Microorganisms are able to reproduce and multiply their negative influence on inhabitants health during certain indoor conditions. Some of the chemical compounds presented in the indoor air belong among potential or evident human carcinogens.

Classic Pettenkofer normative 25 m3.h-1 per person is based on the request to abolish unpleasant body odour evoking strain of depleted air by adhering carbon dioxide concentration 700 ppm. Pettenkofer normative is still a basic value for standards of most developed states. ASHRAE standard is based on it as well.

2.2 What pollutant is the most critical?

Pollutant production generating indoor as a result of people presence is possible to describe physically and to model. The shortness of the air oxygen, whose consumption is also possible to describe physically, can have the negative influence on indoor environment as well. Air amount is 1,06 m3.h-1 per person for the minimal O2 concentration, 8,38 – 9,96 m3.h-1 per person for the optimal relative humidity and 22,5 m3.h-1 per person for the acceptable CO2 concentration. The highest amount of ventilation air is necessary for the acceptable CO2 compliance concentration.

2.3 Carbon dioxide

Carbon dioxide is the most usual air pollutant. Human metabolism, respiration and thermoregulation are the main sources of this pollutant. Respiration is adversely influenced by higher carbon dioxide concentration - already above 15 000 ppm. If its concentration in indoor air enhances above 30 000 ppm, most of people will have headache and dizziness. Concentration above 60 000 – 80 000 ppm leads to lethargy and losing consciousness. According to Czech Government order 178/2001 Sb. maximum acceptable CO2 concentration is 25 020 ppm [5].

2.4 Software for indoor environment modelling and simulation

Software for indoor air quality modelling and simulation are described in Table 1. There are described main characteristics, inputs and results, if the program is multi-zone or simple-zone.

Table 1. Software for indoor environment modelling and simulation

Name	**IDA Indoor Climate and Energy**
Characteristic	a tool for simulation of thermal comfort, indoor air quality and energy consumption in buildings
Inputs	building geometry, thermal characteristics, internal loads and schedules, heating and cooling equipment and system characteristics
Results	zone heat balance, including specific contributions (sun, occupants, equipment, lights), ventilation, heating, cooling, surface transmissions, air leakage, cold bridges and furniture, solar influx, air CO2 and moisture levels, air and surface temperatures, comfort indices, PPD and PMV
Name	**IAQ-Tools**
Characteristic	indoor air quality analysis including troubleshooting "sick" buildings, ventilation and filter design, design for contaminant source control, only simple-zone modelling
Inputs	filter effectivnes, air amount, pollutant production, indoor and outdoor pollutant concentration, contaminants: airborne solid contaminants (asbestos, lead, and particulates), gases (ammonia, carbon dioxide, carbon monoxide, ethane, formaldehyde, hydrogen sulfide, methane, nitrogen oxides, ozone, propane, radon, and sulfur dioxide), bioaerosols (bacteria, fungi, and molds), tracer gases
Name	**COMIS**
Characteristic	air flow distribution model for multizone structures; takes wind, stack and HVAC into account; allows for crack flow, flow through large openings, and single-sided ventilation
Inputs	air-flow network, operating schedule, weather data, pollutant sources
Results	available graphical
Availability	http://www-epb.lbl.gov/comis
Name	**BSim2002**
Characteristic	indoor climate and energy conditions, design heating, cooling and ventilation plants, the geometry of the rooms created in the model graphic editor or imported from CAD drawings, room or rooms are attached to thermal zones by drag and drop in the tree structure of the model BSim 2002 includes standard libraries for: constructions, materials, glass, window frames, people loads, schedules, the user can define new
Inputs	climate data, constructions and materials, heating, cooling, internal loads, moisture load, ventilation systems, automatic control strategies
Results	available weekly, monthly or periodical basis, in tabular or graphic

	form
Name	**CONTAM 2.4**
Characteristic	multizone indoor air quality analysis and ventilation, flowing among particular rooms during natural, hybrid and mechanical ventilation, wind pressure on building facade
Inputs	the quantity airflow and pollutant production, schedules, outdoor pollutant concentration, geometry of zones, ventilation
Results	pollutant concentration, airflow – infiltration, exfiltration, flowing among particular rooms
Availability	http://www.bfrl.nist.gov/IAQanalysis/CONTAMWdesc.htm

3. METHOD - MATHEMATIC MODEL IN PROGRAM CONTAM 2.4

There were chosen three alternatives for simulation of occupied flat. Alternative no. 1 presents flat occupation during weekday, e.g. when mother and her child are at home all the day and father is at work. Alternative no. 2 presents weekend, when all family is at home. Alternative no. 3 describes weekday whit visit in the evening. The plan of the observed flat shows Figure 1. The observed rooms were presented by a living room and a bedroom, their occupation is stated in Fig.2, 3 and 4.

The detected indoor pollutant is carbon dioxide. It was counted with outdoor carbon dioxide concentration 350 ppm and respiration production 19 $l.h^{-1}$ per person. Ventilation air amount for particular spaces is stated in Table 2.

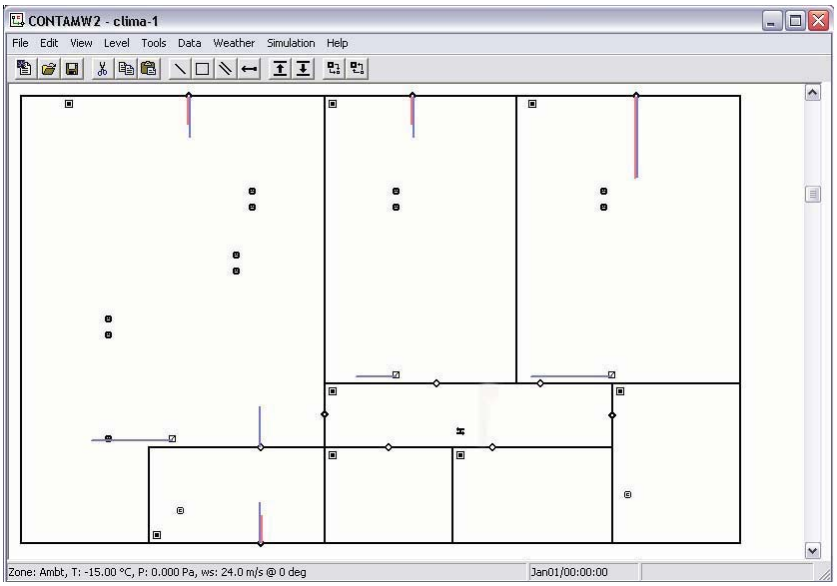

Figure 1. The plan of observed flat

Figure 2. Particular zone occupation for alternative no. 1

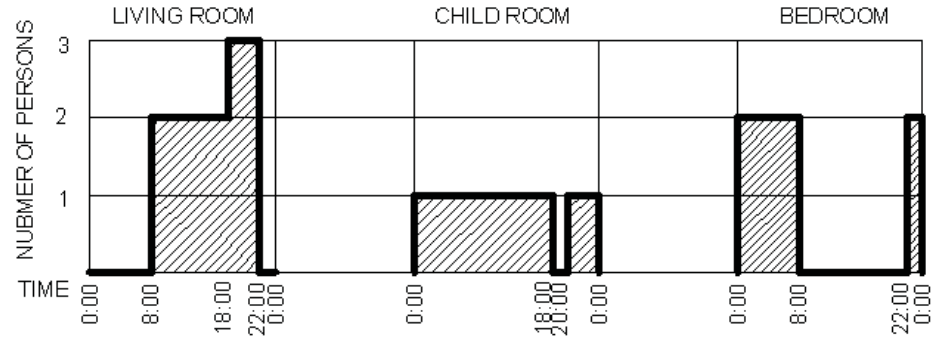

Figure 3. Particular zone occupation for alternative no. 2

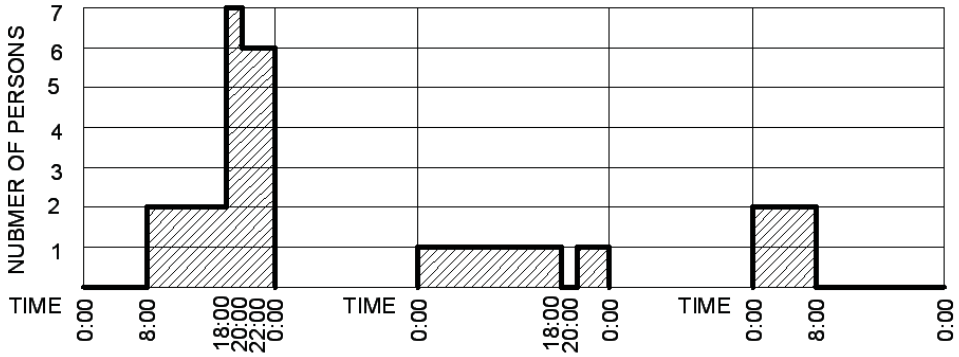

Figure 4. Particular zone occupation for alternative no. 3

Table 2. Ventilation air amount

Zone (room)	Ventilation air amount		
		[$m^3.h^{-1}$]	[$m^3.h^{-1}$ per person]
Living room	Alternative no. 1 and 2 Alternative no. 3	68 155	22,5
Child room		22,5	22,5
Bedroom		45	22,5

4. RESULTS

The carbon dioxide concentration in particular rooms was calculated by program CONTAM 2.4. Figures 5, 6 and 7 show carbon dioxide concentration runs. The results show, that CO_2 concentration run is similar to interior occupation, increasing time of concentration to constant value and decreasing time of concentration to ventilation air concentration depend on room volume. From concentration runs is distinct, that ventilation air amount 22,5 $m^3.h^{-1}$ per person is the necessary air amount for ensuring maximal carbon dioxide concentration 1200 ppm according to EN CR 1752 for Class "C".

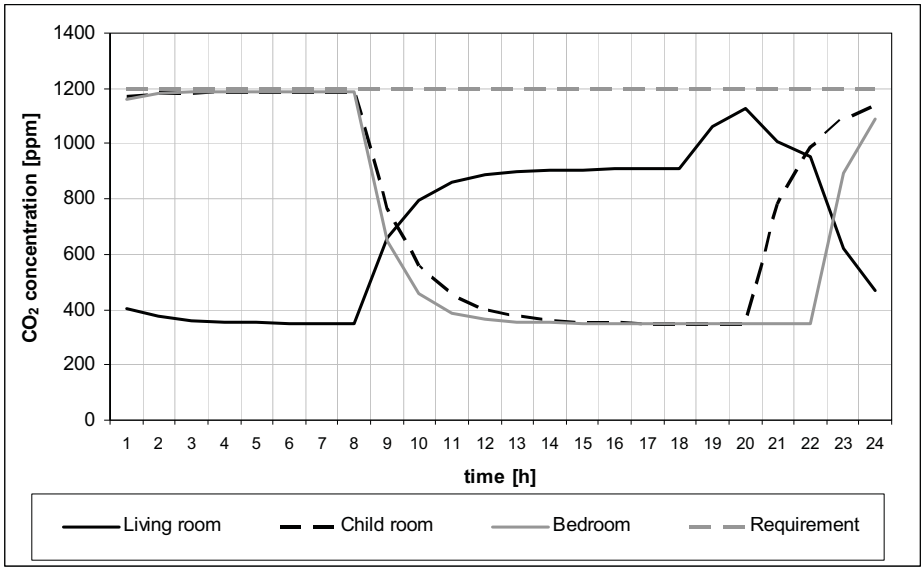

Figure 5. Carbon dioxide concentration runs for alternative no. 1

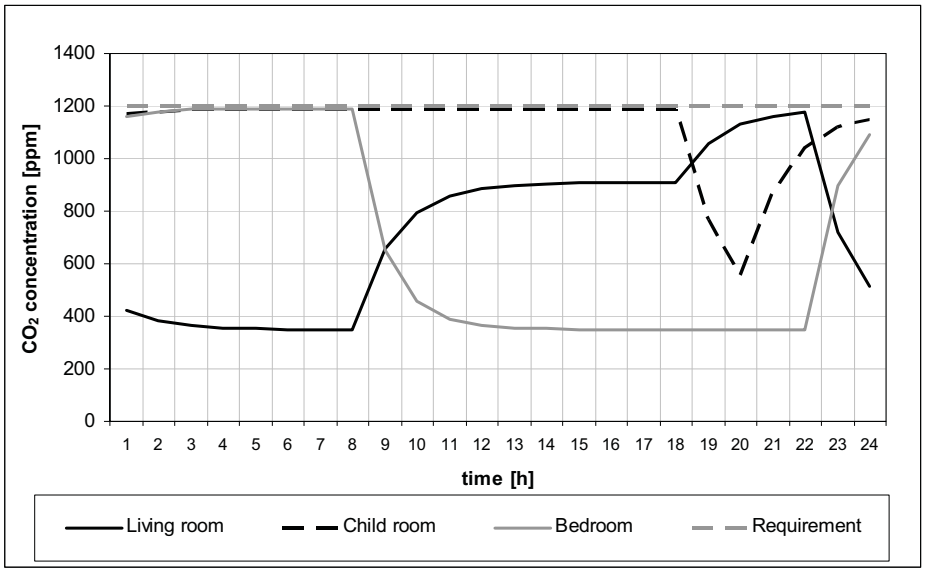

Figure 6. Carbon dioxide concentration runs for alternative no. 2

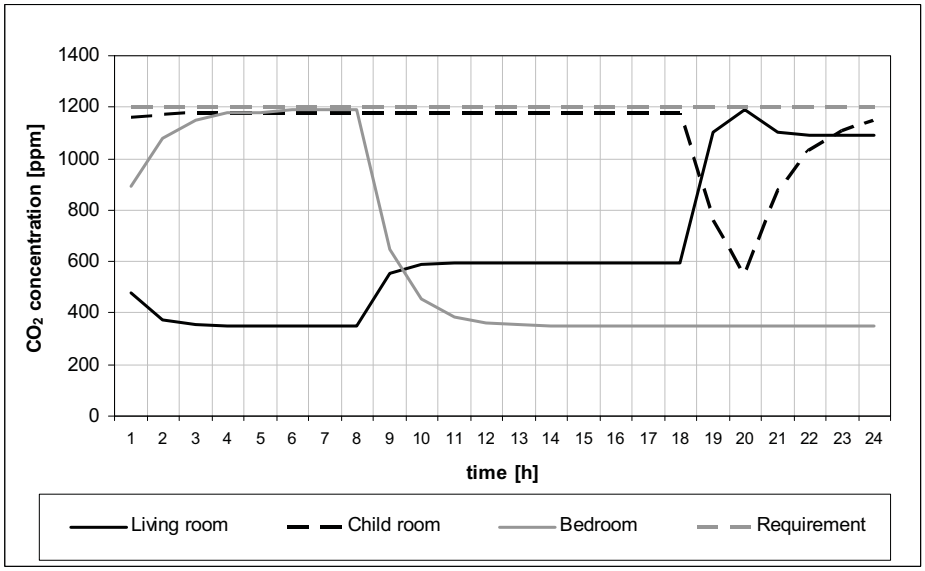

Figure 7. Carbon dioxide concentration runs for alternative no. 3

5. DISCUSSION

The concentration dependence of CO_2 on supplied air amount for alternative no. 3 shows Fig. 7. The maximum CO_2 concentration is 1200 ppm at supply 155 $m^3.h^{-1,}$ it is much higher than in previous alternatives, and this is only for case of a visit. If it would be 68, maximal carbon dioxide concentration will be 2000 ppm for four hours. There is a question, if the short-term exceeding of concentration has an effect for ventilation design. During steady-state air return with more people than expected in the interior causes higher pollutants production. The constant return air volume increases energy losses if the room is empty. The ideal solution is while CO_2 sensor is in each room and air amount is controlled by actual demand.

6. CONCLUSIONS

It was documented that CO_2 concentration is the critical criterion for ventilation air amount design. The results show, that CO_2 concentration runs is similar to interior occupation. Simulation in program Contamw 2.0 showed, that necessary air amount per person for ensuring maximal CO_2 concentration 1200 ppm is 22,5 $m^3.h^{-1}$ per person. It was established that, Pettenkofer normativ 25 $m^3.h^{-1}$ per person is valid.

References

1. Software Contam 2.4
2. Jokl, M. V. *Zdravé obytné a pracovní prostředí*, Academia, Praha, 2002. (in Czech)
3. Energy and buildings, years 1997 – 2003
4. http://www.ubmi.cvut.cz/
5. http://mvcr.iol.cz/sbirka/2001/sb068-01.pdf

ACKNOWLEDGEMETS

This paper presented results supported by Research Plan CEZ MSM 6840770005.

"Computational Civil Engineering 2006", International Symposium
Iaşi, România, May 26, 2006

Some examples of structural optimization problems modelling

Piotr Berkowski

Building Engineering Institute, Faculty of Civil Engineering, Wrocław University of Technology, Wrocław, Wyb. Wyspiańskiego 27, 50-370, Poland

Summary

Some examples of different optimization problems models that were under interest of the author during some past years are presented in a paper. These problems concern: discrete optimization of steel frames with accounting for the second order effects in structural analysis, shape optimization of section under torsion by using BEM, and evolutionary structural optimization method for shape and topology strength optimization.

KEYWORDS: discrete optimization, plane frames, linear analysis, P-delta method, shape optimization, torsion problem, BEM, evolutionary structural optimization.

1. DISCRETE SYNTHESIS OF STEEL FRAMES ACCOUNTING FOR P-DELTA EFFECTS

1.1. Mathematical formulation of the optimization problem

In the analysis and design of multi-storey steel frames it is necessary to consider the influence of nonlinear geometrical effects which are caused by vertical loads acting on horizontal displacements of the structure and on deflections of its columns. These additional effects generally occur in the overturning and torsional moments, and are known as P-delta effects [1]. As these effects are represented by changes in the internal forces distribution over the structure, and by changes in their values, they also have an influence on the results of the minimum-weight design of high-rise frames.

The design problem is formulated as follows [2]:

Obtain the minimum-material volume design of the structure taking into consideration the influence the second-order P-delta effects.

In the proposed optimization model values representing the cross-sectional member dimensions are assumed as a design variable vector **X** and material properties as parameter vector **P**. For the I-welded sections four simple design variables are taken: web plate and flange plate width and thickness. Set of constraints is defined

by design constraints fixed on design variables and by behaviour constraints: displacements, stresses, and local stability in form of the mathematical formulas:

Geometrical constraints: $Q_g(\mathbf{X}, \mathbf{P})$

$$x_{imin} = x_{i1} < x_{in} < x_{imax},\ x_{in} - x_{in-1} = \Delta x,\ x_{imax} - x_{imin} = 2^{q \cdot} \Delta x_i, \tag{1}$$

$$n = 1\ (\min), \ldots, k\ (\max),\ i = i, \ldots j,\ q = 1, 2, ..., I.$$

Stress constraints: $Q_s(\mathbf{X}, \mathbf{P})$

$$\sigma_{k1}(\mathbf{X}, \mathbf{P})/R_{k1} - 1 <= 0,\ \ k = 1, \ldots, d. \tag{2}$$

Local stability geometrical and stress constraints: $Q_{ls}(\mathbf{X}, \mathbf{P})$

$$\sigma_{l2}(\mathbf{X}, \mathbf{P})/R_{l2} - 1 <= 0,\ f_t(\mathbf{X}, \mathbf{P}) <= a_t,\ l = 1, \ldots, d,\ t = 1, \ldots, f. \tag{3}$$

Displacement constraints: $Q_d(\mathbf{X}, \mathbf{P})$

$$v_{mh}(\mathbf{X}, \mathbf{P}) <= v_{mhp},\ v_{nv}(\mathbf{X}, \mathbf{P}) <= v_{nvp},\ m = 1, \ldots, g,\ t = n, \ldots, h. \tag{4}$$

In the equations (1) to (4): x_{imin}, x_{imax}, Δx_i – minimum, maximum, and constant step between design variables; σ, R – current stresses and their permissible values, f, a – current geometrical constraint value and its permissible value, v, v_p – current displacements and their permissible values.

It is obvious that to obtain the required optimal solution – the optimal structure – the following relation must be fulfilled:

$$Q_g \text{ w } Q_s \text{ w } Q_{ls} \text{ w } Q_d \text{ K } \{0\}. \tag{5}$$

As an objective function volume of the material used for a structure is taken. Optimization problem is then formulates in the following term:

Find the design variable vector X* in the feasible set (5) , with parameters **P**, which minimize the value of the global objective function.

1.2. Mathematical programming technique

Well-known discrete programming method called “backtrack” [3] was used to find the optimal vector **X***. This combinatorial method that can solve nonlinear constrained function minimization problem by systematical search procedure was very useful in the presented optimization problem.

1.3. Examples of synthesis process

The process of discrete synthesis of steel frames was implemented in a computer program for second-order analysis. Optimization process was conducted until the difference of values of global objective function for two successive steps was less than the specified tolerance (for example 0,1%). As an example the results of optimization of two-bay three-storey frame are presented in Figures 1 and 2.

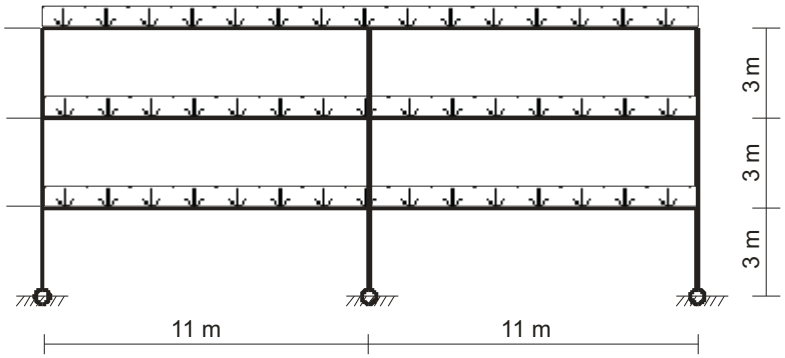

Figure 1. Optimization problem

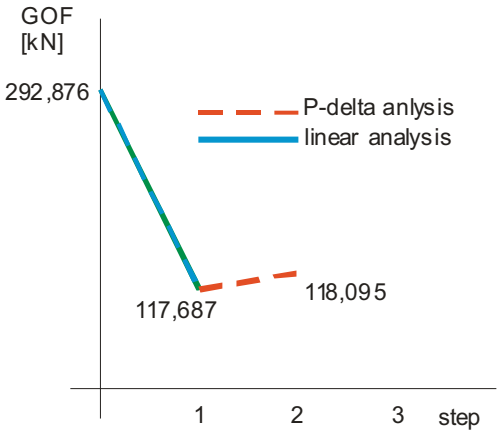

Figure 2. Synthesis results – iteration process

The results of discrete synthesis of steel frames with accounting for P-delta effects in structural analysis shown that for a considered class of structures these effects led to obtain slightly "heavier" structures and, what was more important, led to material and forces redistribution in structural elements. These changes caused overstress in some elements that were optimized with linear analysis.

2. SHAPE OPTIMIZATION OF SECTIONS UNDER SAINT-VENANT TORSION

2.1. Formulation of torsion problem for isotropic solids with BEM

The solution of the Saint-Venant torsion problem was based on that formulated by Gracia [4] and Gracia nad Doblaré in [5, 6], where a general problem of shape optimization of 2D elastic bodies based on the boundary element method was presented.

To formulate the Saint-Venant torsion problem for isotropic and homogenous solids and for multiply-connected domains Ω_i the so-called Prandtl function was used leading to a Poisson equation:

$$\frac{\partial^2 \phi}{\partial x^2} + \frac{\partial^2 \phi}{\partial y^2} = -2 \quad \text{in } \Omega, \ \phi_i = k_i \text{ in } \Gamma_i, i = 0,1,...,N, \tag{6}$$

where N is the number of boundaries Γ_i,

$$\int_{\Gamma_i} \frac{\partial \phi}{\partial \mathbf{n}} d\Gamma_i = -2A_i, i = 1,...,N \tag{7}$$

where:

$$A_i = \frac{1}{2} \sum_{j=1}^{N^i} (\mathbf{r}_j \bullet \mathbf{n}_j) L_j \tag{8}$$

is the area enclosed by each internal boundary, N^i is the number of elements of each internal boundary, L_j is the length of the element 'j', $\mathbf{n}_j$ is the normal to it, and $\mathbf{r}_j$ is the radius-vector between the element and the origin of coordinates.

The introduction of the second Green's identity between the Prandtl function (6) and the fundamental solution of the Laplace equation led to an alternative formulation of Equation (6) in terms of boundary integrals [10,11,12]:

$$c(Q)\phi(Q) + \int_\Gamma \phi \frac{\partial}{\partial \mathbf{n}} (\ln \frac{1}{r}) d\Gamma = \int_\Gamma \frac{\partial \phi}{\partial \mathbf{n}} \ln \frac{1}{r} - \int_\Omega \nabla^2 \phi \ \ln \frac{1}{r} d\Omega \tag{9}$$

where the constant *c* takes values depending on situation of point Q on the boundary and r is the radius-vector joining boundary points and the coordinate system origin.

Using (6) Equation (9) was transformed to the BEM basis:

$$c(Q)\boldsymbol{\phi}(Q) - \int_{\Gamma} \boldsymbol{\phi} \frac{\mathbf{r} \bullet \mathbf{n}}{r^2} d\Gamma = -\int_{\Gamma} \frac{\partial \boldsymbol{\phi}}{\partial \mathbf{n}} \ln r + \int_{\Gamma} (\frac{1}{2} - \ln r)(\mathbf{r} \bullet \mathbf{n}) d\Gamma \qquad (10)$$

and, by the similar way, a formulation for torsional stiffness was obtained:

$$D = -G\left[\frac{1}{4}\int_{\Gamma} r^2 (\mathbf{r} \bullet \mathbf{n}) d\Gamma + \frac{1}{2}\int_{\Gamma} \frac{\partial \boldsymbol{\phi}}{\partial \mathbf{n}} r^2 d\Gamma\right]. \qquad (11)$$

The approximation functions $\boldsymbol{\phi}$ were formulated was by using the simplest constant and linear approximations that led to the torsional stiffness expressed by:

$$D = -G\left[\frac{1}{4}\sum_{i=0}^{N}\sum_{j=1}^{N^{ei}} \int_{\Gamma_j} r^2 (\mathbf{r} \bullet \mathbf{n}) d\Gamma_j + \frac{1}{2}\sum_{i=0}^{N}\sum_{j=1}^{N^{ei}}\sum_{k=1}^{2} q_j^k \int_{\Gamma_j} \boldsymbol{\varphi}_k r^2 d\Gamma_j\right]. \qquad (12)$$

2.2 Formulation of optimization problem

The problem of shape optimization of sections under the Saint-Venant torsion can be stated in the considered case as it was formulated with details in [4, 5, 6, 7]:

Obtain the shape of the section with minimum area having a given torsional stiffness, and that fulfils some constraints related to the section geometry. It should be mentioned that as its dual problem the problem of finding the section with a given area and maximum torsional stiffness could be considered.

These additional constraints are as follows:

- some coordinates of the nodes can be bound;
- some boundary nodes can be fixed;
- the boundaries can not intersect;
- symmetry conditions have to be fulfilled.

The objective function f(**x**) is defined as:

$$f(\mathbf{x}) = \frac{1}{2}\sum_{i=0}^{N}\sum_{j=1}^{N^{ei}} (\mathbf{r}_j \bullet \mathbf{n}_j) L_j, \qquad (13)$$

and the restriction corresponding to the torsional stiffness:

$$h(\mathbf{x}) = D_o + G\left[\frac{1}{4}\sum_{i=0}^{N}\sum_{j=1}^{N^{ei}} (I_j^i)_2 + \frac{1}{2}\sum_{i=0}^{N}\sum_{j=1}^{N^{ei}} q_j (I_j^i)_1\right], \qquad (14)$$

where D is defined by Equation (12), and as design variables **x**, in this first approximation to the optimization problem, the non-restricted boundary node coordinates were taken.

The method used in the optimization problem was based on the feasible direction method and the gradient projection one as it was described in [4, 5]. The restriction imposed on the torsional stiffness was transformed into "the constraint strip" by using the error bound ε_r and though the restriction is satisfied when:

$$(1 - \varepsilon_r) \le \frac{D}{D_o} \le (1 + \varepsilon_r), \tag{15}$$

where D is the torsional stiffness of the current design and D_o is the constraint stiffness. The method of the automatic constraint strip adjusting at each iteration step was applied.

2.3 Interactive graphical program for shape optimization

The overworked interactive program [8] for definition, visualization and modification of the shape optimization problem's data and results consists of two fundamental parts: graphical unit used to define and redefine the problem geometry (graphical pre- and postprocessors) and optimization unit that performs a design process, basing its analysis part on the BEM.

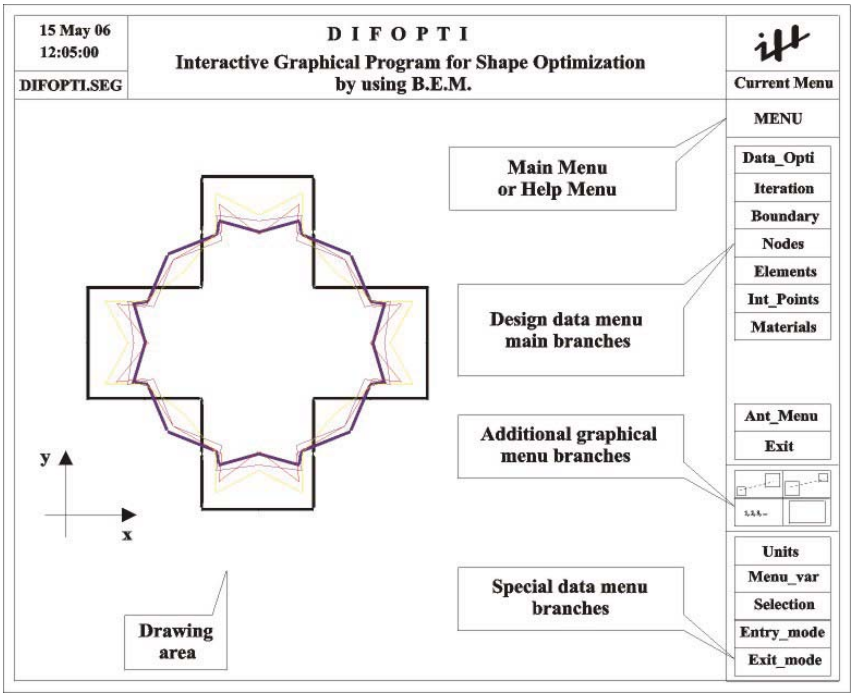

Figure 3. Optimization program graphical interface and section's shape evaluation during optimization process for the so-called "Greek cross"

A general idea of an interactive work with the program consists in giving to a program user a possibility to define graphically the geometry of an initial shape to be optimized and then to have a chance to observe the optimization process at any iteration step. The graphical unit of the program contains a group of geometrical tools (calculating of boundary elements' length, areas closed by boundaries and angles between elements, detection of boundary intersections and mesh redefinition), completed by those of the visual presentation of optimized shapes (drawing of boundaries with different zoom levels, graphical presentation of the objective function and restriction evolution). An example of realized optimization process refers to the shape optimization of simply-connected domain that is so-called "Greek cross" with an obvious final result in the shape of a circle (Figure 3).

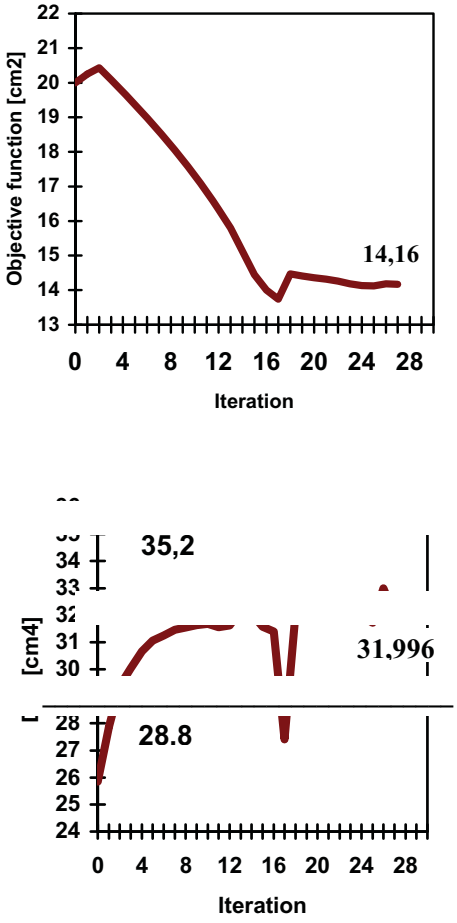

Figure 4. Evaluation of objective function and restriction during optimization

The optimization process converged rapidly with the constraint value D_0/G always inside the constraint strip (Figure 4). However, the boundary of final design is not very smooth because of lack of the mesh redefinition in case of appearance of geometrical mesh irregularities (Figure 3).

3. EVOLUTIONARY STRUCTURAL OPTIMIZATION

3.1. Formulation of the method

Evolutionary Optimization Method (ESO) is based on the simple concept that removing step-by-step inefficient material [9] leads to the optimal shape of the structure. This process is controlled by coefficients that define from which part of the structure, how many, and when the material is removed from the structure. In every case all the restrictions are fulfilled. This method is very useful in shape optimization problems.

This method was applied to solve strength shape optimization problems [9, 10]. Optimization with minimum material criteria leads to structures shaped in accordance with principal stresses trajectories in equivalent shield structure (structural domain) with identical geometrical and boundary conditions as searched structure. ESO process for that kind of problems can be described as follows:

1. Creation of finite element mesh in a initial domain.
2. Structural analysis with FEM to find stress distribution. In cases presented below [8, 9] for plane stress model Huber- von Mises stress was defined:

$$\sigma^{hvm} = \sqrt{\sigma_x^2 + \sigma_y^2 - \sigma_x \cdot \sigma_y + 3 \cdot \tau_{xy}^2} \tag{16}$$

3. Calculation of stresses in every finite element σ_e^{hvm} and definition of material rejection criteria:

$$\sigma_e^{hvm}/\sigma_{max}^{hvm} < RR_i, \tag{17}$$

   where σ_{max}^{hvm} is domain maximum stress value and RR_i is a current rejection ratio (for example 1%).
4. Removal of finite elements with stress that satisfy equation (17) until the process is steady (by assigning zero stiffness value to the element). It means that with the same values of R_i there are no elements that can be deleted.
5. Introducing the so-called "evolutionary rate" ER ($RR_{i+1} = RR_i + ER$) and repetition of FEM and stress analysis, and element removal until new steady stage is reached (for example E = 1%).
6. Optimization process is conducted until, for example, when there are no elements in the domain with stresses $\sigma_e^{hvm} < 25\% \cdot \sigma_{max}^{hvm}$.

3.2. ESO optimization examples

First example is a well-known structural optimization problem of the two-bar frame subjected to a single load placed in the middle of the long domain side. The optimal ratio of H/L can be obtained analytically and is H/L =2 and a structure is a pin-jointed frame.

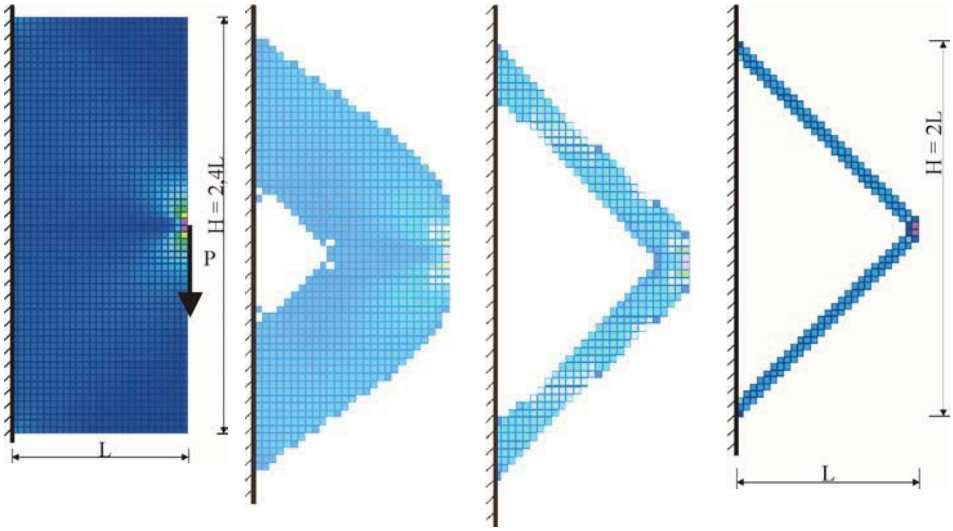

Figure 5. Design domain. ESO solution for R = 5%, 12,5%, and optimal solution for R = 30%.

Second example is ESO solution for a Michell type structure with two fixed ends.

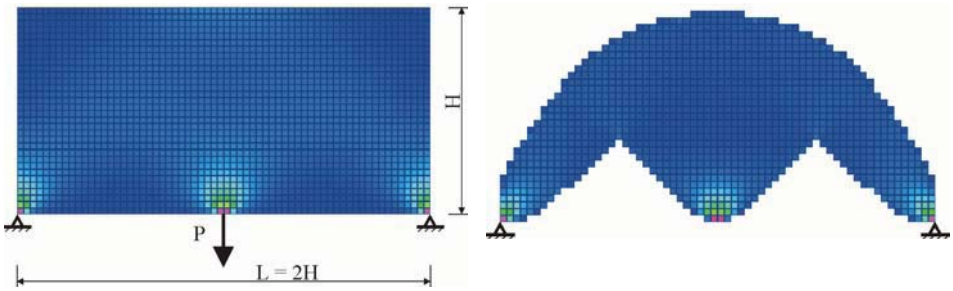

Figure 6. Design domain and ESO solution for R = 5%.

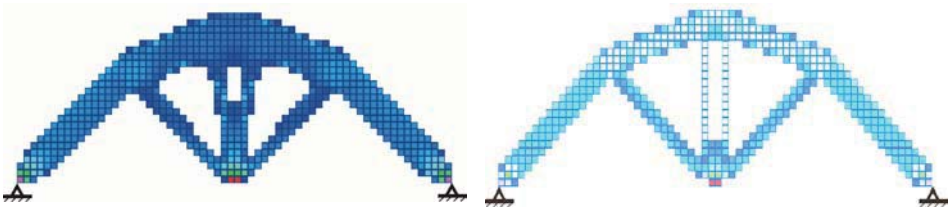

Figure 7. ESO solution for R = 10% and optimal solution for 15%.

4. FINAL REMARKS

A summary of author's interest in different problems of optimization that evaluated from simple discrete frame structural optimization with second order analysis, by shape optimization with BEM to the shape optimization with evolutionary method was presented above.

All the described optimization problems were also introduced into didactic programs in course of structural optimization and computer aided engineering allowing students to know a different way of structural designing.

References

1. Rutenberg, A. A Direct P-Δ Analysis Using Standard Plane Frame Computer Programs*, Comp. & Struct.*, 1-2 (14), 1981.
2. Berkowski, P. Optimization of steel frames taking into account second order structural analysis, *Archiwum Inżynierii Lądowej*, vol. 2, 1988. (in Polish).
3. Farkas, J, *Optimum Design of Metal Structures*, Ellis Horwood Ltd. Publishers, 1984.
4. Gracia, L. *Optimización de Formas en Elasticidad Bidimensional mediante el Método de los Elementos de Contorno*, PhD Thesis, University of Zaragoza, Spain, 1988. (in Spanish).
5. Gracia, L., Doblaré, L. Shape Optimization of Elastic Orthotropic Shafts under Torsion by Using Boundary Elements*, Comp. & Struct.*, vol. 30, No 6, 1988.
6. Gracia, L., Doblaré, M. Shape Optimization by Using B.E.M., *Proc. 10th Conf. B.E.M.*, *(Ed. C. A. Brebbia), Springer-Verlag,* vol. 3, 1988.
7. Espiga, F., Gracia, L., Doblaré, M. Shape Optimization of Elastic Homogenous 2D Bodies by the Boundary Element Method, *Comp. & Struct.*, vol. 33, No 5, 1989.
8. Berkowski, P., Sieczkowski, J., Gracia, L., Doblaré, M. An Interactive Program for Shape Optimization of Sections under Saint-Venant Torsion using Boundary Element Method, *Comp. & Struct.*, vol. 33, No 5, 1989.
9. Xie Y. M., Steven G. P. *Evolutionary structural optimization*, Springer–Verlag, 1997.
10. Berkowski, P. Example of Evolutionary Structural Optimization, *Polioptimization and CAD*, 1997. (in Polish).

Computer simulation on reinforced concrete beams subjected to flexure

Marinela Barbuta[1], Mihai Petru[2], Doina Smaranda Nour[3]

[1]*Assoc.prof.,Civil Engineering Faculty, Technical University „Gh. Asachi" of Iasi, Romania*
[2] *Lecturer,Civil Engineering Faculty, Technical University „Gh. Asachi" of Iasi, Romania*
[3]*Professor, Civil Engineering Faculty, Technical University „Gh. Asachi" of Iasi, Romania*

Summary

The paper presents a computer analyse of flexural behavior of reinforced concrete beams realized with local aggregates, ordinary portland cement and silica fume addition (10%, 15% and 20% replace from cement content).The beams were tested to flexure in laboratory and were determined the mechanical characteristics. The results of tests are presented as load-deflection behavior and cracking propagation. By computer simulation it was shown the same type of failure of beams as the experimental tests.The silica fume addition influences the beam failure, cracking pattern and the value of failure force.

KEYWORDS: computer simulation, addition, beam specimen, flexure test

1.INTRODUCTION

Te computer simulation is used for compare the behaviour of members in laboratory condition and the theoretical one, especially when some components from the mix are varied. The use of silica fume in the concrete composition changes the concrete characteristics and the beam behaviour to flexure /1/ even in the case of ordinary concrete.

2.EXPERIMENTAL PROGRAM

The beam specimen was chosen with a cross-section of 90x120 mm and span of 1500 mm. Fig. 1 illustrates the reinforcement details for specimens.Beams were reinforced with 2 bars of 10 mm diameter and 5 stirrups of 6 mm diameter are placed at the ends of the beam. The structural model and the loads are presented in Fig. 2.

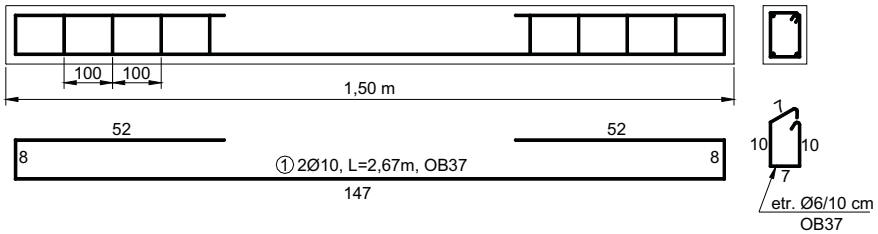

Fig.1 Reinforcement details for beam specimen

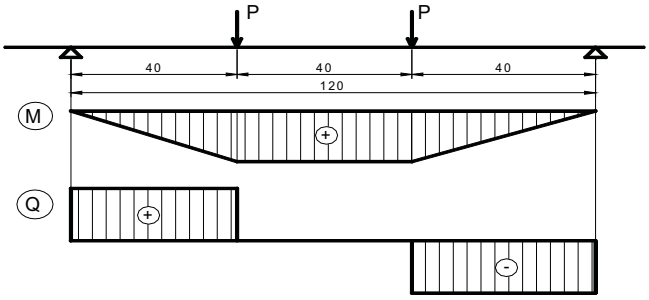

Fig. 2 – Structural model

The concrete poured in the specimens was C16/20 grade, with a cement dosage of about 385 kg/m^3. Portland cement type with compressive strength of 32.5 MPa at 28 days according to Romanian standard was used.

The aggregate was natural sand and gravel with the maximum size of 16 mm. Condensed silica fume used was in different dosage 0,10, 15, 20% by weight of cement as replacement of cement.

3. THEORETICAL ANALYSES

The simulation of loading process is made based on finite element program Cosmos/M. The authors use a small new program to generate the simulation model and to put this model on Cosmos/M application.

The loads are applied step by step. On every step, if appear new cracks the simulation model is changed automatically and the new crack appeared is introduced in the Finite Element Model. The algorithm is showed in Fig. 3. The results are presented in Table 1. Because the number of loading steps is very big, we present in table 1 only a few representative stress maps for different loading steps.

Table 1 – Stress maps for different loading steps

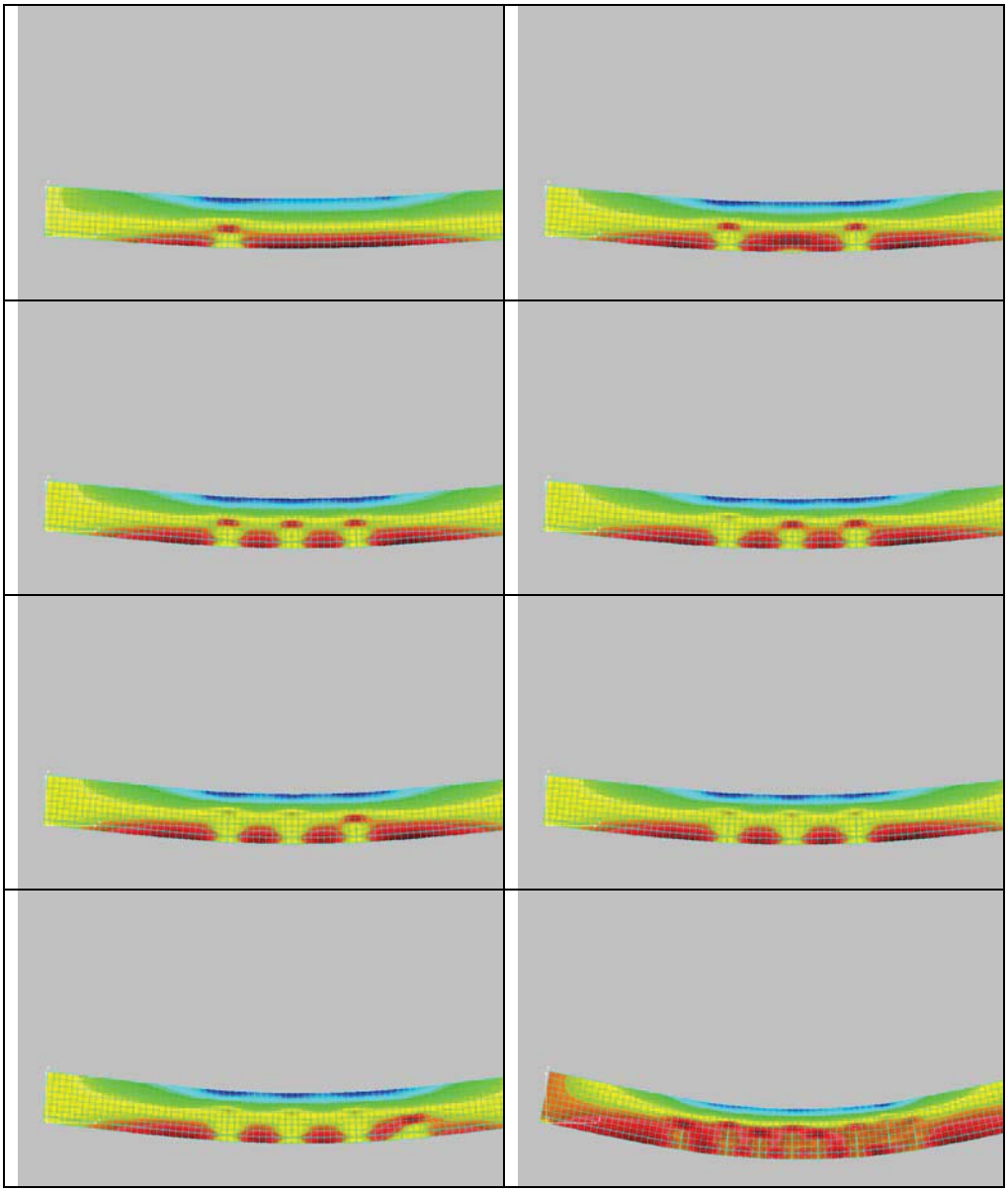

4. EXPERIMENTAL TESTS

Beams, simply supported were subjected to flexure, two-point symmetrical loading was applied to produce a constant moment in the mid-span region, Fig. 2, 4. At

each stage of loading, the deflection at midspan (C3), the compressive concrete strains in the uper fiber of the beam(C1) and the tensile strains in the bottom fiber of the beam (C2) were recorded. The concrete strains were measured using dial gauges with gauge length of 200 mm. The occurence and development of cracks were also observed and recorded.The beam were tested till failure,being compare the experimental type of failure with that given by simulation.

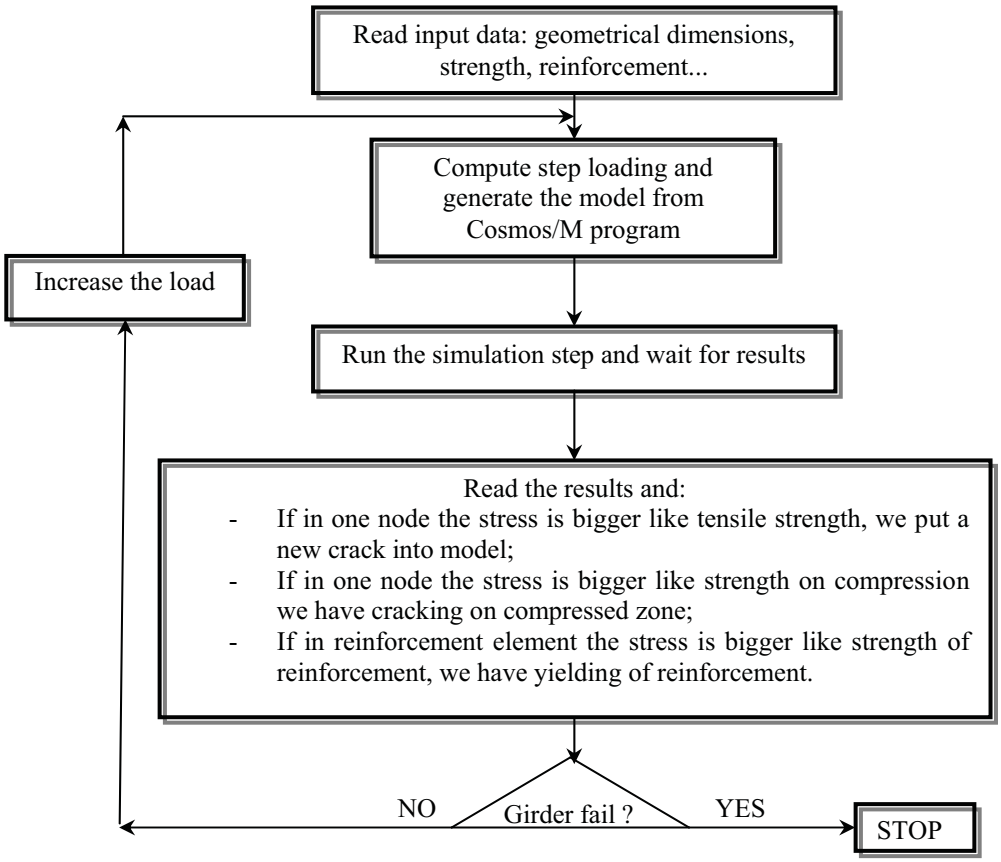

Fig. 3 - Computing algorithm

5. TEST RESULTS AND DISCUSSIONS

The load vs. midspan deflection curves for tested beams are presented in Fig. 5 and the central moment vs. midspan deflection curves are presented in Fig. 6. We can see a good corresponding between experimental and theoretical results.

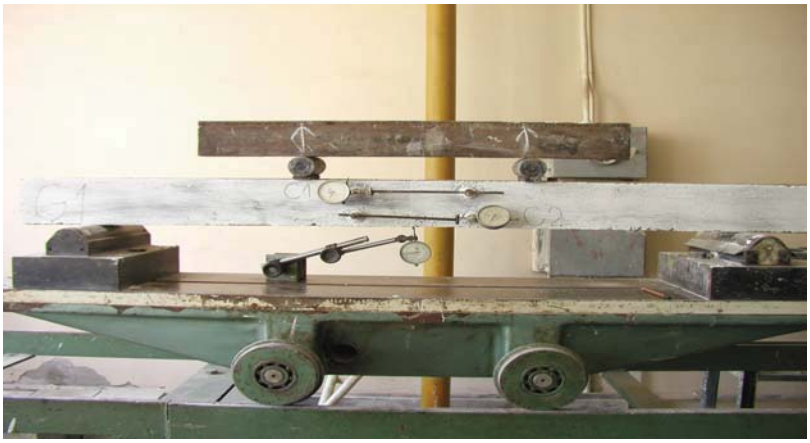

Fig.4. - Tipical experimental set-up

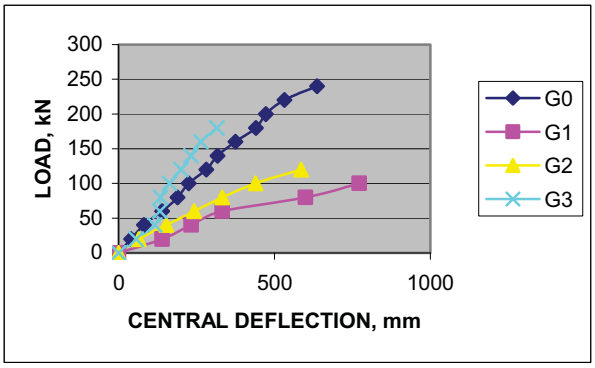

Fig. 5 Load-deflection curves

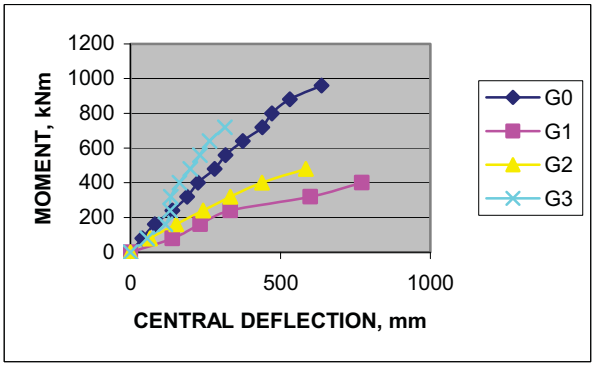

Fig.6. - Midspan moment-curvature for different beams

a)Load-deflection behaviour. Fig. 5 shows typical curves for the beams that were subjected to static load. Prior to cracking, the beams exibited linear elastic behaviour.

We can observe that for the beams with 10% silica fume addition and 15% silica fume addition, a change in slope occurs for a load of about 20 KN; for the beam with 20% silica fume addition the change occurs for a load of about 40 KN and for the beam without addition the change occurs only for a load of about 50 KN. Upper these loads the curves remained linear until the steel reached yield, for all beams.

The bigest deflection at ultimate load presents the beam G1 (with 10% silica fume addition): 772 mm; then the beam G0: 637 mm; after that the beam G2: 585 mm and the smallest deflection was for beam G3: 315 mm.

Among the beams with silica fume addition we observe that beam G3 supported the biggest load: 180 KN.

b)Moment curvature diagrams

In the constant moment zone, near midspan the behavior of beams is basically elastic-plastic Fig. 6, in the case of reduced silica fume addition (beams G1 and G2) and is more elastic in the case of G0 and G3.

c)Cracking

Fig. 7 shows the mode of failure and crack patterns in the beams.

In the case of beam **G1** the cracks are developed especially in the pure bending region, are rare and most of them are inclined.

The compressed concrete is destroyed, the depth at failure is 6 cm.

For the beam **G2** the cracks are vertical, developed in the pure bending region, are reduced as height.

The compressed concrete is crashed, the depth being 5 cm.

Beam **G3** at failure presents cracks, predominant vertical, developed especially in the pure bending zone.

The compressed concrete is completely crushed, the depth is 6 cm.

In the case of beam **G0 (G4)** the cracks are developed on the entire span of the beam: in the central zone are vertical and near supports are inclined. At failure the tension crack reached the crushing zone.

The compressed concrete is less destroyed, the depth being 3,5 cm.

Generally, in the case of beams with silica fume addition, the compressed zone is more destroyed than in the case of beams without silica fume.

Fig. 7 Failure mode and crack pattern

Also, in the case of beams with silica fume addition cracks are not developed to the depth of beams and are not on the entire span of the beam; inclined cracks did not occur. The widths of cracks at failure has values between 1 mm and 1,9 mm.

In the case of beams without silica fume the cracks are closely, more developed toward the compressed zone; the width is bigger, of about 2,3 mm.

The computer simulation indicates the same type of failure as in the experimental tests.

5. CONCLUSIONS

From these researches, the following conclusions result:

(1) The computer simulation shown that the failure of beams occurred with cracks in the pure bending zone and the complete destroy of concrete from the compressed zone; this type of failure is more pronounced in the case of beams with silica fume content.

(2) It appears that silica fume improved the behaviour to shear, because the collapse of beams did not occur through diagonal tension failure (inclined cracks did not occur as in the case of beam without silica fume addition).

(3) The experimental data corresponds to that given by computer simulation (we can observe big deflections of beams, the cracking pattern).

References

1. P. Fidjestol :*Applied Silica Fume Concrete,* Concrete International, November 1993, p.33-36.
2.M. Barbuta, M. Patras: *Properties of hydraulic concrete incorporating large amounts of silica fume,* Bul U.T. Iasi*,* Tom XLIII, Fasc. 1-4, Hidrotehnica,1998, p. 65-72

"Computational Civil Engineering 2006", International Symposium
Iaşi, România, May 26, 2006

Some aspects regarding the design and building of the retaining walls systems made of precast concrete blocks

Nicolae Ungureanu[1], Mihai Vrabie[1], Adrian Moga[2], Cristian Ungureanu[3]

[1]*Department of Structural Mechanics, "Gh. Asachi" Technical University, Iasi, Romania*
[2]*Moinesti Municipium Mayoralty, Romania*
[3]*University of Medicine and Pharmacy „Gr. T. Popa" Iasi, Romania*

Summary

Retaining walls are a large category of engineering structures of multiple uses, having an essential safety ensuring role. The structural systems are varied because the situations and requirements derived from both site conditions and other criteria are varied.

The paper enlarges upon retaining walls systems that use an outstanding amount of precast units and multiple cylindrical vault type structural systems supported by abutments [1], [2]. The paper proposes extending the structural system to retaining walls and develops certain specific issues.

Some considerations regarding structural design are made. Mohr's theory on stress limit state and its use in determining the active and passive soil pressures on retaining walls is being developed.

Rankine's hypothesis, according to which the pressures on surface elements that are parallel to the free surface of the ground have a vertical direction; the horizontal acceleration effect which generates inertia forces in the soil are accounted for. On these grounds the normal and tangential stresses on planes parallel to the back-of-wall ground surface are being expressed.

By using the intrinsic curve corresponding to the sliding plane and the stresses expressed on these planes, Mohr's limit circles, as well as the active and the passive pressures generated by the seismic event on the retaining wall are being determined.

The solving process is an essentially graphic one and allows for the finding of the sliding plane and the main normal stresses as well as the extreme tangential ones in the points of this plane in which the tension state has reached the limit.

KEYWORDS: retaining walls, precast units, structural systems, Mohr's theory, Rankine's hypothesis, limit stress states.

1. INTRODUCTION

Retaining walls are structures of great practical utility. They are included mainly in the category of safety ensuring systems. These walls are widely used on the tracks of traffic ways that cross relatively uneven areas, along water streams, especially when the rivers pass through urban areas where regulation works may be necessary in case landslides need to be controlled. Retaining walls may be also found in certain built-up areas developed on hills or along the rivers, in the vicinity of works of art, e.g. bridges.

The erection of such structures requires a large amount of materials as well as workforce, to say nothing of the additional works done on the building sites. The technologies that use precast units in these structures enable a diminution of the wet works, of forms and, sometimes, even of displacements, as well as an easier operation accompanied by a more efficient control of precast units quality.

Under such conditions, the designing of these retaining systems differs from that of massive masonry walls. A solution, still in use but insufficiently developed, is that of erecting retaining walls with abutments. Essentially, in these systems the ground thrust and other cumulative effects are transmitted to some spaced elements, the abutments. More in-depth analyses demonstrate that these abutments can be built in such a way as to interact with soil masses or rocks, with favorable effects on safety ensuring.

2. PRECAST UNITS

The precast units (blocks) are thus designed so as, when cast in place, to produce a wedging without other additional materials and means [3], [4].

The first member (Fig. 1 a) is shaped like two frustums of pyramid with rectangular bases, the smaller ones being extended to form one unit (Fig. 1 b, c).

The second member (Fig. 1 d) is shaped like also two frustums of pyramid with rectangular bases (Fig. 1 e, f), the greater ones being extended to form a single unit.

The geometric parameters of the precast units can be in a relatively wide range, depending on the geometry of the structure, strength requirements, handling means when placed, coupling mode (mortars, additives, etc.).

In sizing up, all dimensions can be expressed in relation to a single parameter, λ. An example, tested on models [3], [5], without being restrictive, may be:

$$a_1 = \lambda, \quad a_2 = (1{,}1 \div 1{,}2)\lambda, \quad a_3 = (0{,}6 \div 0{,}7)\lambda,$$
$$a_4 = (0{,}5 \div 0{,}8)\lambda, \quad a_5 = (1{,}5 \div 2{,}0)\lambda, \quad a_6 = (0{,}6 \div 1{,}0)\lambda, \tag{1}$$
$$b_1 = (1{,}0 \div 1{,}5)\lambda, \quad b_2 = (1{,}0 \div 1{,}3)\lambda; \quad h = (0{,}8 \div 2{,}0)\lambda$$

Practically, these values have some geometrical constraints.

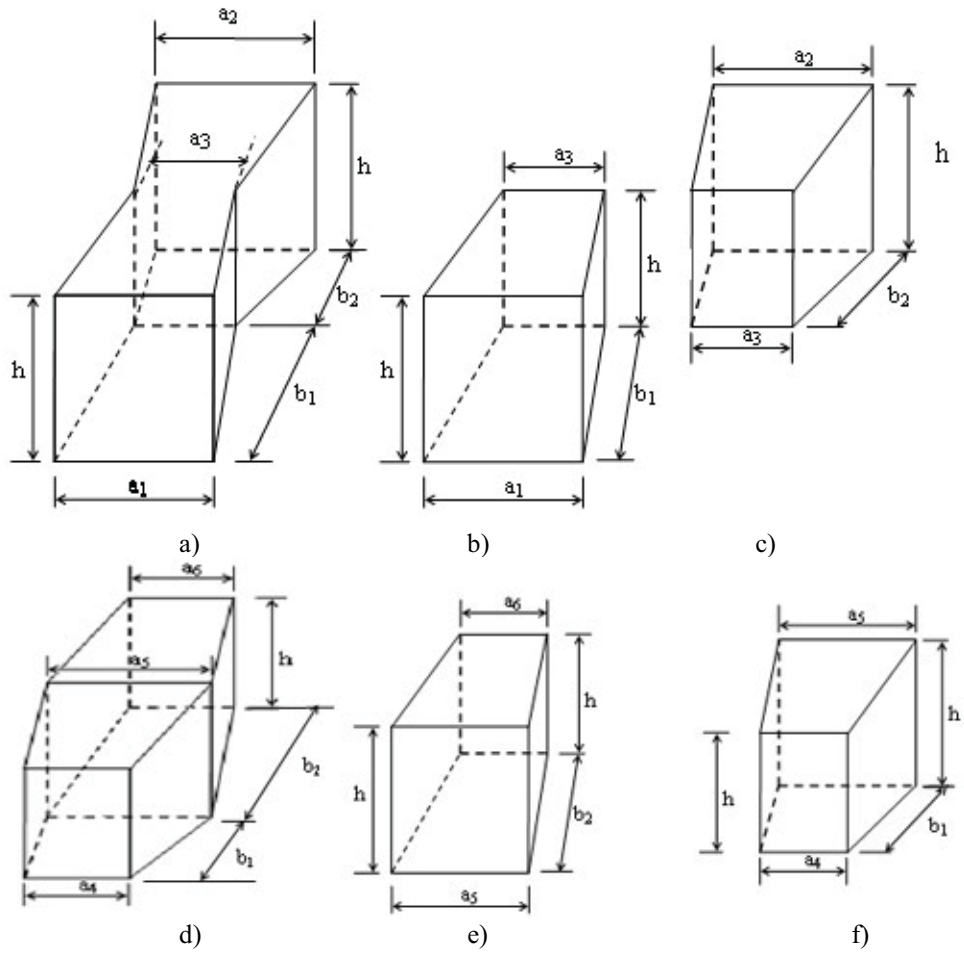

Figure 1. Precast blocks used in the erecting of the retaining wall structure

More complex decisions concerning the sizing of the precast blocks can be taken during structural design work, which depends on the specific site conditions and the envisaged structural system [6]. The paper will focus on the multiple vault abutments system, which has proved to be very efficient.

The precast units may be composed of:

- Concrete (heavy), grades 15 ÷ 25 made up of Portland cement;

- Heavy concrete, grades 15 ÷ 30 with hydraulic cements and additives, especially where water is present (rivers, sea);
- Concrete of lightweight aggregates with common or special cements, depending on the aggregates used, when the precast structure does not contribute with its dead weight to ensure the stability of the retaining wall-ground system.

The precast unit in Fig.1 a and d may be used alone in making the structure or in the other combination, for example member (a) and (e), or (a) and (f).

It is worth mentioning that the precast units may be made using the same formworks, from the unit (a) and (d), by placing the metal or glass plates for delimiting their side.

Likewise, introducing the plate in the central section of element (a) we obtain the elements (e) and (f).

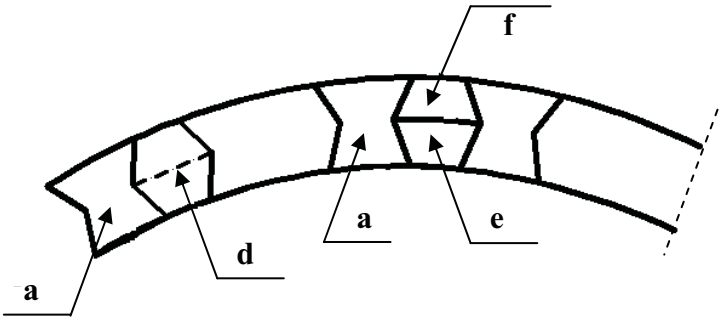

Figure 2. Precasting procedures using a single formwork system

In practice, all types of units described so far can be erected in one formwork by creating separation joints, depending on the requirements of the structural system.

All the units described, or parts of units may be made up of stone by using performant stone cutting equipment, in which case aesthetic shapes are aimed at.

Similar units for certain retaining walls may be made from special ceramics. Where the architectural design requires it, functional and aesthetic details may be considered.

3. STRUCTURES FOR PRECAST RETAINING WALLS

Further on, mention will be made of the vault-shaped retaining walls made up of precast members supported on in-situ cast abutments (Fig. 3).

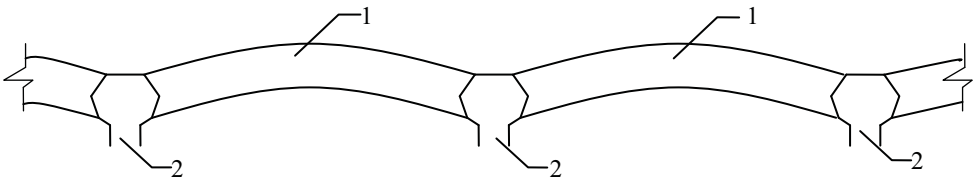

Figure. 3. Plan view of the retaining wall: 1-vaults; 2-abutments

The disposition in plan of the precast units can be seen in Fig. 4.

Figure 4. One example for the disposition in plan of the precast units

The mounting of the precast units may be done with high grade cement mortar and plastifying agents that increase their ductility, adhesiveness, and shear strength, as well as by using specific adhesives instead of mortar.

If the retaining walls have a great height, splayed foundations may be erected under the vaults, their hardening being achieved by in-situ casting of concrete after assembling, which may take several shapes, as presented in Fig.5.

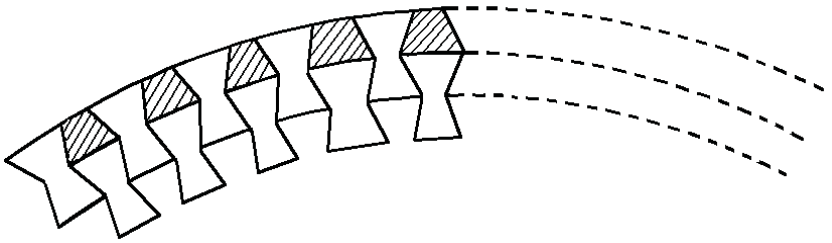

Figure 5. The retaining wall hardening by in-situ casting of concrete

The concrete may be also reinforced along the vertical, while the reinforcement may be anchored to the foundation.

In certain zones, the retaining walls have the characteristics of works of art, and the crowns may be correspondingly treated (Fig. 6 a, b, c). Other architectural elements can be attached, as well, and the abutments are included in this aesthetic conception.

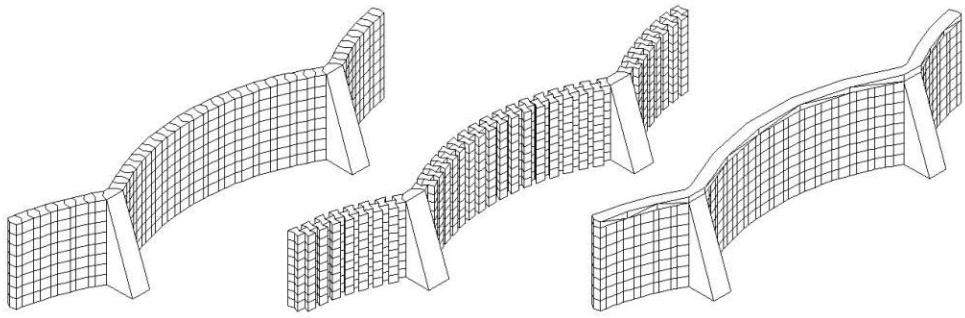

a) b) c)

Figure 6. The retaining walls as works of art

5. SOME PROBLEMS REGARDING THE DESIGN

We consider, first time, that the wall have not the displacements. The vertical pressure and the lateral pressure, from the dead weight of the soil are respectively

$$p_v = \sigma_z = \gamma h \tag{2}$$

and

$$p_h = \sigma_h = \frac{\nu_0}{1-\nu_0}\gamma h = K_0 \gamma h \tag{3}$$

where γ – the unit weight of the soil; ν_0 – Poisson ratio of the soil as elastic bodies; K_0 – the coefficient of lateral pressure of soil; h – the depth.

When a continuous uniformely distributed load q acts on the surface of soil, the pressure p_h is:

$$p_h = K_0(\gamma h + q) \tag{4}$$

The direction of the pressures p_h are the same of the radii of cylindrical wall (Fig. 8a). The axial effort from the cylindrical wall produces by p_h is

$$N = Rp_h = RK_0(\gamma h + q) \tag{5}$$

R being cylindrical radius.

Due to the arch effect, the soil pressures generates forces that self balance on the abutment as well as forces in the vertical plan of the abutments, being taken over by these (Fig. 8b).

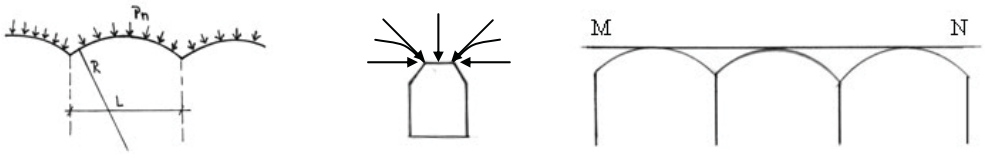

Fig. 8. a) The direction pressure of the soil; b) the arch effect; c) the plane of the pressure

If the retaining wall have a displacement, the active pressures of the soil may be evaluated by Rankine method, considering the pressures on the plane MN (Fig. 8c).

Similarly to the static case, the seismic pressure on a point located on the plane parallel to the back-of-wall ground surface, are vertical (Fig. 9a).

Let us consider the effect of the soil inertia forces given by the horizontal acceleration on the same sections. From the elementary equilibrium equation we can determine the normal and tangential forces on sections that are parallel to the back-of-wall ground surface, in points on the sliding surface, particularly in a point at the base of the wall in which the sliding plane intersects the retaining surfaces (Fig. 9b).

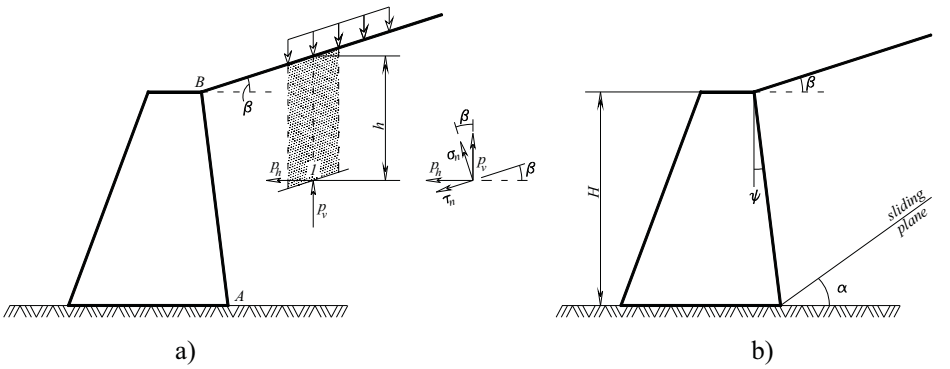

Figure 9. Rankine's hypothesis in the case of seismic action

4. LIMIT STRESS STATE

The limit stress state in a point may be represented by Mohr's circle. Any circle tangent to the intrinsic curve represents a limit stress state.

In the case of a retaining wall where a limit stress state has been reached in the soil, that is, the yielding plane has been formed, in a point which might be point A from the base of the wall the stresses σ_n and τ_n on the section through A, parallel to

the ground surface plane, represents a limit stress state and the point $M(\sigma_n, \tau_n)$ will be situated on Mohr's circle corresponding to yielding.

It is admitted that the soil is cohesive and, by knowing the angle of internal friction φ and cohesion c, the intrinsic curve can be plotted. From a geometrical point of view, we need to draw a circle that passes through the point M and is tangent to the two straight lines.

There are two solutions and through M will pass two circles tangent to the two lines which form the intrinsic curve. The small circle corresponds to the active pressures, while the big one corresponds to the passive ones (Fig. 3).

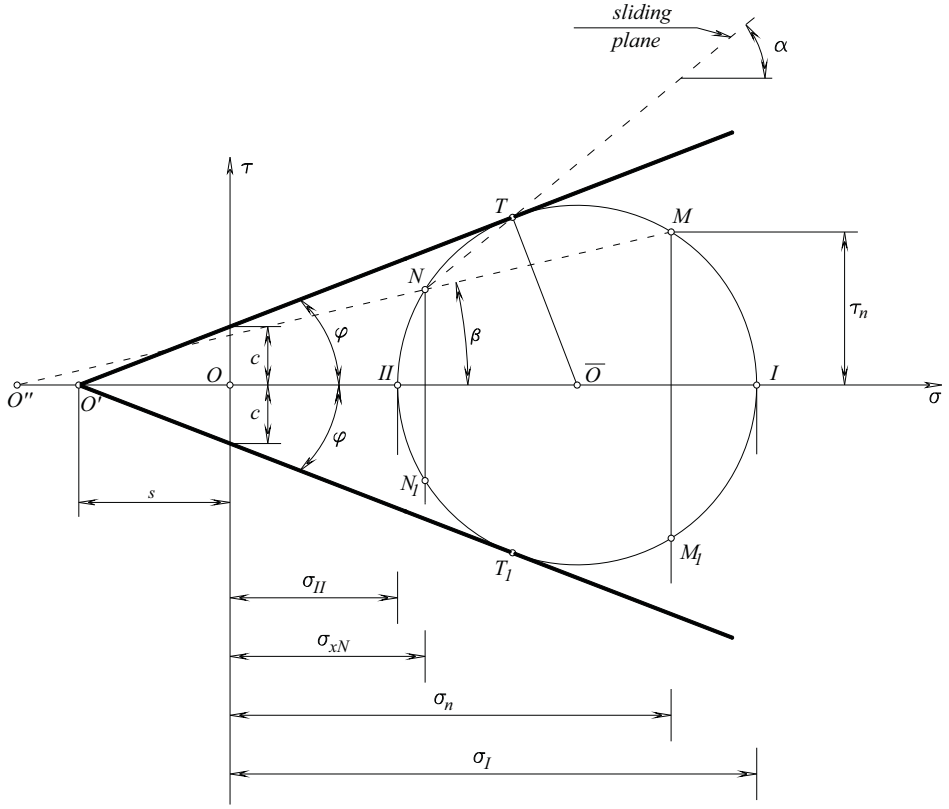

Figure 3 Representation of the limit stress state with Mohr's circle

The line passing through the point M and make the angle β with the horizontal direction (0σ) is parallel to the soil surface plane. This line intersects the circle in the second point N, which is called the circle's pole. This pole has the property that the direction given by the line which connect a point on the circumference with the point N is parallel to the section plane on which act the stresses representing the

point's coordinates. The symmetrical of N against the axis $O\sigma$, the point N_1 on the circle determines the limit stresses $\sigma_{xN_1}, \tau_{xN_1}$ on the face of the wall. As a consequence of equality $\sigma_{xN_1} = \sigma_{xN}$, there follows that:

$$\sigma_{xN} = \sigma_{xN_1} = \overline{\sigma_{xN}}(\gamma + q) \tag{6}$$

and $\overline{\sigma_{xN}} = \overline{\sigma_{xN_1}} = k_{as}$, therefore

$$P_{as} = \frac{1}{2} HK_{as}(\gamma H + 2q) \tag{7}$$

The direction of the yielding plane can be obtained by connecting N with T, and the second plane corresponds to the direction NT_1.

The parallel to NT which passes at the base of the wall and makes the angle α with the horizontal, represents the trace of the sliding plane.

The points I and II determine the main planes on which the tangential stresses are null; σ_I is the maximum stress, and σ_{II} is the minimum stress.

The circle centre has the coordinates $(\frac{\sigma_I + \sigma_{II}}{2}, 0)$, and the radius is equal to $\tau_{\max}$; for the active pressures, it results:

$$R_a = \frac{\sigma_I - \sigma_{II}}{2} \tag{8}$$

In the case of non-cohesive soils, for which $c = 0$, we can draw the circle using $\overline{\sigma_n}$ and $\overline{\tau_n}$ so that to obtain $\overline{\sigma_{xN}} = \overline{\sigma_{xN_1}} = K_{as}$. All the previous reasoning stands valid, with benefic practical consequences. The coefficients K_{as} may be easily determined for different categories of non-cohesive soils.

The cohesive soil can be treated to determine the pressures on the face of the walls as for a non-cohesive soil with the same internal friction angle as of the cohesive one. Using the correspondence theorem, the spherical tensor is superposed on the stress s, applied on the whole contour of the yielding prism, plus a uniform load of intensity s on the back-of-wall free soil surface.

3. CONCLUSIONS

The vault-shaped retaining walls made up of precast units, have several merits, of which mention can be made of:

- manufacturing of precast units in workshops, which ensures the high quality of the products;
- savings in materials: forms and concretes, compared to the current solutions;
- precast unit shapes and the manner of placing them ensure an adequate balance and a high strength, as well as a higher productivity, as compared to the wholly cast "in situ' retaining walls;
- large possibilities to ensure the stability of the structure, due both to the arch effect and the transmission of stresses to the abutments;
- the retaining walls, by their shapes and the details that can be associated to, belong to the works of art with a significant aesthetic value;
- adaptability to varied relief shapes.

By designing precast retaining walls shaped as vaults supported on abutments and taking account of the specific locations, various other merits of these systems can be enhanced.

Extending the use of limit stress state by means of Mohr's circle allows us to obtain a graphic solution of the way pressures on retaining walls are determined using Rankine's hypothesis, extended for the case of seismic action. The solving is relatively simple and general for the gravity and assimilated retaining walls. It may be used in both cohesive and non-cohesive soils. The coefficients of earth pressure may be determined for both active and passive pressures.

References

1. Ungureanu, N., Popovici, N. *New constructive types of filter dams on torrent beds*, Proc. of the Jubilee Scientific Session of the Hydrotechnical Engineering Faculty ,"Gh. Asachi" Polytechnic Institute, Iasi, 1978.
2. Ungureanu, N., Băloiu, V., Popovici, N. *Precast arched filter dam structure for torrent beds correction*, Patent no.75275 (1980), Romania.
3. Popovici, N., Ungureanu, N. *Essais sur modèles de travaux hidrotechniques préfabriqués pour l'aménagement des torrents*, Polytechnic Institute Bulletin, Iasi, vol. XXVI (XXX), Fasc.3-4, SectionV- Civil Engineering Architecture.
4. Ungureanu, N., Popovici, N. *Une structure en arc des elements prefabriques pour les barrages utilises dans l'amenagement des torrents*, Polytechnic Institute Bulletin., Iasi, vol. XXVIII (XXXII), Fasc. 1-4, 1982, pp. 57-60.
5. Boariu C. *On the stress and stability of underground structures during construction works and in operation*, Doctoral thesis, "Gh. Asachi" Technical University, Iasi, 2000.
6. Huang Tien-kuen *Mechanical Behavior of Interconnected Concrete-Block Retaining Wall,* Journal of Geotechnical and Geoenvironmental Engineering, vol. 123, No. 3, March 1997, pp. 197-203.
7. Ungureanu, N., Vrabie M., Moga A., Ungureanu C. *Precast Vault Shaped Retaining Walls Systems*, International Technical-Scientific Conference "The Real Problems of the Urbanism and Territory Arrangement", 30 sept. – 1 oct. 2004, Chişinău, Moldova, vol. I, pp. 214-219.
8. Caquot, A., Kerisel, J. *Tratat de mecanica pământurilor*, Ed. Tehnică, Bucureşti, 1968 (traducere din limba franceză)
9. Clayton, C.R.S. *Retaining Structures,* Thomas Telford, London, 1993.

10. Clough, G.W., Duncan, S.M. *Earth Pressures* – Foundation Engineering Handbook H.Y. Fang, Ed. Chapman &Hall Ltd. New York, 1994.
11. Greco, V. *Stability of Retaining Walls against Overturning,* Journal of Geotechnical and Geoenvironmental Engineering, Vol. 123, Issue 8, pp. 778-780, August 1997.
12. Lungu, I., Stanciu, A., Boți, N. *Probleme speciale de geotehnică şi fundații,* Ed. Junimea, 2002.
13. Moga, A. *Asupra conformării şi calculului unor elemente şi structuri plane şi spațiale folosite în construcțiile de sprijinire,* Teza de doctorat, Univ. Tehnică „Gh. Asachi" Iaşi, 2005.
14. Sparacio, R., Chianesse, E. *Structture di sostegmo in presenza di accelerazioni di sisma*, Conferenza tenuto al corso di perfezionamento il 30 Gennaio 1975, Universita de Napoli, 1976.
15. Stanciu, A. *Une generalisation de la theorie de Coulomb pour le calcul de la poussee e de la butee des terres,* Revue Francaise de Geotechnique, no. 50, pp. 39-59, 199
16. *** *Efectele acțiunii dinamice a pământului asupra construcțiilor de reținere (ziduri de sprijin, construcții subterane, hidrotehnice),* Contract 835/1981, lista CNST, nr. 103/1982, ICCPDC Iaşi, resp. ing. Gh. Palamaru, I.P. Iaşi – Catedra de Mecanica Construcțiilor, resp. N. Ungureanu.

"Computational Civil Engineering 2006", International Symposium
Iaşi, România, May 26, 2006

Modeling and evaluation of seismically induced damages by functional and stochastic models

Adrian Vulpe[1], Alexandru Carausu [2]

[1] *Dept. of Structural Mechanics,* [2] *Dept. of Mathematics,*
"Gh. Asachi" Technical University of Iasi

Summary

In this paper we further develop some (of our) earlier approaches to the modeling of damage effects induced by earthquake motions in structures. A large variety of damage indices and damage functionals have been proposed and applied in seismic damage studies. The selection of one or another analytic model naturally depends on the nature of the structure and also on the earthquake load characteristics. As regards the mathematical nature of the models proposed and/or used in structural reliability and seismic risk assessment, the fragility curves and various vulnerability functionals have been rather widely used. We propose a more extensive employment of mathematical models based upon stochastic processes as more specific tools for modeling the structural response and damage effects induced by seismic motions.

Keywords: seismic damages, damage index, stochastic models, seismic fragility

1. INTRODUCTION

The analysis of the degree or state of damage is essential for the estimation of the remaining lifetime and also for rehabilitation / retrofitting decisions and programs. But – even in the design – the evaluation or prediction of potential structural damage during the expected lifetime is an important issue. Appropriate analytical and probabilistic damage models must be selected in order to perform a realistic analysis / evaluation.

A large variety of damage indices or indicators have been proposed and used for damage quantification for specific categories of structures. In general, they are scalar functions whose values may be related to specific structural damage states or levels [1], [2], [3], [4]. Naturally, the models selected for the quantification basically depend on the nature of the structure and also on the expected adverse actions from the environment, at the site of the system under analysis, able to affect its stability or service capacity. The effects of earthquake actions are – probably – among the most dangerous for the structures, industrial facilities, bridges and dams, etc.

In order to define the collapse or another type of failure for components and structures, it is necessary to define and use damage parameters which are relevant for the strength and deformation capacity of structures under cyclic loads in the inelastic domain. These parameters are the arguments of a real scalar function that synthetically characterizes the degree of damage experienced by the structure. Such a function is – mathematically speaking – a damage functional. If only two damage states are taken into account, the failure and the absence of plastic damage, such a functional may be normalized so as to take value 1 in the former case and value 0 in the latter one. If several degrees of damage are admitted, it may take any values in the interval [0,1].

The most commonly used damage parameter has been the ductility. The evaluation of the structural safety is evaluated by comparing the maximum plastic excursion and the allowable value, considering only one cycle with the largest plastic deformation and neglecting the others [5], [6]. Another class of models consider the hysteretic energy as the damage parameter and the collapse is assumed to occur when the structure dissipates an energy equal to (or higher than) a limit value. The methods based on such models take into account the contribution to energy dissipation of all cycles independently from the cycle amplitude. Conversely, it has been experimentally and practically proved that the cycles with limited plastic deformation are of no practical relevance to the degree of damage sustained.

An approach that combines the knowledge on ductility and energy has been developed in several papers by E. Cosenza et al. [7], [8], [9]. In fact, earlier approaches of this type, due to Banon & Veneziano [2], respectively Park & Ang [3], are integrated in an extended formulation. However, not of all these methods for damage arrive to probabilistic evaluations for the damage levels of a structure induced by earthquake excitations. The most specific classes of models for the probabilistic assessment of earthquake effects on structural systems are those involving seismic fragility and vulnerability formats.

The fragility of a component or structure is essentially its probability of failure conditional on a certain intensity of ground motion at its site. The vulnerability formats can also take into account the level of damage induced by previous earthquakes (or other factors like aging) for predicting the future damage events under expected earthquakes of certain intensities.

Therefore the concept of vulnerability seems to be better suited for seismic damage evaluation. In the next section we present an evaluation of the damage models which are compatible with the use of fragility and vulnerability concepts. A widely accepted ground motion parameter PGA (peak ground acceleration) is replaced by parameters like MMI and MSK intensities.

A specific fragility model is thus obtained, in terms of events that consist in reaching a certain damage category over a scale of three to five damage levels. Then we present a way to enrich the vulnerability models by taking into account

the magnitude and the maximum seismic intensity in the evaluation of the damage rate for certain classes of structures, also involving some attenuation laws. Some possibilities to incorporate stochastic processes into damage models are addressed in the last section of the paper. We thus extend our earlier investigations on (seismically induced) damage modeling and analysis of papers [10], [11] and [12], [13].

2. SEISMIC DAMAGE INDICATORS AND DAMAGE FUNCTIONALS

The steps to be followed in defining a damage functional are formulated by Cosenza *et al* in [9] as follows :

(*i*) Definitions of parameters d_i which are considered as important / relevant to the definition of progressive collapse.

(*ii*) Definition of the values $\mathbf{d}_Y$ and $\mathbf{d}_U$ assumed by the state vector at the beginning of structural system yielding and at collapse under cyclic loads, respectively.

(*iii*) Introduction of a normalized damage functional D, defined on the space of the state vectors $\mathbf{d} = [d_1 \ldots d_i \ldots d_m]$; this function should assume a value of 0 at the beginning of yielding and a value of 1 at failure, and it should increase as damage increases.

(*iv*) Evaluation of the value assumed by the functional, with reference to the structure examined and for the expected seismic events; the seismic checking will be satisfied if it results in $D < 1$.

It follows from (*iii*) that a damage functional would have to be analytically expressed as a function of the damage state vector $\mathbf{d}$, that is $D = \varphi(\mathbf{d})$ where φ **:** $\Delta \rightarrow [0,1]$ is a function from the space of (the possible values of) the damage parameters $d_1, \ldots, d_i, \ldots, d_m$ to the unit interval.

This formulation is quite general, so far. Yet we may raise here the problem of the nature of the selected damage parameters from the probabilistic point of view. If at least one of them has a random nature then the damage functional itself becomes random. Clearly, all of the damage parameters may be random with specific distributional assumptions accepted for modeling their random behavior. Let us denote by F_i the *cdf* (cumulative distribution function) of the random parameter d_i. Then the *cdf* of the damage functional D will be defined by

$$F_D(\delta) = P(D \leq \delta) = P(\varphi(d_1, \ldots, d_i, \ldots, d_m) \leq \delta). \tag{1}$$

The evaluation of the probability in Eq. (1) will clearly depend not only on the distributions assumed for the random components of $\mathbf{d}$ (i.e., for the arguments of

φ) but also on the analytic nature of this function. This problem will be examined (in more detail) in the next section.

Let us now see a couple of examples of damage indicators or functionals considered in some references dealing with seismic damage modeling. The cinematic ductility is defined in [7-9], for a SDOF structure with EPP behavior, by

$$d = \mu_s = \frac{x_{\max}}{x_y} \tag{2}$$

where $x_{\max}$ is the maximum plastic excursion and x_y is the yielding displacement. The value of this damage parameter is equal to 1 at yielding (this value is denoted $d_y = 1$) while the value at collapse is d_u = the maximum allowable value of ductility $\mu_{u,mon} = x_{u,mon} / x_y$ where $x_{u,mon}$ is the maximum displacement determined by monotonic tests. If $x_{\max}$ is taken in absolute value then Eq. (2) gives the cyclic ductility. An analytic form for a normalized damage functional is proposed in [7-9] by

$$D = \begin{cases} 0 & \text{for } d \le d_y, \\ \left(\dfrac{d - d_y}{d_u - d_y} \right)^{\alpha} & \text{for } d_y < d \le d_u, \ \alpha > 0. \end{cases} \tag{3}$$

It is easy to see that this damage functional takes values in the interval [0,1], and it effectively depends on a single damage parameter d given by Eq. (2), but also on the parameters d_y, d_u and α. The first two of them are the characteristic values of d at yielding / collapse considered in step (*ii*) while α is a parameter involved in the analytic form of function φ. The domain of φ is $\Delta = [0, d_u]$. However, this simple example shows that a more exact formulation for the function φ would need to extend its argument(s) so as to include some parameters**:** $D = \varphi(\mathbf{d},\boldsymbol{\theta})$.. The corresponding form of the normalized damage functional in terms of kinematic or cyclic ductility is

$$D_{\mu} = \frac{\mu - 1}{\mu_{u,mon} - 1}. \tag{4}$$

Many hysteretic models for the damage evaluation are formulated in terms of the plastic dissipated energy E_h: the structural collapse is assumed to occur when the total dissipated energy reaches or increases beyond a limit value $E_{u,mon}$. Even in this case, the allowable amount of energy that can be dissipated can be obtained by means of a monotonic analysis which evaluates just the limit value $E_{u,mon}$. The hysteretic ductility is defined [7-9] as

$$\mu_e = \frac{E_h}{F_y x_y} + 1 \tag{5}$$

where F_y is the maximum force to which the structure can be subjected. The corresponding (energy-based) damage functional D_E has just the form in Eq. (4) with μ replaced by μ_e and $\mu_{u,mon}$ by $\mu_{e,mon}$.

Combinations of the ductility-based damage indicators with energy-based indicators were proposed. Among the best known are the methods due to Banon & Veneziano and to Park & Ang, respectively. Their original formulations may be expressed in terms of the ductility / energy parameters just presented above. The B&V method leads to the damage functional

$$D_{BV} = \sqrt{\left(d_1^*\right)^2 + \left(d_2^*\right)^2} \quad \text{with} \quad d_1^* = d_1 - 1 \;\&\; d_2^* = a(d_2)^b \tag{6}$$

where a and b are two parameters which are specific to the structural problem and have to be determined experimentally. The two damage parameters that occur in Eq. (6) are $d_1 = \mu_s$ (see Eq. (2)) and $d_2 = 2(\mu_e - 1)$ (see Eq. (5)). Therefore, the function φ corresponding to the Banon-Veneziano damage functional of Eq. (6) is

$$D_{BV} = \varphi(d_1, d_2) = \sqrt{(d_1 - 1)^2 + (a d_2^b)^2}\,. \tag{7}$$

In the (d_1^*, d_2^*) plane, the circles centered at the origin define the lines with equal collapse probability as it follows from the Banon-Veneziano functional in (6).

The Park-Ang damage functional is defined as a linear combination of the maximum displacement and the plastic dissipated energy ; its expression is given by

$$D_{PA} = \frac{x_{max}}{x_{u,mon}} + \beta \frac{E_h}{F_y x_{u,mon}} = \frac{\mu_s + \beta(\mu_e - 1)}{\mu_{u,mon}}\,. \tag{8}$$

The physical interpretation of the Park-Ang damage functional is based on the assumption that, under plastic dissipation of energy, the collapse does not occur when the the kinematic / cyclic ductility reaches the ultimate value of the monotonic test $\mu_{u,mon}$ but the fraction β of the hysteretic ductility μ_e must be added to the former ductility. This factor β may be considered as a free deterioration parameter that characterizes the structural elements. Since $\mu_{u,mon}$ is experimentally determined for a certain structure or component and it does not depend on the maximum EPP displacement x_{max} we may consider it as a

structural parameter rather than a damage indicator ; if we denote it by η the analytic expression of the function φ corresponding to the Park-Ang damage functional of Eq. (8) is

$$D_{\mathrm{PA}} = \varphi\,(d_1, d_2) = \frac{d_1 + \beta\, d_2 \;/\; 2}{\eta}. \tag{9}$$

The damage parameters d_1 and d_2 have been previously defined. It is remarked in [9] that D_{PA} is not a normalized damage functional since it does not provide the value 0 for $x_{\max} = x_y$ and the value 1 in the case of failure.

Many other damage indicators (or parameters) are considered in the literature on seismic damage assessment. We do not intend to present and discuss very many of them. As we have already mentioned, different damage measures based on hysteretic models may be even not comparable since the differences in their formulations may follow from the different nature of the structures under analysis. However, a comparison between B-V, P-A functionals and the damage functional by the plastic fatigue method is presented in [9]. Let us remark, so far, that the general form of a damage functional with the function φ that occurs in Eq. (1) may be retrieved in the examples just presented; yet, its analytical expression may depend not only on the damage parameters like d_1 and d_2 but also on some parameters: $\theta_1 = = a$ & $\theta_2 = b$ in Eq. (6), respectively $\theta_1 = \beta$ & $\theta_2 = \eta$ in Eq. (9). This gives a ground for the general form to be suggested for a damage functional, namely $D = \varphi\,(\mathbf{d}\,,\,\boldsymbol{\theta})$. It is clear that the damage parameters have a random nature since they are associated with the seismic response of the structure which is, in fact, the output to the random input consisting of the seismic ground motion at the site of the structure. But, besides this source of randomnes, some (or all) of the parameters in $\boldsymbol{\theta}$ may be uncertain. Moreover, even the analytical form of the function φ would have to be considered as uncertain, even when it is derived on the ground of experimental results or by the analysis of response to actual or artificial earthquake accelerograms. This distinction between randomness and uncertainty is usual in the seismic fragility models. We approach such problems in the next two sections of the paper.

3. PROBABILISTIC ASSESSMENT OF SEISMIC DAMAGE IN HYSTERETIC STRUCTURES

We have just discussed the problem of the randomness of the *damage indicators* (or parameters, as they are termed in [9]), that is, of the components of the vector

$$\mathbf{d} = (d_1, \ldots, d_i, \ldots, d_m).$$

It is clear that the evaluation of the probability in Eq. (1) cannot be accomplished without assuming certain probabilistic distributions for the random damage indicators. On another hand, the condition of the normalized damage functional to take only the $0 - 1$ values seems to be too restrictive since a rather widely accepted and used functional like D_{PA} has not been normalized. In order to avoid this limitation, we may let φ to take any positive value. As we have mentioned, the function defining the damage measure also depends (in general) on a set of parameters $\boldsymbol{\theta} \in \Theta$. Hence the general form of this function is $\varphi : \Delta \times \Theta \rightarrow [0,\infty)$.

There are many studies and even computer codes for the damage state assessment of a structure in terms of qualitative (or "linguistic") degrees of damage like, e.g., (no damage, moderate damage, heavy damage, collapse). These scales for damage levels vary from a reference to another. Other scales include an additional level, namely "slight damage" between "no damage" and "moderate damage". If a damage measure D taking values in $[0,1]$ is used then the five levels of damage severity may be assigned to the respective intervals described in Table 1 that follows.

Table 1. The intervals for a normalized damage measure over a five levels scale

Damage level	No damage	Slight damage	Moderate damage	Severe damage	Collapse
Interval for D	[0 , 0.1)	[0.1 , 0.25)	[0.25 , 0.4)	[0.4 , 0.8)	[0.8 , 1]

This scale is the revised form (by Ang, in 1993) of the scale proposed by Park, Ang & Wen in 1985. The value of 0.4 is taken as the limit of damage beyond which the structure is not repairable.

From the probabilistic point of view, it is relevant to evaluate the probability that a certain structural member or structure will reach a certain damage level under an estimated structural response induced by an earthquake of an estimated intensity & duration. If a damage functional $D = \varphi(d, \theta)$ is used, with its cdf $F_D(\delta)$, then the probability that the damage level of the structure will fall within an interval like those suggested in Table 1 will be given by

$$P(\delta_k \le D < \delta_{k+1}) = F_D(\delta_{k+1} + 0) - F_D(\delta_k + 0). \tag{10}$$

The notation for the arguments of $F_D(\,)$ in Eq. (10) stand for the right lateral limits.

The evaluation of the probability in Eq. (10) would be not possible without some distributional assumption on the random parameters in $\mathbf{d} = (d_1, \ldots, d_i, \ldots, d_m)$. Indeed, the inequality under the probability in the left-hand side of Eq. (10) can be rewritten as

$$\delta_k \le \varphi(d_1, d_2, \ldots, d_m ; \theta_1, \theta_2, \ldots, \theta_\ell) < \delta_{k+1}. \tag{11}$$

If we assume that all the damage parameters are random variates with the respective *cdf*'s (cumulative distribution functions) $F_1, \ldots, F_i, \ldots, F_m$ or with the *pdf*'s (probability distribution functions) $f_1, \ldots, f_i, \ldots, f_m$ then the probability that the damage parameter d_i takes values in a specified interval $[a_i, b_i]$ can be expressed as

$$P(a_i \le d_i \le b_i) = \int_{a_i}^{b_i} f_i(x)\,dx = \int_{a_i}^{b_i} dF_i(x) = F_i(b_i) - F_i(a_i). \tag{12}$$

The probabilities of Eqs. (12) for $i = 1, 2, \ldots, m$ can be used for the evaluation of the probability in Eq. (10) provided the event in Eq. (11) can be assembled from the component events as those that occur in (12). Even when certain probabilistic distributions are accepted for $d_1, \ldots, d_i, \ldots, d_m$ this problem may be not too simple. Its solution also depends on the shape of function φ as well as on the values of the parameters $\boldsymbol{\theta}$ which explicitly occur in Eq. (11). In many cases, these parameters are considered as deterministic but their values are estimated by regression analysis, as in a paper by Han and Wen. A limit state function can be easily obtained from a damage functional φ as in Eq. (11). If a failure threshold δ^* is selected (for instance $\delta^* = 0.4$) then the limit state function can be defined by

$$g(\mathbf{d}, \boldsymbol{\theta}) = \delta^* - D = \delta^* - \varphi(\mathbf{d}, \boldsymbol{\theta}). \tag{13}$$

The failure event will be characterized by $g(\mathbf{d},\boldsymbol{\theta}) \le 0$ while the survival of the structure will correspond to the converse inequality $g(\mathbf{d},\boldsymbol{\theta}) > 0$. We include an example to illustrate a possible solution to the evaluation of probabilities as in Eqs. (10) & (13) at the end of this paper.

Another way for a probabilistic evaluation of the nonlinear behavior of RC members consists in effectively using vectors of damage parameters $\mathbf{d}$ and not necessarily taking such a vector as the argument of the function φ. Such a vector is assumed to be time-dependent and it characterizes the state of the system in the space Δ of the damage parameters.

An approach of this kind was considered (in [2]) by Banon & Veneziano. Six damage indicators were analyzed, namely the rotation ductility μ_θ, the curvature ductility μ_φ, the damage ratio DR, the flexural damage ratio FDR, the *normalized cumulative rotation* NCR, and the *normalized dissipated energy* E_n. Among them, FDR and E_n were found to be the most relevant. They are defined and redenoted below, resulting in a vector damage function:

$$\begin{cases} \text{FDR} = K_f \,/\, K_r = d_1, \\ \mathrm{E_n} = \int_0^t M(\tau)\,\theta(d\tau) \,\Big/\, \frac{1}{2} M_y\, \theta_y = d_2(t), \end{cases} \tag{14}$$

where K_f = the initial flexural stiffness, K_r = the reduced secant stiffness, $M(\tau)$ is the yield moment (at time τ), $\theta(d\tau)$ is the rotational increment of the inelastic spring at one end of the member during the time interval $(\tau\ ,\ \tau + d\,\tau)$, M_y = the yield moment, and θ_y = the rotation at yielding ; t is the time elapsed from the beginning of loading. The corresponding vector damage function is

$$\mathbf{d}(t) = [\, d_1(t)\ \ d_2(t)\,] \ . \tag{15}$$

The initial value of $\mathbf{d}$ is $\mathbf{d}\,(0) = [1 \quad 0]$ and it corresponds to the point $A\,(1,0)$ in the $(d_1\ ,\ d_2)$ plane. The current point P in this plane is considered to represent a damage state, that is the state of the system at time t . Two hazard functions are also considered in [2], namely

$$\lambda_1(d_1\ ,\ d_2\ ,\ d_2'_1) \ \ \&\ \ \lambda_2(d_1\ ,\ d_2\ ,\ d_1'_2)\ ,$$

where $d_2'_1$ denotes the derivative of d_2 with respect to d_1 , and similarly for the second function. A line integral from A to P, denoted by I_L , is involved in defining the survival failure probability of the structural member as follows **:**

$$I_L = I_{AP} = \int_A^P \lambda_1(d_1, d_2, d_1'_2)\, dd_1 + \lambda_2(d_1, d_2, d_1'_2)\, dd_2 \ ; \tag{16}$$

$$P(\text{survival}) = \exp(-I_L)\ ,\ P(\text{failure}) = 1 - \exp(-I_L)\ . \tag{17}$$

In our paper [11] we presented evaluations for the integral in Eq. (16) without neglecting the third arguments of the two hazard functions (as it is done in [2]) ; in fact, this integral can be evaluated in the $(d_1{*}, d_2{*})$ plane where the new variables are connected to the original ones according to the transformations in Eqs. (6).

We also considered the progressive failure in a structure (consisting of several member with hysteretic behavior); the structural probability of failure / survival was evaluated on the basis of the assumption that the mean distance from the origin to the failure points is Weibull-distributed.

4. FRAGILITY AND VULNERABILITY MODELS FOR SEISMIC DAMAGE ASSESSMENT

Fragility models applied to seismic damage evaluation

We approached the use of fragility models in structural damageability assessment in our papers [12] and [13]. The models and formulas presented in the previous sections of this paper allow for more detailed characterizations of the seismic damage reached by a structure with hysteretic behaviour in terms of the severity classes, using adapted fragility models. Since the 80's when the fragility concept was introduced, mainly for the PSA (probabilistic safety assessment) of the NPPs, the fragility-based models have undergone a significant development and a wider use for the seismic risk evaluation of various classes of structures. In general, the relationship *ground motion intensity versus structural damage* induced thereby characterizes the level of damage to a particular class of structures as a function of a ground motion parameter.

A number of $n + 1$ damage states are considered by A.Singhal in [16], which are the components of a damage state vector. We denote this vector by $\boldsymbol{\delta} = (\delta_0, \delta_1, \ldots, \delta_n)$, with the warning that is basically different from the vector $\mathbf{d}$ whose components were distinct damage parameters (or indicators); the components of the former vector, that is δ_i's, may be taken as the points determining the partition of the range for the damage measure D; for instance, they may be equal to the values in Table 1 if D is a normalized damage functional (in the terminology of [6], [7], [8]). This damage measure is assumed to be a random variable. A "classical" fragility curve describes the probability of failure conditional on a certain ground motion intensity. For the probabilistic damage evaluation, it has to characterize the probability of reaching a damage state at a specified ground motion level. Formally, we define the probabilities

$$p_{ik} = P(D \in [\delta_{i-1}, \delta_i) \mid M = m_k) \tag{18}$$

where D is a random (normalized) damage measure and M is a random ground motion intensity parameter. Eq. (18) gives a similar (but not identical) way to efine fragilities proposed in [16]. The intervals that occur under the probability operator are just the same as in Eq. (10).

These "damage fragilities" are clearly the probabilities of Eq. (10) conditional on the event that the seismic intensity M (denoted by Y in [16]) belongs to a certain intensity class. Clearly, it has been implicitly assumed a discretization of the range where this ground motion parameter takes its possible values. Hence, the event $M = m_k$ should be replaced by $M \in [m_{k-1}, m_k)$.

Certainly, we may accept continuous values for m in $[0\,,\infty)$ or $[0\,,\sup M)$. In most of the typical fragility models the seismic input parameter is the PGA capacity A, that is the peak ground acceleration corresponding to the failure of the system. In the general case, the random variable M is represented as

$$M = \widetilde{M}\ \varepsilon_R\ \varepsilon_U \quad \text{with}$$

$$\text{Med}[M] = \widetilde{M},\ \text{Med}[\varepsilon_R] = \text{Med}[\varepsilon_U] = 1,\ \sqrt{\text{Var}[\varepsilon_R]} = \beta_R,\ \sqrt{\text{Var}[\varepsilon_U]} = \beta_U. \tag{19}$$

These three parameters in Eqs. (19) are sufficient for expressing the seismic fragility of the structure in the double log-normal format by the *cdf* defining the failure probability conditional on the median seismic capacity C, and by the *pdf* that accounts for the random variability of C around its median **:**

$$P_f(m) = \Phi\left[\frac{\ln(m/C)}{\beta_R}\right] \quad \text{with}$$

$$f_C(c) = \frac{1}{\sqrt{2\pi}\,\beta_U\,c}\exp\left[-\frac{1}{2}\left(\frac{\ln(c/\widetilde{C})}{\beta_U}\right)^2\right] \tag{20}$$

where Φ is the standard normal *cdf* and the variabilities due to randomness (of the response) and to uncertainty (in the theoretical model for C) are accounted for by the standard deviations in Eqs. (19). Fragility curves for a global damage index, defined as a weighted sum of element damage indices, were derived for RC structures of lower / higher rise by A.Singhal [16]. The damage functional there used was an equivalent form of Park & Ang damage index (similar to that of Eq. (9)). Its analytic expression is

$$D = \frac{\theta_m}{\theta_u} + \frac{\beta}{M_y\,\theta_u}\int dE \tag{21}$$

Using the general form of a damage functional (see Eq. (11)), we may write it as

$$D = \varphi\,(dE\,;\,\theta_m, \theta_u, \beta, M_y)$$

where θ_m = the maximum positive or negative plasting hinge rotation, θ_u = ultimate hinge rotation capacity under monotonic loading, β is a model parameter (evaluated to be = 0.15), Q_y = the calculated yield strength, and dE = the incremental dissipated hysteretic energy. More details on this damage index may be found in [15]. On the basis of 100 artificial ground motions and using

IDARC2D & DRAIN-2DX programs, a nonlinear dynamic analysis was performed by A.Singhal resulting in the fragility curves for the P&A damage index of Eq. (21), with the spectral acceleration taken for the seismic input parameter ($m = S_a$).

The observed building damage data from earthquakes makes possible to update the values of the parameters by the Bayesian method, on the basis of a vector $Z = (z_1, \ldots, z_n)$ of statistical evidence. More details on this Bayesian updating of fragilities are given in [16]. The probability that the damage to a structure exceeds a certain damage threshold δ_i at specified levels of the ground motion m_k is expressed by

$$Q_{ik} = P(D \geq \delta_i \mid M = m_k). \tag{22}$$

With reference to the *cdf* that occurs in Eq. (10), and also introducing the parameters $\boldsymbol{\theta}$, it is easy to see that the probabilities in Eq. (22) can be rewritten as

$$Q_{ik} = 1 - F_D(\delta_i - 0 \mid M = m_k, \boldsymbol{\theta}) \tag{23}$$

As regards the probabilities for the damage measure D to fall exactly in the interval that defines a damage severity level, they are given by

$$q_{ik} = P(\delta_i \leq D < \delta_{i+1} \mid M = m_k, \boldsymbol{\theta}) =$$

$$= F_D(\delta_{i+1} - 0 \mid M = m_k, \boldsymbol{\theta}) - F_D(\delta_i - 0 \mid M = m_k, \boldsymbol{\theta}). \tag{24}$$

These probabilities can be expressed in terms of the fragility model defined in Eqs. (20). The ground motion intensity m_k can be, for instance, the PGA, the PGV, or the MMI intensity at the site. We do not give explicit expressions for the damage fragilities in Eq. (24) ; we presented such expressions in [13]. Four fragility curves are plotted in Fig. 1 of that reference, with the interval for the damage index partitioned into five severity classes ; they are drawn by means of the median D curve.

The probabilities in Eqs. (24) can be found as the lengths of the intervals on the $(O\ q)$ axis determined by the projections on this axis of the fragility curve segments cut by the segments of the median damage index line in the (S_a, D) plane.

Vulnerability models for seismically damaged structures

The concept of seismic vulnerability is similar to that of seismic fragility. Roughly speaking, it expresses a measure of the likelihood of failure (or severe damage) of a structure caused by strong earthquakes. As in the case of the fragility concept, the notion of vulnerability has not a unique and generally accepted definition. A classification and review of the vulnerability methods is presented in a report by

M.Dolce *et al.* to the *10 ECEE* Conf. (Vienna, 1994). During the last decades, several investigations and results on the seismic vulnerability analysis have been accomplished by the research group led by H. Sandi at INCERC – Bucharest. In his paper [17] it is emphasized the importance of the damage probability assessment for already damaged structures in seismically active areas (like Romania with its major seismic source in Vrancea).

Let us conclude that the models for the seismically induced damages based on both damage indices or functionals, respectively on fragility curves, may be termed as *functional models*. For the former class of models this is quite obvious. As regards the fragility curves, they are – in fact – the graphs of conditional cumulative distribution functions, hence their nature is also *functional* but – at the same time – distributional : certain probabilistic distributions are implicitly assumed for the PGA median capacity and for the repartition of the median. In most cases, the double lognormal format is accepted and used.

5. STOCHASTIC MODELS FOR SEISMIC DAMAGES OF STRUCTURES

Other approaches to the probabilistic assessment of the damage state of a structural component / structure consist in the use of stochastic processes. In fact, the deterioration of a structure during an earthquake is actually a time-dependent process. Many of the hysteretic models in use avoid considering this dependence of time explicitly. However, the cumulative damage indices are closer to such a time-dependent approach, since the accumulation of dissipated energy grows with the time and the number of cycles in structural response.

The same remark holds for the fatigue models. An intermediate approach consists in considering the number of peaks or zero crossing in the response process; alternatively, the number of hysteretic cycles may be taken into account. These numbers are, clearly, more or less proportional to the time T = duration of the structural response to a seismic ground motion.

In the most frequently applied aseismic design practices, it is common to reduce the linear elastic design forces and thus to allow a few inelastic excursions in the structural response during a severe earthquake shaking. The structure is required to be sufficiently ductile to withstand these excursions without collapse. Anderson and Bertero [18] showed that the large amplitude accelerations may not always cause significant damage by driving the structure into the non-linear range, whereas many successive non-linear excursions of relatively smaller amplitudes may be more damaging during earthquakes of longer duration. A model based on the order statistics of the response peaks is used in [19] to consider the damage

accumulation from several random nonlinear excursions and to associate the ductility with the total damage due to these excursions.

A notion that may provide a bridge between the models based on damage indicators / functionals and those involving the stochastic processes is that of *damage spectrum*. We found it in the reference [20] by Y. Bozorgnia and V.V. Bertero. A damage spectrum represents the variation of a damage index (DI) versus structural period for a series of inelastic SDOF systems subjected to an earthquake ground motion. The DIs considered by these two authors are normalized, that is their range is the [0,1] interval. This is the case, for instance, with the damage functional D in Eq. (3). The two authors propose improved damage spectra. The first of them (denoted DI_1) is a weighted sum of the normalized plastic deformation and the normalized hysteretic energy ; the second DI is DI_2 = another weighted sum of the normalized plastic deformation and the normalized hysteretic velocity. These improved damage spectra can better quantify the damage potential of the recorded ground motion. They are based on normalized response quantities of a series of inelastic SDOF systems. They provide simple means for considering the demand and capacity related to strength, deformation and energy dissipation of the structural system. They will be zero if the response remains elastic, i.e., no significant damage is expected, and will be unity when the maximum deformation capacity is reached under monotonic deformation. We intend to go deeper with the study of the properties and possible applications / extensions of these improved DIs in a future investigation.

6. CONCLUDING REMARKS

In this paper we have gone a little further with our earlier approaches to the modeling and analysis of seismically induced damages. The most typical among our papers – on this line – is Ref. [13} and we have even had to recall some discussions and formulae from this paper. But there exists a very rich literature on these topics and the variety of damage indices to quantify the effect of seismic motions on structures is quite large. We appreciate as being necessary a deeper involvement of the stochastic processes in modeling and analysis of seismically induced damages in structural systems.

References

1. Mahin, S.A. and Bertero, V.V., "An evaluation of inelastic seismic design spectra," *J. of Structural Division*, ASCE, Vol.107, 1981, pp. 1777-1795.
2. Banon, H. and Veneziano, D., "Seismic safety of reinforced concrete members and structures," *Earthquake Engineering and Structural Dynamics*, Vol. 10, 1982, pp.179-193.
3. Park, Y.J. and Ang, A-H.S., "Mechanistic seismic damage model for reinforced concrete," *J. of Structural Engineering*, ASCE, Vol. 111, 1985, pp. 722-739.

4. Krawinkler, H. and Zohrei, M., "Cumulative damage in steel structures subjected to earthquake ground motions," *Computers & Structures*, Vol. 16, 1983, pp. 531-541.
5. Uang, C.M. and Bertero, V.V., "Evaluation of seismic energy in structures," *Earthquake Engineering & Structural Dynamics*, Vol. 19, 1990, pp. 77-90.
6. Powell, G.H. and Allahabadi, R., "Seismic damage prediction by deterministic methods: concepts and procedures," *Earthquake Engineering & Structural Dynamics*, Vol. 19, 1990, pp. 77-90.
7. Cosenza, E., Manfredi, G. and Ramasco, R., "An Evaluation of the Use of Damage Functionals in Earthquake-Resistant Design," *Proc. Of the Ninth European Conference on Earthquake Engineering*, Vol. A, pp. 303-312, Moscow, Russia, 1990.
8. Cosenza, E. and Manfredi, G., "Seismic Analysis of Degrading Models by Means of Damage Functions Concept," *Proc. Of Workshop on Nonlinear Seismic Analysis of Reinforced Concrete Buildings*, pp. 77-92, Bled, Slovenia, July 1992.
9. Cosenza, E., Manfredi, G. and Ramasco, R., "The use of damage functionals in earthquake engineering: a comparison between different methods," *Earthquake Engineering & Structural Dynamics*, Vol. 22, 1993, pp. 855-868.
10. Vulpe, A. and Carausu, A., "Seismic Reliability Analysis of Reinforced Concrete Structures with Progressive Failure," *Proc. of International Symposium Re-Evaluation of Concrete Structures – Reliability and Load Carrying Capacity*, pp. 249-258, Copenhagen - Lyngby, Denmark, June 1988.
11. Vulpe, A. and Carausu, A., "Evaluation of Seismic Damageability of Structures Using Fragility Models and Damage Risk Matrices," *Transactions of the Fourteenth SMiRT Int. Conference*, Vol. 10, Div. M, pp. 175-182, Lyon, France, August 1997.
12. Vulpe, A., Carausu, A. and Vulpe, G.E., "Use of Fragility Models and Damage Risk Matrices in Structural Damageability Evaluation," *Proc. of the 12th World Conference on Earthquake Engineering*, Paper 2726, pp. 1-8, Auckland, New Zealand, January-February 2000.
13. Vulpe, A., Carausu, A. and Vulpe, G.E., "Earthquake induced damage quantification and damage state evaluation by fragility and vulnerability models. *Transactions* ***SMiRT 16***, Washington DC, August 2001, Paper # 1650, 1-8.
14. Singhal, A., "Stochastic Damage Estimation in Reinforced Concrete Frames," *Proc. Of the Eleventh World Conference on Earthquake Engineering*, Paper 1863, pp. 1-8, Acapulco, Mexico, June 1996.
15. Ang, A.H-S., "Seismic Damage Analysis of Reinforced Concrete Buildings," Chapter 6, *Stochastic Methods in Structural Dynamics* (G.I. Schueller & M. Shinozuka, Eds.), Martinus Nijhoff Publ., Dordrecht-Boston-Lancaster, 1987.
16. Singhal, A. and Kiremidjian, A.S., "Bayesian updating of fragilities with application to RC frames," *J. of Structural Engineering,* Vol. 124, 1998, pp. 922-929.
17. Sandi, H. "A Format for Vulnerability Characteristics of Damaged Structures," *Proc. of the Eleventh European Conference on Earthquake Engineering*, pp. 1-8 (on CD-ROM), Paris, France, 1998, Balkema Publ.House.
18. Anderson, J.C. and Bertero, V.V., Seismic Performance of an Instrumented Six Story Steel Building," Report No. UCB-EERC 91/11, Univ. of California – Berkeley, 1991.
19. Basu, B. and Gupta, V.K., "A probabilistic assessment of seismic damage in ductile structures," *Earthquake Engineering & Structural Dynamics*, Vol. 24, 1993, pp. 1333-1342.
20. Bozorgnia, Y. and Bertero, V.V. "Estimation of damage potential of recorded earthquake ground motion using structural damage indices. *Proc. of the 12th European Conference on Earthquake Engineering*, London, September 9-13, 2002, Paper Ref. 475, pp. 1-8 (on CD-ROM), Elsevier Science Ltd.

"Computational Civil Engineering 2006", International Symposium
Iaşi, România, May 26, 2006

Design of compressed elements simulated with elements of initial deflection equivalent to buckling curves A,B,C

[1]Mihai Coveianu, [2]Daniel Bîtcă

[1,2]*Catedra de Construcţii Metalice , Universitatea Tehnică de Construcţii Bucureşti, România*

Summary

This paper introduces a proposal for the calculation design of compressed elements. The basic idea is that an element has a bearing capacity given by the buckling curves A, B, C, proven experimentally, and this element can be replaced with an equivalent element having an initial deflection f_0. On this element a non linear geometric calculation is performed (using design software, e.g. SAP2000, Images3D, or software developed by this paper's authors, etc). After performing the iterations, if the element does not lose the stability (it finds the equilibrium position) then it is enough to perform resistance checking for bending and axial force at the half length of the element. This calculation is valid if the torsion (the section rotation because of the failure of stability given by the bending-torsion) can not appear. A multi segment model of an element (20 segment element) has been modeled, it was loaded with an axial force $N=\varphi \times A \times R$ and by tests it was found a deflection corresponding to an unit effort equal to R (by a non linear calculation). This was found at the half length of the element. In order to justify the method the case of a double hinged element with different slenderness of 143,118 and 92 was solved. The conclusions are that the stability checking can be replaced with the resistance checking (bending with axial force, the efforts coming from an non linear geometric calculation) if the element has an initial defection of l/700 on curve A, l/400 for curve B, and l/300 for curve C.

Secondly, this model of calculation design is performed in the second part of this paper for some compressed columns, tested at The Steel Structure Tests Laboratory – Steel Structures Department, between April 10 and 14, 2006. The elements were square pipes (120x120x5) with a length of 4500 mm. The purpose of this test in the laboratory was to verify the behavior of a pipe made of bended and then welded steel sheet and to establish its position in one of the buckling curves. The results of these tests were compared with the method described in the paper and an equivalent deflection was proposed for this type of sections.

KEY WORDS: buckling, compressed elements, square steel pipes.

1. FOREWORD

This paper shows the calculation design of a compressed element by a calculation software. The most of the approaches consist of performing a static linear calculation and with the resulted efforts to perform stability checking. Those can be made manually or automatically. This is not far from the reality in most of the cases (but not 100%) but this is not something that uses fully the calculation power of the computers.

Errors can appear though because the buckling lengths of the structure are unknown (as a matter of fact this is a special problem and entire papers can be written on this subject only). The 2 order effects can be estimated correctly only with a few rare software. The c coefficient in the verification relation (the verification of compressed and bended elements from STAS 10108/0-78) which is related to the bending moment diagram distribution is also not very easy to asses. And eventually, the buckling from axial force on one direction is added to the buckling on the other direction from the bending moment.

2. ESTIMATION OF THE EQUIVALENT DEFLECTION FOR EACH BUCKLING CURVE

All the difficulties stated in the introduction can be eliminated using the method describes in the following part (using a calculation software). This is about a method that is comprised also in other codes but only as a recommendation. The ideal element is replaced with an element which has an initial deflection. With this element a nonlinear geometric calculation is performed. After performing the necessary iterations (if the structure does not lose its stability, because this is highlighted by the software) it is enough to do resistance checking at bending with axial force. This calculation is valid if the torsion of the section can not appear.

So, the only matter is estimating the initial deflection f_0, because the bearing capacity of the element depends on it. In this paper an estimation method of this deflection is given. We start with the assumption that a double hinged element has the capacity

$$N_{cap}=\varphi \times A \times R \qquad (1)$$

where φ is calculated using the buckling curves A, B. C given in STAS 10108/0-78.

A multi segment model of a double hinged element (20 segment elements) has been modeled and by tests it was found a deflection corresponding to a unit effort equal to R (by a non linear calculation). This was found in a segment at the half length of the element. In order to convince you about the truth of this method a case of an element with the slenderness of 143, 118 and 92 was solved (I30 profile

with a length of 17, 14 and 11 m stressed in relation with the strong axis - curve A). The calculation model has 21 joints and 20 line elements. The verifications are for the element no 10 at the half to the initial element.

In the next pages the results of double hinged element with a deflection of $f_0 = l/700$ is presented.

The element with a slenderness of 143 has a bearing capacity of:

$$N_{cap}=\varphi \text{ x } A \text{ x } R = 0.364 \text{ x } 6910 \text{ x } 240 = 603.6 \text{ kN}=60.36 \text{ tf} \quad (2)$$

By loading the element with the initial deflection of l/700 with N=60.3 tf, the resulting unit stress is described below (the bending moment in element no 10 is M=10 tf·m):

$$\sigma = \frac{N}{A} + \frac{M}{W} = \frac{603 \times 10^3}{6910} + \frac{0.1 \times 10^9}{653 \times 10^3} = 240.4 \frac{N}{mm^2} \quad (3)$$

The element with the slenderness of 118 has a bearing capacity of:

$$N_{cap}=\varphi \text{ x } A \text{ x } R = 0.500 \text{ x } 6910 \text{ x } 240 = 829.0 \text{ kN}=82.90 \text{ tf} \quad (4)$$

Considering the double hinged element loaded with this effort the resulting unit stress id described below (the bending moment is 8.05 tf·m):

$$\sigma = \frac{N}{A} + \frac{M}{W} = \frac{829 \times 10^3}{6910} + \frac{0.805 \times 10^8}{653 \times 10^3} = 243.4 \frac{N}{mm^2} \quad (5)$$

The element with the slenderness of 92 has a bearing capacity of:

$$N_{cap}=\varphi \text{ x } A \text{ x } R = 0.675 \text{ x } 6910 \text{ x } 240 = 1119.4 \text{ kN}=111.94 \text{ tf} \quad (6)$$

Considering the double hinged element loaded with this effort the resulting unit stress id described below (the bending moment is 5.23 tf·m):

$$\sigma = \frac{N}{A} + \frac{M}{W} = \frac{1194 \times 10^3}{6910} + \frac{0.523 \times 10^8}{653 \times 10^3} = 242.0 \frac{N}{mm^2} \quad (7)$$

The result of these tests is the possibility of neglecting the stability checking and performing only the resistance checking (in the same conditions in which the non linear geometric calculation was performed). It can be stated also that in order to reach the bearing capacity the element will show big defections 142.77 and 31 mm meaning 1/120 and l/180. This kind of deflections can be clearly seen so the failure is not coming with any previous warning as stated in a large number of specialty books. The advantages are then obvious. There is no need of a stability checking

that contains terms not easy to asses (especially the buckling curves). Moreover, the software calculation can solve exactly complex structures with a large number of elements. A figure to be remembered is the initial deflection of $f_0=l/700$ that is equivalent of the buckling curve A in the Romanian Standard.

In the following part the same problem is solved for the buckling curve B (the calculation was performed with the same section even if the section is classified in curve A) By tests the deflection resulted $f_0=l/400$. For space reasons only all this calculation is not fully presented, it can be found at position 1 in the bibliography.

In the same method the problem was solved for the buckling curve C (the calculation was performed with the same section even if the section is classified in curve A). By tests the deflection resulted $f_0=l/300$.

In figure 1 the buckling curves A, B,C are presented and also 9 points resulted from the calculation proposed by the authors (with initial deflections of *l/700* for the buckling curve A, *l/400* for the buckling curve B and *l/300* for C) calculated for slenderness of (λ) 92, 118 and 143. This points are practically on the curves A, B and C , the differences being very small. The differences are presented in table 1.

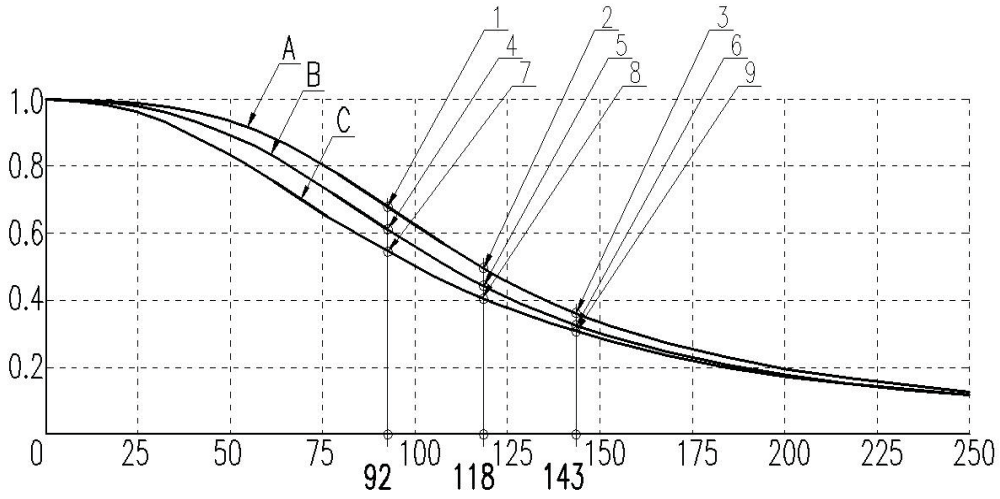

Figure 1. Graphic representation of the results obtained from the calculation proposed by the authors

Table 1. Differences between STAS and the proposed method (in percentage)

Point	λ	Difference [%]
1	92	0.8
2	118	1.2
3	143	0.1
4	92	4.1
5	118	2.5
6	143	2.7
7	92	0.5
8	118	0.5
9	143	2.5

By *Difference [%]* we understand the procentual difference between the calculation model proposed by the authors and the classic model from STAS 10108/0-78.

As a conclusion, the proposal can be that for each of the curves A,B and C an imperfection to be introduced as an initial deflection according to the tabel below. We must say that in reality the element does not have this initial deformation but his recommended deformation solves also the matter of remanent tensions. Even so, the final deflection of the element will result from a non linear calculation because the remanent tensions decrease the rigidity of the element.

Tabel 2. Initial deflections equivalent to buckling curves A, B, C

Curve	f_0
A	1/700
B	1/400
C	1/300

3. INITIAL DEFLECTION FOR COMPRESSED ELEMENTS WITH A SQUARE PIPE STEEL SECTION

In this chapter a reference is made to the square pipe section resulted by bending and welding of a steel sheet. In the standard at law (10108/0-78) the square pipe section is obtained by hot rolling and it is classified in the buckling curve A. Because the section realized by welding is a recent procedure it is not included in the standard at law for the moment. This is the reason why compressed columns have been tested (section 120x120x5 and a length of 4500mm), at The Steel Structure Tests Laboratory – Steel Structures Department between April 10-14, 2006.

The capable stress obtained was around 32-33tf (6 tests have been performed)

Capable stress (taking into account also the slenderness is λ =97.67)

Curve A:

$$N_{cap}=\varphi \text{ x } A \text{ x } R = 0.634 \text{ x } 2290 \text{ x } 240 = 348.5 \text{ kN}=34.85 \text{ tf} \quad (8)$$

Curve B:

$$N_{cap}=\varphi \text{ x } A \text{ x } R = 0.569 \text{ x } 2290 \text{ x } 240 = 312.7 \text{ kN}=31.27 \text{ tf} \quad (9)$$

Curve C:

$$N_{cap}=\varphi \text{ x } A \text{ x } R = 0.510 \text{ x } 2290 \text{ x } 240 = 280.3 \text{ kN}=28.03 \text{ tf} \quad (10)$$

Iti is noticed that the value resulted by tests lead to a buckling curve between the curves A and B from the STAS 10108/0-78.

The authors propose for this elements made of welded square pipe a initial deflection f_0=l/500. The following table is presented where ***u*** is the shortening of the element under compression, ***v*** is the deflection at half length (v_e being the value measured experimentally), and the unit stresses N/A (from axial force) and M/W (from bending moment)

Table 3. Values of the deflections and tensions obtained experimentally and by design calculation

N [t·f]	u [mm]	v [mm]	v_e [mm]	N/A [N/mm^2]	M/W [N/mm^2]	N/A+M/W [N/mm^2]
10	1.03	2.52	0.40	43.6	13.9	57.5
20	2.10	6.87	2.60	87.3	38.1	125.4
30	3.31	16.21	11.10	131.0	90.5	221.5
31	3.46	17.76	15.00	135.4	99.2	234.6
32	3.61	19.52	18.40	139.7	109.1	248.8
33	3.77	21.52	24.60	144.1	120.3	264.4

In figure 2 values of ***N*** and ***v*** are presented. They are resulted experimentally and also by calculations. The correct approach of the model proposed by the authors can be noticed from the figure below. The initial deflection is l/500.

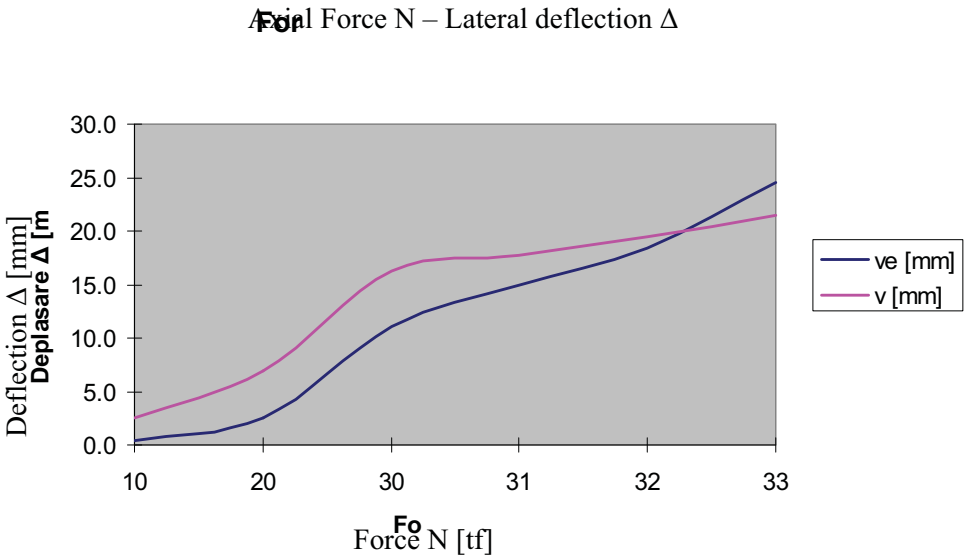

Figure 2. Diagram N-Δ resulted experimentally and by calculation

4. CONCLUSIONS

As a conclusion a proposal of introducing an imperfection as an initial deflection according to the table below can be made for each of the curves A,B,C and also for the square pipe steel sections. It must be underlined that in reality the element does not have this initial deformation but this (recommended) deformation solves also the effect of residual tensions. Even so, the final deflection of the element will be resulted from a non linear calculation because the residual tensions decrease the rigidity of the element.

Table 4. Initial equivalent deflection of the sections classified in the buckling curves A , B, C according to STAS 10108/0-78 and square pipe steel section

Curve	f_0
A	1/700
B	1/400
C	1/300
Square Pipe Section	l/500

For the ordinary calculation of the square pipe welded steel section the (self assuring) classification is on the curve B or more exactly by interpolation between A and B.

References

1. Coveianu, M. *Contribuţii la calculul geometric neliniar al structurilor metalice alcătuite din bare (Teza de Doctorat)*, Universitatea Tehnica de Construcţii, Bucureşti, 1998. (in Romanian)
2. Bănuţ, V. *Calculul neliniar al structurilor*, Editura Tehnică, Bucureşti, 1981. (in Romanian)
3. Mazilu, P. *Statica construcţiilor vol.1*, E.S.A.C., Bucureşti, 1955. (in Romanian)
4. Mazilu, P. *Statica construcţiilor vol.2*, Editura Tehnică, Bucureşti, 1959. (in Romanian)
5. Pătrâniche, N., Siminea, P., Chesaru, E. *Construcţii metalice*, Editura Didactică şi Pedagogică, Bucureşti, 1982. (in Romanian)

"Computational Civil Engineering 2006", International Symposium
Iaşi, România, May 26, 2006

Studies regarding the computation of vibrating frequencies for steel taintor (radial) gates

[1]Adrian Prodescu, [2]Daniel Bîtcă

[1,2]*Steel Structures Departament , University of Civil Engineering, Bucharest, Romania*

Summary

Steel taintor gates are mobile elements used in hydraulic structures for the partially or totally closing-opening of some spillways or for controlling the water level on upstream, controlling the water discharge and for the evacuation of the floatable debris, ice and alluviums.

Water, excepting hydraulic pressure on the gate, may have hydrodynamic effects when flowing, if the gate is totally or partially opened. These hydrodynamic effects may be dangerous and it could reflect to principal hydraulic structure. Amplification of gate vibration is happened when the water edge pulsating frequencies is around the gate eigenfrequency. In the sequel of this fact, the determination with precision of this frequencies is very helpful, to avoid the undesired process. In this paper it was elaborated the mathematic mesh for a deep radial gate. Using this model, a modal analysis has been made considering different models for the border (bearing) conditions.

KEYWORDS: radial gate, eigenvalues, eigenfrequency, bearing conditions

1. STUDY'S OBJECT

In this paper it is analyzed a deep radial gate, which have dimensions 4,00x4,00m, located on 20,00m depth.

The structure of the gate is in main part made by steel sheet with 10mm thickness. The structure of radial gate is presented in figure 1.

Without the resistance steel structures, the radial gate is composed by sealing device, made by rubber profile type P (see figure 2). This study was intent on determinate the influence of accurate modeling the bearing conditions about eigenvalues and eigenfrequencies of the gate. It was analized the influence of lateral sealing device who remains in contact with the piers of dam, in time of gate maneuvering.

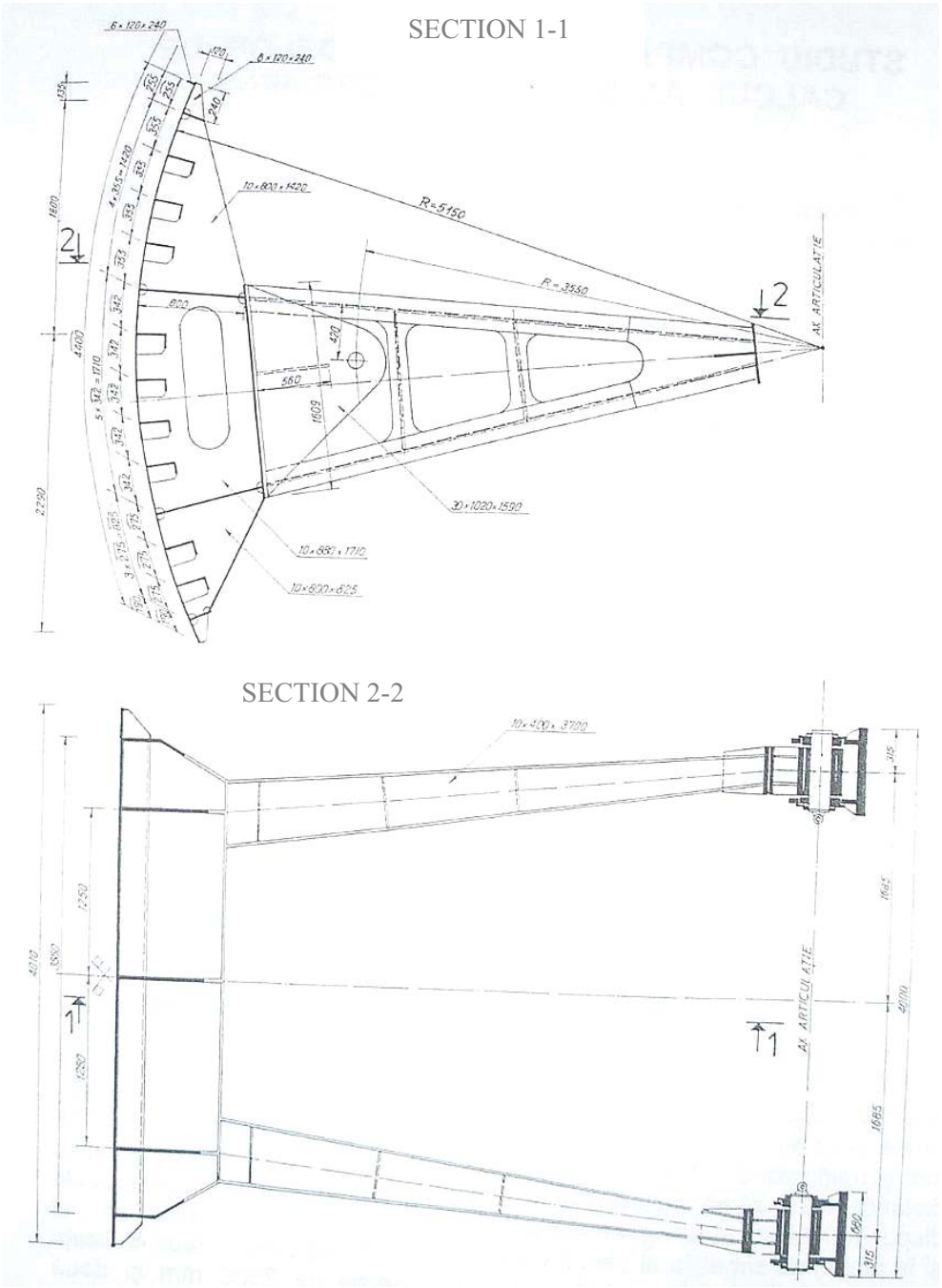

Figure 1. The structure of analized radial gate

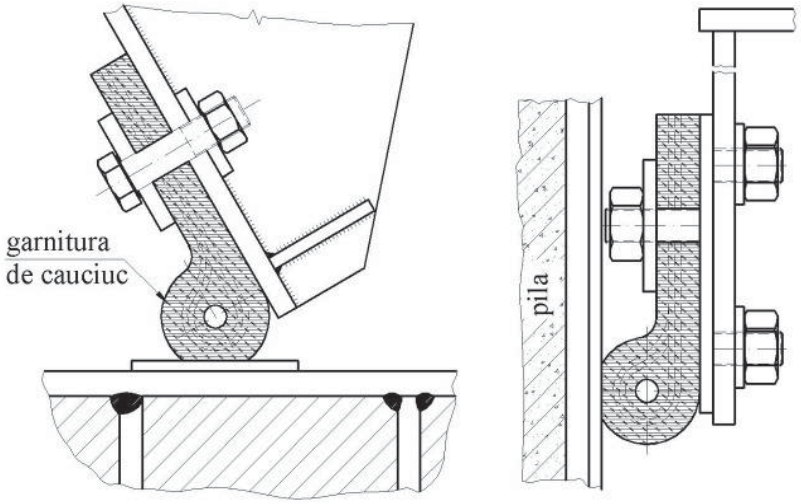

Figure 2. The sealing device: bottom pack and lateral seal pack

Considering variability of Young's modulus value for rubber according miscellaneous sources (literature, internet) three hypotheses were analyzed, namely:

- hypothesis 1, when the lateral sealing is neglected;

- hypothesis 2, when the lateral sealing is meshed in and the rubber Young's modulus is considered with value $E_c = 30$ N/mm^2;

- hypothesis 3, when the lateral sealing is meshed in and the rubber Young's modulus is considered with value $E_c = 300$ N/mm^2;

2. THE MESH OF THE STRUCTURE

In order to perform the modal analysis in the hypotheses described above, one has been built a finite element mesh. The mesh contains about 3400 thin shell elements with bending capabilities. The hydraulic cylinder was meshed using beam elements. For these elements, the Young's modulus was affected (E_h=10000N/mm²) in order to take into account the compressibility of the hydraulic oil. The cylinder was considered to be hinged by the gate.

Figure 3 shows the mesh of the taintor (radial) gate.
The modal analysis was made using the version 9. 0. 3 of SAP 2000 software.

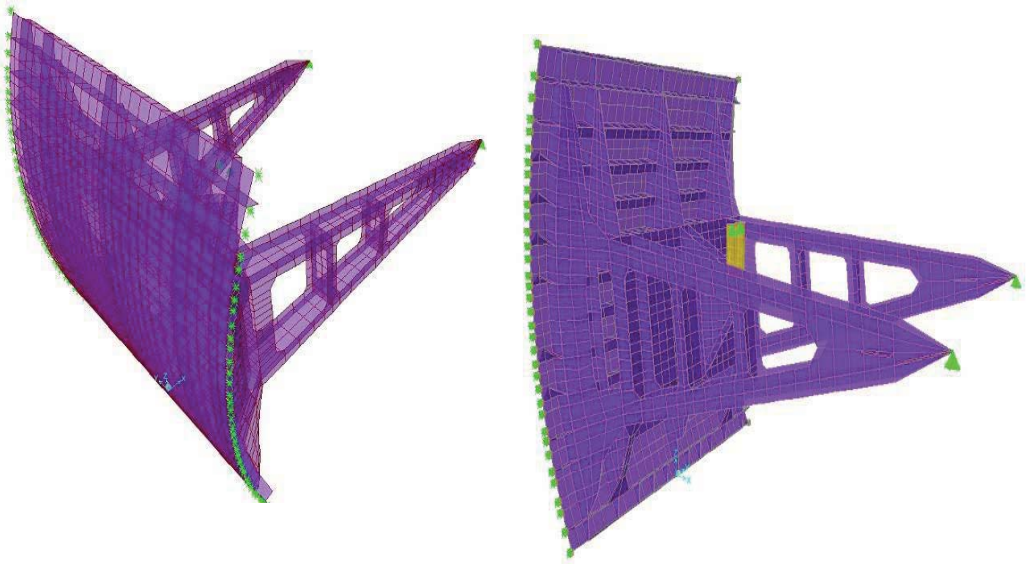

a) b)

Figure 3. The mesh of the structure; a) view from upstream; b) view from downstream

For the mesh of the sealing devices from the laterals of the gate, bar elements which can only take compression were used.

The mesh of these devices was made taking into account the different values of the mechanical characteristics for various types of rubber. In the bibliography there are encountered values between 10 and 100 N/mm^2 for the Young's modulus of the rubber.
Taking into account that the mesh of the sealing was made using bar elements while the sealing devices are continuous, the Young's modulus of the rubber considered in the mesh was affected by the ratio between the effective length of the sealing and the length of the meshed sealing. Thus results values between 30 and 300 N/mm^2 for the Young's modulus. In order to reveal the influence of the value of the Young's modulus of the sealing rubber, both extreme values shown above were used in the modal analysis.

3. THE RESULTS OF THE ANALISYS. CONCLUSIONS

The first 24 eigenvalues were studied for the three bearing hypotheses. The values of the natural periods and eigenfrequencies are listed in Table 1.

Table 1. Natural periods and eigenfrequencies

Mode	Natural periods [s]			Eigenfrequencies [Hz]		
	hyp. 1	hyp. 2	hyp. 3	hyp. 1	hyp. 2	hyp. 3
1	0,164	0,151	0,126	6,099	6,601	7,920
2	0,081	0,077	0,054	12,286	12,996	18,611
3	0,051	0,050	0,046	19,798	20,165	21,797
4	0,020	0,020	0,020	49,783	50,013	51,005
5	0,017	0,017	0,017	57,901	57,924	58,021
6	0,016	0,017	0,017	62,438	59,913	60,299
7	0,015	0,016	0,016	68,890	61,444	62,500
8	0,014	0,016	0,016	71,053	62,465	62,563
9	0,013	0,014	0,014	74,873	68,994	69,266
10	0,013	0,014	0,014	79,120	71,347	72,616
11	0,012	0,013	0,013	80,064	74,951	75,432
12	0,012	0,013	0,013	84,581	79,264	79,390
13	0,011	0,012	0,012	92,868	80,135	80,244
14	0,010	0,011	0,011	96,805	93,214	94,598
15	0,010	0,010	0,010	103,681	96,974	97,069
16	0,009	0,009	0,009	108,566	106,542	107,009
17	0,007	0,009	0,009	133,369	110,108	113,817
18	0,007	0,007	0,007	146,843	140,489	143,349
19	0,006	0,007	0,007	176,025	147,798	149,522
20	0,005	0,005	0,005	203,169	193,911	192,049
21	0,004	0,004	0,004	241,896	226,347	223,514
22	0,003	0,004	0,004	320,718	280,820	282,008
23	0,002	0,002	0,002	486,145	469,925	469,925
24	0,001	0,001	0,001	911,577	841,751	841,043

A detailed comparative analysis of the first three significant eigenvalues was made. In fig. 4, 5 and 6 one can compare the vibration modes for these three eigenvalues for each bearing hypotheses.

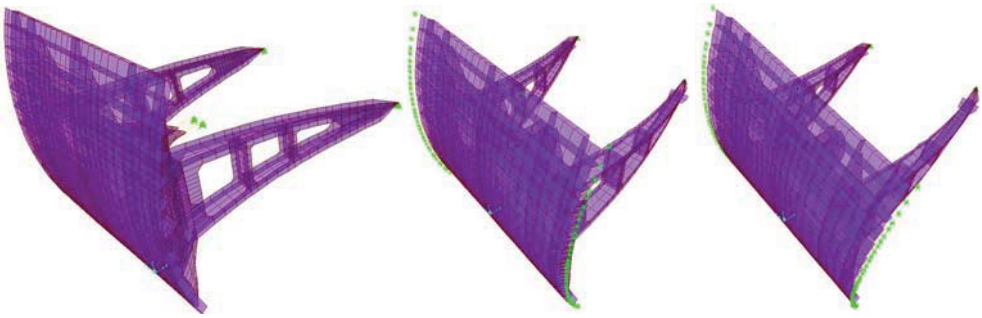

Hypothesis I Hypothesis II Hypothesis III

Figure 4. Vibrating mode 1

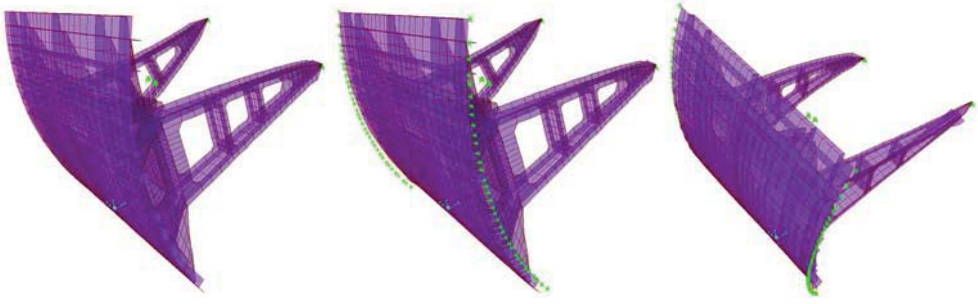

Hypothesis I Hypothesis II Hypothesis III

Figure 5. Vibrating mode 2

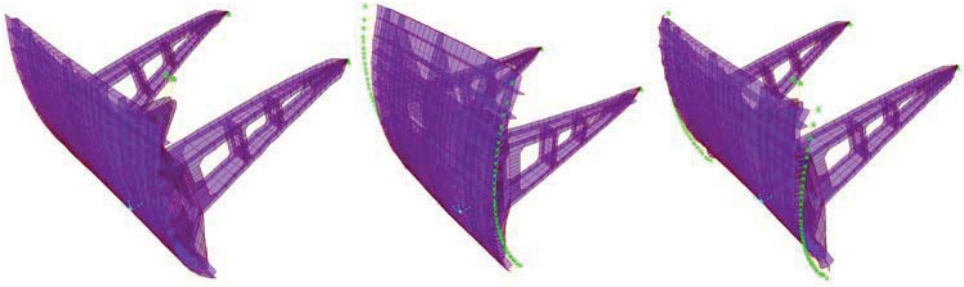

Hypothesis I Hypothesis II Hypothesis III

Figure 6. Vibrating mode 3

From the previous figures one can see that the presence of the sealing devices in the mesh does not affect essentially the vibration modes; the directions of the oscillations are the same in each mode.

By comparing the diagrams from fig. 7 and 8, one can notice that the values of the natural periods and frequencies of the gate are affected by the bearing conditions. The modifications are more important for those modes in which the main vibrations occur on the left bank - right bank direction, causing the compression of the sealing devices. As an example, in the first mode the eigenfrequency grows with 8÷13 percent depending on the Young's modulus considered, while the frequencies of 3rd to 5th modes were slightly affected by the bearing conditions because the vibrations occur on the upstream - downstream direction.

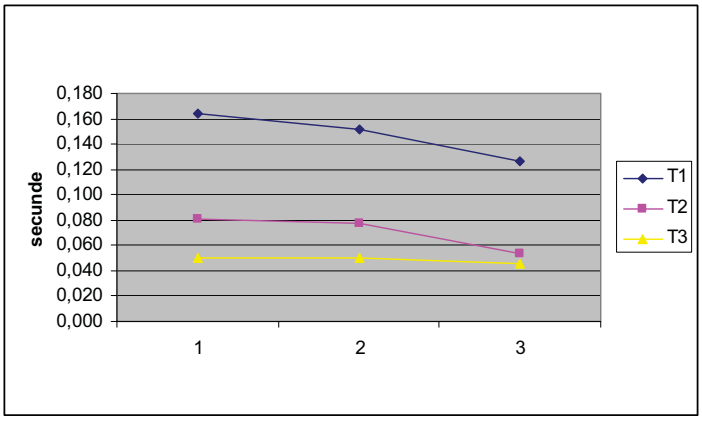

Figure 7. First vibrating periods variation according to the three hypothesis

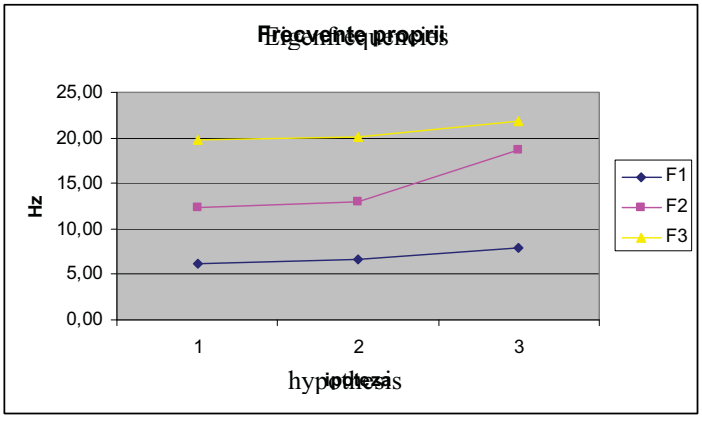

Figure 8. First eigenfrequencies variation according to the three hypothesis

As a conclusion, the correct mesh of the bearing conditions for the modal analysis of a hydraulic radial (taintor) gate especially affects the frequencies which cause compression of the sealing devices. This influence is important bearing in mind that the values are affected mainly in the fundamental (first) vibration mode.

For the analyzed gate, the influence of the mesh of the bearing conditions is between 8...13 %. These values can not be neglected, especially because they could increase for the little size hydraulic gates.

References

1 Prodescu, A. *Acuratețea modelelor de calcul folosite la analiza stavilelor segment*, Teză de doctorat, Universitatea Tehnica de Construcții, Bucureşti, 1998 (in Romanian)

2 Beleş, I; Răduică, N. *Construcții metalice şi elemente de construcții; Stavile metalice* Institutul de Construcții Bucureşti 1979 (in Romanian)

"Computational Civil Engineering 2006", International Symposium
Iaşi, România, May 26, 2006

Teaching and learning Applied Mechanics by aid of computers

Ioana Anca Vlad

Department of Structural Mechanics, "Gh. Asachi" Technical University, Iasi, 700050, Romania

Summary

Actual trends in teaching of Applied Mechanics emphasise a mathematical modelling approach that requires students to possess knowledge of physical systems and the governing laws. Mathematical Programming Media, mainly MathCAD, Matlab, and Mathematica may represent a strong tool for improving the quality of teaching and learning in various fields of the technical higher education, where Applied Mechanics is required. Freshmen' lack in applying usual mathematical notions requires also improved teaching methods of those subjects requiring a strong mathematical base.

Students are now intensively browsing on Internet, more than 3-4 years ago, and the on-line applets and other applications that are available, may stimulate them to create their applications and solutions, aided by instructors.

The paper describes the ways of employing and managing these tools by both involved parts: teaching staff and students in Civil Engineering.

KEYWORDS: Applied Mechanics, Theory of Elasticity; MathCAD, computer-assisted learning.

1. INTRODUCTION

The quality assurance criteria in the higher education include for academic programme important tasks of the academic structures and specific procedures /1/. These criteria contribute to an institutional culture oriented to quality and success, where the student is considered an involved part, as Bologna declaration stated, in opposition to the traditional approach that considers the student as an interested part, sometimes being not completely involved.

According to the new concept, the university becomes an institution that offers education, creates skills and success-oriented performance according the specific and new demands of the labour market.

The Applied Mechanics is an engineering science, which underlies much of the practice of civil and mechanical engineering, and it is an important component in materials science, aerospace engineering, geophysics, architecture and other fields.

Bologna process contributed, in the engineering educational field to the curricula re-thinking. In this respect, teaching Applied Mechanics, i.e. Strength of Materials, Theory of Elasticity, Structural Statics and Dynamics, requires suitable tools for helping students to a faster understanding and data processing, as well as for developing students' skills of solving rough theoretical problems and for performing stress analysis of modern structures.

2. CHANGING STUDENTS' PERCEPTION

2.1 The Target Group

Curran and Moscardini /3/ used the term "mathematically unadapted," to cover those students, which have good academic potential, but poor mathematical and modelling skills, as lack of the high school instruction. These students will not be capable to clearly understand explanations, or a simple graph, to make the logical connexion between numbers to algebra and to solve their home assignments and examination papers. Poor mathematical skills will generally lead to lack of confidence, and sometimes, to the abandon of the engineering study.

Some students in Civil Engineering have a humanistic background and often they are not able to relate mathematics to reality, simple differential equations to the actual phenomena described.

2.2 Looking Backward

10-15 years ago, most courses in our field (Statics, Strength of Materials, Theory of Elasticity and Plates, Applied Physics) have used computers for relatively routine calculations and for report writing. Occasionally computers have been used in the laboratory for simple simulations or data logging. Not often were computers used to help teach and visualize fundamental concepts, or to fully explore the alternatives of an interesting case study, or design project.

2.3 New Mathematical Tools

New information technologies bring with them not only challenges and problems but also the perspective of many benefits. Effectiveness of teaching and learning, and thus the quality of educational experiences, can be significantly enhanced for both student and teacher. In addition, we can develop important new ways to organize the many topics and details of educational programs.

Some of the new tools that can assist in teaching and learning are the advances in symbolic computation for mathematics and modeling, new simulation systems for analysis and design, Internet tools and last but not least, the mathematical programming media, enabling faster understanding, graphic presentations, etc. Concurrent to the emergence of these new tools has been the huge developments in

the computer-human interface, which are providing by GUI the access without the need of mastering sophisticated programming and control procedures.

2.4 Perspective

The new tools make possible avoiding the massive volume of simple mathematical manipulation in solving basic illustrative problems and physical models, thus gaining students' confidence to tackle mathematical models, and not only. Since the new curriculum enables students to gain advanced information about Matlab, MathCAD and other, we may estimate that their modelling skills will be improved and they will be interested in learning other recommended useful software, related to the engineering field.

3. TO A BETTER STUDENT-INSTRUCTOR DIALOGUE

This dialogue starts in the classroom, but now, the Internet plays a specific role: web pages are recommended by the instructor, the quizzes, take-home examination papers and the laboratory works are posted on own teachers' web pages. The electronic mail becomes a usual tool in the information dissemination and dialogue.

Very fast looking through the main chapters of the Theory of Elasticity we may discover that all old and terrifying-for students subjects could gently handled and presented "in a new coat" using computers.

3.1 Internet Tools

Starting from the fundamental assumptions, stated by the 19th century famous for the scientific world scholars, but completely unknown for freshmen, Internet provides information about those scholars' lives and about their work. Pictures may help, too. Sites of main Encyclopaedias, as well as those of well-known Universities (Cambridge, Berkeley) are also helpful.

Also, there may be found free on-line educational applets and software for the stress and strain states, like Visual Mechanics/2/, DrBeamPro/2/, Beam2D, or Rod2D/3/, but these tools may have a weak point, requiring computers in every laboratory. At our recommendation, students also use them at home, or in the Campus network. A virtual laboratory may acquire interesting software and simulation movies regarding to the photoelasticity phenomenon and its applications to the stress states study, as samples may be found on the Cambridge University site. The fundamental equations of the Applied Mechanics involve Calculus, Analytical and Differential Geometry and other branches of the Mathematics. Here, FORTRAN /2/, Pascal, and C programming languages are helpful in plotting surfaces, contour curves, Mohr circles, as well as for handling numerical and energy-based methods. Unfortunately, nowadays students in Civil Engineering are

not very skilful and keen of programming languages, since more friendly-user tools are available.

When discuss topics about mechanical properties and experimental studies, instructor's movies about experimental techniques, as well as those of well-known facilities providers (Phillips, Vishay, etc) may be employed, too.

The Internet provides information about new structural systems and famous mega-structures, so that, looking for them students become more interested and motivated.

3.2 Role of the Mathematical Programming Media in Teaching and Learning

The students' feedback requires solving many problems, as well as data processing in the classroom, and during home assignments. Solving Applied Mechanics problems, in general and those of the Theory of Elasticity, as a particular case must enable finding the main functions involved, of stress, strain, and displacements, as boundary-value problems. For teaching purposes known functions may be chosen, otherwise available algorithms of the numerical and variational methods may be handled to build own computer codes for solutions. A short example of using MathCAD to demonstrate a particular problem of the plane Elasticity, instead of performing time-consuming partial derivatives by hand is below presented.

3.3 MathCAD Case Study /1/

The stress tensor component functions in a prismatic dam acted by the hydrostatic pressure and body (gravitational) forces are given. Requirements: fulfilment of Navier equations and that of the fundamental compatibility equation in terms of stresses. MathCAD code has been chosen since average students faster assimilate it. Principal stresses at a given level are required, too.

Let $\mathbf{T}_\sigma$ is the stress tensor for a plane state. The stress components include the body force effects.

Step 1: Define the constants: water and concrete specific weights γ_w ; γ_c, dam width, b, level x_0 measured from the top.

Step 2: Stress functions (input data):

$$\sigma_x(x,y) := \frac{\gamma_w}{4b^3}\cdot\left(x^3\cdot y - 2\cdot x\cdot y + 1.2\cdot b^3\cdot x\cdot y\right) \tag{1}$$

$$\sigma_y(x,y) := -\gamma_w\cdot x\cdot\left(0.5 + \frac{y^3}{4\cdot b^3} - 3\cdot\frac{y}{4\cdot b}\right) \tag{2}$$

$$\tau_{xy}(x,y) := \gamma_w \cdot \frac{\left(b^2 - y^2\right)}{8 \cdot b^3} \cdot \left[3 \cdot x^2 - \left(b^2 + y^2\right) + 1.2 \cdot b^2\right] \tag{3}$$

Step 3: Define first order partial derivatives

$$Dsx(\sigma_x, x, y) := \frac{d}{dx}\sigma_x(x,y) \qquad Dtx(\tau_{xy}, x, y) := \frac{d}{dx}\tau_{xy}(x,y) \tag{4}$$

$$Dsy(\sigma_y, x, y) := \frac{d}{dy}\sigma_y(x,y) \qquad Dty(\tau_{xy}, x, y) := \frac{d}{dy}\tau_{xy}(x,y) \tag{5}$$

Step 4: Define second order partial derivatives

$$DDsx(\sigma_x, x, y) := \frac{d^2}{dx^2}\sigma_x(x,y) \; DDysx(\sigma_x, x, y) := \frac{d^2}{dy^2}\sigma_x(x,y) \tag{6}$$

$$DDsy(\sigma_y, x, y) := \frac{d^2}{dy^2}\sigma_y(x,y) \; DDysy(\sigma_y, x, y) := \frac{d^2}{dy^2}\sigma_y(x,y) \tag{7}$$

Step 5: Substitute for Navier equations: $\begin{bmatrix} \frac{\partial}{\partial x} & \frac{\partial}{\partial y} \end{bmatrix} \cdot \mathbf{T}_{\boldsymbol{\sigma}} = \mathbf{0}$ (8)

There were defined two sums *c(x,y)* and *d(x,y)* :

$$\begin{aligned} c(x,y) &:= Dsx(\sigma_x, x, y) + Dty(\tau_{xy}, x, y) \\ d(x,y) &:= Dtx(\tau_{xy}, x, y) + Dsy(\tau_{xy}, x, y) \end{aligned} \tag{9}$$

If these quantities were symbolically evaluated, both results are equal to zero. Thus, equations (8) were satisfied.

Step 6: Substitute for the compatibility equation in terms of stresses:

$$\Delta(\sigma_x + \sigma_y) = \left(\frac{\partial^2}{\partial x^2} + \frac{\partial^2}{\partial y^2}\right)\left[\sigma_x(x,y) + \sigma_y(x,y)\right] = 0 \tag{10}$$

Define the Laplace operator like:

$$\Delta(x,y) := DDsx(\sigma_x, x, y) + DDysx(\sigma_x, x, y) + DDsy(\sigma_y, x, y) + DDysy(\sigma_y, x, y)$$

$$ans := if(\Delta \neq 0, 1, 0) \tag{11a, b}$$

Finally, it resulted: $ans = 0$, thus stresses are accurate. Principal stresses and directions are the eigenvalues and eigenvectors of $\mathbf{T}_\sigma$. Thus, we may simply found them using well-known computer codes, MathCAD, Matlab, Maple or Mathematica functions, instead of solving algebraic 3rd degree equations and linear system of equations and loosing the final goals due to a huge volume of work.

Remark:

Deterministic numerical solutions belong to FEM and BEM methods, the most powerful domain for solving almost any Applied Mechanics problem, at a higher level of studies (master and PhD school, or research and industry). We may

observe that even sophisticated codes use now Matlab or Mathematica, due to their functions and compact form.

3. CONCLUSIONS

The short example suggests a possibility of improving the quality of teaching and learning in a specific field of the Applied Mechanics, aided by computers.

This implies permanent dialogue with students, upgrading of knowledge and improving skills for the practical use of computer languages and mathematical programming media.

The virtual laboratory requires an own portfolio of applets, software and expert systems, as well as slide presentations, correlated with classical teaching tools and laboratory.

References

1. Vlad, I.A., *The Plane Elasticity*, Editura Societății Academice Matei Teiu Botez , Iaşi, 2005.
2. Beer, F.P., Johnston, Russell E., R. *Mechanics of Materials, Book and Instructor's Manual,* McGraw-Hill, Inc., New York, 1993.
3. Curran, D.A.S., Moscardini, A.O., Middleton, W., Innovative Application of CAL to the Teaching of the Mathematically Unadapted, in *Computer Aided Training in Science and Technology*, Editors: Oñate, E., Suarez, B., and al., Barcelona, 1990.
4. http://mathworld.wolfram.
5. http://www.drbeam.com/Visual Mechanics
6. http:// www. engilab.com/beam2d

"Computational Civil Engineering 2006", International Symposium
Iaşi, România, May 26, 2006

New screed materials for external thermal insulation composite systems

Nikol Žižková

Institute of Technology of Building Materials and Components, Faculty of Civil Engineering, Brno University of Technology, Brno, 602 00, Czech Republic

Summary

Thermal insulation of buildings is an actual topic during present days when energy and fuel prices rise up. Thermal insulation of building facades consists from thermal insulation layer, its fixing and protective layer. This article is focusing the topic of reusing the waste for production of new polymercemente materials which can be used for such facades thermal insulation systems.

The goal of this work was to explore the possibility of using selected waste byproducts in the manufacture of new polymer-modified mortar – in particular, dry adhesives and screeding material to apply insulation sheeting materials in external thermal insulation composite systems, while at the same time maintaining the maximum possible filler for the desired characteristics.

In the course of the research, observation was made of the influence of the waste byproducts under study on mechanics and chemical characteristics that is to say on the microstructure of polymer-modified mortar adhesive and screeding mixtures. It is absolutely necessary to use computers for evaluation of results obtained during the performed tests.

KEYWORDS: External Thermal Insulation Composite Systems (ETICS), waste, recycling, polymercement mixture.

1. INTRODUCTION

The negative fallout from incautious handling of waste byproducts from human economic activity on the environment, as well as on man, provides good motivation to seek out new means of liquidating waste. Both ecological and economic reasons lead us to focus on the problem of waste in the building sector and how waste byproducts can be recycled in the manufacture of new construction materials.

The disadvantage of the polymer-modified mortar, which is currently available on the market, is its high price. This price is due chiefly to the use of expensive additives but high-quality compounds taken from non-renewable natural materials

are also a factor. One possible way to postpone the exhaustion of non-renewable natural resources, and at the same time lower the price of production, is to take advantage of a wide range of waste byproducts, which are both high quality and carry a low price tag.

As high as possible ratio of recycled materials to be used, to prefer reusable sources and to keep as much supply of raw material for future [1] – those are the major directions towards to the main point of (SUR) Sustainable development in the Czech Republic. There is one possibility to keep the non-reusable sources (raw materials) to use secondary material sources e.g. waste material.

The Czech Law No. 188/2004 – Waste Operation Law shows how to solve this problems. This law prefers using so called material using of waste instead of other waste using. This article is giving an example how primary materials can be replaced by selected waste materials which can be considered as secondary material sources.

The results investigated and published by Czech Ecology Institute shows 37% of the whole amount of waste is reused as secondary material in the Czech Republic within present days. Building materials industry represents one of the branches which is able to use civil engineering waste and industrial waste as well.

2. THERMAL INSULATION COMPOSITE SYSTEMS

According to placement thermal insulation systems can be divided to exterior and interior. According to implementation and material solution they can be divided to plaster, prefabricated and contact solutions. Basic layers used in External Thermal Insulation Composite Systems (ETICS) see Figure 1 consists of base layer, glue/binding agent, thermal insulation, raw plugs, battens, reinforcement layer (reinforcement layer consists of screed and bracing mesh), surface treatment and auxiliary elements (auxiliary elements are the products for corners finishing, expansion joints, etc).

Binding agent is determined to affix thermal insulation on base. Screed mass and bracing mesh (bracing mesh is made of glass fiber usually) gives together reinforcement layer. In some cases according to manufacturer directions the screed layer can represent both binding agent and screed layer. Reinforcement layer is fundamental for securing mechanical properties, stability and service life of contact thermal insulation systems.

In this article the materials for fixing the thermal insulation layer and the materials for using as reinforcing layer were observed. Those fixing and kniffing materials are produced often as dry mix, during the production of dry mix is redispersible polymer added (as polymer part) into final material.

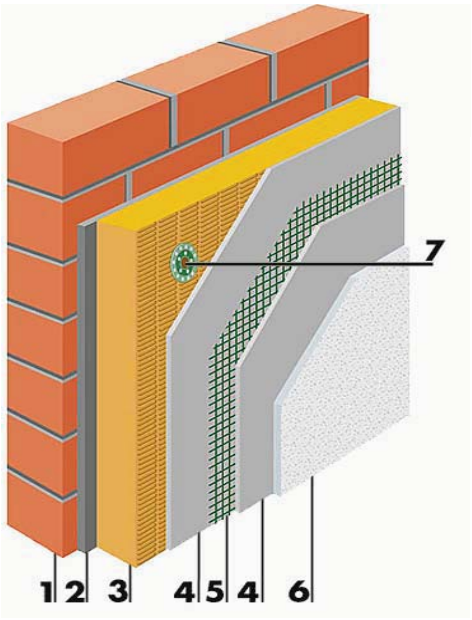

1 Masonry
2 Binding agent
3 Thermal insulation
4 Screed mass
5 Bracing mesh
6 Surface treatment
7 Raw plug

Figure 1. Basic layers ETICS [2]

3. SELECTED RESULTS

3.1. Used materials

Aggregate – crushed limestone, firestone sand, fly-ash, waste from crushed limestone flushing

Binding agent – cement CEM I 52,5 R

Additives – special admixtures named generally as additives. These contain redispersible copolymer EVA, stabilizing agent and defoamer

3.2. Observed properties

Main observed properties of screed and fixing layer observed during initial period were processibility (according to Czech Standard ČSN 722441) and adhesiveness. Adhesiveness to concrete was measured according to Czech Standard ČSN 732577 and adhesiveness to polystyrene thermal insulation layer was measured according to Technical Rules - CZB 2001. Other observed values were strengths (according to Czech Standard ČSN EN 12808-3), frost resistance coefficient (according to

Czech Standard ČSN 722452) and thermal conductivity coefficient (according to Czech Standard ČSN EN 993-14).

The results acquired when gradually part of filling agent was replaced by fly-ash and after washing waste from crushed limestone, the quantity of 20, 40, 60 and 80% are showed on Figures 2 a 3. To have a comparison the mix with no waste material was tested – marked as S/R.

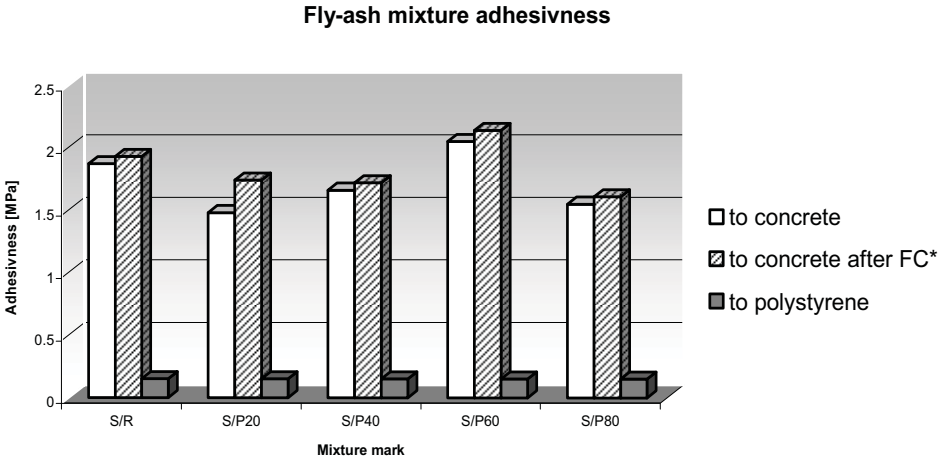

*FC – 25 Freezing Cycles

Figure 2. Fly-ash mixture adhesiveness

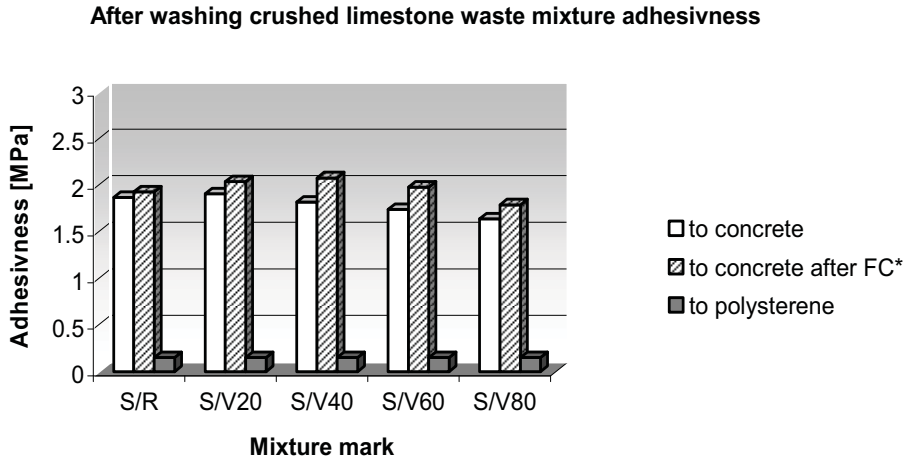

*FC – 25 Freezing Cycles

Figure 3. Adhesiveness after washing waste from crushed limestone mixture

Tests were realized with putty coats in order to clear also the fracture characteristic of these mixtures. This can be of importance for instance in the case of thermally stressed materials. The measured results are in the Table 1. This test was realized in cooperation with the Building Testing Institute at the Faculty of Civil Engineering, Brno University of Technology.

Table 1. Fracture charakteristic

Mixture mark	Static modulus of elasticity E	Fracture toughness	Energy of the crak	Fracture performance
	GPa	$MPa.m^{1/2}$	$J.m^{-2}$	$J.m^{-2}$
S2	13,54	0,4928	19,43	11,72
S1	12,29	0,6718	36,74	23,55
S11	9,68	0,5734	34,01	22,50

The fracture characteristics are in particular the modulus of elasticity, the energy to fraction and the fracture toughness. The fracture characteristics complete the classical information concerning the material in form of strength characteristics. The fracture characteristics were determined by the analysis of data obtained by the Three – Point – Bending – Test (see Fig. 2). The beams 40x40x160 mm were loaded by three points bending and in the same time the couples of load and deflection values were recorded [3].

Figure 2. Three-Point-Bending-Test

The fracture toughness is a constant of the material or also the critical value at which the material will be failed before the front of the crack in the case of its unstable spread. This characteristic gives an account of the material properties in the area allocated by the increasing arm of the dependence between load and deflection. The higher is the load, the more resistant is the material against the spread of the crack.

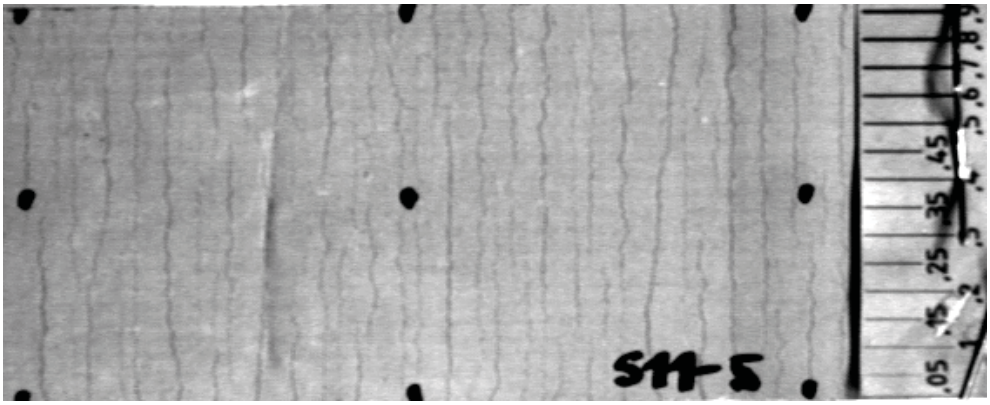

Figure 3. Reference screed mixture with elongation of 1.5% in the direction of the warp

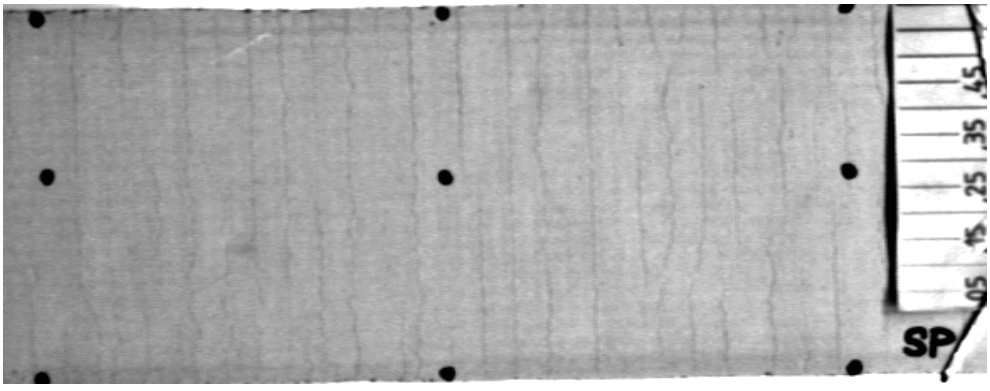

Figure 4. Screed mixture with s fly-ash (20%) with elongation of 1.5% in the direction of the warp

The mowing power is the energy necessary for the spread of the crack. The value of this energy depends on the fracture toughness and on the modulus of elasticity. The fracture performance represents the energy consumption during the process of fracture. The results in Table 1 show, that the most fragile material is the mixture S2, the parameters of mixtures S1 and S11 are almost identical.

The use of waste from crushed limestone washing and of fly ash can increase the adhesion especially after the freeze/thaw cycles, the compression and the bending

strength, the frost resistance and the thermal conduction coefficient. The addition of fly ash can reduce the extent and the number of cracks. Figure 3 shows the reinforcing layer formed by meshwork and the reference putty coat (it contains only quartz sand and ground limestone) with elongation of 1.5%. The reinforcing layer with the meshwork and putty coat with the addition of fly-ash (20%) and also with the prolongation of 1.5% you can find in Figure 4.

The determination of cracks size in the reinforcing layer by the tensile test is for every tested mixture examined on six samples, (three samples in the direction of the warp and three in the direction of the weft). The formation of cracks and the cracks development was monitored for the given value of relative deformation. The Videoextensometer was used for the measurement and the archiving of the material surface actual state during the tensile test.

The principle of the measuring device is to pick up the visual field by the CDD camera and the digitalization of the image. The optical spots were monitored by the special software, which enables to examine the change of the plane coordinates spots [4]. The samples containing the fly ash showed a decrease of cracks frequency and size in the case of 0.5, 1.0 and also 1.5% prolongation in the direction of both the warp and the weft.

4. CONCLUSIONS

One can say, based on the results acquired in the frame of this article the selected waste materials as stated after washing waste from crushed limestone and power plant fly-ash can modify polymercemente stuff.

When the substitution of original material by waste material is appropriate the new material is having the same or even better properties than reference materials. New materials for external thermal insulation composite systems are ecologically and economically evidently beneficial.

Acknowledgements

This work was published with the financial support of the research project: MSM 0021630511 "Progressive Building Materials with Utilization of Secondary Raw Materials and their Impact on Structures Durability" and project of Ministry of industry and trade of Czech Republic FT-TA2/076: "Progressive Arrangement of Building Materials and Components for Surface Treatment with Utilization of Secondary Raw Materials".

References

1. www.ceu.cz, Czech Ecological Institute
2. www.heizkosten-einsparen.de
3. Keršner, Z., Schmid, P., Stibor, M., Kaltenbacher, T. Charakteristic lengths of materials for coating of heat insulation of bulding, *Křehký lom*, AV ČR, Brno, 2001
4. Schmid, P., Kešner, Z., Stibor, M. Experimental stress analysis and fracture charakteristic of upper surface of thermal isolation, *Construmat 2001 – Conference about structural materials*, BUT, Brno, 2001, ISBN 80-214-1936-9

"Computational Civil Engineering 2006", International Symposium
Iaşi, România, May 26, 2006

Coating of concrete structures exposed to corrosive media

Vít Petránek

Brno University of Technology, Faculty of Civil Engineering, Institute of Technology of Building Materials and Components, Veveri 95

Summary

The paper describes research and development of protective materials based on polymer resins. Instead of usual filler, ground quartz sand, several types of industrial wastes were used. Main aim of the research was to determine the most suitable type of industrial waste material, its treatment and last but not least amount of filler. On the contrary to silicate coatings the polymer-based coatings are not so "sensitive" to chemical composition of the filler. Paper describes methodology, carried out tests, results and possible outcome of the research.

Key words: Concrete, corrosive media, protection, polymer coatings.

1. INTRODUCTION

The lifetime of reinforced concrete construction work is substantially limited by the amount of deterioration and chiefly by the corrosion of reinforcement. The causes of reinforced concrete deterioration can be various. In general, aggressive media can be divided according to the types that affect concrete:

- Aggressive gases and vapors with acidic character (CO_2, SO_2, N_xO_y, H_2S etc.),
- Aggressive waters and solutions,
- Hygroscopic solid substances,
- Microbiological effects,
- Mineral fats and oils,
- Stray current that effect reinforcement.

2. STRATEGY OF PROTECTION

The question of protection of reinforced concrete structures depends on the corrosive surroundings to which these structures are exposed to. Protection of concrete structures can be realized in different ways:

- Change of operational and exposure conditions
- Improvement of physical properties of repair materials for original concrete
- Influencing the electrochemical behavior
- Application of different types of surface treatment

In this paper, the development of surface treatment is discussed. Several effective methods are; coatings, membranes, and impregnation paints. Surface protection of concrete structures is an expensive secondary measure. A significant part of the costs is the price of the material. One of the possibilities to reduce the price is the choice of less expensive material, but which still provides sufficient protection to the structure. Another possibility is to replace part of the binder with filler. For further price reduction and for ecological benefits, the utilization of industrial waste materials as filler in coatings was suggested.

3. THE METHODOLOGY OF TESTS

At the Institute of Technology of Building Materials and Components, in the framework of research, the problems of the investigated protective coating types were tested. Those that utilize waste materials instead of usual fillers. Tested coatings can be divided into two main groups; silicate coatings and polymer coatings. Polymer coatings are based on polyester, vinyl-ester and polyurethane. They are designed for special applications where the concrete is exposed to a strong corrosive medium. The selection of materials was directed by local accessibility, by urgency of processing or liquidation, and by current known limits of utilization possibility. Admittedly, the waste materials are from local sources and their actual technical properties differ from all other materials, but on the basis of this research it is possible to deduce generally applicable dependences for the same waste materials from other localities.

3.1. Description of individual waste materials used in paints

Fly ash - Fly ash from electrostatic precipitators was used in this work. In this fly ash there are two main components: mullite and β-quartz. Chemical composition is relatively stable SiO_2 57%, Al_2O_3 29%, Fe_2O_3 6,2%, TiO_2 2% , CaO 1,7%, MgO , K_2O 1,8%. Bulk density: 2060 kg/m^3, specific surface: 270 m^2/kg

Slag - Ground blast furnace slag is a granulated material formed by quick cooling of blast furnace slag during the production of iron. The blast furnace slag is very important in the building industry. Chemical composition is variable CaO (30-50%), SiO_2 (30-43%), Al_2O_3 (5-18%), MgO (1-15%), Bulk density: 2810 kg/m^3, specific surface: 380 m^2/kg.

Wastes from the washing of crushed aggregates - In brief, this waste material called "washing waste" is formed during the washing of crushed aggregates in the quarry. It is mainly the production of washed standard sand. The formed slurries accumulate and then are brought to a stock-pile.

The washing waste has the same mineralogical and chemical composition as the washed sand. The mineralogical and chemical composition depends on the locality of the source. The grain size composition depends on the kind of mineral, the crushing technology, and the method of treatment and separation. The chemical compositions of both samples of washing wastes are given in Table 1.

Table 1. Chemical analyses of waste washings

Compound	Sample 1 Amount %	Sample 2 Amount %
Insoluble material	59.5	91.47
CaO	0.82	1.19
Al_2O_3	0.4	1.39
Fe_2O_3	1.17	1.92
pH	8.5	8.2

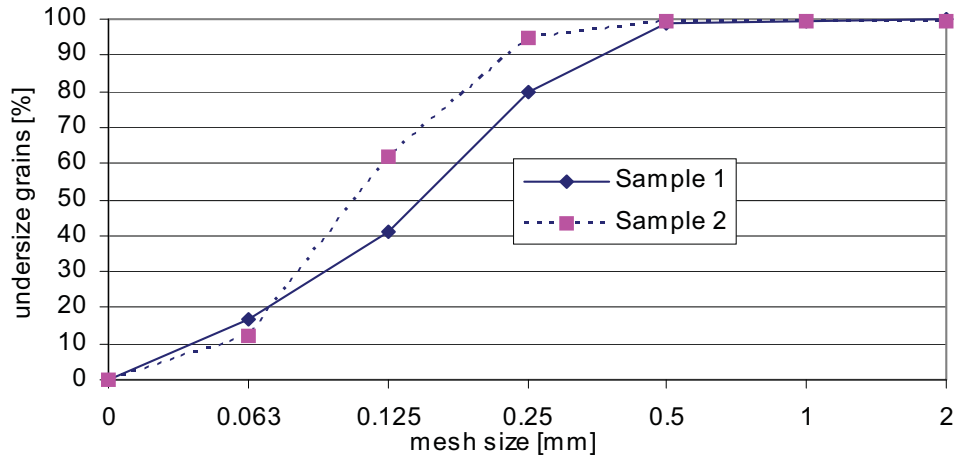

Figure 1. Sieve analysis of washing wastes

Properties of two kinds of material having different properties: Bulk density: Sample 1 = 2170 kg/m^3 Sample 2 = 2690 kg/m^3, Bulk density (jarred): Sample 1 = 1470 kg/m^3 Sample 2 = 1420 kg/m^3.

Minerals determined by X-ray analysis: Sample 1: β-quartz, feldspar, muscovite, kaolinite Sample 2: β-quartz, feldspar, muscovite, kaolinite, gehlenite, montmorillonite.

3.2. Binders

The experimental work was divided according to three types of binders:

- Vinyl-ester (VE)
- Polyester (UP)
- Polyurethane (PUR)

3.3. Application of coatings and proposed proportions

For all proportions, the coatings were applied by a paint brush on vibro-pressed concrete paving bricks 200 x 200 mm. The composition of the vibro-pressed concrete paving bricks corresponds with requirements for concrete as substrate for testing surface treatment of building structures.

The methodology used for polymer coating is divided into two phases – the 1st phase is selection of most preferable proportions and the 2nd phase is determination of selected coating properties. In the 1st phase, proportions adjusted by the increasing quantity of filler by 5%, in order to determine the effect of filler quantity for constant quantity of binder on individual properties. The 1st phase includes also the testing of basic properties and the selection of most preferable proportions by means of an optimization process for further modification of coatings. In the 2nd phase – tests were performed with coatings following selected proportions to determine their properties.

The method was chosen in order to describe the changes in the coatings behavior, from the minimum up to the maximum percentage filling.

4. TEST RESULTS

The consistency of fresh coating is an important property. It is influenced by the properties of the binder and the amount of used filler. For consistency test results of polymer coatings filled with waste materials see Fig. 2.

Very important property of coatings is bond to the substrate. All tested coatings had, due to high quality binder, very good results (see Fig. 3).

The character of polyurethane coating significantly differs from polyester and vinyl-ester resin. The high viscosity of the binder limited the filling considerably. This caused a thick of the coating, which can be considered even as excessive. From another point of view this property can be evaluated very positively because the protective coatings perfectly cover small unevenness of the surface. With increasing quantity of filler, the coatings quickly lose their self-leveling properties after application. For this reason the maximum filling was only 30% in the case of

a coating filled with slag, 20% with washing wastes, and 20% with fly ash, optimal filling was even lower (see Fig. 2).

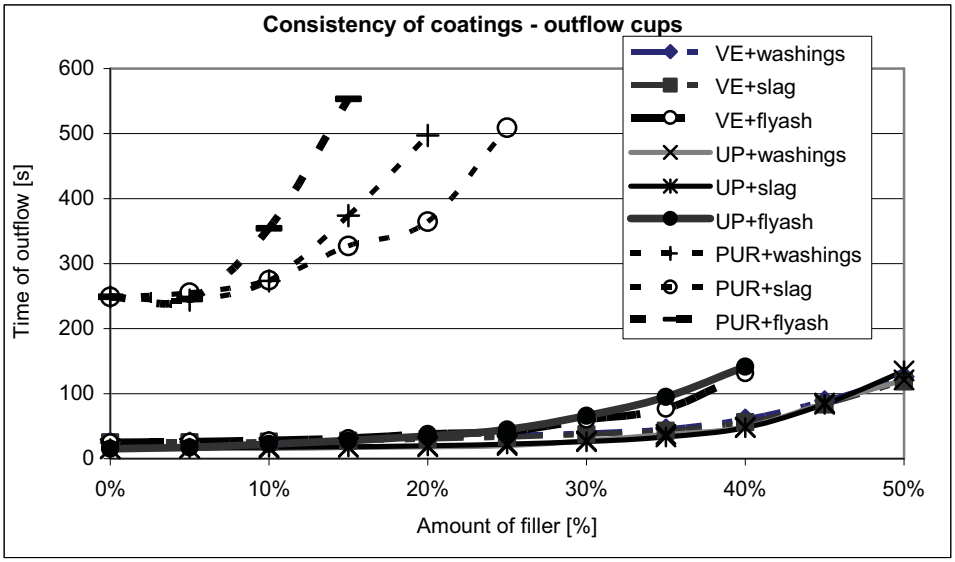

Figure 2. Consistency of polymer coatings in fresh state

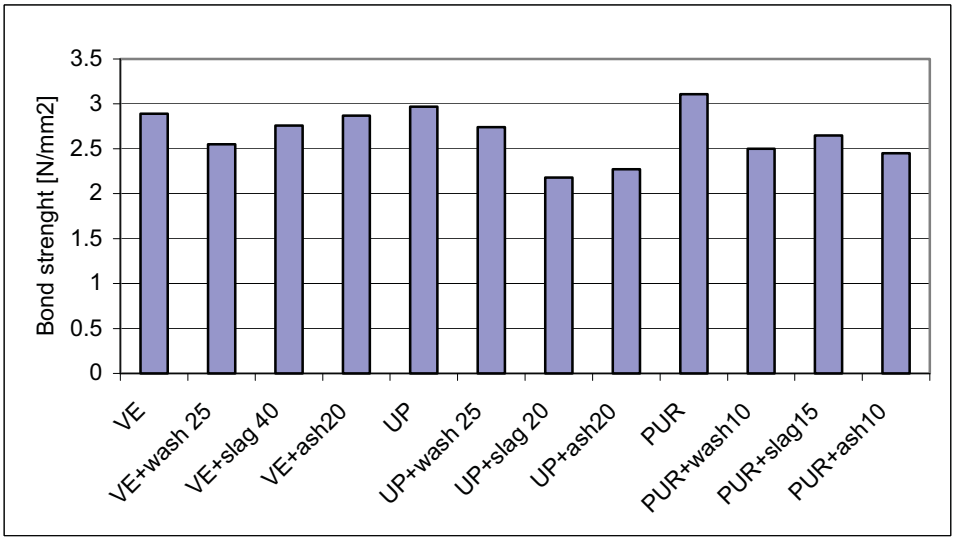

Fifure 3. Bond strength of polymer coatings to concrete surface. VE+wash25 – VE binder filled with 25 % of waste washings. Other abbreviations are analogous

The polyester and vinyl-ester coatings enabled maximum filling up to 50% owing to low viscosity. This meant in the case of transparent vinyl-ester that it obtained covering properties, became non-transparent. The micro-hardness of these resins significantly exceeds the micro-hardness of tested polyurethane. Results often exceed the values of reference samples. The vinyl-ester resin had self-leveling properties even with high percentage of filling with all types of binders and no traces after application with brush were formed.

It was found that if polyester and vinyl-ester were used without filler the gelatinization takes place as a rapid exothermic reaction. The temperature increases up to 60ºC and quick curing and considerable shrinkage takes place. When fillers are added, the curing reaction is not so rapid and the shrinkage is reduced. The shrinkage influence on thin-layer materials is not so significant and the shrinkage is further limited by the addition of fillers.

5. CONCLUSION

Filer materials commonly used in coating at the present time are fine ground limestone or ground pure quartz sand. The use of industrial waste materials as a substitute for these fillers was proven and verified for the development of protective coatings. Besides the environmental benefits, this would also have a positive economic effect.

The result of the work verified that the filling with selected raw waste materials has no significant effect on the properties of the coating itself up to a relatively high degree of filling. All test result values exceeded the values required for coatings by relevant standards or technical conditions. The limiting factor for filling the binder is the workability of the fresh coating. The research of long term durability of these coating applications on real structures is in progress.

For the most advantageous utilization of wastes the following proportions were selected:

- Vinilester + 40% slag, with similar properties as VE + 25% washing wastes
- Polyester + 25% washing wastes
- Polyurethane + 15% slag

In contrast with silicate coatings, the noted proportions of polymeric coatings have more general validity because the polymer binders are not as sensitive concerning the type and the properties of fillers, except for significant changes of pH value. The mentioned proportions for polymer coatings can be used even for other fillers with similar grain size distribution.

Acknowledgement

This paper was prepared with financial support from grant of the Czech Grant Agency 103/05/P262, entitled: “Thin layer protection systems for concrete exposed to special environment” and from the research project CEZ - MSM 0021630511, entitled: “Progressive Building Materials with Utilization of Secondary Raw Materials and their Impact on Structures Durability”.

Literature

[1] Drochytka, R., Petranek, V. Atmospheric Concrete Deterioration. In Concrete Structures in the 21st Century. Japan Concrete Institute, FIB Conference, 1st ed. Osaka, 2002, vol. 2, 10 p..

[2] Petranek, V., Hudec, P. Silicate Coatings with Waste Materials. In proceedings of. WTA International Conference, 1st ed., Brno: VUT Brno, 2003, ISBN 80-02-01538-X

[3] Petranek, V Kohutova, N., Surface Treatment as the Final Stage of Concrete Repair Works In proceedings of VI. International Conference OTMC, 1st ed., Zagreb: University of Zagreb, 2003, ISBN 953-96245-5-X, pp. 234-241

[4] Petránek, V., Hudec, P. Protection of Concrete by Silicate Coating with the use of Waste Raw Materials. Conference proceeding of EUROMAT, Lausanne, Switzerland, [online], 2002 http://webdb.dgm.de/tagprog/FMPro.

"Computational Civil Engineering 2006", International Symposium
Iaşi, România, May 26, 2006

Iassy contributions to the development of Earthquake Engineering

Daniel Diaconu[1], Dumitru Vasilescu[2], Gheorghe Palamaru[2]
Constantin Mihai[2], Adrian-Constantin Diaconu[2], Tudorel Popa[2]

[1]*Romanian Association for Earthquake Engineering*
[2] *National Institute for Research & Development in Civil Engineering, INCERC – Branch of Iassy*

To the Blessed Memory of Professor Anton Şesan

Summary

The contributions of Iassy to the development of earthquake engineering, experimental testing facilities and investigations regarding determination of the dynamic characteristics of structures and peculiarities of seismic response of various categories of civil, industrial, agricultural, energetic, utility or unicate constructions of national importance are described in this paper.

1. GENERAL CONSIDERATIONS

The research activity in the field of earthquake engineering has been carried out in Iassy both within the Branch of National Institute for Research & Development in Civil Engineering (INCERC) and the Faculty of Civil Engineering. Various closed cooperation in the field have been also undertaken with other university research centers and national or districtual building design institutes. That activity has served to the major needs for the design and construction industry in this country including development of experimental base of investigation, the evaluation of the seismic protection levels of existing constructions and the rehabilitation of hazardous buildings to current design standards. A special attention has been given to developing facilities with a variety of testing capabilities to gain practical understanding of seismic design problems and to maximize the effectiveness and usefulness of the results for the profession.

In this context, it should be mentioned that the year 2006 has a double significance to the civil engineers from the city of Iassy:

- This year is the 65th anniversary of the Civil Engineering Faculty of Iassy (originally founded on November 1941 within the Polytechnic Institute of Iassy);
- Also, this year is the 50th anniversary of the INCERC Branch of Iassy (originally founded on June 1956 as a part of the Institute for Researches

and Studies in Constructions, ICSC, Bucharest). INCERC – Iassy was founded under the initiative of Professor Anton Şesan with the support of both central authorities and several prominent scientific personalities.

The main fields of activity in which research engineers of Iassy have brought significant contributions refer to two major directions in Civil Engineering namely: (i) **Seismic protection** of building structures and (ii) **Thermal insulation** and energy conservation in buildings.

The research activity has developed in a larger variety of concerns mainly after 1960, when the first programmable shaking table (1966) and the Hygrothermal Research Station (1972) were put into operation, followed by the construction of a new base for experimental investigation in Podu Roş zone (1985).

2. CONTRIBUTIONS

2.1 Determination of dynamic characteristics of structures

The first action undertaken by the Iassy research staff, with major implications to quantification of seismic response of structures, was the assessment of a methodology for experimental determination of the dynamic characteristics of building structures, using as excitation either the ground microtremors or a rotating weight vibration generator. As long as the fundamental period is used as an index value in determining the lateral forces and the response displacements, it was considered necessary to develop a workable and reliable method to establish this index. The methodology and main results obtained were first published in 1962 and then reported at the Fourth World Conference on Earthquake Engineering held in Chile in 1969 (Fig. 1). The proposed experimental procedures have been developed and improved continuously being used even today to detection of structural deficiencies or as a method of controlling the quality of strengthening works.

2.2 Civil Engineering structures

The following categories of structures were tested under various loading conditions to check their aseismic compliance:

(a) **Large panel structures** with five levels (ground floor and four stories above) in honeycomb or celullar system, as well as nine level reinforced concrete structures with vertical load-bearing cores (Fig. 2).

The strength and deformability capacities of large panels were determined under horizontal and vertical static loads and the horizontal and vertical joints were tested under dynamic-seismic actions (I, II, III and IV generations of systems with various types of connections). A major concern in the design and construction of

large panel structures has been the increase of plan layout flexibility and solution of various problems regarding the performance of their connections under strong earthquake motions. To develop a better understanding of the effects of high intensity seismic loading on the postelastic behavior of these systems, portions of full scale structures and scale models of relatively large geometric dimensions were tested up to failure and the behavior of their joints was observed with special care. Based on the results obtained in this investigation, some recommendations were made pursuing to eliminate the discontinuities within the structural walls and to improve the overall response of the structure.

(b) **Masonry structures** made of simple brick, reinforced with steel mesh or polymeric grid and having reinforced concrete pillars and monolithic or precast floors. The important role of floor overcasting was emphasized in this investigation.

A research program concerning the seismic behavior of masonry infill frames was initiated at INCERC Iassy in 1990 and continued for the next six years. The experiments involved two types of infill panels: reinforced and unreinforced clay brick masonry panels.

Twenty-two specimens were tested using both monotonically increasing and cyclic loads. The behavior of the subassemblies was carefully observed from the elastic range up to failure. The ultimate objective of the research program was to evaluate the way in which infill masonry panels affect the lateral stiffness, strength and deformation capacity of the frame and to determine the degree in which the strengthening procedure based on jacketing the both sides of the panel by reinforced mortar succeeds in restoring the lateral stiffness and strength capacity of the damaged subassemblies. Perhaps the most adequate method of strengthening an old masonry building is to improve the connection from wall to floor and roof diaphragms and in some cases improve the diaphragm action in addition to the rehabilitation of the damaged walls to achieve the desired seismic design level.

(c) Five-story **structures made of three-dimensional precast components** having dimensions of a room and assembled by means of vertical prestressing rods (Fig. 3). The studies carried out on this system have shown the importance of interaction among the three-dimensional structural members to the overall seismic response and concluded that the tested prestressing system is not necessary to improve the structural behavior.

(d) **Monolithic or partially prefabricated framed structures** with ground floor and ten stories, with or without “soft shear walls” (Fig. 4). The investigation performed on structural models at relatively large geometric scale and on full scale subassemblies have indicated the importance of the story drifts and damping to the oscillation filtering effects along the structure height. Another important aspect arisen from this study refer to the stiffness and lateral reinforcement of the short,

normal and long columns as well as the specific problems regarding the detailing and reinforcement of the beam-column joint etc.

(e) Partially prefabricated **lamellar framed structures** with ground floor and eight stories (Fig. 5). The column cross section is elongated in both directions (L, T or + shaped columns) providing more flexibility of plan layout and larger free spaces at the ground floor level. On the other hand, the prefabrication of the beams and floor units, as well as the casting the monolithic columns in special steel formworks allow an industrialized execution of these buildings. The experimental studies on individual lamellar shaped columns and the testing of several structural models on the shaking tables have shown the importance of a proper shear reinforcement of the columns to make them capable to withstand the vertical sliding among their wings and to reduce story drifts. The performance of the tested models and the behavior of some lamellar buildings during actual earthquakes provide evidence to support the view that this structural system can be designed to withstand severe seismic earthquake motions expected in seismic regions of Romania.

On the other hand, the use of lamellar columns in conjunction with flat slab frames, although it may result in more economical structures, should be used with precautions in seismic zones. The testing of a five story reinforced concrete model representing an office building consisted of monolithic lamellar columns and precast flat slabs indicated less ductility and excessive story drifts compared to fully framed lamellar structures under similar excitation intensity.

(f) **Structures with monolithic vertical diaphragms and precast flat slabs** (Fig. 6). The investigation of this system included the experimental study of the behavior of the shear walls reinforced according to classical practice or diagonally as well as the behavior of their lintels constructed also in two reinforcement variants. The influence of the lintel stiffness and the type of the wall-floor connection to the structural wall behavior were also studied. Another aspect investigated refers to the consequence of a flexible ground floor to the overall behavior of the structure.

(g) **Structures with frames and thinned structural walls and structures with central or multiple cores** (Fig. 7). The reinforced concrete cores are either monolithic or prefabricated, assembled by prestressing. The studies performed on various types of structural arrangements of walls and cores showed the importance of structural layout to the torsional response and the influence of core coupling to frames to the behavior under lateral loading.

(h) **Rural buildings made up of local materials** (Fig. 8) whose seismic resistance is conditioned by a proper interaction of the structural components and a suitable jacketing the walls with mortar reinforced by a wire mesh or a polymeric grid.

Using the testing facilities existing at INCERC - Iassy, a three dimensional full scale adobe structure was tested under simulated seismic excitations producing a substantial amount of damage in the component elements. The structure was

strengthened by jacketing the walls on both sides with wire meshes (Ø2.5 mm / 5 cm) interconnected by crossties introduced in drilled holes. The thickness of the poured mortar was 3 … 4 cm and the specified compressive strength was 2.5 N/mm2 (strength class M25). The upgraded structure was tested again in the similar conditions to those of the original structure. The experimental results clearly emphasized the effectiveness of the applied strengthening solution.

2.3 Industrial structures

2.3.1 Single-story and multi-story industrial buildings

The elaboration of a typified fully prefabricated system of single-story and multi-story industrial buildings characterized by higher speed of erection lead to the necessity of checking the seismic adequacy of a large series of construction systems, functional modules, structural subassemblies and joints.

Several structural models (Fig. 9) representing fully prefabricated single-story buildings were constructed and tested by means of large capacity shaking table. The main difference among the experimental structures consisted in the roof solution. In the case of the first model tested, the roof was made of reinforced concrete surface member alternating with openings for skylight. The roof of the second model consisted only precast beams in both longitudinal and transversal direction thus providing a relatively flexible diaphragm at the roof level. The spaces among beams were used for steel skylights or opaque zones disposed alternately.

The experimental program also included the shaking table test of a single story structure with prestressed columns having ring-shaped cross section (Fig. 9).

The tested structures exhibited specific inelastic behavior and failure patterns. A realistic evaluation of their inelastic seismic response depends not only on the hysteretic characteristics of its vertical load-resisting elements but also on the behavior of connections which determines the interaction of all structural members. It should mentioned that based on the experimental findings, the calibration of the seismic coefficient, Ψ, of the design code was undertaken for the first time in conjunction with the single-story industrial buildings, using dynamic criteria.

As regard multi-story structures for industrial buildings, a large variety of models were investigate starting from a simple two-story system with larger spaces at the upper story to more complicated multi-story systems including framed structures, structural wall structures or reinforced concrete core structures, consisting mainly of precast components.

All scale models incorporated the main features of the actual three-dimensional prototypes they represented and were designed to resist the combined service gravity loads and seismic lateral forces based on the requirements of a seismic code similar to Eurocode 8.

The major objectives of that investigation were to study experimentally the seismic behavior of some particular types of standard precast constructions and to formulate specific design guidelines for their structural systems. Another objective of the research was to investigate simple design analytical models that may be used in predicting inelastic seismic response of reinforced concrete structures. Because the design guidelines should be performance-based, response prediction of a structure to earthquake excitations, and especially prediction of lateral displacements by which structural performance can be judged, is of considerable practical importance. The design recommendations were developed using the information from both the experimental and analytical investigation.

2.3.2 Special constructions

For special typified constructions (Fig. 11a, 11b), as the 25-60 m3 capacity surface tanks made of polyesters reinforced with glass fibers, 5000-10000 m3 capacity surface tanks made of precast concrete members assembled by prestressing and 60000- 80000 m3 capacity steel tanks as well as for a series of elevated water tanks with capacities varying from 150 to 750 m3, a large research program has been conducted at the INCERC Iassy to obtain experimental data on the effect of linear and nonlinear interaction of liquid sloshing with containers and supported structure and to evaluate more realistically the $P - \Delta$ effect on the stability and resistance capacity of the supporting pillars with circular cross sections. The reinforcement distribution within cross sections was found to influence considerably the postelastic behavior of the elevated tank structure. The amount of confinement significantly affects the mechanical characteristics of concrete. Mechanisms of confinement for circular and rectangular sections differ.

2.4 Unique constructions of national importance

To achieve a better understanding of the seismic behavior of some unique constructions of national importance, as Bucharest subway and several large thermocentral power plants, some analytical and experimental research works have been performed at the INCERC Iassy as a part of a larger national program. The program included seismic analysis of the Rovinari (Fig. 12 a) and Chişcani thermocentral power plant structures as well as various structures of the Cernavoda nuclear power plant and some specific design guidelines and recommendations were formulated using the information from both the experimental and analytical investigation. Before such results were used to formulate design recommendations, they were carefully evaluated in terms of the level of structural performance expected and realistic estimates of the severity of inelastic deformational demands required of structural components in various soil-construction systems accounting for site seismicity.

Other design instructions or methodologies were prepared for buried pipelines (Fig 12 b), retaining walls and buried or surface constructions subjected to explosions.

The synthesis of these studies led to the conclusion that the maximum dynamic response of buried (underground) constructions is obtained due to the relative displacements, depending of the characteristics of the excitation source (harmonic, seismic, explosion) and the soil mass surrounding the structure. Despite advancements in this field, significant gaps still remain in our understanding because of the complexity of seismic response of constructions and the multitude of structural systems, configurations and details encountered in practice.

2.5 Seismic isolation; equipment-structure interaction

Base isolation is an alternative antiseismic design strategy. In general, an isolation system incorporates both flexibility and energy-absorbing capacity. Flexibility in the horizontal direction will increase the fundamental period of the structure beyond the range of periods which dominate the seismic response, so that the earthquake-induced loading will be decreased. However, the low stiffness of the isolation system could cause the displacements of the building to become too large. Hence, the isolation system should have some energy-absorbing capacity which, in addition to attenuating the transmission of energy into the building, will also reduce the structural displacement.

The complex theoretical and experimental studies on seismic isolation systems and equipment–structure interaction were conducted on a new conceptual basis by using both passive and active elements to dissipate energy induced into the structure during a severe earthquake action. Based on these studies, some methodologies were elaborated for passive isolating systems at foundation level (Fig. 13a) by using reinforced neoprene bearings and simple neoprene plugs as well as kinematic isolating systems by using concrete ellipsoids reinforced with metallic fibers. It should be mentioned that an experimental multistory building isolated with such ellipsoids was constructed in Iassy.

The large variety of structural damping-energy dissipation systems (Fig. 13b) investigated at the INCERC Iassy may be grouped in the following categories:

-directional dissipation devices

-inertial dissipation devices

- dissipation walls

- dissipation links

- rigidity plate dissipation systems

For all these isolation systems, specific modeling techniques or design instructions were developed.

Many buildings such as hospitals, power plants, telephone exchanges and pumping stations for water or gas pipelines contain essential equipment which must be

designed to be integral with the primary structure under earthquake-induced loading and must continue to operate in the aftermath of a severe earthquake. These aspects were also investigated in the frame of the antiseismic design strategy.

2.6 Rehabilitation of the existing buildings

The rehabilitation of hazardous structures to current design standards has been performed within the national program of restoration of existing stock of buildings.

One of the first category of structures investigated with the view of rehabilitation, refers to masonry buildings constructed in various periods of time in our country. For this category of structures, some strengthening methods and procedures verified experimentally were drawn up. The main strengthening method consisted in jacketing the walls with mortar or micro-concrete spraying, the reinforcement being either a steel wire mesh or a polymeric grid (Fig 14a).

In the case of large panel structures constructed during the early period in our country, a special jacketing method was applied in conjunction with reinforced concrete pillars and horizontal framework at the exterior joints, anchored at the floor level by means of prestressed cables and thus improving the rigidity of the floor diaphragm (Fig. 14b). The both methods have the advantage that does not necessitate the evacuation of the inhabitants during the strengthening works.

In designing the strengthening system the basic engineering approach should be to make use of the existing elements to as great an extent as possible. Of a great importance is also the proper selection of the new materials used in the rehabilitation works and the evaluation of the behavior of a composite element or structure consisting of old materials and new added materials.

Based on analysis of structural degradation indices, the rehabilitation of reinforced concrete frame and structural wall structures was solved by jacketing as well as by introducing some masonry or reinforced concrete rigidity panels into the existing structure, thus providing some stiffening diaphragms with controlled degree of rigidity.

2.7 Improvement of the dynamic-seismic interaction among different building materials and members

Starting from the current knowledge related to the mechanical characteristics and performance of building materials under seismic loading conditions, emphasis was placed on the following problems:

a. Studies on the mechanical connection between the reinforcing bars and the concrete with a special attention given to bond-slip relationships and anchorages of smooth and deformed bars under dynamic loading conditions.

b. Studies on the design and behavior of concrete members reinforced with rigid reinforcement of thin-walled section which, compared to hot rolled sections, reduce steel consumption by approximately 30%.

c. Dynamic modeling of connections between prefabricated elements and their influence upon seismic forces and stress and strain state of the structure.

d. Experimental investigation on the behavior of composite floor systems (reinforced concrete deck and rolled steel beams acting together by means of various types of shear connectors).

e. Analysis of experimental hysteretic loops obtained on various monolithic or prefabricated structural members, joints, subassemblages, and structures enabled the calibration of several hysteretic models with a large practical utilization.

f. Energy based concepts, derived from experimental findings, for evaluation of structural degradation (representing an important aspect in structural retrofitting).

2.8 Seismic qualification of technological equipment and facilities

INCERC Iassy has conducted experimental studies and theoretic generalizations regarding seismic qualification of a wide range of individual technological equipment and industrial installations considered as independent units. These studies referred to seismic behavior of energetic equipment (Fig. 15), chemical industry installations and petroleum industry equipment. Below is a list of the main systems qualified seismically during the last three decades:

a. Electric switchers (230 KV, 400 KV, 750 KV)

b. Simple and double electric separators

c. AC transformers (400 KVA – 400 MVA)

d. Reactant coils (tested in laboratory or in situ)

e. Medium and high voltage cells

f. Bearings for aerial lines of AC transport

g. Automation panels

h. Accumulator battery and gas reductions

i. Tight penetrations for nuclear power plants, security transducers etc.

The seismic tests were performed according to the required product procedures and specifications. In some cases the tests were conducted under voltage charge.

2.9 Cooperation

The staff of the INCERC Iassy also performed research works for partners of other countries on a contractual base (V.R.B. – Venezuela, Jacobson & Widmark – Sweden) as well as bi-lateral cooperation and exchange of information with prestigious similar institution working in the field of earthquake engineering or related fields (Earthquake Engineering Research Center of the University of California at Berkeley, ISMES –Bergamo, LNEC - Lisboa, Tniisk –Moscow, Iziis - Scopje Newmark Research Laboratory of the University of Illinois at Urbana-Champaign, Beijing Institute of Architectural Design). The participation of the INCERC Iassy to all European and World Conferences on Earthquake Engineering starting from 1969 should be also mentioned here. Other participations refer to various professional symposia and conferences as ERES (Earthquake Resistant Engineering Structures-International Conference) and Romanian National Conference on Earthquake Engineering.

In this context, it should be mentioned that the Faculty of Civil Engineering and the INCERC Iassy organized at Iassy a Conference on Earthquake Analysis of Structures with international participation during September 1970 (Fig. 16) which was the first conference on this subject organized in Romania. At this conference participated 11 countries with 21 contributions, apart from 40 contributions from Romania.

Also, the INCERC Iassy participated at various international programs of research in structural engineering organized by PNUD – UNESCO, UNDRO, CAER, INCO-COPERNICUS, PECO ERBEV-ECOLAND, BECEP-IC etc.

All mentioned achievements were possible due to the realization of a proper experimental base that included seismic shaking tables of 60 Kgf, 1 tf, 15 tf, 140 tf capacities, vibration generators, and multiple testing facilities for static and dynamic loading conditions. Besides, the attention given to the development of feasible and reliable methods of investigation contributed also to these achievements.

It is hoped that research activities in this field will get new dimensions by finalizing the investment started in 1985 (and postponed due to the lack of financial support). That investment comprises enhanced facilities for testing full scale structures and assemblies of structural elements and includes large capacity earthquake simulators (I-5 tf, I-30 tf, I-200 tf, I-1000 tf) which are in various stages of construction (Fig. 17).

References

INCERC - Branch of Iassy, Research reports and publications, 1966 - 2005

DYNAMIC CHARACTERISTICS

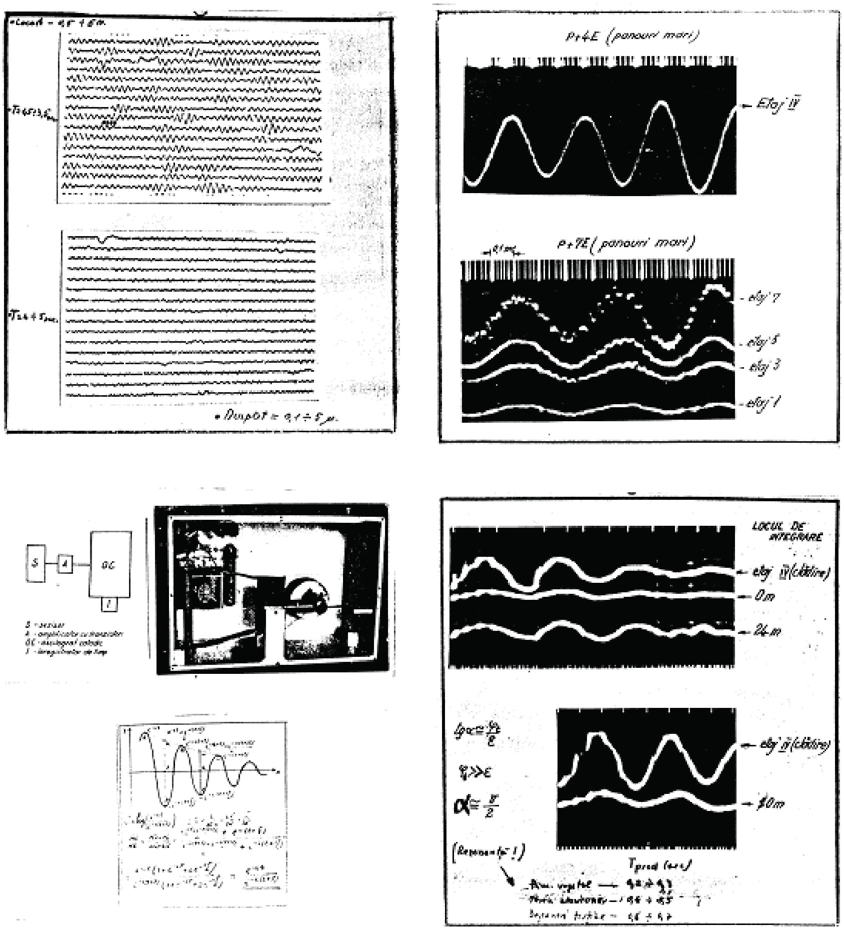

Natura terenului de fundație	Tipul constr. și localitatea	T transversal (sec) Tmed	Diferențe %	Tmin ÷ Tmax	T longitudinal (sec) Tmed	Diferențe %	Tmin ÷ Tmax
Aluvionar [illegible]	PM (P+4E) [illegible]	0,301	100	0,300÷0,308	0,282	100	0,254÷0,310
Loessoidal	PM (P+4E) [illegible]	0,272	-10	0,264÷0,279	-	-	-
Praf nisipos-argilos	PM (P+4E) [illegible]	0,223	-26	0,220÷0,226	-	-	-
Argilă [illegible]	PM (P+4E) [illegible]	0,217	-28	0,210÷0,226	-	-	-
Aluvionar	PM (P+4E) [illegible]	0,254	-16	0,238÷0,272	0,209	-25	0,200÷0,210
Loessoidal	[illegible]	0,226	-26	0,217÷0,244	0,17	-40	0,182÷0,182
Loessoidal	[illegible]	0,261	-14	0,242÷0,265	0,207	-27	0,204÷[illegible]
Argilă [illegible]	[illegible]	0,275	-9	0,262÷0,290	0,243	-14	0,213÷0,262
Loessoidal	[illegible]	0,326	+7	0,319÷0,340	0,248	-12	0,230÷0,278
Aluvionar	idem	0,332	+8,5	0,287÷[illegible]	0,280	-1	0,267÷0,290
—	PM (P+9E) București	0,408	-	0,408÷0,411	0,380	-	0,379÷0,382
—	[illegible]	0,508	-	0,481÷0,515	0,480	-	0,460÷0,488

−35% ÷ +35% Tscade ≈ 10%

$T_r \approx 0,25$ sec

Figure 1

Figure 2

Figure 3

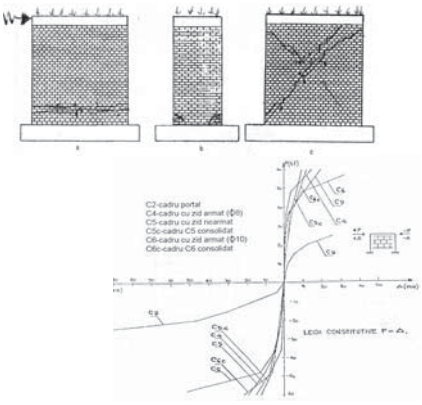

Figure 4

Figure 5

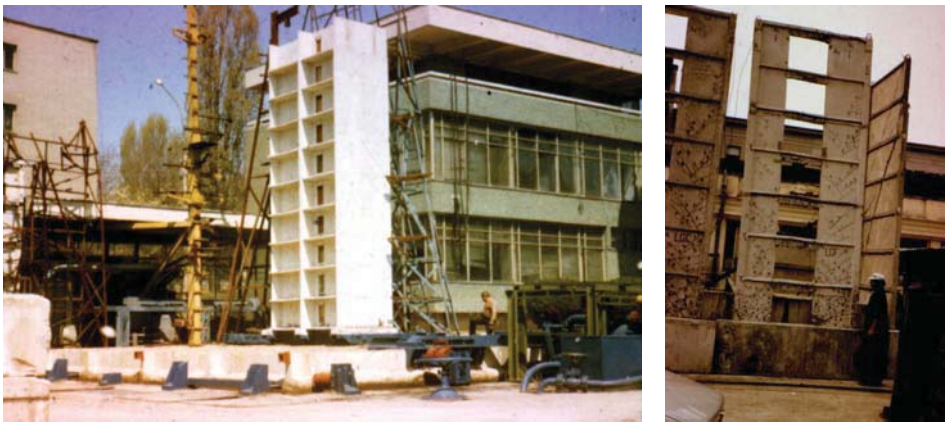

Figure 6

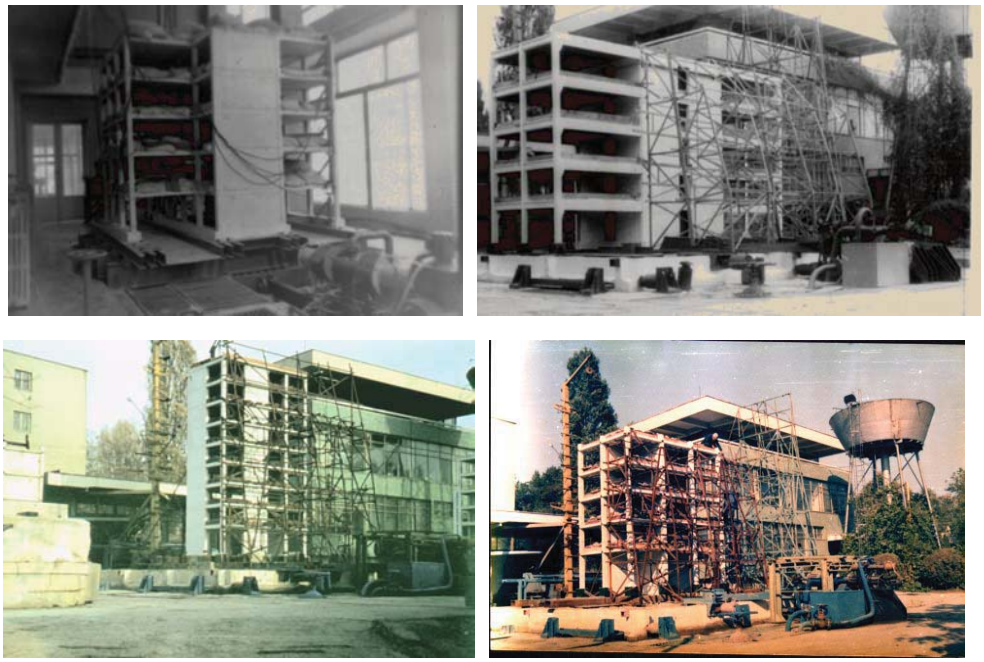

Figure 7

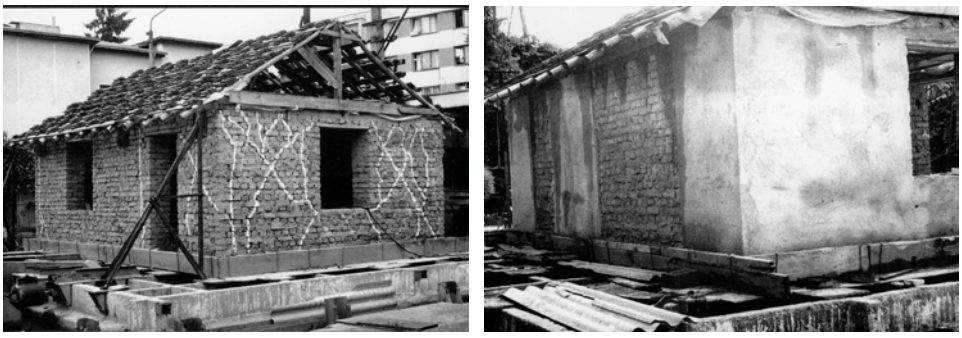

Figure 8

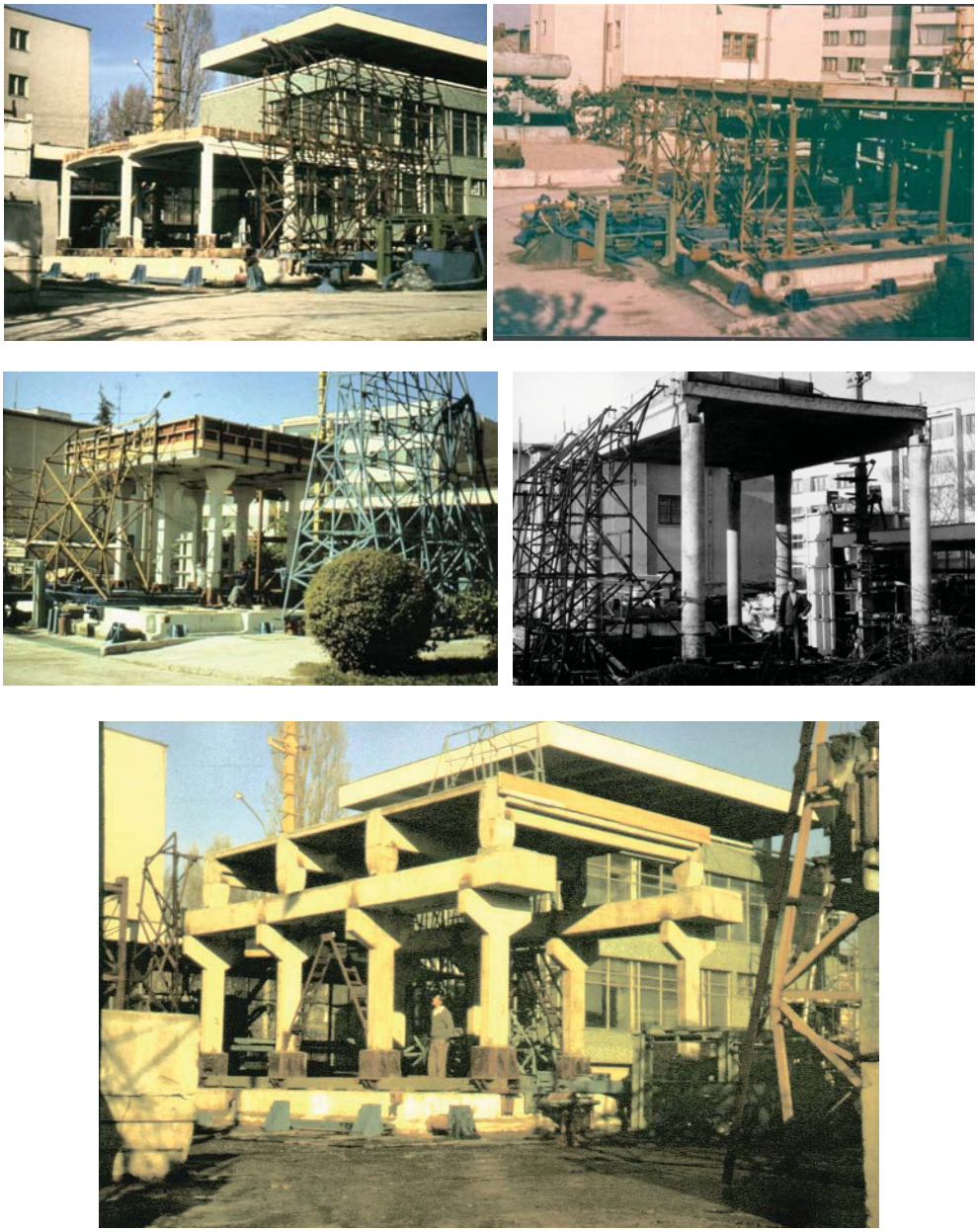

Figure 9

Figure 10

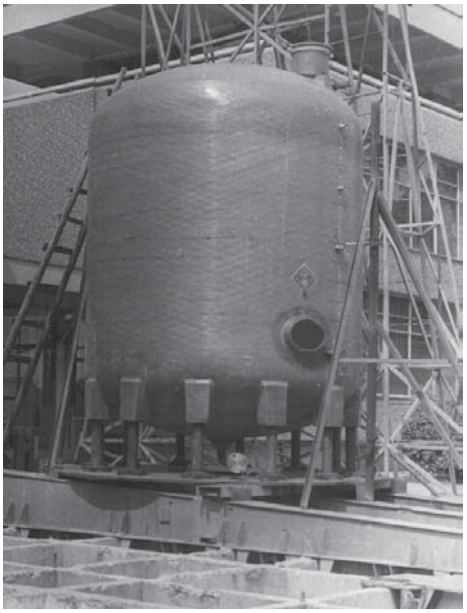

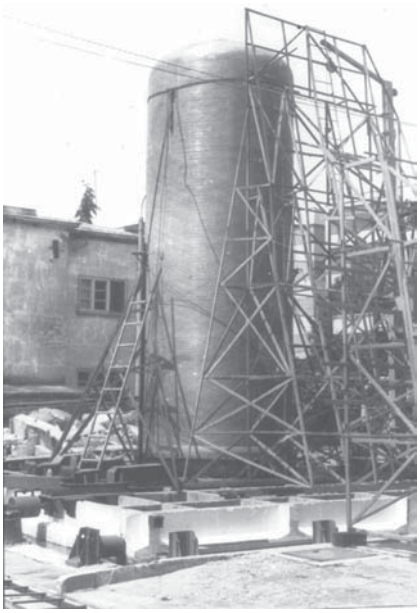

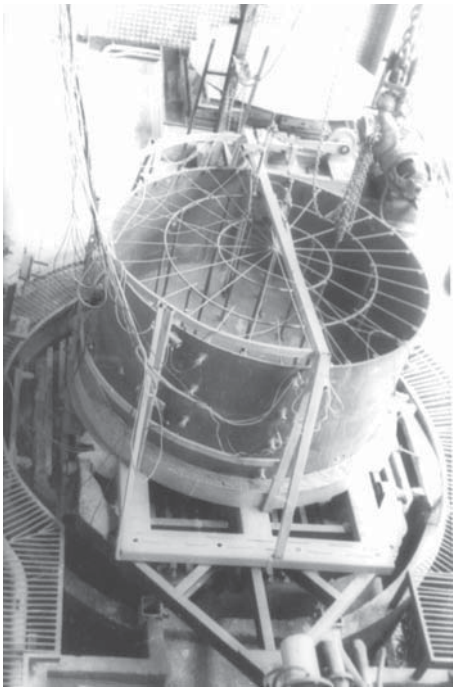

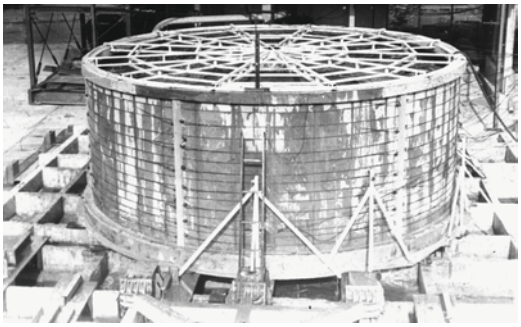

Figure 11a

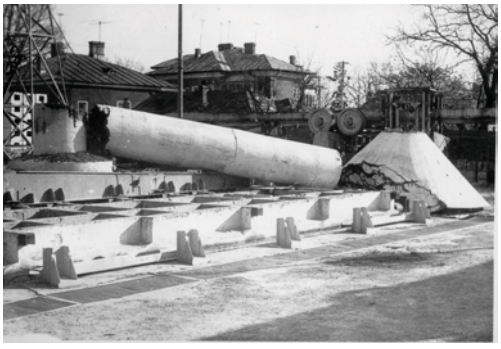

Figure 11b

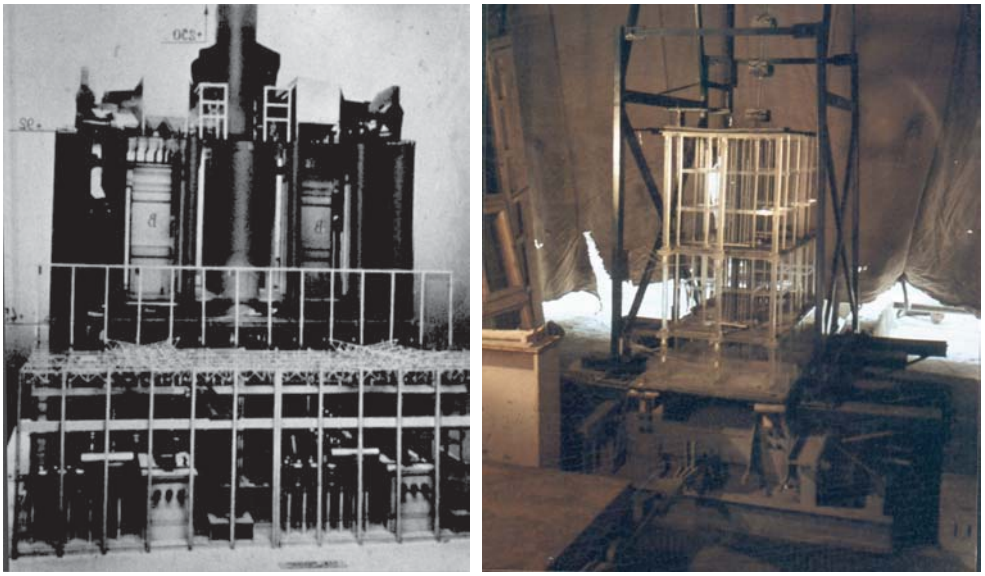

Figure 12a

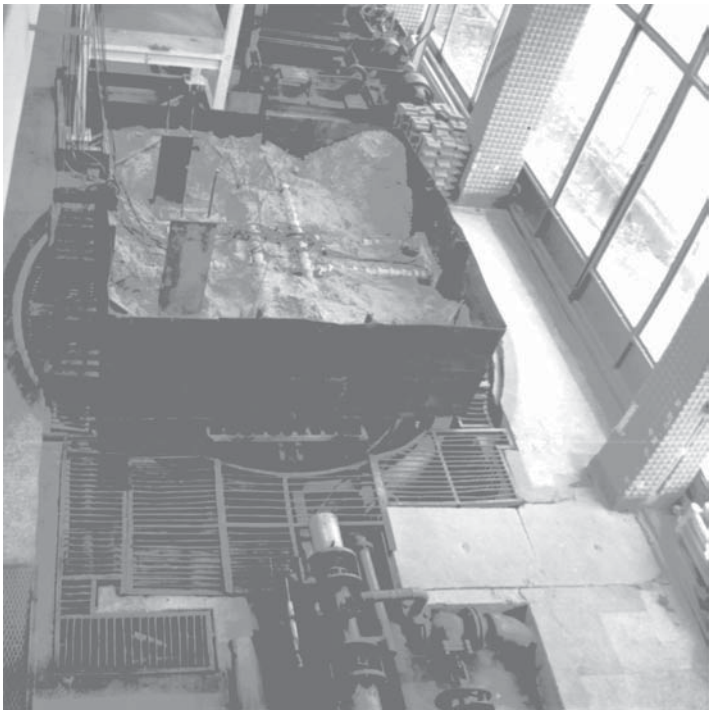

Figure 12b

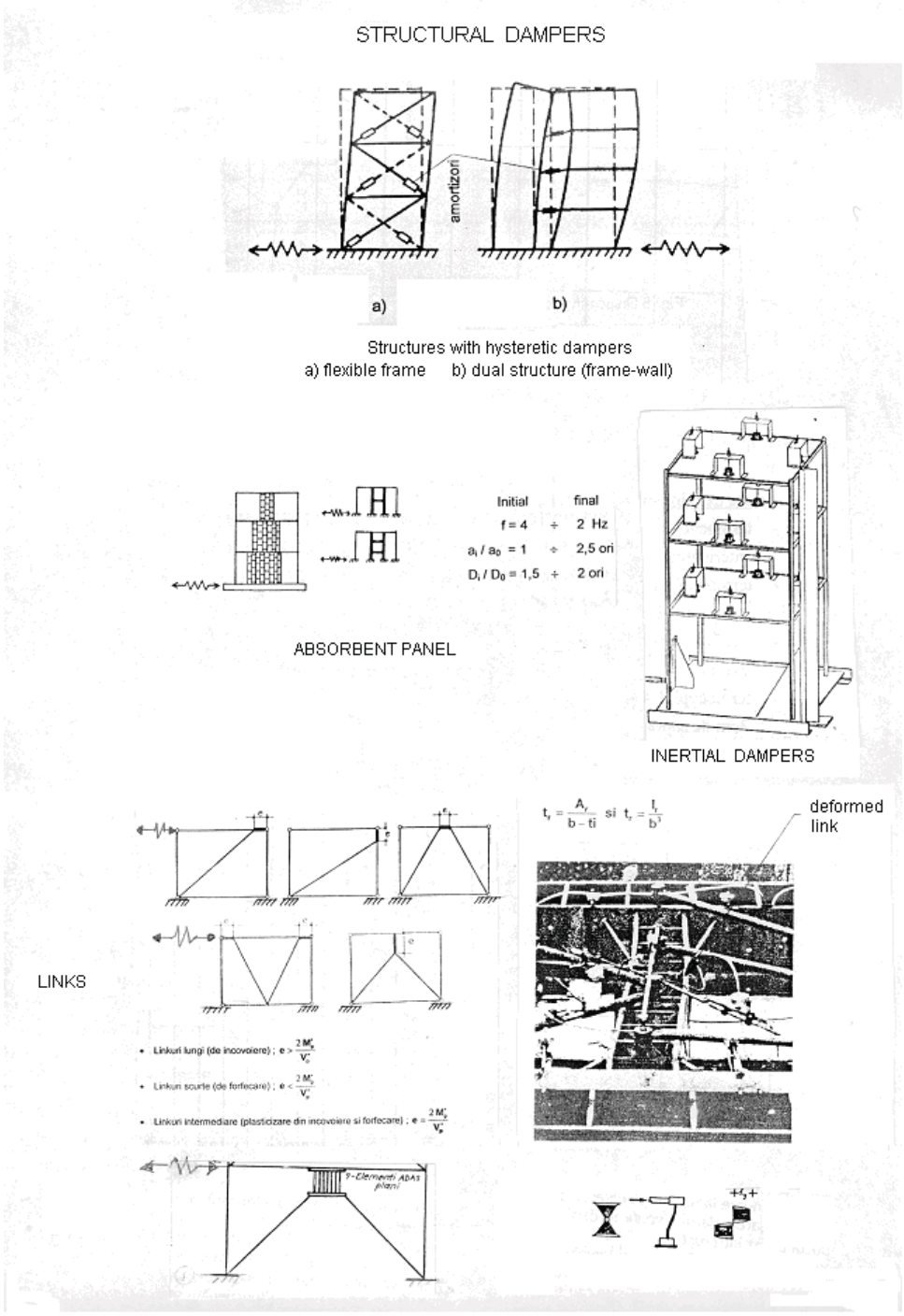
STRUCTURAL DAMPERS
amortizor
a)
b)
Structures with hysteretic dampers
a) flexible frame b) dual structure (frame-wall)
Initial final
f = 4 ÷ 2 Hz
$a_i / a_0 = 1$ ÷ 2,5 ori
$D_i / D_0 = 1,5$ ÷ 2 ori
ABSORBENT PANEL
INERTIAL DAMPERS
LINKS
deformed link
$t_f = \frac{A_f}{b - ti}$ si $t_i = \frac{I_i}{b^3}$
• Linkuri lungi (de incovoiere) ; $e > \frac{2M_p}{V_p}$
• Linkuri scurte (de forfecare) ; $e < \frac{2M_p}{V_p}$
• Linkuri intermediare (plasticizare din incovoiere si forfecare) ; $e = \frac{2M_p}{V_p}$
9-Elemenfi ADAS plani

Figure 13a

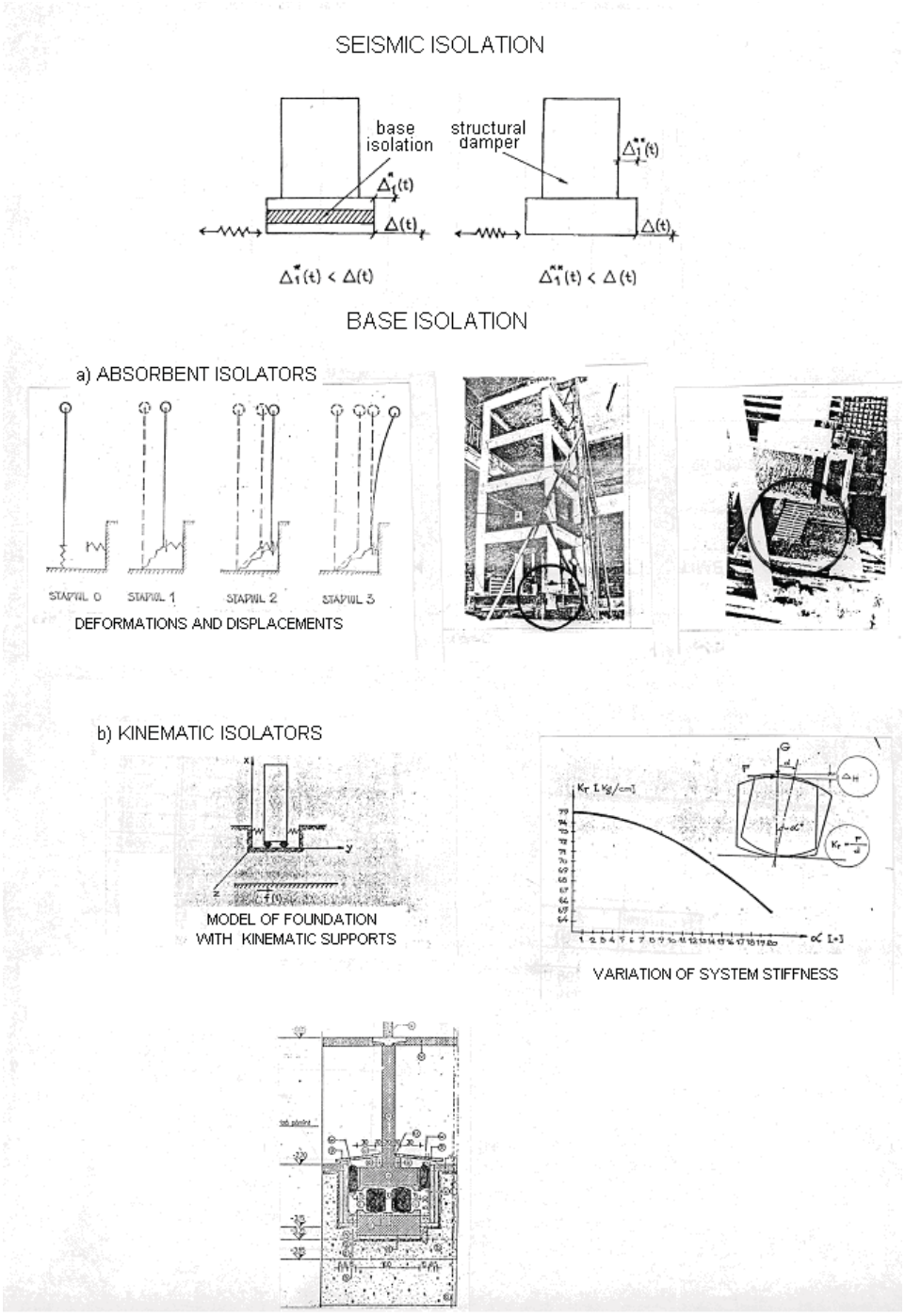
SEISMIC ISOLATION
base isolation
structural damper
BASE ISOLATION
a) ABSORBENT ISOLATORS
STAPWL 0
STAPWL 1
STAPWL 2
STAPWL 3
DEFORMATIONS AND DISPLACEMENTS
b) KINEMATIC ISOLATORS
MODEL OF FOUNDATION
WITH KINEMATIC SUPPORTS
VARIATION OF SYSTEM STIFFNESS

Figure 13b

Figure 14a

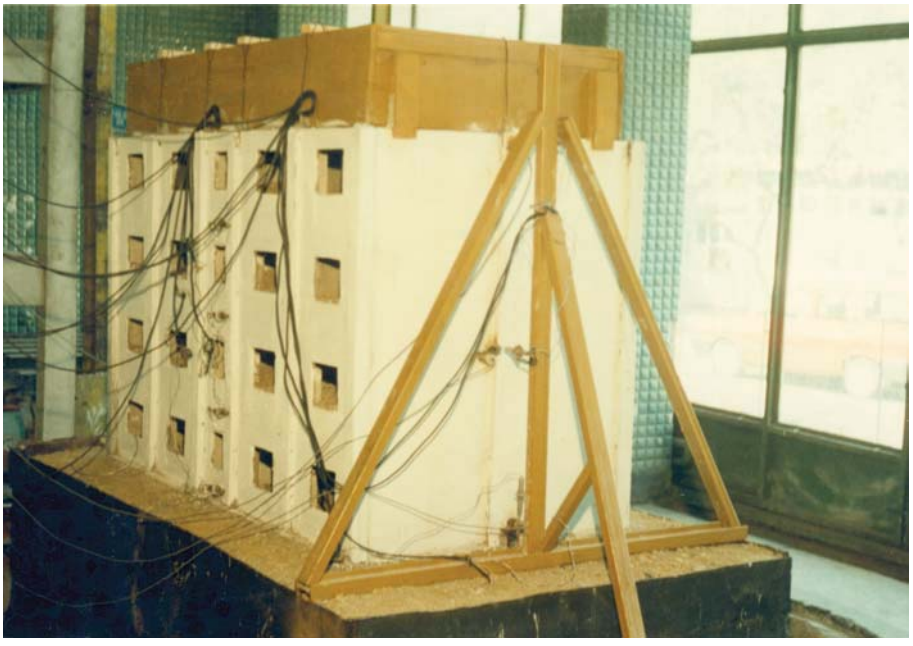

Figure 14b

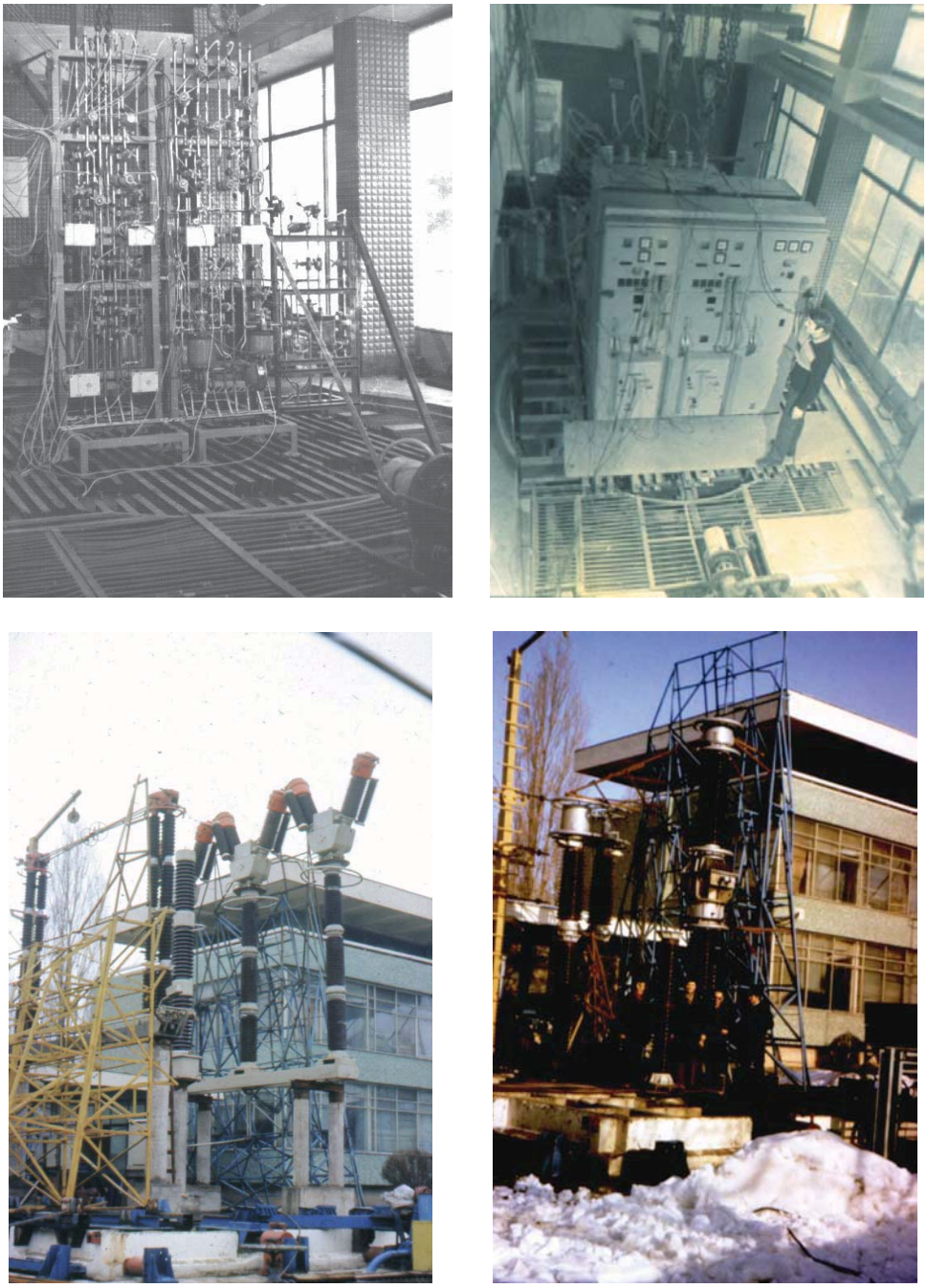

Figure 15

Figure 16

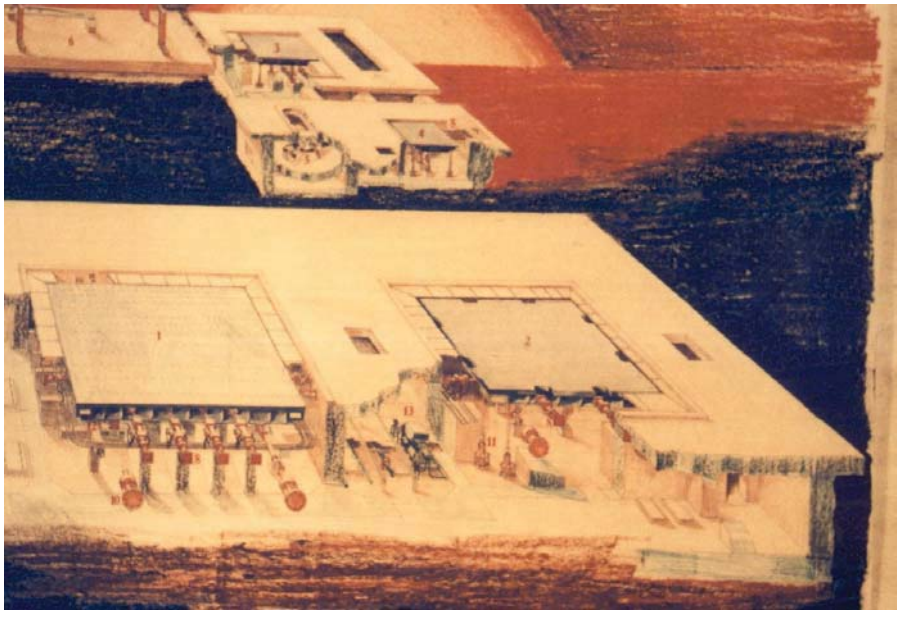

Figure 17

"Computational Civil Engineering 2006", International Symposium
Iaşi, România, May 26, 2006

Real-time damage monitoring system by modal testing of highway bridges

Cristian-Claudiu Comisu

Department of Bridges, Faculty of Civil Engineerig, Technical University "Gh. Asachi", Iasi, code 700050, Romania

Summary

The mobile laboratory will have a complete set of equipment and calculation technique in order to accomplish the following objectives:

1. *The dynamic testing of bridges with two electrodynamic vibrators.*
2. *The determination of the dynamic characteristics*
3. *The 3D model of the structure of the tested bridge*
4. *The process of calibration of the 3 D calculation model*
5. *The permanent process of comparison*
6. *The diagnosis of the structure in due time. When receiving the warning signal, the direct consequence is the immediate redirecting of the attention on the 3-D calculation calibrated model.*
7. *The application of the bridge protection protocol. The protocol includes a series of scenarios:*
   - *7.1. Beginning with the most simple which consists in taking the protection measures against fog or glaze on the bridge*
   - *7.2. Continuing with the more complicated scenarios which consist in requiring speed limitation, enlarged distance between the vehicles, closing certain traffic lanes.*
   - *7.3. Ending with the most serious cases which may consist in a traffic ban and adopting protection measures in accordance with the traffic.*

The advantages offered by the application of the program are:

1. *The possibility of prompt intervention*
2. *The possibility of taking decisions in due time.*
3. *The optimized administration of the highway bridges.*

KEYWORDS: bridge, structural health monitoring, damage detection, active sensing, experimental modal analysis & vibration testing, system identification, signal processing, probabilistic & statistical analysis.

1. INTRODUCTION

The construction of a mobile laboratory for dynamic testing and real-time online diagnosis of highway bridges is a response to the immediate necessity of quick intervention of a technically qualified entity to take decisions in due time concerning the nature of the interventions on bridges in case of great emergency.

At this moment in most countries of European Community, the methodology applied in these instructions for establishing the technical state of a bridge is based especially on visual observations, having in this way a great amount of subjectivity in appreciating the value of the quality and functionality index. Besides the disturbing action on the traffic, the methodology applied at this time in Romania and other countries of European Community has another series of major disadvantages, such as:

1. The low precision in indicating the moment of appearance, the evolution and the moment in which a critical point is reached during the process of deterioration that can be observed on the structure.

2. The observations are made exclusively visual without any possibility of receiving information about the gravity of the structural degradation process.

3. The high costs for providing access in hard accessible areas of the technical personnel which establishes the technical state.

4. The current unemployment of the testing and especially of the dynamic equipment which affects in serious way the precision of establishing the technical state of the bridge in a certain moment.

5. The great time interval between the moment in which the technical state is established and the decision of intervention, in case of major structural degradation which can seriously affect the safety and traffic comfort on the highway.

6. In Romania there is no protocol meant to assure the results continuity and correlation between the stages of establishing the technical state.

7. There is no possibility to determine the exact time interval in which the bridge can still be exploited until the next stage of intervention.

8. There is no possibility for optimized administration of the financial resources by rational planning of repair and maintenance works.

Appling the modal testing and diagnosis of highway bridges by creating a mobile laboratory, leads to elimination of any deficiency of the current methodology used at this time in Romania and allows it to become compatible with the technical requirements specified by the technical standards applied in the European Community.

The modal test method is being developed with the intent of using them as a fundamental tool for detecting bridge damage or deterioration. This process involves basic structural stimulus/response testing and Fourier analysis to construct a number of frequency response functions (FRF). These FRF's contain the information to characterize the structural behavior by providing the natural frequencies of vibration, as well as the corresponding deflection mode shapes and damping estimates. Using these parameters, a direct estimate of the flexibility matrix can be determined. By examining changes in the flexibility matrix, damage or deterioration can be more easily detected than by examining the global mode shapes. In essence, the flexibility matrix appears to be significantly more sensitive to small changes in structural behavior.

In 1993, Professor Varlam from the Faculty of Civil Engineering in Iasi, Romania, sustains his doctorate paper entitled: "**On the behavior of reinforced concrete bridge structures during dynamic action**", under the scientifically of direction of Professor A. Negoita. The studies and the researches have allowed for the first time in Romania to establish a dynamic research methodology of bridges with the help of a vibrator built by professor Varlam which is capable to excite bridge structures with forces determined as value, frequency and position.

Figure 1. The electodynamic vibrator built by professor Varlam from the Bridges Laboratory of the Faculty of Civil Engineering in Iasi.

The electrodynamic vibrator for site testing of bridge structures which is in functioning state at the Faculty of Civil Engineering in Iasi, is able to roll on wheels of its own and can be connected to a trailer truck. At the back of the truck, the pumping and a set electric welding are installed, assuring in this way the

functioning independence of the testing equipment towards the national electric power network.

Figure 2. The stand for dynamic testing of bridge models at great scale

The vibrator has 3 hydraulic cylinders, covers a frequency range between 0.5 and 10 Hz and has a dynamic force of up to 1200 daN/10 Hz. Because the methodology is simple and economical, it opened the way for the use of modern dynamic testing methods of road bridges.

The interest for applying a modal testing and monitoring system is an up-to-date matter and the numerous studies, research programs and scientific manifestations of the last few years underline the increased attention given to this matter on the international level. Important research groups from the European Union **(Switzerland, Germany, Great Britain, Italy, Denmark, France**) but also from the **USA, Canada and Japan**, have begun since 1996 the implementation of important research programs whose results have already been communicated in conferences organized in this field of activity.

The most intense research in this field, both concerning the financial resources and the size of the involved research groups are made in USA and Canada. The research group from the **University of Cincinati Infrastructure Institute (UCII)** already has a testing and diagnosis laboratory for highway bridges. The bridges` modal testing is based on the use of the drop hammer studies and electrodynamic vibrators. The research group has also developed a calculation program dedicated to the 3 D modulation of the tested bridge structure, based on the finite elements method. The calibration of the calculation model is based on the experimental data

obtained after the modal testing and helps to establish the technical state of the bridge and the remaining exploitation time.

2. BENEFITS

The benefits offered by the implementation of the program are:

1. The possibility of prompt intervention because of the mobility of the modal testing laboratory and structural diagnosis. The laboratory must be conceived and equipped in such way that it can reach any bridge in a determined time interval established on the criteria of minimal disturbance of the traffic on the part of the highway in question. This feature becomes very important in case of terrorist attack or a natural calamity (earth quake, serious accidents involving human victims)

2. The possibility of taking decisions in due time. The process of modal testing, of calculation of the dynamic characteristics, of calibration of the 3-D calculation model, of comparison with the values calculated in the previous stage and of launching the warning signal, must follow a quick and precise procedure. The decision of launching the warning signal and of beginning the protection protocol of the bridge must be an exact, precise process without any trace of human subjectivity.

3. The optimized administration of the highway bridges. The existence in the computers memory of a 3-D calibrated calculation model allows the diagnosis of the technical state of the bridge in due time. The calculation model allows the identification of the type of degradation, its position on the structure, the gravity of the process so that one may establish with precision:

3.1. The time interval in which the tested bridge can still be used in accordance with the traffic safety and comfort.

3.2. The type of the necessary repairing process (amount of material, labor and equipment)

3.3 The best distribution of financial resources

3. OBJECTIVES, DELIVERABLES AND EXPECTED SCIENTIFIC IMPACT

The research program has as goal the creation of a mobile laboratory with a complete set of equipment and calculation technique in order to accomplish the following objectives:

1. Dynamic testing of bridges with two electrodynamic vibrators. The modal testing will be made every 5 years for the functional bridges or after special events – terrorist attack, earthquakes, accidents by striking the structural elements of the bridge, exceptional transportation.

2. The determination of the dynamic characteristics (own values and vectors, damping characteristics) with the help of electronic equipment and a calculation program dedicate to modal analysis.

3. The 3D modulation of the tested bridge structure with the help of a specially designed calculation program based on the method of finite elements.

4. The calibration process of the 3D calculation model is made in the auto laboratory in due time and consists in comparing the model's theoretical dynamic characteristics with those of the real structure obtained at the site. In successive stages the theoretical dynamic values of the 3D model are changed until these will be equal to the experimental ones, case in which the model is considered calibrated.

On the occasion of the preliminary reception of the bridge (time To) a dynamic testing is performed together with a 3D modulation and calibration of the model based on the dynamic characteristics gathered at the site. In this case, the calibration of the model is made only modifying the mechanical characteristics taken into account when making the calculation model, assuming that in the phase of preliminary reception the bridge does not have flaws or major degradation.

All the following calibrations of the 3D calculation models will be made successively at the time Ti and will consist both in modifying the mechanical characteristics of the materials (due to rheological process of shrinkage and slow flow of the concrete, the relaxation of the fitting, the corrosion of the fitting and concrete carbonization) and in modifying the structural geometrical characteristics (due to a splitting process, displacement, deformation or vibration of the structure) in comparison with the calculation model calibrated in the previous testing phase at the time Ti – 1.

5. The permanent comparison process in due time of the characteristics calculated at the moment of the bridge testing (time Ti) with those calculated in the previous testing stage (time Ti – 1)

If as a result of the modal analysis one does not identify a significant difference between the values of the dynamic characteristics, the bridge is diagnosed as being in a satisfactory technical state in comparison with the previous technical state. If there is a difference between the values, a warning signal is to be launched.

6. The diagnosis of the structure in due time. When receiving the warning signal, the direct consequence is the immediate redirecting of the attention on the 3-D calculation calibrated model. The study of the calculation model must indicate the

type of the identified degradation process, its position on the structure and its gravity. The visualization of the affected structure can help the diagnosis process by confirming the observations made after the analysis of the calculation model.

7. The application of the bridge protection protocol. The structural protection protocol can be integrated in the procedures mentioned above, or it can be conceived as a completely separate procedure, the strategy function established by The National Roads Administration.

The protocol includes a series of scenarios:

-Beginning with the most simple which consists in taking the protection measures against fog or glaze on the bridge

-Continuing with the more complicated scenarios which consist in requiring speed limitation, enlarged distance between the vehicles, closing certain traffic lanes, the immediate announcement of the fire fighters, the traffic police and the ambulance.

- Ending with the most serious cases which may consist in a traffic ban and adopting protection measures in accordance with the traffic.

4. SCIENTIFIC PROGRAMME AND INNOVATION

The process of modal testing and diagnosis of bridges has 5 stages:

The dynamic testing of bridges

The determination of the dynamic characteristics

The comparison of the dynamic characteristics calculated at the site

The structure’s diagnosis

The bridge protection protocol.

The 3D modulation stages of the bridge structure and calibration of the calculation model can occur parallel to stage 3 and emerge in stage 4 of structural diagnosis.

Assembling these stages in a complex process, able to contain the modal testing and structural diagnosis procedure, provides the necessary conditions for creating a completely new entity in the bridge management system.

In stage 1, we suggest a methodology of modal testing using an electrodynamic vibrator and a series of equipment made of accelerometers, power amplifiers, signal analyzer and a graphical recording device.

In stage 2, the dynamic characteristics are determined using signal analyzers FFT. Stage 2 takes place within the bridge perimeter simultaneously to the testing process.

In stage 3, there are compared the values of the dynamic characteristics determined in the current stage with those determined during the previous testing for the same characteristics.

In stage 4 the diagnosis of the tested structure has two activities.

In activity 4.1 the diagnosis of the bridge is made by comparing the values of the dynamic characteristics determined in different stages of the bridge testing. If as a result of the comparing process one does not identify a significant difference of the values of the dynamic characteristics, the bridge is diagnosed as being in a satisfactory technical state. If there is a difference between the values, the bridge is diagnosed as being in an unfit technical condition and a warning signal is to be launched.

This activity is followed by activity 4.2 in which the diagnosis of the structure is made with the help of a 3D calculation model using a specially designed calculation program based on the method of finite elements.

The process of electronic modulation of the structure is made only once during the first dynamic testing of the bridge in question and the information is saved permanently in the central computer. On occasion of each bridge testing, the 3D calculation model is recalibrated, process which has to make the values of the calculated dynamic characteristics and the measured ones coincide. The calibration has as consequence the direct identification of the calculation model, and on the real structure the identification of a degrading process, regarding its position and manifestation level.

In the moment in which the warning signal is launched, begins an analyzing procedure of the 3-D calculation model in order to identify the position, and the gravity of the degradation process which led to a significant alteration of the values of the dynamic features. In this way the diagnosis of the technical state of the structure is made with a maximum of accuracy and precision, knowing the type of the degradation process, its exact position on the structure and the gravity or its size.

In stage 5 begins the structure protection protocol. The protocol's main concern is the fulfillment of the immediate traffic protection measures, and in the second phase the repair and consolidation works, which in this case are correctly dimensioned concerning the amount of work, material and the necessary equipment. In the same time the protocol provides the optimization of the financial resources.

The organization of the testing and diagnosis of bridges in these 5 stages will allow the functioning of the mobile laboratory so that it can fulfill the following major requirements:

- The possibility of prompt intervention

- The possibility of taking decisions in due time
- The optimized administration of the highway bridges.

5. CONCLUSIONS

The use of a mobile testing and bridge diagnosis laboratory on a highway section involves:

1. The optimized administration of the financial resources dedicated to the bridges` maintenance and repair. The significant drop of the resources used for this sector, allows them to be redirected to other sectors such as the investment one.

2. The optimization of the maintenance and repairing works leads to an increased duration of exploitation of the bridge in question, which allows the achievement of benefits that can be redirected towards the investment sector.

3. The maintenance for a long time in a good technical state of the bridges on a highway section, for which are necessary only current maintenance works, leads to the traffic fluidization on that highway sector.

4. The implementation of this testing and diagnosis system for highway bridges, regarded as a standard process for establishing the technical state, demands the use of a modal testing equipment and calculation programs made abroad and involves a technological transfer towards the users, the opportunity to create new working places and opens new perfection possibilities.

References

1. Aktan A. E., Hunt V. J., Lally M. J., Stillmaker R. B., (1994) Field Laboratory for Modal Analysis and Condition Assessment of Highway Bridges, Structural Dynamics Research Laboratory at the University of Cincinnati, Proc., 12th IMAC.
2. Aktan, A.E., Chuntavan, C., Toksoy, T., Lee, K.L., (1992) Bridge Nondestructive Evaluation by Structural Iden-tification, Proc., 3rd NSF Workshop on Bridge Eng. Res. in Progress, Dept. of AMES, UC San Diego,.
3. Aktan, A.E., Chuntavan, C., Toksoy, T., Lee, K.L., (1993) Structural Identification of a Steel-Stringer Bridge for Nondestructive Evaluation, Transportation Research Board, Record 1393.
4. Aktan, A.E., Chuntavan, C., Toksoy, T., Lee, K.L., (1994) Modal Testing for Structural Identification and Condition Assessment of Constructed Facilities, Proc., 12th IMAC.
5. Aktan, A.E., Zwick, M.J., Miller, R.A., Sharooz, B.M., (1992) Nondestructive and Destructive Testing of a Decommissioned RC Slab Highway Bridge and Associated Analytical Studies, Transportation Research Board, Record 1371.
6. Agardh, L., Modelling (1993) Soft Impacts for Vibrational Ex-citation of Civil Engineering Structures, Swedish Natl. Testing and Res. Inst., Nordtest Tech. Rep. 201.
7. Comisu, Cristian Claudiu, (2006) Sistem integrat de monitorizare pentru îmbunătățirea durabilității structurilor de poduri inteligente. Program de cercetare Facultatea de Construcții si Instalații Iaşi, cod CNCSIS 438. (in Romanian)

8. Comisu, Cristian Claudiu, (2006) Sistem integrat de monitorizare permanenta pentru îmbunătățirea durabilității structurilor de poduri inteligente. Program de cercetare Facultatea de Construcții si Instalații Iaşi, cod CNCSIS 438. (in Romanian)
9. Comisu, Cristian Claudiu, (2006) Mobile Laboratory for dynamic Testing and Diagnosis of Highway Bridges, COST Reseach proposal.
10. Comisu, Cristian Claudiu, (2006) Laborator mobil pentru testarea dinamica si diagnosticarea in timp real a podurilor pentru autostrăzi, Material transmis la concursul Premii AIPCR 2007, Tema – Siguranța circulației. (in Romanian)
11. Hunt, D.L, Weiss, S.P., West, W.M., Dunlap, T.A., (1999) Freesmeyer, S.R., Development and Implementation of a Shuttle Modal Inspection System, Sound and Vibration Magazine, August.
12. Tomoyuki. I., (2004) Development of Takenaka Mobile Laboratory, Intelligent Structures - 2, Monitoring and Control, ed., Wen, Y.K., Elsevier Publ., 218-227.

"Computational Civil Engineering 2005", International Symposium
Iaşi, România, May 26, 2005

Useful calculation of buckling length for steel columns

Dragos Voiculescu

Department of Steel Structures, University of Civil Engineering, Bucharest, Romania

Abstract

The paper presents the Microsoft Excel computer program for the calculation of buckling length for steel columns in different types of structures. These values can be used afterwards in the process of sizing and checking of the column sections with other computer programs. The program purpose is to give the written part in the design process for the steel columns of a structure.

KEYWORDS: Computer program, buckling length, Microsoft Excel.

1. INTRODUCTION

This paper presents a computer program, realized using Microsoft Excel, for the calculation of the buckling lengths of HE steel columns. The program can be used for any column HE section and for any type of support at the ends. The determination is done sequentially on the two directions of buckling y and respectively z, using relations from the international design practice. As the purpose of the program is to give directly the calculation sheet, the language used in it is Romanian.

2. PROGRAM PRESENTATION

2.1 Determination of the buckling length in y-y plane

In order to establish the buckling length of the column in y-y plane (Fig.1) we must enter the type of supports at the column ends in y-y plane.

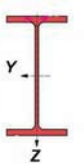

Figure 1. The buckling planes of the column

All the possible types of supports are introduced using a dynamic window which gives a higher degree of simplicity in usage. (Fig.2).

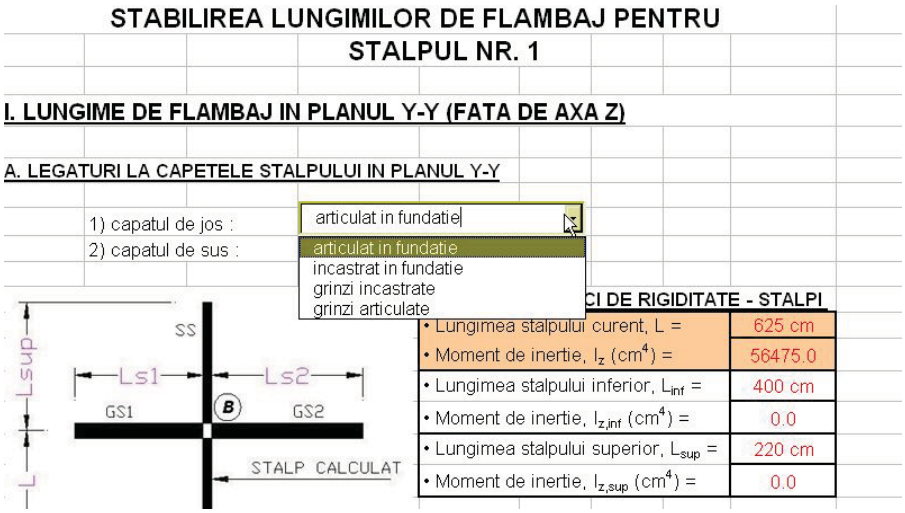

Figure 2. Introducing the supports at the column ends

After establishing the end supports, we should introduce the stiffness characteristics of the neighboring beam and column elements in y-y plane. (Fig.3).

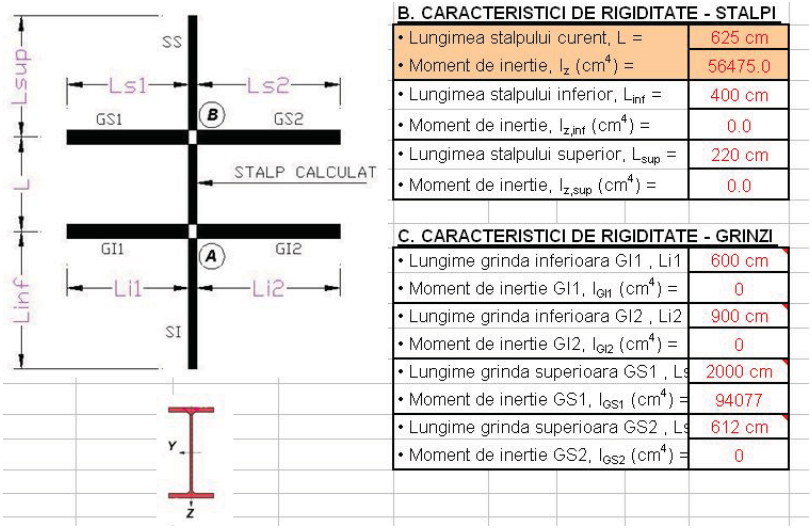

Figure 3. Introduction of stiffness characteristics of adjacent beams and columns

After this step, we will establish the column type in a dynamic window (Fig.4).

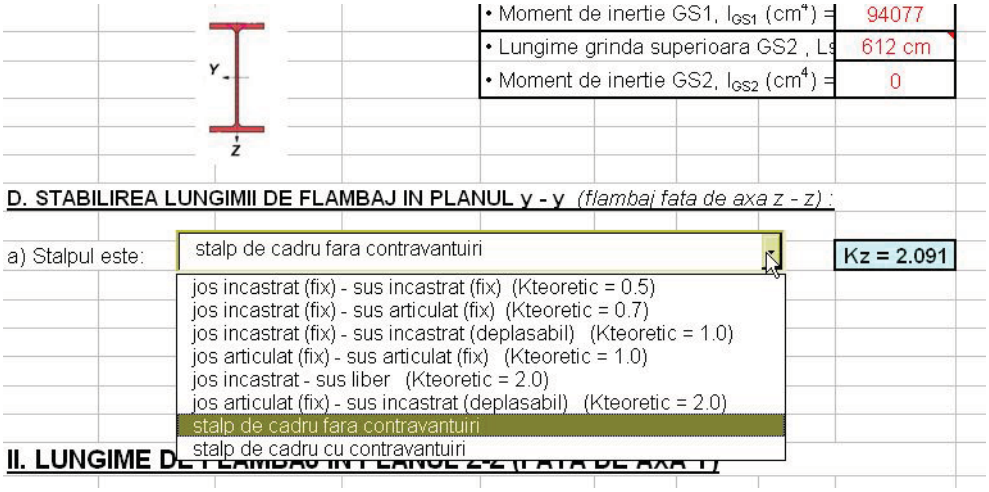

Figure 4. Establishing the column type

After completing these initial data, in case the column is a moment frame column or part of a braced structure, we go in "LUCRU" worksheet of the program where all data is read automatically (see Fig.5). For the calculation of G_A and G_B factors the program is using the following relation:

$$G = \frac{\sum \frac{I_{stalp}}{L_{stalp}}}{\sum \frac{I_{grinda}}{L_{grinda}}} \tag{1}$$

Then the value of K_z buckling factor is given by the equation:

$$\frac{G_A \cdot G_B}{4}\left(\pi/K\right)^2 + \frac{G_A + G_B}{2}\left[\left(1 - \frac{\pi/K}{\tan\left(\pi/K\right)}\right)\right] + 2\left(\frac{\tan\left(\pi/2K\right)}{\pi/K}\right) = 1 \tag{2}$$

The calculation is done afterwards using the Microsoft Excel „GOALSEEK" function and the program sends the final value of the buckling factor in the main worksheet, which may be used to calculate the buckling length of the column.

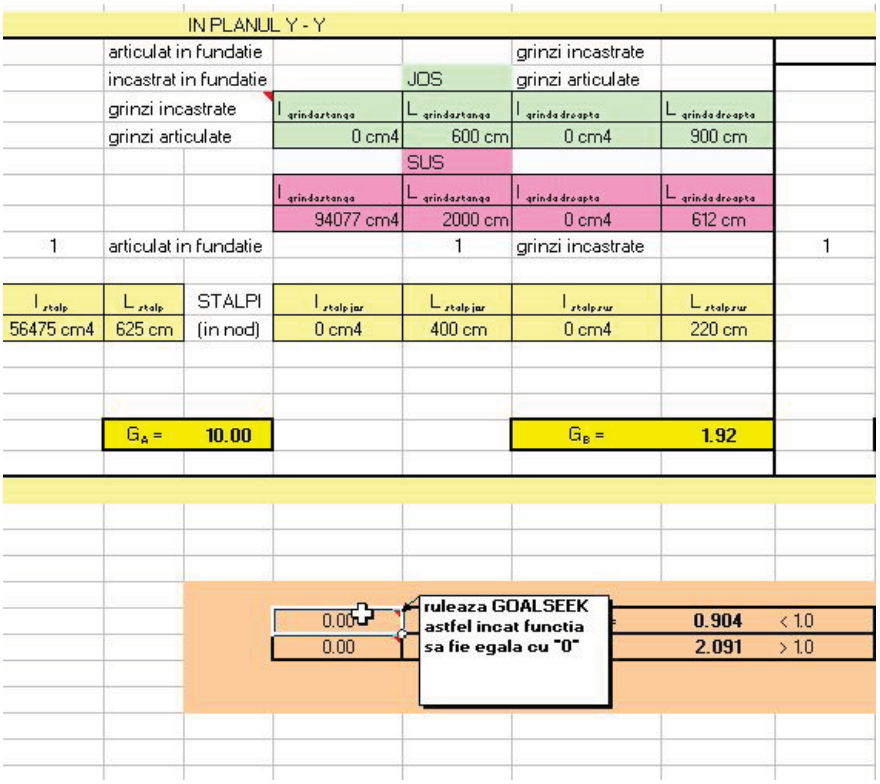

Figure 5. Values of G factors and calculation of the buckling factor

2.2 Determination of the buckling length in z-z plane

In the orthogonal plane, z-z, the calculation is realized following the same steps as presented above, in z-z plane.

2.3 Results

The calculation results are centralized in a final table to give the possibility of using them in the column sizing programs. The column buckling length is obtained by multiplying the column length with the correspondent buckling factors (Fig.6).

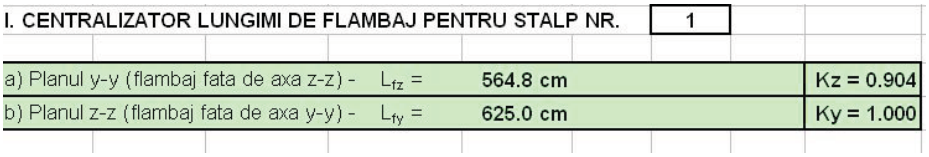

Figure 6. Buckling length table

3. CONCLUSIONS

The program is very easy to use and very useful in the design process of steel columns. It is the preliminary step before entering in a sizing program and gives the possibility of economic sizing of the steel columns. As it was intended to give the design calculation sheets, the language used in it is Romanian, but my intention is to make it in English, too.

References

1. Canadian Institute of Steel Construction, *Handbook of Steel Construction*, Universal Offset Limited, Markham, Ontario 1993.
2. R. Englekirk, *Steel Structures*, John Wiley&Sons, Singapore, 1994.

"Computational Civil Engineering 2005", International Symposium
Iaşi, România, May 26, 2005

"HE" column sizing under complex actions

Dragos Voiculescu, Daniela Preda

Department of Steel Structures, University of Civil Engineering, Bucharest, Romania

Abstract

The paper presents the Microsoft Excel computer program for the design of "HE" columns. All the checks are done after STAS10108/0-78 but they will be updated for European Union codes.

KEYWORDS: HE column design; Microsoft Excel.

1. INTRODUCTION

The program is giving the calculation sheet for the design of "HE" columns. Initially we have to input the steel grade of the column and its length (fig.1).

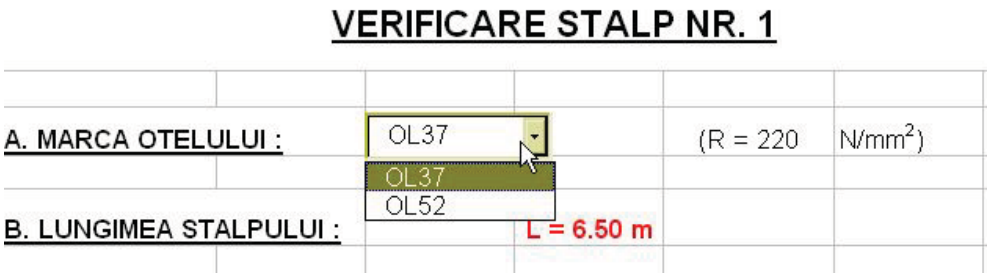

Figure 1. Initial data

Afterwards we must complete a table with the stresses resulted from the static calculation.

Also we have to choose a column size from the "HE" database of the program, using a dynamic window.

Automatically all the geometrical data of the section of the column will be prompted in a table. This data will be used for the strength and stability checks. (Fig.2)

C. EFORTURI MAXIME (CU SEMNELE LOR) :

	Forta axiala N (kN)	Moment $M_{y,1}$ (kNm)	Moment $M_{y,2}$ (kNm)	Moment $M_{z,1}$ (kNm)	Moment $M_{z,2}$ (kNm)	Forta taietoare T_y (kN)	Forta taietoare T_z (kN)
I. N_{max}, M_{yc}, M_{zc}	415.0	0.0	1.2	0.0	0.1	0.2	0.9
II. N_c, M_{ymax}, M_{zc}	167.0	0.0	77.0	0.0	1.0	0.1	23.2
III. N_c, M_{yc}, M_{zmax}	0.0	1.0	0.0	1.0	0.0	0.0	0.0

D. PROFIL UTILIZAT

HE 240 A

HE 240 A
HE 240 AA
HE 240 B
HE 240 M
HE 260 A

h (mm)	t_w (mm)	b (mm)	t_f (mm)	A (cm^2)
230	7.5	240	12	76.84
W_y (cm^3)	**W_z (cm^3)**	**I_y (cm^4)**	**I_z (cm^4)**	**G (kg/ml)**
675.1	230.7	7763	2769	60.30

Figure 2. Stresses and size tables

After the section size is chosen, we introduce the buckling length factors, computed with another program. The program calculates then the buckling length of the column in the y-y and z-z planes. Using the data input, the program calculates then the slenderness of the column and the buckling factors (Fig.3)

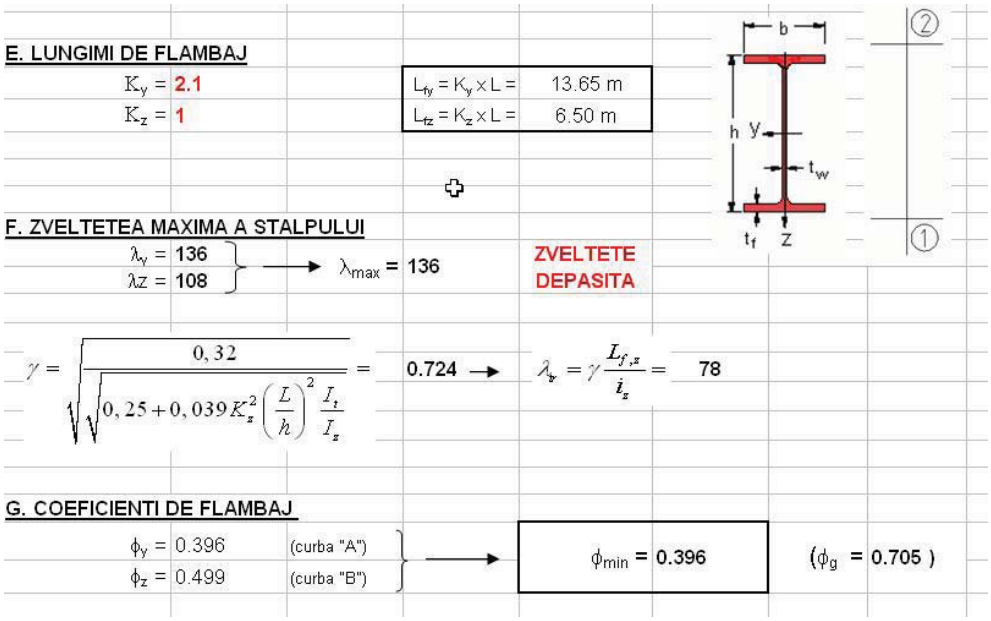

Figure 3. Buckling length and factors

2. CHECKS

2.1 Strength check

Strength check is done in all characteristic points of the section using the relations presented in figure 4.

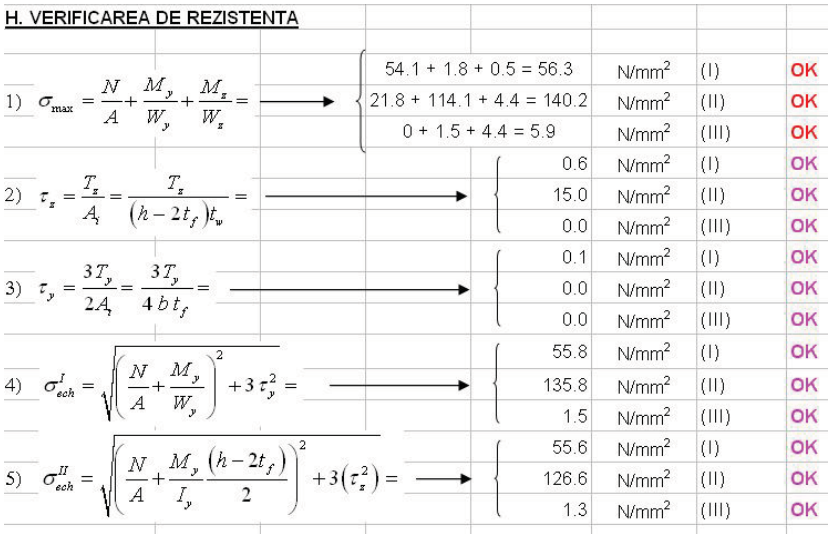

Figure 4. Strength checks

2.2 General stability check

According to the stresses introduced in the table, the program computes the values of the moment reduction factors and checks the stability. (fig.5)

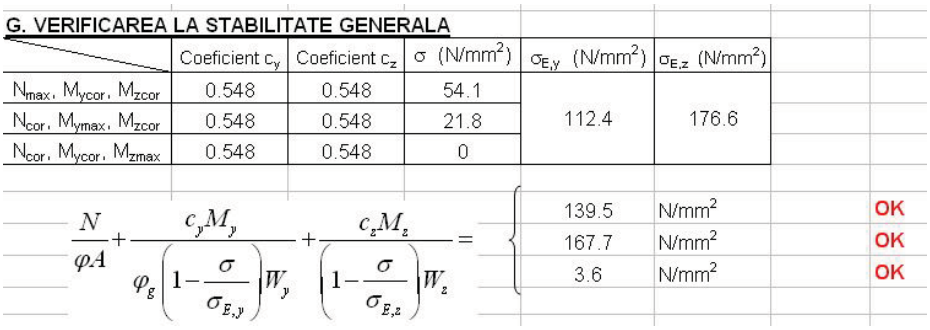

Figure 5. General stability check

3. CONCLUSIONS

The program is easy to use and very user friendly. As the intention was to create the calculation sheets in the design process, the language used was Romanian, but in the near future it will be upgraded with an English language translation.

References

1. *STAS 10108/0-78*, Bucuresti 1978 (in Romanian).

"Computational Civil Engineering 2006", International Symposium
Iaşi, România, May 26, 2006

Trends of actual computer assistance for laboratory studies in boundary layer wind tunnel

Elena-Carmen Teleman[1], Elena Axinte[2], Radu Silion[3]

[1,2,] *Civil Engineering Department, Faculty of Construction, "Gh. Asachi" Technical University, Iaşi, 700050, Romania*
[3]*Faculty of Computers and Automatics, "Gh. Asachi" Technical University, Iaşi, 700050, Romania*

Summary

The modern research studies dealing with wind action and different shapes of constructions are developed mainly based on boundary layer wind simulations. These studies, along with measurements at natural scale and assisted by advanced computer aids are extremely important for the structural engineer in the phase of conception and design of a certain structure.

The paper presents some of the results of using techniques of study the wind simulation based on computer aid in the boundary layer wind tunnel from the Laboratory of Structural Aerodynamics

KEYWORDS: boundary layer wind tunnel, wind structure simulation, wind spatial turbulence, power spectral densities, length scales of the wind turbulence.

1. INTRODUCTION

From the climatic point of view, the last decades of the XX century were characterized by dramatic changes at the level of planetary wind patterns. Although difficult to evaluate de wide panel of consequences, at least a brief quantification of these uneasy events may be lightened by the economic losses. In their "8th Biennial Scruton Lecture" in 2003 the British Wind Engineering Society had reported that between 1950 and 2002 losses due to severe wind storms "have spiraled" from 11 to 104 billion dollars and the number of these major storms increased from 7 in the first decade to 42 during the last ones [1].

In parallel, the last half-century was a period of great development of the wind engineering and the study of the aerodynamics of constructions all over the world. Huge steps forward were made in understanding the complexity of the wind climate and the wind flow structure. The structural designers are important beneficiaries of these achievements because the major problems engendered by the interaction between wind and constructions find their solutions. After devastating

disasters that affected in the last century various structures all over the world and after repeated serious economic losses the structural engineer knows he has an unyielding enemy he has to fight, which is the action of the wind upon the construction.

2. MODERN APPROACHES OF THE ASSESSMENT OF WIND LOADING

The classic approaches of studying the interaction between the wind flow in the proximity of the earth surface, called boundary layer of the natural wind and the structures immersed in this layer is based on three aspects: wind climate, boundary layer and structures itself and several steps were made in time in order to find the best assessment of their interaction [2].

The structure and its environmental conditions are taken as a whole at the impact with the structure of the wind in a given placement. The key is to have sufficient data that enable the model the wind climate based on probabilistic parameters, retaining those corresponding to the extreme-value and the peak loading coefficients from measurements on structures (at natural scale or on models).

Still, there are not yet developed fully convenient standard methods for the dynamic structures to replace the quasi-static admittance method and the problem is solved particularly by ad-hoc modeling.

The evaluation of the wind action upon the constructions according to the most advanced standard methods knows two main general approaches, both being sufficiently accurate. One of these refers to the analysis of the behavior of the structure considering the mechanical characteristics of the construction, the basic concept being the reduction of both forces and displacements to the spectral density of power. The method responds mainly to the necessity of the structural engineer to design the main structure against global effects of the wind action. But in order to be fully convinced that this method leads to an evaluation of a good accuracy, both the wind turbulence spectrum and the admittance function must indeed converge into realistic description of the design response of the structure (fig. 1)

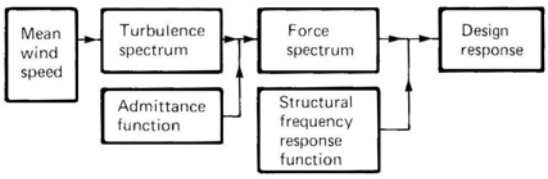

Fig.1. Aerodynamic admittance method of analysis of structures to wind loading- Cook[2]

3. ELEMENTS FOR MODELING THE WIND FLOW FIELD

3.1. Wind structure

The nature of the atmospheric boundary layer of the wind flow on the surface of the earth is in the center of the modern researches and since its direction was found to change only a few degrees up to 180 m above the ground, the mathematic description of the flow is based on its constant vector, the mean wind velocity *V(z)* which depends on the height *z* and on the fluctuating velocities, which in a Cartesian system of coordinates will be expressed with the help of three functions, *v(x,y,z,t*), *u(x,y,z,t)* , *w(x,y,z,t)*. The expression of the wind field will then be:

- in the longitudinal direction: $V(z)+v(x,y,z,t)$ (1)

- in the lateral direction: $u(x,y,z,t)$ (2)

- in the vertical direction: $w(x,y,z,t)$ (3)

showing clearly that turbulence is an additional dynamic part of the wind velocity; the instantaneous value of speed being affected longitudinally by this turbulence. The influernce of the lateral and vertical components of turbulence is much more reduced, for this reason the longitudinal instantaneous value of the speed being the only one considered in the general cases in the evaluation of the wind impact on the constructions.

The mean wind velocity is described by the wind profile on the surface of the ground and some important laws of variation were imposed by the afferent models: the logarithmic profile based on von Karman'constant, used by EC1, the empirical power law profile, the mathematical model of Harris and Deaves, using the Coriolis parameter. These relationships must cope with two amendments:

1) they must be easy to apply by the designing engineer;
2) they must fit the experimental data, either obtained by measurements on site or by modeling in the wind tunnel.

The design load of the wind on the construction is obtained starting from the reference wind velocity which, up to now being determined on the basis of previous data, doesn't take into account a possible and predictable „greenhouse effect" when estimating the extreme winds. On this point, the future will leave space for unpleasant but necessary corrections.

Due to the different traditional procedures of estimating the extreme winds (based on wind velocity or pressure velocity) and to the lack of correlation between the meteorologists and the engineers regarding basic physical wind parameters, confusion is still present needing better harmonizing methods through out all the countries entering in the European Union.

3.2. Wind turbulence

The three turbulence components in relationships (1)…(3) are random values probabilistically described by: standard deviation, time scales, power spectral density functions that define the frequency distribution and normalized co-spectra that specify the spatial correlation.

Up to 200 m above the ground, the distribution of the turbulence components is esteemed to be Gaussian with a zero mean value. Still, in the tails of the distribution, the turbulence components pop out from the range of ± r.m.s. Among other errors in the evaluation process, this may have severe implication on the evaluation of the maxima values of local pressures (and suctions) on the surface of the constructions [3].

The frequency distribution of the turbulence component v is described by the non-dimensional power spectral density function $F_N(z,n)$ defined as:

$$F_N(z,n) = \frac{nS_v(z,n)}{\sigma_v^2(z)} \tag{4}$$

where:

n- frequency [Hz]

$\sigma_v(z)$- standard deviation of the longitudinal componenet fo wind turbulence;

$S_v(z, n)$ - power spectrum of the along-wind turbulence component. The energy of the turbulence is generated in the large eddies corresponding to the low frequencies and dissipated in small eddies corresponding to high frequency domain. In between there is the inertial sub-range where the turbulent spectrum doesn't depend on the mechanisms of generation and dissipation and which find itself an equilibrium in transferring the produced energy.

Several shapes are given for the power spectral density function by reference researchers in the domain: Kaimal et al., Simiu, Davenport, Harris. EC1 uses a particular shape of the Kaimal spectrum longitudinal component a simple spectral form, adequate for most common structures for whom the fundamental natural frequency of vibration is higher than the frequency corresponding to the lower end of the inertial sub-range. Structures having very low natural frequencies, like flexible off-shore structures, tall slender and light structures, light bridges will be analyzed with spectral density functions having a more accurate representation of the low frequency range. [3].

3.3 The time scales and the integral length scales

The material manifestation of the spatial turbulence of the wind flow consists in vortices of various dimensions and energy which are responsible for the gusts that

hit the surface of the obstacles. Information about virtually the quantity of energy produced and dissipated through wind turbulence is given by the autocorrelation and cross correlation functions.

The mathematic expression of the autocorrelation function, $K_v^T(z, t)$ is the value of the product of the turbulence component v at the time t and the one at the time $t+\tau$, averaged on the interval of time $T-\tau$ and measured in the same place in the Cartesian coordinates space:

$$K(\tau) = \frac{1}{T-\tau}\int_0^T v(x,y,z,t)\cdot v(x,y,z,t+\tau)dt \tag{5}$$

and it is used to be expressed and plotted under its normalized form:

$$k(\tau) = \frac{K(\tau)}{\sigma_v^2} \tag{6}$$

It is evident that for $\tau=0$, $k(\tau)=1$. We normally assume that the flow is homogeneous on the horizontal direction and in this light the autocorrelation function is regarded as the characteristic time of memory of the turbulent velocity v and since it depends only on the height z and on the interval of times τ it is known as the time scale T(z), that is the scale of eddies on the time domain. For $\tau << T(z)$, measurements of v at the time t will define very well v at the time $t+\tau$ but only very little information will give if $\tau >> T(z)$ so the definition of the time scale would have the form:

$$T(z) = \int_0^\infty k_v^T(z,\tau)\cdot d\tau \tag{7}$$

The normalized autocorrelation function has a good approximate description ($\tau >0$):

$$k_v^T(z,\tau) = e^{\left(-\frac{\tau}{T(z)}\right)} \tag{8}$$

The cross correlation function gives us information about the spatial variation of the turbulence of the unidirectional flow at the time t, describing the variation of the velocity $v(t)$ in two different points and depending on the distance between these two last:

$$k(x,\Delta x) = \frac{1}{\sigma_{v,x}\cdot\sigma_{v,x+\Delta x}}\cdot\int_0^\infty v(x,y,z,t)\cdot v(x+\Delta x,y,z,t)dx \tag{9}$$

Integral length scales are measures of the sizes of vortices, defining an averaged size of gust in a specific direction and the expression of the length scale is similar to the time scale using the cross correlation function:

$$L_v^x = \int_0^\infty k_v(z, \Delta x) dx \tag{10}$$

So the longitudinal integral length scale is equal to the time scale multiplied by the mean wind velocity: $k_v(z, \Delta x) = k_v^T(z, \tau)$ for $\Delta x = V(z) \cdot \tau$ and accordingly, $L_v^x(z) = V(z) \cdot T(z)$. There are 9 integral length scales according to the spatial turbulence components *v*, *u*, *w* and the three Cartesian directions *x*, *y*, *z*.

The integral length scales are determined with accuracy with full scale measurements procedures. Nevertheless, when the conditions impose, they may be determined by modeling the wind in boundary layer tunnels, providing adequate techniques of data acquisition are used. A mathematical law of variation is rather difficult to be found because of the extensive scatter of the data. EC1 [4] uses the Counihan's empirical relationship for a range of 10-240 m:

$$L_v^x = C \cdot z^m \tag{11}$$

where *C* and *m* depend on roughness length z_0 and both *z* and L_v^x are expressed in meters, so in fact integral length scales decrease with the increase of the surface roughness.

The other length scales are expresses as a function of longitudinal integral length scale L_v^x:

$$L_v^y \approx 0.3 L_v^x; L_v^z \approx 0.2 L_v^x. \tag{12}$$

The expression proposed by Counihan is correct only for very long upstream fetch, about 50 km but most of the structures are placed in sites with several variation of terrain category. Although there isn't yet set up a procedure accurate enough for the practical design work, the integral length scale is used by EC1.

4. MEASUREMENTS IN THE BOUNDARY LAYER WIND TUNNEL

4.1. Acquisition technique

Modeling the wind impact on structures in the laboratory is still found to be a very reliable way of finding the necessary data during the designing process of the constructions, otherwise strongly recommended by all the codes for practice for

wind loading on structures. The simulation of the wind turbulent flow is the first and main step towards a credited set of data obtained from the measurements of the wind pressures on the surface of the buildings, also forces, moments and other dynamic effects on structures or on parts of structures.

The laboratory of Structural Aerodynamics is equipped with on open return circuit tunnel, SECO 2. The atmospheric boundary layer is simulated according to Counihan methods, and implies the model of vertical profile of the mean wind velocity, the velocity spectrum, the turbulence intensity scale for a specific terrain category.

The fluctuant wind pressures are measured with the help of a chain of devices [5]

Between the years 1994 - 2000 many studies were developed in SECO 2 wind tunnel aiming to provide all the experience and data neccessary fo the determination of fluctuating wind local pressures on the surface of the rigid models of different constructions[5], [6].

All the amount of aquisition represented two categories of data:

- data of the wind climate and the turbulence of the boundary layer;
- fluctuating local pressures on the surface of the constructions.

These sets of data had to be stocked and processed (correction, calibrations etc) based on the statistic laws. In this respect another set of programs was developed under MATLAB.

4.2. Power spectral densities analysis

It is demonstrated that both the correlation and the spectrum functions satisfy the Fourier integral transformation :

$$S(n) = 4\int_0^{\infty} K(\tau)\cdot \cos 2\pi n\cdot \tau \cdot d\tau \tag{13}$$

and Davenport [ ] showed that numerous spectra satisfy the following relationship:

$$K(\tau) = \int_0^{\infty} S(n)\cdot \cos 2\pi n\cdot \tau \cdot dn \tag{14}$$

Based on this assumption, the data obtained from the measurements may be used to determine the power spectral densities in the longitudinal direction of the wind flow using the computer program, for exemple the program MATLAB-TST_PSD.M which is able to trace the normalized spectrum of the wind local pressure on the surface of the model [5].

4.3. Turbulence intensity analysis

The turbulence intensity scale is determined by measurements of the spatial components of the wind turbulence directly introduced in the relationship (5) for different specific heights above the ground. During several stages of the research studies the turbulence intensity was determined and compared with some known relationships

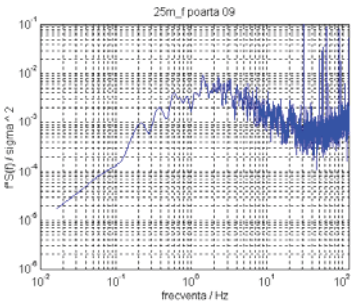

Fig.3. Spectral power of a local pressure signal described under the MATLAB program [5]

In fig.4 there are plotted the values obtained via measurements in the tunnel in comparison with:

- polynomial approximating function (program under MATLAB);

- Deaves and Harris relationship [5];

- two correction functions under the same program.

4.4. Cross correlation of the longitudinal and transversal turbulence

In the process of modelling the parameters of the wind profile is is very important to determine the integral length scales which will further on give information about the dimensions of the vortices with respect to the dimensions of the building imersed in that particular boundary layer. It was already discussed the influence of the dimensions of these vortices upon the dynamic behavior of the building under wind gusts (figure 5).

The spatial cross correlation is usually determined longitudinally and transversally in the cross section of the tunnel where the model of the building will be placed. Pressure measurements are conducted simultaneously in two different point, the first being fixed and the other moving every 5 cm longitudinall and transversally, covering a square surface of 55 cm length to 35 cm width, in the middle of the cross section of the tunnel. The plotted results are for z = 15 cm above the floor of the tunnel. The slight non symmetry of the transversal cross correlation with respect to the central axis show the influence of the access door but it is not relevant for the testing area, considering the dimensions of the model of the building [6].

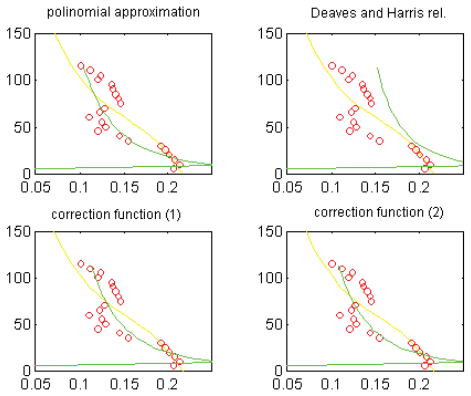

Fig. 4 Graphical representation of the theoretical functions of aproximation of the turbulence intensity (red- values obtained from measurments; yellow- graphical aproximation of the line; green- functions decribed mathematically by the program [5]

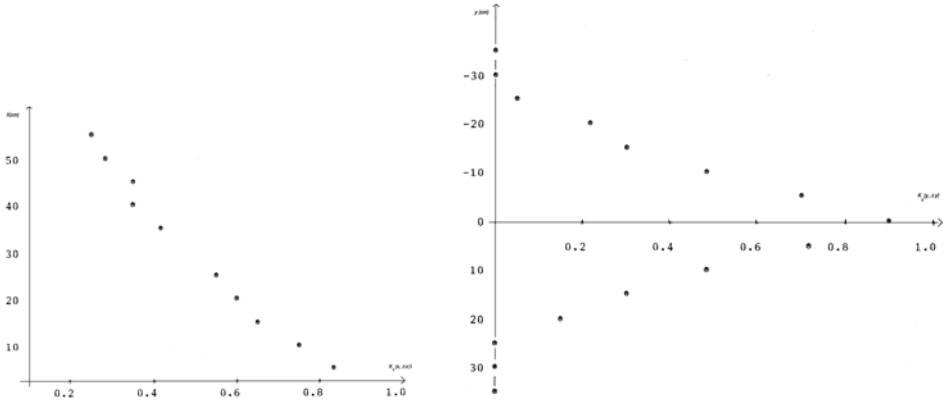

a b

Fig. 5 a, b. Correlations obtained in the boundary layer wind tunnel SECO 2 during the process of modelling the wind turbulent flow (z=15 cm): a)- longitudinal correlations; b)- transversal correlations [6]

5. CONCLUSIONS

Modelling of the wind structure in boundary layer wind tunnel is not a very easy task, the laws of similarity must be respected and the parameters of the flow must be compared and calibrated in order to obtain realistic values of pressure coefficients. The wind flow characteristics: wind profile, power spectral density, turbulence intensity and the length scales are the basic elements of modelling the

wind flow around the building. Together with the aerodynamic and mechanical characteristics of the building itself they model the structural response to wind action. In order to accomplish a succesful analysis of the wind dynamic pressures on the building, the model of the turbulent flow must be as accurate as possible.

The results obtained from the numerous tests in the tunnel SECO 2 in the last decade represent a huge experience of the researchers implied in the field of aerodynamic of structures.

The modern design codes to wind loading on structures and in particular EC1 which will be adopted by Romanian specialists, are increasing in accuracy but they are not easy to be applied by the structural engineer. They are more complicate, they need far more information about the wind in a certain environment and they often reccomend the study of the models in the boundary layer wind tunnel.

The meteorology is a science that evoluates very rapidly nowadays and new models are proposed for the study of the global wind changing nature. Structural engineer must cope with all these aspects in order to insure the security of both the occupants of the building and of the structure itself during the designing process.

References

1. Smith, B., Wyatt, T., *Structures, Dynamics and Wind –a 10th review*, 8th Biennial Scruton Lecture 2003, Wind Engineering Society, London, U.K.
2. Cook, N. J., *The designer's guide to wind loading of building structures*, Part 1 &2, BRE , Butterworths, 1985, ISBN 0408008709
3. Dyrbye, C., Hansen, S. O., *Wind Loads on Structures*, John Wiley&Sons Copyright, 1997, ISBN ISBN 0471956511
4. Eurocode 1- Actions on structures; Part 1-4. General actions-wind actions
5. Teleman, E.-C., *Contributions to the concept and design of the multistorey steel structures*, Ph.D. thesis, Iasi 2000
6. Axinte, E. &al.- *Studiul conditiilor de experimentare si a metodelor de masura in tunel cu strat limita rpivind actiunea dinamica a vantului asupra constructiilor si actualizarea tuneluilui SECO 2*, Contract nr. 37/1998, Grant 452/1998, tema 49 (in Romanian)

"Computational Civil Engineering 2006", International Symposium
Iaşi, România, May 26, 2006

The importance of databases for the efficient exploitation of bridges within an administrative unit

Constantin Ionescu, Raluca Popa

Department of Structural Mechanics, "Gh. Asachi" Technical University of Iaşi, România

Summary

This paper presents a way to organize information obtained through a process of collecting, storing and transforming data concerning the network of roads and bridges of an administrative unit.

The type of information discussed herein pertains to the number and length of communal, county and national roads, and to the bridges along these roads (with details concerning the structural types, lengths, openings, crossed streams, etc.). The resulting information is structured in five tables.

The study will be followed-up and extended, and its results will be used to manage the existing network and to develop the transportation infrastructure, with respect to bridges, in the administrative unit of interest.

The essential aspects that must be carefully considered by any researcher are: the variety of the data bases, the accuracy and reliability of stored data, the methods of transforming data into information, and the access to or usage of data bases.

KEYWORDS: Bridge, road, database, stream, flooding.

1. INTRODUCTION

The transportation infrastructure represents a valuable national asset that must be adequately exploited and passed on to the next generations in a satisfactory state.

The decision makers' responsibility is heightened by the fact that the good functioning of the entire economy in a given administrative unit depends upon its transportation infrastructure, in which art works are included.

Proper maintenance of bridges in an administrative unit is conditioned by the actions of the network administrator with respect to art work consolidation and maintenance [4]. In order to make these actions efficient, the technical state of the bridges must be systematically and regularly assessed, both globally and subsystem-wise. Meeting this goal requires the development and implementation of inventory, audit and evaluation programs. The purpose of such software is to

establish the present and future capacity of the infrastructure to handle the needs and purposes it was designed for [1].

Existing data enables the development of strategies, programs, projects and solutions. However, substantial financial resources are required to accomplish this. The necessary administrative budget is the sum of all projects' values. Obviously, as common practice around the world reveals, funds are always scarce and many projects compete simultaneously.

The decision is difficult. The projects with the greatest benefits must always be selected. By 'benefits' we mean not only the financial value, but also time, cost, fuel consumption, spare parts and so on.

Bridge maintenance and consolidation programs cannot be developed unless the network administrator has the appropriate data base software for monitoring the technical state and the evolution of all the bridges in the network. Creating and efficiently exploiting databases requires systematic thinking and an algorithmic approach. The usage of computers as working norm is imposed by the growing complexity of algorithms and the growing size of databases. Therefore, computerizing the whole sphere of knowledge and decision-making is imminent [3].

The present paper is a germane effort toward organizing data and information pertaining to an administrative unit's network of roads and bridges through databases.

2. NOTES ON DATA BASES. EXAMPLES

It is known that a data base represents an integrate assembly of data, structured and heeled with a description of the structure.

A data base system is necessary in order to scientifically exploit road networks like the one presented in Table 1. This system must contain structured data identifying bridges, topographic data, geographic data, data on the technical state of the bridges, library data, etc.

The library database will contain information about useful standards and normatives, compendiums and monographs about designing, exploiting, maintaining, auditing and evaluating the costs and technical performance of bridges.

The bridge identification data includes the name of the bridge, its position on the road, the closest city, the construction year, the dimension and elements of the bridge, and so on.

Tab.1. Information concerning the road networks

	DC	DJ	DN
Total number of roads	124	44	8
Total length of the roads in the administrative - territorial unit [km]	644.415	758.580	407.228
Minimal length of a road [km]	0.510	1.650	1.913
Maximal length of a road [km	22.026	68.163	121.369
Medium length of a road[km]	5.197	17.240	80.904

Tables 2, 3 and 4 present information (adapted data) on the bridges of the road network (communal, county-level and national) of an administrative unit. Figure 1 presents the technical state of one of the bridges over Moldova River after a pile was eroded.

Tab.2. Information concerning bridges on the common road network

Total number of bridges	131
Total length of bridges [m]	2699.20
Medium length of bridges [m]	21.83
Obstacle crossed: ▪ river [number] ▪ creek [number] ▪ another obstacle (stream, valley), [no.]	▪ 6: o Bistrita river, crossed three times, o Bârlad river crossed 4 times; ▪ 44: o creek Cuejdiu crossed 7 times, o Grințieș and Dalia creek crossed 6 times ▪ 7
Biggest length of a bridge[m]	204, over Ozana river, in Dumbrava
Biggest opening of a bridge [m] ▪ Cantilever beam	125; over Moldova river in Boteşti

The bridge engineer needs information on the bridge area, emplacement and interaction surfaces. [3] Such information refers to the evolution of geological processes and to the mechanical and physical properties of the rocks. Information is used to determine the founding conditions and to ensure the bridge stability. Also it is necessary to obtain information on the water stream crossed: the design discharges and corresponding levels, the bed's roughness, the elements of the bed's morphology, and so on. Table 5 contains flooding information from the administrative unit studied.

As to geotechnical information, the engineer must know the cross section of the river bed in the bridge area, and the details of the ground layers (terrain type, geotechnical and physical properties). In this respect, special attention must be paid to the set-up of water courses crossed by bridges.

Tab. 3. Information on the bridges in the county roads network

Total number of bridges	167
Total length of bridges [m]	3936.095
Medium length of bridges [m]	23.57
Obstacle crossed: ▪ river [number] ▪ creek [number] ▪ another obstacle (stream, valley), [no.]	▪ 7: o Siret river crossed 5 times, o Bârlad river crossed 4 times; ▪ 80: o Dămuc river crossed 7 times o Sabasa, Balaz and Hangu creeks crossed 6 times each ▪ 9
Biggest length of a bridge[m]	▪ 314, over Siret river, in Ion Creangă ▪ 306, over Moldova river, in Tupilați
Biggest opening of a bridge [m] ▪ Boxed continuous girder	87; over Siret river in Sagna, L_{tot}=215 m (58+87+58)

The database concerning the technical state is important for the bridge exploitation process (maintenance, repairs and consolidations). This type of information is related to the bending state, the cracking state and the impairment (degradation) state (see Fig. 1). Information is obtained from the study of various phenomena such as: corrosion, interaction with the environment, erosion, and so on. These phenomena are studied by qualified persons who periodically assess the technical

state of the bridge by means of quality indexes, surveillance, extended inspections, audits and other means.

Fig.1. Technical state of one of the bridges over Moldova river after infrastructure's erosion

Tab. 4. Statistics on the bridges from the national roads network

Total number of bridges	122
Total length of bridges [m]	6758.08
Medium length of bridges [m]	55.39
Obstacle crossed: ▪ river [number] ▪ creek [number] ▪ another obstacle (stream, valley), [no.]	 4 44 49
Biggest length of a bridge[m]	669, over Poiana Teiului Lake
Biggest opening of a bridge in structural types ▪ braced arch [m] ▪ built-in arch [m] ▪ built-in vault [m] ▪ two-hinged vault [m] ▪ slab on two supports [m] ▪ girder on two supports [m] ▪ continuous girder [m] ▪ Gerber girder [m]	 72.4; r. Bistrița,in Bicaz 31.6; Valley, in Bicaz 29; Lake, Poiana Teiului 14.7; Vale, in Bicaz 12,1; Neagra creek, in Neagra 32.5; Valea Bubei, in Chirițeni 42.5; r. Bistrița, in Lunca 27.5; r. Siret, in Gîdinți
Exploitation duration: ▪ biggest [years, construction year] ▪ smallest [years, construction year]	 58, 1948 17, 1989
Medium duration of exploitation of the bridges [years]	41

Tab. 5. Flooding in the studied area

Years in which flooding took place	▪ 1970, 1971, 1975, 1977, 1978, 1979 ▪ 1985 ▪ 1991, 1992, 1997, 1998, 1999 ▪ 2000,2001, 2002, 2003, 2004, 2005
Cause of the flooding	▪ Effusions ▪ Bank erosion ▪ Slops ▪ Discharges from slopes
Examples of water streams that caused flooding	▪ Topolița creek: 1975, 1985; Petricani area ▪ R. Bicaz: 1995, 2002; Bicaz Chei village area ▪ R. Bistrița: 2002, 2003, 2004; Fărcaşa villages area ▪ Zahorna creek: 1972, 2005; Girov and Verşeşti areas

CONCLUSIONS

1. As outlined above, the bridge's management system must have essential data and information on which to rely, in order to arrive at the right, optimal and most efficient decision. The data bases are vital instruments for the bridge management system.
2. Transportation infrastructure development in an administrative unit demands perfect knowledge of the network's state, spanning over a variety of aspects: the evolution of structural types of bridges under exploitation, the erosion caused by water streams, flooding, relief, and so on.

References

1. Scînteie, R., Baze de date şi algoritmi pentru căi de comunicație, Editura Societății Academice „Matei-Teiu Botez", Iaşi, 2003 (in Romanian)
2. Ionescu, C., O propunere - zona podului public, Revista: „Drumuri şi Poduri", nr. 28 (97), oct. 2005 (in Romanian)
3. Ionescu, C., Scînteie, R., Informational Flows in Bridges Engineering; Proceedings of the International Conference, Constructions 2003, Volume 4 – Road, Bridges and Railways, Editura Argonaute &Napoca Star, Cluj-Napoca, 2003 (in Romanian)
4. Ionescu, C., Scînteie, R., Evaluarea stărilor tehnice ale podurilor prin metode matematico-euristice, Probleme actuale ale urbanismului şi amenajării teritoriului, Conferință tehnico-ştiințifică internațională, Chişinău, 2004 (in Romanian)

"Computational Civil Engineering 2006", International Symposium
Iaşi, România, May 26, 2006

Information and dissemination in Bridge Engineering

Constantin Ionescu, Alina Nicuță

Department of Structural Mechanics, "Gh. Asachi" Technical University of Iași, România

Summary

The paper brings into consideration the methodology of the technical-scientific creation act in the Bridge Engineering Area. The creation process has three main steps: information, technical-scientific creation and results dissemination.

Any author (researcher, postgraduate etc.) can access multiple information channels such as treaties, monographs, journals and most recently the INTERNET. There is also the possibility to establish connections, by electronic mail with any researcher in the world.

A great importance has the results dissemination. This process has a double role: to spread the research results and to establish the research quality.

KEYWORDS: Bridge Engineering, information, creation, dissemination.

1. INTRODUCTION

Nowadays in the same time with the information flow (data, information, knowledge), the society knew another development of the strategies and methods of knowledge dissemination in the scientific and technical areas.

Any scientific of technical process means a chain of three systems: the information system, the creation system and the dissemination system, fig.1.

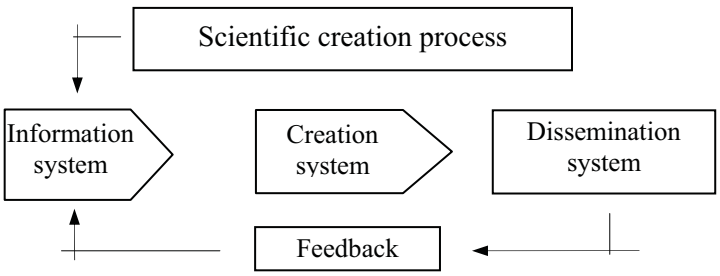

Fig. 1. Creation process

2. THE INFORMATION SYSTEM

In order to analyze the information system is necessary to evaluate the resources of this process. Beside the financial and human materials we must consider another resource, the knowledge (information or data).

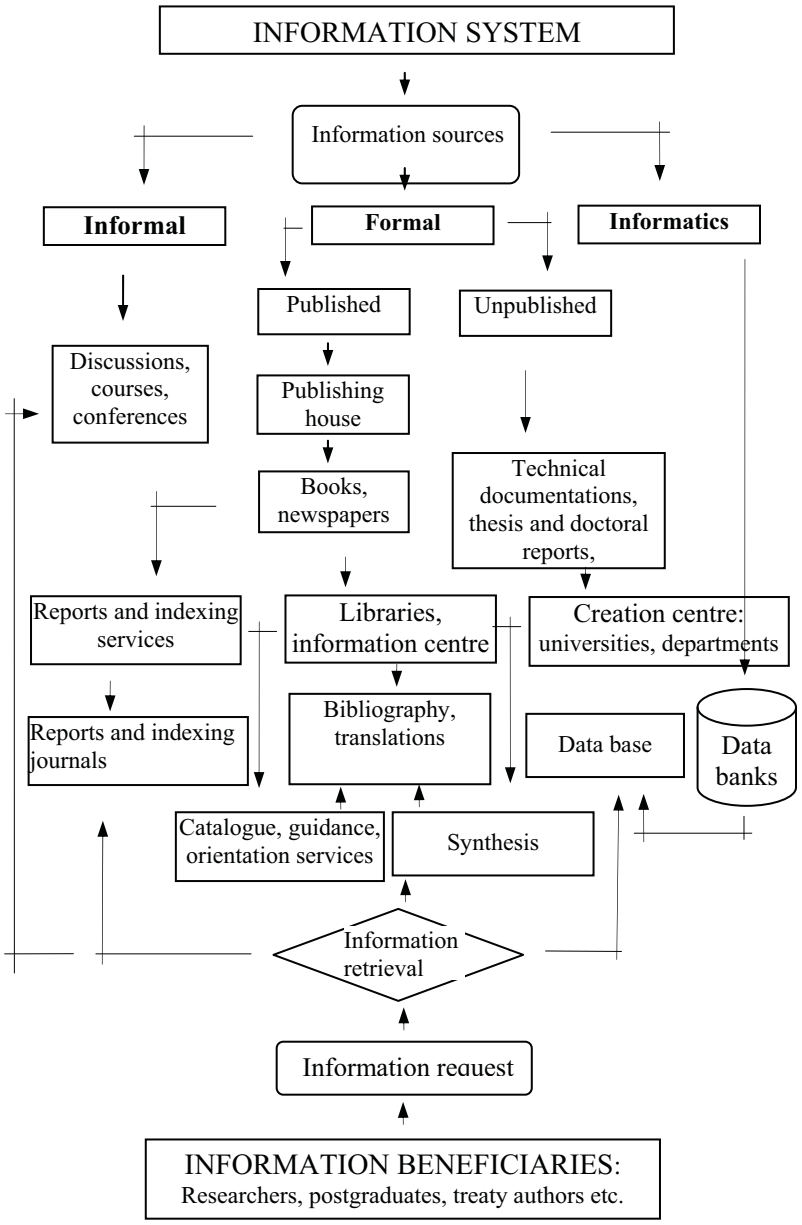

Fig. 2. Information channels system

In the information flow society the information must be considered the most important resource. The information are the „product" of the information systems which are based on the automatically adaptation of the data with the help of the electronic computers.[1].

The information sources are: informal, formal and informatics, fig.2. Trey have a classic nature (paper printed), or modern nature (informatics) and are obtained in Academic or technical areas.

The informal sources contain scientific discussions, academic discourses and conferences. The formal sources are books, treaties, monographs, newspapers, published information and unpublished sources such as technical discussions, papers or postgraduate thesis.

The informatics sources form the data bases and can be directly accessed from a simple computer, through INTRANET, in a firm or by INTERNET, globally.

The information creation system, fig.3., refers to two different activities: the information acquisition from different sources and the information dissemination by different information channels.

The documents after an analytical and/or synthetically adaptation are transformed in information and given to the beneficiaries free access.

The beneficiaries can receive a straight answer to the information request by accessing the documentation fund or the information memory (research engines).

The information act quality depends on the quality of the three classical resources: material, financial and human, but also a new resource, specific to the information era, the knowledge.

3. THE DISSEMINATION SYSTEM

The dissemination is a post creation process. Any information beneficiary (researcher, postgraduate, treaty, monograph's author, etc.) must become also a knowledge producer. His work is recognized only by dissemination in academic area, by publications, fig. 4 and 5 or in the technical area by projects.

The information quality is connected with the newspaper importance where there have been disseminated, newspapers category, fig.6. or the publishing house, where a treaty or book was published.

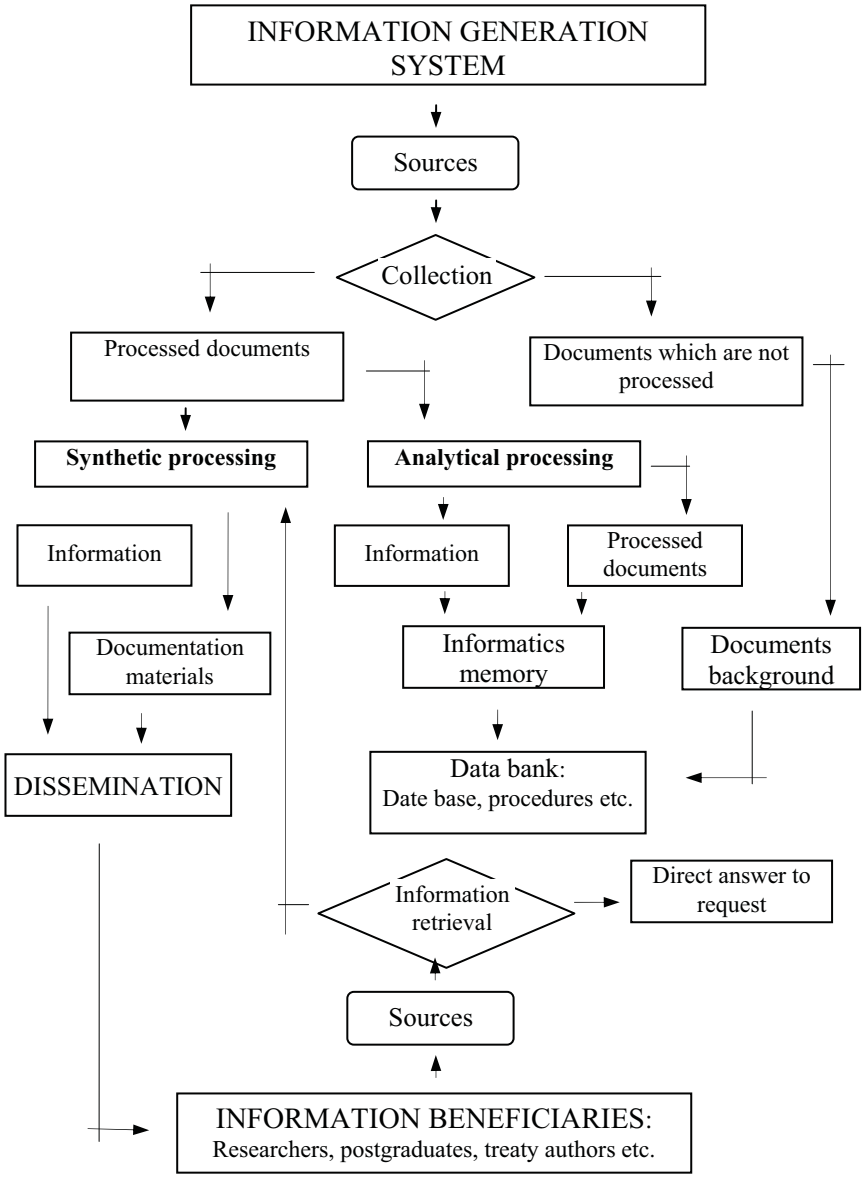

Fig. 3. Information and documentation system

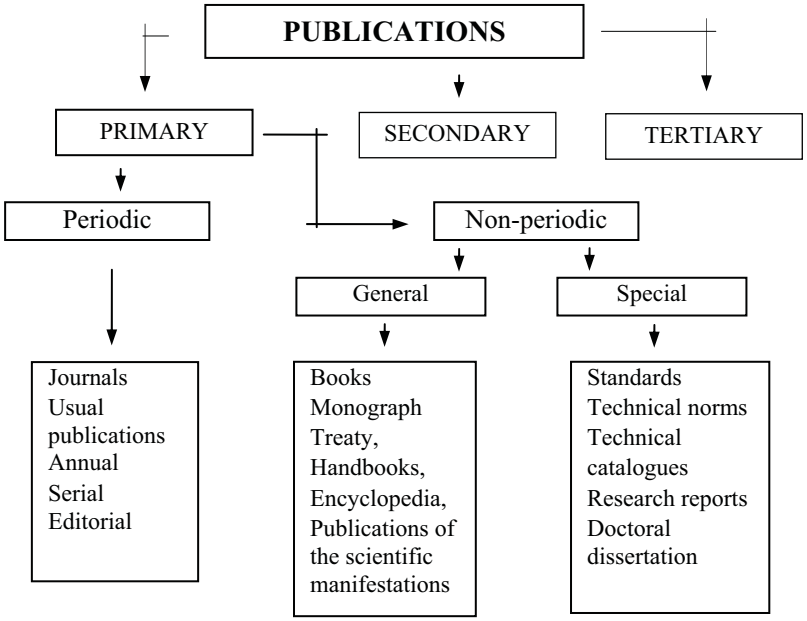

Fig.4. Primary publications

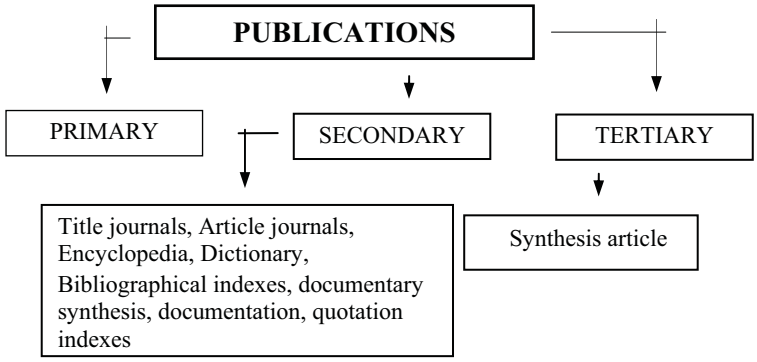

Fig.5. Secondary and tertiary publications

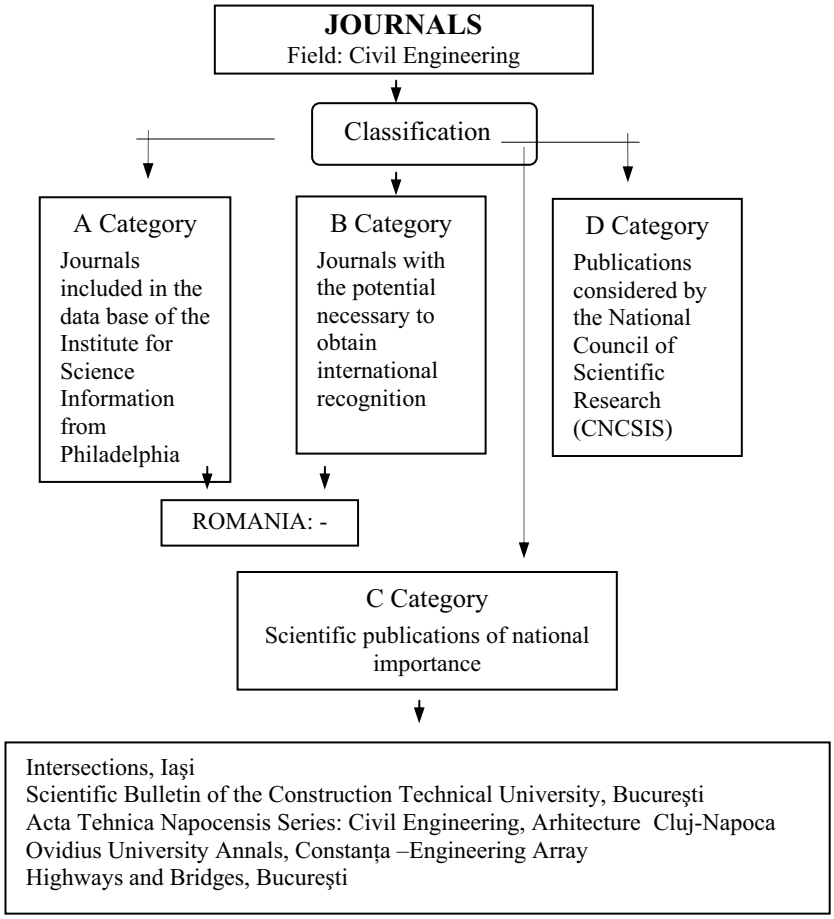

Fig. 6. The Romanian journals classification according to CNCSIS

References

1. Vasilescu, Petre, *Discrepanța generațiilor în informatică*, Editura Ştiințifică şi Enciclopedică, Bucureşti, 1985 (in Romanian)
2. Păunescu, E., Badea-Dincă, N., Stăicuț, E., *Informatizarea societății – un fenomen inevitabil?*, Editura Ştiințifică şi Enciclopedică, Bucureşti, 1985 (in Romanian)
3. Gherghel, N., *Cum să scriem un articol ştiințific*, Editura Ştiințifică, Bucureşti, 1996 (in Romanian)
4. Holban Horia, *Tehnica cercetării ştiințifice*, Editura Graphix, Iaşi, 1994 (in Romanian)
5. Ionescu, C., Unele considerații privind informatizarea proiectării podurilor, *Zilelele Academice Timişene (Infrastructuri eficiente pentru transporturi)*, Editura Mirton, Timişoara, 1999. (in Romanian)

"Computational Civil Engineering 2006", International Symposium
Iaşi, România, May 26, 2006

Steps to Structural Robotics implementation

Fideliu Păuleț-Crăiniceanu

Department of Structural Mechanics, "Gh. Asachi" Technical University, Iaşi, 700050, România

Summary

Recent advances in computational tools (hardware and software) raise the hope that more improvements in Civil Engineering could take place, too. These advances refer (among many other) to very high speed processors (e.g. 500 GHz) very large storage capacities (of terabytes orders), sophisticated and safer computer wireless networks, new structural software etc. If one is adding the new materials, new technologies, new sensors, new design tools and philosophy, the only logical result is that the Civil Engineering must be also at the edge of profound changes.

The paper is continuing previous researches into a quite newly proposed domain, Structural Robotics. This domain of Structural Mechanics is aiming to autonomous structures, adaptable to changes in loads, functions, materials, structural theories and practice etc. In Structural Robotics, Structural Control is just a component.

Because the nature is using structures with active hinges, a proposal for introducing active hinges into Civil Engineering structures has been made. In this study, the active hinges are now implemented in some simple, planar structures in order to verify the needs for devices, energy, power and computation.

Though researches are at the beginning, promising analytical results have been obtained.

KEYWORDS: structural robotics, active control, seismic protection.

1. INTRODUCTION

The hardware and software of computers are daily suffering improvements that raise the hope that more improvements in Civil Engineering could take place, too.

New advances in computational tools refer (among many other) to: very high speed processors (e.g. 500 GHz processors are already in the laboratories of important producers and 1000GHz processors are in the views); very large and fast storage capacities (of terabytes orders); sophisticated and safer computer wireless networks; new structural software etc.

Also, appearance of other facts should be noticed: new materials (e.g. composite materials, memory shape materials, fluids with controllable viscosity, plastic materials etc), new technologies (especially computer based ones, strong and fast actuators with multiple high control circuits), new sensors (with better accuracy, fast enough to avoid time delays, wireless connected), new design tools (e.g. software integrating all stages in constructions' realization) and new philosophies (as Structural Active Control, Intelligent Building etc).

Even if conservative people would like to avoid this, the only logical consequence of the above statements is that the Civil Engineering must be also at the edge of profound changes. Of course the rhythm of changes in Civil Engineering is slower than that in Computer Science.

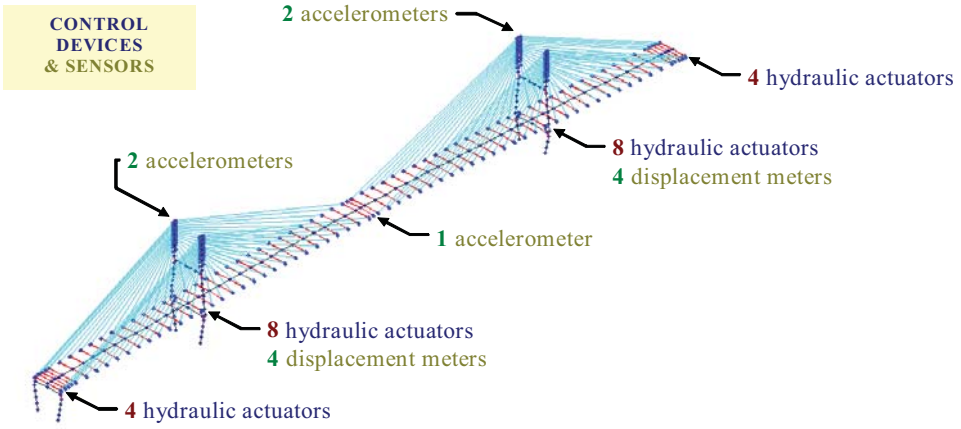

Figure 1. Example of Structural Active Control use [8]

In order to cope with and to integrate the changes imposed by today's scientific and technical society, a new sub-domain of Structural Mechanics was proposed: Structural Robotics [1]. This domain is aiming to obtain autonomous structures, adaptable to changes in loads, functions, materials, technologies, structural theories and practice etc. Robotic structures should to be robotized (i.e. to contain robots) and have robotic behavior: they must have only little human interventions though major decisions (as partial/total demolition and/or reconstruction, changes in some elements, automatic redesign, adapting to new norms and to new field data etc) might be taken.

As predicted by author, [2], though many different especially technical obstacles should be removed, the only important factor remaining to be solved remains the large, independent energy and power needed to operate such structures. Of course, the energy crises will be more and more frequent in the near future and, surely, new ways to solve them will be obtained.

In Structural Robotics, Structural Control is just a component. Author's quite important experience into this field, e.g. [2-11], together with observed literature, e.g. [12-23], were the bases for trying new optics in Structural Mechanics for Civil Engineering (i.e. the introduction of the Structural Robotics concept).

Structural Active Control is a relatively new sub-domain in Structural Engineering. Though the field have been introduced from 1972, [24], practical applications are still far from being implemented other then experimentally.

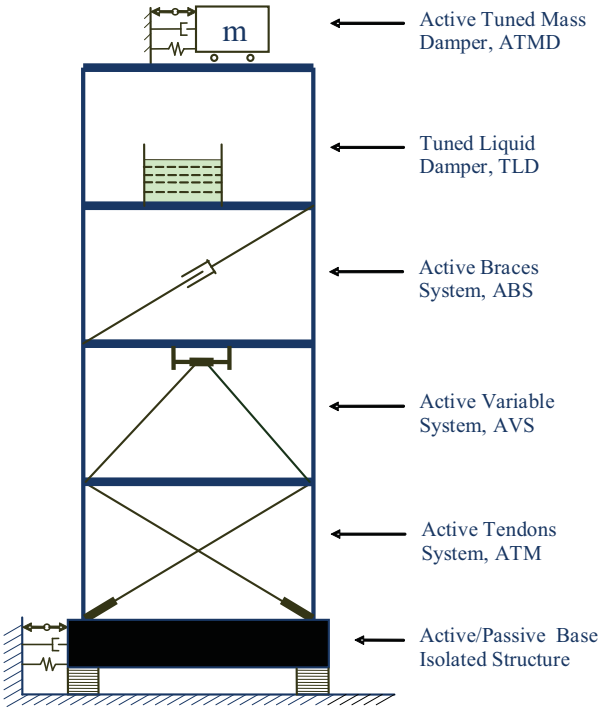

Figure 2. Use of some structural control systems [27]

Even from the early researches it was found that passive control is cheaper and easier to apply [25,26] but the efficiency is hard to prove and limited [27]. Figure 2 is presenting a concept for using some control means.

In contrast, active control implies large costs and difficulties in application because of laborious design, experimental work, special means and devices, inter-disciplinary task teams, monitoring etc. However, in principle, active control can assure the maximum protection of structure with the means and energy the beneficiaries want to spend. Figure 1 shows a case for using structural active control for a long cable-stayed bridge [8].

Of course, combinations of active and passive control should always be in the views or researchers [28].

Anyone could observe that the nature is using structures with active hinges. Therefore, a proposal for introducing active hinges into Civil Engineering structures has been made [29].

In this paper the aim is to have active hinges implemented in some simple, planar structures in order to verify the needs for devices, energy, power and computation, [30].

2. ACTIVE CONTROL APPROACH

For structural active control strategy, the classical optimal control [13,17] with proposed energy based parameters calculations [5] is used.

Supposing that the control actions are a function of the states, i.e. $\mathbf{u}(t) = -\mathbf{K}(t)\mathbf{x}(t)$ then the goal is to obtain the feedback gain matrix $\mathbf{K}(t)$ to minimize a performance index J defined by

$$J = \frac{1}{2}\int_0^{t_f} \left[\mathbf{x}'(t)\mathbf{Q}\mathbf{x}(t) + \mathbf{u}'(t)\mathbf{R}\mathbf{u}(t)\right]dt \tag{1}$$

where $\mathbf{Q}$ and $\mathbf{R}$ = weighting matrices. The prime sign in Equation (1) means a transpose. $\mathbf{Q}$ and $\mathbf{R}$ show the relative importance of minimizing the states (structural response) or the actuating forces. The first is $2n \times 2n$ -dimensional and the second is $m \times m$ -dimensional, where m is the number of the actuators.

The first term in the brackets of Equation (1) can be written as energy expression, and thus leading to minimization of the energy of the structural response. This is obtained if the weighting matrix $\mathbf{Q}$ is composed from the structural mass matrix $\mathbf{M}_1$ and stiffness matrix $\mathbf{K}_1$, in the form

$$\mathbf{Q} = \begin{bmatrix} \mathbf{K}_1 & 0 \\ 0 & \mathbf{M}_1 \end{bmatrix} \tag{2}$$

The weighting matrix $\mathbf{R}$ can be taken as a diagonal matrix with terms showing the relative importance between the active devices (or their strategic positions in the structure, their performances, etc.), i.e.

$$\mathbf{R} = \mathrm{diag}\{r_1 \ldots r_m\} \tag{3}$$

where $r_1 \ldots r_m$ are the corresponding relative importance factors for actuators. If all of these factors are equal, then the matrix $\mathbf{R}$ becomes easier to generate, $\mathbf{R} = r\mathbf{I}$, with $\mathbf{I}$ being the identity matrix.

For implementing this strategy, the FEM problem was solved by the help of a free FEM computer program adapted for structural active control, [3]. Verifications, comparisons of results, pre or post-processing of data were made using programming environments and their components [31,32]. Other improvements of the method (as taking into account the time delay, reduced order observer and reduced order approach of the entire structure) have been analyzed and implemented in strategies, too, [7-10].

3. STRUCTURAL ACTIVE HINGES

As shown in chapter 1 of this study, the examples from natural environment are showing that the living beings usually have active hinges (as knees and elbows). These hinges allow very good adaptation to various kinds of loads.

Based on above observation, a proposal of structural active hinges has been made [29]. Figure 3 is showing the proposed Structural Active Hinges (SAH) development. At the left an implementation using linear actuators, with active forces, $F_a(t)$, is proposed. At the right of the same figure, the version using active moments, $M_a(t)$, and corresponding rotational actuators, is presented.

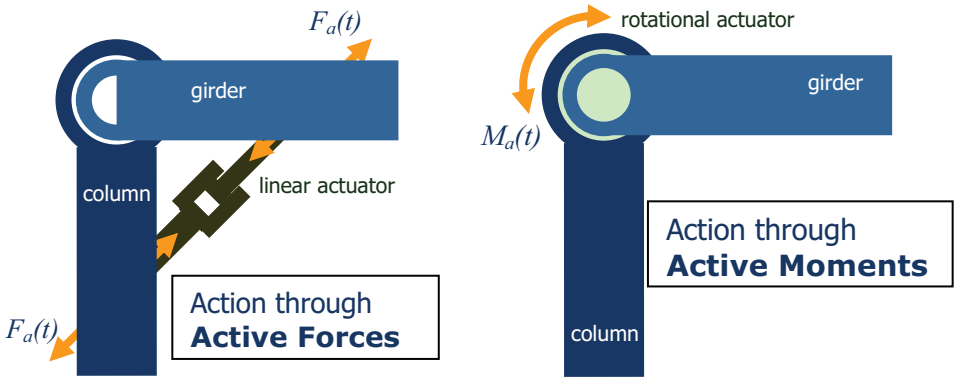

Fig.3 Structural Active Hinges development, SAH [29]

For practical application of such general structural active devices, actuators market is showing multiple and consistent solutions. Manufacturers are providing reliable, fast enough, highly accurate, and somehow affordable linear and rotational actuators, see for example [33].

However, a drawback of the whole problem is that the manufacturers are not numerically showing the internal dynamics of their actuators, creating the task to model the controlled system a quite hard work.

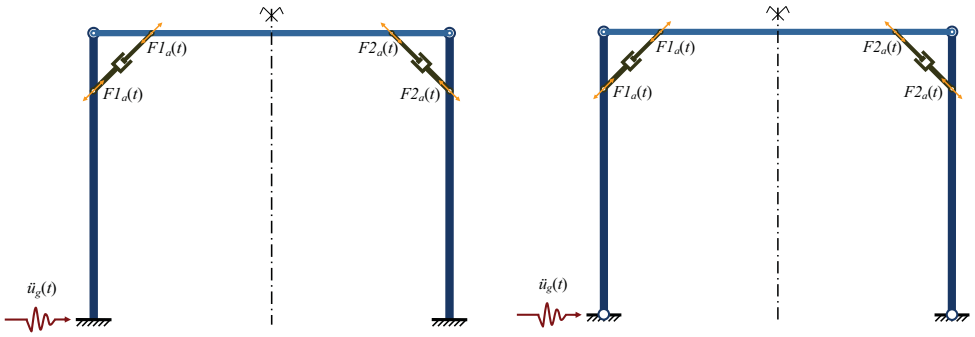

Figure 4. Simple, one span and one level, structures with active control

Therefore, the models taking into account are supposing perfect response of actuators which can be seen as a first stage into simulation of practical, very realistic, implementations.

4. STRUCTURAL ACTIVE HINGES IMPLEMENTATION

Though a complex analysis of implementation for the proposed style of devices should be done, only first stages of such task have been realized. In Figure 4 simple, one span and one level, structures with active control are presented. Linear actuators are implemented.

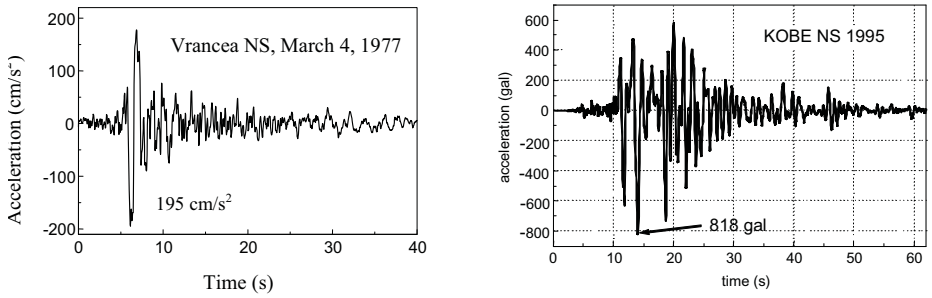

Figure 5. Example of external actions (time-history seismic accelerations)

Figure 5 is showing two examples of time-history seismic accelerations used in numerical simulations: the Romanian earthquake located in Vrancea seismic area, from March 4, 1977, NS acceleration component with 195 cm/s^2 peak; and the

Japanese major earthquake from Kobe, January 17, 1995, NS acceleration component with 818 cm/s^2 peak.

The aim is to use structures designed in such a manner that they are reliable from the point of view of comfort and safety even during strong earthquakes. This type of structures should present only minor damages that would not stop or interrupt the activities inside the buildings after the earthquakes. Of course life and safety of people inside must be totally protected.

Results from first analyses show effectiveness of the methodology and devices. Structural response can be reduced to 70-30% from the non-active state (and that could be considered a passive state). This structural response is monitored in different terms as: accelerations, velocities, displacements, rotations, bending moments, shear forces, stresses etc.

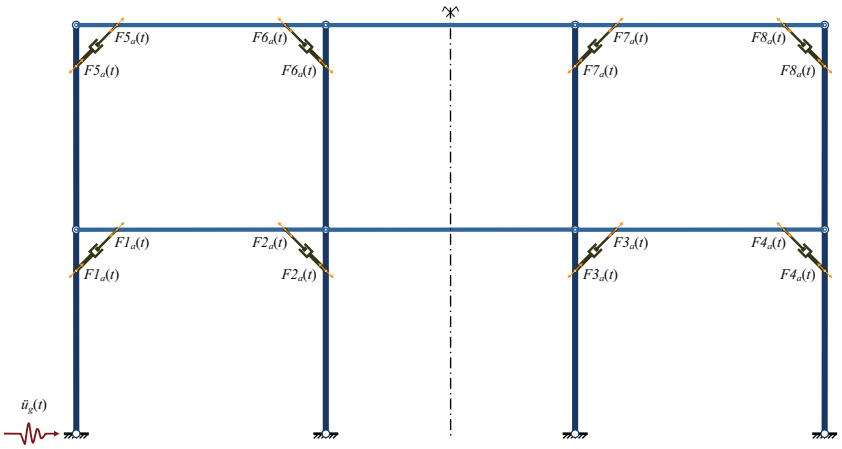

Figure 6. Hinged frame (mechanism), regulated by structural control systems

Figure 6 shows a hinged frame (a mechanism), regulated by structural control systems. As in the case of structures shown in Figure 4, the structure can be seen as passive controlled if now actuator is active and actively controlled when actuators are used. This building is still under analytical investigations.

For future works, additional to structures like that in Figure 6, rotational actuators are in the views. Also, three-dimensional numerical studies should be performed.

5. CONCLUSIONS

The general goal of the author is to show that a new concept, Structural Robotics, can be implemented in Civil Engineering. Components of this new concept are studied, for the time being, as separated and necessary steps.

Some progresses were done when Structural Active Control has been intensively and extensively studied. The newly introduced Structural Active Hinges are detailed and shown to be practically realizable.

Analytical models and numerical applications to simple structures are presented and good results are obtained. Future directions are also seen.

Acknowledgements

The author is in debt to Romanian National University Research Council (CNCSIS) that supported in part, through the Grant code no. 540/27637/2005, some researches presented in this paper.

References

1. Paulet-Crainiceanu, F., Structural Robotics, *Information Processing for Damaged Assessment,* Proceedings of the First Romanian American Workshop în Structural Engineering, June 25-30, 1999, Iasi, Romania, Iasi, pages 43-52, "Al. I. Cuza" University Press, 1999
2. Miyata T., Yamada H., Păuleț-Crăiniceanu, F., Active Structural Control For Cable Bridges Under Earthquake Loads, *MOVIC, Proceedings of The Third International Conference on Motion and Vibration Control, Chiba, Japan, September 1-6, 1996*, K. Nonami, T. Mizuno (eds.), Vol. 2, pp. 53-58, 1996
3. Paulet-Crainiceanu, F., *Active Control Approach for Long Span Bridge Responses to Strong Earthquakes*. Doctoral Thesis. Yokohama National University, Yokohama, Japan, 1997
4. Păuleț-Crăiniceanu, F., Atanasiu, G.M., Optimal active control for large three-dimensional FEM models, *Eleventh European Conference on Earthquake Engineering, CNIT, Paris la Défense, France, September 6-11, 1998* (Compact Disk)
5. F. Paulet-Crainiceanu. Seismic response control of long cable-stayed bridges. *Proceedings of the Second World Conference on Structural Control,* June 28 - July 1, 1998, Kyoto, Japan. Vol. 2, pages 959-964, Chichester, John Willey & Sons, 1999
6. F. Paulet-Crainiceanu. Structural active control for buildings and bridges în seismic areas. în J.H. Zang, X.N. Zang, editors, ICAPV2000, *Proceedings of the International Conference on Advanced Problems în Vibration Theory and Applications*, June 19-22, 2000, Xi'an, China, pages 147-151, Beijing, Science Press, 2000
7. Păuleț-Crăiniceanu, F., Rodellar J., Monroy C., Control Settings and Performance Analysis of an Optimal Active Control Method for Cable Bridges, *ECCM-2001, The 2nd European Conference on Computational Mechanics, June 26-29, 2001, Cracow, Poland* (CD-ROM, Datacomp)
8. Bakule, L., Păuleț-Crăiniceanu, F., Rodellar, J., Decentralized Control Design for Cable-Stayed Bridge Benchmark, *Proceedings of the 2002 American Control Conference*, Vol. 4, IEEE, Piscataway, pp. 3046-3051, 2002
9. Bakule, L., Păuleț-Crăiniceanu, F., Rodellar, J.: Reliable Control Design for Cable-Stayed Bridge Benchmark, *Proceedings of the American Control Conference Denver, Colorado, June 4-6, 2003*, IEEE 2003, CD-ROM, pag. 5040-5045
10. Păuleț-Crăiniceanu, F., Rodellar, J. Optimal seismic response control of a long span cable-stayed bridge for a benchmark problem, *Intersections/Intersections* International Journal, Vol I, 2004, No.7, *Bridges World*, pp. 27-35, www.ce.tuiasi.ro/intersections
11. L. Bakule, F. Paulet-Crainiceanu, J. Rodellar, J.M. Rossell: Overlapping Reliable Control for a Cable-Stayed Bridge Benchmark, *IEEE Transactions on Control Systems Technology*, vol.13, No.4, July 2005, pp.663-669

12. Negoiță, Al. (coord.), *Inginerie Seismică*, (*Earthquake Engineering*), Editura Didactică şi Pedagogică, Bucureşti, 1985 (in Romanian)
13. Soong, T.T., *Active Structural Control: Theory and Practice*. Longman Scientific & Technical, New York (1990)
14. Meirovitch, L., *Dynamics and Control of Structures*, John Wiley & Sons, New York, 1990
15. Housner, G.W., Soong, T.T., Masri, S.F., Second Generation of Active Structural Control in Civil Engineering, *Proceedings of the First World Conference on Structural Control*, Los Angeles, California, USA. Vol. 1: Panel 3-18, 1994
16. Constantinou, M.C., Seismic Isolation Systems: Introduction and Overview, în Passive and Active Structural Vibration Control în Civil Engineering, *CISM Courses and Lectures No.345*, Springer Verlag, Wien, New York, 1994, 81-96
17. Yang, J.N., Li, Z., Vongchavalitkul, V., Generalization of Optimal Control Theory: Linear and Nonlinear Control. *Journal of Engineering Mechanics*, Vol. 120., 1994
18. *Proceedings of the First World Conference on Structural Control*, Los Angeles, California, USA, Vol 1-4, 1994
19. *Proceedings of the Second World Conference on Structural Control,* June 28 - July 1, 1998, Kyoto, Japan. Vol. 2, pages 959-964, Chichester, John Willey & Sons, 1999
20. *Proceedings of the Third World Conference on Structural Control, 7-12 April 2002, Como, Italy, John Wiley & Sons, Chichester*, 2003, ISBN 0-471-48980-8
21. *Journal of Structural Control*, vol. 10, no.3+4, 2003, ISSN 1122-8385
22. Voicu, M., *Introduction in Automation*, 2nd edition, Polirom, Iaşi, 2002 (in Romanian)
23. Filipescu, A., Stamatescu, S., *System Theory: analysis and synthesis of linear system in structural approach*, Matrix Rom, Bucureşti, 2002 (in Romanian)
24. Yao, T.P.J., Concept of structural control. *Journal Structural Division,* 98, No. St7, 1567-1574, 1972
25. Budescu, M., *Contribuții privind izolarea seismică a structurilor*, *(Contributions regarding seismic isolation of structures),* Doctoral Thesis, Plytechnic Institute of Iasi, 1980 (in Romanian)
26. Olariu I., Olariu F., Sarbu D., Structural Control for Seismic Loads Using PRB System, *Proceedings of the Second World Conference on Structural Control, Kyoto, Japan*, John Willey & Sons, Chichester, 1999, I, 173-180
27. Păuleț-Crăiniceanu, F., Active versus passive control of seismic response for Civil Engineering Structures, *Memoriile Secțiilor Ştiințifice*, Seria IV, Tom XXI/1998, Editura Academiei Române, Bucureşti, 2001, pp.197-215
28. Păuleț-Crăiniceanu, F., Wolfe R., Caffrey J., Masri S., An Experimental Study of an Adaptive Momentum Exchange Device for Structural Control Applications, *Second European Conference on Structural Control, 2ECSC*, ENPC, Champs-sur-Marne, France, July 3-6, 2000
29. Păuleț-Crăiniceanu, F., Structures with active hinges, a step to Structural Robotics, *Computational Civil Engineering 2005*, Editura Societății Academice "Matei-Teiu Botez", Iasi, 2005, pp. 246-256
30. Păuleț-Crăiniceanu, F., Research Report. Grant A2276, *Journal of Sciences Politics and Scientology*, Special Issue 2006, pp.1-8 (in Romanian)
31. *Matlab. User's Guide*. The MathWorks Inc., (1999).
32. *Control System Toolbox. User's Guide*, The MathWorks Inc., (1999).
33. MTS Systems Corporation, USA: *www.mts.com*.

ISBN (10) 973-7962-89-3
ISBN (13) 978-973-7962-89-8

MANIFESTARI STIINTIFICE